

**Electrosynthesis and Functionalization of
Dehydroamino Acids and their Application in the
Total Synthesis of Darobactin A**

**Inaugural-Dissertation
to obtain the academic degree
Doctor rerum naturalium (Dr. rer. nat.)**

submitted to the Department of Biology, Chemistry, Pharmacy
of Freie Universität Berlin

by

MARCEL GAUSMANN

2023

The present work was carried out in the period from December 2019 to July 2023 at the Institute of Chemistry and Biochemistry of the Freie Universität Berlin, Department of Biology, Chemistry, and Pharmacy under the direction of Prof. Dr. Mathias Christmann.

Parts of this project have already been published in:

M. Gausmann, N. Kreidt, M. Christmann, *Org. Lett.* **2023**, *25*, 2228–2232.

Chapter 5.8 of the Experimental Section was reprinted (adapted) with permission from M. Gausmann, N. Kreidt, M. Christmann, Electrosynthesis of Protected Dehydroamino Acids. *Org. Lett.* **2023**, *25*, 2228–2232, [DOI: 10.1021/acscorglett.3c00403](https://doi.org/10.1021/acscorglett.3c00403). Copyright 2023 American Chemical Society.

1st reviewer: Prof. Dr. Mathias Christmann

2nd reviewer: Prof. Dr. Christian Hackenberger

Date of defense: 2nd November 2023

Acknowledgments

First, I would like to thank Prof. Dr. Mathias Christmann for the opportunity to realize my doctoral studies in his research group and for trusting me to pursue my own paths during this challenging research with a high level of freedom and responsibility. His excellent, supportive guidance and fruitful discussion constantly encouraged me to overcome the challenges encountered in this project, not only scientifically, but also personally.

I am grateful to Prof. Dr. Christian Hackenberger to be the second reviewer for this dissertation and for his supportive feedback on the published work.

I want to thank all former and present members of the Christmann group for their support and encouragement during my work, creating a welcoming working atmosphere.

My special gratitude belongs to Bence Hartmayer for his excellent companionship in Lab 24.02 and the endless – sometimes funny, sometimes inspiring – discussions about anything and everything to pass the time during long lab days. We are a great team and our Trash Friday playlist will be fondly remembered. Thank you Jan-Hendrik Dickoff for taking over the Lab, you are a worthy successor and we had a great time together.

I thank Dr. Reinhold Zimmer for his scientific and organizational support throughout the years, you are indispensable for this group. I acknowledge Christiane Groneberg for her open door, fruitful discussions, and separation of various compounds.

The NMR department is acknowledged for carrying out hundreds of analyses over the years. Special thanks belong to Anja Peuker and Gregor Drendel for their professional measurements of numerous ge-NOESY spectra.

I would like to thank Jan-Hendrik Dickoff, Lorenz Wiese, Kamar Shakeri, and Zhen Wang for proofreading my thesis.

Last but not least, I want to express my deepest gratitude to my friends and family, especially Lisa Brunsmann and Amina Moshtaha, for supporting me and cheering me up in these critical times.

Finally, I deeply appreciate the loving support, empathy, and patience of Aradhana Sharma, while writing this thesis.

Declaration of Independence

Herewith I certify that I have prepared and written my thesis independently and that I have not used any sources and aids other than those indicated by me. I also declare that I have not submitted the dissertation in this or any other form to any other institution as a dissertation.

Marcel Gausmann

Berlin, 14th August 2023

“The saddest aspect of life right now is that
science gathers knowledge faster
than society gathers wisdom.”

– Isaac Asimov

Abstract

The structural unique natural product darobactin A demonstrated a novel mode of action against drug-resistant Gram-negative bacteria. With the bismacrocyclized heptapeptide posing a promising lead structure, the total synthesis of this compound could enable the development of a new class of antibiotics.

This work describes various synthetic approaches towards the key bond formation within its unique macrocycle, namely the construction of a β -hydroxytryptophan moiety and the formation of an unprecedented C-C bond between the β -position of the lysine and the C6-position of a central indole moiety. The asymmetric construction of the β -hydroxytryptophan was demonstrated by development of a SHARPLESS asymmetric aminohydroxylation protocol. Construction of the C-C bond was realized *via* the HECK-reaction of a 6-bromotryptophan and various dehydroalanine derivatives. Installation of the lysine side-chain was studied on a model substrate using a subsequent HECK reaction of Troc-allylamine with a brominated dehydroamino acid derivative.

The extensive use of dehydroamino acids within this work and limited synthetic methods towards their synthesis inspired the development of an electrocatalysis by electrochemical, NaCl-mediated α -methoxylation of amino acids carbamates followed by Brønsted-acid catalyzed elimination of methanol.

The method not only allowed the scalable, economic access of dehydroamino acids, but also the synthesis of novel 2-aminoproline and 2-aminopipercolic acids by cyclization of methoxylated lysine and ornithine derivatives, respectively.

Dehydroamino acids pose a versatile synthetic handle for the functionalization of complex biomolecules and the synthesis of non-canonical amino acids. Hence, their functionalization towards the synthesis of L-quisqualic acid and highly substituted 2-pyrazoline amino acids was investigated. A powerful [2+3]-cycloaddition of diazo compounds and dehydroamino acids was demonstrated using DABCO as a nucleophilic catalyst.

Kurzzusammenfassung

Der strukturell einzigartige Naturstoff Darobactin A zeigt einen neuartigen Wirkmechanismus in seiner Aktivität gegen multiresistente, Gram-negative Bakterien. Das bismacrozyklisierte Heptapetid stellt eine vielversprechende Leitstruktur dar und die erfolgreiche Totalsynthese dieser Verbindung könnte zur Entwicklung einer neuen Antibiotika-Klasse führen.

Diese Arbeit beschreibt verschiedene Synthesewege zur Darstellung des zentralen Makrocyclus. Schlüsselschritte sind der Aufbau der β -Hydroxytryptophan-Substruktur und die Knüpfung der anspruchsvollen C-C-Bindung zwischen dem β -Kohlenstoff des Lysins und der C6-Position des zentralen Indols.

Die enantioselektive Synthese des β -Hydroxytryptophans konnte durch die Entwicklung einer asymmetrischen SHARPLESS Aminohydroxylierung erreicht werden. Die außergewöhnliche C-C-Bindung wurde durch die HECK-Reaktion eines 6-Bromotryptophans mit verschiedenen Dehydroalanin-Derivaten verwirklicht. Anschließende HECK-Reaktion mit Troc-Allylamin ermöglichte die Einführung der Lysin-Seitenkette an einem Modellsubstrat.

Der intensive Einsatz von Dehydroaminosäuren und die Einschränkungen der verfügbaren Synthesemethoden führten zur Entwicklung einer neuen elektrochemischen Synthesemethode dieser Substratklasse. Die NaCl-vermittelte α -Methoxylierung von Aminosäure-Carbamaten gefolgt von der säurekatalysierten Eliminierung von Methanol ermöglichte den Zugang zu einer Vielzahl verschiedener Dehydroaminosäuren. Durch die beschriebene Methode konnten außerdem neue 2-Aminoprolin und 2-Aminopipicolinsäure-Derivate synthetisiert werden.

Dehydroaminosäuren stellen einen wertvolles Motiv für die Funktionalisierung von komplexen Biomolekülen dar und ermöglichen die Synthese unnatürlicher Aminosäuren. Die potentielle Synthese des Excitotoxins L-Quisqualsäure mittels konjugierter Addition von 1,2,4-Oxadiazolidion, sowie die Herstellung neuartiger, hochsubstituierter 2-Pyrazolin-Aminosäuren wurden untersucht. Dabei stellte sich die Nukleophil-katalysierte [2+3]-Cycloaddition von Diazoverbindungen an Dehydroaminosäuren als wertvoller Zugang zu 2-Pyrazolin-Aminosäuren heraus.

Content

1. Introduction	1
1.1. The Natural Product Darobactin A.....	1
1.2. Dehydroamino Acids	10
1.3. Electroorganic Synthesis	17
1.4. Pyrazolines	24
2. Objectives	27
3. Results	29
3.1. Studies towards the Total Synthesis of Darobactin.....	29
3.2. Electrosynthesis of Protected Dehydroamino Acids	64
3.3. Synthesis of Quisqualic Acid.....	77
3.4. Synthesis of Highly Substituted 2-Pyrazoline Amino Acids	80
4. Conclusion and Outlook	91
5. Experimental Section	95
5.1. General Methods	95
5.2. Template-assisted C6-Indole Functionalization of the Eastern Fragment.....	97
5.3. Synthesis of a 6-Triflyl Tryptophan	107
5.4. Sharpless Asymmetric Aminohydroxylation	111
5.5. Synthesis of Boc- Δ Lys(Troc)-OMe (72)	115
5.6. C6-Indole Bond Formation via Heck Reaction.....	118
5.7. Installation of the Lysine Side Chain	131
5.8. Electrosynthesis of Protected Dehydroamino Acids	139
5.9. Synthesis of Quisqualic Acid.....	166
5.10. Synthesis of 2-Pyrazoline Amino Acids.....	168
6. References	177
7. Appendix	185
7.1. List of Abbreviations	185
7.2. NMR Spectra	188
7.3. HPLC/GC Traces	314
7.4. Crystallographic Data.....	316

1. Introduction

1.1. The Natural Product Darobactin A

1.1.1. Discovery and Biological Activity

Darobactin A (**1**) was first isolated in 2019 by LEWIS *et al.* from *Photorhabdus khanii* and detected in 15 different species of *Photorhabdus*, a genus of bioluminescent, gram-negative bacteria.^[1] These bacteria are symbionts of nematodes and colonize their gut biomes. The nematodes are entomopathogenic, invading insect larvae and releasing the *Photorhabdus* bacteria. Consequently, the bacteria produce toxins and kill the insect, typically within 48 hours. The insect cadaver represents a source of nutrition for both the bacteria and the nematode, constituting their mutualistic relationship.^[2] During this process, the bacteria produce antibiotics to compete with invading microorganisms.

The natural product darobactin A (**1**) was isolated by HPLC and fractions were identified by Bioassays. The authors elucidated the structure by mass-spectroscopy and extensive NMR studies, revealing a modified heptapeptide with the sequence Trp¹-Asp²-Trp³-Ser⁴-Lys⁵-Ser⁶-Phe⁷ (Figure 1.1).

The heptapeptide is cyclized by two unusual crosslinks, a C7-indole-O-benzyl ether bridge between Trp¹ and Trp³ and a C-C bond between the C6-indole of Trp³ and β -carbon of Lys⁵. Together, these crosslinks form a bismacrocyclic core consisting of a 15-membered western ring and a 14-membered eastern ring. These macrocycles are highly strained, causing non-canonical atropisomerism of both rings, arising from the hindered rotation of the indole rings. In the naturally occurring atropisomer, both indole-nitrogen direct to the same face of the bismacrocyclic core. The orientation of the indoles was determined by extensive ROESY studies in comparison to DFT models of the four possible atropisomers.^[1]

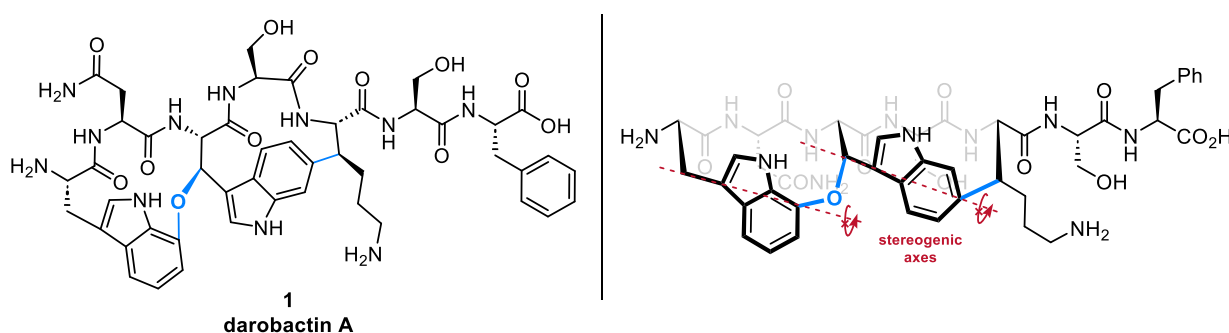


Figure 1.1: Structure of darobactin A (**1**, left) with the unusual crosslinks highlighted in blue. The non-canonical atropisomerism is caused by two stereogenic axes through the indole rings, arising from their hindered rotation (right).

Darobactin A showed high activities against various clinically relevant Gram-negative bacteria, including drug-resistant strains of *P. aeruginosa*, *K. pneumoniae*, *E. coli*, and *S. sonnei* with a minimum inhibitory concentration (MIC) of 2-4 $\mu\text{g mL}^{-1}$.^[1] The compound was equally active against polymyxin-, extended-spectrum β -lactamase- and carbapenem-resistant clinical isolates. It was inactive against Gram-positive bacteria, and importantly, showed no activity against most Gram-negative gut commensals, e.g. the symbiotic bacteria of the genus *Bacteroides*.^[3] This remarkable selectivity is unprecedented and prevents

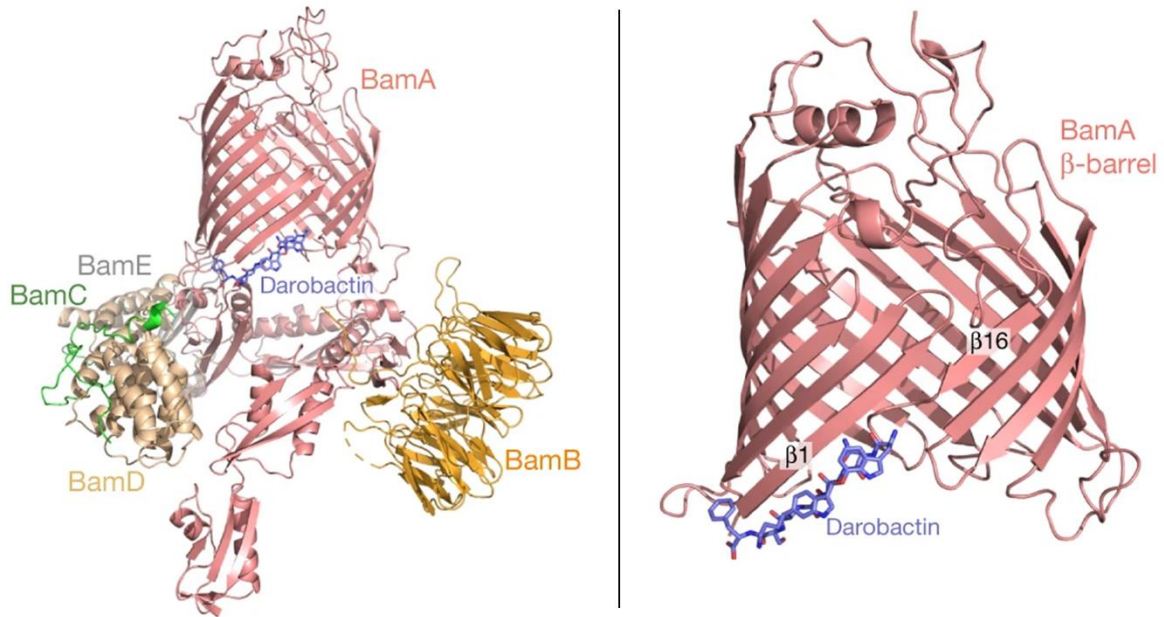


Figure 1.3: Structure of the BAM complex with bound darobactin resolved by cryo-EM with a resolution of 3.0 Å (left). Crystal structure with a resolution of 2.3 Å of the BamA β -barrel with darobactin A bound to the interaction site at the β 1-strand (right). Reproduced with permission from Springer Nature.^[8]

The native function of the BAM complex is the biogenesis of outer membrane proteins (OMPs). BamA is responsible for the folding and insertion of the OMP (Figure 1.4). Typically, the BamA protein recognizes a β -signal of the OMP nascent chain at the dynamic lateral gate in its center, initiating the folding and subsequent insertion of the OMP into the outer membrane of Gram-negative bacteria.^[8-10] Darobactin binds to this lateral gate, locking it in a lateral-closed conformation and hinders the access of other β -signal peptides.^[11]

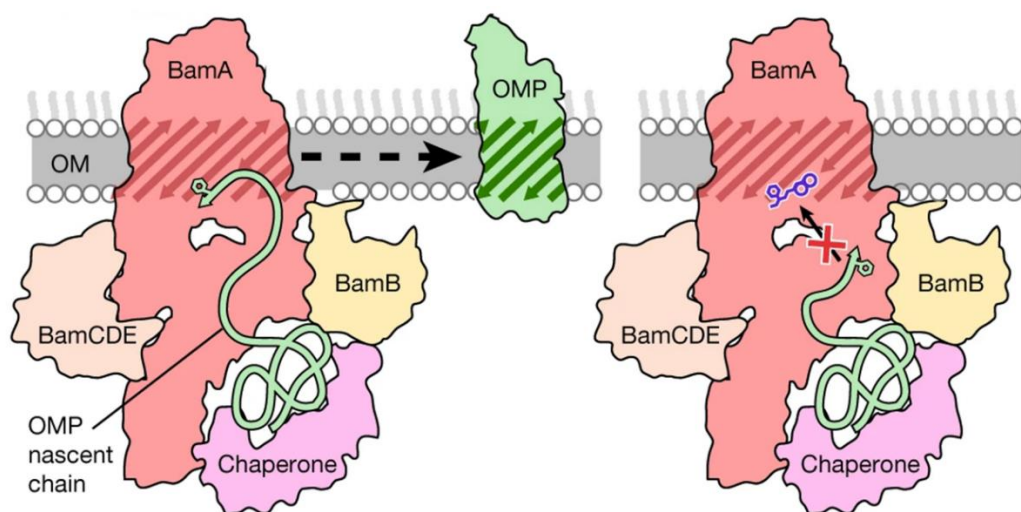


Figure 1.4: The native function of the outer membrane protein BamA in the BAM complex of Gram-negative bacteria. Recognition of the β -signal of the OMP nascent chain at the lateral gate in the center of BamA leads to folding and insertion of the OMP into the membrane (left). Darobactin A (**1**) binds to the β -signal binding site at the lateral gate, preventing the folding and insertion of OMPs into the membrane (right). Reproduced with permission from Springer Nature.^[8]

The lateral gate has an unusual physicochemical nature, as its composed of lipidic, peptidic, and aqueous components. Darobactin must have evolved to adapt to this specific binding site, mutation experiments assessed a high robustness against mutations of the BAM complex.^[8]

1.1.3. Biosynthesis and Biosynthetic Engineering Efforts

The biosynthetic gene cluster (BGC) of darobactin was first identified by LEWIS *et al.* by sequencing the genome of the native host bacterium *P. khanii*.^[1] The gene cluster consists of six open reading frames, starting with a global translation inhibitor *relE* and followed by *darA-E* (Figure 1.5).

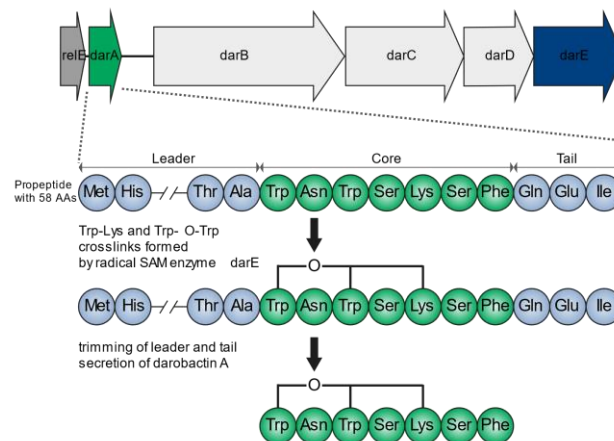
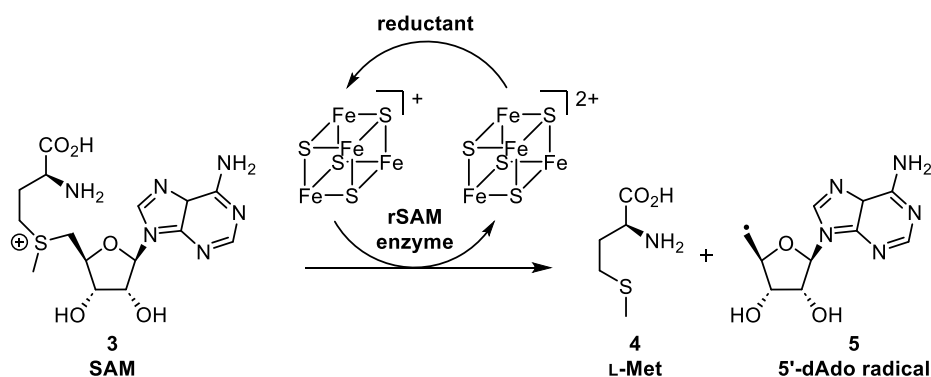


Figure 1.5: The biosynthetic gene cluster (BGC) of darobactin A (1) consisting of the global translation inhibitor *relE*, the propeptide encoding gene *darA*, the ABC-type transporter genes *darB*, *darC*, and *darD*, and the encoding gene for the rSAM enzyme. Translation of *darA* synthesizes the darobactin A propeptide, post-translational crosslinks are formed by the rSAM enzyme forming the bismacrocyclic. Trimming of the leader and tail sequence leads to the secretion of darobactin A (1).

The biosynthesis commences with a propeptide consisting of 58 amino acids, encoded by *darA*. The following three frames *darB*, *darC*, and *darD* encode for an ABC-type trans-envelope exporter system and *darE* encodes for a radical S-adenosyl methionine (rSAM) enzyme, which catalyzes the Trp-Lys and Trp-O-Trp crosslink formation.

After translation of the propeptide, composed of a leader sequence, the darobactin core consisting of the seven natural amino acids, and a Gln-Glu-Ile tail, the two crosslinks are formed by post-translational modification by the rSAM enzyme.

This superfamily of enzymes consists of 700 million unique sequences and is known to carry out over 100 different radical reactions involving the 5'-dAdo radical.^[12-13] Although the mechanism for the formation of the 5'-dAdo radical **5** (Scheme 1.1) is thoroughly investigated,^[14] the exact mechanism for the Trp-Lys and Trp-O-Trp is an area of active research.^[15-16]



Scheme 1.1: Generation of a reactive 5'-dAdo radicals by radical SAM enzymes.^[13]

Given the novel mode of action and its promising antibiotic profile as a lead structure, great efforts, not only towards its total synthesis but also towards the engineering of a biosynthetic pathway were made.

The native producer strain showed a low production titer of $\leq 3 \text{ mg L}^{-1}$ for darobactin A, uneconomic for industrial-scale fermentation.^[1] In 2021, MÜLLER *et al.* developed a production platform for various darobactin derivatives using modified BGCs of darobactin in the cheap and reliable *E. coli* BL21 strain.^[17-18] They could improve the production titer to 13.4 mg L^{-1} in 3 days. Independently, SCHÄBERLE *et al.* were able to increase to production titer to $>30 \text{ mg L}^{-1}$ in 2 days using an *E. coli* Rosetta™ (DE3) production system.^[19]

They were able to produce 17 new darobactin derivatives and conducted SAR studies using MIC assays of the crude extracts to compare their antibacterial activity (Figure 1.6).

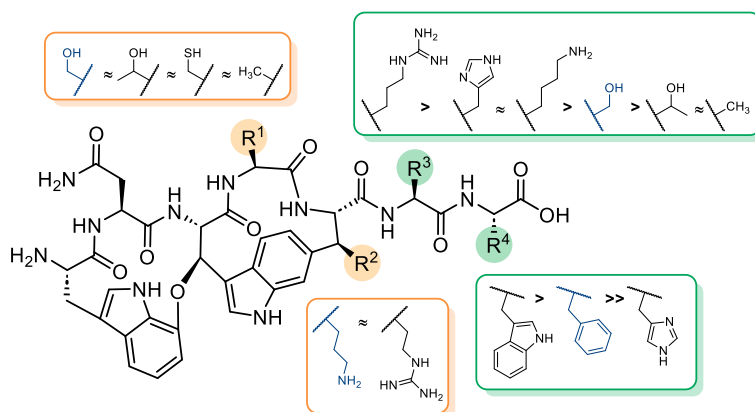


Figure 1.6: Summarized results of the SAR study conducted by MARLOVITS, HERRMANN, and MÜLLER *et al.* using biosynthetic engineering and antibacterial activity measurements by MIC assays of the crude extracts.^[18]

Although this procedure did not allow the measurement of precise MIC values, important insights were gained by a comparison of the different structural modifications. Whereas the replacements of the amino acids Ser⁴ and Lys⁵ did not alter the antibacterial activity significantly, the replacement of the modification of the 6th amino acid Ser⁶. The use of amino acids with positively charged side chains, e.g. Arg, His, or Lys drastically increased its bioactivity. Additionally, the replacement of Phe⁷ with Trp increased its potency.

1.1.4. Reported Total Synthesis

The discovery of darobactin attracted a lot of attention in the scientific community. Not only the novel mode of action and antibacterial profile but also the unique structure posed a challenge for synthetic chemists from all over the world.

In 2022, three years after its discovery, the first total synthesis of darobactin A was disclosed by a joint venture of the SARLAH group and the Department of Process R&D at Merck under the lead of PETRONE and PATEL *et al.*^[20] Independently, BARAN *et al.* published a total synthesis featuring the same key-steps for the macrocyclizations, two atroposelective LAROCK indole syntheses.^[21]

Notably, both groups revealed their failed cyclization approaches via different media, demonstrating very similar retrosynthetic endeavors (Figure 1.7).^[20-23]

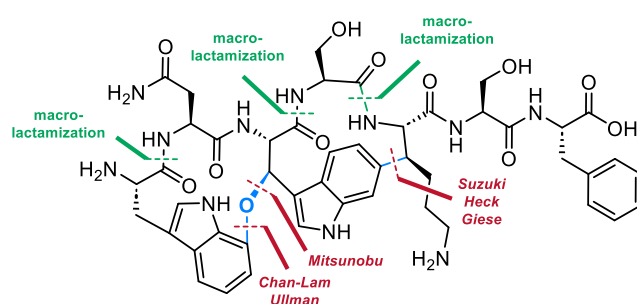
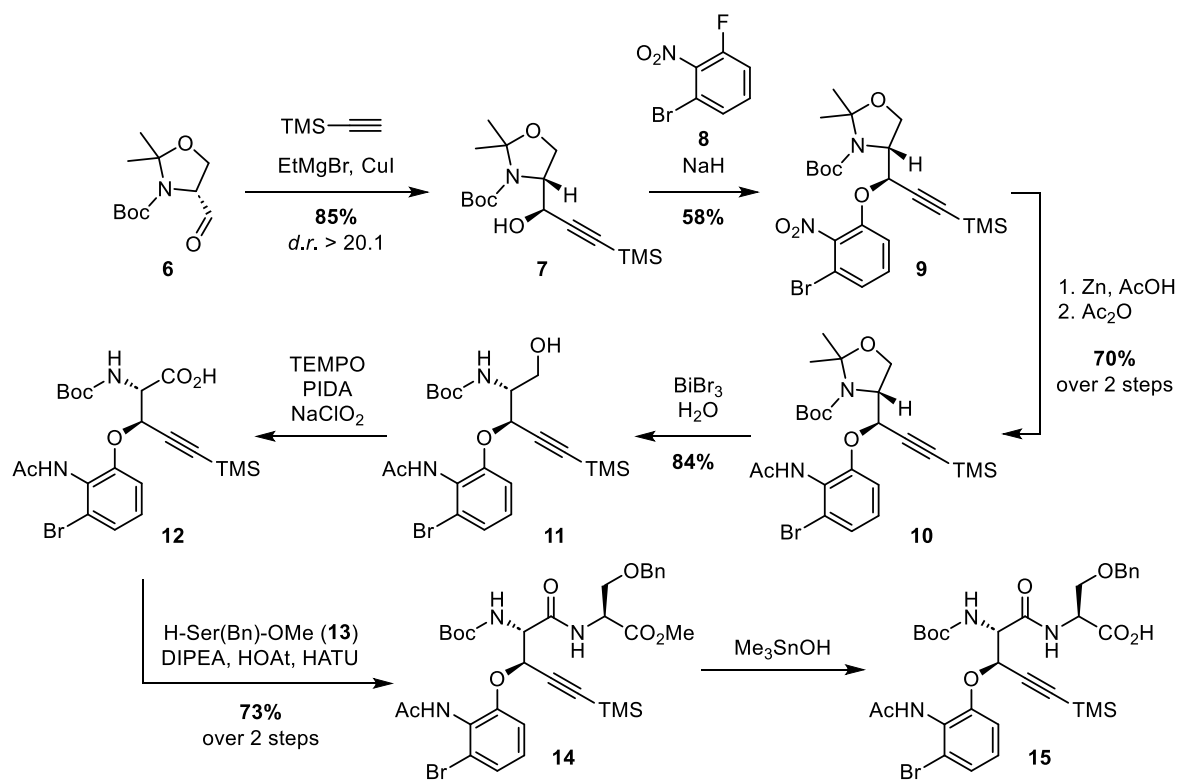


Figure 1.7: Summary of the failed cyclization approaches for the macrocycles of darobactin A (1).

While the attempted macrolactamizations favored the formation of dimers over cyclization, HECK- and SUZUKI-cross-coupling approaches for the formation of the Trp³-Lys⁵ C-C bond were successful, but led to the exclusive formation of the undesired atropisomer.

The final approach of SARLAH, PETRONE and PATEL *et al.* commenced with the synthesis of dipeptide **15** (Scheme 1.2). Starting with the diastereoselective addition of TMS-acetylene to Garner's aldehyde (**6**), nucleophilic aromatic substitution at the fluorobenzene **8** provided nitroarene **9**. Reduction of the nitro-group and subsequent acetylation afforded acetanilide **10**. Cleavage of the oxazolidine moiety with bismuth bromide gave the amino alcohol **11** which was oxidized to the corresponding amino acid **12** using ZHAO's modification of the ANELLI oxidation.^[24] Peptide coupling with H-Ser(Bn)-OMe (**13**) followed by ester hydrolysis with Me₃SnOH afforded the dipeptide building block **15**.

Scheme 1.2: Synthesis of dipeptide 15 by SARLAH, PETRONE and PATEL *et al.*^[20]

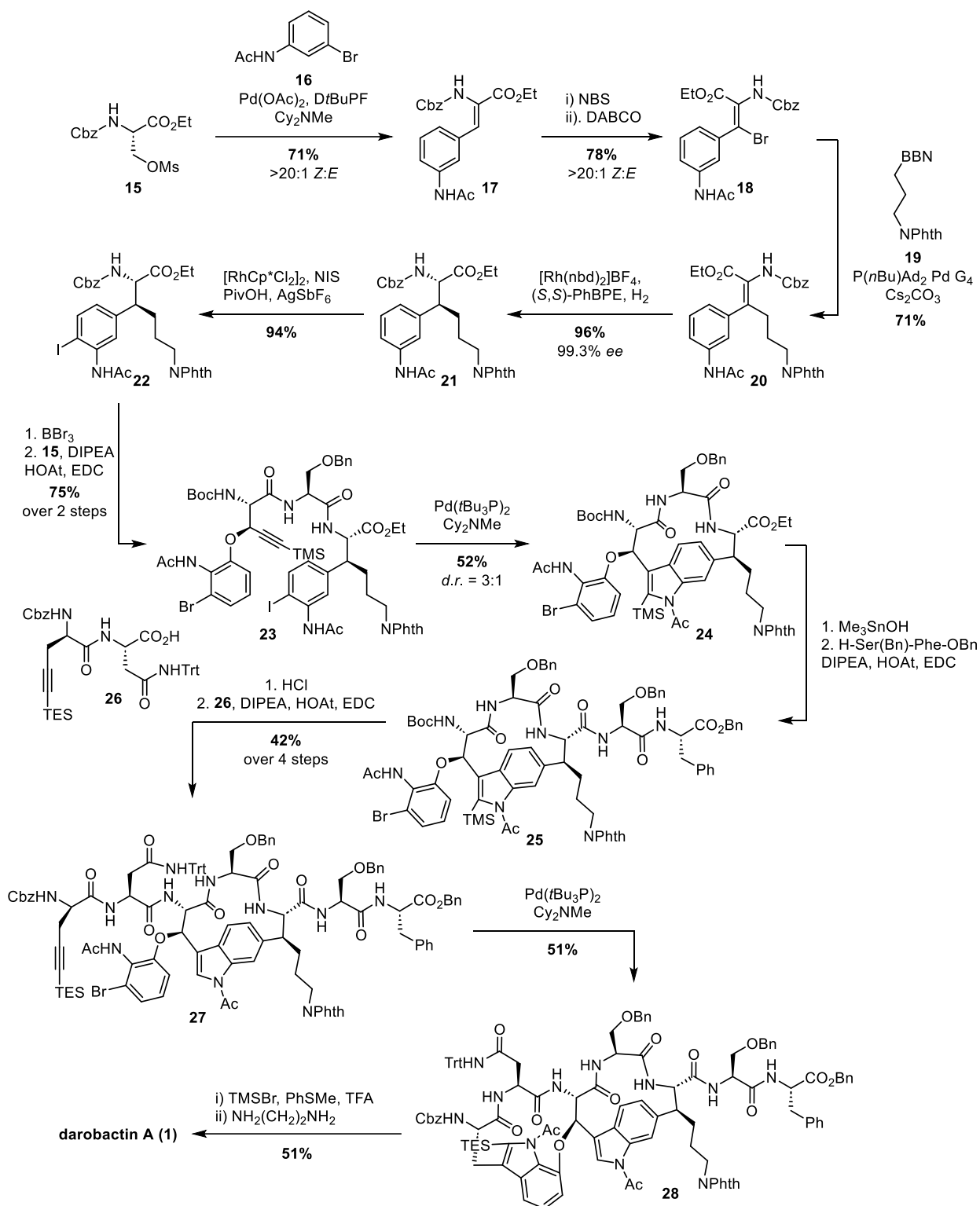
The synthesis of the next major building block introduces the lysine moiety resembling the C6-indole β -C bond between Trp³ and Lys⁵ of darobactin A. The synthesis began with mesylated Cbz-Ser(Ms)-OEt (**15**) (Scheme 1.3). *In situ* elimination of the mesylate and HECK reaction of the dehydroalanine in solution with 3-bromoacetanilide (**16**) afforded the non-canonical dehydroamino acid (dhAA) **17** in 71% yield and excellent (*Z*)-selectivity. Bromination at the β -position gave vinyl bromide **18** which underwent a SUZUKI reaction with 9-BBN functionalized propyl phthalimide **19**. Extensive high-throughput screening identified [Rh(nbd)₂]BF₄ / (S,S)-PhBPE as a suitable catalyst-ligand system for the high-pressure asymmetric hydrogenation of the dhAA **20** with excellent enantioselectivity and yield.

To allow a distinction of the two haloacetanilides for the envisioned LAROCK cyclizations, the installation of an iodide on the eastern acetanilide enabled a predefined LAROCK cyclization cascade based on the higher reactivity of the iodide over the bromide. The C-H iodination of **21** was achieved by an *ortho*-iodination protocol developed by GLORIUS *et al.*^[25] Deprotection of the benzyl carbamate of **22** using BBr₃ followed by peptide coupling with building block **15** afforded cyclization precursor **23**.

Preliminary LAROCK cyclization studies revealed that a preceding formation of eastern macrocycle was strictly necessary to achieve the desired atroposelectivity in both cyclizations. The slower oxidative addition of the bromide over the iodide allowed the sequencing of the ring formations by temperature control.

The eastern macrocycle was formed at 40 °C forming **24** with an atroposelectivity of 3:1 favoring the desired atropisomer. Hydrolysis of the terminal ester and peptide coupling with H-Ser(Bn)-Phe-OBn afforded the pentapeptide **25**. Acid-promoted deprotection of the *N*-terminus followed by peptide coupling with alkynyl-dipeptide **26** introduced the alkyne function for the western macrocycle, which was formed by cyclization of **27** using the established protocol at 80 °C furnishing the bismacrocyclic core of darobactin A.

Deprotection of the nine remaining protection groups from **28** was orchestrated in a single pot by acidic/LEWIS acidic removal of the TES, Trt, Cbz, and the three benzyl groups followed by cleavage of the phthalimide and the two acetyl groups using ethylene diamine. Darobactin A (**1**) was synthesized in 16 steps (longest linear sequence).

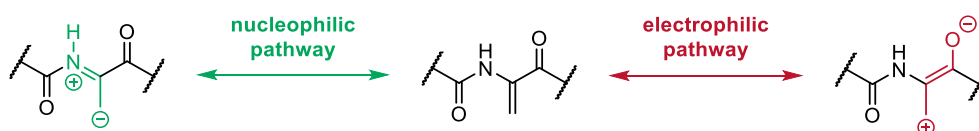
Scheme 1.3: Total synthesis of darobactin A (1) reported by SARLAH, PETRONE and PATEL *et al.*^[20]

1.2. Dehydroamino Acids

1.2.1. Properties of Dehydroamino Acids

α,β -Dehydroamino acids (dhAAs) are non-canonical amino acids and are not encoded in the genetic code of naturally occurring organisms. Yet, peptides containing dhAAs are abundant in nature, often arising by posttranslational modification of serine, threonine, and cysteine residues.^[26-27]

The structure of dhAAs features a double bond between the α - and β -carbon, resulting in a planar geometry with restricted flexibility. The φ - and ψ - torsion exhibit a *trans*-geometry, making dhAAs strong turn inducers in the peptide chain. Additionally, the electron-donating effect of the amide nitrogen in combination with the electron-withdrawing carbonyl group represents a complex electronic architecture, allowing a wide range of chemical transformations. Depending on the conditions, either the electron-rich character of the enamide or the electrophilicity of the β -carbon, conjugated to the carbonyl function, can be exploited, i.e. in polar addition reactions (Scheme 1.4).



Scheme 1.4: Unique electronic structure of dhAAs.

1.2.2. Naturally Occurring Dehydropolptides and their Biological Activities

The presence of dhAAs in dehydropolptides has drastic effects on their conformation and biological activity. Due to their restricted conformation and the planar geometry, the structural and proteolytic stability of the peptide is increased, allowing tighter target complementarity.^[26, 28-30]

While dehydroalanine and dehydrobutyrine can be incorporated by enzymatic dehydration of serine or threonine, respectively, natural products with other dhAAs are extremely rare.^[27] Most dhAA-containing peptides are isolated from bacteria, but fungi and sponges, as well as other sources have been reported (Figure 1.8).^[27]

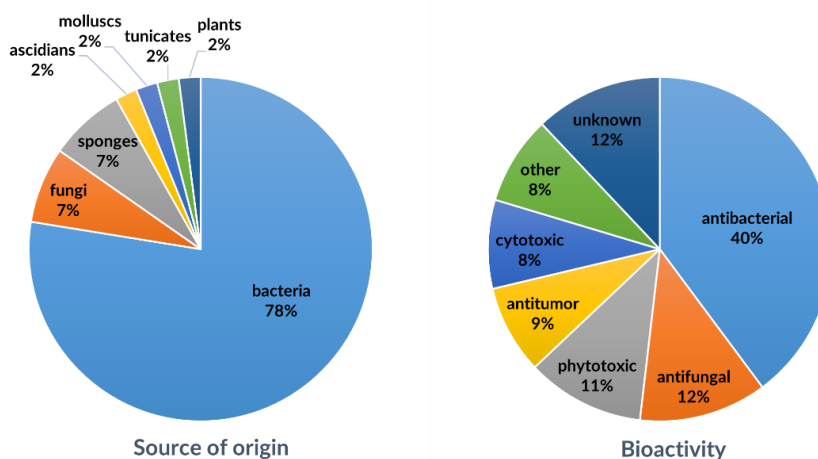


Figure 1.8: Source of origin and bioactivity of dhAA-containing peptides.^[27]

More than half of the isolated peptides exhibit antibacterial and antifungal activities (Figure 1.8), and several peptides have been used as lead structures for antibiotics.

Thiazolyl peptide antibiotics are an important class of dhAA-containing antibiotics with >80 members containing its characteristic substructure, a macrocycle with a central pyridine/piperin ring substituted with three thiazoles. Two prominent examples are thiocillin (**29**) and thiostrepton (**30**) (Figure 1.9).

While both of these structures show potent antibacterial activities, they suffer poor pharmacokinetics, limiting their therapeutic use.^[31-32] Their pharmacological profile could be improved by gene editing and site-selective functionalization of the dehydroalanine residues.^[31-34]

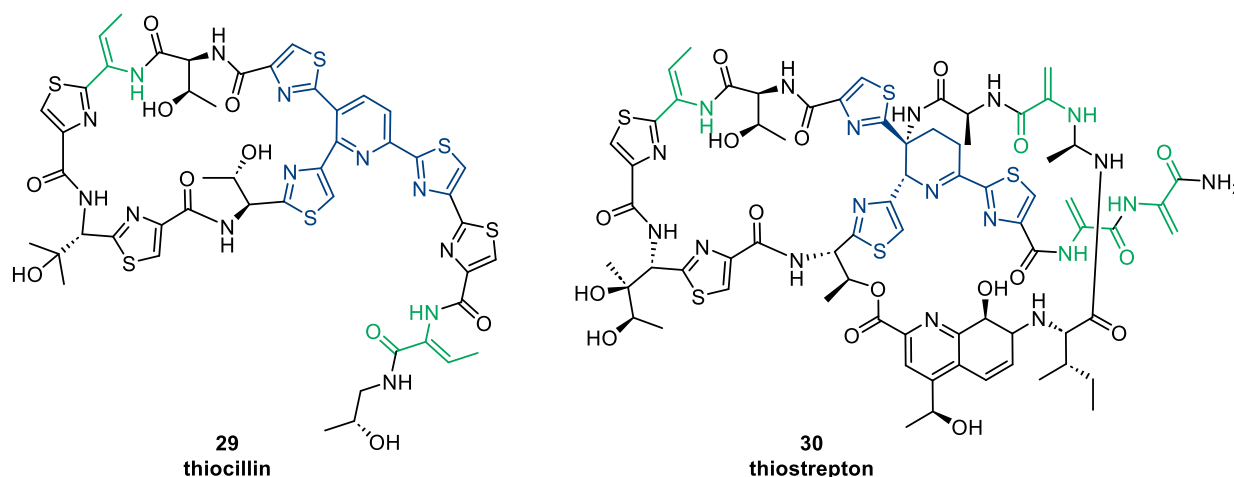
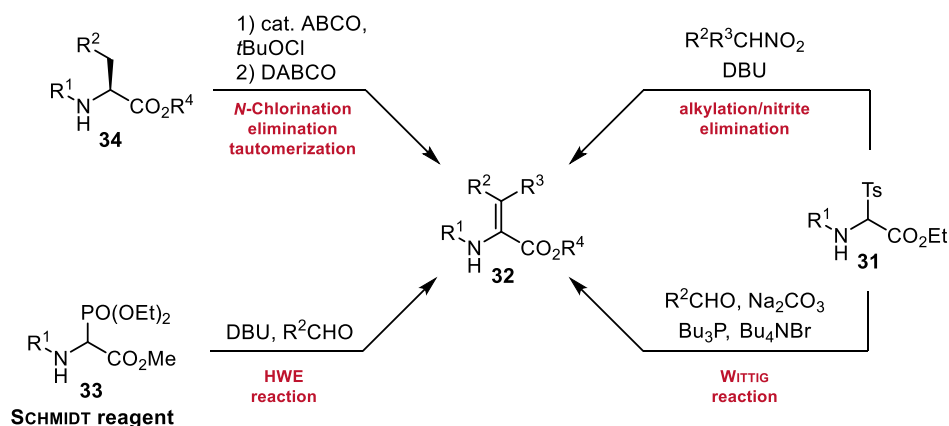


Figure 1.9: Structures of the thiazolyl peptide antibiotics thiocillin (**29**) and thiostrepton (**30**).

1.2.3. Synthesis of Dehydroamino Acids

Inspired by nature, dehydroalanine, and dehydrobutyryne derivatives are accessible by dehydration from their respective serine and threonine derivatives.^[35-36] While enzymes phosphorylate the hydroxy functions using ATP followed by H^+ or Mg^{2+} activation and base-induced elimination to generate the desaturated amino acids,^[37] chemists transform the hydroxy function into common leaving groups, e.g. mesylates or carbonates to facilitate the elimination reaction. Additionally, the conversion of cysteines or selenocysteines can afford dehydroalanines.^[38-39]

In contrast, the synthesis of other dhAAs remains challenging, as β -hydroxyamino acids are not readily accessible by synthetic methods. KINOSHITA *et al.* reported two methods using *N*-Cbz-tosyl glycines (**31**) and nitro compounds^[40] or aldehydes^[41] in an alkylation/nitrite elimination-cascade or Wittig-type reaction, respectively (Scheme 1.5). These approaches allow access to a variety of substituted dhAAs **32** but are limited in the protective groups on the tosyl glycine derivative and the accessibility of their respective coupling partners.

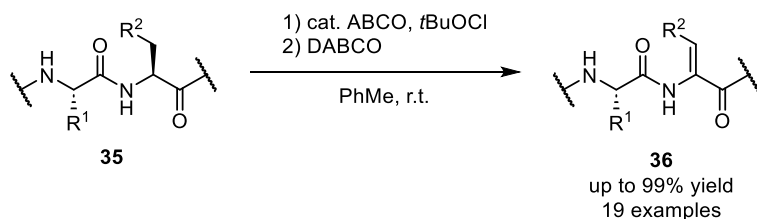


Scheme 1.5: Synthetic approaches towards dhAAs.

An alternative strategy utilizes the SCHMIDT reagent (**33**) in HORNER-WADSWORTH-EMMONS reactions.^[42-43] The method was shown to be quite flexible, a large variety of dhAAs can be accessed, if the corresponding aldehyde is accessible. The *N*-Cbz protected reagent is commercially available, but other derivatives have to be synthesized by modifications of the reagent as the reagent synthesis does not tolerate other protective groups like *tert*-butyl carbamates.^[44]

Few direct desaturations of the corresponding saturated amino acids have been reported. In one of the first reports of dhAAs in 1977, SCHMIDT *et al.* reported a direct synthesis of dhAAs from the corresponding amino acids **34** using an *N*-chlorination, dehydrochlorination, and rearrangement sequence.^[45]

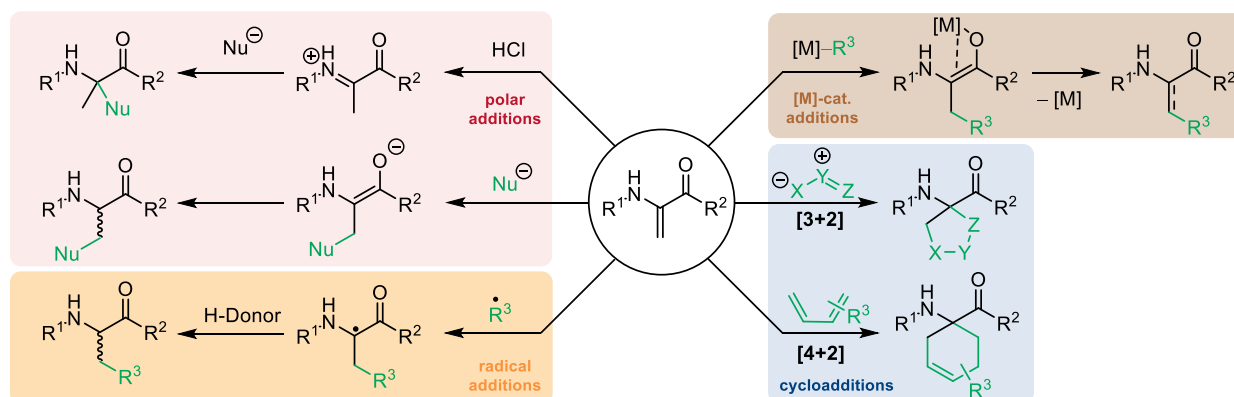
However, the method found limited application due to the use of reactive *t*BuOCl and challenging *N*-protection of the sensitive enamines. NANJO and TAKEMOTO *et al.* revisited the reaction and applied a similar *N*-chlorination protocol using quinuclidine as a catalyst for the selective late-stage desaturation of aliphatic peptides of type **35** (Scheme 1.6).^[46] Unfortunately, carbamate-protected residues were not desaturated under these conditions.



Scheme 1.6: Late-stage desaturation of peptides by NANJO and TAKEMOTO *et al.*^[46]

1.2.4. Functionalization of Dehydroamino Acids

The unique electronic structure of dhAAs offers a plethora of chemical transformations to modify dhAAs, dhAA-containing peptides, and natural products (Scheme 1.7).



Scheme 1.7: Reaction types and selectivities for the functionalization of dhAAs.

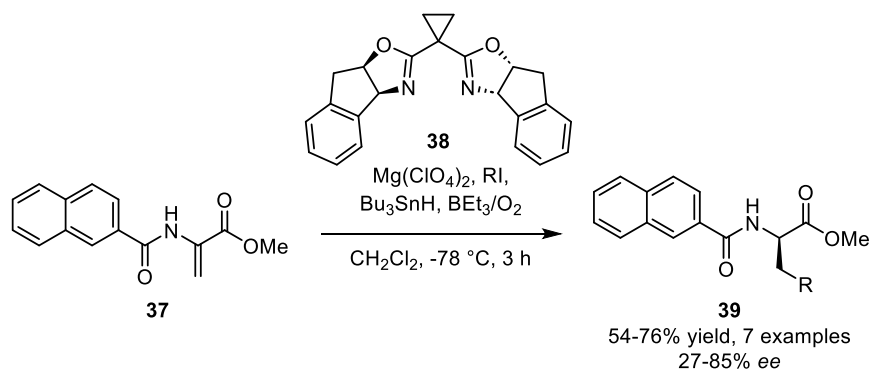
Depending on the reaction conditions, polar, nucleophilic additions can be performed with α - or β -selectivity. In slightly acidic media, the enamine-character dominates and protonation of the β -position, followed by nucleophilic addition to the imine leads to α,α -disubstituted amino acids.^[26] However, due to the acidic conditions, the α -substitution is limited to non-basic nucleophiles, e.g. electron-rich aryls, halogens, or thiols.^[47-48]

Nucleophilic β -substitution is readily used in total synthesis and widely reported in academic literature. Conjugate additions can be achieved under very mild conditions with high chemoselectivity and yields, e.g. thiols, amines, malonates, and electron-rich aryls undergo addition at room temperature using K_2CO_3 as a mild base.^[49] Although many methods for the conjugate addition of nucleophiles on dhAAs have been reported, stereoselective additions remain challenging.

DhAAs demonstrate outstanding SOMO-philicity and readily undergo radical addition at the β -carbon, forming an α -radical. The α -radical is highly stabilized due to the captodative effect between the nitrogen and carbonyl-function. Quenching with H-Donors gives β -substituted amino acids selectively.

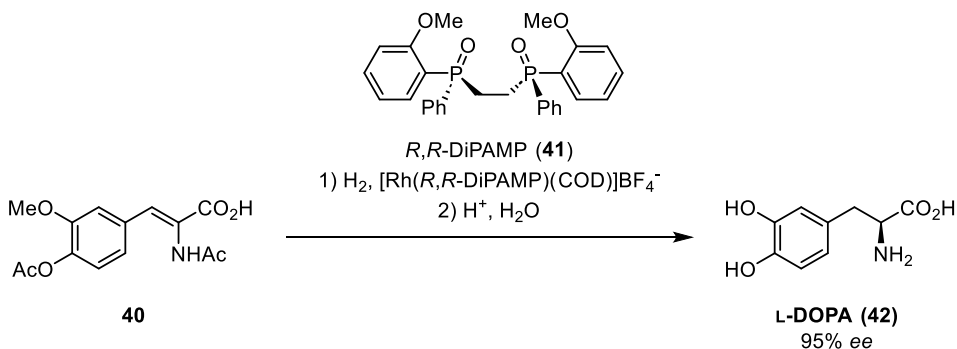
While at the beginning of the century, the radical initiation under mild conditions posed a major obstacle, with the rise of photoredox-catalysis, mild methods for radical generation became accessible, and the radical addition to dhAAs found widespread application for the site-selective modification of dehydropeptides and the synthesis of unnatural amino acids.^[50-54]

Again, achieving stereoselectivity remains a major hurdle, but promising results on simple systems were reported by SIBI *et al.*^[55] Using $Mg(ClO_4)_2$ as a catalyst and a bisoxazoline ligand **38** they achieved reasonable enantioselectivities for the addition of alkyl iodides to dehydroalanines (Scheme 1.8).

Scheme 1.8: Radical conjugate addition with enantioselective H-atom transfer reported by SIBI *et al.*^[55]

While polar and radical conjugate additions to dhAA suffer from low enantioselectivities, transition metal-catalyzed reactions with dhAAs benefit from the highly ordered transition states using appropriate ligands.

In fact, the 2001 Nobel prize was given to KNOWLES for the asymmetric hydrogenation of dhAA **40** towards the synthesis of L-DOPA (**42**), a drug used in the clinical treatment of Parkinson's disease (Scheme 1.9).^[56]

Scheme 1.9: Asymmetric hydrogenation by KNOWLES for the industrial synthesis of L-DOPA (**42**).^[56]

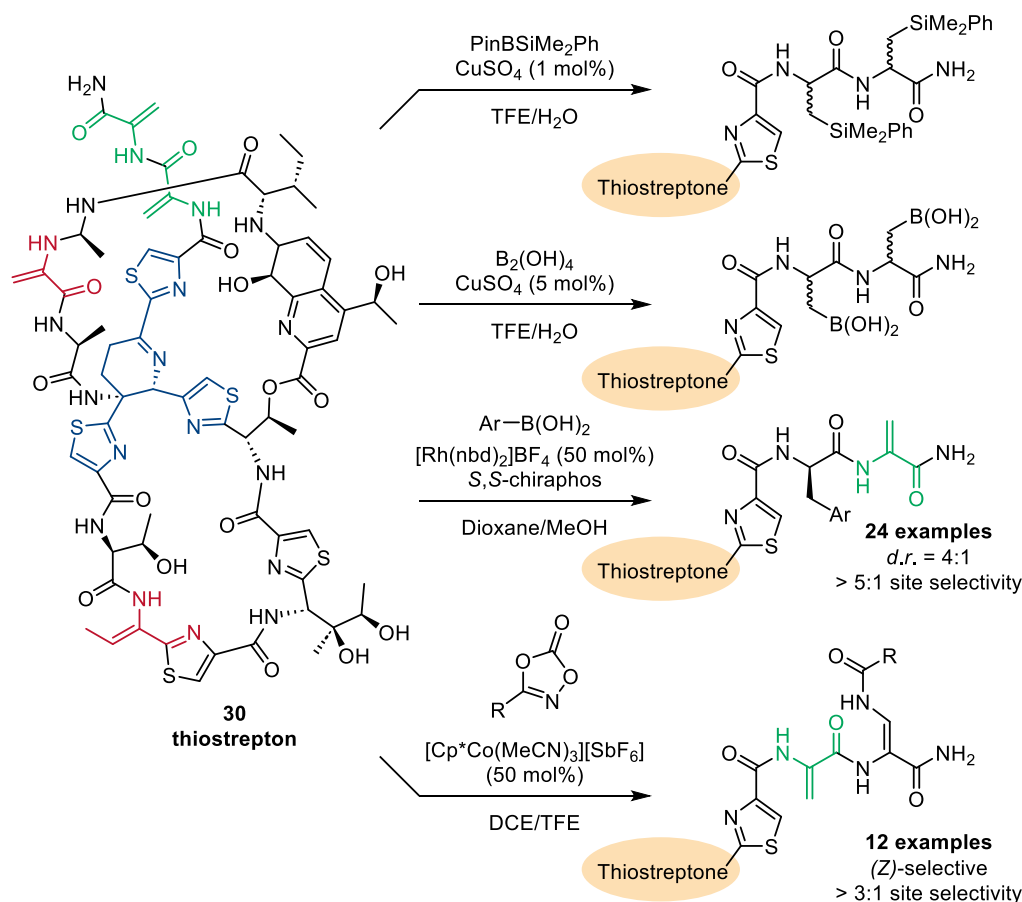
After its discovery, the asymmetric hydrogenation reaction found wide application for the asymmetric synthesis of amino acids, however, the reaction was limited to dhAAs with small protecting groups, e.g. acetyl or formyl, carbamates were difficult to hydrogenate.^[57]

Fortunately, with the recent development of powerful phosphine-phosphite ligands, the asymmetric hydrogenation of carbamate-protected dhAAs became feasible.^[58-59]

DhAAs can be readily halogenated in the β -position using *N*-halosuccinimides.^[60] The corresponding vinyl halides can be employed in common cross-coupling reactions, e.g. SUZUKI or SONOGASHIRA reactions.^[61-63] In contrast, the HECK reaction with dhAAs as the olefinic substrate experienced more extensive use, e.g. in the total synthesis of clavicipitic acids,^[64] or the synthesis of pyridylalanines and dehydrophenylalanines.^[65-66]

Newest methodologies focus on the modification of dehydroalanine-containing peptides, especially thiostreptone (**30**). Cu(II)-catalyzed β -Silylation and β -borylation, Co(III)-catalyzed β -amidation and Rh(I)-catalyzed conjugate arylation using boronic acids has been demonstrated to modify the complex thiopeptide

antibiotic with various site-selectivity, tolerating the abundance of functional groups within the molecule (Scheme 1.10).^[32-34]

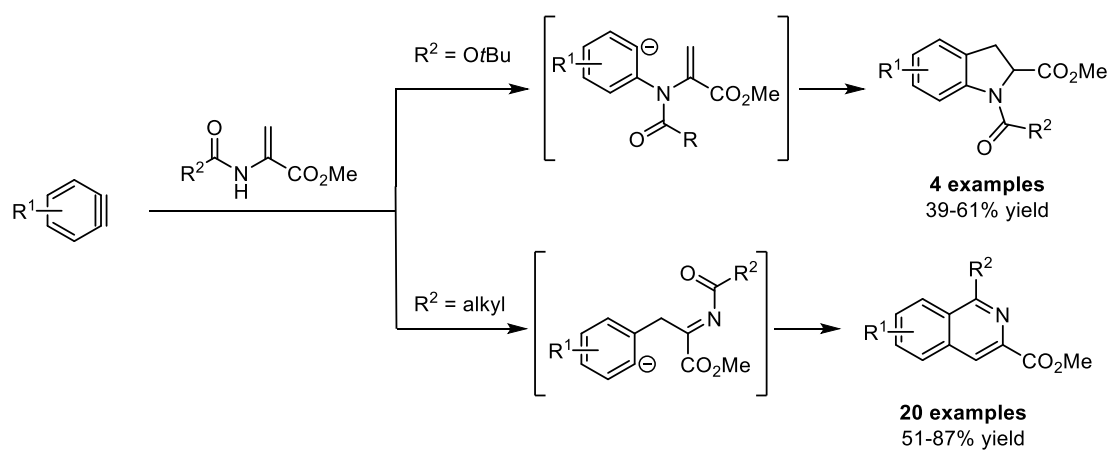


Scheme 1.10: Various site-selective modifications of the antibiotic peptide thiostrepton (**30**). The dehydroalanine and dehydrobutyridine moiety within the bismacrocyclic (red) were retained within all reported methods.^[32-34]

Given the unique electronic nature of dhAAs, they readily react in cycloadditions.

Interestingly, although they commonly participate as the 2π -partner given their olefinic character,^[67-68] a report by STOLTZ *et al.* demonstrates that they are also capable to react as pseudo-1,3-dipoles (3π) and even as the 4π -partner when the nitrogen and acyl-substituent are involved, respectively.^[69]

In their work, they developed a divergent access of substituted indolines and isoquinolines by cycloaddition of *N*-acyl dhAAs with arynes. While carbamate-protected dhAAs undergo cycloaddition as a 3π -partner, forming indolines, enamides underwent [4+2] cycloaddition with arynes forming isoquinolines (Scheme 1.11).



Scheme 1.11: Orthogonal syntheses of indolines and isoquinolines by STOLTZ *et al.*^[69]

1.3. Electroorganic Synthesis

1.3.1. History of Electroorganic Reactions

With the discovery and research of electricity by the end of the 18th century, scientists became aware of the concept of electrolysis, a cheap and simple method to conduct redox reactions. Starting with the electrolysis of inorganic compounds, chemists started to investigate the electrolysis of organic compounds.

The field of electroorganic chemistry was born with the discovery of the Kolbe reaction, a C–C homocoupling reaction that occurs by electrochemical decarboxylation of carboxylates, leading to radicals that undergo dimerization.^[70] Although the field was popular at that time, the interest in electroorganic chemistry subsided quickly, probably due to a lack of understanding of fundamental processes and a high entry barrier.^[71]

With the development and increased availability of electronic equipment, electroorganic chemistry experienced a renaissance and was fueled by the urgent need for green and sustainable chemical processes since the turn of the millennium (Figure 1.10).

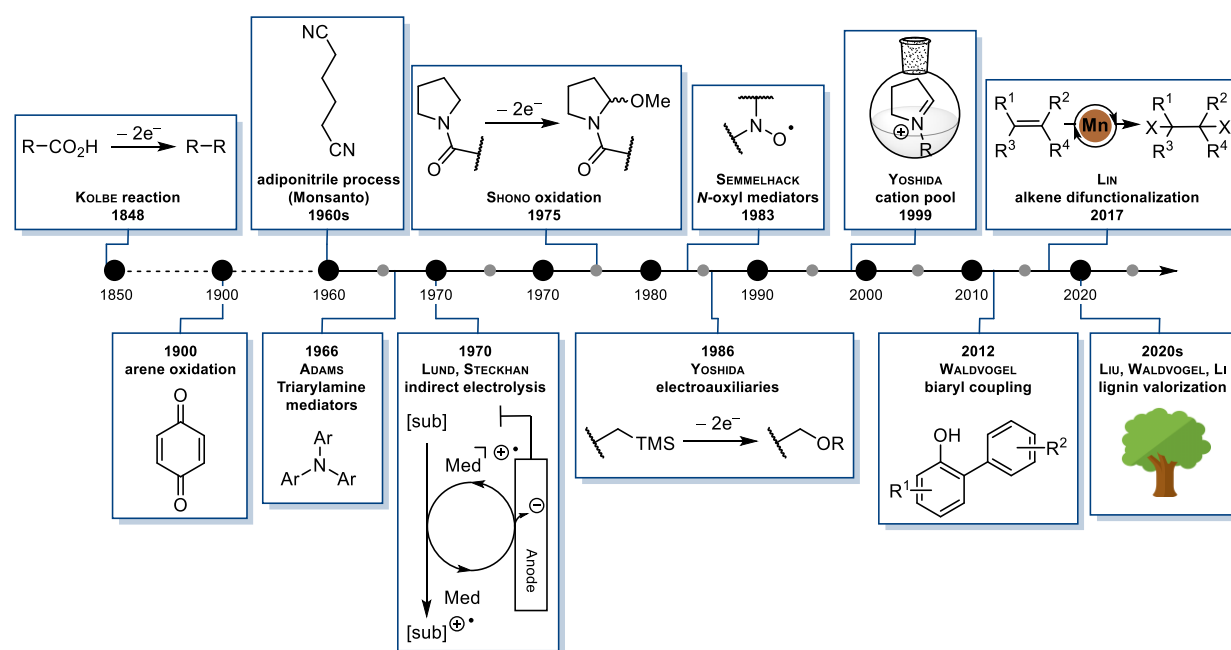


Figure 1.10: Milestones in the field of electroorganic chemistry throughout history.

In the middle of the 20th century, the first electrosynthetic processes were developed and implemented, e.g. the adiponitrile process by Monsanto.^[72] The electrochemical process allows large-scale access to the valuable Nylon 66 precursor using readily available acrylonitrile and steel electrodes.

The discovery of triarylamine mediators in 1966 and the extensive research on indirect electrolysis by LUND and STECKHAN *et al.* unlocked new potentials in the field, as the use of mediators often offers higher selectivities under milder reaction conditions compared to direct processes. Additionally, indirect electrolysis often lowers the required energy input as electrode inhibition can be mitigated.^[73-75]

A key method in electroorganic synthesis, the SHONO oxidation was discovered in 1975. The method allows the α -functionalization of alkyl amides and carbamates and found wide application in organic synthesis.^[76] Due to the low oxidation potential of alkyl amides, the mild conditions, and the valuable reaction products for medicinal chemistry, the transformation represents the most studied and utilized electroorganic transformation in academic literature.^[77]

In 1986, Yoshida *et al.* developed and described a new concept for electrochemical transformation, the utilization of electroauxiliaries, e.g. the trimethyl silanes.^[78] The increased HOMO energy level of C–Si and C–Sn bonds enabled site-selective redox transformations of redox-sensitive molecules.

Additionally, the group coined two new concepts for electroorganic synthesis and developed a variety of methods based on the concepts of “cation pool” and “cation flow” chemistry.^[79-80]

In the cation pool-methods, carbocations are electrochemically generated and accumulated at low temperatures in the absence of nucleophiles. The subsequent addition of a nucleophile in the absence of electricity allows the direct oxidative carbon-bond formation with redox-sensitive nucleophiles.

The newest developments focus on challenging transformations, e.g. the direct phenol-arene coupling developed by Waldvogel *et al.*,^[81] or the difunctionalization of alkenes with azides, halides, or CO₂.^[82] Notably, the difunctionalization of alkenes can be performed by merging shuttle reactions with paired electrolysis, e.g. enabling the dichlorination of alkenes using polyhalogenated waste products as a feed stock. The method is used to recycle lindane, a persistent organic pollutant with global quantities of 4 to 7 million tons.^[82]

Given the urgent need for aromatic, renewable feedstocks for the chemical industry, major efforts are conducted to depolymerize and valorize lignin towards organic chemicals. Many electrochemical methods for both, the depolymerization and the anodic oxidation of technical, organosoluble lignin have been demonstrated and are subject of current research.^[83]

1.3.2. Concepts and Parameters

Compared to regular transformations, electroorganic reactions have very different parameters influencing reactivities and selectivities. While a conventional redox-reaction uses (often stoichiometric) reagents and forms by-products, electrochemical methods use electrons as traceless redox equivalents.

The electrochemical reaction is conducted in an electrochemical cell, consisting of an anode (oxidation) and a cathode (reduction) submerged in an electrolyte and connected to a power supply providing a potential between the two electrodes (Figure 1.11).

In contrast to reagent-based chemistry, the oxidation and reduction event can be spatially separated by a diaphragm, providing a sufficient charge-flow to ensure charge neutrality is given.^[70] The majority of electroorganic methods are oxidation processes, hence, the anode reaction often receives the most attention, however, it is important that a process needs electrolytic conversion on both electrodes. In

general, the favored reaction represents the reaction with the lowest Gibbs free energy between oxidation and reduction.^[84]

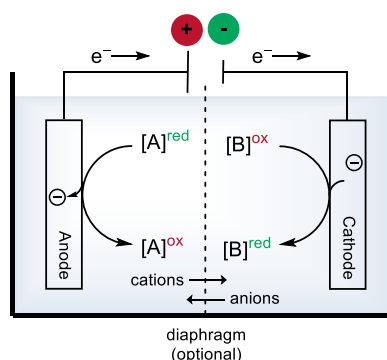
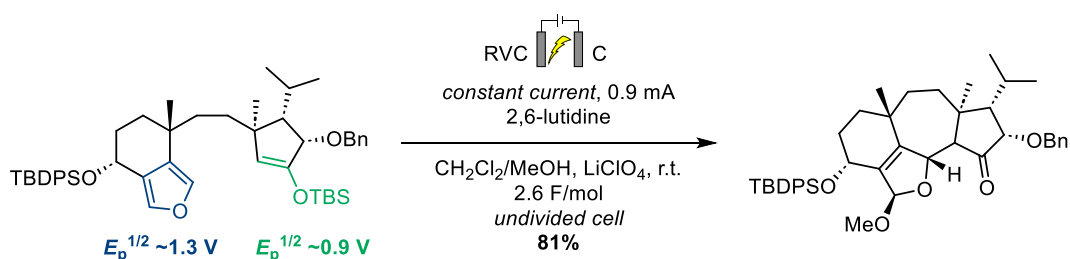


Figure 1.11: Representation of a basic electrolytic reaction.

The cell voltage refers to the applied potential on the electrodes and is affected by various overpotentials on the electrode (e.g. electrode interface, gas evolution), the resistivity of the electrolyte and separator, and the oxidation potential of the substrate. Determination of the redox potential of the substrate requires the use of a third standardized reference electrode.^[84]

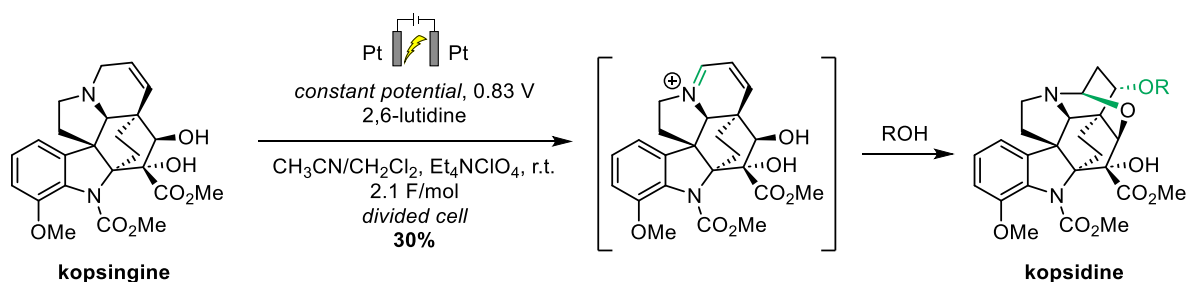
Electrochemical reactions can be conducted with direct current (DC) or alternating current (AC) and under constant potential (potentiostatic) or constant current (galvanostatic).

Most electrosynthetic transformations are performed under galvanostatic conditions. The galvanostatic reaction can be performed with two electrodes, however, while the substrate concentration subsides, the cell voltage increases, allowing undesired reactions to become dominant. However, careful conversion control can mitigate this problem and good selectivities can be achieved, as showcased in the total synthesis of guanacastepene E by TRAUNER *et al.* in 2006 (Scheme 1.12).^[85]



Scheme 1.12: Anodic oxidative ring-closure of a seven-membered ring in the synthesis of guanacastepene E under galvanostatic conditions.^[85]

In contrast, a potentiostatic reaction requires a third reference electrode and a potentiostat. This potential-control enables “dialing-in” the oxidative strength and can lead to very selective processes, tolerating a wide array of functional groups. An impressive example is the electrochemical oxidation of aspidofractinine-type alkaloids with pendant nucleophilic alcohols (Scheme 1.13).^[86]



Scheme 1.13: Anodic oxidation of kopsingine under potentiostatic conditions, tolerating nucleophilic groups.^[86]

Although the potentiostatic mode suppresses side overoxidations, it is usually avoided as the decreased current and conversion rate towards the end of the electrolysis leads to conversion problems and makes scale-up highly difficult.^[84]

Another concept to consider is indirect electrolysis using redox mediators (Figure 1.12). Mediators often improve the efficiency of electrochemical reactions, as the mediator acts as an electron-shuttle between the heterogeneous electron-surface and the homogeneously dissolved substrate, maintaining a constant oxidation potential and concentration at the electrode surface compared to direct electrolysis. Modification of the mediator often allows modification of the chemoselectivity.^[87]

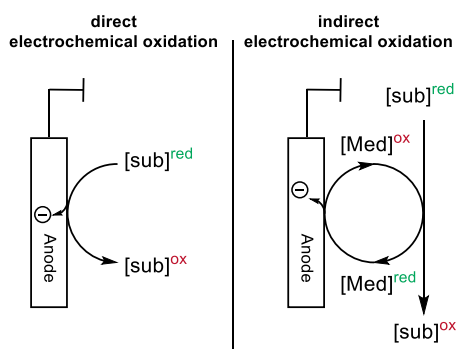
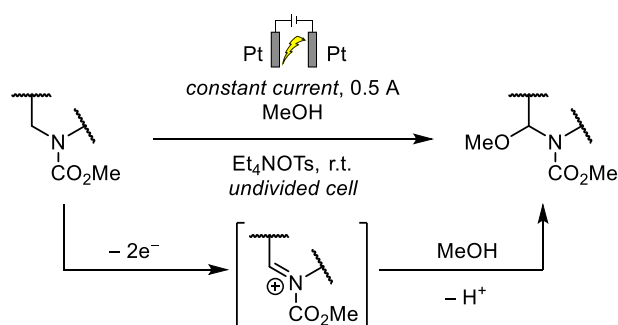


Figure 1.12: Comparison of a direct electrolysis (left) and an indirect electrolysis (right) using a redox mediator.

Besides these key concepts, a variety of parameters have to be considered when designing electroorganic reactions, which are usually not of great concern in conventional transformations. These include electrolyte and substrate concentration, electrode material and geometry, inter-electrode distance, electrode tilt angle, activity and roughness of the electrode surface, stirring speed, ohmic heating, cell voltage, and current among others. Efforts were made trying to demystify these parameters and many pitfalls can be avoided by keeping the parameter set consistent and reproducible during the screening process.^[88]

1.3.3. SHONO Oxidation

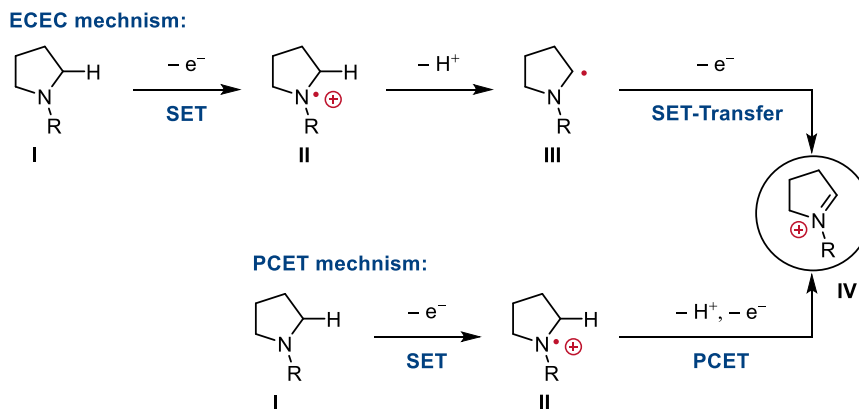
The SHONO oxidation represents a powerful method for the C–H functionalization of carbamates. It has been extensively studied since its discovery by SHONO *et al.* in 1975 (Scheme 1.14).^[76]



Scheme 1.14: Reaction conditions and mechanism of the SHONO oxidation reported in 1975.^[76]

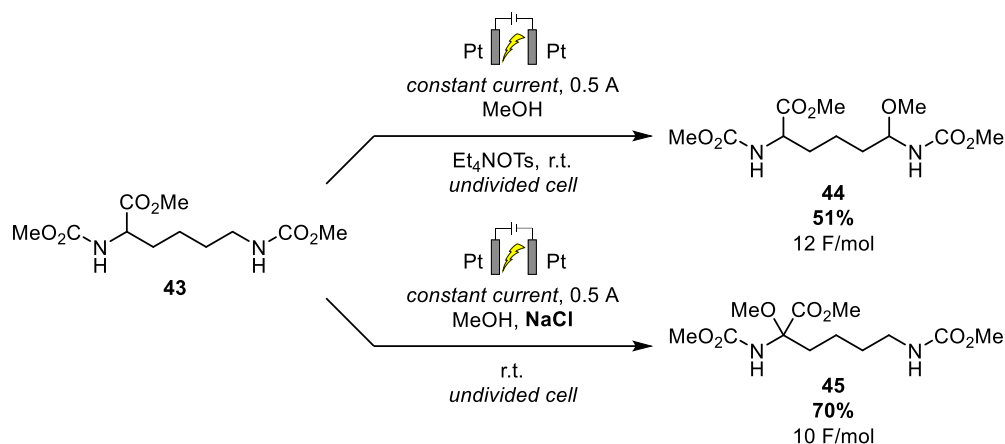
In the original report, the anodic oxidation of various methyl carbamates was described. The anodic oxidation forms an iminium ion, which undergoes a nucleophilic addition by the solvent methanol, forming a α -methoxylated carbamate.

The reaction mechanism is still a topic of debate, as the formation of the key intermediate, the iminium ion **IV**, can be explained either by electrochemical-chemical-electrochemical-chemical (ECEC) events or by SET-transfer followed by a concerted proton-coupled electron transfer (PCET) (Scheme 1.15).^[89]



Scheme 1.15: Two different mechanisms discussed in the literature: The ECEC mechanism and the PCET mechanism.^[89]

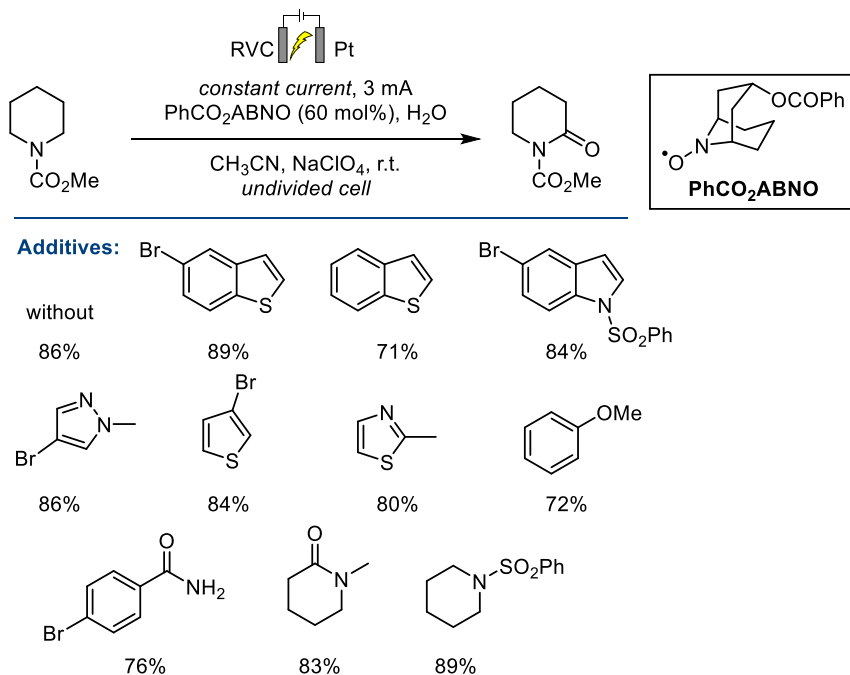
SHONO *et al.* extended the substrate scope to amides and electron-deficient amino acid carbamates.^[9, 90] Interestingly, studies on lysine bismethylcarbamate revealed a reversal of regioselectivity, if sodium chloride was used as a mediator (Scheme 1.16). The reaction under the reported conditions without mediator afforded ϵ -methoxylated lysine **44** in 51% yield, whereas running the reaction in the presence of sodium chloride led to selective formation of the α -methoxylated product **45** in 70% yield.^[90]



Scheme 1.16: Change in regioselectivity of the anodic oxidation of lysine **43** in presence of NaCl observed by SHONO *et al.*^[90]

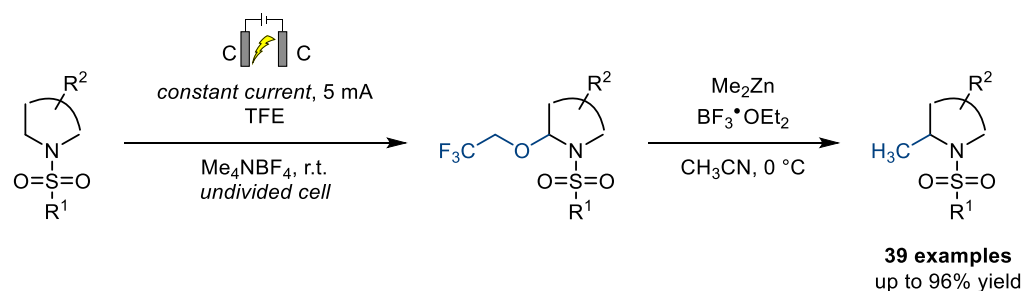
SHONO-type processes attracted attention as a robust method for the functionalization of peptides and drug-like molecules.^[89, 91-93] Detailed investigations to turn the process into indirect electrolysis were conducted by STAHL *et al.*^[94]

The use of PhCO₂ABNO as a mediator enabled outstanding functional group tolerance, as demonstrated in experiments with various nucleophilic and redox-sensitive additives (Scheme 1.17).



Scheme 1.17: Development of an indirect SHONO-type oxidation enabled exceptional functional group tolerance. The yields of the reaction conducted in the presence of redox-sensitive additives were not affected.^[94]

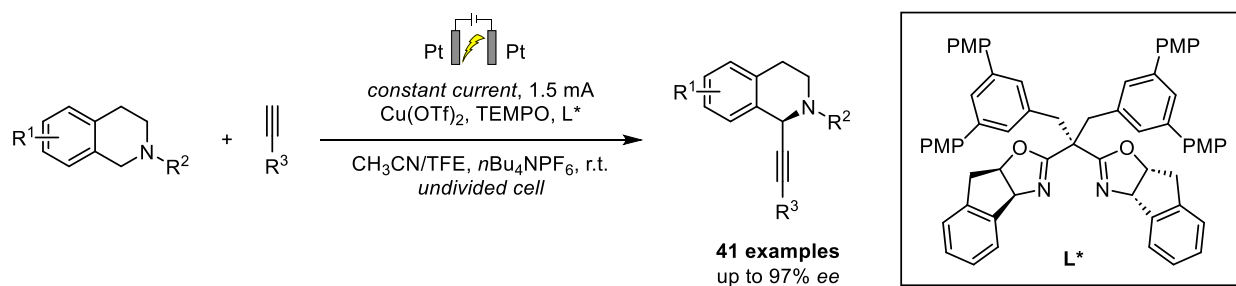
In recent studies, the use of 2,2,2-trifluoroethanol (TFE) as a solvent was exploited to install a labile trifluoroethyl-ether on various drug-like molecules, acting as a reactive functional group for the selective installation of methyl groups (Scheme 1.18).^[89]



Scheme 1.18: SHONO-type process using TFE as a solvent enabled the selective functionalization of drugs by subsequent methylation.^[89]

Other developments focus on the generation and accumulation of the iminium-ion as a cation-pool at low temperatures, followed by the addition of various nucleophiles.^[79-80]

SHONO-type processes were also coupled with transition-metal catalysis. In an impressive example, Cu(II)/TEMPO catalysis enabled the enantioselective installation of alkynes to tetrahydroisoquinolines (Scheme 1.19).^[95]



Scheme 1.19: Enantioselective alkylation of tetrahydroisoquinolines in a SHONO-type process coupled with Cu(II)/TEMPO catalysis.^[95]

1.4. Pyrazolines

1.4.1. Properties of Pyrazolines

Pyrazolines are a class of five-membered heterocyclic compounds featuring two adjacent nitrogen atoms. They resemble the dihydro derivative of pyrazoles with one endocyclic double bond. Although three tautomers exist, the 2-pyrazoline scaffold is by far the most studied and prevalent scaffold due to its stability compared to the other forms.

Calculations of the relative energies show that 1-pyrazolines are still in a small energy range of 8.5 kJ/mol, while the 3-pyrazoline tautomer is clearly unfavored with a relative energy of 55.1 kJ/mol for its lowest energy conformer (Figure 1.13).^[96]

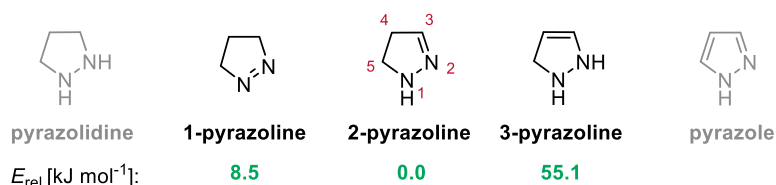


Figure 1.13: Pyrazoline tautomers and their relative energies calculated by BLANCO *et al.* using B3LYP calculations.^[96]

2-Pyrazolines are weak bases, protonation occurs selectively at the N1 site, with a proton affinity of 889 kJ mol⁻¹, corresponding to a basicity between ammonia (854 kJ mol⁻¹) and pyridine (930 kJ mol⁻¹).^[96]

1.4.2. Biological Activity of Pyrazoline-Derivatives

Pyrazoline scaffolds pose an omnipresent motif in drug discovery. Their widespread use as an isostere of other heterocycles, e.g. imidazoles, thiazoles, tetrazoles, isoxazoles, and others allow the modulation of the physicochemical properties and biological profiles of lead structures.^[97-99] Additionally, substituted pyrazolines demonstrate a wide spectrum of biological activities such as anticancer,^[100-103] anti-inflammatory,^[104] antitubercular,^[105] antidepressant,^[106] antibacterial,^[107] antimalarial^[108-109] or antidiabetic.^[110-111]

This versatility positions many of these compounds in the top 200 small molecule drugs by retail sales in 2022, 18 of the 200 drugs contained pyrazoline or pyrazole scaffolds.^[112] Well-established drugs include the antipyretic metamizole (**46**), the non-steroidal anti-inflammatory drug (NSAID) celecoxib (**47**), one of the few drugs for the specific treatment of amyotrophic lateral sclerosis (ALS), edaravone (**48**), the antiobesity drug rimonabant (**49**) and axitinib (**50**) used for the treatment of renal cell carcinoma and other tumor types (Figure 1.14).

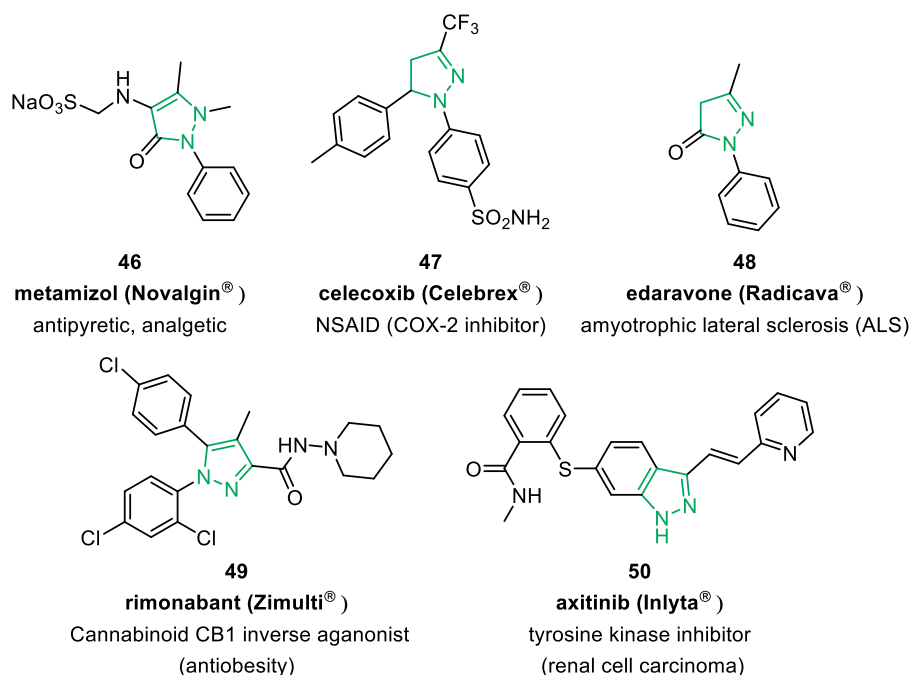


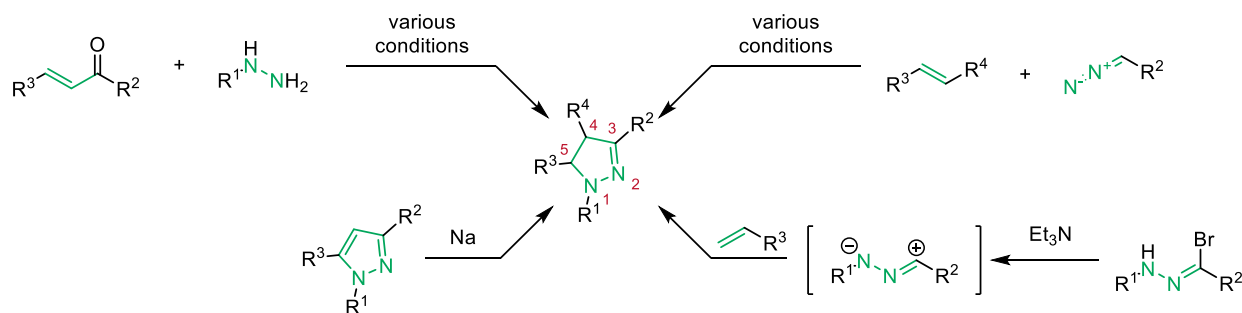
Figure 1.14: Pyrazoline and pyrazole-containing drugs.

1.4.3. Synthesis of Pyrazolines

Various structure-activity studies of pyrazoline drugs demonstrated a strong influence of the substitution pattern.^[97] 1,3,5-Trisubstituted pyrazolines are well explored and studied as the available synthetic routes allow easy access to this pattern (Scheme 1.20).

The first preparation of 2-pyrazolines was described by KNORR and BLANK *et al.* in 1885 by reduction of 1,3-diphenyl-5-methylpyrazole with elemental sodium in ethanol.^[113] The most common synthesis method is the cyclization of chalcones, α,β -unsaturated ketones, or aldehydes with hydrazines.^[114-116]

Although the reaction usually requires harsh conditions and is limited to few functional groups ($R^1, R^2 = \text{H}$, alkyl, Ar, $R^3 = \text{alkyl, Ar}$), it remains the dominant synthesis method for 2-pyrazolines due to their simple protocols and cheap starting materials.

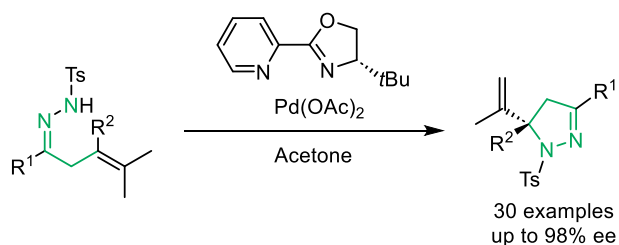


Scheme 1.20: Common methods for the synthesis of 2-pyrazolines.

The [2+3]-cycloaddition of alkenes and diazo compounds allows a mild access to 3,4,5-trisubstituted pyrazolines with great functional group tolerance. The reaction affords 1-pyrazolines which spontaneously convert to or have to be isomerized to 2-pyrazolines. Tri- or tetrasubstituted olefins are usually not tolerated.^[117-118]

In contrast, the 1,3-dipolar cycloaddition of nitrile imines allows the direct access of 2-pyrazolines. The nitrile imines are typically prepared *in situ* by dehydrohalogenation of hydrazonyl halides with Et₃N.^[115, 119]

Despite their widespread use in medicinal chemistry and decades of research, the synthesis of 4,4- and 5,5-disubstituted pyrazolines, as well as the preparation of enantioenriched C4- and C5-substituted 2-pyrazolines remains challenging and are areas of active research. A recent breakthrough by YANG and ZHANG *et al.* enabled the asymmetric synthesis of 2-pyrazolines bearing a quaternary C5-stereocenter utilizing a Pd-catalyzed Aza-WACKER-type cyclization (Scheme 1.21).^[120]



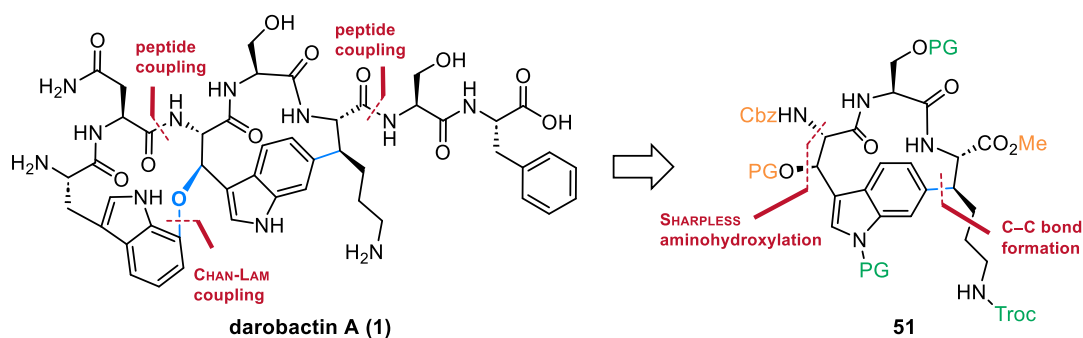
Scheme 1.21: Asymmetric Aza-Wacker-type cyclization for the synthesis of 2-pyrazolines bearing a quaternary stereocenter.^[120]

2. Objectives

Antibiotic resistance poses an urgent threat to global health, associated with 5 million deaths worldwide in 2019.^[121] Infections with Gram-negative bacteria are especially hard to treat due to their impenetrable outer membrane.

The novel mode of action of the natural product darobactin A (**1**) offers outstanding selectivity and displays high potency against various drug-resistant strains of Gram-negative bacteria. Hence, darobactin A (**1**) represents an attractive target as a lead structure for the development of a novel class of antibiotics. Total synthesis of this molecule could give access to substantial material quantities and would facilitate derivatization to improve its activity and proteolytic stability.

In the following work, first synthetic approaches toward darobactin A (**1**) were investigated. Retrosynthetic analysis identified the unique Trp-Ser-Lys macrocycle **51** as the key building block featuring two benzylic stereo centers (Scheme 2.1).



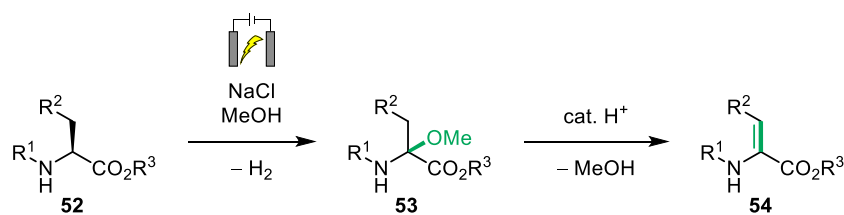
Scheme 2.1: Retrosynthetic analysis of darobactin A (**1**) leads to the Trp-Ser-Lys macrocyclic building block **51**.

For the stereoselective construction of the hydroxytryptophan-moiety, the development of a SHARPLESS asymmetric aminohydroxylation will be a major goal of this work.

The unique C-C bond between the lysine and C₆-indole could be installed by an asymmetric reductive HECK-reaction, Template-assisted Pd(II)-catalyzed C-H olefination or HECK-reaction followed by hydrogenation. All of these approaches can be traced back to a dhAA moiety, either in the form of a dehydrolysine or a dehydroalanine-containing peptide.

DhAAs are a class of non-canonical amino acids with unique reactivity. Despite their abundance in natural products and their utility for late-stage diversification, available methods for their synthesis are limited.

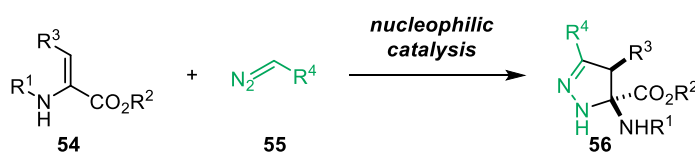
Therefore, the development of a direct synthesis of dehydroamino acids **54** from their corresponding amino acid carbamates **52** using an electrochemical α -methoxylation followed by acid-catalyzed elimination of methanol was envisaged (Scheme 2.2).



Scheme 2.2: Electrosynthesis of protected dhAAs (**54**).

The proposed method could offer a simple, scalable access to dhAAs as an economic alternative to previous approaches.

With an established general access to various protected dhAAs, unprecedented functionalization of this versatile substrate class should be investigated, e.g., the cycloaddition with diazo compounds **55** could afford highly substituted 2-pyrazoline amino acids **56** (Scheme 2.3).



Scheme 2.3: Proposed cycloaddition of dhAAs **54** with diazo compounds **55** forming highly substituted 2-pyrazolines **56**.

Given the prevalence of 2-pyrazolines in active pharmaceutical ingredients,^[112] this unprecedented class of amino acids could be used for the modification of peptides or the development of new small-molecule drugs.

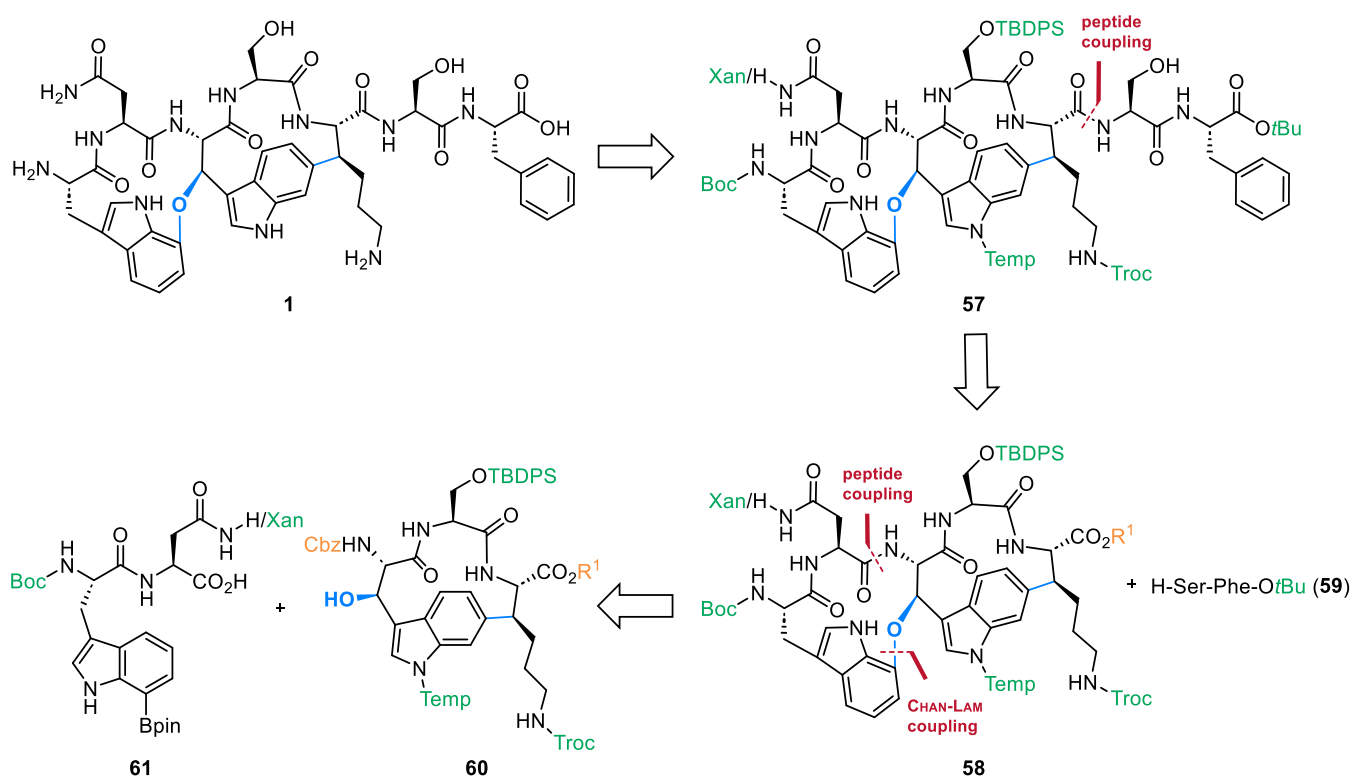
3. Results

3.1. Studies towards the Total Synthesis of Darobactin

3.1.1. Retrosynthetic Analysis of Darobactin A

The retrosynthetic analysis of darobactin A (**1**) identified the central tryptophan as the pivotal building block, bearing the two key connections, the C7-Indole benzylic ether, and the C-C-bond between the β -position of the lysine and the C6 of the indole.

A convergent synthesis separating the molecule into three building blocks was envisaged (Scheme 3.1).



Scheme 3.1: Retrosynthetic analysis of Darobactin A (**1**). Separation into building blocks east and west. "Permanent" (green) and "temporary" (orange) protecting groups are highlighted.

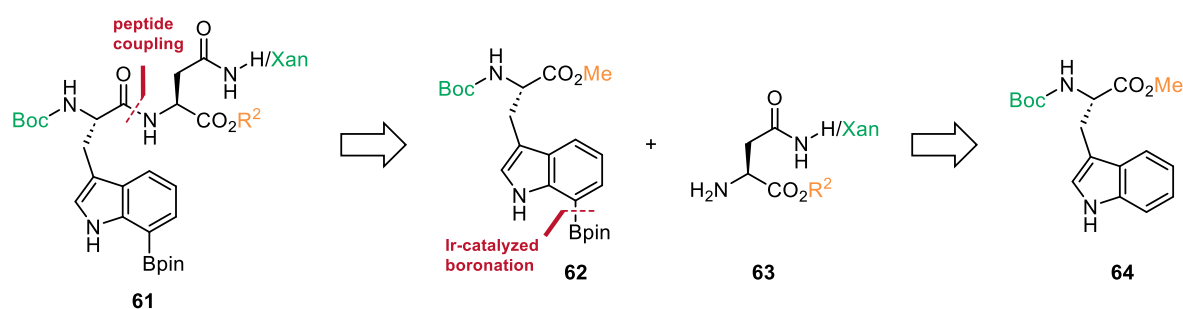
To accommodate the plethora of nitrogen and oxygen functional groups, the protective group strategy is delicate and separated into two types of protective groups. The "permanent" protecting groups need to tolerate the various reaction conditions over the long linear sequences of the individual building blocks and should be deprotected in as few steps as possible releasing the final heptapeptide darobactin A.

The "temporary" protecting groups are used for the transitional protection of intermediates, e.g. the protection of amines and carboxylic acids before amide bond constructions. These functional groups are designed to be orthogonal to the permanent protecting groups and only have to tolerate the conditions within a short linear sequence.

The Troc-group on the lysine and the sulfonamide template on the central indole should survive most transformations and can be specifically deprotected using mild single electron reductions e.g. the zinc-acetic

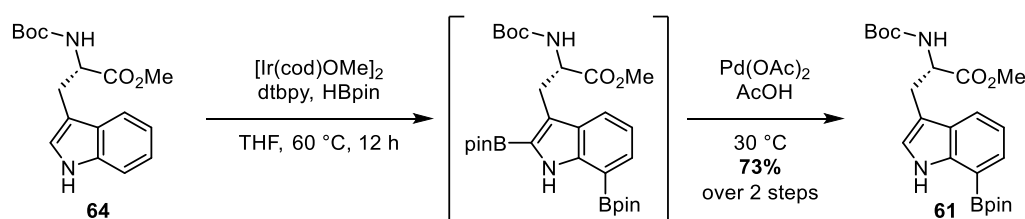
acid system or electrolysis. Other permanent protective groups include a *tert*-butyl ester at the phenyl alanine and other acid-labile protective groups, e.g. 9-xanthenyl (Xan) on the asparagine amide and Boc at the *N*-terminus.

The globally protected natural product **57** can be deconstructed by late-stage peptide coupling of the C-terminal H-Serin-Phe-OtBu dipeptide (**59**). Bismacrolactam **58** can be transformed into western building block **61** and eastern building block **60** utilizing a Chan-Lam transformation as the key step and peptide coupling of C7-boronated tryptophan and a β -hydroxytryptophan motif. The functionalized Boc-Trp-Asp-Dipeptide **61** can be formed by peptide coupling (Scheme 3.2).



Scheme 3.2: Retrosynthetic analysis of western building block **61**.

The necessity of the asparagine amide protection has to be evaluated, as the amide might be prone to react as a nucleophile in the Chan-Lam coupling. Xan-protected asparagine is commercially available and integrates into the global protection group strategy. Building Block **61** is literature known and could be obtained by C7-Boronation of Boc-Trp-OMe (**65**) utilizing the bisboronation/protodeboronation protocol developed by MOVASSAGHI *et al.* (Scheme 3.3).^[122]

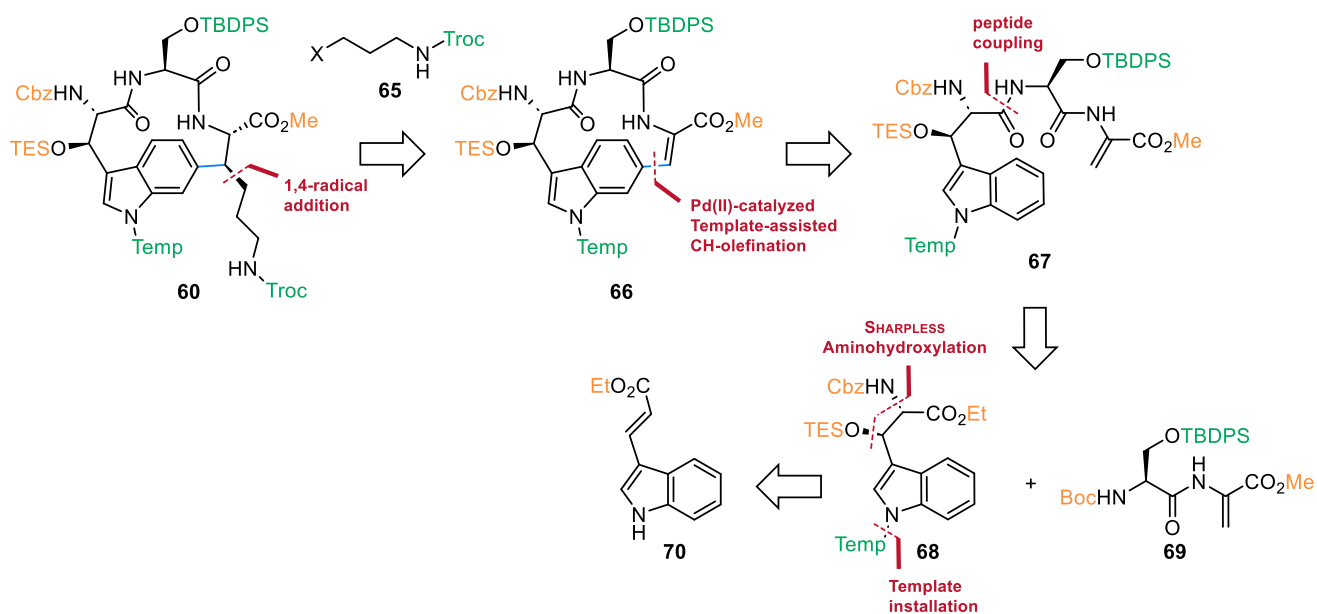


Scheme 3.3: Protocol for the C7-boronation of Boc-Trp-OMe (**64**) reported by MOVASSAGHI *et al.*^[122]

Construction of the eastern building block **60** faces multiple synthetic challenges as it bears the two posttranslational stereocenters at the β -positions of β -hydroxytryptophan and lysine, respectively. Whilst the stereocenter at the tryptophan could be installed by SHARPLESS asymmetric aminohydroxylation, the C-C coupling to the lysine forms the second stereocenter.

This C6-indole functionalization poses a major challenge, as regioselective C6-functionalization is known to be notoriously difficult, due to the lack of reactivity of this position in electrophilic substitutions combined with the fact, that it is the most distant position from the nitrogen and C3-position of the indole, the common anchor point for directing groups.

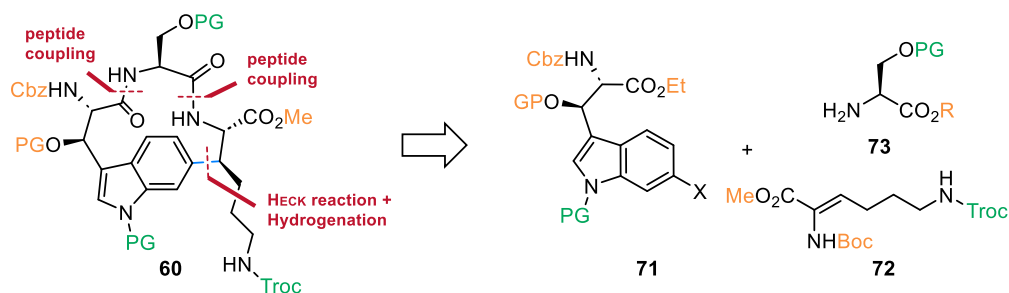
Two different approaches were considered. The ambitious approach utilizes a U-shaped template developed by MOVASSAGHI and YU *et al.* to perform a Pd(II)-catalyzed C–H-activation of the C6-position, enabling an intramolecular C6-olefination with a dehydroalanine moiety (Scheme 3.4).



Scheme 3.4: Retrosynthetic analysis of the eastern building block **60**.

Next, the lysine side chain could be introduced by radical conjugate addition of 3-halopropyl carbamate **65** to unsaturated macrolactam **66**, which is accessed by the template-assisted olefination. Tripeptide **67** can be derived from the desaturated dipeptide Boc-Ser(TBDPS)- Δ Ala-OMe (**69**), offering good convergence. β -Hydroxytryptophan **68** suggested a SHARPLESS asymmetric aminohydroxylation for the introduction of both stereocenters utilizing literature known indole **70** after installation of the sulfonamide template on the nitrogen.

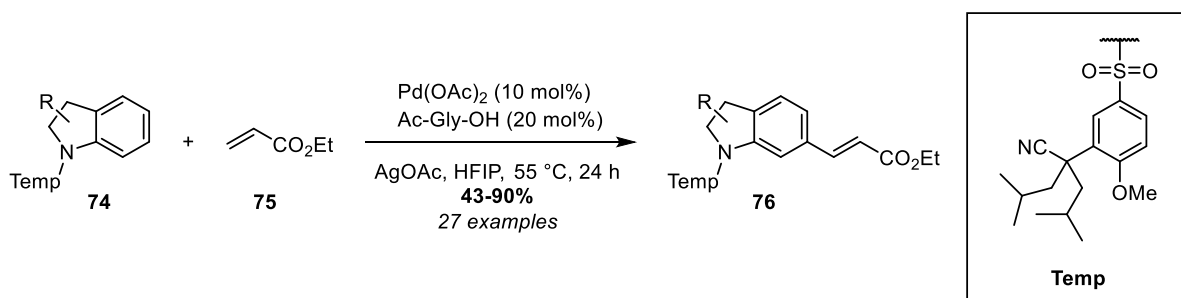
A more conservative approach utilizes the HECK transform to deconstruct the eastern building block **60** into C6-halogenated tryptophan **71** and dehydrolysine **72** as coupling partners (Scheme 3.5). Tryptophan **71** could be synthesized analogous to the previous approach, starting from commercially available 6-Bromoindole or by preparation of 6-Triflylindole by triflation of 6-Hydroxyindole. The use of a triflate would facilitate an asymmetric reductive HECK-reaction, as the cationic pathway enhances stereoselectivity as no dissociation of chiral phosphine ligands is required.^[123]



Scheme 3.5: Retrosynthetic analysis of western building block **60** utilizing the HECK transformation.

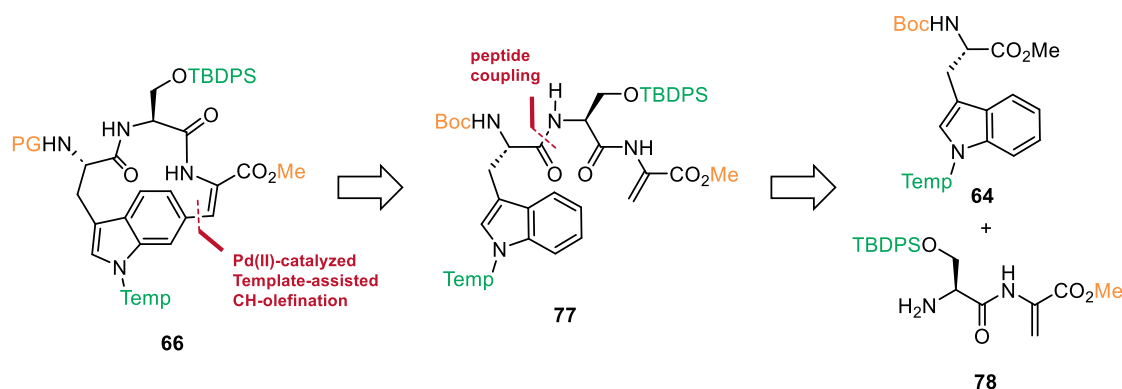
3.1.2. Template-assisted C6-Indole Functionalization of the Eastern Fragment

An ambitious approach towards the synthesis of the eastern building block **60** exploits the Pd(II)-catalyzed C–H olefination developed by MOVASSAGHI and YU *et al.*^[124] Their method showed promising results in the C6-olefination of various indolines utilizing a nitrile-functionalized sulfonamide template on the indoline nitrogen (Scheme 3.6). The U-shaped template enabled the C6-functionalization of indolines with various olefins showing regioselectivities of up to 20:1 (C6:others). The method features high functional group tolerance, including C2,3-fused rings, spiro rings at C3, piperidines, pyrroloindolines, and diketopiperazines.



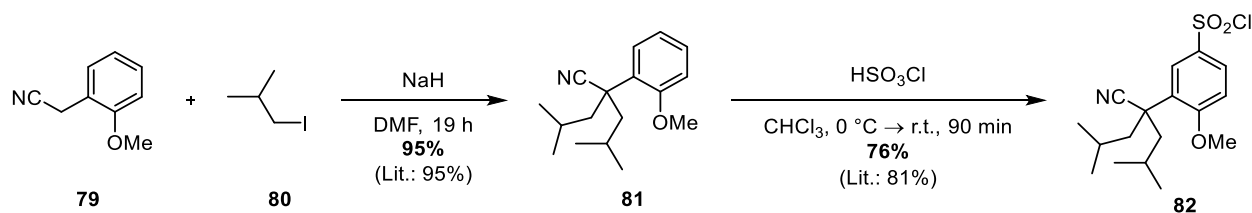
Scheme 3.6: Pd(II)-catalyzed C–H olefination of indolines developed by MOVASSAGHI and YU *et al.*^[124]

To evaluate this ambitious, yet elegant approach towards the ring closure of the eastern building block, non-hydroxylated tryptophan tripeptide **77** was used as a readily accessible model substrate (Scheme 3.7).



Scheme 3.7: Retrosynthetic analysis of the non-hydroxylated intermediate **66**.

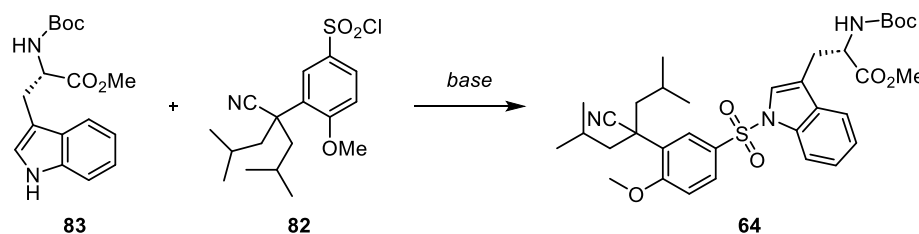
The sulfonyl chloride **82** utilized for the introduction of the template was synthesized according to the reported procedure by MOVASSAGHI and YU *et al.* (Scheme 3.8).



Scheme 3.8: Synthesis of the template sulfonyl chloride **82** according to the reported procedure by MOVASSAGHI and YU *et al.*^[124]

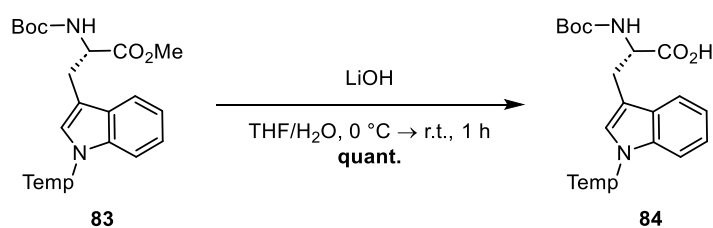
Alkylation of commercially available anisol **79** with isobutyl iodide **80** was achieved in 95% yield. Chlorosulfonation afforded TempCl **82** in good yield. Installation of the template on Boc-Trp-OMe (**83**) was investigated using a variety of bases (Table 3.1).

Table 3.1: Installation of the sulfonamide employing different bases.



Entry	Base	Solvent	T	t	Conversion (Yield)
1	NaH	THF	r.t.	16 h	0%
2	NaH	THF	50 °C	2 d	8%
3	NaOH/ <i>n</i> Bu ₄ NHSO ₄	CH ₂ Cl ₂	r.t.	16 h	0%
4	<i>n</i> BuLi	THF	-78 °C → r.t.	17 h	Full (81%)

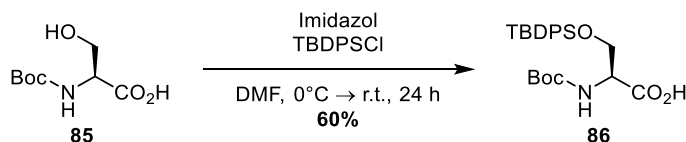
Surprisingly, the strong base NaH, commonly used for the introduction of the tosyl-group on indoles, was not sufficient to sulfonylate the nitrogen, even at elevated temperatures of up to 50 °C in THF (entries 1 and 2). Sodium hydroxide in a phase-transfer-system in anhydrous CH₂Cl₂ was unsuccessful (entry 3), but lithiation of the indole using *n*BuLi afforded Boc-Trp(Temp)-OMe (**64**) in 81% yield (entry 4). Saponification using LiOH furnished Boc-Trp(Temp)-OH (**84**) in quantitative yield (Scheme 3.9).



Scheme 3.9: Saponification of Boc-Trp(Temp)-OMe (**83**).

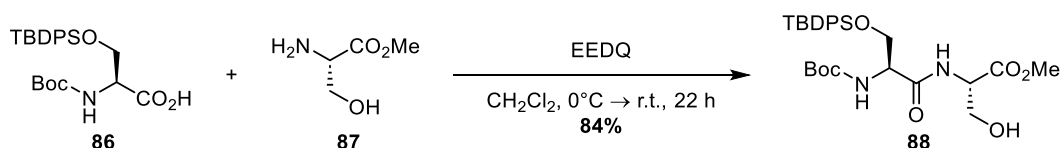
For the synthesis of the unsaturated dipeptide H-Ser(TBDPS)-ΔAla-OMe (**78**) a peptide coupling of Boc-Ser(TBPDS)-OH (**86**) with H-Ser-OMe (**87**) followed by mesylation and base-induced elimination to introduce the dehydroalanine moiety was envisioned.

Silylation of Boc-Ser-OH (**85**) with TBDPSCI afforded the silylated amino acid **86** in 60% yield (Scheme 3.10).



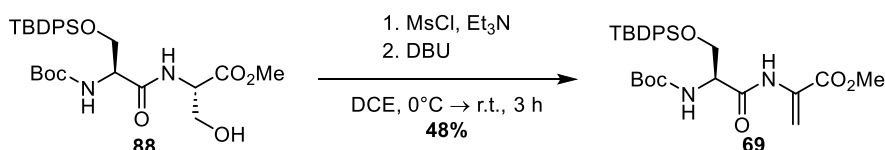
Scheme 3.10: Synthesis of Boc-Ser(TBDPS)-OH (**86**).

While coupling of serines with common coupling reagents like carbodiimides, uronium or phosphonium reagents requires protection of the hydroxyl group, 2-ethoxy-1-ethoxycarbonyl-1,2-dihydroquinoline (EEDQ) allows coupling of serines with unprotected hydroxyl-function.^[125] Hence, coupling of Boc-Ser(TBDPS)-OH (**86**) with H-Ser-OMe (**87**) was enabled using EEDQ and gave Boc-Ser(TBDPS)-Ser-OMe (**88**) in 84% yield (Scheme 3.11).



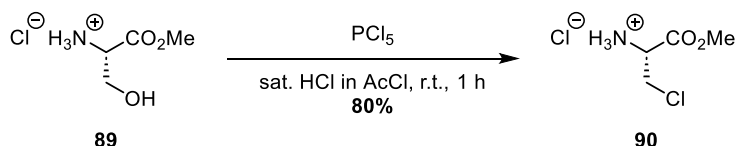
Scheme 3.11: Coupling of unprotected H-Ser-OMe (**87**) enabled by EEDQ.

Dehydration of dipeptide **88** could be achieved by mesylation and elimination with DBU in a one-pot procedure (Scheme 3.12).



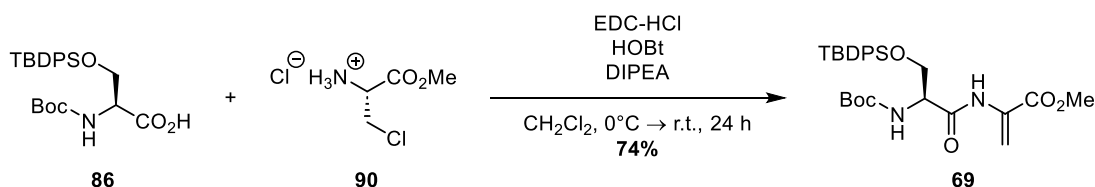
Scheme 3.12: Dehydration of dipeptide **88**.

Given the moderate yield of 48%, a different approach using chloroalanine **90** as dehydroalanine precursor was pursued. Chloroalanine methyl ester (**91**) was synthesized *via* PCl₅ chlorination of H-Ser-OMe hydrochloride (**90**) in HCl-saturated, anhydrous acetyl chloride as a solvent to prevent *N*-chlorination (Scheme 3.13).^[126]



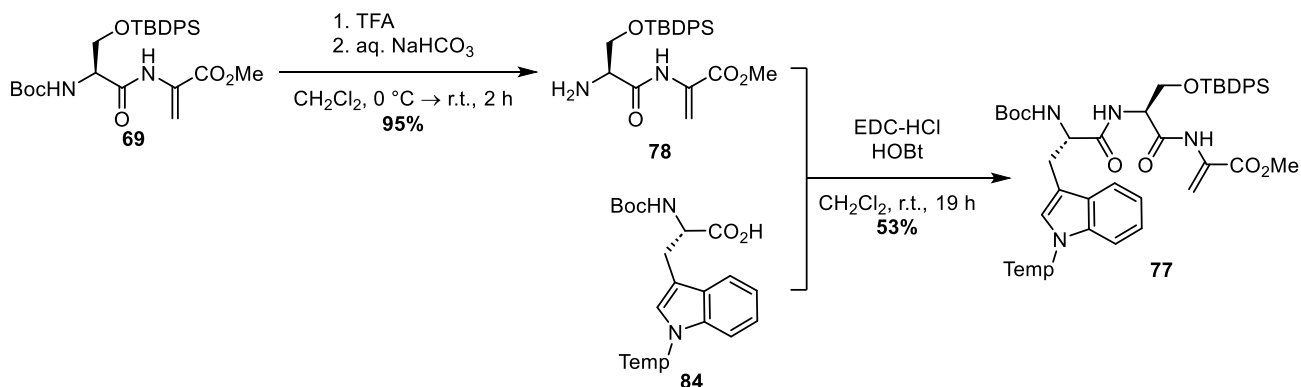
Scheme 3.13: Synthesis of chloroalanine **90**.

The protocol afforded spectroscopically pure chloroalanine **90** in 80% yield without further purification steps. Pleasantly, peptide coupling using EDC and DIPEA as the coupling agent and base, respectively, furnished the desired Boc-Ser(TBDPS)-ΔAla-OMe (**69**) in 74% yield without the need for an additional elimination step (Scheme 3.14).



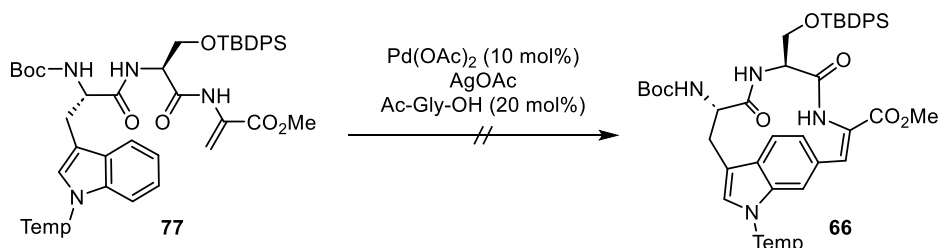
Scheme 3.14: One-pot construction of the Boc-Ser(TBDPS)- Δ Ala-OMe dipeptide (**69**).

Formation of the chloroalanine-dipeptide was not observed throughout the reaction, suggesting that dehydrochlorination of the amide is faster than the nucleophilic attack of the amine to the active ester during peptide coupling. Deprotection of the *N*-terminus was performed using TFA/CH₂Cl₂, and full conversion was achieved after 3 h at room temperature. It is important to note, that isolation of the TFA-salt was possible, but traces of excess TFA resulted in fast product decomposition. Therefore, isolation of the free amine using a NaHCO₃-wash was mandatory. While still not stable upon prolonged storage, immediate use of the free amine **78** allowed the synthesis of tripeptide **77** in moderate yield using EDC/HOBt (Scheme 3.15). These instabilities are probably attributed to the dehydroalanine moiety, which is prone to acid-catalyzed polymerization as well as nucleophilic attack of the primary amine.



Scheme 3.15: Final steps towards the synthesis of tripeptide **77**.

With the model tripeptide **77** in hand, the Pd(II)-catalyzed intramolecular C–H olefination was investigated (Scheme 3.16).



Scheme 3.16: Attempted Pd(II)-catalyzed ring closure of the eastern building block.

Employing the reported conditions with Pd(OAc)₂ as catalyst, Ac-Gly-OH as ligand and AgOAc as oxidant, the cyclization was attempted in dry HFIP. However, no conversion of the tripeptide **77** was observed after

refluxing for 24 h. To access higher temperatures, the reaction was repeated in refluxing toluene, but even at these elevated temperatures for 24 h, no conversion was observed. Fortunately, the starting material demonstrates high-temperature stability and could be recovered.

The low reactivity could be accounted to different factors. As the initial report of MOVASSAGHI and YU *et al.* was only reported for various indolines and C2,3-fused indoles, the template may require structural modification. More important, the conformational rigidity of the peptide chain could pose a problem, as the equilibrium of the amide bonds will be favored for the *s-trans* conformation. To overcome this problem, a solution could be the introduction of an oxazolidine as a molecular hinge, effectively acting as a pseudo-proline (Figure 3.1).^[127]

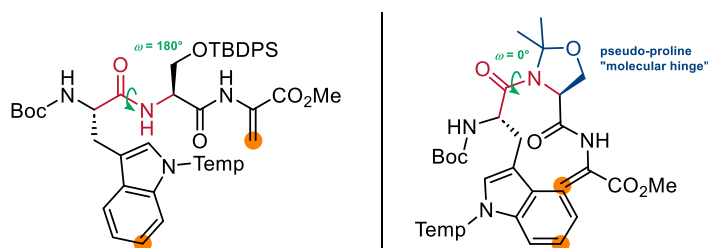


Figure 3.1: Conformation of a *s-trans*, *s-trans* tripeptide compared to a *s-cis*, *s-trans* tripeptide forced by the introduction of a pseudo-proline as a molecular hinge.

In the synthesized tripeptide **77**, both amide bonds most likely exhibit a torsion angle $\omega = 180^\circ$ (*s-trans* conformation). Installation of an oxazolidine moiety would subject the amide bond much more readily to isomerize to the *s-cis* ($\omega = 0^\circ$) conformation. Ring opening of the oxazolidine under acidic conditions should reestablish the serine.

Taking a step back, the intermolecular olefination of the tryptophan **83** should be tested, before starting this synthetic endeavor. Therefore, an olefination of Boc-Trp(Temp)-OMe (**83**) with simple olefins and dehydroalanine was attempted (Table 3.2).

Unfortunately, olefination with Ac- Δ Ala-OMe (**91**) using the reported conditions was not successful (entry 1). Repeating the reaction in a closed vial at 90 °C resulted in the decomposition of the starting material (entry 2). The authors optimized their reaction using ethyl acrylate **92** as a model substrate, however, olefination of tryptophan **83** with this olefin was not achieved (entry 3).

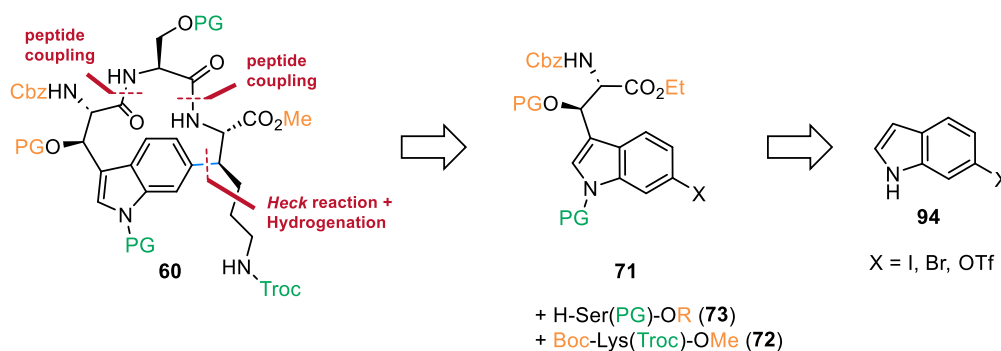
Modification of the reaction conditions, e.g. running the reaction in a dry oxygen atmosphere (entry 4) or using acetic acid as an additive (entries 4 and 5) showed no conversion with dehydroalanine **91**. In consequence, the template-assisted Pd(II)-catalyzed C–H olefination method was considered unsuitable for C6-olefination of tryptophan **83**.

Table 3.2: Attempted olefination of tryptophan **83** using various olefins, oxidants, solvents and additives.

Entry	Olefin	Oxidant	Additive	Solvent	T	Result
1	91	AgOAc	Ac-Gly-OH	HFIP	56 °C	s. m. recovered
2	91	AgOAc	Ac-Gly-OH	HFIP	90 °C	decomposition
3	92	AgOAc	Ac-Gly-OH	HFIP	56 °C	s. m. recovered
4	91	O ₂	AcOH	Xylene	100 °C	s. m. recovered
5	91	AgOAc	AcOH	Xylene	100 °C	s. m. recovered

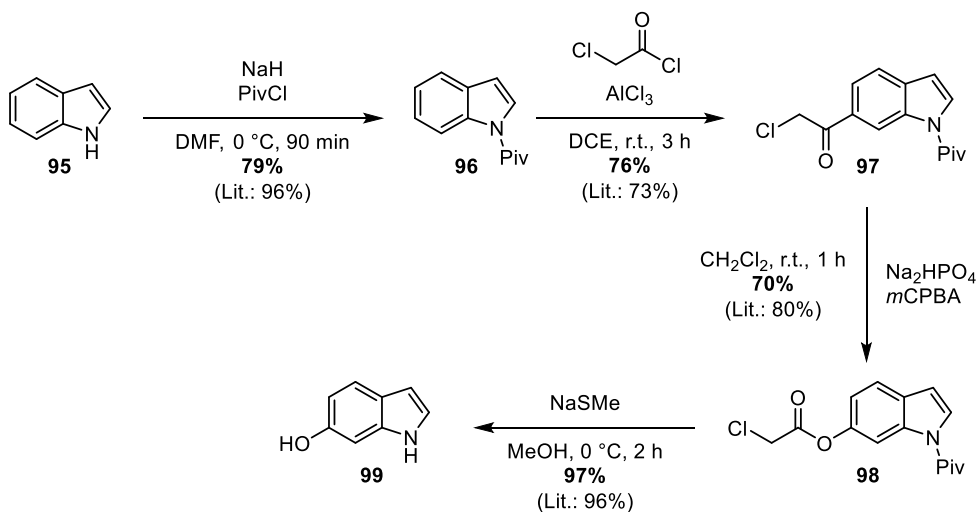
3.1.3. Synthesis of a 6-Triflyl Tryptophan

To investigate the C6-carbon bond formation via the HECK transformation, pre-functionalized indoles were investigated. As potential aryl (pseudo)halide starting materials, 6-iodo-, 6-triflyl, and 6-bromoindole were considered (Scheme 3.17).

**Scheme 3.17:** Retrosynthetic analysis of eastern building block **60** with a HECK transformation as a key step.

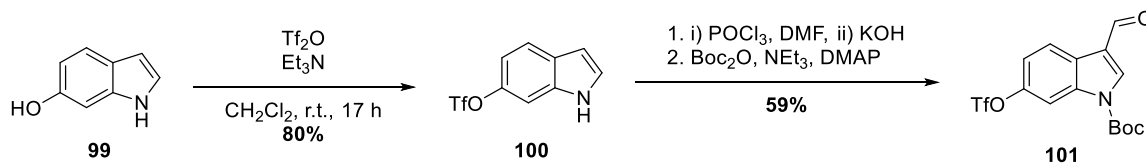
While 6-iodoindole and 6-bromoindole would favor a neutral mechanistic path for the HECK reaction, 6-triflylindole would offer access to a cationic HECK reaction.^[123] This opens the possibility of an asymmetric hydrogenative HECK coupling with dehydrolysine, installing the stereocenter at the β -position without the need for challenging asymmetric hydrogenation of a tetrasubstituted double bond. It is well known, that the cationic pathway is essential for high asymmetric induction, as both phosphines remain bound in the catalytic system.^[123, 128-131] Therefore, 6-triflylindole was investigated first.

Albeit 6-hydroxyindole **99** is commercially available (~100€/g), the starting material was synthesized using the well-established procedure by TERANISHI *et al.*^[132] Herein, pivaloylation of the indole allows regioselective FRIEDEL-CRAFTS chloroacetylation of the 6-position (Scheme 3.18). BAEYER-VILLIGER oxidation using *m*CPBA and simultaneous deprotection of the resulting chloroacetate and pivaloyl group gave 6-hydroxyindole (**99**) in 41% yield over four steps on a multigram scale.



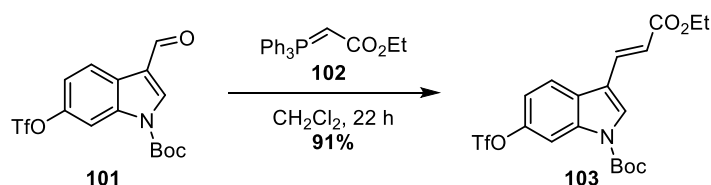
Scheme 3.18: Synthesis of 6-hydroxyindole **99** according to a protocol reported by TERANISHI *et al.*^[132]

With substantial quantities of 6-hydroxyindole (**99**) in hand, triflation was achieved using Tf₂O and Et₃N in 80% yield (Scheme 3.19). The stability of 6-triflylindole (**100**) was limited, even at room temperature, therefore VILSMEIER-HAACK formylation was conducted immediately, followed by subsequent Boc-protection of the nitrogen. Again, the formylated 6-triflylindole demonstrated high reactivity and decomposed quickly upon purification by silica chromatography or storage in neat form, easily detected by a change of color from colorless to dark red. Therefore, Boc-protection had to be performed immediately after workup affording carbamate **101** in 59% over two steps as a bench-stable, colorless solid.



Scheme 3.19: Reaction sequence towards bench-stable carbaldehyde **101**.

Carbaldehyde **101** was subjected to a WITTIG olefination using commercially available ylide **102**, affording α,β -unsaturated ester **103** as a single *E*-isomer in excellent yield (Scheme 3.20). The (*Z*)-isomer was not observed.



Scheme 3.20: WITTIG olefination of carbaldehyde **101**.

Approaching the first key step of the building block synthesis, the SHARPLESS asymmetric aminohydroxylation was investigated.

3.1.4. SHARPLESS Asymmetric Aminohydroxylation

The SHARPLESS asymmetric aminohydroxylation is a powerful reaction for the enantioselective construction of *syn*-vicinal protected amino alcohols using simple alkenes as starting materials.^[133]

Although the reaction mechanism is related to the frequently employed SHARPLESS asymmetric dihydroxylation, the introduction of two different functional groups adds significant complexity, as regioselectivity of the reaction becomes a major concern.^[134]

While the dihydroxylation reaction almost always utilizes the (DHQ)₂PHAL ligand or its pseudoenantiomeric counterpart, (DHQD)₂PHAL, the ligand choice becomes an important parameter for the SHARPLESS asymmetric aminohydroxylation. Drastic effects on the regioselectivity have been observed for different ligand cores,^[135] hence a variety of ligand cores will be investigated (Figure 3.2).

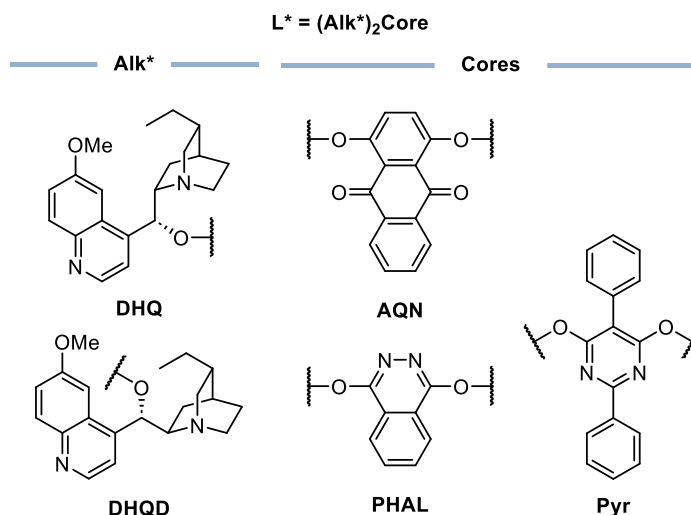
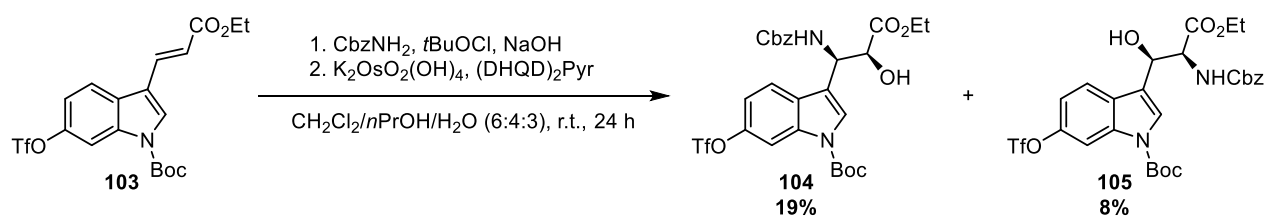


Figure 3.2: Ligands of the type (Alk*)₂Core used for the SHARPLESS asymmetric aminohydroxylation.

The first aminohydroxylations conducted with substrate **103** exposed multiple problems. First of all, the reaction is very susceptible to oxygen, light, and stoichiometry of the reagents, e.g. excess base, super- or substoichiometric quantities of the *t*BuOCl shuts down conversion almost completely. Because *t*BuOCl is a very reactive reagent and prone to decomposition, fresh preparation before the reaction and/or titration of

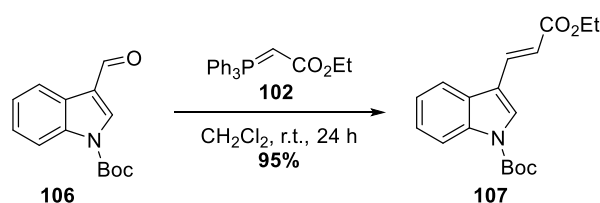
stored batches is mandatory. The use of properly calibrated transfer syringes for reagent dosing and freeze-pump-thaw-degassing of all solutions was strongly required.

Secondly, the starting material **103** was not soluble in the specific *n*PrOH/H₂O mixture, which is commonly used for these kinds of transformations, requiring the addition of a third solvent affecting the reaction rate significantly.^[133] With these measures, the first aminohydroxylation using (DHQD)₂Pyr and benzyl carbamate could be achieved (Scheme 3.21). Unfortunately, the reaction gave unsatisfactory yields and low regioselectivity of 2.4:1.



Scheme 3.21: First successful aminohydroxylation of **103** gave low yields and regioselectivities.

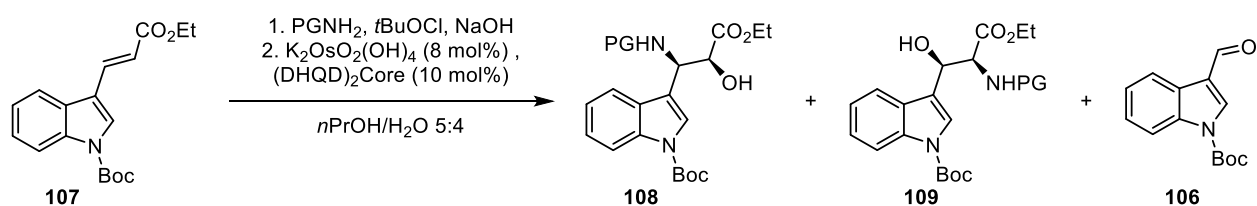
To further optimize the selectivity and yield of this reaction, the reaction was optimized using the unfunctionalized indole **107**, as the triflate group was not expected to alter the selectivities significantly. The test substrate was accessible by WITTIG olefination of *N*-Boc-protected indole-6-carbaldehyde (**106**) in excellent yield (Scheme 3.22).



Scheme 3.22: Synthesis of test substrate **107**.

The optimization was commenced using different carbamates and (DHQD)₂AQN as a ligand. As the chlorination step makes the reaction very elaborate, the use of bench-stable Fmoc-NHCl was tested (Table 3.3, entry 1), as successful SHARPLESS asymmetric aminohydroxylations with this easily accessible compound have been reported by TAYLOR *et al.*^[136] The reaction afforded the desired benzylalcohol **109** in good yield, however, the reaction rate was quite slow, and full conversion could not be achieved.

Unfortunately, the product decomposed within minutes after isolation, making it unsuitable for further investigations.

Table 3.3: Optimization of the SHARPLESS asymmetric aminohydroxylation using different carbamates, ligands, and solvent systems.

Entry	Carbamate	Core	Solvent	t	Rec. s. m. 107	Yield Benzylamine ^a	Yield Benzylalcohol
1	FmocNHCl ^b	AQN	<i>n</i> PrOH/H ₂ O 5:4	21 h	55%	n.d.	45%
2	BocNH ₂	AQN	<i>n</i> PrOH/H ₂ O 5:4	2 h	-	5%	17%
3 ^c	CbzNH ₂	AQN	<i>n</i> PrOH/H ₂ O 5:4	2 h	-	32%	44% 94% <i>ee</i> ^d
4	CbzNH ₂	Pyr	<i>n</i> PrOH/H ₂ O 5:4	23 h	-	traces	traces 95% <i>ee</i> ^d
5	CbzNH ₂	PHAL	<i>n</i> PrOH/H ₂ O 5:4	3 h	-	85% >99% <i>ee</i> ^d	Traces
6	CbzNH ₂	Et ₃ N	<i>n</i> PrOH/H ₂ O 5:4	25 h	20%	15%	24%
8 ^c	CbzNH ₂	AQN	<i>i</i> PrOH/H ₂ O 5:4	2 h	-	31%	35%
9 ^c	CbzNH ₂	AQN	<i>t</i> BuOH/H ₂ O 5:4	2 h	-	32%	33%
10 ^c	CbzNH ₂	AQN	CH ₃ CN/H ₂ O 5:4	2 h	-	-	-

[a] Contains inseparable CbzNH₂, yield recalculated by ¹H NMR-analysis.

[b] The *N*-chlorocarbamate was added as a solid, instead of *in situ* chlorination using *t*BuOCl.

[c] Reduced catalyst and ligand loading of 4 mol% and 5 mol%, respectively.

[d] Determined by chiral HPLC using racemic standards obtained from entry 6.

The use of *tert*-butyl carbamate led to a complex product mixture and therefore low yield (entry 2). Additionally, the carbaldehyde **106** was obtained in 10% yield, probably formed by retro-aldol reaction of **109** or retro-MANNICH reaction of **108**. Benzyl carbamate gave the desired benzylalcohol **109** in 44% yield and 94%*ee* (entry 3).

With sufficient material of both regioisomers in hand, 2D NMR analysis was performed to assign the two isomers. Unfortunately, the assignment of the signals for these isomers was not straightforward, as the α - and β -CH exhibit similar coupling patterns to heteroatoms in both isomers. However, the HMBC cross-coupling signals of the α - and β -CH of compound **109** posed convincing evidence for the assignment as the benzylamine **108**, given, that H11 clearly shows coupling to carbamate C15 as well as C2, C3, and C9 of the indole ring, while for H10 only coupling to C3 was observed (Figure 3.3). The only detail contrary indicating

the benzylalcohol was the lower intensity of the C3-H10 compared to the C3-H11 coupling, as for the 3J -coupling a significantly higher intensity should be observed.

The assignment was revoked weeks later when a crystal structure of the opposing triflate-functionalized isomer was obtained by X-ray single crystal analysis.

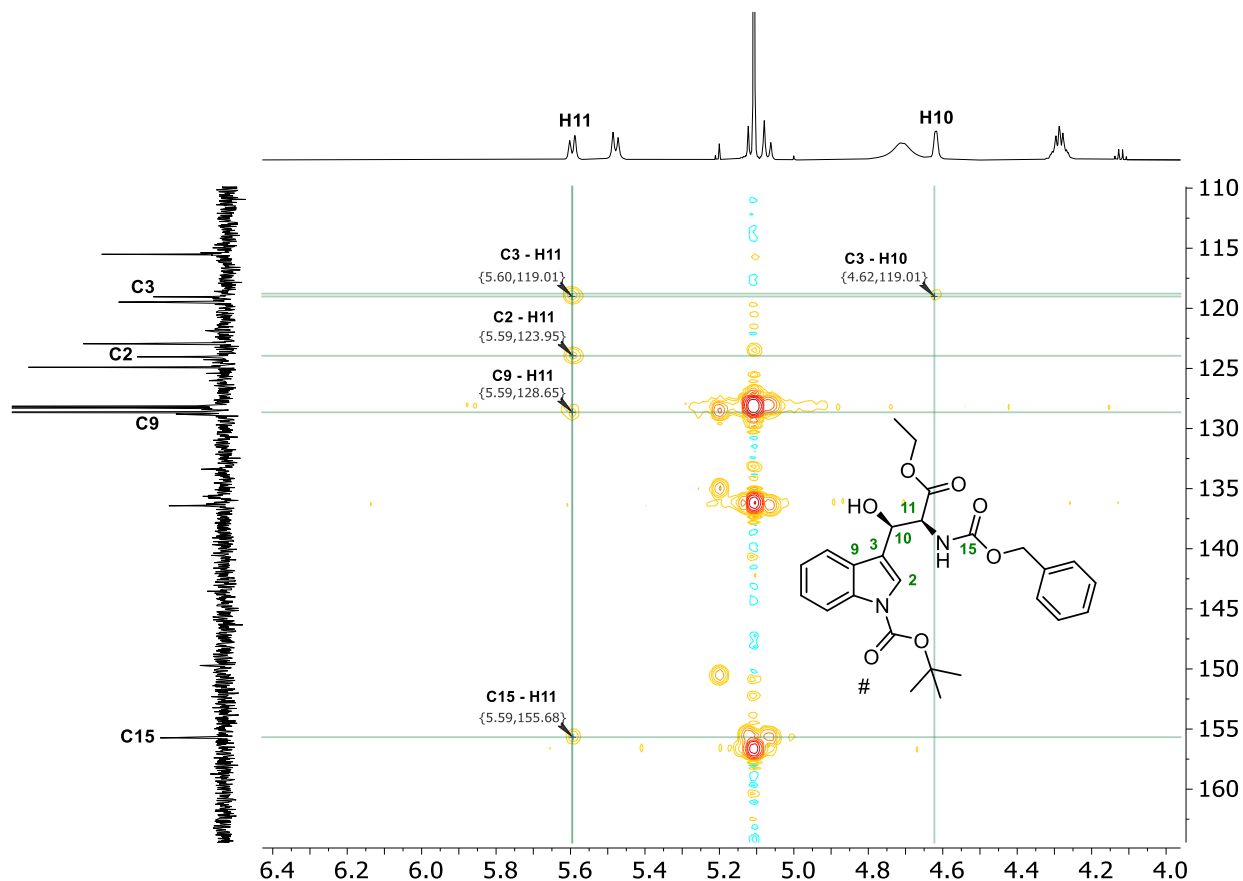
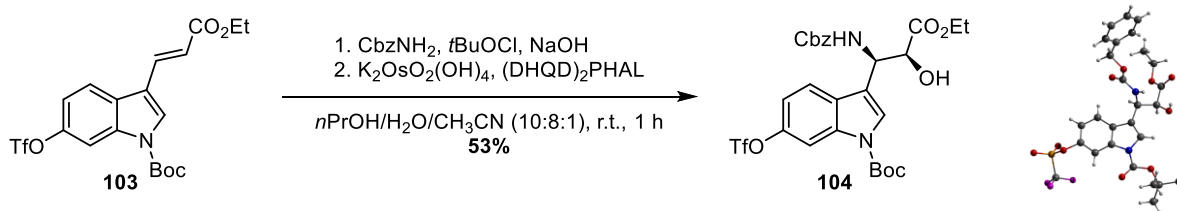


Figure 3.3: Section of the HMBC Spectrum of compound **109**, initially assumed as benzylamine **108**, but later determined as the desired benzylalcohol **109** by X-ray single crystal analysis of the opposing regioisomer of the triflate derivative.

Based on this misleading assignment of isomers, a better regioselectivity of the reaction was aspired. Therefore, different ligand cores were examined, as they are known to change the regioselectivity of the aminohydroxylation dramatically.^[135] Indeed, using PHAL instead of AQN as the ligand core rendered the reaction almost completely regioselective towards benzylamine **104** in 85% yield and 99%*ee* (entry 5).

Enantioselectivities were determined by preparation of the racemates using Et₃N as the ligand (entry 6). To conclude the optimization, different alcohol/water mixtures were tested to increase the solubility of the substrate (entries 8-10). However, *n*PrOH still gave the best results among the tested alcohols, while decomposition was observed in CH₃CN.

Application of the optimized reaction conditions on the triflate derivative using (DHQD)₂PHAL (entry 5) afforded benzylamine **104** in 53% yield (Scheme 3.23).

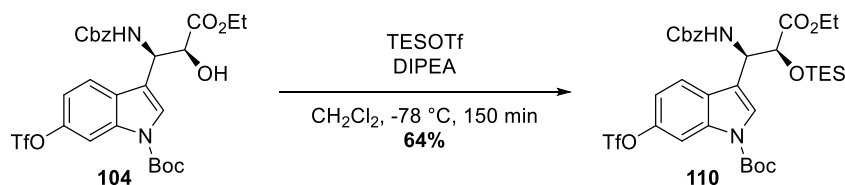


Scheme 3.23: Application of the optimized reaction conditions to the triflate derivative **104**. The crystal structure of the product was obtained weeks after the experiment and revoked the initial assignment as the benzylalcohol regioisomer **105**.

In contrast to the model substrate, the triflate was not soluble in the optimized solvent mixture, therefore small amounts of CH₃CN had to be added to the reaction mixture. The crystal structure was obtained weeks after the experiment, revoking the expected constitution as previously discussed.

Unfortunately, running the reaction with Et₃N as a ligand in order to prepare a racemate, did not afford any product. However, running the same HPLC method as for the previous derivatives showed a single peak. Based on the previous results and the good chromatographic separation of the enantiomers of compound **108**, high enantioselectivity can be assumed.

X-ray single crystal analysis elucidated the absolute configuration as α -(S), β -(R) as aspired for the synthesis of the functionalized (S)-tryptophan. Silylation of the secondary alcohol **104** was performed using TESOTf at -78 °C to prevent deprotection of the Boc group under the LEWIS acidic conditions and gave silyl ether **110** in 64% yield (Scheme 3.24).



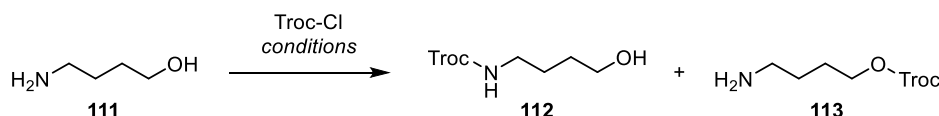
Scheme 3.24: Silylation of secondary alcohol **104**.

With substrate **110** in hand, a C-C coupling towards the formation of the lysine-indole carbon bond was envisioned. As a suitable substrate, Boc- Δ Lys(Troc)-OEt **72** was synthesized.

3.1.5. Synthesis of Boc- Δ Lys(Troc)-OMe (72)

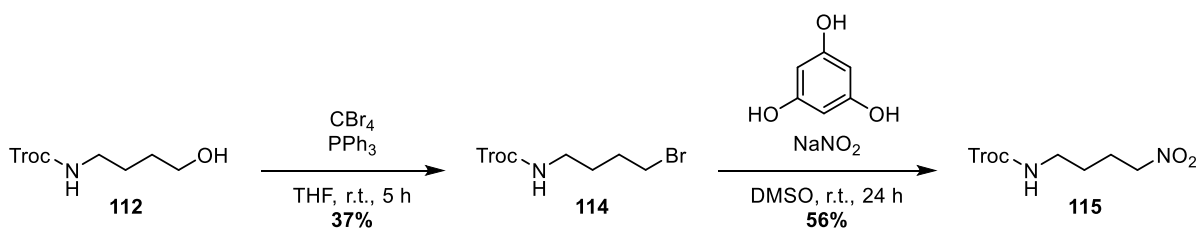
The synthesis commenced with the chemoselective protection of 4-aminobutanol (**111**) (Table 3.4). Surprisingly, the use of NaHCO₃ as a weak base in a biphasic system (SCHOTTEN-BAUMANN method) resulted in poor chemoselectivity despite slow syringe pump addition of TrocCl over 3 h (entries 1 and 2). In contrast, the use of aqueous NaOH-solution as reaction medium in combination with slow addition of TrocCl over 1 h increased the regioselectivity dramatically, affording carbamate **112** in 81% yield on a gram-scale (entry 4).

Table 3.4: Reaction optimization for the chemoselective N-Troc protection of 4-aminobutanol (**111**).



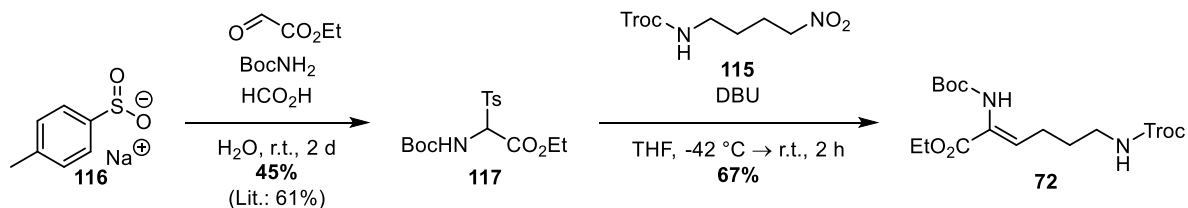
Entry	Conditions	Yield	
		N-protected 112	O-protected 113
1	NaHCO ₃ , Et ₂ O/H ₂ O, 0 °C → r.t., 24 h	50%	35%
2	NaHCO ₃ , Et ₂ O/H ₂ O, 0 °C, 24 h, syringe pump addition TrocCl (3 h), 24 h	32%	24%
3	NaOH, H ₂ O, 0 °C → r.t., 19 h	86%	13%
4	NaOH, H ₂ O, 0 °C → r.t., 21 h, syringe pump addition TrocCl (1 h)	81%	-

Subsequential APPEL-reaction gave bromide **114** in 37% yield (Scheme 3.25). The low yield can be attributed to its high volatility, causing significant product loss upon evaporation of the solvent used in chromatography.



Scheme 3.25: Synthesis of nitro compound **115**.

Introduction of the nitro-group was achieved by nucleophilic substitution using phloroglucinol and sodium nitrite. Glycine tosylate was obtained from a three-component reaction using sodium *p*-toluene sulfinate **116**, ethyl glyoxal, and *tert*-butyl carbamate in formic acid (Scheme 3.26). The compounds were subjected to the alkylation/nitrite elimination conditions reported by KINOSHITA *et al.* and gave (*Z*)-Boc- Δ Lys(Troc)-OEt (**72**) in 67% yield. Formation of the (*E*)-isomer was not observed.



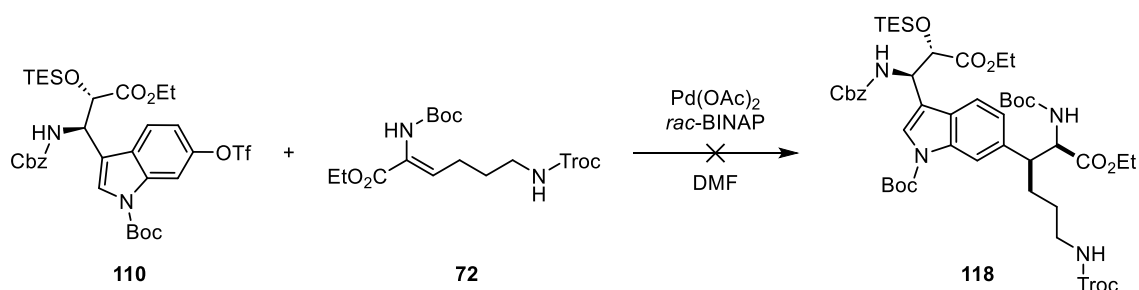
Scheme 3.26: Synthesis of Boc- Δ Lys(Troc)-OEt (**72**) based on the method reported by KINOSHITA *et al.*^[40]

3.1.6. Reductive HECK Reaction

As previously discussed, the use of a triflate offers the possibility of an asymmetric reductive HECK-coupling to install the C6-indole-lysine C-C bond and defines the stereocenter at the α - and β -position of lysine in a single step.

With Boc- Δ Lys(Troc)-OEt (**72**) and triflate **110** on hand, the feasibility of a reductive HECK-coupling for the formation of the C6-indole-lysine C-C bond was evaluated (Table 3.5). Unfortunately, employing common conditions for this transformation, e.g. by using proton sponge (entry 1) or sodium formate (entry 2) as H-donor and base simultaneously, did not promote any conversion of the substrates. For the combination of Et₃N and formic acid, hydrogenolysis of the benzyl carbamate was observed, but no C-C bond formation could be achieved (entry 3).

Table 3.5: Attempted reductive HECK coupling of dehydrolysine **72** and triflate **110**.



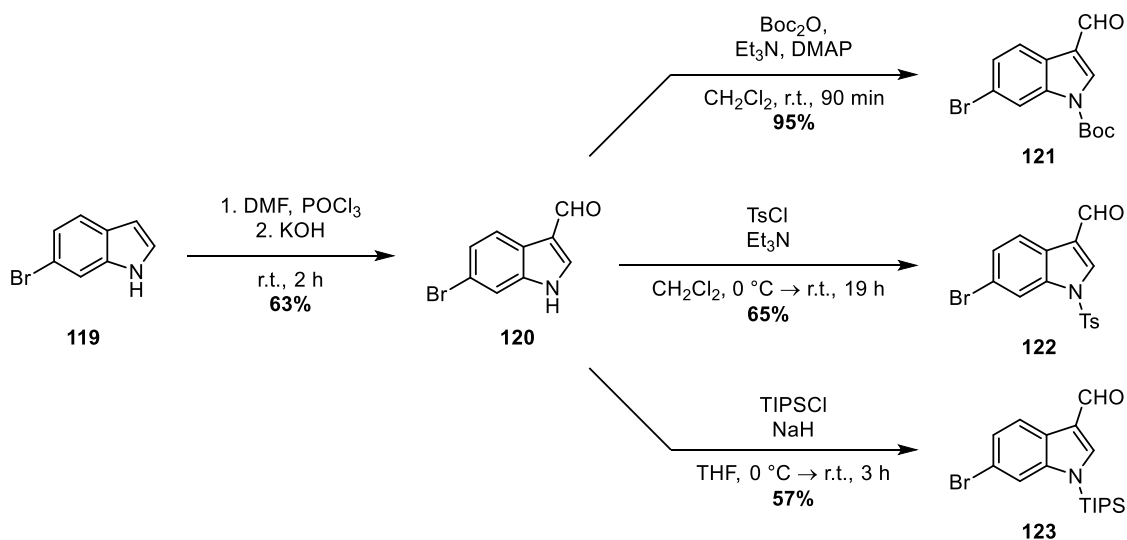
Entry	Base	H-Donor	T	Result
1	Proton sponge	Proton sponge	100 °C	No conversion
2	NaHCOO	NaHCOO	100 °C	No conversion
3	Et ₃ N	HCOOH	70 °C	Cbz-deprotection

Reaction conditions: Triflate **110** (0.01 mmol, 1.00 eq.), Boc- Δ Lys(Troc)-OMe (**72**, 1.10 eq.), base (2.00 eq.), Pd(OAc)₂ (5 mol%), *rac*-BINAP (10 mol%), degassed, dry DMF (0.1 M).

3.1.7. C6-Indole Bond Formation via HECK Reaction

An extensive screening campaign using a variety of simple test substrates was commenced. As the cationic reductive HECK reaction using the triflate derivative **110** was unsuccessful, the use of the more accessible bromide was taken into consideration to unlock the neutral pathway of the HECK reaction.

Therefore, commercially available 6-bromoindole **119** was formylated and *N*-Boc protected as previously described. In contrast to the triflate derivative, the unprotected indole derivative **120** was stable and could be isolated in good yields. In addition, to modulate the electronic properties of the indole, the tosyl- and TIPS- protected derivatives **122-123** were synthesized (Scheme 3.27).

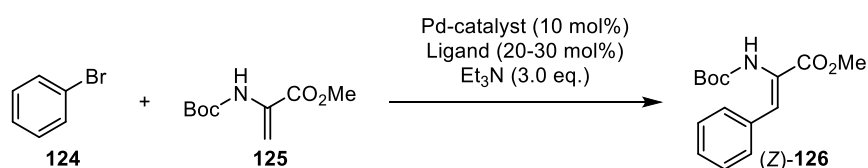


Scheme 3.27: Formylation and various protections of 6-bromoindole (**119**).

To test the suitability of dhAAs as substrates, the simple coupling of bromobenzene and Boc- Δ Ala-OMe (**125**) was conducted (Table 3.6).

Fortunately, coupling of this arylbromide was no challenge, demonstrating the suitability of Boc- Δ Ala-OMe (**125**) as an olefinic substrate for the HECK-reaction. While conducting the reaction in DMF at 90 °C gave 44% yield (entry 1), lowering the temperature to 80 °C (entry 2) afforded (*Z*)-Boc- Δ Phe-OMe (**126**) in 61% yield. The configuration was determined by ¹H-NOESY. The (*E*)-isomer was not observed.

Change of the catalyst, ligand, and switching the solvent to CH₃CN did not alter the yield significantly (entry 4). Moreover, running the reaction with electron-rich P(2-furyl)₃ as a ligand, did not give the desired product (entry 3).

Table 3.6: Reaction screening for the HECK-reaction of bromobenzene (**124**) with Boc- Δ Ala-OMe (**125**).

Entry	Catalyst	Ligand	solvent	T	t	Result
1	Pd(OAc) ₂	PPh ₃	DMF	90 °C	17 h	44%
2	Pd(OAc) ₂	PPh ₃	DMF	80 °C	24 h	61%
3	Pd ₂ (dba) ₃	P(2-furyl) ₃	DMF	90 °C	19 h	Complex mixture
4	Pd ₂ (dba) ₃	P(oTol) ₃	CH ₃ CN	80 °C	24 h	62%

Next, the olefination of 6-bromoindoles was investigated (Table 3.7).

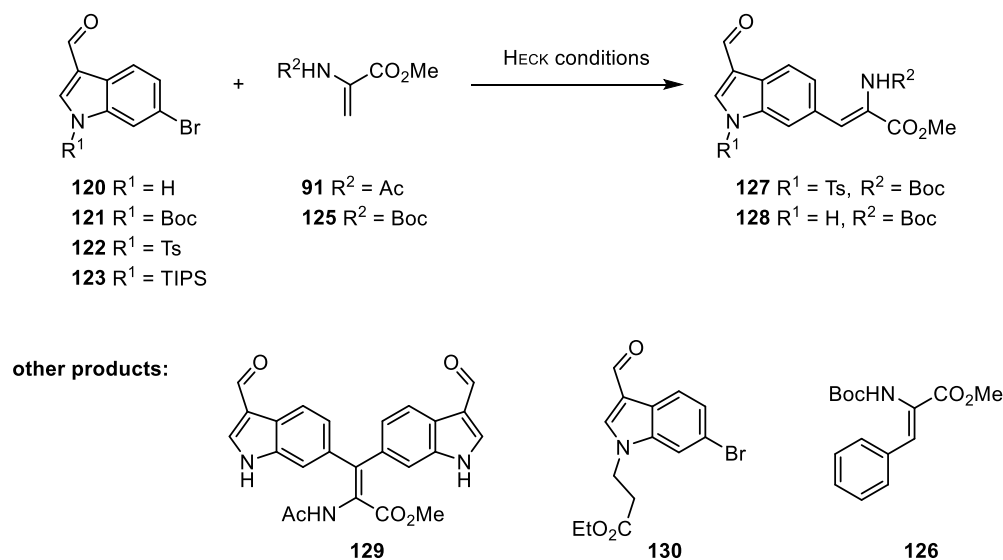
Employing similar conditions to the olefination of indole **121** and Ac- Δ Ala-OMe as optimized before (entry 1), a new product was isolated. NMR-Analysis suggested showed a 1:2 ratio of the methyl ester and acetyl signals compared to the indole signals, without showing any olefinic signals, suggesting structure **129**. However, ESI-MS did not detect the expected mass.

The loss of the Boc group presented the first major obstacle in this campaign, as the protecting group on the indole turned out to be unexpectedly labile. Running the reaction with the weaker NaHCO₃/*n*Bu₄NBr base system yielded 11% of deprotected starting material **120**, while not showing any other products (entry 2).

Lowering the temperature to 60 °C prevented the loss of the Boc-group, however, no conversion was observed (entry 3). As the loss of the Boc-group is not necessarily problematic, the reactions were repeated with unprotected indole bromide **120**, however, running the reaction with Et₃N (entry 4) led to decomposition even at lower temperatures, while the weaker base system did not show any conversion (entry 5).

Additionally, ethyl acrylate was tested as a simpler olefin, which led to 1,4-addition at the indole nitrogen instead of C6-olefination (entries 6-7). The olefination with ethyl acrylate could not be achieved with the Boc-protected indole derivative, again, deprotection and 1,4-addition of the indole nitrogen competed over the C6-olefination (entry 8).

To modulate the electron-density of the indole, the electron-rich TIPS-protected as well as the electron-poor Ts-protected derivatives were investigated. C6-olefination of the TIPS-derivative **123** could be achieved, albeit only the deprotected product **128** could be obtained (entry 11). Surprisingly, 18% of (Z)-Boc- Δ Phe-OMe (**126**) was obtained as a major side product, probably arising from the thermal decomposition of the PPh₃ ligand.^[137]

Table 3.7: Screening campaign for the C6-olefination of 6-bromoindoles.

Entry	Ar-Br R ¹	Alkene R ²	Catalyst Ligand	Solvent T	Base Additives	Rec. s.m.	Result
1	121 Boc	91 Ac	Pd(OAc) ₂ PPh ₃	DMF 90 °C	Et ₃ N	n.d.	21% 129
2	121 Boc	91 Ac	Pd(OAc) ₂ PPh ₃	DMF 90 °C	NaHCO ₃ <i>n</i> Bu ₄ NBr	n.d.	11% 120
3	121 Boc	91 Ac	Pd(OAc) ₂ PPh ₃	DMF 60 °C	Et ₃ N	n.d.	No conversion
4	120 H	91 Ac	Pd(OAc) ₂ PPh ₃	DMF 60 °C	Et ₃ N	n.d.	Decomposition
5	120 H	91 Ac	Pd(OAc) ₂ PPh ₃	DMF 60 °C	NaHCO ₃ <i>n</i> Bu ₄ NBr	n.d.	No conversion
6	120 H	Ethyl acrylate	Pd(OAc) ₂ PPh ₃	DMF 60 °C	NaHCO ₃ <i>n</i> Bu ₄ NBr	-	52% 130
7	120 H	Ethyl acrylate	Pd(OAc) ₂ PPh ₃	CH ₃ CN 60 °C	NaHCO ₃ <i>n</i> Bu ₄ NBr	-	67% 130
8	121 Boc	Ethyl acrylate	Pd(OAc) ₂ PPh ₃	CH ₃ CN 60 °C	NaHCO ₃ <i>n</i> Bu ₄ NBr	59%	15% 130 , 8% 120
9	120 H	Ethyl acrylate	Pd(OAc) ₂ PPh ₃	DMF 60 °C	Et ₃ N	-	Decomposition
10	121 Boc	Ethyl acrylate	Pd(OAc) ₂ PPh ₃	DMF 60 °C	Et ₃ N	n.d.	No conversion
11	123 TIPS	125 Boc	Pd(OAc) ₂ PPh ₃	DMF 90 °C	Et ₃ N	n.d.	11% 128 , 18% 126
12	121 Boc	125 Boc	Pd ₂ (dba) ₃ P(2-furyl) ₃	DMF 60 °C	NaOAc	53%	32% 120

Table 3.7: Continued.

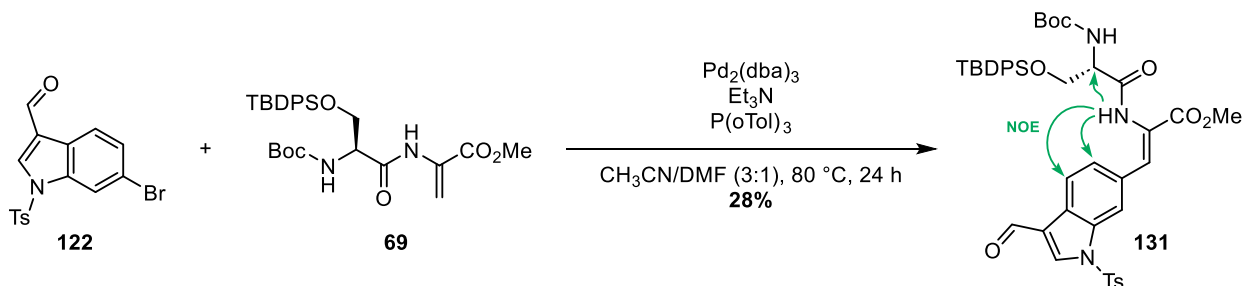
Entry	Ar-Br R ¹	Alkene R ²	Catalyst Ligand	Solvent T	Base Additives	Rec. s.m.	Result
13	121 Boc	125 Boc	Pd ₂ (dba) ₃ XPhos	DMF 60 °C	Cs ₂ CO ₃	-	Decomposition
14	122 Ts	125 Boc	Pd(OAc) ₂ PPh ₃	DMF 60 °C	Et ₃ N	n.d.	No conversion
15	122 Ts	125 Boc	Pd(OAc) ₂ PPh ₃	CH ₃ CN 90 °C	Et ₃ N	32%	10% 127
16	122 Ts	125 Boc	Pd(OAc) ₂ XPhos	CH ₃ CN 80 °C	Et ₃ N	n.d.	No conversion
17	122 Ts	125 Boc	Pd XPhos G2	CH ₃ CN 80 °C	Et ₃ N	n.d.	20% conv.
18	122 Ts	125 Boc	Pd(OAc) ₂ P(oTol) ₃	CH ₃ CN 80 °C	Et ₃ N	n.d.	10% conv.
19	122 Ts	125 Boc	Pd₂(dba)₃ P(oTol)₃	CH₃CN 80 °C	Et₃N	21%	36% 127
20	122 Ts	125 Boc	Pd ₂ (dba) ₃ P(oTol) ₃	CH ₃ CN 80 °C	Na ₂ CO ₃	n.d.	No conversion
21	122 Ts	125 Boc	Pd ₂ (dba) ₃ P(2-furyl) ₃	CH ₃ CN 80 °C	Et ₃ N	n.d.	No conversion
22	122 Ts	125 Boc	Pd ₂ (dba) ₃ P(Cy) ₃	CH ₃ CN 80 °C	Et ₃ N	n.d.	No conversion
23	122 Ts	125 Boc	Pd ₂ (dba) ₃ XPhos	CH ₃ CN 80 °C	Et ₃ N	n.d.	No conversion
24	122 Ts	125 Boc	Pd(PPh ₃) ₄	CH ₃ CN 80 °C	Et ₃ N	n.d.	No conversion

Reaction conditions: Ar-Br (0.05 mmol, 1.00 eq.), alkene (1.30 eq.), base (2.00 eq.), Pd-catalyst (10 mol% Pd), ligand (20-30 mol%), degassed, dry solvents (0.1-0.2 M), closed vial, 16-24 h.

In contrast to the Boc- and TIPS-derivative, the electron-poor Ts-protected indole **122** demonstrated higher stability. While in DMF at 60 °C using Pd(OAc)₂/PPh₃ showed no conversion (entry 14), the formation of **127** in 10% yield proceeded when the reaction was performed in CH₃CN at 90 °C (entry 15). The conversion was not complete, 32% of starting material alongside traces of deprotected indole **120** were isolated after 16 h. To improve the yield and conversion, different catalyst/ligand systems were tested (entries 16-19).

While Pd Xphos G2 as a precatalyst and Pd(OAc)₂ showed some conversion, switching the system to Pd₂(dba)₃/P(oTol)₃ (entry 19) improved the conversion and yield significantly to 36% (46% brsm). Further optimizations using an inorganic base (entry 20) or by using different ligands (entries 21-23) were not successful.

The applicability of the optimized reaction conditions was tested on the Boc-Ser(TBDPS)- Δ Ala-OMe (**69**) dipeptide (see chapter 3.1.1 for the corresponding synthesis). The dipeptide was insoluble in CH₃CN but sufficient solubility could be achieved by addition of 25% DMF. Full conversion was observed after 24 h at 80 °C and the HECK product **131** was obtained in 28% yield (Scheme 3.28). A plethora of compounds was observed on TLC, but the difficult separation and complexity of the spectra did not allow the identification of the side products.

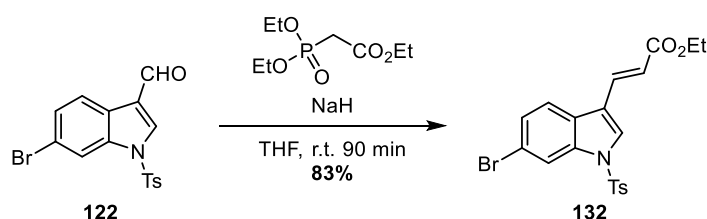


Scheme 3.28: Application of the optimized HECK protocol using Boc-Ser(TBDPS)- Δ Ala-OMe (**69**) as the olefinic substrate.

The product could be characterized as the single (*Z*)-isomer by ¹H ge-NOESY experiments. Excitation of the NH proton showed a magnetization transfer of 0.7%, 0.9%, and 1.8% for the H₄, H₅ protons of the indole and the serine α -proton, respectively. In contrast, irradiation of the methyl ester protons showed no significant NOEs >0.05%.

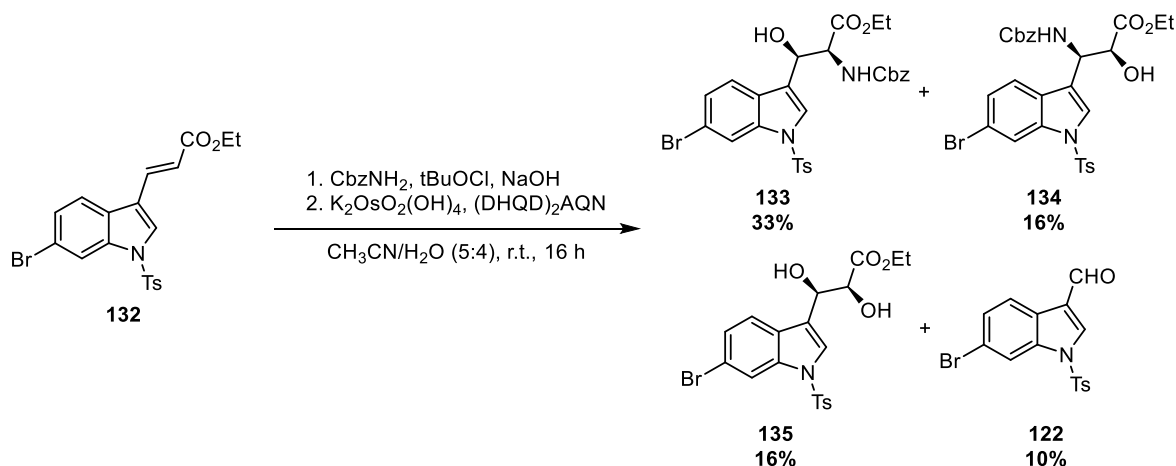
After identification of the tosyl-group as an appropriate protecting group and conditions for the HECK-reaction in hand, the synthesis of the tripeptide was conducted starting from tosylated 6-bromoindole derivative **122** in order to attempt an intramolecular HECK-reaction using the optimized conditions.

For economic and availability reasons, a HORNER-WADSWORTH-EMMONS reaction was performed using triethyl phosphonoacetate instead of a WITTIG reaction with ylide **102** as shown previously (Scheme 3.29). The reaction afforded olefin **132** in good yield as a single diastereomer.



Scheme 3.29: HORNER-WADSWORTH-EMMONS-reaction of aldehyde **122**.

Unfortunately, employing the previously optimized conditions was not suitable, as the tosyl-derivative is insoluble in *n*PrOH, *s*BuOH, *n*BuOH, *t*BuOH, methoxymethanol, and 4:1 ROH/CH₃CN mixtures thereof. Hence, CH₃CN had to be used as the solvent, albeit decomposition was observed with previous substrates. With the reversal of the regioisomeric assignment (see chapter 3.1.4), the reaction was performed with (DHQD)₂AQN as the ligand favoring the benzylalcohol derivative **133** (Scheme 3.30).



Scheme 3.30: SHARPLESS aminohydroxylation of **132**.

Benzylalcohol **133** could be successfully obtained and isolated in 33% yield. While the regioselectivity improved compared to the model system (2:1 cf. 1.4:1, Table 3.3, entry 3), new problems emerged due to the electron-withdrawing tosyl-group.

Firstly, significant amounts of dihydroxylation product **135** were obtained. Secondly, indole **122** was isolated in 10% yield, whose formation can be attributed to either Retro-aldol reaction of **133** or Retro-MANNICH reaction of **134**. All attempts to synthesize a racemate using Et₃N failed, however, HPLC-analysis using the optimized conditions for the C6-H derivative **109** showed a single peak without shoulder, suggesting a high enantiopurity.

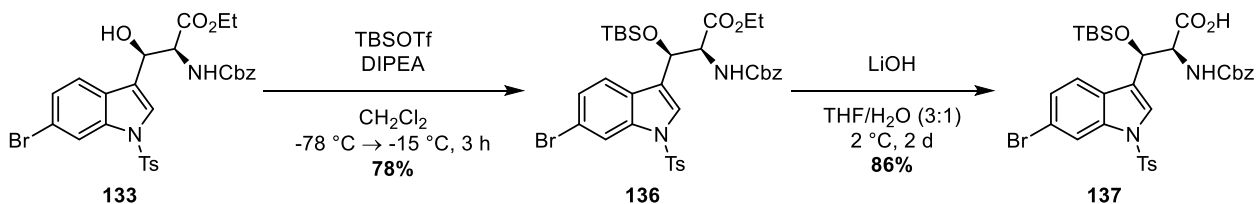
To conclude the experiences with the SHARPLESS aminohydroxylation, while representing a powerful method for installation of the hydroxy-group in an enantioselective fashion and crucial for the envisioned synthesis of darobactin, the reaction poses a major bottleneck for the synthesis.

Disadvantages are the low yields and high ligand loadings of the expensive ligand (DHQD)₂AQN with fluctuating commercial availability (while commercially available from Sigma-Aldrich in 2020, the ligand became commercially unavailable in Germany in 2021 until the time of writing this thesis). Given the current results, 130 mg of ligand are necessary to synthesize 500 mg of benzylalcohol **133**, attempted recovery of the ligand was not successful.

Given the TBDPS group on the H-Ser(TBDPS)-ΔAla-OMe, an installation of a TES-group on the tryptophan would require selective deprotection of the secondary TES ether in the presence of a primary TBDPS ether. While there are literature precedents that this might be successful,^[138] chemoselectivity problems were anticipated by slightly adjusting the protective group strategy.

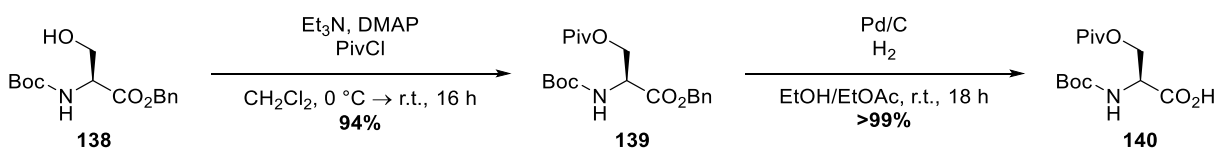
The use of a primary pivaloyl ester in the dipeptide H-Ser(Piv)-ΔAla-OMe (**142**) allows simultaneous deprotection of the primary alcohol and the indole in a single step using basic, nucleophilic conditions and allows the use of a more robust TBS-group for the secondary alcohol on the tryptophan.

Therefore, the synthesis was continued by TBS-protection of the alcohol, silyl ether **136** was obtained in 78% yield. Saponification of the ethyl ester furnished carboxylic acid **137** in 86% yield (Scheme 3.31).



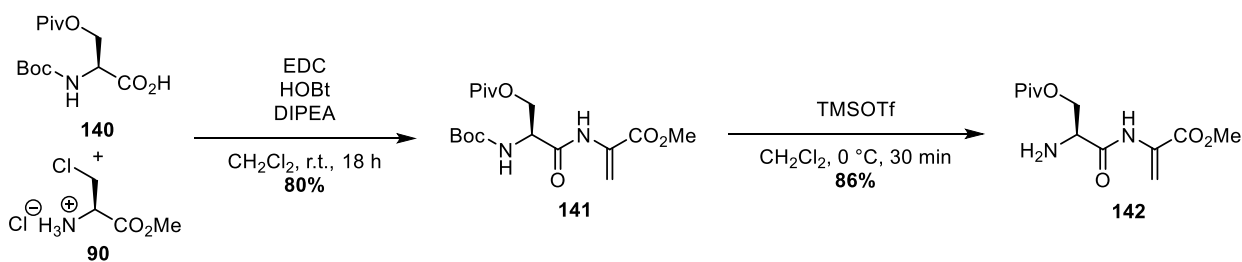
Scheme 3.31: TBS-protection and saponification of the ester function of **133**.

The dipeptide H-Ser(Piv)- Δ Ala-OMe (**142**) was prepared analogously to the TBDPS derivative. The pivaloyl group was installed on commercially available Boc-Ser-OBn, followed by hydrogenolysis of the benzyl ether in excellent yields (Scheme 3.32).



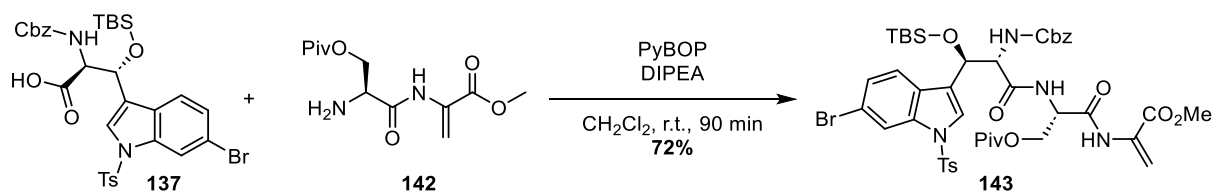
Scheme 3.32: Synthesis of Boc-Ser(Piv)-OH (**140**).

Peptide coupling with chloroalanine **90** using the established one-pot conditions delivered Boc-Ser(Piv)- Δ Ala-OMe (**141**) in a comparable yield of 80% (Scheme 3.33). Cleavage of the Boc-group under neutral conditions using TMSOTf gave primary amine **142** in good yield. It is important to note, that deprotection using TFA followed by basic workup, as applied for the TBDPS-derivative (cf. XX) gave three spots on TLC. The addition of HSiEt₃ as a carbocation scavenger resulted in hydrosilylation of the dehydroalanine moiety.



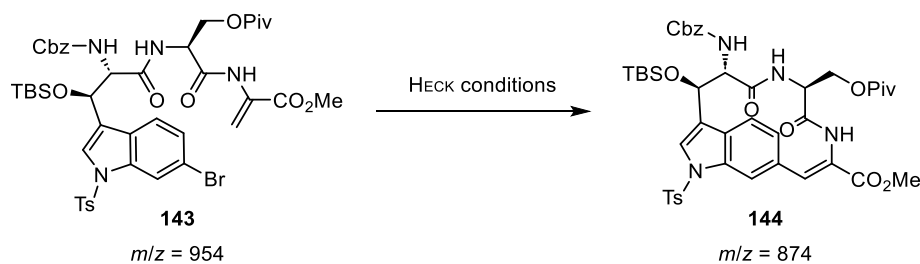
Scheme 3.33: One-pot peptide coupling and elimination.

Given the moderate yield of 52% using EDC/HOBt as coupling reagents and the higher steric demand of tryptophan **137** compared to tryptophan **84** (see chapter 3.1.2), more reactive reagents were tested. While the uronium agent COMU gave the product in 23% yield, the use of the reactive phosphonium reagent PyBOP gave tripeptide **143** in 72% yield after 90 min (Scheme 3.34).



Scheme 3.34: Peptide coupling of highly functionalized tryptophan **137** and H-Ser(Piv)- Δ Ala-OMe (**142**).

With tripeptide **143** in hand, the intramolecular HECK-cyclization was investigated (Table 3.8). The reactions were performed on a 5 mg-scale, due to the complexity and high molecular weight of the product, ¹H-NMR alone did not give useful information, therefore, all crude products of the reactions were analyzed by ESI-MS.

Table 3.8: Attempted cyclization of tripeptide **143** implementing various HECK conditions.

Entry	Catalyst Loading	Ligand Loading	Base Additives	Solvent T	Conversion	Result
1	Pd ₂ (dba) ₃ (10 mol%)	P(oTol) ₃ 60 mol%	Et ₃ N	CH ₃ CN 80 °C	Partial	Complex mixture, only polar products
2	Pd ₂ (dba) ₃ (10 mol%)	P(oTol) ₃ 60 mol%	Et ₃ N	DMF 80 °C	Full	Complex mixture, Loss of OMe Signal
3	Pd XPhos G2 (10 mol%)	-	K ₂ CO ₃	DMF 80 °C	Full	<i>m/z</i> not found
4	Pd(OAc) ₂ (20 mol%)	P(2-furyl) ₃ 40 mol%	Et ₃ N	PhMe 100 °C	Full	<i>m/z</i> not found
5	Pd(OAc) ₂ (20 mol%)	XPhos 40 mol%	Cs ₂ CO ₃	PhMe 100 °C	Full	<i>m/z</i> < 685
6	Pd(OAc) ₂ (10 mol%)	dppp 20 mol%	K ₂ CO ₃	PhMe 100 °C	Full	Dehalogenation
7	Pd(OAc) ₂ (20 mol%)	PPh ₃ 60 mol%	Et ₃ N (50 vol%)	PhMe 100 °C	Full	<i>m/z</i> < 600
8	Pd(OAc) ₂ (20 mol%)	BINAP 120 mol%	Ag ₂ CO ₃	CH ₃ CN 80 °C	No	-
9	Pd(OAc) ₂ (13 mol%)	P(oTol) ₃ 38 mol%	Ag ₂ CO ₃	NMP 90 °C	Partial	<i>m/z</i> not found
10	Pd ₂ (dba) ₃ (10 mol%)	PPh ₃ 80 mol%	DIPEA Ag ₃ PO ₄	NMP 90 °C	Full	<i>m/z</i> not found
11	Pd(OAc) ₂ (20 mol%)	-	NaHCO ₃ Bu ₄ NCl, 4Å MS	CH ₃ CN 80 °C	No	-
12	Pd(OAc) ₂ (32 mol%)	-	NaHCO ₃ Bu ₄ NCl	NMP 90 °C	Full	Complex mixture, Aldehyde Signals
13	Pd(OAc) ₂ (20 mol%)	PPh ₃ 40 mol%	NaHCO ₃ Bu ₄ NCl	CH ₃ CN/H ₂ O 80 °C	No	-
14	Pd(CH ₃ CN) ₂ Cl ₂ (21 mol%)	P(<i>n</i> Bu) ₃ 200 mol%	K ₂ CO ₃	NMP 90 °C	Full	Only baseline spots
15	Pd ₂ (dba) ₃ (22 mol%)	AsPh ₃ 116 mol%	DIPEA	NMP 90 °C	No	-

Reaction conditions: Tripeptide **143** (5.0 μmol, 1.00 eq.), base (5.00 eq.), degassed, dry solvents (0.01 M), closed vial, 20 h.

The optimized conditions for the intermolecular reaction did not yield the desired macrolactam, a complex mixture of very polar products was obtained (entry 1). Changing the solvent to DMF gave similar results, notably the methyl ester signal was lost in ¹H-NMR, indicating deprotection/decomposition of the

dehydroalanine moiety (entry 2). A variety of ligands was tested, but the product mass was not observed in any of the crude products (entries 3-6). Interestingly, the use of the dppp-ligand resulted in the formation of a product with a mass of $m/z = 899$, which would correspond to the $[M+2H+Na]^+$ ion, implying dehalogenation of the starting material (entry 6).

Forcing the reaction to operate *via* the cationic pathway by the addition of silver salts (OVERMAN conditions), e.g. Ag_2CO_3 showed low conversion (entries 8-9) and or did not form the desired product if DIPEA was added as an additional base (entry 10).

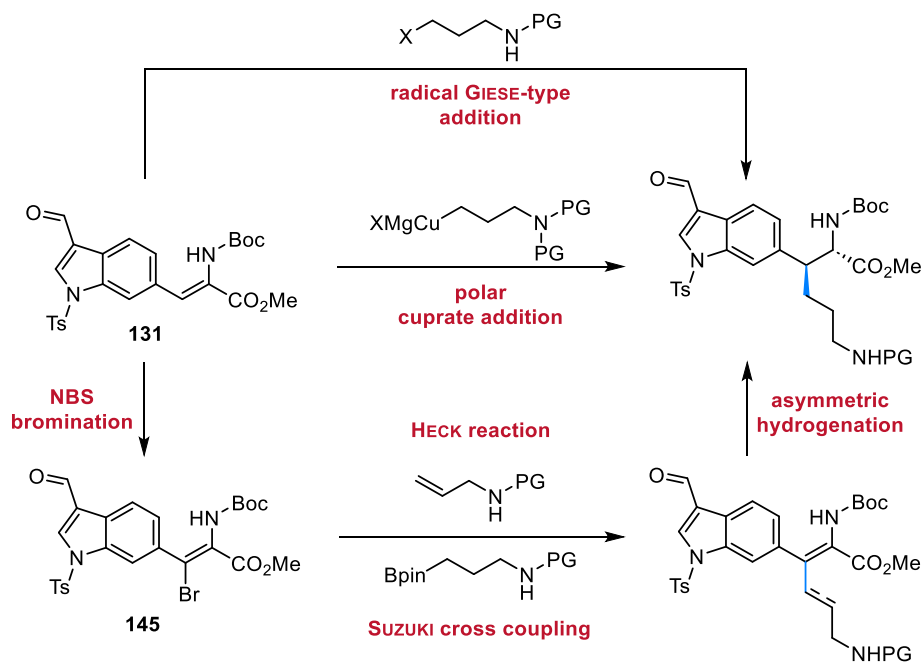
Running the reacting under strictly anhydrous JEFFEREY conditions in an attempt to lower the reaction temperature did not show any conversion (entry 11) or led to decomposition if NMP was used as the solvent instead of CH_3CN (entry 12). Aqueous JEFFEREY conditions showed no conversion (entry 13) and application of highly reactive $P(nBu)_3$ only showed baseline spots, indicating the decomposition of the starting material (entry 14).

The use of $AsPh_3$, which displays a very narrow Tolman cone angle of approx. 100° (cf. PPh_3 145°),^[139] did not give any conversion (entry 15).

With these results and the published total syntheses of darobactin in the meantime,^[20-21] the cyclization *via* HECK reaction was no longer investigated.

3.1.8. Installation of the Lysine Side Chain

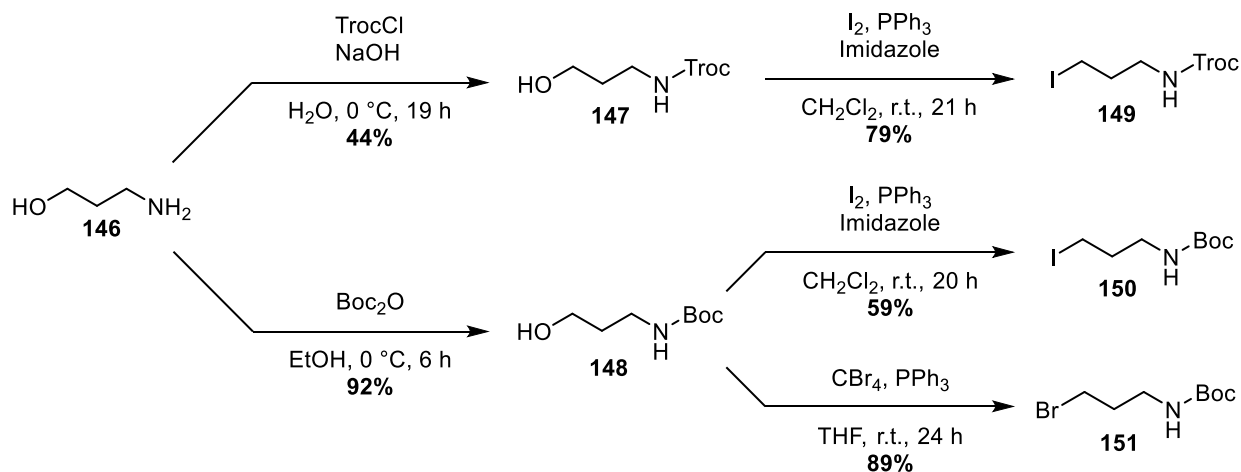
As the reductive HECK reaction could not be achieved, new approaches toward the installation of the lysine side chain had to be investigated. Given the reactivity of dhAAs, three viable options were considered (Scheme 3.35).



Scheme 3.35: Three approaches towards the installation of the lysine side-chain, exemplified starting from HECK-product **131**.

Firstly, the pronounced SOMO-philicity of dHAAs should allow radical conjugate addition of alkyl halides in a GIESE-type reaction. Secondly, polar 1,4-addition of a cuprate to the MICHAEL system should be attempted, however, the basicity of the reagents results in a risk of N-H deprotonation. Finally, the formation of a vinylhalide and subsequent cross-coupling or HECK-reaction could achieve the aspired C-C bond formation.

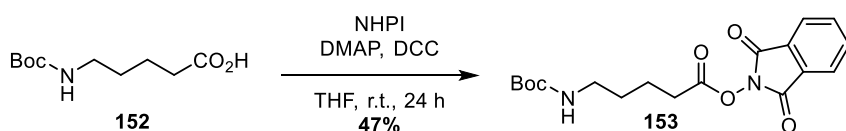
To assess the most elegant approach, the radical 1,4-addition, three alkyl halides were synthesized starting from 3-aminopropanol (**146**) (Scheme 3.36).



Scheme 3.36: Synthesis of alkyl halides as radical precursors.

While selective Troc-protection of the amine **146** gave carbamate **147** in a moderate yield of 44%, protection using the less reactive Boc₂O afforded *tert*-butyl carbamate **148** in an excellent yield of 92%. Both derivatives were synthesized as the stability of the Troc-group during the radical formation step was uncertain.^[140] Hence, while the Troc-group would integrate more flexibly into the given protective group strategy, the Boc-group is reportedly stable under radical conditions and a late-stage addition to the dehydroalanine moiety would not interfere with this strategy.^[140]

The alcohols **147** and **148** were transformed into the alkyl halides **149-151** using APPEL conditions in good to high yields. Additionally, an *N*-Hydroxyphthalimide (NHPI) derivative was synthesized by STEGLICH esterification of Boc-GABA-OH (**152**) (Scheme 3.37).



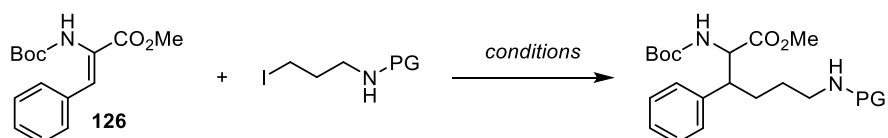
Scheme 3.37: STEGLICH esterification of Boc-GABA-OH (**152**) with NHPI.

The radical addition was attempted using (*Z*)-Boc- Δ Phe-OMe (**126**) as a readily accessible test system. Classical GIESE conditions using azobisisobutyronitrile (AIBN) as a radical initiator were applied to all four radical precursors (Table 3.9, entries 1-4). Unfortunately, no alkylation was observed in these reactions, both

starting materials, the radical precursors and (Z)-Boc- Δ Phe-OMe (**126**), were detected by $^1\text{H-NMR}$ of the crude product. This indicates, that the radical generation was not successful.

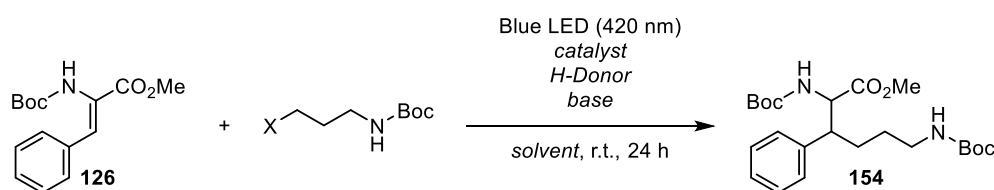
Alternatively, alkylation by Ag_2O -mediated proton-coupled electron transfer (PCET) as described by COA *et al.* was attempted but no conversion was observed (entry 5).^[141]

Table 3.9: Attempted radical 1,4-addition to (Z)-Boc- Δ Phe-OMe (**126**) using various radical precursors.



Entry	Precursor	Radical generation	H-Donor	Conditions	Result
1	Troc-Iodide 149	AIBN	Bu_3SnH	CH_2Cl_2 , reflux, 9 h	no conversion
2	Iodide 150	AIBN	Bu_3SnH	PhMe, reflux, 5 h	no conversion
3	Bromide 151	AIBN	Bu_3SnH	PhMe, reflux, 5 h	no conversion
4	NHPI ester 153	AIBN	Bu_3SnH	PhMe, reflux, 5 h	no conversion
5	Bromide 151	Ag_2O	-	CH_3CN , reflux, 9 h	no conversion

In the past decade, photocatalysis using cyclometalated ruthenium and iridium complexes drastically developed.^[142] Typically, these 18-electron complexes can be excited by blue light and produce stable photoexcited states with long lifetimes. These long-lived states allow bimolecular quenching under formation of radicals, e.g. by dehalogenation of alkyl halides. Therefore, a variety of common photocatalysts were tested for the alkylation of dHAA **126** (Table 3.10). As the irradiation source, a 30 W high-power COB-LED (420 nm) was used.

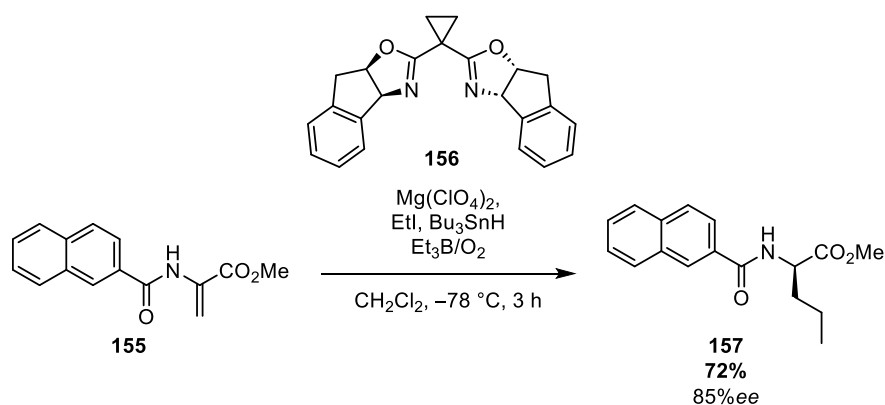
Table 3.10: Reaction conditions tested for the photocatalyzed alkylation of (Z)-Boc- Δ Phe-OMe (**126**).

Entry	X	Catalyst	H-Donor	Solvent Base	Conv. to 154	E/Z 126
1	I	[Ir(dtbbpy)(ppy) ₂] ₂ PF ₆	Hantzsch ester	DMSO/H ₂ O -	-	1:1
2	I	[Ru(bpy) ₃](PF ₆) ₂	Hantzsch ester	DMSO/H ₂ O -	-	1:3
3	CO ₂ Nphth	[Ir(dtbbpy)(ppy) ₂] ₂ PF ₆	Hantzsch ester	DMSO/H ₂ O -	-	1:1
4	CO ₂ Nphth	[Ir(dtbbpy)(ppy) ₂] ₂ PF ₆	Hantzsch ester	CH ₂ Cl ₂ DIPEA	-	1:1
5	CO ₂ Nphth	[Ir(dF(CF ₃)ppy) ₂ (dtbpy)]PF ₆	Hantzsch ester	CH ₃ CN K ₂ CO ₃	-	1:1
6	CO ₂ Nphth	[Ir(dF(CF ₃)ppy) ₂ (dtbpy)]PF ₆	(Me ₃ Si) ₃ SiH	CH ₃ CN K ₂ CO ₃	-	1:1
7	Br	[Ir(dtbbpy)(ppy) ₂] ₂ PF ₆	(Me ₃ Si) ₃ SiH	CH ₃ CN K ₂ CO ₃	-	1:1
8	Br	[Ir(dF(CF ₃)ppy) ₂ (dtbpy)]PF ₆	1,4- Cyclohexadiene	CH ₃ CN K ₂ CO ₃	-	1:1
9	Br	[Ru(bpz) ₃](PF ₆) ₂	1,4- Cyclohexadiene	CH ₃ CN K ₂ CO ₃	-	1:9
10	I	[Ru(bpy) ₃](PF ₆) ₂	(Me ₃ Si) ₃ SiH	CH ₃ CN K ₂ CO ₃	-	1:3

In all reactions, the radical formation was indeed successful, the radical precursors were not detected after the reaction. However, no formation of the alkylated product was observed, instead partial isomerization of (Z)-Boc- Δ Phe-OMe (**126**) to its (E)-isomer alongside the formation of propyl carbamates were detected by ¹H-NMR of the crude mixture. The degree of isomerization was typically 50% for the Ir(I) catalysts and 10% to 25% for the Ru(II) catalysts.

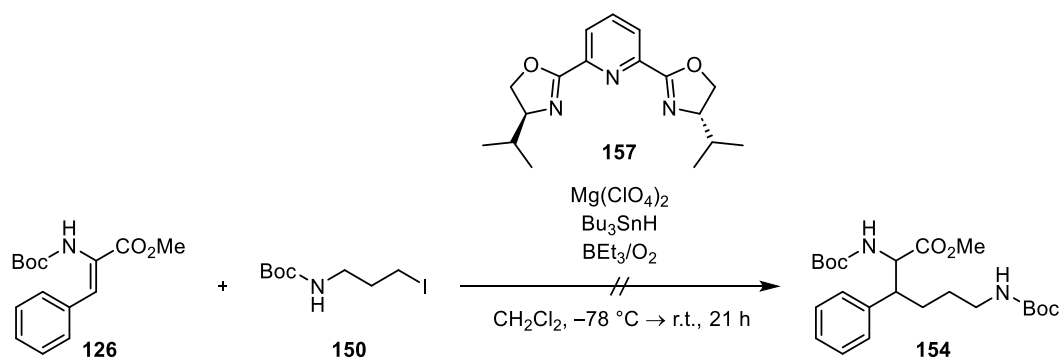
The selective contra-thermodynamic isomerization of (Z)-dHAAs would pose a very valuable method to access (E)-dHAAs. However, attempts to increase the degree of isomerization over 50% utilizing various photocatalysts, incl. the catalysts shown, riboflavin and thioxanthone, failed. This indicates similar triplet-energies of the geometric isomers, infringing the precondition for directionality *via* deconjugation.^[143] Non-conjugated dHAAs, e.g. Boc- Δ Lys(Troc)-OMe (**72**) did not isomerize under these conditions.

Another promising protocol for the installation of the lysine side-chain was reported by SIBI *et al.*^[55] They achieved a 1,4-radical addition of ethyl iodide to dehydroalanine derivative **155** followed by enantioselective H-atom transfer to the resulting glycine radical (Scheme 3.38).



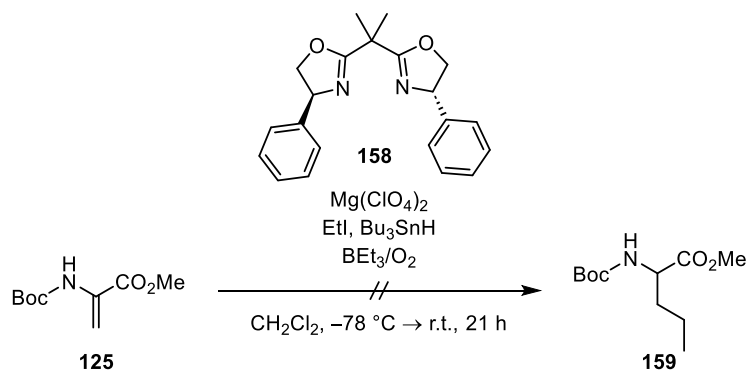
Scheme 3.38: Enantioselective alkylation of dehydroalanine **155** reported by Sibi *et al.*^[55]

As the BOX-ligand **156** was not available, the reaction was conducted using BOX-ligand **157** and iodide **150** (Scheme 3.39).



Scheme 3.39: Attempted alkylation of Boc- Δ Phe-OMe (**126**) inspired by the protocol reported by Sibi *et al.*^[55]

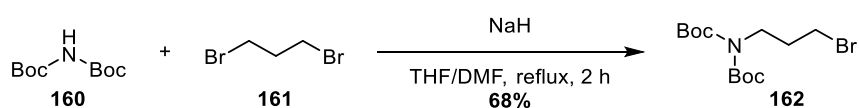
After 3 h at $-78\text{ }^\circ\text{C}$, no conversion was observed and the reaction was continued at room temperature for 18 h. No product formation was observed and iodide **150** was still detected *via* TLC. Application of similar conditions for the addition of ethyl iodide to Boc- Δ Ala-OMe (**125**) resulted in a complex product mixture, but the formation of the alkylated product **159** was not observed (Scheme 3.40).



Scheme 3.40: Attempted alkylation of Boc- Δ Ala-OMe (**125**) with Etl .

This result indicates that either the large bite-angle BOX-ligand **158** (110.6° cf. 104.7° for **156**)^[144] or the presence of an aryl amide is crucial for the reaction to proceed.

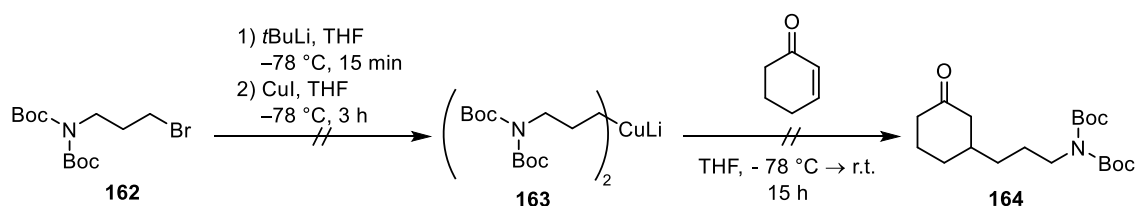
While polar 1,4-addition of cuprates is a reliable method for the alkylation of small molecules, e.g. terpenes, the formation of cuprates is limited to base-stable substrates. Typically, the pK_a value of amides or carbamates is lower than the pK_a value of the lithium or magnesium organyls used for the preparation of the GILMAN or NORMANT cuprate. Hence, for the attempted polar addition, a bisprotected bromopropyl amine **162** was synthesized by alkylation of di-*tert*-butyliminodicarboxylate (**160**) with 1,3-dibromopropane (**161**) (Scheme 3.41).



Scheme 3.41: Synthesis of bisprotected bromopropyl amine **162**.

The preparation of a NORMANT cuprate was investigated using bromide **162**. In the first step, formation of the GRIGNARD reagent was attempted using commercially available magnesium turnings. However, refluxing in dry Et₂O or THF for several hours, preactivation by iodine, and initiation using 1,2-dibromoethane or ultrasonic baths did not get the GRIGNARD reaction started. As a last resort, RIEKE's magnesium was prepared from anhydrous MgCl₂, anhydrous potassium iodide, and elemental potassium in dry, degassed refluxing THF.^[145] However, even the resulting highly activated magnesium did not lead to formation of the GRIGNARD reagent.

Consequently, the preparation of a GILMAN cuprate was tested by lithium-halogen exchange using *t*BuLi. Treatment of bromide **162** with *t*BuLi for 15 min at -78 °C and subsequent addition of anhydrous CuI led to quantitative formation of GILMAN cuprate **163** (Scheme 3.42).



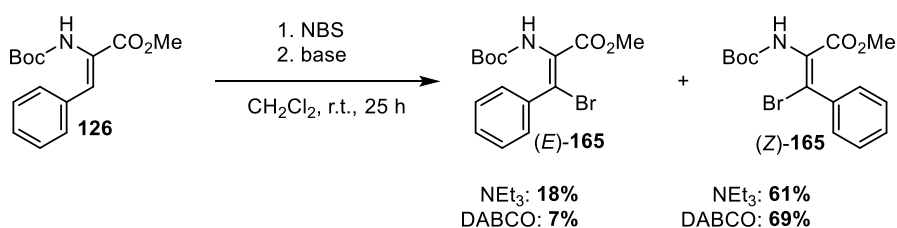
Scheme 3.42: Attempted preparation of GILMAN cuprate **163**. Addition to cyclohexenone to validate formation of **163**, failed.

The GILMAN test did not detect any remaining organolithium species.^[146] To validate the successful formation of the GILMAN cuprate, a small amount was subjected to cyclohexenone and the crude reaction product was analyzed. No conjugate addition product and no bromide **162** were detected, suggesting that cuprate **163** did not form and instead side reactions during the lithiation step occurred.

Therefore, this approach was not further investigated. In a third approach, alkenylation via HECK reaction followed by hydrogenation was tested. In principle, two approaches can be envisioned, the coupling of an

alkyl halide to the dhAA or the installation of a bromide on the dhAA scaffold and coupling of the vinyl bromide with allylcarbamates. Albeit the direct coupling of an alkyl halide would be an elegant method and recent advances in this area enabled acrylate substrates, the substrate scopes remain rather limited. [147] Hence, the more reliable method of a classical MIZOROKI-HECK reaction was investigated starting with the bromination of the test substrate (Z)-Boc-ΔPhe-OMe (**126**).

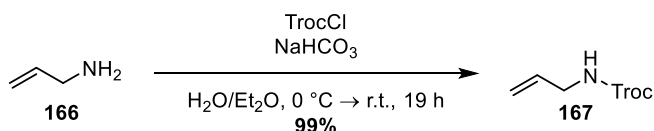
The bromination of (Z)-Boc-ΔPhe-OMe (**126**) was achieved using NBS and an amine base. While the use of Et₃N as the base showed a 3:1 selectivity towards the (Z)-isomer, the diastereoselectivity could be improved significantly to 10:1 using the bicyclic base DABCO (Scheme 3.43).



Scheme 3.43: Bromination of (Z)-Boc-ΔPhe-OMe (**126**) using two different amine bases.

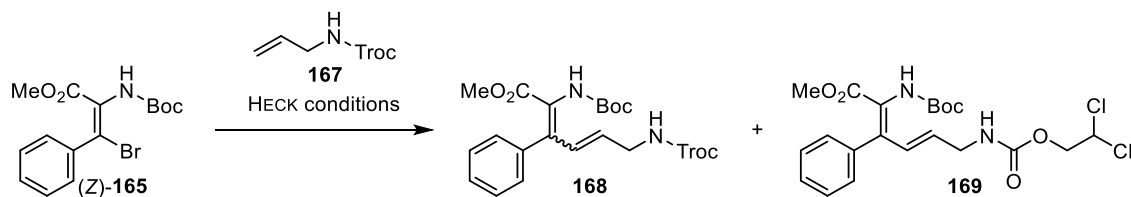
As asymmetric *syn*-hydrogenation after olefination of the (Z)-configured isomer would yield both stereocenters in the desired configuration for the total synthesis of darobactin, the observed selectivity was advantageous to access darobactin.

The coupling partner for the aspired MIZOROKI-HECK reaction, 2,2,2-trichloroethyl allylcarbamate (**167**), was synthesized by protection of allylamine (**166**) with TrocCl in quantitative yield (Scheme 3.44).



Scheme 3.44: Synthesis of , 2,2,2-trichloroethyl allylcarbamate (**167**).

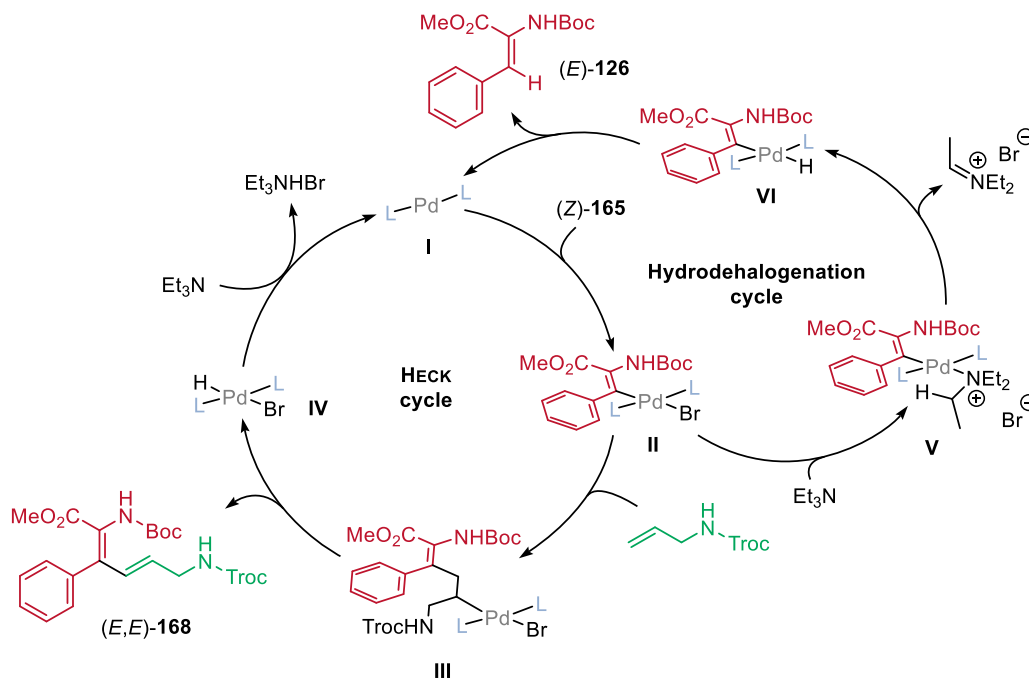
The olefination of dehydrophenylalanine (Z)-**165** was attempted using various HECK conditions (Table 3.11).

Table 3.11: Screening of suitable reaction conditions for the olefination of (Z)-165.

Entry	Catalyst	Ligand	Base	Solvent	Result
1	Pd(OAc) ₂	XPhos	Et ₃ N	NMP	Formation (E)-Boc-ΔPhe-OMe (126)
2	Pd(OAc) ₂	SPhos	Cs ₂ CO ₃	NMP	Complex mixture
3	Pd(OAc) ₂	SPhos	DIPEA	CH ₃ CN	Complex mixture
4	Pd ₂ (dba) ₃	P(oTol) ₃	Ag ₃ PO ₄	CH ₃ CN	No conversion
5	Pd ₂ (dba) ₃	P(oTol) ₃	DIPEA	NMP	Complex mixture
6	Pd ₂ (dba) ₃	P(oTol) ₃	DIPEA	DMF	13% 168 (d.r. 3:1 (E,E)/(Z,E), 14% 169)

Reaction conditions: Bromide (Z)-165 (0.1-0.2 mmol, 1.00 eq.), olefin 167 (1.50 eq.), base (3.00 eq.), Pd-catalyst (20 mol% Pd), ligand (40 mol%), degassed, dry solvent (0.1 M), 80 °C, 24 h.

The use of Et₃N as a base resulted in hydrodehalogenation of the bromide under the formation of (E)-Boc-ΔPhe-OMe (**126**) (entry 1). This side reaction is a common phenomenon in Pd-catalyzed reactions (Scheme 3.45).^[148-150]

**Scheme 3.45:** Proposed mechanism of the hydrodehalogenation as a side reaction of the catalytic Heck reaction.

The side product can be explained by halogen replacement of the intermediate **II** after oxidative addition of the vinyl bromide (*Z*)-**165** to the palladium complex **I**. The formed *N*-complexed palladium species **V** undergoes β -hydride elimination under release of triethyliminium bromide and formation of hydride complex **VI**. Reductive elimination of (*E*)-**126** regenerates the PdL₂ complex **I** of the primary catalytic cycle.

Application of Cs₂CO₃ as an inorganic base and DIPEA as a non-nucleophilic base (entries 2-3) resulted in complex product mixtures. Application of the Pd₂(dba)₃/P(*o*Tol)₃ system with Ag₃PO₄ to access the cationic pathway was not successful and did not show any conversion. Finally, using the system with DIPEA in DMF was successful (entry 5). Unfortunately, the yield of 13% was low and the reaction showed only moderate diastereoselectivity of 3:1 (*E,E*)/(*Z,E*). This effect is likely due to thermal isomerization as the *Z*-configuration is thermodynamically favored as observed previously.

Additionally, the Troc-group demonstrated only limited stability, the hydrodehalogenated product **169** was isolated in 14% yield. The identity of this product was proven by 2D-NMR spectroscopy and isotope distribution analysis by high resolution ESI-MS (Figure 3.4). The calculated intensities for the hydrodehalogenated derivative **169** with two chlorine atoms matched the observed intensities.

These results suggest the unexpected oxidative addition of the CCl₃-group to the Pd complex followed by hydrodehalogenation (Scheme 3.45).

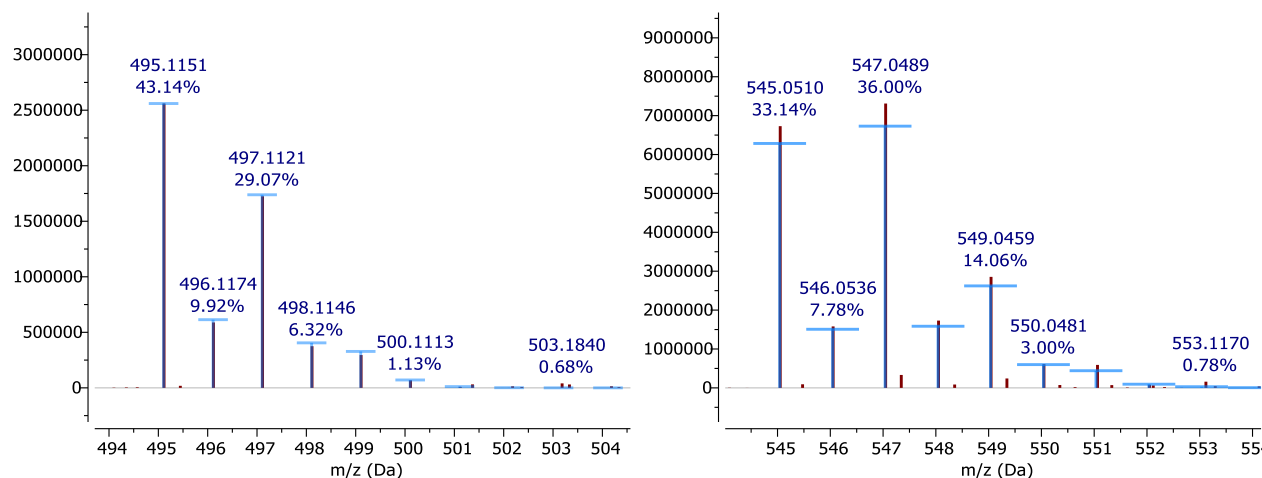


Figure 3.4: Isotope distribution of side product **169** (left) containing two Cl-atoms and the product **169** (right) containing three Cl-atoms. Red: Observed Intensities, Blue: calculated intensities

With these results on hand, it was shown that the lysine side-chain can be successfully introduced by bromination of the dhAA moiety followed by HECK-reaction with allyl carbamates. The yield could be improved by utilization of a different terminal protecting group. A late-stage introduction of the side-chain should allow the replacement of the Troc-group with a Boc-group, when the dhAA is incorporated in the peptide chain, preserving orthogonality of the protective group strategy.

Asymmetric hydrogenation of dhAAs is described in the literature,^[57, 59] and the method was successfully employed on a similar motif in the total synthesis of darobactin by PATEL, PETRONE, and SARLAH *et al.*, which was published in the meantime (for the reported total synthesis see section 1.1.4).^[20]

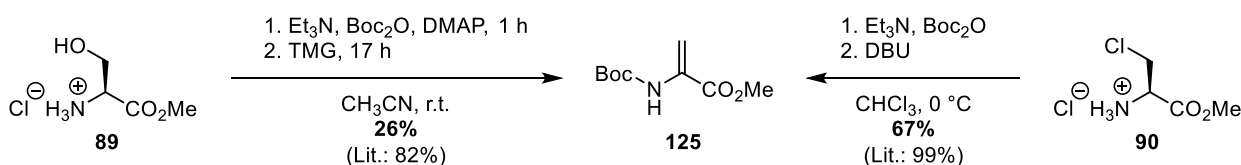
Hence, no further investigations towards the total synthesis of darobactin were conducted.

3.2. Electrosynthesis of Protected Dehydroamino Acids

3.2.1. NaCl-mediated α -Methoxylation of Amino Acid Carbamates

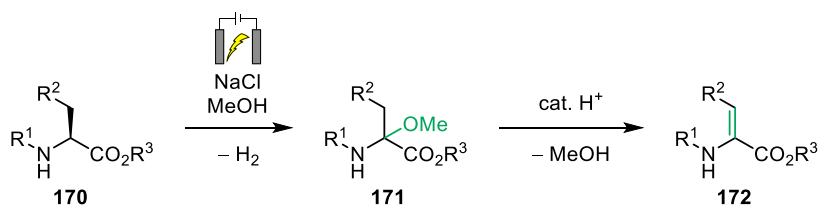
During the darobactin project, several dhAAs, especially alanine and lysine derivatives were synthesized. Whilst the dehydroalanine derivative Boc- Δ Ala-OMe (**125**) is commercially available, despite its simplicity, it is quite expensive with 100-140€/g (Sigma Aldrich, abcr). Therefore, compound **125** was synthesized from H-Ser-OMe HCl (**89**) according to a protocol reported by FERREIRA *et al.* (Scheme 3.46).^[35] However, multiple attempts to reproduce the literature yield of 82% failed with the highest achieved yield of 26%.

Another synthesis reported by TAMURA *et al.* starting from chloroalanine **90** provided the product in acceptable yield of 67%.^[151] However, the preparation protocol of chloroalanine **90** requiring harsh chlorination conditions using PCl₅ in HCl-saturated AcCl as solvent prohibited large-scale preparation of this compound.^[126]



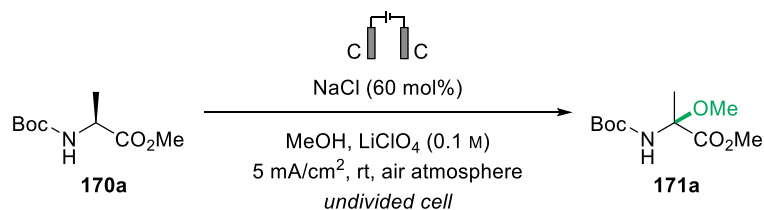
Scheme 3.46: Two synthetic approaches towards Boc- Δ Ala-OMe (**125**) were tested.

These results and the lack of preparation methods for dehydrolysine derivatives, due to the limited stability of GAB-Aldehydes encouraged the development of new synthetic methods towards dhAAs. Inspired by the SHONO oxidation, a powerful C-H-oxidation method for the alkoxylation of various carbamates, an electrochemical α -methoxylation of amino acid carbamates followed by acid-catalyzed elimination of methanol was envisioned (Scheme 3.47).



Scheme 3.47: Aspired protocol for two-step synthesis of dhAAs **54** from their corresponding amino acid carbamates **52**.

Albeit α -methoxylation of electron-deficient and sterically unhindered amino acid methyl carbamates was described by SHONO *et al.*,^[90] a new protocol had to be developed to oxidize sterically demanding carbamates, e.g. *tert*-butyl carbamates. Hence, the investigation was commenced using commercially available Boc-Ala-OMe (**170a**) as a model substrate to establish suitable conditions for electrochemical oxidation (Table 3.12).

Table 3.12: Optimization of the Reaction Conditions.^a

Entry	Deviation from standard conditions	F/mol	Conversion ^b (yield)
1	None	4	Full (99%)
2	No NaCl	4	Trace
3	0.05 M substrate	10	25%
4	0.1 M substrate	4	77%
5	No LiClO ₄	4	Full (83%)
6	No LiClO ₄ , LiCl instead of NaCl	6	Full (89%)
7	No LiClO ₄ , Bu ₄ NCl instead of NaCl	10	55%
8	<i>n</i> Bu ₄ PF ₆ instead of LiClO ₄ , no NaCl	4	Trace
9	Et ₄ NBF ₄ instead of LiClO ₄ , no NaCl	4	Trace
10	Et ₄ NBF ₄ instead of LiClO ₄	4	Trace
11	2,2,2-trifluoroethanol instead of MeOH	4	No conversion
13	Reaction under argon sweep	4	Full (99%)

^aReaction conditions: **170a** (1.0 eq., 0.3 M), NaCl (0.6 eq.), LiClO₄ (0.1 M), 8.2 mm graphite electrodes, $J = 5 \text{ mA/cm}^2$, 4 F/mol, rt, air atmosphere.

^bConversion determined by GC-MS.

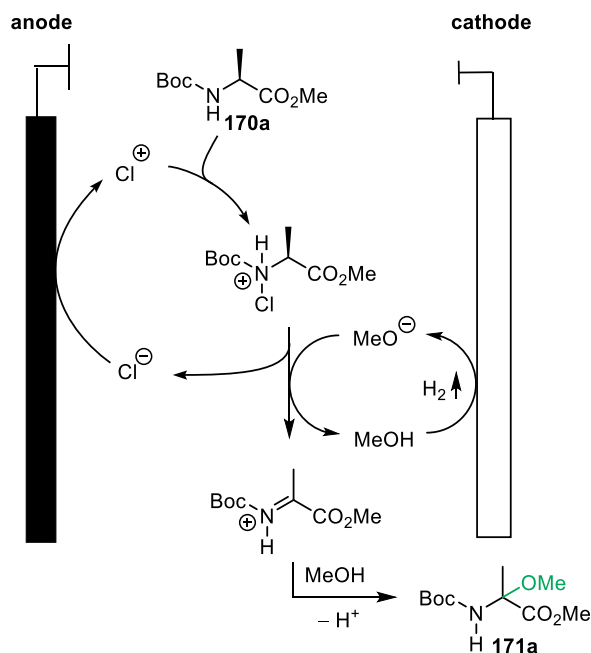
Reaction optimization using 8 mm graphite rods used for welding revealed that the addition of NaCl (60 mol%) as a mediator, LiClO₄ as conducting salt, and a high substrate concentration (0.3 M) in MeOH furnished the desired product in quantitative yield after 4 F/mol, showing a faradaic efficiency of 50% (entry 1).

Testing a variety of conditions showed, that the addition of NaCl was crucial for the reaction to occur (entry 2). Lowering the concentration was detrimental to the faradaic efficiency of the reaction (entries 3-4). This effect is a frequently reported problem in electroorganic chemistry,^[88] due to the required mass transport of the substrate/mediator to the electrode surface.

The use of NaCl as the only conducting salt, without the addition of LiClO₄ was successful, however, the product was obtained in a significantly lower yield of 83% (entry 5). This may be partially explained by the

lithium cations in solution, as the reaction proceeded with LiCl in 89% yield (entry 6) and gave 55% conversion if only Bu₄NCl was used as the catalyst and conducting salt (entry 7). Attempts to replace the LiClO₄ with less problematic conducting salts, e.g. nEt₄NBF₄, failed (entry 10). A replacement of MeOH with 2,2,2-trifluoroethanol in order to install a better leaving group was not successful (entry 11), probably due to the limited solubility of NaCl.

Based on these results and literature precedents,^[90, 152] the reaction is likely to occur *via* N-chlorination, dehydrochlorination, and addition of methanol as the mechanism of action (Scheme 3.48).



Scheme 3.48: Proposed mechanism for the NaCl-mediated SHONO type oxidation of Boc-Ala-OMe (170a).

To evaluate this mechanism, cyclic voltammograms in anhydrous, degassed MeOH were recorded using a glassy carbon working electrode and two platinum wires as reference and counter electrodes (Figure 3.5).

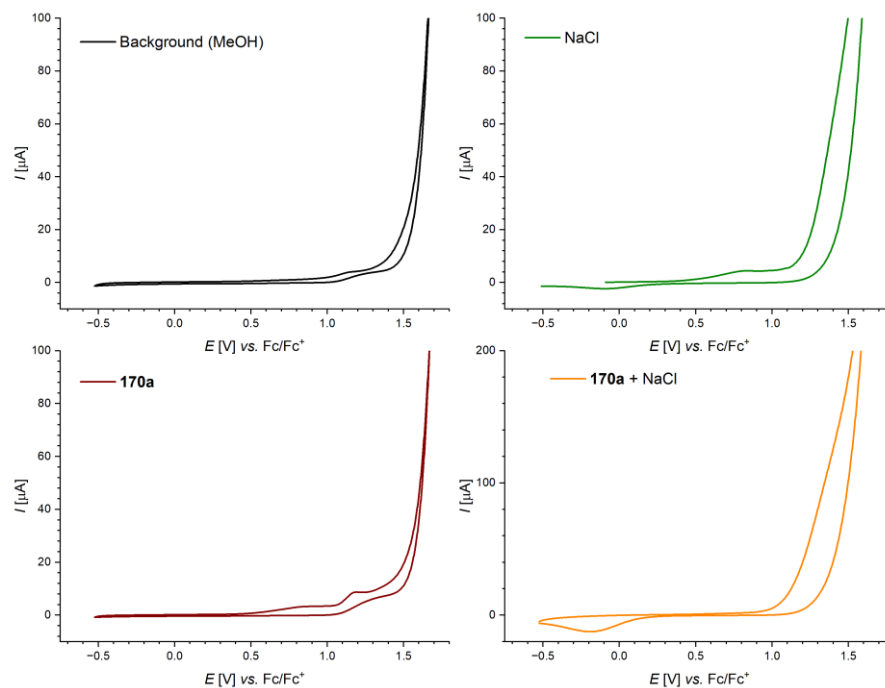
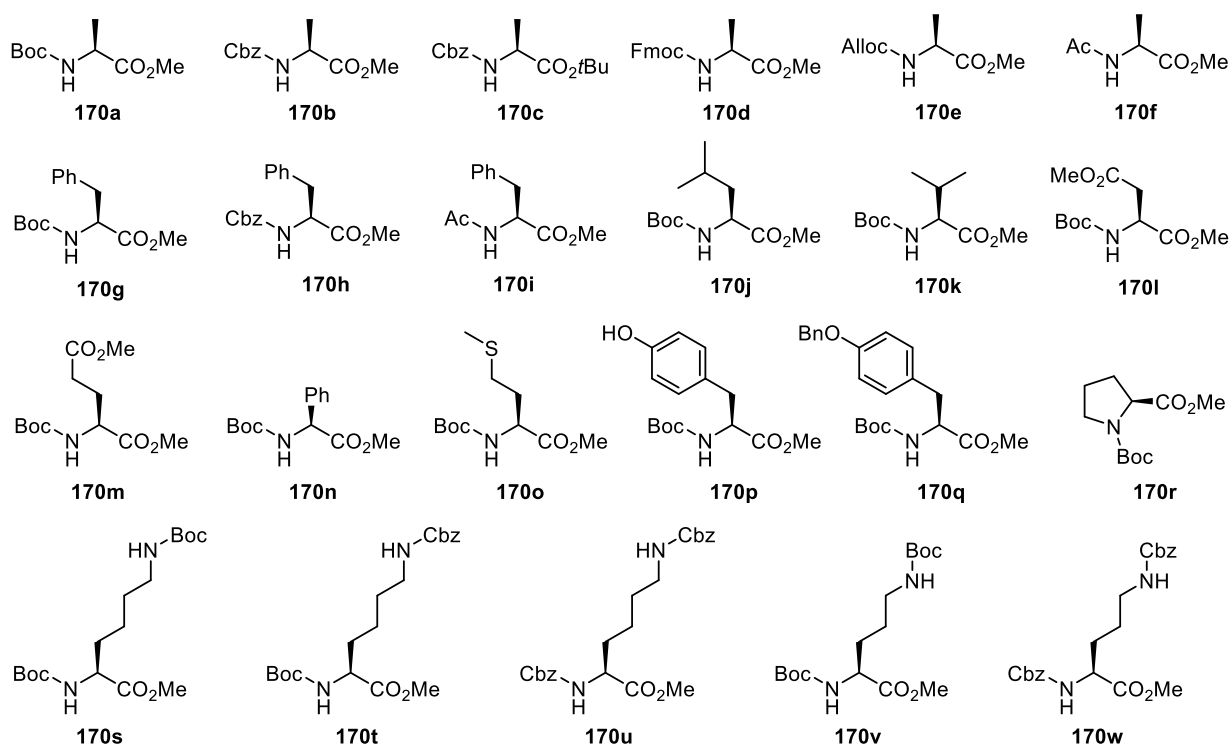


Figure 3.5: Cyclic voltammograms.

Herein, a comparison of the MeOH background scan and scan of the substrate **170a** revealed, that no significant oxidation occurs within the oxidation window of the solvent of up to 1.5 V. In contrast, a scan of NaCl clearly showed some oxidation event starting from 0.7 V and the reaction mixture showed a high current flow starting from 1.0 V.

With the established reaction conditions in hand, a variety of literature known starting materials **170a-1p** were synthesized according to common procedures for amine protections^[153-158] and esterifications^[159-163] of amino acids (Table 3.13).

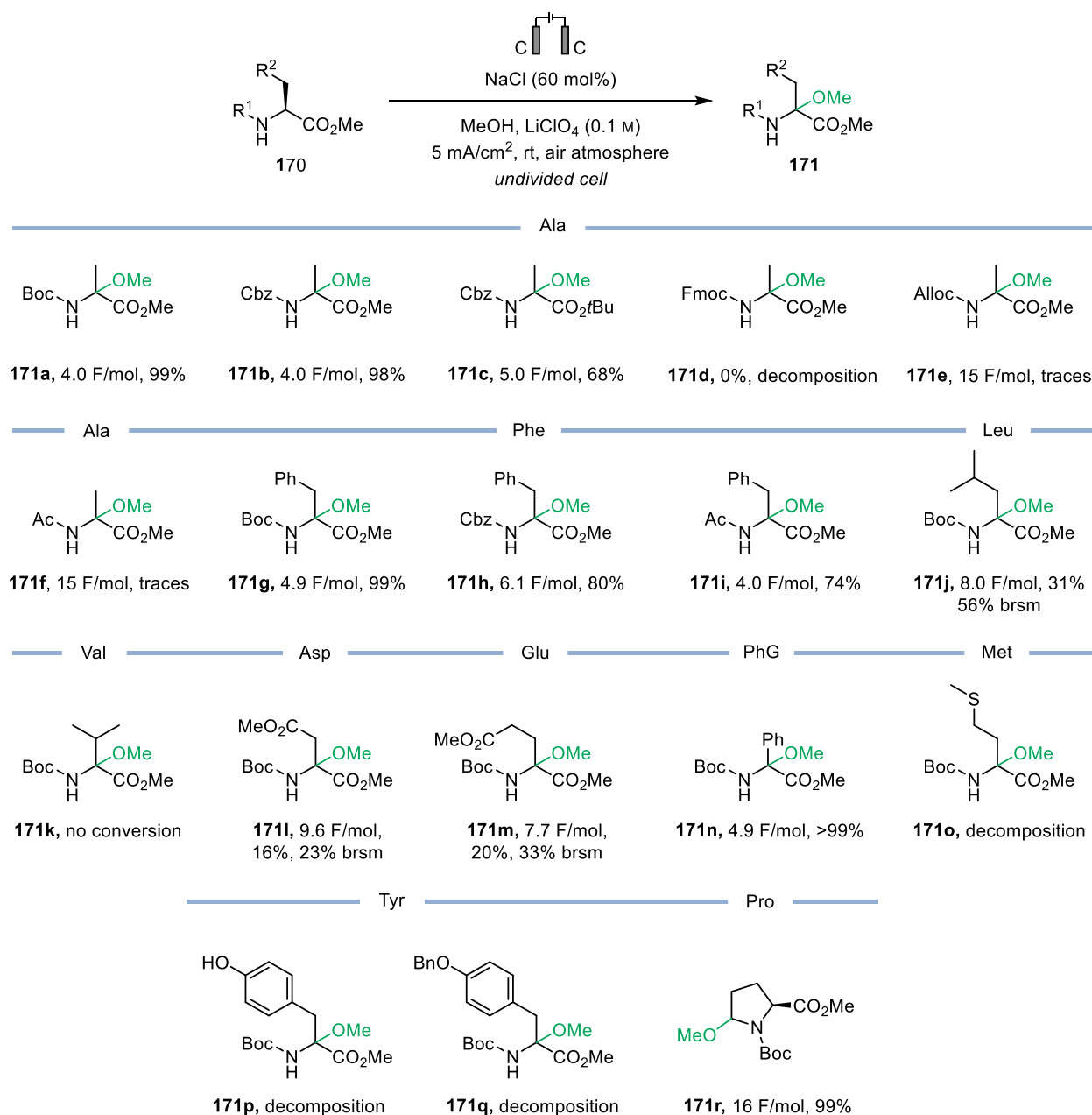
Table 3.13: Starting materials tested.



Exploration of the substrate scope (Table 3.14) demonstrated that *tert*-butyl and benzyl carbamates are well tolerated and gave clean conversions for their corresponding alanine derivatives (**170a-c**).

In contrast, Fmoc-protected **170d** decomposed under the given reaction conditions. Formation of 9-methylidene-9*H*-fluorene was observed by GC-MS of the reaction mixture, suggesting a base-induced deprotection caused by the generated methoxide ions. Sterically demanding *tert*-butyl ester could be converted with a minor decrease in faradaic efficiency and yielded the methoxylated derivative **171c** in 68% yield.

Alloc- and acetyl-protections were not tolerated for alanine, only traces of product were observed in crude NMR, even after 15 F/mol. Surprisingly, acetyl protection was tolerated for the phenylalanine-derivative **170i**. The lack of reactivity of Ac-Ala-OMe (**170f**) could be attributed to its strong tendency for aggregation in solution.^[164]

Table 3.14: Scope and limitations of the NaCl-mediated SHONO-type oxidation.

^aReaction conditions: substrate **170a-r** (4 mmol, 1 equiv), 60 mol% NaCl, MeOH (0.3 M), 0.1 M LiClO₄, 5 mA/cm² constant current, graphite anode and cathode.

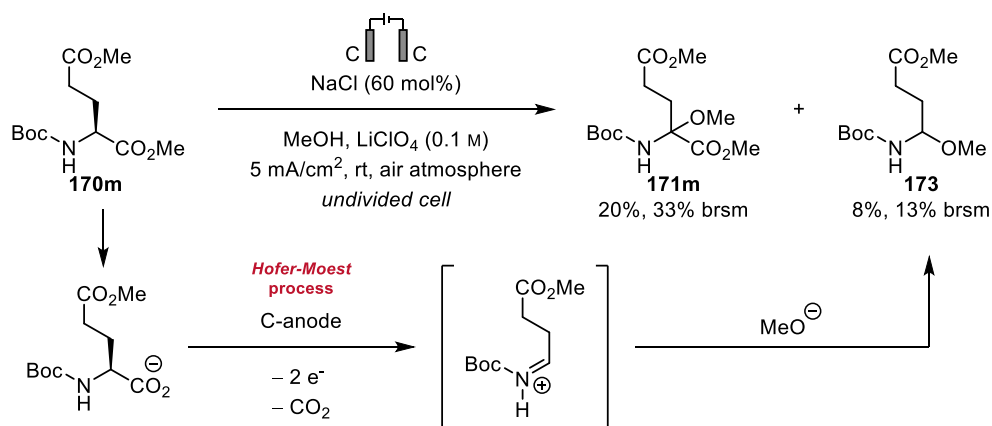
Whereas alanine and phenylalanine derivatives generally showed good faradaic efficiencies, sterically more demanding substrates like leucine (**170j**), asparagine (**170l**) and glutamine (**170m**) derivatives often stopped before full conversion was achieved. This conversion stagnation can be attributed to a variety of factors negatively impacting the mass transport to the electrode surface.

Generally, the larger steric bulk in β -substituted amino acids makes transport through the HELMHOLTZ double layer less likely, especially with diminishing substrate concentration at higher conversions. Additionally, in some cases, product buildup at the electrode surface could decrease the area of the active surface.

A frequent reversal of electrode polarity, e.g., every 15 min using a microcontrolled H-bridge assembly may mitigate this problem but was not investigated during this work.

Notably, electrolysis of Boc-Glu-OMe (**171m**) afforded significant amounts of the HOFER-MOEST-type product **3j** (Scheme 3.49). In a HOFER-MOEST process, carboxylate ions undergo decarboxylative oxidation on the anode forming carbocations, which undergo rapid addition with alcohols, a reaction also known as abnormal KOLBE reaction.^[165-166]

Albeit no carboxylic acids were present in the starting material, due to the vicinity of the second ester, a partial nucleophilic deprotection by the abundant chloride ions assisted by lithium cations could be the source of the carboxylate intermediate.



Scheme 3.49: Observed side product **3j** probably caused by a HOFER-MOEST process as a side reaction.

While phenyl glycine **170n** showed excellent faradaic efficiency and quantitative yield, the β -branched amino acid carbamate Boc-Val-OMe (**170k**) showed no conversion. Methoxylation of methionine **170o** was not successful, instead, signs of the sulfoxide were observed *via* GC-MS, indicating that the thioether function exhibits a lower redox potential than the chloride ions present. Unfortunately, tyrosines **170p** and **170q** were not tolerated, rapid decomposition was observed even for the O-benzylated derivative **170q**. Electrolysis of Boc-Pro-OMe (**170r**) showed selective methoxylation at the less hindered 5-position of the pyrrolidine ring.

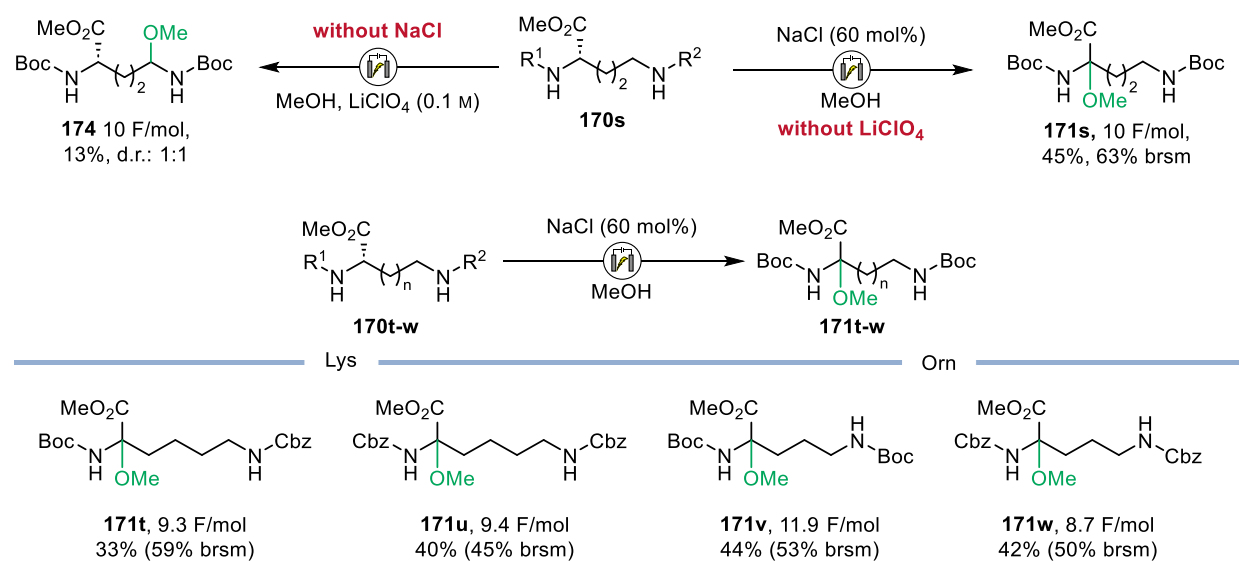
To make the process viable for large-scale preparation of **171a**, the setup was scaled up using six graphite rods instead of two, connected in parallel with alternating polarity to ensure a constant interelectrode-gap of 5 mm (see Experimental Section 5.8.2 for a graphical guide). The reaction proceeded cleanly after 7.6 F/mol in 86% yield (17 g) without further purification, however, a polarity switch after 3 F/mol was necessary to drive the reaction to full conversion, suggesting significant product adsorption at the electrode surface.

For the total synthesis of darobactin A, dehydrolysine derivatives should be accessed, however, as the corresponding 4-aminobutyraldehydes are very unstable, synthesis *via* HORNER-WADSWORTH-EMMONS-olefination was not suitable. Albeit the synthesis of Boc- Δ Lys(Troc)-OMe (**72**) *via* the alkylation/nitrite elimination method by KINOSHITA *et al.* was successful (Scheme 3.26), the required nitro compound had to

be synthesized in three steps from the rather expensive starting material 4-aminobutanol (**111**, Scheme 3.25).

Hence, developing a direct access to dehydrolysines from their saturated counterparts was coveted. Application of the optimized protocol to Boc-Lys(Boc)-OMe (**170s**) gave an inseparable mixture of α -, ϵ - and dimethoxylated products. To increase the regioselectivity, studies without the LiClO₄ were conducted and afforded the α -methoxylated derivative **171s** regioselectively in 45% yield (63% brsm). In contrast, running the reaction without NaCl resulted in regioselective ϵ -methoxylation, albeit in a low yield of 13% (Table 3.15).

Table 3.15: Regioselectivity of the anodic oxidation of lysine and ornithine derivatives.

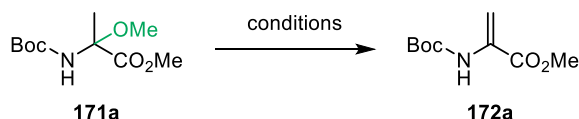


Encouraged by these results, orthogonally protected Boc-Lys(Cbz)-OMe (**170u**) was subjected to electrolysis and gave the desired product with a slightly decreased yield of 33% (59% brsm) due to incomplete conversion. The substrate scope could be extended to ornithines **170v-w**, as well as bis(benzylcarbamate) protected derivatives in similar yields. The shorter side chain of ornithines showed little influence on the reaction in terms of faradaic efficiency, yield, and regioselectivity.

3.2.2. Synthesis of Dehydroamino Acids via Brønsted-acid Catalyzed Elimination of Methanol

Whilst for less sensitive enecarbamates, elimination can be achieved using NH_4Cl at high temperatures (100–160 °C) under solvent-free conditions,^[9] this procedure was not viable for the synthesis of dhAAs due to their high susceptibility to polymerize.^[167-168] Therefore, different BRØNSTED and LEWIS acids as well as bases were tested to eliminate methanol from **171a** in THF-sol. (Table 3.16).

Table 3.16: Screening of various BRØNSTED and LEWIS acids as well as bases for the elimination of MeOH from **171a**.



Entry	Reagent	Conditions	Result
1	AcOH	THF, 50 °C, 19 h	no conversion
2	NH_4Cl	THF, reflux, 19 h	no conversion
3	Amberlyst® 15	THF, 50 °C, 4 h	polymerization
4	Amberlyst® 15	THF, r.t., 4 h	polymerization
5	HCl	3:1 THF / 1 M HCl, 3 h	deprotection
6	PPTS	THF, reflux, 4 h	96% yield
7	$\text{BF}_3 \cdot \text{OEt}_2$	THF, r.t., 2 h	polymerization
8	$\text{Ti}(\text{O}i\text{Pr})_4$	THF, r.t., 19 h	no conversion
9	SnCl_2	THF, r.t., 19 h	no conversion
10	AlMe_3	THF, r.t., 1 h	decomposition
11	DBU	THF, 50 °C, 19 h	partial conversion
12	KOtBu	THF, r.t., 19 h	partial conversion

The preliminary tests showed that neither AcOH, nor NH_4Cl were acidic enough to achieve any conversion upon reflux in THF (entries 1 and 2).

In contrast, the cation-exchange resin Amberlyst® 15 led to rapid polymerization at room or elevated temperatures (entries 4 and 5). Treatment of **171a** with dilute HCl cleaved the acid labile Boc-group (entry 5). For LEWIS acids, $\text{BF}_3 \cdot \text{OEt}_2$ and AlMe_3 presented to be too strong, leading to polymerization and decomposition (entries 7 and 10), whereas $\text{Ti}(\text{O}i\text{Pr})_4$ and SnCl_4 were not too weak to achieve elimination. Bases like DBU and KOtBu showed partial conversion, however, full conversion could not be achieved even with a 3-fold excess of base (entries 11 and 12).

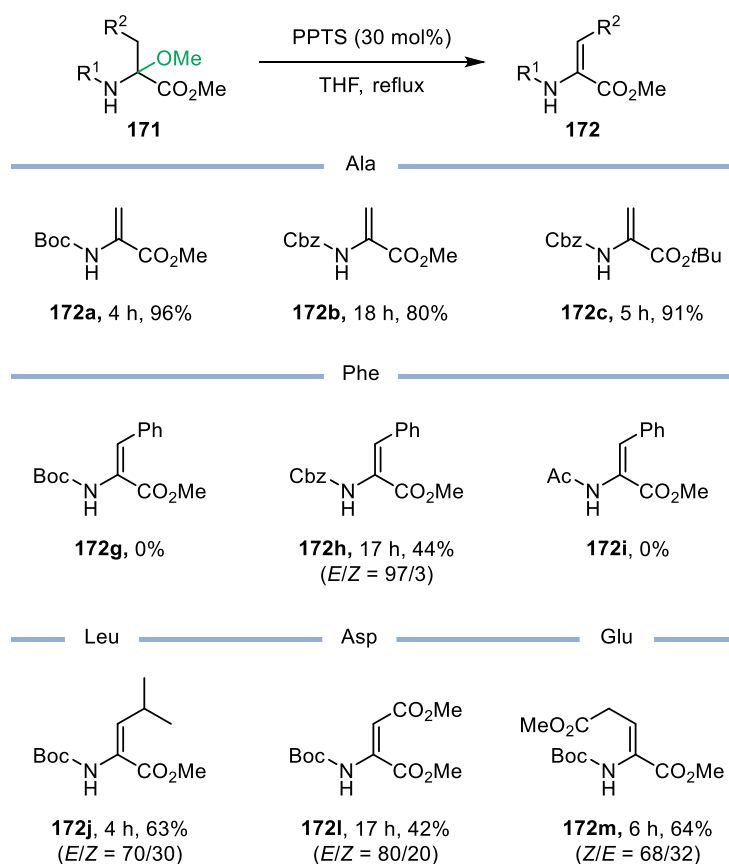
Finally, pyridinium *para*-toluenesulfonate was discovered as the sweet spot between the elimination of the methoxy-group and deprotection/polymerization of the acid-labile *tert*-butylcarbamate (entry 6). The product was afforded in 96% yield without the need for chromatographic purification.

Application of the optimized conditions using 30 mol% PPTS in refluxing THF afforded spectroscopically pure dehydroalanine derivatives **172a-c** in excellent yield after aqueous workup. Elimination of **172a** could be achieved on a 70 mmol scale in virtually quantitative yield. The PPTS catalyst could be recovered by simple filtration of the reaction mixture upon cooling, making the process highly economical for large-scale preparation.

It is important to note, that while this procedure gave pure dehydroalanines, the neat products (typically oils) are very prone to polymerization if handled at room temperature for a prolonged period of time, hence extensive drying at the rotary evaporator or the high vacuum line have to be performed with great care. Generally, the product stability could be increased by addition of 100 ppm 4-methoxyphenol as a stabilizer, continuous storage at -20 °C under argon, or handling in solution. For β -substituted dhAA derivatives these issues were not observed.

The protocol was applied to the α -methoxylated products **2e-j** (Table 3.17). All stereoisomers could be separated by column chromatography and configurations were determined by gradient-enhanced ^1H -NOESY experiments (see Appendix).

Table 3.17: PPTS-catalyzed elimination reaction towards dhAA derivatives.

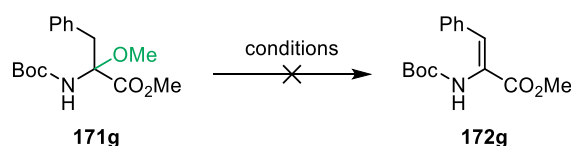


Whereas conjugated products, e.g., Cbz- Δ Phe-OMe and Boc- Δ Asp-OMe (**172l**) were formed with high to excellent (*E*)-selectivity, non-conjugated Boc- Δ Glu-OMe (**172m**) was formed in moderate (*Z*)-selectivity.

Elimination of **2h** favored the formation of (*E*)-Boc- Δ Leu-OMe (**172j**), probably due to steric repulsion of the bulky residue and the *tert*-butyl carbamate. In case of Boc- Δ Phe-OMe (**172g**) no product was isolated, due to rapid polymerization, probably caused by deprotection of the conjugated enamine.

Similarly, for Ac- Δ Phe-OMe (**172i**), rapid polymerization was observed. Attempts to eliminate **171g** using other reagents, failed (Table 3.18).

Table 3.18: Attempted elimination towards **172g**.

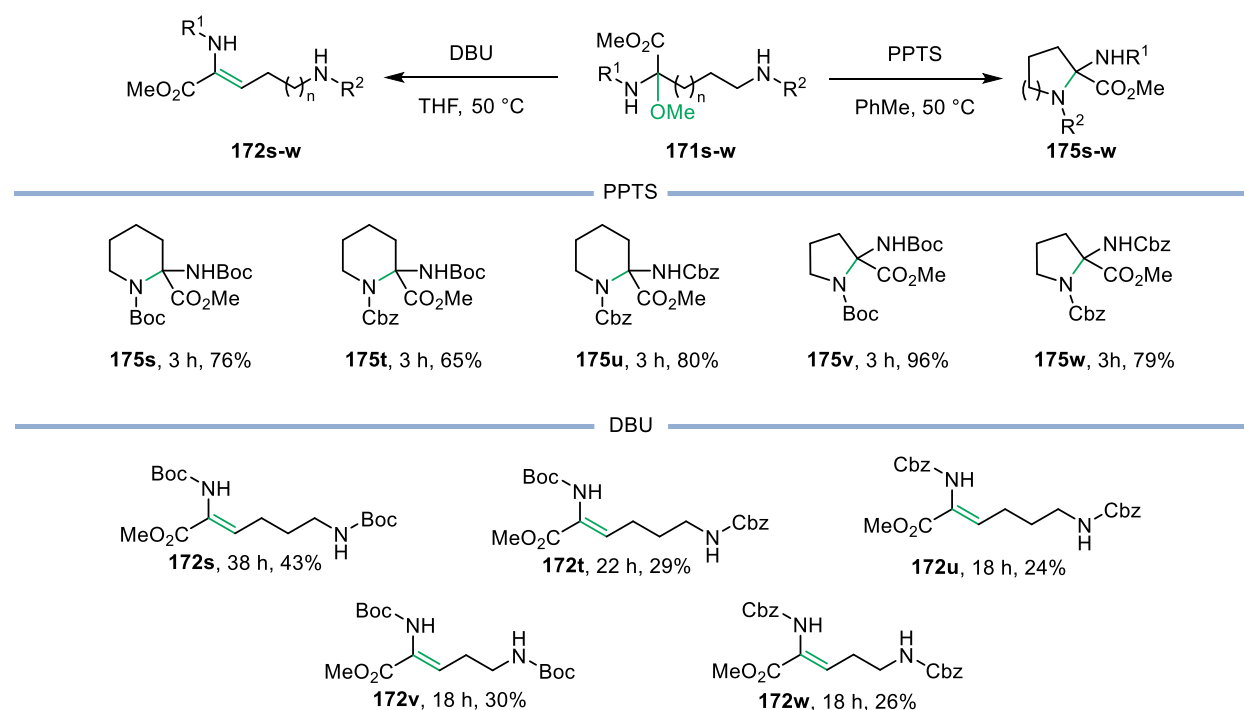


Entry	Reagent	Conditions	Result
1	PPTS	THF, 50 °C, 2 h	Polymerization
2	PPTS	THF, r.t., 2 h	Polymerization
3	HNEt ₃ Cl	THF, r.t., 2 h	Polymerization
4	AcOH	THF, 50 °C, 2 h	No conversion
5	4 Å MS	THF, 50 °C, 2 h	No conversion
6	LiClO ₄	Et ₂ O, r.t., 2 h	No conversion
7	ZnCl ₂	CH ₂ Cl ₂ , r.t., 2 h	No conversion
8	BF ₃ -OEt ₂	CH ₂ Cl ₂ , r.t., 2 h	Polymerization
9	DBU	CH ₂ Cl ₂ , r.t., 2 h	56% conversion

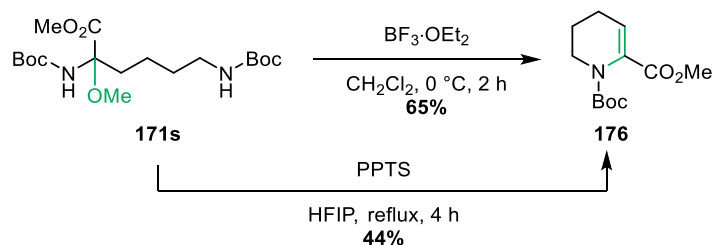
Even very mild acidic conditions, e.g., PPTS at room temperature or HNEt₃Cl resulted in rapid polymerization (entries 2-3). Attempted base-mediated elimination using DBU resulted in 56% conversion after 2 h determined by GC-MS (entry 9), however, the amount of product diminished after prolonged reaction time, demonstrating the lability of the substrate.

Surprisingly, application of the protocol to the lysine and ornithine derivatives **2l-2p** revealed a different reactivity (Table 3.19).

Instead of the formation of their respective dhAA derivatives, cyclization of the side chain afforded new 2-aminoproline and 2-aminopiperic acid scaffolds **5l-5p** in excellent yields. Albeit these may pose valuable products for medicinal chemistry, solvent effects to favor elimination over intramolecular cyclization were investigated on lysine derivative **2l**. However, no formation of **4l** could be observed in toluene, methanol, or HFIP.

Table 3.19: Diversification of α -methoxylated ornithine and lysine derivatives.

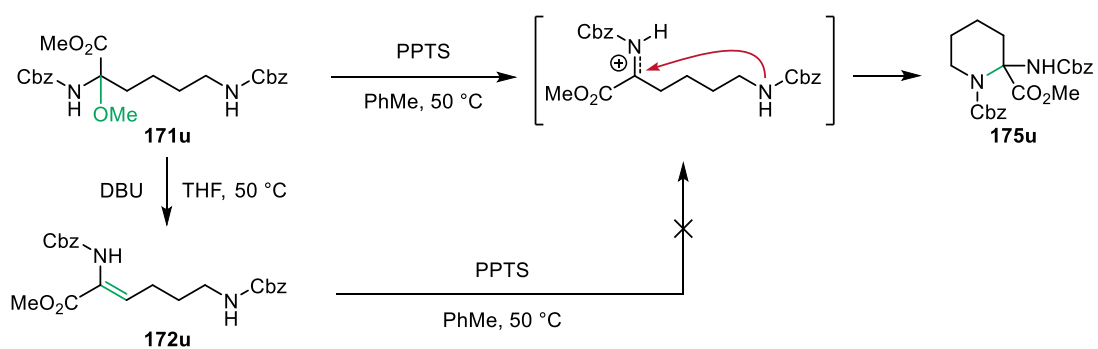
While in toluene, cyclized product **175s** was obtained in 76% (cf. 65% in THF), protic solvents like MeOH or HFIP showed no formation of **172s** or **175s**. Instead, subsequent elimination of the α -carbamate function gave rise to dehydropipecolic acid **176** in 44% yield using HFIP (Scheme 3.50). The same product was obtained in 65% yield upon treatment with $\text{BF}_3\text{-OEt}_2$.

**Scheme 3.50:** Synthesis of 2-dehydropipecolic acid **176**.

As acidic conditions did not yield the desired dehydrolysines and dehydroornithines **172s-w**, the base-induced elimination using DBU was revisited. The reaction at 50 °C in THF yielded the desired dehydrolysines and dehydroornithines **172s-w** in moderate yields of 24-43% (Table 3.19).

Elimination afforded the (*Z*)-isomers selectively, the (*E*)-isomers were not observed. The moderate yields can be attributed to transesterification of the α -carbamate function with the released methanol, the corresponding methyl analogs were isolated in yields of 13-32%.

To investigate the mechanism of the cyclization reaction, Cbz- Δ Lys(Cbz)-OMe (**172u**) was subjected to the acidic protocol (Scheme 3.51).



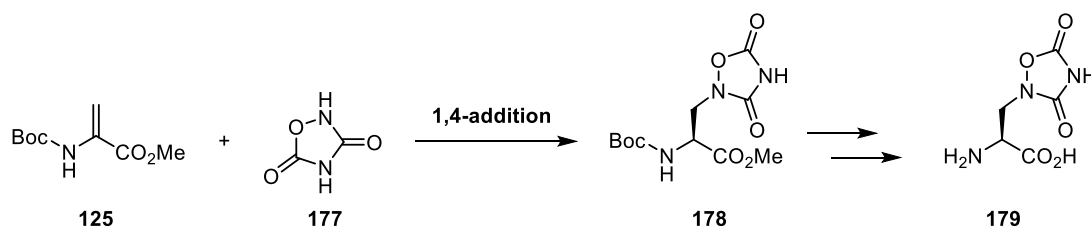
Scheme 3.51: Mechanistic investigation of the formation of cyclized product **175u**. The formation was not observed when **172u** was treated with the PPTS protocol.

Formation to **175u** was not observed, indicating that **172u** is not the precursor of the cyclized product, and cyclization is probably caused by intramolecular addition to a carbocation/iminium intermediate.

3.3. Synthesis of Quisqualic Acid

3.3.1. Biological Activity of L-Quisqualic Acid

With an economic protocol for the gram-scale synthesis of dehydroalanines in hand, new approaches toward the synthesis of unusual amino acids utilizing the unique reactivities of dhAAs were investigated. In this project, L-quisqualic acid (**179**) was identified as a valuable target, as it should be readily accessible by 1,4-addition of 1,2,4-oxadiazolidine-3,5-dione (**177**) (Scheme 3.52). Activation of the dhAA **125/172a** using chiral reagents could afford the unusual amino acid enantioselectively. Alternatively, the product could be resolved by enzymatic resolution or diastereomeric recrystallization using chiral acids, e.g. mandelic acid or chiral amines, upon deprotection.

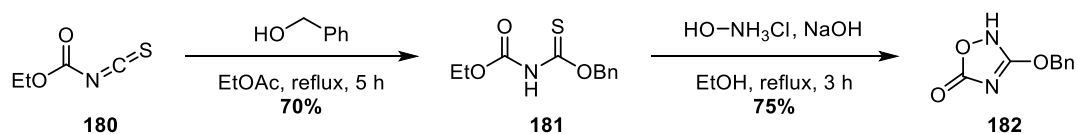


Scheme 3.52: Aspired 1,4-addition of 1,2,4-oxadiazolidine-3,5-dione (**177**) to Boc-ΔAla-OMe (**125**).

L-Quisqualic acid (**179**) was first isolated from the seeds of *Quisqualis indica* in 1976,^[169] a ligneous vine used in traditional Chinese medicine.^[170] The amino acid is one of the most potent AMPA receptor agonists reported, a substrate class known as ampakines. The AMPA receptor is an ionotropic transmembrane receptor with glutamate as its natural substrate.^[171] Binding of ampakines results in fast excitatory synaptic transmission in the central nervous system, while glutamate opens the ion channel for a short period (1 ms),^[172] L-quisqualic acid opens the channel for 8.5 ms while exhibiting an EC_{50} value of 16.3 μ M (cf. Glutamate: 296 μ M).^[173-174] This makes L-quisqualic acid a highly potent excitotoxin and it is routinely used for the selective destruction of neurons in the brain or spinal cord.^[174-176]

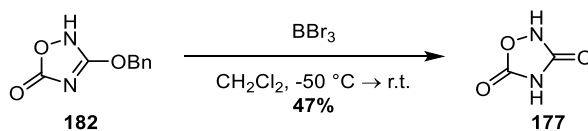
3.3.2. Synthesis of 1,2,4-Oxadiazolidione (**177**)

The nucleophile for the envisioned 1,4-addition, 1,2,4-oxadiazolidine-3,5-dione (**177**), was synthesized in three steps, starting from ethoxycarbonyl isothiocyanate (**180**) (Scheme 3.53).^[177] Nucleophilic addition of benzylalcohol gave thionourethane **181** in 70% yield after recrystallization from Et₂O. Condensation of hydroxylamine hydrochloride resulted in cyclization to afford oxadiazolidine **182** in 75% yield after purification by simple acid-base extraction of the vinylogous acid.



Scheme 3.53: Synthesis of oxadiazolidine **182**.

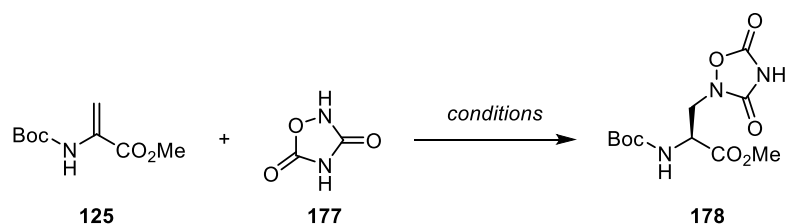
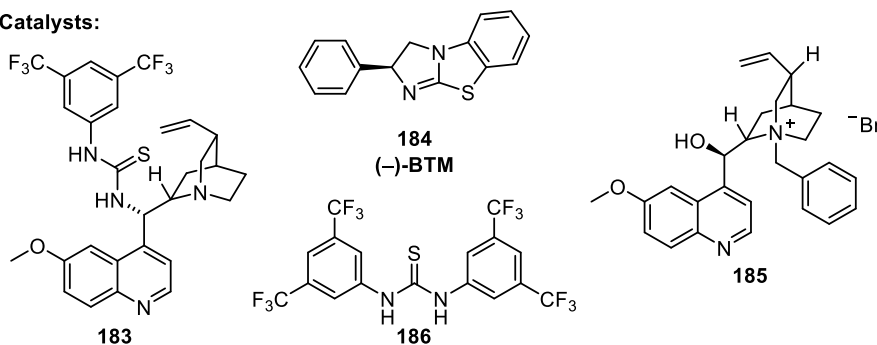
Finally, debenylation using BBr_3 at low temperatures gave 1,2,4-oxadiazolidine-3,5-dione (**177**). The moderate yield of 47% can be attributed to losses during recrystallization on a 200 mg-scale.



Scheme 3.54: Debenzylation of oxadiazolidine **182**.

3.3.3. Conjugate Addition of 1,2,4-Oxadiazolidione (**177**) to Boc- Δ Ala-OMe (**125**)

With the nucleophilic substrate **177** in hand, its conjugate addition to Boc- Δ Ala-OMe (**125**) was attempted (Table 3.20). First, a variety of bases was investigated (entries 1-3), however, no conversion of the starting materials was observed. In order to run the reaction with asymmetric induction, the bifunctional catalyst **183** was investigated (entries 4-6), as it allows simultaneous activation of the dhAA and nucleophile by hydrogen bonding and deprotonation/LEWIS base catalysis, respectively. This method poses a common strategy to realize enantioselective conjugate additions.^[178-182] Unfortunately, no conversion was observed for the given substrates, therefore chiral nucleophiles (entry 7), phase-transfer- (entry 8) and thiourea-catalysts (entry 9) were tested, without success. Finally, multiple LEWIS-acids (entries 10-13) were tested, but again, no conversion was observed.

Table 3.20: Attempted 1,4-addition of oxadiazolidine **177** to Boc- Δ Ala-OMe (**125**) using various reagents, catalysts and activation modes.**Catalysts:**

Entry	Catalyst	Loading	Solvent	T	t	Conversion
1	Et ₃ N	1.0 eq.	PhMe	r.t.	5 d	-
2	Et ₃ N	1.3 eq.	CH ₃ CN	r.t. → 80 °C	1 d	-
3	K ₂ CO ₃	2.3 eq.	CH ₃ CN	50 °C → 90 °C	2 d	-
4	183	20 mol%	Et ₂ O	r.t.	3 d	-
5	183	20 mol%	CH ₃ CN	r.t.	1 d	-
6	183	20 mol%	PhMe	r.t.	1 d	-
7	(-)-BTM (184)	20 mol%	Et ₂ O	r.t.	3 d	-
8	PTC 185	5 mol%	Wasser/Toluol	r.t.	1 d	-
9	Schreiner Cat. (186)	20 mol%	Et ₂ O	r.t.	3 d	-
10	ZnBr ₂	20 mol%	CH ₃ CN	r.t.	1 d	-
11	InCl ₃	20 mol%	CH ₃ CN	r.t.	1 d	-
12	Yb(OTf) ₃ ·H ₂ O	20 mol%	CH ₃ CN	r.t.	1 d	-
13	Sc(OTf) ₃	20 mol%	CH ₃ CN	r.t.	1 d	-
14	I ₂	10 mol%	CH ₃ CN	r.t.	1 d	-

These results indicate only a weak nucleophilicity of the oxadiazolidine **177**, probably due to the abundance of electron-withdrawing groups in the heterocycle, particularly the neighboring carbonyl group.

3.4. Synthesis of Highly Substituted 2-Pyrazoline Amino Acids

3.4.1. Optimization of the [2+3]-Cycloaddition of dhAAs and Diazo Compounds

The 2-pyrazoline scaffold is an omnipresent motif in pharmaceutically active ingredients and poses a highly valuable substrate class (cf. chapter 1.4).

The newly developed electrosynthesis of dhAAs (cf. chapter 3.1.8) offers simple, scalable access to various dhAAs which could be transformed into a new class of 2-pyrazoline amino acids by 1,3-dipolar cycloaddition with diazo compounds. To polarize the double bond, a nucleophilic activation of the double bond was envisioned to drive the reaction to favor the formation of 2-pyrazolines instead of cyclopropanes.

First test experiments using DABCO as a nucleophilic catalyst, Boc- Δ Ala-OMe as the test substrate, and ethyl diazoacetate (EDA) delivered promising results with the formation of 2-pyrazoline derivative **188** alongside formation of cyclopropane (**Scheme 3.55**).



Scheme 3.55: First 1,3-cycloaddition of EDA (**187**) and Boc- Δ Ala-OMe (**125**).

Albeit the reaction only showed 36% conversion, the dehydroalanine reacted cleanly to the two products, no other by-products were observed. 2-Pyrazoline **188** and cyclopropanes **189** were obtained in 14% and 17% yield, respectively. Separation of the two diastereomeric cyclopropanes, formed in a 1:2 ratio, was not possible by flash chromatography, due to virtually identical R_f values. The identity of pyrazoline **188** could be proven by X-ray crystallography (Figure 3.6).

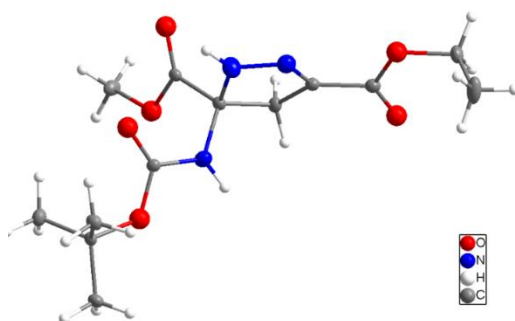


Figure 3.6: Crystal structure of pyrazoline **188**.

Based on this promising result, an extensive optimization campaign was conducted to suppress the cyclopropane formation and achieve higher conversion. Screening experiments were conducted in closed vials on a 0.2 mmol scale and yields were determined by quantitative NMR using ethylene carbonate as an

internal standard. The optimization commenced with the investigation of various nucleophilic catalysts and loadings (Table 3.21).

Table 3.21: Reaction optimization using different catalysts and catalyst loadings.

Catalysts:

Entry	Catalyst	Loading	Conv.	Pyrazoline 188		Cyclopropane 189	
				Yield ^a (brsm)	Isolated Yield	Yield ^a (brsm)	<i>cis</i> : <i>trans</i>
1	-	-	49%	0%	-	38% (78%)	38:62
2	ABCO	20 mol%	47%	29% (62%)	-	20% (43%)	57:43
3	184	20 mol%	53%	14% (26%)	9%, 8% <i>ee</i>	43% (61%)	26:74
4	190	20 mol%	71%	15% (21%)	18%, 9% <i>ee</i>	n.d.	n.d.
5 ^b	183	20 mol%	72%	22% (31%)	17%, 6% <i>ee</i>	17% (24%)	51:49
6 ^b	185	20 mol%	85%	25% (29%)	19%, 1% <i>ee</i>	31% (37%)	30:70
7	DABCO	10 mol%	54%	20% (37%)	-	9% (17%)	57:43
8	DABCO	20 mol%	50%	26% (52%)	-	12% (24%)	59:41
9	DABCO	40 mol%	45%	29% (64%)	-	18% (40%)	54:46
10	DABCO	100 mol%	52%	25% (48%)	-	12% (23%)	48:52

Reaction conditions: 0.2 mmol scale, 1.1 eq. EDA, 50 °C, 70 h, closed vial

^a determined by quantitative NMR with ethylene carbonate as internal standard, ^b 96 h

The control experiment (entry 1) in the absence of catalysts showed significant formation of the cyclopropane product **184** after 70 h at 50 °C and can be likely attributed to the thermal decomposition of EDA under the formation of the carbene, resulting in cyclopropanation of the starting material. The formation of pyrazoline **188** was not observed.

Albeit the two diastereomers of cyclopropane **189** were chromatographically inseparable, the signals could be distinguished by NMR-spectroscopy and assigned by suitable ^1H -GOESY experiments (Figure 3.7).

A strong NOE-effect of 6.1% was observed for the NH after irradiation of the methine-proton of the *trans*-isomer. This NOE-effect was absent in the *cis*-isomer. Notably, a strong shift of the NH-proton was observed due to the hydrogen-bonding of the amine proton to the ethyl ester function (*cis*: 5.15 ppm, *trans*: 2.10 ppm).

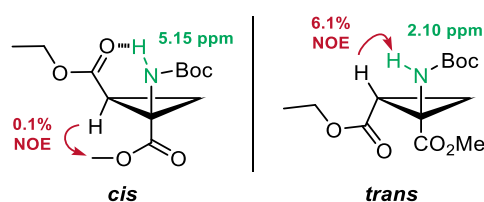
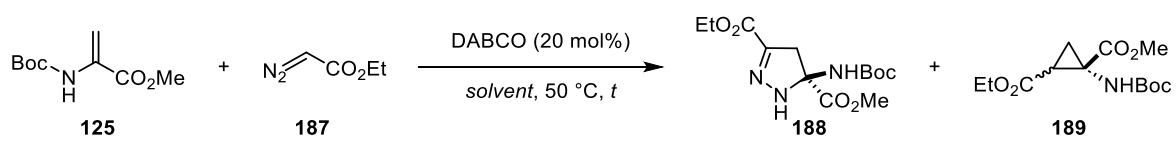


Figure 3.7: Structural assignment of the cyclopropane diastereomers.

The use of quinuclidine (ABCO) rendered the reaction less product selectivity compared to DABCO (cf. entries 3 and 8). Asymmetric catalysts (entries 3-8) were tested but gave only marginal enantiomeric excess of up to 9% *ee*. Screening of the DABCO loading (entries 7-10) revealed a catalyst loading of 20-40 mol% as the sweet spot, however, the conversion, yield, and chemoselectivity did not alter significantly between the catalyst loadings of 10-100 mol%.

Next, a screening of various solvents was conducted (Table 3.22). The results showed a clear trend in chemoselectivity. While apolar aprotic solvents, e.g. toluene (entry 2), favored the formation of the cyclopropanes, the product selectivity increased with rising polarity of the solvent, peaking with the use of polar, aprotic solvents like DMSO, DMPU, and DMF (entries 7-9). No formation of cyclopropanes was observed, hence the yield based on recovered starting material was almost quantitative.

Albeit the use of alcoholic solvents (entries 4-6), e.g. MeOH, EtOH, HFIP, favored the formation of pyrazolines over cyclopropanes, transesterification, and decomposition byproducts were observed, decreasing the overall yield. The diastereoselectivity of the cyclopropane formation was unaffected by solvent effects, except for CH_3CN (entry 10) favoring the *cis*-isomer in a 7:3 ratio.

Table 3.22: Reaction optimization using different solvents.


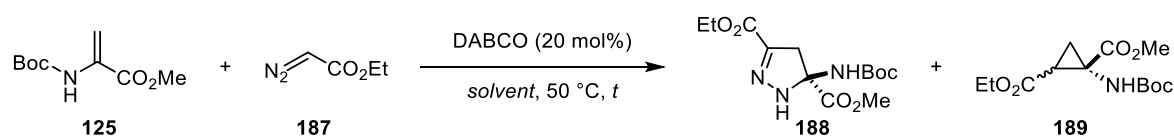
Entry	Solvent	ET_{30}	t	Conv.	Yield ^a		<i>cis</i> : <i>trans</i>
					Pyrazoline 188 (brsm)	Cyclopropane 189 (brsm)	
1	CHCl ₃	39.1	70 h	50%	26% (52%)	12% (24%)	59:41
2	PhMe	33.9	70 h	72%	25% (35%)	44% (62%)	48:52
3	THF	37.5	70 h	61%	41% (67%)	12% (20%)	50:50
4	EtOH	51.8	70 h	78%	61% (78%)	7% (9%)	46:54
5	MeOH	55.4	40 h	81%	50% (62%)	3% (4%)	50:50
6	HFIP	65.3	40 h	71%	11% (15%)	n.d.	n.d.
7	DMSO	45.1	40 h	55%	49% (89%)	0%	-
8	DMPU	36.1	40 h	63%	65% (103%)	0%	-
9	DMF	43.2	40 h	61%	60% (98%)	0%	-
10	CH ₃ CN	45.6	40 h	74%	45% (61%)	5% (7%)	69:31

Reaction conditions: 0.2 mmol scale, 1.1 eq. EDA, DABCO (20 mol%), 50 °C, closed vial

^a determined by quantitative NMR with ethylene carbonate as internal standard

The optimization was continued by screening the concentration for the two most promising solvents, CH₃CN and DMF compared to CHCl₃ (Table 3.23). The reaction rate drastically increased at higher concentrations (entries 3, 6, and 9).

Finally, running the reaction at 50 °C in DMF with 0.5 mol/L completed the reaction in 67 h (entry 10) and gave the desired product in 88% NMR yield and 49% isolated yield after column chromatography. The formation of cyclopropanes **189** in 7% yield over this prolonged reaction time indicated the thermal decomposition of pyrazoline **188** under the release of nitrogen.

Table 3.23: Reaction optimization using different solvents and concentrations.

Entry	Solvent	<i>c</i>	<i>t</i>	Conv.	Pyrazoline 188	Cyclopropane 189	<i>cis</i> : <i>trans</i>
					Yield ^a (brsm)	Yield ^a (brsm)	
1	CHCl ₃	0.1 M	70	19%	20% (105%)	18% (96%)	54:46
2	CHCl ₃	0.2 M	70	50%	26% (52%)	12% (24%)	57:43
3	CHCl ₃	0.5 M	70	70%	38% (54%)	24% (35%)	
4	CH ₃ CN	0.2 M	70	74%	45% (61%)	5% (7%)	69:31
5	CH ₃ CN	0.2 M	40	57%	42% (70%)	4% (7%)	60:40
6	CH ₃ CN	0.5 M	40	80%	70% (88%)	7% (9%)	53:47
7	DMF	0.2 M	40	61%	60% (98%)	0%	-
8	DMF	0.2 M	18	33%	33% (100%)	0%	-
9	DMF	0.5 M	18	56%	53% (95%)	0%	-
10	DMF	0.5 M	67	100%	88%	7%	59:41

Reaction conditions: 0.2 mmol scale, 1.1 eq. EDA, DABCO (20 mol%), 50 °C, closed vial

^a determined by quantitative NMR with ethylene carbonate as internal standard

3.4.2. Thermal Analysis of 2-Pyrazoline **188**

This hypothesis of thermal nitrogen-loss was tested by thermal characterization of the product using simultaneous thermogravimetric and differential-scanning-caloric analysis (TG-DSC).

Within this measurement, a sample of 2-pyrazoline **188** was heated gradually in a crucible from 25 °C to 200 °C for approximately 2 h, while measuring the heat flux compared to a reference crucible. During the experiment, the mass was constantly recorded (Figure 3.8).

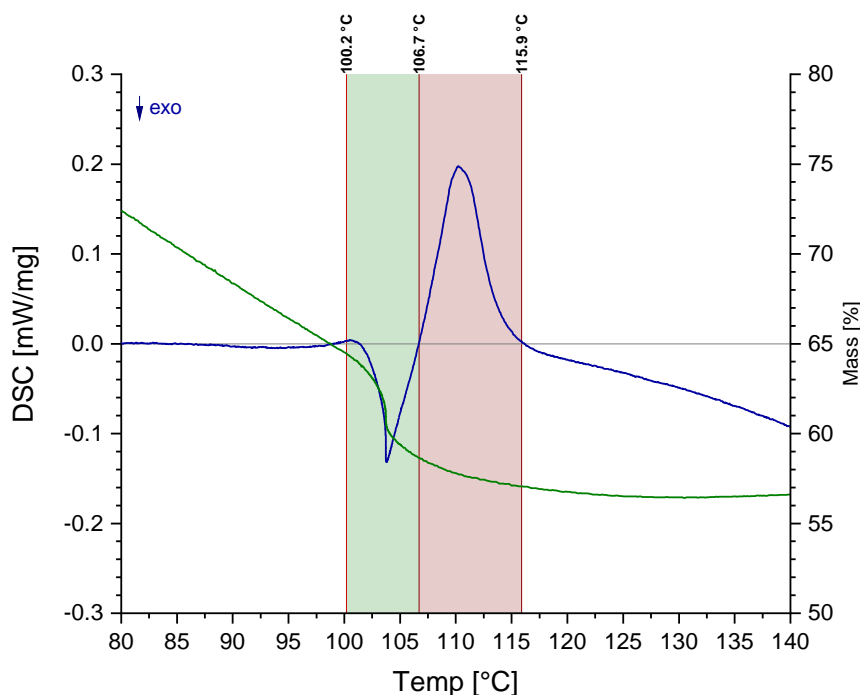


Figure 3.8: TG-DSC analysis of pyrazoline **188**. Green curve: mass loss; blue curve: heat flux relative to reference crucible; green area: exothermic nitrogen loss; red area: melting of the sample.

The sample showed a mass loss of 7% between 100 and 106 °C, correlating with an exothermic event with an enthalpy of $\Delta H = -11.4$ kJ/mol. The observed mass loss is in good agreement with the calculated mass loss of 8.9% for the formation of cyclopropane **189**. Unfortunately, an overlapping endothermic event was observed from 106.7 to 115.9 °C.

Independent measurement of the melting point of 112.6 to 113.6 °C confirmed, that the event represents the melting of the sample. Consequently, the overlap of these two thermic events causes the observed enthalpy of $\Delta H = -11.4$ kJ/mol to be lower than the reaction enthalpy of the nitrogen loss due to a lack of isolation from the endothermic melting process. The overlap of these processes is not unlikely, as the formation of an eutectic mixture of pyrazoline **188** and cyclopropane **189** can be assumed. The observed, but not isolated, melting enthalpy was determined to be between $\Delta H_m = 8.0$ kJ/mol to $\Delta H_m = 8.8$ kJ/mol for pyrazoline **188** and cyclopropane **189**, respectively.

The formation of cyclopropane **189** after the thermal analysis was proven by $^1\text{H-NMR}$ of the crucible residue after the measurement (Figure 3.9).

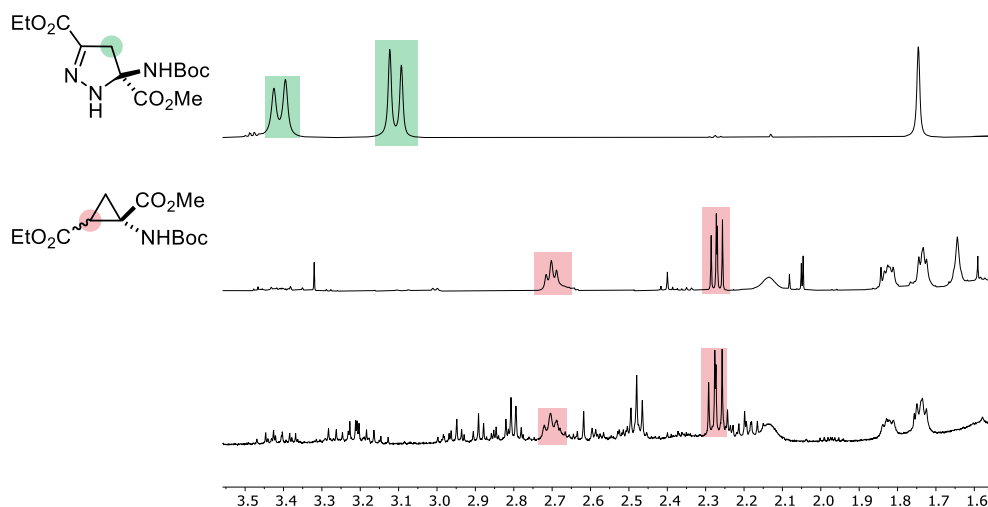
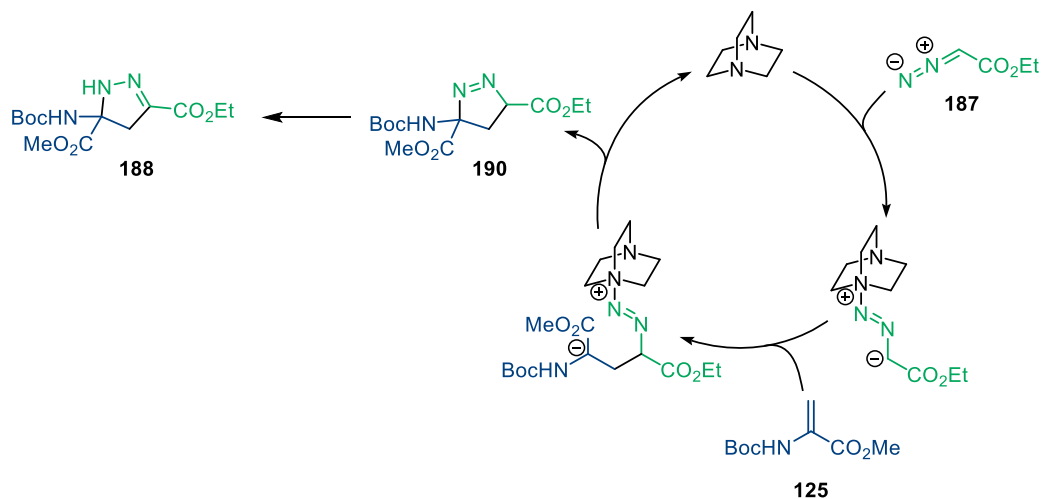


Figure 3.9: $^1\text{H-NMR}$ of pyrazoline **188** (top), cyclopropane **189** (middle), and the crucible residue (bottom) after thermal analysis from 25 to 200 °C.

Based on the results of the reaction optimization, the formal 1,3-dipolar cycloaddition is considered to follow a nucleophile-catalyzed pathway (Scheme 3.56). A similar mechanism was proposed for the cycloaddition of EDA to alkenes by KRISHNA *et al.*^[118]

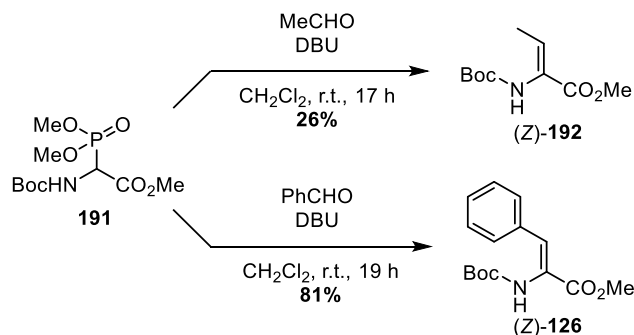


Scheme 3.56: Proposed mechanism for the nucleophile catalyzed formal 1,3-dipolar cycloaddition of EDA (**187**) to Boc- Δ Ala-OMe (**125**).

Herein, DABCO activates EDA (**187**) by nucleophilic addition to the terminal nitrogen. 1,4-Addition of the resulting triazene intermediate to Boc- Δ Ala-OMe (**125**) forms an enolate that cyclizes under the release of the DABCO catalyst, forming 1-pyrazoline **190**. The 1,3-H shift gives the thermodynamically favored 2-pyrazoline **188**.

3.4.3. Extending the Substrate Scope of the Reaction

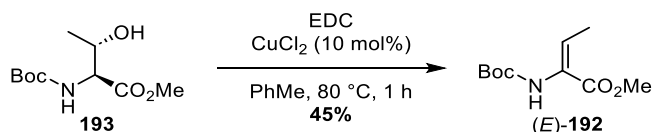
With the established procedure, the scope of potential dHAAs was explored. First, methyl- and phenyl-substituted derivatives were investigated. Using the commercially available SCHMIDT reagent **191**, (*Z*)-Boc- Δ Abu-OMe (**192**) and (*Z*)-Boc- Δ Phe-OMe (**126**) were prepared in a HORNER-WADSWORTH-EMMONS reaction (Scheme 3.57). Whereas the reaction using acetaldehyde afforded (*Z*)-Boc- Δ Abu-OMe (**192**) in 26% yield, the reaction with benzaldehyde proceeded smoothly and gave (*Z*)-Boc- Δ Phe-OMe (**126**) in an excellent yield of 81%.



Scheme 3.57: HWE-reaction of Schmidt reagent **191** with acetaldehyde and benzaldehyde.

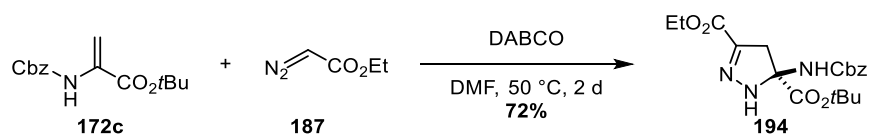
To evaluate the stereospecificity, the (*E*)-isomer of Boc- Δ Abu-OMe (**192**) was also prepared based on a procedure by SAI *et al.*^[183] Herein, Boc-Thr-OMe (**193**) is dehydrated using EDC and catalytic CuCl₂. Noteworthy, the authors stated, that the commonly used EDC hydrochloride was too weak to overcome the thermodynamic instability of the (*E*)-isomer and gave the (*Z*)-isomer in high selectivity.

As only the hydrochloride salt was available, an *in situ* preparation of anhydrous EDC by treatment of its dry hydrochloride solution with dry ammonia gas, followed by inert filtration of the ammonium chloride and extensive degassing was conducted. The reaction afforded (*E*)-Boc- Δ Abu-OMe (**192**) diastereoselectively in moderate yield (Scheme 3.58).



Scheme 3.58: Dehydration of Boc-Thr-OMe (**193**) using EDC to access (*E*)-Boc- Δ Abu-OMe (**192**).

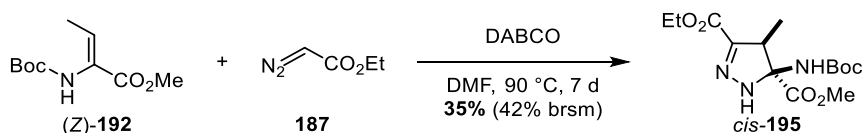
Additionally, Cbz- Δ Ala-OtBu (**172c**), synthesized by the developed electrosynthesis (see section 0), was tested to access an orthogonally protected pyrazoline derivative. The Cbz-group as well as the *tert*-butyl ester were tolerated and gave pyrazoline **194** in 72% yield after 2 d at 50 °C in DMF (Scheme 3.59).



Scheme 3.59: Synthesis of orthogonally protected pyrazoline **194**.

The pyrazoline **194** features three different protecting groups and should allow selective deprotection of either ester as well as the carbamate for follow-up chemistry.

While the reactions of unsubstituted dehydroalanines with EDA proceeded at a reasonable rate to full conversion, the dehydrobutyridine derivative (*Z*)-**192** manifested a drastic decrease in reaction rate. Running the reaction of (*Z*)-**192** for 7 d at 90 °C only gave incomplete conversion. The product could be isolated in 35% yield (42% brsm) and the starting material was recovered (Scheme 3.60). Only the *cis*-diastereomer of pyrazoline **195** was observed, indicating a stereospecific reaction.



Scheme 3.60: Stereospecific cycloaddition of EDA and (*Z*)-**192**.

Due to the prolonged reaction time at these elevated temperatures, a competing decomposition of EDA is likely to occur, impeding full conversion. While this may be mitigated by the subsequent addition of EDA throughout the reaction time, a different approach by microwave heating was investigated.

The reaction was heated in a microwave to 70 °C for 20 h and the pressure of the microwave vial was recorded. Unfortunately, a linear increase in overpressure from 0 to 4.5 bar over the course of the reaction was observed, indicating the expected EDA decomposition. The conversion after 20 h compared to regular heating at 70 °C was 13% and 4%, respectively.

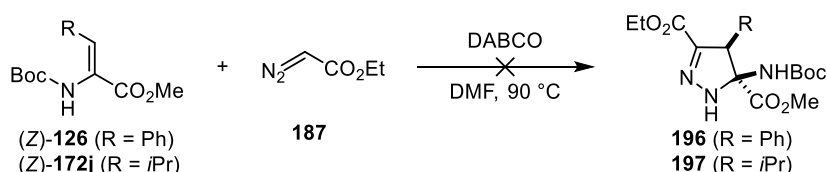
A comparison of the reaction mixture clearly shows the decomposition under microwave irradiation, while the EDA remains reasonably stable at 70 °C under conventional heating conditions (Figure 3.10).



Figure 3.10: Color of the reaction mixture after 20 h at 70 °C using microwave heating (left) and conventional heating (right).

Applying the protocol to the thermodynamically disfavored (*E*)-isomer (*E*)-**192** gave the *trans*-isomer *trans*-**195** selectively in 30% yield (67% brsm). However, the isomerized starting material (*Z*)-**192** was isolated in 16% yield alongside 40% of the employed isomer (*E*)-**192**.

As expected, the use of sterically more demanding dhAAs, e.g. (Z)-Boc- Δ Phe-OMe (**126**) or (Z)-Boc- Δ Leu-OMe (**172j**), demonstrated poor reactivity, only traces of product could be observed *via* crude $^1\text{H-NMR}$, even after several days at 90 °C (Scheme 3.61).



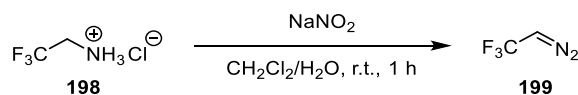
Scheme 3.61: Application of the protocol to sterically demanding dhAAs failed.

To assess the generality of the method and to pursue a greater substrate scope, the use of more nucleophilic diazo compounds was considered.

EDA is readily available in an almost pure form ($w = 87\%$ in CH_2Cl_2) and although it shows limited thermal stability, it cannot sustain detonation.^[184-185] For that reason, it is one of the few diazo compounds used on an industrial scale, e.g. in the synthesis of clofencet (plant growth regulator) or in various cyclopropanations.^[186-187] However, its stability correlates to decreased nucleophilicity compared to other diazo compounds.^[188-189]

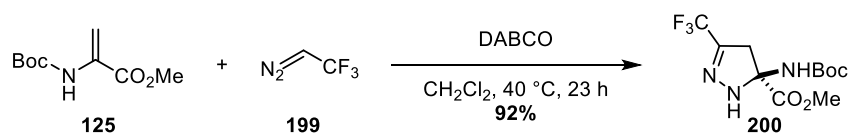
The use of more nucleophilic, semi-stabilized diazo compounds, e.g. diazo acetonitrile, phenyl-, trifluoromethyl-, trimethylsilyl diazomethane, should be taken into consideration to achieve the aspired cycloaddition reaction at milder temperatures, higher reaction rates, and broader substrate scope. In recent decades, *in situ* preparation or flow protocols allow the preparation and handling of these energetic materials in small quantities with reduced safety risks.^[190-194]

The investigation was commenced by the preparation of trifluoromethyl diazomethane (**199**) in solution by treating a suspension of trifluoroethylammonium chloride (**198**) with sodium nitrite in a $\text{CH}_2\text{Cl}_2/\text{H}_2\text{O}$ mixture (Scheme 3.62). All of the following reactions were carefully conducted on a small scale with appropriate safety measurements.



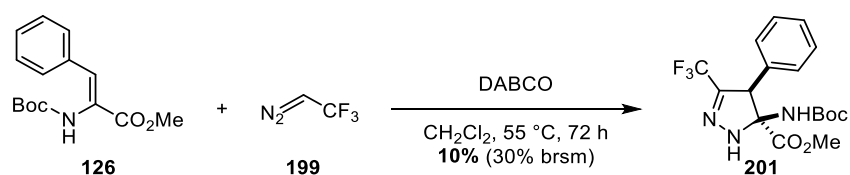
Scheme 3.62: Preparation of a trifluoromethyl diazomethane (**199**) solution.

The solution was added to Boc- Δ Ala-OMe (**125**) and (Z)-Boc- Δ Phe-OMe (**126**). The reaction with the model substrate **125** proceeded cleanly in 23 h at 40 °C and afforded the pyrazoline **200** in 92% yield (Scheme 3.63).



Scheme 3.63: Synthesis of 2-pyrazoline **200**.

In contrast, conversion was sluggish for the dehydrophenylalanine derivative **126**, but elevating the temperature to $55\text{ }^\circ\text{C}$ showed 30% conversion after 72 h. The product **201** was isolated in 10% (30% brsm) yield and the starting material was recovered (Scheme 3.64).

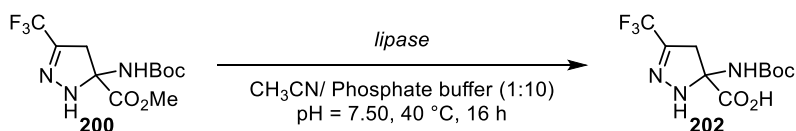


Scheme 3.64: Synthesis of highly substituted 2-pyrazoline **201**.

Both reactions exhibited stereospecificity and no cyclopropanes were observed. This result demonstrates, that with semi-stabilized diazo compounds, higher substituted 2-pyrazolines may be accessible.

This class of 2-pyrazoline 5-amino acids was not reported before and given the abundance of 2-pyrazoline moieties in active pharmaceutical ingredients, the biological activity of these compounds should be assessed. Additionally, subsequent deprotection of the amino acid functions could allow the installation into peptides and follow-up chemistry.

To investigate a potential enzymatic resolution by ester hydrolysis, pyrazoline amino acid **200** was subjected to various lipases (Scheme 3.65).



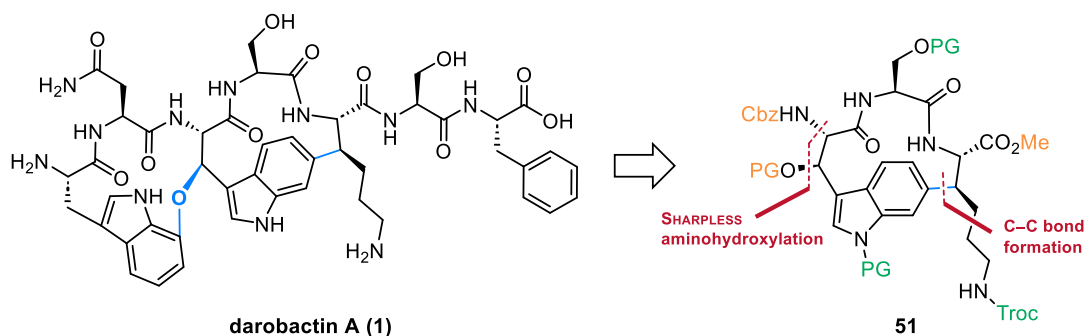
Scheme 3.65: Enzymatic resolution by ester hydrolysis of racemate **200** failed, full conversion to carboxylic acid **202** was observed. *C. rugosa*, *C. antarctica*, and Lypozyme TL TM[®] were tested.

Three different lipases, *C. rugosa*, *C. antarctica*, and the immobilized Lypozyme TL TM[®] were tested under mild conditions of $40\text{ }^\circ\text{C}$ and a carefully controlled pH of 7.5 throughout the reaction.

After 16 h, the reaction mixtures were analyzed via TLC and ^1H and ^{19}F -NMR of the crude product after acidification and extraction. All three lipases showed full conversion ester **200** to carboxylic acid **202** and residual methyl ester **200** was not detected, hence both enantiomers were hydrolyzed and the racemic resolution under the given conditions failed.

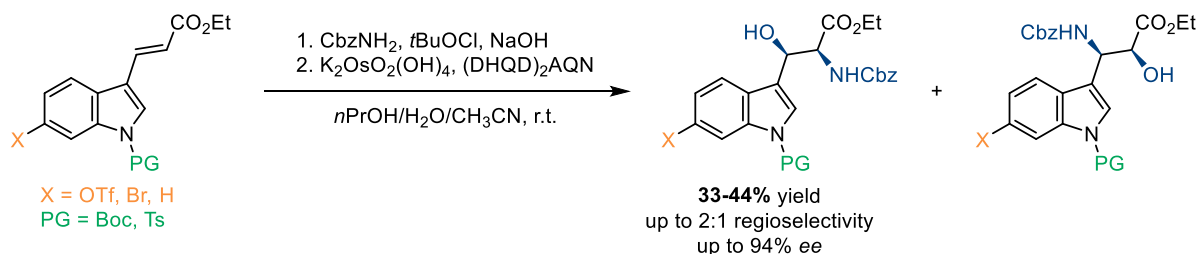
4. Conclusion and Outlook

The natural product darobactin A (**1**) represents a promising lead structure for the development of a novel class of antibiotics, given its unique mechanism of action. The total synthesis of the natural product was the overarching objective of this thesis. The retrosynthetic analysis identified a Trp-Ser-Lys macrocycle **51** as the pivotal building block for its total synthesis, bearing two key challenges, the stereoselective construction of the β -hydroxytryptophan moiety and the construction of the unique C-C bond between the lysine and the C6-position of the central indole (Scheme 4.1).



Scheme 4.1: Retrosynthetic analysis of darobactin A (**1**) identified macrocycle **51** as the pivotal building block for its total synthesis.

Firstly, a SHARPLESS asymmetric aminohydroxylation of indole derivatives was developed (Scheme 4.2).



Scheme 4.2: Stereoselective construction of the β -hydroxytryptophan utilizing a SHARPLESS asymmetric aminohydroxylation.

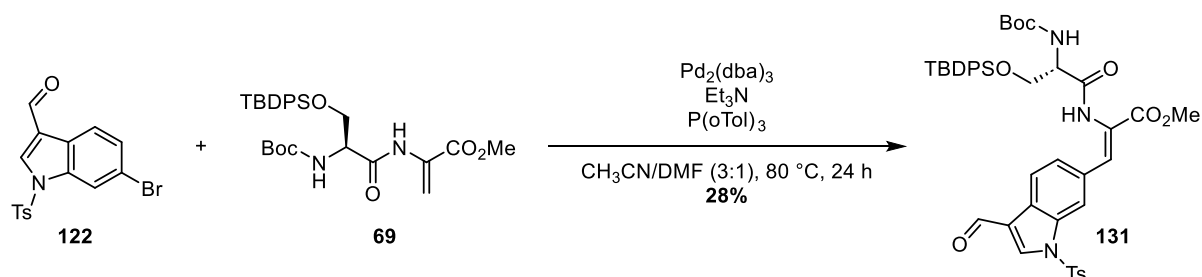
Extensive reaction optimization revealed a dominant formation of the undesired regioisomers as a major challenge. The regioselectivity could be reversed using the (DHQD)₂AQN ligand and specific solvent mixtures.

Various approaches toward the C-C bond formation between the central tryptophan and the β -carbon of the lysine were investigated. The attempted Template-assisted Pd(II)-olefination of Boc-Trp(Temp)-OMe (**64**) could not be realized, neither dehydroalanines nor ethyl acrylate as a simple model substrate reacted under various reaction conditions. Studies towards the C-C bond formation *via* reductive HECK-reaction of C6-triflyl tryptophans with orthogonally protected Boc- Δ Lys(Troc)-OMe (**72**) demonstrated low reactivity of the dehydrolysine as an olefinic substrate.

Finally, a HECK-protocol was developed to realize the pivotal C-C bond between the C6-position of 6-bromoindole **122** and various dehydroalanines. The experimental studies revealed, that Boc-protection

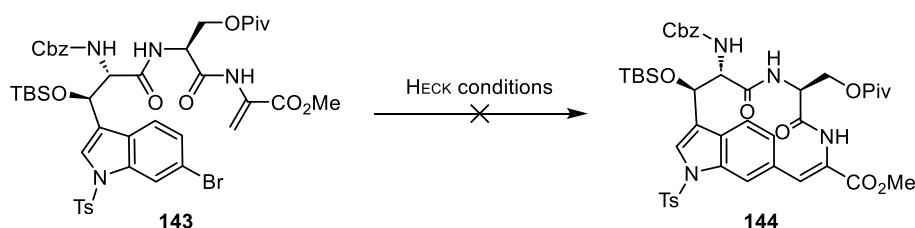
of the indole was not suitable, the protecting group was too labile at the elevated temperatures and basic conditions employed in the aspired HECK-transformations.

As an alternative, the protection of the indole-nitrogen as a sulfonamide showed increased stability. Screening of various catalyst-ligand systems identified $\text{Pd}_2(\text{dba})_3 / \text{P}(\text{oTol})_3$ as a superior system for various dehydroalanines, most notably the dehydropeptide Boc-Ser(TBDPS)- Δ Ala-OMe (**69**), demonstrating excellent (*Z*)-selectivity (Scheme 4.3).



Scheme 4.3: Heck reaction of 6-bromindole **122** with dehydropeptide Boc-Ser(Piv)-DAla-OMe (**69**).

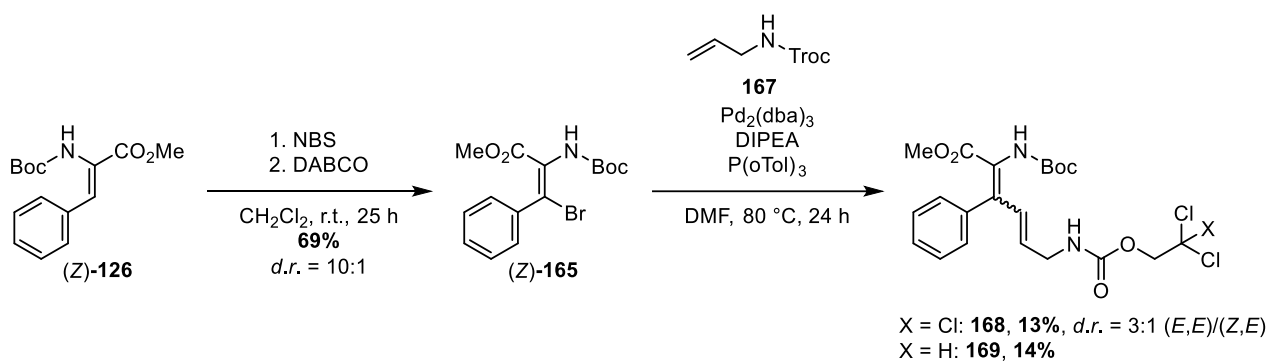
For the construction of the eastern macrocycle of darobactin A (**1**), the optimized conditions, among others, were applied to cyclization precursor **143**. However, the formation of the strained macrocycle **144** was not observed under the tested conditions (Scheme 4.4).



Scheme 4.4: Attempted intramolecular HECK cyclization of precursor **143**.

The utilization of dehydroalanines instead of dehydrolysine for the C-C bond formation necessitated the late-stage introduction of the lysine side chain. Initial attempts using radical conjugate additions, e.g. classical GIESE-type conditions or addition of radicals generated under visible-light photoredox catalysis, and polar 1,4-additions turned out to be challenging.

Lastly, bromination of the dhAA followed by HECK-reaction with Troc-allylamine (**167**) achieved the aspired C-C bond formation on Boc- Δ Phe-OMe (**165**) as a model substrate. However, hydrodehalogenation at the protecting group was observed as a major side reaction (Scheme 4.5).

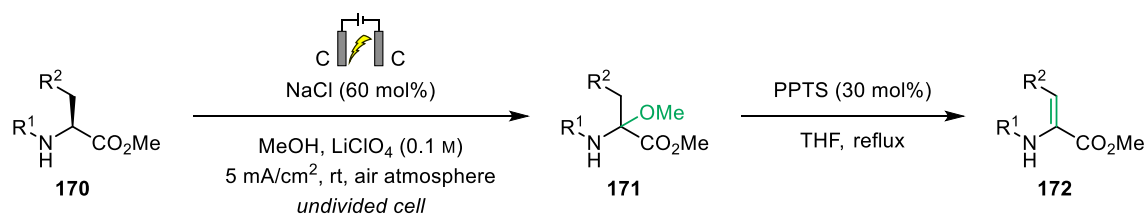


Scheme 4.5: Introduction of the lysine side-chain by bromination of model substrate Boc- Δ Phe-OMe ((Z)-126) followed by HECK reaction with allyl amine **167**.

With the demonstration of these key transformations towards the total synthesis of darobactin A (**1**) and due to the publication of two independent total syntheses by PATEL, PETRONE, and SARLAH *et al.* and BARAN *et al.* in 2022,^[20-21] the investigations towards the total synthesis of darobactin A were discontinued.

Through the employment of several dhAAs within the investigated transformations, several synthetic methods for their synthesis were evaluated. Albeit dhAAs have proven to be excellent handles for the functionalization of peptides and natural products, available methods towards their synthesis are limited. Hence, the development of a new direct synthesis of dhAAs from their corresponding amino acid carbamates was aspired.

A NaCl-mediated electrochemical oxidation process was developed to α -methoxylate amino acid carbamates. A subsequent PPTS-catalyzed elimination enabled the atom-economic synthesis of a variety of carbamate-protected dhAAs (Scheme 4.6). The electrochemical reaction was realized with a simple setup using inexpensive graphite electrodes and could be demonstrated on a decagram-scale in the synthesis of Boc- Δ Ala-OMe (**172a**).

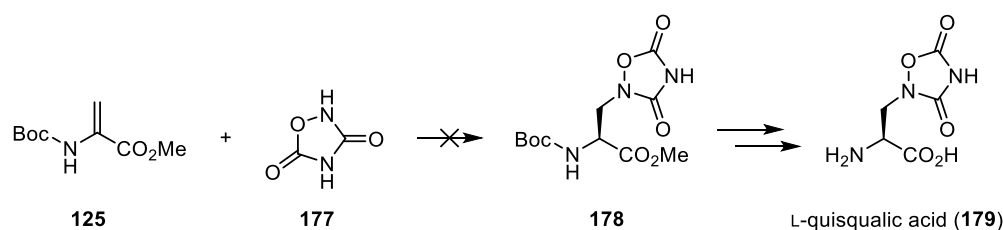


Scheme 4.6: Electrosynthesis of protected dhAAs (**172**).

Surprisingly, application of the acid-catalyzed conditions to α -methoxy lysines and ornithines led to cyclization thereof, forming new 2-aminoproline- and 2-aminopipercolic acid derivatives in excellent yield. The corresponding dehydrolysines and dehydroornithines were accessed by base-induced elimination of methanol.

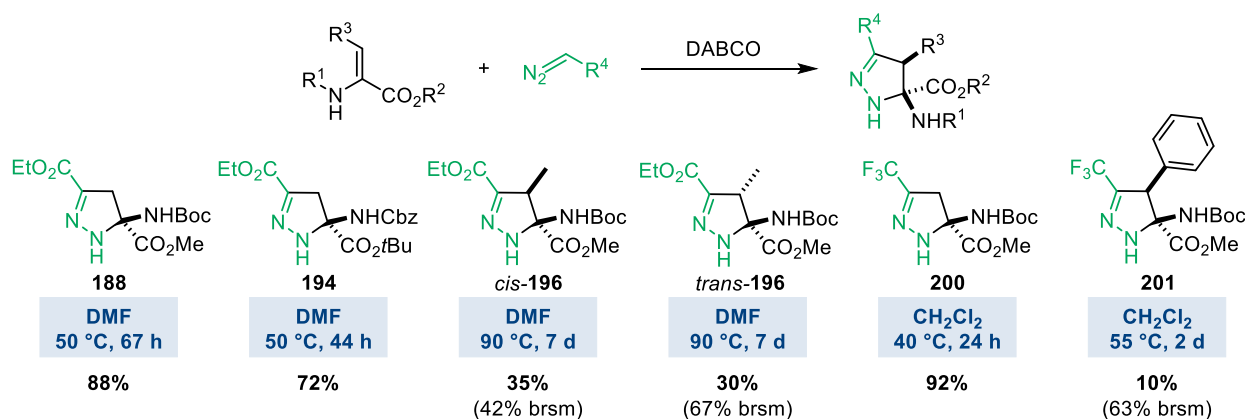
With a new general access to protected dhAAs in hand, functionalization of this versatile substrate class was investigated. Besides the previously stated HECK-reactions, the conjugate addition of 1,2,4-oxadiazolidione (**177**) towards the synthesis of the valuable excitotoxin, L-quisqualic acid (**179**), was

investigated. Unfortunately, the heterocycle demonstrated weak nucleophilicity, and no conversion was observed under nucleophilic, phase-transfer-, LEWIS-acid-, thiourea-, and bifunctional catalysis (Scheme 4.7).



Scheme 4.7: Attempted conjugated addition of 1,2,4-oxadiazolidione (177) towards the synthesis of L-quisqualic acid (179).

As a final project of this work, the access to a new class of highly substituted 2-pyrazolines amino acids by nucleophile-catalyzed [2+3] cycloaddition of diazo compounds was developed (Scheme 4.8).



Scheme 4.8: Synthesis of highly substituted 2-pyrazoline amino acids.

The formation of cyclopropane byproducts could be suppressed by extensive reaction optimization, leading to high substrate concentration and the use of polar aprotic solvents as crucial factors for the formation of 2-pyrazolines with stabilized diazo compounds, e.g. ethyl diazoacetate. The substrate scope was extended to β-substituted dhAAs, tolerating benzyl and *tert*-butyl carbamates as well as methyl- and *tert*-butyl esters. The cycloaddition of trifluoromethyl diazomethane with Boc-ΔAla-OMe (125) could be achieved in 92% yield under mild conditions.

Preliminary studies towards enzymatic resolution of the 2-pyrazolines using lipases were not successful, but further investigations towards their resolution, e.g. based on crystallization of diastereomeric salts or using different enzymes, could lead to separation of the pharmaceutically valuable enantiopure amino acids.

Additionally, the higher reactivity observed for trifluoromethyl diazomethane provides a promising outlook for the substrate scope of other semi-stabilized diazo compounds.

Further studies towards the installation of the 2-pyrazoline amino acid moiety on complex dehydropeptides, e.g. thiostrepton or nisin A, should be conducted.

5. Experimental Section

5.1. General Methods

Solvents and Reagents

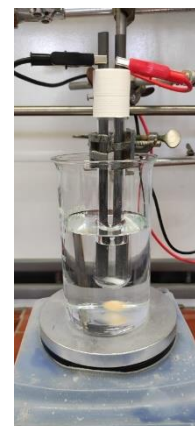
All air and moisture-sensitive reactions were performed under an argon atmosphere (Argon 4.6, 99.996%) provided by the company *Air Liquide*. Used glass equipment was dried by a heat gun under vacuum (10^{-3} mbar) and flushed with argon three times. Syringes and needles were flushed three times with argon before use.

All reagents were provided by commercial suppliers (*Acros Organics, Alfa Aesar, Carbolution, Carl Roth, Fisher Chemical, Merck, Sigma Aldrich*) and used without further purification unless otherwise stated. Dry solvents (THF, Et₂O, CH₂Cl₂, toluene) were obtained through an MB SPS-800 solvent system from the company *MBRAUN* and stored with 3 Å or 4 Å molecular sieves. DIPEA, Et₃N, and DBU were dried over CaH₂ and distilled under an argon atmosphere. NBS was recrystallized from boiling H₂O, dried in a vacuum desiccator, and stored under light exclusion. DABCO was recrystallized from EtOH/*n*-hexane and dried under a vacuum over CaCl₂. The solvents EtOAc, Et₂O, MeOH, CH₂Cl₂, and pentane were distilled through rotary evaporation prior to use.

Solvents were removed under reduced pressure by a rotary evaporator at 40 °C. Oil pump vacuum was used to remove residual solvents. Room temperature refers to 23 °C.

Electrochemistry

The power supply unit LSP-1403 by the company *VOLTCRAFT* was used, which was connected to graphite electrodes (8.2 mm) by *Polymet* through banana connectors (4 mm) and crocodile clips. The electrodes were spaced apart by 5 mm using a 3D-printed PLA holder. A beaker with room temperature water was used as a thermal reservoir to prevent a rise in temperature during the reaction.



Cyclic voltammetry

Cyclic voltammograms were obtained using a *Gamry Interface 1010E* using a glossy carbon disk working electrode, Pt wire as the counter electrode, and Pt wire as the pseudoreference electrode. Each measurement was referenced to ferrocene as an internal standard.

Microwave-Irradiation

Reactions under microwave-heating were irradiated in a *Biotage Initiator+* using 5 mL vials.

Thin Layer Chromatography (TLC)

TLC was performed using ALUGRAM Xtra SIL G/UV₂₅₄ plates by *Macherey-Nagel*. Visualization was performed under UV-light ($\lambda = 254$ nm), potassium permanganate stain (1.5 g KMnO₄, 10 g K₂CO₃, and 1.25 mL 10% NaOH-solution in 200 mL H₂O), anisaldehyde stain (135 mL EtOH, 5 mL conc. H₂SO₄, 1.5 mL AcOH, 3.7 mL *p*-anisaldehyde) or ninhydrin stain (1.5 g ninhydrin in 100 mL *n*-butanol and 3 mL AcOH).

Column Chromatography

Purification by flash chromatography was performed with silica gel 60 Å (35 – 70 µm) by the company *Macherey-Nagel*. The column was pressurized by 0.5 bar with compressed air. Automated flash chromatography was performed on a CombiFlashR_f system, using RediSepR_f silica gel columns by the company *Teledyne ISCO*.

Nuclear Magnetic Resonance Spectroscopy (NMR)

All spectra were measured on a *JEOL ECX 400* (400 MHz), *Bruker Avance 500*, *JEOL ECP 500* (500 MHz), *Varian INOVA 600* (600 MHz), or *Bruker Avance 700* (700 MHz), using deuterated solvents by the company *Eurisotop*. All spectra were measured at 298 K. Chemical shifts were reported in ppm and referenced according to the signal TMS as an internal standard. Signal multiplicities were abbreviated as follows: s = singlet, d = doublet, t = triplet, q = quartet, p = quintet, dp = doublet of quintet, m = multiplet or as combinations of the abbreviations to describe complex multiplicities. Coupling constants *J* are given in Hertz (Hz). Assignments of the respective signals were done by suitable 2D experiments (¹H, ¹H-COSY; ¹H,¹³C-HSQC; ¹H,¹³C-HMBC; ¹H-ge-NOESY). All spectra were analyzed using *MestReNova 14.1.1*.

Fourier-Transform Infrared Spectroscopy (FT-IR)

FT-IR spectra were measured using a FT-IR 4100 system by the company *JASCO*. The wavenumbers are given in cm⁻¹.

Optical Rotation

Optical rotations were measured on a *JASCO P-2000* polarimeter at 589 nm in 100 mm quartz-glass cells. The solvent, temperature, and concentration (g/100 mL) are indicated for each measurement.

High-Performance Liquid Chromatography (HPLC)

The determination of enantiomeric excesses were determined using an *Agilent 1200 series* HPLC on chiral stationary phase. Analytes were detected using a diode-array-detector.

Gas Chromatography with coupled Electron Ionization Mass Spectroscopy (GC-MS)

GC-MS was performed on an *Agilent 7890A* system with a *VL MSD 5975C* mass detector. The electron impact ionization was realized at 70 eV. Helium gas was used as carrier gas with a flow of 1.4 mL/min and pressure of 0.3 bar. *Agilent 19091S-4335 HP-5 MS* (30 m x 0.25 mm x 0.25 µm) was used as capillary tube.

Mass Spectrometry (HR-MS)

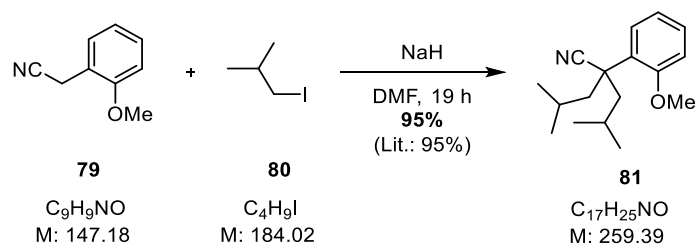
High resolution mass spectrometry was performed on an *AGILENT 6210* ESI-TOF-spectrometer. The electro spray method was used as ionization method.

Thermogravimetric Analysis – Differential Scanning Calorimetry (TG-DSC)

The differential scanning calorimetry measurements were performed using *NETZSCH STA 449F3 Jupiter*, alumina crucibles (85 µL) with pierced lids and nitrogen purge gas flow of 250 mL/min.

5.2. Template-assisted C6-Indole Functionalization of the Eastern Fragment

5.2.1. 2-(2-Methoxyphenyl)-4-methyl-2-propylpentanenitrile (**81**)



A 100 mL Schlenk-flask was charged with nitrile **79** (2.50 g, 17.0 mmol, 1.00 eq.) in dry DMF (38 mL). The solution was cooled to 0 °C and NaH (60% in mineral oil, 2.04 g, 51.0 mmol, 3.00 eq.) was added in portions over 20 min. Iodide **80** (5.9 mL, 51.0 mmol, 3.00 eq.) was added and the solution was allowed to warm up to room temperature and stirred for 19 h. The reaction mixture was treated with sat. aq. NH_4Cl -sol. (15 mL), diluted with 60 mL water, extracted with Et_2O (3 x 60 mL), the combined organic phases were washed with brine (100 mL), dried over Na_2SO_4 and the solvent was removed under reduced pressure. The product **81** (4.18 g, 16.1 mmol, 95%, Lit.: 95%) was obtained as colorless crystals.

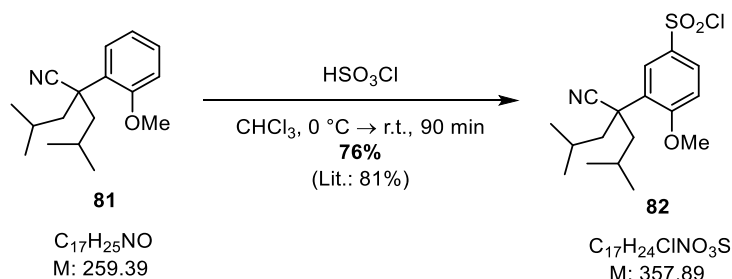
$R_f = 0.3$ (*n*-pentane).

$^1\text{H NMR}$ (500 MHz, CDCl_3) $\delta = 7.67$ (dd, $J = 7.7, 1.7$ Hz, 1H), 7.30 (ddd, $J = 8.1, 7.2, 1.7$ Hz, 1H), 6.97 (td, $J = 7.6, 1.2$ Hz, 1H), 6.86 (dd, $J = 8.2, 1.2$ Hz, 1H), 3.82 (s, 3H), 2.36 (dd, $J = 13.9, 5.6$ Hz, 2H), 1.75 (dd, $J = 13.9, 6.8$ Hz, 2H), 1.60 – 1.47 (m, 2H), 0.95 (d, $J = 6.7$ Hz, 6H), 0.62 (d, $J = 6.7$ Hz, 6H) ppm.

$^{13}\text{C NMR}$ (126 MHz, CDCl_3) $\delta = 157.5, 130.2, 129.2, 125.1, 124.7, 121.0, 111.6, 55.2, 55.2, 47.3, 26.0, 23.8, 23.6$ ppm.

The analytical data of compound **81** is in agreement with the literature.^[124]

5.2.2. TempCl (**82**)



A 50 mL flask was charged with anisol **81** (4.11 g, 15.8 mmol, 1.00 eq.) and CHCl_3 (15 mL) and cooled to 0 °C. Chlorosulfonic acid (6.2 mL, 93.1 mmol, 5.88 eq.) was added dropwise and the solution was stirred for 30 min at 0 °C. The cooling bath was removed and stirring was continued for 1 h. The reaction mixture was poured on 150 g ice and the phases were separated. The aqueous phase was extracted with CH_2Cl_2 (3 x 50 mL), the combined organic phases were dried over Na_2SO_4 , filtered and the solvent was removed under

reduced pressure. The crude product was purified by column chromatography (SiO₂, *c*-hexane/EtOAc 9:1 → 3:1) affording sulfonyl chloride **82** (4.32 g, 12.1 mmol, 76%, Lit.: 81%) as a colorless solid.

R_f = 0.65 (*c*-hexane/EtOAc = 2:1).

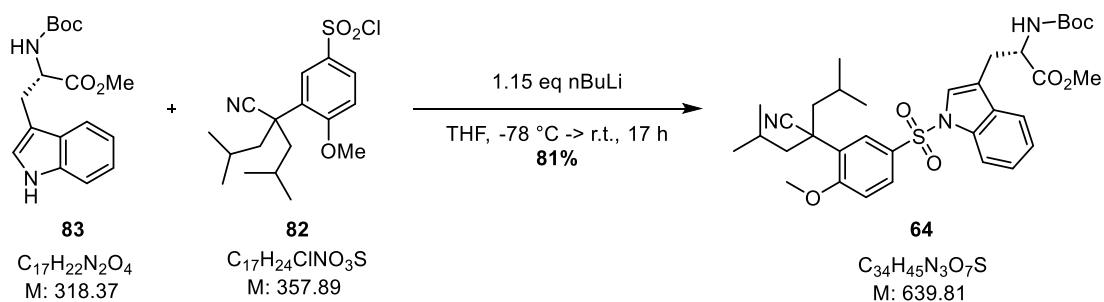
¹H NMR (500 MHz, CDCl₃) δ = 8.32 (d, J = 2.4 Hz, 1H), 8.03 (dd, J = 8.8, 2.5 Hz, 1H), 7.05 (d, J = 8.9 Hz, 1H), 3.98 (s, 3H), 2.29 (dd, J = 14.2, 5.7 Hz, 2H), 1.83 (dd, J = 14.1, 6.8 Hz, 2H), 1.60 – 1.46 (m, 3H), 0.96 (d, J = 6.7 Hz, 6H), 0.67 (d, J = 6.7 Hz, 5H).

ppm.

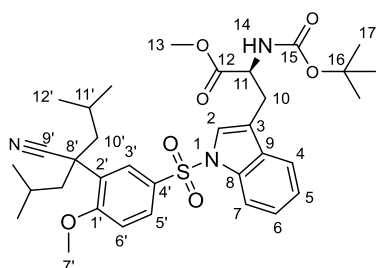
¹³C NMR (101 MHz, CDCl₃) δ = 164.7, 136.7, 129.5, 128.9, 127.3, 123.6, 111.9, 56.3, 46.8, 26.1, 23.8, 23.6 ppm.

The analytical data of compound **82** is in agreement with the literature.^[124]

5.2.3. Boc-Trp(Temp)-OMe (**64**)



A 50 mL Schlenk flask was charged with Boc-Trp-OMe (**83**, 0.821 mg, 2.58 mmol, 1.00 eq.) in dry THF (17 mL) and cooled to -78 °C. *n*-BuLi (2.32 M, 1.3 mL, 2.96 mmol, 1.15 eq.) was added. TempCl **82** (1.20 g, 3.35 mmol, 1.30 eq.) in dry THF (6 mL) was added dropwise to the reaction mixture and the solution was allowed to warm up to room temperature overnight. After 17 h, sat. aq. NH₄Cl-sol. (20 mL) was added and most of the THF was removed under reduced pressure. The mixture was extracted with EtOAc (3 x 50 mL), the combined organic phases were washed with brine (100 mL), dried over Na₂SO₄, filtered and the solvent was removed under reduced pressure. The crude product was purified by column chromatography (SiO₂, *c*-hexane/EtOAc 9:1 → 4:1) affording Boc-Trp(Temp)-OMe (**64**, 1.34 g, 2.09 mmol, 81%) as a colorless solid.



R_f = 0.59 (*n*-pentane/EtOAc = 2:1).

m.p. = 56.5-57.0 °C.

$^1\text{H NMR}$ (600 MHz, CDCl_3) δ = 8.10 (d, J = 2.3 Hz, 1H, H3'), 7.97 (d, J = 8.3 Hz, 1H, H4), 7.78 (dd, J = 8.7, 2.4 Hz, 1H, H5'), 7.42 (d, J = 2.3 Hz, 1H, H7), 7.35 (s, 1H, H2), 7.31 (ddd, J = 8.3, 7.2, 1.2 Hz, 1H, H5), 7.20 (t, J = 7.6 Hz, 1H, H6), 6.85 (d, J = 8.7 Hz, 1H, H6'), 5.08 (d, J = 7.9 Hz, 1H, NH), 4.61 (q, J = 6.2 Hz, 1H, H11), 3.82 (s, 3H, H7'), 3.67 (s, 3H, H13), 3.19 (ddd, J = 49.6, 14.7, 5.5 Hz, 2H, H10), 2.15 (ddd, J = 14.2, 7.1, 5.8 Hz, 2H, H10'a), 1.67 (dt, J = 14.2, 6.3 Hz, 2H, H10'b), 1.44 (d, J = 13.9 Hz, 9H, H17), 1.30 – 1.17 (m, 2H, H11'), 0.78 (dd, J = 11.9, 6.7 Hz, 6H, $\text{H}_{\text{Rot}12'}$), 0.41 (d, J = 6.7 Hz, 3H, $\text{H}_{\text{Rot}12'}$), 0.35 (d, J = 6.6 Hz, 3H, $\text{H}_{\text{Rot}12'}$) ppm.

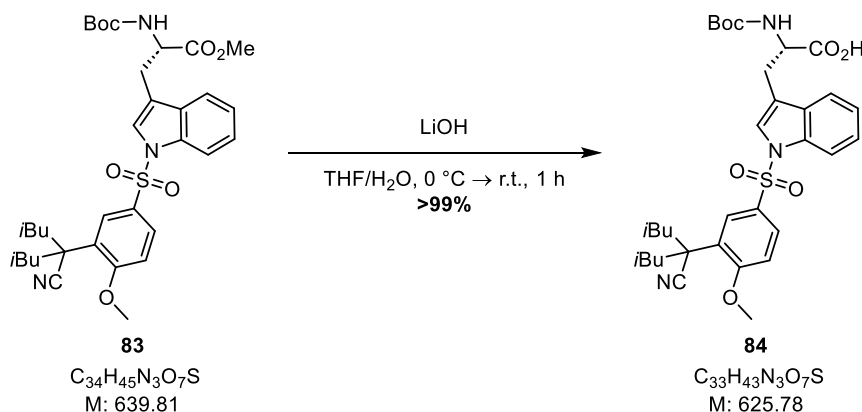
$^{13}\text{C NMR}$ (151 MHz, CDCl_3) δ = 172.1 (1C, C12), 161.4 (1C, C1'), 155.2 (1C, C9'), 135.3 (1C, C8), 131.3 (1C, C9), 129.9 (1C, C4'), 128.8 (1C, C5'), 128.7 (1C, C3'), 126.6 (1C, C2'), 125.3 (1C, C5), 124.7 (1C, C2), 123.5 (1C, C6), 123.1 (1C, C3), 122.3 (C6), 119.5 (1C, C7), 118.1, 114.1 (1C, C4), 111.7 (1C, C6'), 80.2; 79.9 (1C, C16), 55.9 (1C, C7'), 53.8 (1C, C11), 52.5 (1C, C13), 47.1 (1C, C8'); 46.8 (2C, C10'), 28.5 (3C, C17), 27.8 (1C, C10), 25.9 (2C, C11'), 23.5; 23.4 (4C, C12') ppm.

IR (neat): $\tilde{\nu}$ = 3390 (b), 2956 (w), 2931 (w), 1746 (w), 1714 (m), 1495 (m), 1449 (m), 1367 (m), 1263 (m), 1172 (vs), 1117 (w), 1097 (w), 1018 (w), 976 (w), 746 (m) cm^{-1} .

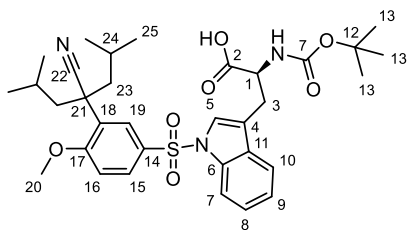
$[\alpha]_{\text{D}}^{23}$ (c = 0.925, CHCl_3) = +20.659.

HRMS (ESI): m/z calculated for $\text{C}_{34}\text{H}_{45}\text{N}_3\text{NaO}_7\text{S}^+$ ($[\text{M}+\text{Na}]^+$): 662.2870; found: 662.2873.

5.2.4. Boc-Trp(Temp)-OH (**84**)



A 10 mL flask was charged with Boc-Trp(Temp)-OMe (**83**, 150 mg, 0.234 mmol, 1.00 eq.) in THF/Water (4:1, 2.5 mL) and cooled to 0 °C. LiOH (16.8 mg, 0.703 mmol, 3.00 eq.) was added and stirring was continued for 1 h. The reaction mixture was diluted with water (10 mL) and extracted with Et_2O (20 mL). The aqueous phase was cooled to 0 °C, acidified to pH = 3 using 1 M HCl and extracted with EtOAc (3 x 20 mL). The combined organic phases were dried over Na_2SO_4 , filtered and the solvent was removed under reduced pressure affording spectroscopically pure Boc-Trp(Temp)-OH (**84**, 147 mg, 0.234 mmol, >99%) as a colorless solid.



$R_f = 0.43$ (*c*-hexane/EtOAc = 3:1).

$^1\text{H NMR}$ (600 MHz, CDCl_3) $\delta = 7.99$ (s, 1H, H19), 7.89 (dd, $J = 9.0$ Hz, 2.7 Hz, 2H, H10 & H15), 7.53 – 7.44 (m, 2H, H5 & H7), 7.29 (t, $J = 7.8$ Hz, 1H, H9), 7.21 (t, $J = 7.6$ Hz, 1H, H8), 6.88 (d, $J = 8.7$ Hz, 1H, H16), 5.17 (d, $J = 7.5$ Hz, 1H, NH), 4.65 (d, $J = 6.8$ Hz, 1H, H1), 3.83 (s, 3H, H20), 3.26 (ddd, $J = 55.8$ Hz, 15.0 Hz, 5.3 Hz, 2H, H3), 2.15 (ddd, $J = 14.2$ Hz, 8.5 Hz, 5.8 Hz, 2H, H23b), 1.73 – 1.66 (m, 2H, H23a), 1.46 (s, 9H, H13), 1.34 – 1.31 (m, 2H, H24), 0.80 (d, $J = 6.6$ Hz, 3H, $\text{H}_{\text{Rot}25}$), 0.77 (d, $J = 6.6$ Hz, 3H, $\text{H}_{\text{Rot}25}$), 0.45 (d, $J = 6.6$ Hz, 3H, $\text{H}_{\text{Rot}25}$), 0.38 (d, $J = 6.7$ Hz, 3H, $\text{H}_{\text{Rot}25}$) ppm.

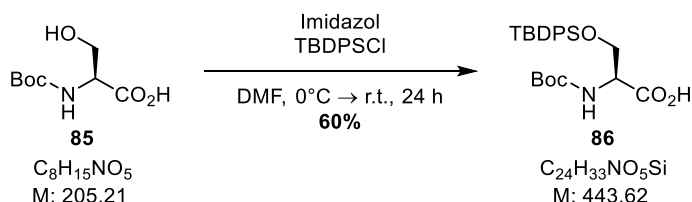
$^{13}\text{C NMR}$ (151 MHz, CDCl_3) $\delta = 175.1$ (C2), 161.4 (C7), 155.5 (C17), 135.1 (C6), 131.3 (C11), 129.7 (C14), 129.0 (C15), 128.4 (C19), 126.5 (C18), 125.2 (C9), 124.8 (C5), 123.3 (C8), 119.6 (C4), 118.08 (C22), 113.92 (C10), 111.78 (C16), 81.88; 80.44 (C12), 55.84 (C20), 53.62 (C1), 47.13 (C21), 46.59; 46.52 (C23), 28.40 (C13), 27.96; 27.52 (C3), 25.83 (C24), 23.41; 23.32 (C25) ppm.

IR (neat): $\tilde{\nu} = 3334, 3116, 3006, 2958, 2928, 2871, 1713, 1596, 1576, 1493, 1262, 1171, 1117, 1096, 1057, 1019, 975, 856, 820, 749$ cm^{-1} .

$[\alpha]_D^{23}$ ($c = 2.450, \text{CHCl}_3$) = +19.416.

HRMS (ESI): m/z calculated for $\text{C}_{33}\text{H}_{43}\text{N}_3\text{NaO}_7\text{S}^+$ ($[\text{M}+\text{Na}]^+$): 648.2714; found: 648.2687.

5.2.5. Boc-Ser(TBDPS)-OH (**86**)



A 25 mL Schlenk flask was charged with Boc-Ser-OH (**85**, 0.455 g, 2.22 mmol, 1.00 eq.) and imidazole (0.604 g, 8.87 mmol, 4.00 eq.) in dry DMF (10 mL). The solution was cooled to 0 °C and TBDPSCI (1.5 mL, 2.44 mmol, 1.10 eq.) was added slowly. The reaction was allowed to warm up to room temperature and stirred for 24 h. The reaction mixture was treated with water (15 mL) and Et_2O (30 mL). The phases were separated and the aqueous phase was extracted with Et_2O (3 x 20 mL). The combined organic phases were dried over Na_2SO_4 , filtered and the solvent was removed under reduced pressure. The crude product was purified by column chromatography (SiO_2 , *c*-hexane/EtOAc 19:1 → 4:1) affording Boc-Ser(TBDPS)-OH (**86**, 0.594 g, 1.35 mmol, 60%) as a colorless solid.

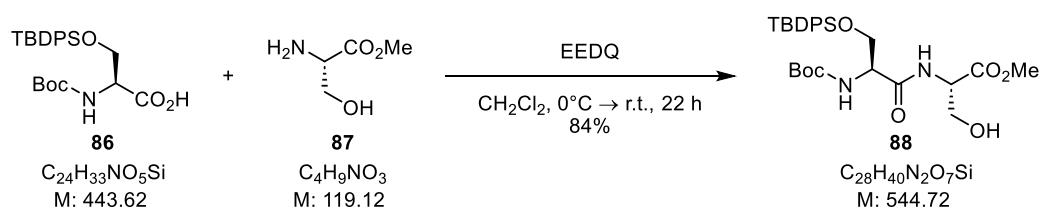
$R_f = 0.79$ (*n*-pentane/EtOAc = 1:1).

$^1\text{H NMR}$ (600 MHz, CDCl_3) $\delta = 7.67 - 7.58$ (m, 4H), 7.47 - 7.32 (m, 6H), 5.79 (s, 1H), 5.39 (d, $J = 8.6$ Hz, 1H), 4.44 (dt, $J = 8.3, 3.4$ Hz, 1H), 4.18 - 4.07 (m, 1H), 3.91 (dd, $J = 10.3, 3.4$ Hz, 1H), 1.46 (s, 9H), 1.03 (s, 9H) ppm.

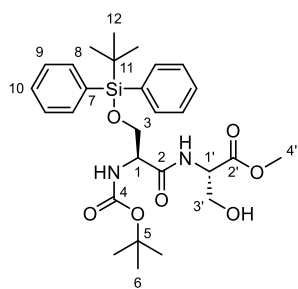
$^{13}\text{C NMR}$ (126 MHz, CDCl_3) $\delta = 175.9, 155.7, 135.7, 135.6, 133.0, 132.6, 130.1, 130.1, 128.0, 80.4, 64.5, 55.5, 28.5, 26.9, 19.4$ ppm.

The analytical data of compound **86** is in agreement with the literature.^[195]

5.2.6. Boc-Ser(TBDPS)-Ser-OMe (**88**)



A 25 mL Schlenk flask was charged with Boc-Ser(TBDPS)-OH (**86**, 0.272 g, 0.613 mmol, 1.00 eq.), H-Ser-OMe (**87**, 95.0 mg, 0.797 mmol, 1.30 eq.) in dry CH_2Cl_2 (8 mL) and cooled to 0°C . EEDQ (0.243 g, 0.981 mmol, 1.60 eq.) was added and the solution was allowed to warm up to room temperature. After 24 h, the mixture was diluted with EtOAc (20 mL) and washed with aq. HCl (0.5 M, 2x 10 mL). The organic phase was dried over Na_2SO_4 , filtered and the solvent was removed under reduced pressure. The crude product was purified by column chromatography (SiO_2 , *c*-hexane/EtOAc 1:0 \rightarrow 10:1) affording Boc-Ser(TBDPS)-Ser-OMe (**88**, 0.280 g, 0.514 mmol, 84%) as a colorless solid.



$R_f = 0.6$ (*c*-hexane/EtOAc = 10:1).

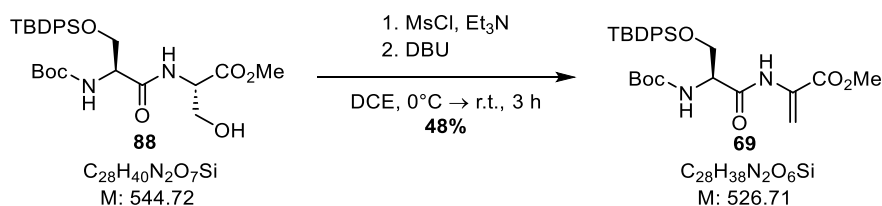
$^1\text{H NMR}$ (600 MHz, CDCl_3) $\delta = 7.64$ (d, $J = 7.1$ Hz, 4H, H9), 7.43 (t, $J = 7.2$ Hz, 2H, H10), 7.40 (t, $J = 7.4$ Hz, 4H, H8), 7.24 (NH), 5.30 (NH), 4.66 (s, 1H, H1), 4.26 (s, 1H, H_{Rot3a}), 4.08 (dt, $J = 10.3$ Hz, $J = 3.2$ Hz, 1H, H1'), 3.95 (s, 2H, H3), 3.83 (dd, $J = 10.5$ Hz, $J = 5.3$ Hz, 1H, H_{Rot3b}), 3.76 (s, 3H, H4'), 1.44 (s, 9H, H6), 1.06 (s, 9H, H12) ppm.

$^{13}\text{C NMR}$ (151 MHz, CDCl_3) $\delta = 170.9$ (C2), 170.6 (C2'), 155.8 (C4), 132.9 (C7), 132.7 (C9), 130.1 (C8), 128.0 (C10), 80.6 (C5), 64.1 (C1'), 63.4 (C3), 56.4 (C1), 55.3 (C3'), 52.9 (C4'), 28.4 (C6), 26.9 (C12), 19.4 (C11) ppm.

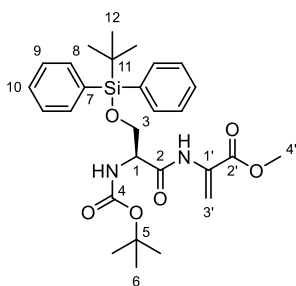
IR (neat): $\tilde{\nu} = 3350, 2954, 2858, 1744, 1668, 1498, 1366, 1167, 1112, 757, 703$ cm^{-1} .

$[\alpha]_D^{23}$ ($c = 1.065$, CHCl_3) = +6.657.

HRMS (ESI): m/z calculated for $\text{C}_{28}\text{H}_{40}\text{N}_2\text{NaO}_7\text{Si}^+$ ($[\text{M}+\text{Na}]^+$): 567.2497; found: 567.2494.

5.2.7. Boc-Ser(TBDPS)- Δ Ala-OMe (**69**)

A 25 mL Schlenk flask was charged with Boc-Ser(TBDPS)-Ser-OMe (**88**, 255 mg, 0.468 mmol, 1.00 eq.) and dry DCE (12 mL) and cooled to 0 °C. Et₃N (0.16 mL, 1.17 mmol, 2.50 eq.) was added, the solution was stirred for 10 min and MsCl (0.72 mL, 0.94 mmol, 2.00 eq.) was added. The solution allowed to warm up to room temperature and stirred for 3 h. DBU (0.35 mL, 2.34 mmol, 5.00 eq.) was added and stirring was continued for 24 h. All volatiles were removed under reduced pressure and the residue was taken up in CH₂Cl₂ (15 mL), washed with aq. citric acid (10%, 15 mL), sat. aq. NaHCO₃-sol. (2 x 15 mL) and brine (15 mL). The organic phase was dried over Na₂SO₄, filtered and the solvent was removed under reduced pressure. The crude product was purified by column chromatography (SiO₂, *c*-hexane/EtOAc 9:1) affording Boc-Ser(TBDPS)- Δ Ala-OMe (**69**, 117 mg, 0.223 mmol, 48%) as a colorless solid.



R_f = 0.6 (*c*-hexane/EtOAc = 10:1).

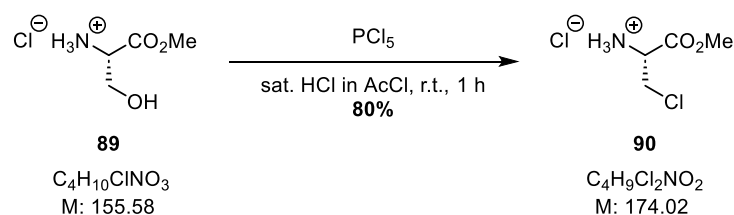
¹H NMR (600 MHz, CDCl₃) δ = 8.56 (s, 1H, NH), 7.61 (d, J = 7.2 Hz, 4H, H8), 7.43 (dt, J = 6.7 Hz, J = 2.9 Hz, 2H, H10), 7.38 (td, J = 7.4 Hz, J = 3.2 Hz, 4H, H9), 6.67 (s, 1H, H3'a), 5.94 (s, 1H, H3'b), 5.30 (s, 1H, NH), 4.31 (s, 1H, H_{Rot}3a), 4.09 (d, J = 10.1 Hz, 1H, H_{Rot}3b), 3.83 (s, 3H, H4'), 3.80 (d, J = 4.4 Hz, 1H, H1), 1.46 (s, 9H, H6), 1.04 (s, 9H, H12) ppm.

¹³C NMR (151 MHz, CDCl₃) δ = 169.5 (C2), 167.7 (C4), 164.3 (C2'), 135.6 (C8), 132.9 (C7), 130.8 (C1'), 130.1 (C10), 128.0 (C9), 109.5 (C3'), 80.7 (C5), 64.2 (C1), 57.0 (C4'), 53.7 (C3), 28.4 (C6), 26.9 (C12), 19.3 (C11) ppm.

IR (neat): $\tilde{\nu}$ = 3385, 3071, 2931, 2857, 1689, 1520, 1325, 1164, 1110, 904, 823, 702 cm⁻¹.

$[\alpha]_D^{23}$ (c = 1.235, CHCl₃) = -11.506.

HRMS (ESI): m/z calculated for C₂₈H₃₉N₂O₆Si⁺ ([M+H]⁺): 527.2546; found: 527.2534.

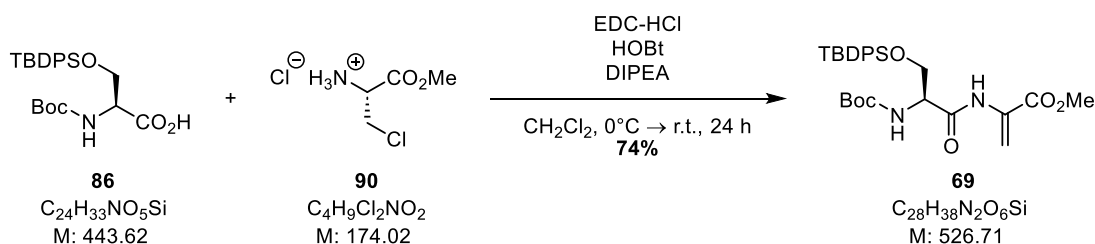
5.2.8. 3-Chloro-L-alanine methylester hydrochloride (**90**)

A 100 mL three-necked flask equipped with a dropping funnel and valve was connected to a washing bottle filled with CaCl_2 using PTFE tubing, connected to a second 50 mL three-necked flask equipped with a teflon tube connected to a bubbler. The 100 mL flask was used for dry HCl generation and was charged with NaCl, the dropping funnel was charged with conc. H_2SO_4 (10 mL). The second flask was used for the reaction, charged with AcCl (16 mL) and cooled to 0 °C. HCl was generated by dropwise addition of H_2SO_4 to NaCl over 10 min to saturate AcCl with HCl. After gas formation subsided, the whole apparatus was flushed with a slow stream of Ar. H-Ser-OMe HCl (**89**, 2.00 g, 12.9 mmol, 1.00 eq.) was added to the reaction flask under vigorous stirring. PCl_5 (2.94 g, 14.1 mmol, 1.10 eq.) was added in three portions, the reaction was allowed to warm up to room temperature and stirring was continued for 1 h. Toluene (20 mL) was added and the precipitate was filtered, washed with toluene (2 x 20 mL) and *n*-pentane (20 mL). The product was dried under reduced pressure affording chloroalanine **90** (1.79 g, 10.3 mmol, 80%) as a colorless solid.

^1H NMR (500 MHz, D_2O) δ = 4.69 (dd, J = 4.5, 3.3 Hz, 1H), 4.21 (dd, J = 12.9, 4.5 Hz, 1H), 4.09 (dd, J = 12.9, 3.2 Hz, 1H), 3.89 (s, 3H) ppm.

^{13}C NMR (126 MHz, D_2O) δ = 167.9, 54.3, 54.1, 41.9 ppm.

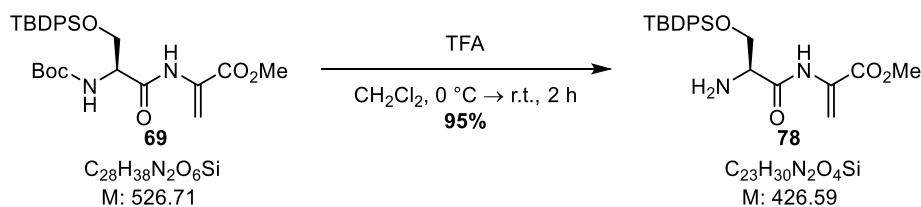
The analytical data of compound **90** is in agreement with the literature.^[126]

5.2.9. Boc-Ser(TBDPS)- Δ Ala-OMe (**69**)

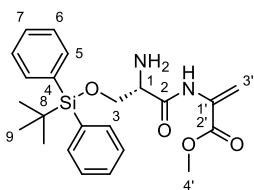
A 25 mL Schlenk flask was charged with Boc-Ser(TBDPS)-OH (**86**, 0.487 g, 1.10 mmol, 1.00 eq.), chloroalanine **90** (0.248 g, 1.43 mmol, 1.30 eq.) and HOBt (0.223 g, 1.65 mmol, 1.50 eq.) in dry CH_2Cl_2 (8 mL). The reaction mixture was cooled to 0 °C and EDC-HCl (0.442 g, 2.31 mmol, 2.10 eq.) followed by DIPEA (0.56 mL, 3.23 mmol, 4.50 eq.) were added. The reaction was allowed to warm up to room temperature and stirred for 24 h. The reaction mixture was diluted with EtOAc (20 mL), washed with aq. HCl (0.5 M, 2 x 10 mL), dried over Na_2SO_4 , filtered and the solvent was removed under reduced pressure. The crude product was purified by column chromatography (SiO_2 , *c*-hexane/EtOAc 1:0 → 4:1) affording Boc-Ser(TBDPS)- Δ Ala-OMe (**69**, 430 mg, 0.816 mmol, 74%) as a colorless solid.

The analytical data of the product is in agreement with the analytical data of experiment 0.

5.2.10. H-Ser(TBDPS)- Δ Ala-OMe (78)



A 10 mL Schlenk flask was charged with dipeptide **69** (150 mg, 0.285 mmol, 1.00 eq.) in 5 mL dry CH_2Cl_2 . The solution was cooled to 0 °C and TFA (0.32 mL, 4.28 mmol, 15.0 eq.) was added dropwise. The reaction mixture was stirred for 2 h, concentrated under reduced pressure and immediately diluted with EtOAc (10 mL). The organic phase was washed with sat. aq. NaHCO_3 -sol. (10 mL), water (10 mL), brine (10 mL), dried over Na_2SO_4 , filtered and the solvent was removed under reduced pressure affording free amine **78** (115 mg, 0.270 mmol, 95%) as a colorless oil.



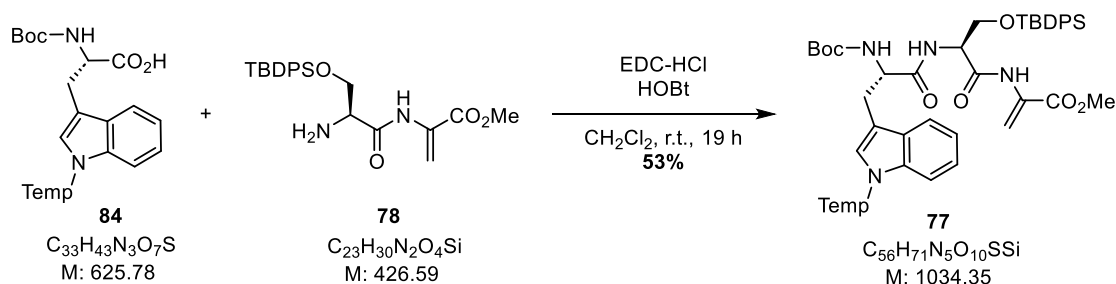
$^1\text{H NMR}$ (600 MHz, CDCl_3) δ = 7.65 – 7.62 (m, 4H, H5), 7.45 – 7.41 (m, 2H, H7), 7.40 – 7.36 (m, 4H, H6), 6.63 (s, 1H, H3'a), 5.89 (d, J = 1.7 Hz, 1H, H3'b), 3.98 – 3.95 (m, 1H, $\text{H}_{\text{Rot}3\text{a}}$), 3.91 – 3.87 (m, 1H, $\text{H}_{\text{Rot}3\text{b}}$), 3.85 (s, 3H, H4'), 3.55 (dd, J = 5.9 Hz, 4.0 Hz, 1H, H1), 1.84 (s, 2H, NH_2), 1.05 (s, 9H, H9) ppm.

$^{13}\text{C NMR}$ (151 MHz, CDCl_3) δ = 171.9 (C2), 164.4 (C2'), 135.50; 135.48 (C5), 133.1; 132.86 (C4), 130.94 (C1'), 129.81 (C7), 127.77; 127.75 (C6), 109.4 (C3'), 66.0 (C1), 57.3 (C4'), 52.7 (C3), 26.8; 26.6 (C9), 19.3 (C8) ppm.

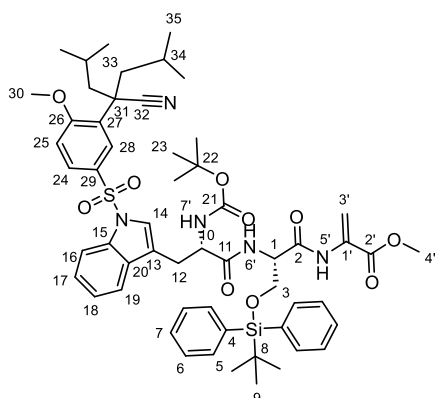
IR (neat): $\tilde{\nu}$ = 3074, 2931, 2857, 1685, 1638, 1513, 1444, 1323, 1112, 825, 746 cm^{-1} .

$[\alpha]_{\text{D}}^{25}$ (c = 0.745, CHCl_3) = -12.000.

HRMS (ESI): m/z calculated for $\text{C}_{23}\text{H}_{31}\text{N}_2\text{O}_4\text{Si}^+$ ($[\text{M}+\text{H}]^+$): 427.2048; found: 427.2034.

5.2.11. Boc-Trp(Temp)-Ser(TBDPS)- Δ Ala-OMe (**77**)

A 25 mL Schlenk flask was charged with Boc-Trp(Temp)-OH (**84**, 125 mg, 199 μmol , 1.00 eq.), H-Ser(TBDPS)- Δ Ala-OMe (**78**, 85.0 mg, 199 μmol , 1.00 eq.) and HOBT (50.0 mg, 370 μmol , 1.50 eq.) in dry CH_2Cl_2 (10 mL). The reaction mixture was cooled to 0 °C and EDC-HCl (88.0 g, 459 μmol , 2.10 eq.) was added. The reaction was allowed to warm up to room temperature and stirred for 19 h. The reaction mixture was diluted with EtOAc (30 mL), washed with aq. HCl (0.5 M, 3 x 10 mL), dried over Na_2SO_4 , filtered and the solvent was removed under reduced pressure. The crude product was purified by column chromatography (SiO_2 , *c*-hexane/EtOAc 2:1) affording Boc-Trp(Temp)-Ser(TBDPS)- Δ Ala-OMe (**77**, 109 mg, 105 μmol , 53%) as a colorless solid.



$R_f = 0.30$ (*n*-pentane/EtOAc = 3:1).

m.p. = 92.0-93.5 °C.

$^1\text{H NMR}$ (600 MHz, CDCl_3) δ = 8.38 (s, 1H, $\text{NH}5'$), 8.04 (d, $J = 2.4$ Hz, 1H, H28), 7.92 (d, $J = 8.2$ Hz, 1H, H19), 7.77 (dd, $J = 8.8$ Hz, 2.4 Hz, 1H, H24), 7.60 – 7.56 (m, 4H, H5), 7.47 – 7.44 (m, 1H, H16), 7.44 (s, 1H, H14), 7.42 (ddt, $J = 7.2$, 5.2 Hz, $J = 1.6$ Hz, 2H, H7), 7.39 – 7.35 (m, 4H, H6), 7.24 (ddd, $J = 8.4$, 7.2 Hz, 1.1 Hz, 1H, H18), 7.10 (t, $J = 7.4$ Hz, 1H, H17), 6.95 – 6.85 (m, 1H, $\text{NH}6'$), 6.88 – 6.80 (m, 1H, H25), 6.60 (s, 1H, H3'a), 5.96 (d, $J = 1.4$ Hz, 1H, H3'b), 5.12 – 4.97 (m, 1H, $\text{NH}7'$), 4.52 (td, $J = 6.7$, 3.8 Hz, 1H, H10), 4.49 – 4.45 (m, 1H, $\text{H}_{\text{Rot}3}$), 4.05 – 3.97 (m, 1H, $\text{H}_{\text{Rot}3}$), 3.81 (s, 3H, H4'), 3.80 (s, 3H, H30), 3.63 – 3.54 (m, 1H, H1), 3.23 – 3.14 (m, 1H, $\text{H}_{\text{Rot}12}$), 3.17 – 3.05 (m, 1H, $\text{H}_{\text{Rot}12}$), 2.13 (dt, $J = 14.3$, 5.5 Hz, 2H, $\text{H}_{\text{Rot}33}$), 1.66 (ddd, $J = 14.3$, 7.1, 3.3 Hz, 2H, $\text{H}_{\text{Rot}33}$), 1.40 (s, 9H, H23), 1.20 (ddd, $J = 26.8$, 13.0, 6.5 Hz, 2H, H34), 1.01 (s, 9H, H9), 0.77 (d, $J = 6.7$ Hz, 3H, $\text{H}_{\text{Rot}35}$), 0.75 (d, $J = 6.7$ Hz, 3H, $\text{H}_{\text{Rot}35}$), 0.38 (d, $J = 6.6$ Hz, 3H, $\text{H}_{\text{Rot}35}$), 0.35 (d, $J = 6.6$ Hz, 3H, $\text{H}_{\text{Rot}35}$). ppm.

^{13}C NMR (151 MHz, CDCl_3) δ = 171.8 (C2), 168.6 (C2'), 164.2 (C11), 161.5 (C21), 155.7 (C26), 135.9; 135.8 (C5), 135.6 (C15), 132.9; 132.7 (C4), 131.13 (C20), 131.09 (C1'), 130.30; 130.29 (C7), 130.2 (C29), 129.1 (C24), 128.7 (C28), 128.23; 128.18 (C6), 126.7 (C27), 125.5 (C18), 125.1 (C14), 123.7 (C17), 123.3 (C13), 119.8 (C16), 118.6 (C32), 114.3 (C19), 111.9 (C25), 110.2 (C3'), 80.9 (C22), 64.0 (C1), 56.0 (C4'), 55.7 (C30), 53.7 (C10), 53.2 (C3), 47.3 (C31), 46.92; 46.91 (C33), 28.52; 28.47(C23), 27.1 (C12), 26.1; 26.0 (C9), 23.64 (C34), 23.60; 23.57 (C35), 19.5 (C8). ppm.

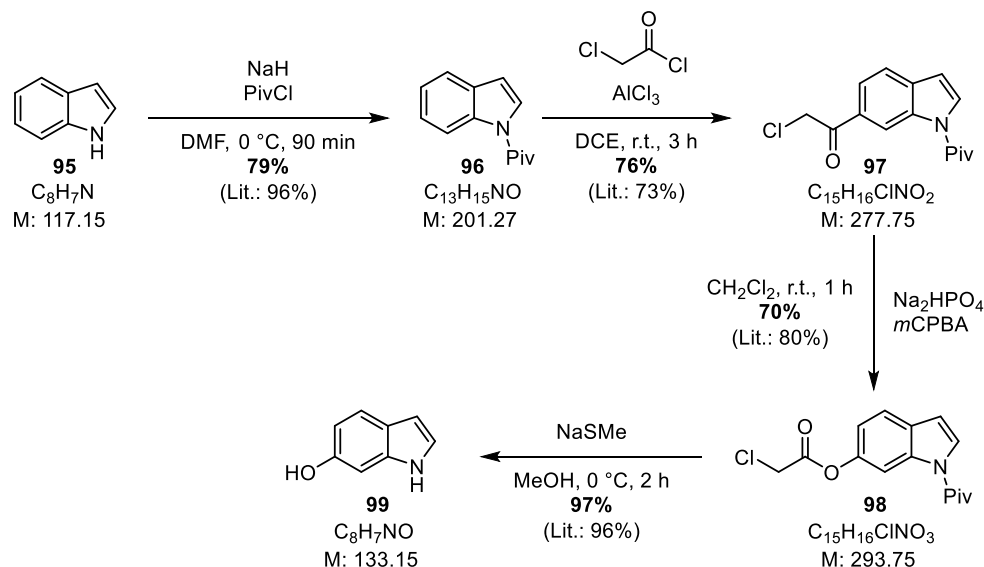
IR (neat): $\tilde{\nu}$ = 3310, 2956, 2858, 1696, 1656, 1518, 1446, 1367, 1261, 1172, 1114, 1019, 824, 745, 706 cm^{-1} .

$[\alpha]_{\text{D}}^{25}$ (c = 0.500, CHCl_3) = +4.800.

HRMS (ESI): m/z calculated for $\text{C}_{56}\text{H}_{72}\text{N}_5\text{O}_{10}\text{SSi}^+$ ($[\text{M}+\text{H}]^+$): 1034.4764; found: 1034.4767.

5.3. Synthesis of a 6-Triflyl Tryptophan

5.3.1. 6-Hydroxyindole (**99**)



6-Hydroxyindole (**99**) was synthesized according to the procedure by TERANISHI *et al.*^[132] Starting from indole (**95**, 10.0 g, 85.4 mmol), pivaloylation afforded indole **96** (13.6 g, 67.6 mmol, 79%). Chloroacetylation of indole **96** (3.93 g, 19.5 mmol) gave the acetylated derivative **97** (4.11 g, 14.8 mmol, 76%). BAEYER-VILLIGER oxidation of **97** (10.1 g, 36.4 mmol) afforded indole **98** (7.41 g, 25.2 mmol, 70%). Deprotection of indole **98** (2.38 g, 8.09 mmol) provided 6-hydroxyindole (**99**, 1.04 g, 7.83 mmol, 97%) as a colorless solid.

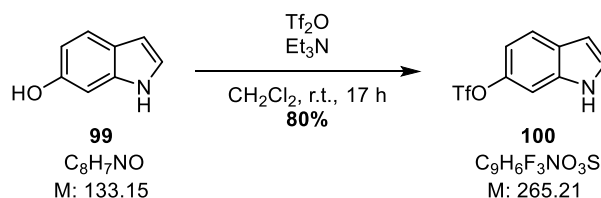
$R_f = 0.2$ (*c*-hexane/EtOAc = 4:1).

1H NMR (600 MHz, MeOD- d_4) $\delta = 7.33$ (dd, $J = 8.5, 0.6$ Hz, 1H), 7.03 (d, $J = 3.2$ Hz, 1H), 6.80 (dt, $J = 2.1, 0.8$ Hz, 1H), 6.59 (dd, $J = 8.5, 2.2$ Hz, 1H), 6.31 (dd, $J = 3.2, 0.9$ Hz, 1H) ppm.

^{13}C NMR (151 MHz, MeOD- d_4) $\delta = 153.8, 138.6, 124.0, 123.3, 121.5, 110.3, 102.1, 97.5$ ppm.

The analytical data of 6-hydroxyindole (**99**) is in agreement with the literature.^[132]

5.3.2. 1H-Indol-6-yl trifluoromethanesulfonate (**100**)



A 100 mL Schlenk flask was charged with 6-hydroxyindole (**99**, 2.00 g, 15.0 mmol, 1.00 eq.) and dry CH_2Cl_2 (40 mL). The solution was cooled to 0 °C and dry Et_3N (4.2 mL, 30.0 mmol, 2.00 eq.), followed by Tf_2O (freshly distilled from P_2O_5 , 3.0 mL, 18.0 mmol, 1.20 eq.) were added dropwise. The reaction mixture was allowed to warm up to room temperature and the reaction mixture was poured into aq. HCl (1 M, 100 mL) and stirred for 5 min at room temperature. The phases were separated and the aqueous phase was extracted

with CH₂Cl₂ (50 mL). The combined organic phases were dried over MgSO₄, filtered and the solvent was removed under reduced pressure. The black crude product was purified by column chromatography (SiO₂, *n*-pentane/EtOAc 7:1) to afford triflate **100** (3.18 g, 12.0 mmol, 80%) as a pale yellow solid.

R_f = 0.4 (*c*-hexane/EtOAc = 4:1).

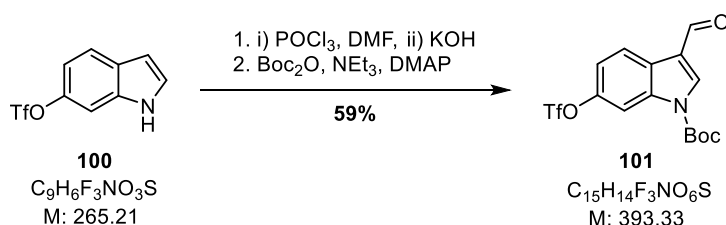
¹H NMR (600 MHz, CDCl₃) δ = 8.31 (s, 1H), 7.65 (d, *J* = 8.6 Hz, 1H), 7.34 (dd, *J* = 2.3, 1.1 Hz, 1H), 7.31 (td, *J* = 2.9, 2.3, 0.9 Hz, 1H), 7.04 (dt, *J* = 8.6, 1.6 Hz, 1H), 6.60 (ddt, *J* = 3.2, 2.0, 1.0 Hz, 1H) ppm.

¹⁹F NMR (565 MHz, CDCl₃) δ = -72.62 ppm.

¹³C NMR (151 MHz, CDCl₃) δ = 145.6, 135.2, 127.8, 126.6, 121.9, 119.0 (q, 320.9 Hz), 113.5, 104.4, 103.2 ppm.

IR (neat): $\tilde{\nu}$ = 3450, 1458, 1417, 1344, 1208, 1139, 1103, 1090, 946, 875, 809, 728 cm⁻¹.

5.3.3. *tert*-Butyl 3-formyl-6-(((trifluoromethyl)sulfonyl)oxy)-1*H*-indole-1-carboxylate (**101**)



A 25 mL Schlenk tube was charged with dry DMF (3 mL) and cooled to 0 °C. POCl₃ (0.28 mL, 3.00 mmol, 1.50 eq.) was added dropwise and the solution was stirred for 30 min. The starting material **100** (0.530 g, 2.00 mmol, 1.00 eq.) dissolved in dry DMF (2 mL) was added over 15 min using a syringe pump. The reaction mixture was allowed to warm up to room temperature and stirring was continued for 90 min. The reaction mixture was treated with aq. KOH-sol. (20%, 4 mL). The mixture was heated to reflux for 3 h and cooled down to room temperature. The mixture was partitioned between sat. aq. NaHCO₃-sol. (80 mL) and EtOAc (80 mL). The phases were separated and the aqueous phase was extracted with EtOAc (2 x 50 mL). The combined organic phases were washed with brine (80 mL), dried over Na₂SO₄, filtered and the solvent was removed under reduced pressure. The residue was taken up in CH₂Cl₂ (3 mL) and Boc₂O (0.480 g, 2.20 mmol, 1.10 eq.) followed by Et₃N (0.56 mL, 4.00 mmol, 2.00 eq.) were added. DMAP (48.8 mg, 0.40 mmol, 0.20 eq.) was added and the solution was stirred for 1 h at room temperature. The solvent was removed under reduced pressure and the crude mixture was purified by column chromatography (SiO₂, *c*-hexane/EtOAc 9:1 → 4:1) affording carbaldehyde **101** (0.460 g, 1.17 mmol, 59%) as colorless crystals.

R_f = 0.5 (*c*-hexane/EtOAc = 2:1).

¹H NMR (500 MHz, CDCl₃) δ = 10.10 (s, 1H), 8.36 (dd, *J* = 8.7, 0.5 Hz, 1H), 8.32 (s, 1H), 8.15 (d, *J* = 2.3 Hz, 1H), 7.30 (dd, *J* = 8.7, 2.3 Hz, 1H), 1.72 (s, 9H) ppm.

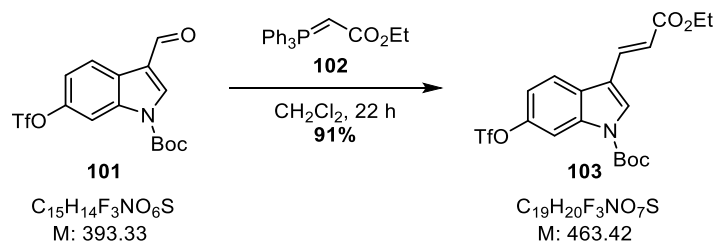
¹⁹F NMR (471 MHz, CDCl₃) δ = -72.56 ppm.

¹³C NMR (126 MHz, CDCl₃) δ = 185.4, 148.3, 147.8, 137.8, 135.8, 126.0, 123.6, 121.1, 118.2, 109.3, 87.0, 28.1 ppm.

IR (neat): $\tilde{\nu}$ = 3139, 2982, 2935, 2822, 1752, 1681, 1616, 1589, 1550, 1476, 1421, 1397, 1373, 1350, 1321, 1301, 1256, 1207, 1136, 1086, 920, 868, 842, 767, 741, 722 cm^{-1} .

HRMS (ESI): m/z calculated for $\text{C}_{15}\text{H}_{14}\text{F}_3\text{NNaO}_6\text{S}^+$ ($[\text{M}+\text{Na}]^+$): 416.0386; found: 416.0410.

5.3.4. *tert*-Butyl (*E*)-3-(3-ethoxy-3-oxoprop-1-en-1-yl)-6-(((trifluoromethyl)sulfonyl)oxy)-1*H*-indole-1-carboxylate (**103**)



A 5 mL Schlenk tube was charged with carbaldehyde **101** (0.250 g, 0.636 mmol, 1.00 eq.), ylide **102** (0.266 g, 0.763 mmol, 1.20 eq.) and dry CH_2Cl_2 (3 mL). The solution was stirred for 22 h at room temperature, filtered through a silica plug (2 cm) and the solvent of the filtrate was removed under reduced pressure. The crude product was purified by column chromatography (SiO_2 , *c*-hexane/*EtOAc* 19:1 \rightarrow 6:1) affording acrylate **103** (0.267 g, 0.576 mmol, 91%) as a colorless oil.

R_f = 0.5 (*c*-hexane/*EtOAc* = 4:1).

^1H NMR (500 MHz, CDCl_3) δ = 8.19 (s, 1H), 7.94 (s, 1H), 7.87 (d, J = 8.7 Hz, 1H), 7.79 (dd, J = 16.1, 0.7 Hz, 1H), 7.27 – 7.24 (m, 1H), 6.51 (d, J = 16.2 Hz, 1H), 4.29 (q, J = 7.1 Hz, 2H), 1.69 (s, 9H), 1.36 (t, J = 7.1 Hz, 3H) ppm.

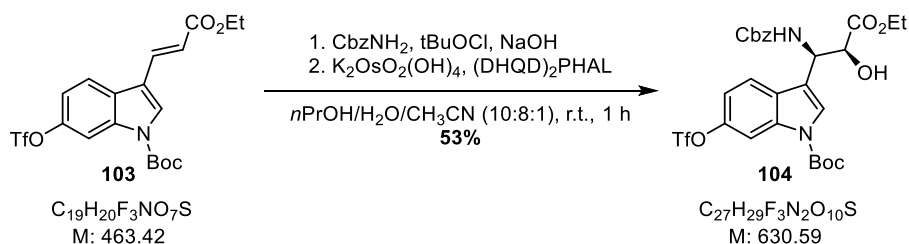
^{19}F NMR (565 MHz, CDCl_3) δ = -72.6 ppm.

^{13}C NMR (151 MHz, CDCl_3) δ = 167.2, 148.6, 147.3, 136.0, 135.3, 129.9, 127.8, 121.3, 120.0, 118.6, 117.9, 117.1, 116.6, 109.5, 86.0, 60.7, 28.2, 14.5 ppm.

IR (neat): $\tilde{\nu}$ = 2983, 2937, 1746, 1713, 1639, 1474, 1443, 1422, 1370, 1243, 1211, 1151, 1092, 1043, 977, 928, 852 cm^{-1} .

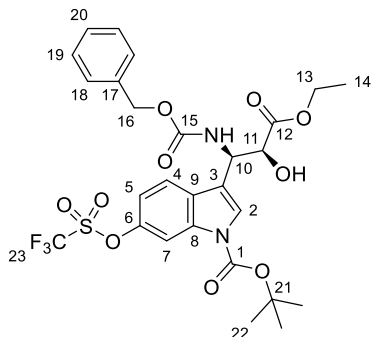
HRMS (ESI): m/z calculated for $\text{C}_{19}\text{H}_{20}\text{F}_3\text{NNaO}_7\text{S}^+$ ($[\text{M}+\text{Na}]^+$): 486.0805; found: 486.0808.

5.3.5. *tert*-Butyl 3-(((1*R*,2*S*)-2-(((benzyloxy)carbonyl)amino)-3-ethoxy-1-hydroxy-3-oxopropyl)-6-(((trifluoromethyl)sulfonyl)oxy)-1-indole-1-carboxylate (**104**)



Compound **104** was prepared according to **GP1** starting from **103** (150 mg, 0.325 mmol, 1.00 eq.), benzyl carbamate (152 mg, 1.00 mmol, 3.10 eq.), potassium osmate dihydrate (9.54 mg, 25.8 μmol , 0.08 eq.),

*t*BuOCl (110 μ L, 0.971 mmol, 3.00 eq.), (DHQD)₂PHAL (25.2 mg, 32.3 μ mol, 0.10 eq.), sat. aq. NaOH-sol. (0.40 M, 2.47 mL, 0.987 mmol, 3.05 eq.), *n*PrOH (3.34 mL), CH₃CN (0.33 mL) and water (0.20 mL). After 1 h, full conversion was observed. Column chromatography (SiO₂, *c*-hexane/EtOAc 9:1 \rightarrow 5:1) afforded protected benzylamine **104** (108 mg, 0.171 mmol, 53%) as colorless crystals.



m.p. = 129.4-130.6 °C.

R_f = 0.43 (*c*-hexane/EtOAc = 2:1).

¹H NMR (700 MHz, CDCl₃) δ = 8.11 (s, 1H, H7), 7.80 (s, 1H, H2), 7.72 (d, *J* = 8.7 Hz, 1H, H4 or H5), 7.38 – 7.28 (m, 5H, H18, H19, H20), 7.18 – 7.13 (m, 1H, H4 or H5), 5.57 (d, *J* = 9.8 Hz, 1H, NH), 5.44 (d, 3*J* = 9.8 Hz, 1H, H11), 5.09 (Ψ q, *J* = 8.0 Hz, 2H, H16), 4.59 (d, 3*J* = 4.0 Hz, 1H, H10), 4.35 – 4.24 (m, 2H, H13), 3.36 (d, *J* = 4.0 Hz, 1H, OH), 1.67 (s, 9H, H22), 1.31 (t, 3*J* = 7.1 Hz, 3H, H14) ppm.

¹⁹F NMR (565 MHz, CDCl₃) δ = -72.56 ppm.

¹³C NMR (176 MHz, CDCl₃) δ = 172.7 (1C, C12), 155.7 (1C, C15), 149.1 (1C, C1), 147.1 (1C, C6), 136.3, 135.2, 128.7, 128.4, 128.2, 126.2 (1C, C2), 120.8 (1C, C4 or C5), 119.9, 119.1, 118.1, 116.4 (1C, C4 or C5), 109.2 (1C, C7), 85.2 (1C, C21), 72.5 (1C, C10), 67.3 (1C, C16), 63.1 (1C, C13), 49.5 (1C, C11), 28.2 (3C, C22), 14.2 (1C, C14) ppm.

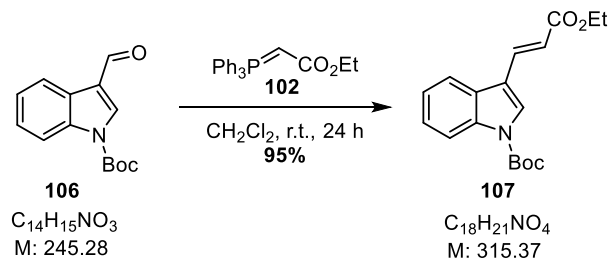
IR (neat): $\tilde{\nu}$ = 3349, 2983, 2934, 1738, 1615, 1523, 1472, 1445, 1422, 1330, 1294, 1245, 1214, 1143, 1117, 924 cm⁻¹.

$[\alpha]_D^{25}$ (*c* = 0.820, CHCl₃) = -22.34.

HRMS (ESI): *m/z* calculated for C₂₇H₂₉F₃N₂NaO₁₀S⁺ ([M+Na]⁺): 653.1387; found: 653.1385.

5.4. SHARPLESS Asymmetric Aminohydroxylation

5.4.1. *tert*-Butyl (*E*)-3-(3-ethoxy-3-oxoprop-1-en-1-yl)-1*H*-indole-1-carboxylate (**107**)



A 25 mL Schlenk tube was charged with carbaldehyde **106** (0.600 g, 2.45 mmol, 1.00 eq.) in dry CH_2Cl_2 (13 mL). Ylide **102** (0.937 g, 2.69 mmol, 1.10 eq.) was added and the solution was stirred for 24 h at room temperature. The solution was filtered over a silica plug (3 cm), the solvent was removed under reduced pressure and the crude product was purified by column chromatography (SiO_2 , *c*-hexane/EtOAc 19:1 → 9:1) to give ester **107** (0.731 g, 2.32 mmol, 95%) as a colorless solid.

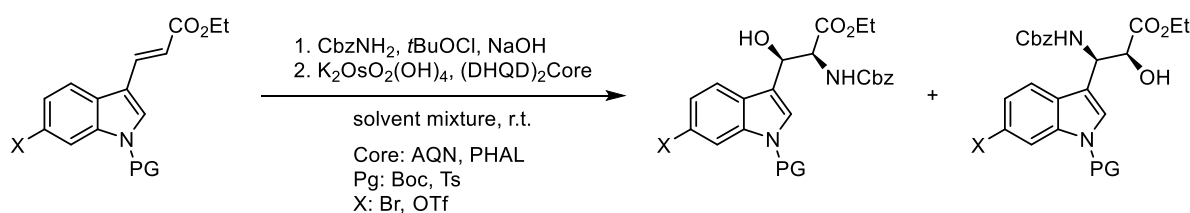
$R_f = 0.6$ (*c*-hexane/EtOAc = 4:1).

$^1\text{H NMR}$ (500 MHz, CDCl_3) $\delta = 8.20$ (d, $J = 8.2$ Hz, 1H), 7.92 – 7.77 (m, 3H), 7.38 (ddd, $J = 8.4, 7.2, 1.3$ Hz, 1H), 7.36 – 7.31 (m, 1H), 6.54 (d, $J = 16.1$ Hz, 1H), 4.28 (q, $J = 7.1$ Hz, 2H), 1.68 (s, 9H), 1.36 (t, $J = 7.1$ Hz, 3H) ppm.

$^{13}\text{C NMR}$ (126 MHz, CDCl_3) $\delta = 167.6, 149.3, 136.5, 136.4, 128.8, 128.0, 125.4, 123.7, 120.4, 117.6, 116.9, 115.7, 84.8, 60.5, 28.3, 14.5$ ppm.

The analytical data of compound **107** is in agreement with the literature.^[196]

5.4.2. General Procedure for the SHARPLESS Asymmetric Aminohydroxylation (GP1)

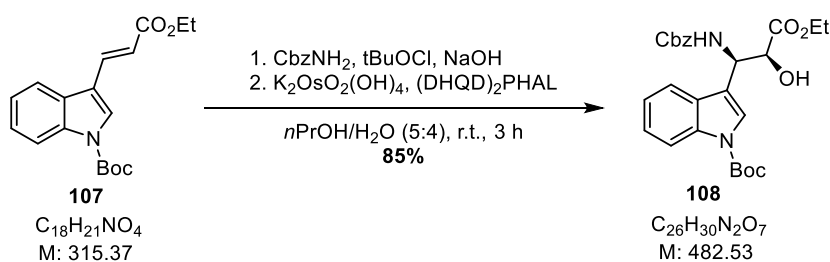


Caution! The reaction is oxygen- and light sensitive, therefore all solutions and solvents, incl. aq. NaOH-sol. (0.40 M), *n*PrOH, CH_3CN and water were degassed by three FPT cycles freshly before use. Additionally, the stoichiometry has to be very precise, e.g. excess/substoichiometric base has a negative impact on the reaction, measurements using calibrated equipment (**calibrated** Eppendorf syringes or graduated pipettes, instead of syringes) is encouraged. The quality of *t*BuOCl can vary from batch to batch and may diminish upon prolonged storage. Therefore, *t*BuOCl was freshly prepared and titrated using iodometric redox titration.

A Schlenk flask was charged with benzyl carbamate (3.10 eq.), aq. NaOH-sol. (0.40 M, 2.95 eq.), *n*PrOH (1.55 mL/mmol carbamate) and cooled to 0 °C. Freshly synthesized *t*BuOCl (purity >96%, 3.00 eq.) was

added dropwise over 2 min, the reaction was allowed to warm up to room temperature and stirred for 30 min. The ligand, (DHQD)₂Core (0.10 eq.) dissolved in *n*PrOH and/or CH₃CN (31.8 mL/mmol ligand) was added in one portion, followed by addition of the starting material (1.00 eq.), dissolved in *n*PrOH and/or CH₃CN (19.0 mL/mmol starting material). Subsequent addition of potassium osmate dihydrate (0.08 eq.) dissolved in aq. NaOH-sol. (0.40 M, 0.10 eq.) and water (25 mL/mmol osmate) results in a pale green suspension. The reaction mixture was stirred under light exclusion at room temperature and treated with sat. aq. NaHSO₃-sol. (40 mL/mmol) at 0 °C for 30 min. *n*PrOH and/or CH₃CN were removed under reduced pressure and the aqueous phase was extracted with EtOAc (3 x 10 mL/mmol). The combined organic phases were washed with water (10 mL/mmol), sat. aq. NH₄Cl-sol. (10 mL/mmol), brine (10 mL/mmol), dried over Na₂SO₄, filtered and the solvent was removed under reduced pressure. The crude product was purified by column chromatography (SiO₂, *c*-hexane/EtOAc).

5.4.3. *tert*-Butyl 3-((1*R*,2*S*)-1-(((benzyloxy)carbonyl)amino)-3-ethoxy-2-hydroxy-3-oxopropyl)-1*H*-indole-1-carboxylate (**108**)



Compound **108** was prepared according to **GP1** starting from **107** (31.5 mg, 0.100 mmol, 1.00 eq.), benzyl carbamate (46.9 mg, 0.310 mmol, 3.10 eq.), potassium osmate dihydrate (2.95 mg, 8.00 μ mol, 0.080 eq.), *t*BuOCl (33.9 μ L, 0.300 mmol, 3.00 eq.), (DHQD)₂PHAL (7.79 mg, 10.0 μ mol, 0.10 eq.), sat. aq. NaOH-sol. (0.40 M, 0.763 mL, 0.305 mmol, 3.05 eq.), *n*PrOH (1.20 mL) and water (0.20 mL). After 3 h, full conversion was observed. Column chromatography (SiO₂, *c*-hexane/EtOAc 9:1 \rightarrow 3:1) afforded protected benzylamine (41.0 mg, 85.0 μ mol; 85%, >99% *ee*) as a colorless solid.

*R*_f = 0.5 (*c*-hexane/EtOAc = 2:1).

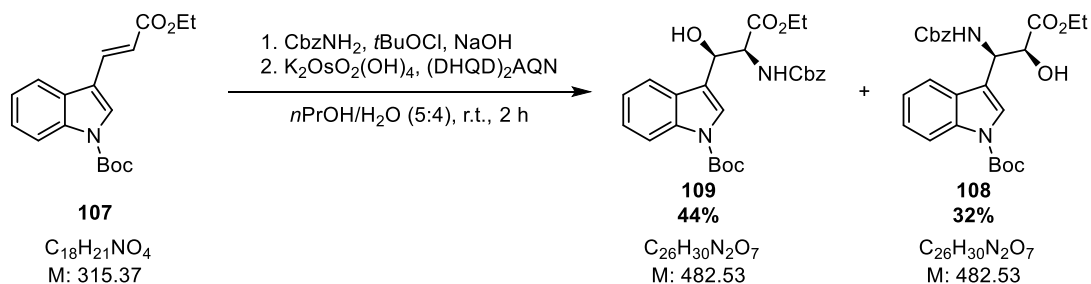
¹H NMR (600 MHz, CDCl₃) δ = 8.14 (s, 1H), 7.72 – 7.62 (m, 2H), 7.43 – 7.28 (m, 6H), 7.24 (d, *J* = 7.5 Hz, 1H), 5.60 (d, *J* = 9.7 Hz, 1H), 5.46 (d, *J* = 9.8 Hz, 1H), 5.09 (q, *J* = 12.3 Hz, 2H), 4.62 (s, 1H), 4.29 (qq, *J* = 7.5, 3.4 Hz, 2H), 3.32 (s, 1H), 1.66 (s, 9H), 1.31 (t, *J* = 7.2 Hz, 3H) ppm.

¹³C NMR (151 MHz, CDCl₃) δ = 173.0, 155.7, 149.7, 136.4, 128.6, 128.3, 128.1, 124.9, 124.0, 122.9, 119.5, 119.0, 115.5, 84.1, 72.4, 67.2, 62.9, 49.9, 28.3, 14.2 ppm.

IR (neat): $\tilde{\nu}$ = 3614, 2955, 2912, 2876, 1726, 1654, 1512, 1454, 1417, 1328, 1260, 1222, 1171, 1083, 1051, 1017, 981, 846 cm⁻¹.

HRMS (ESI): *m/z* calculated for C₂₆H₃₀N₂NaO₇⁺ ([M+Na]⁺): 505.1945; found: 505.1968.

5.4.4. *tert*-Butyl 3-((1*R*,2*S*)-2-(((benzyloxy)carbonyl)amino)-3-ethoxy-1-hydroxy-3-oxopropyl)-1*H*-indole-1-carboxylate (**109**)



Compound **109** was prepared according to **GP1** starting from **107** (31.5 mg, 0.100 mmol, 1.00 eq.), benzyl carbamate (46.9 mg, 0.310 mmol, 3.10 eq.), potassium osmate dihydrate (1.47 mg, 4.00 μmol , 0.04 eq.), tBuOCl (33.9 μL , 0.300 mmol, 3.00 eq.), (DHQD)₂AQN (4.29 mg, 5.00 μmol , 0.05 eq.), sat. aq. NaOH-sol. (0.40 M, 0.763 mL, 0.305 mmol, 3.05 eq.), *n*PrOH (1.20 mL) and water (0.20 mL). After 2 h, full conversion was observed. Column chromatography (SiO₂, *c*-hexane/EtOAc 9:1 \rightarrow 3:1) afforded the desired protected benzylalcohol **109** as an inseparable mixture with benzyl carbamate (*w*=54% (determined by NMR), 39.3 mg, 43.5 μmol ; 44%) as a colorless solid. Additionally, benzylamine **108** (15.3 mg, 31.6 μmol , 32%, 94% *ee*) was isolated.

Benzylalcohol **109**:

R_f = 0.5 (*c*-hexane/EtOAc = 2:1).

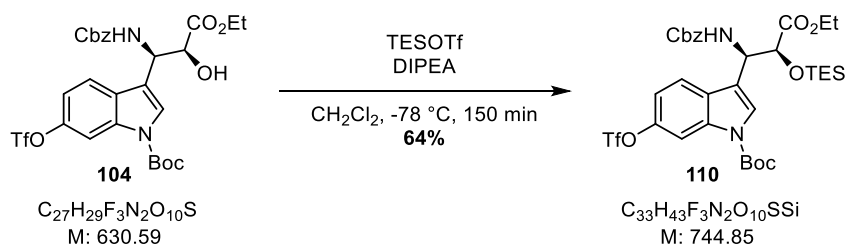
¹H NMR (600 MHz, CDCl₃) δ = 8.14 (s, 1H), 7.63 (dd, *J* = 10.5, 5.6 Hz, 2H), 7.41 – 7.19 (m, 7H), 5.75 (d, *J* = 9.0 Hz, 1H), 5.52 (d, *J* = 3.8 Hz, 1H), 5.03 (q, *J* = 12.3 Hz, 2H), 4.86 – 4.71 (m, 1H), 4.22 (tt, *J* = 10.4, 5.3 Hz, 2H), 2.96 (d, *J* = 4.5 Hz, 1H), 1.65 (s, 9H), 1.25 (t, *J* = 7.2 Hz, 3H) ppm.

¹³C NMR (151 MHz, CDCl₃) δ = 170.9, 156.9, 156.5, 136.2, 135.7, 128.7, 128.6, 128.4, 128.3, 128.1, 124.9, 123.6, 122.9, 119.8, 119.4, 115.5, 84.1, 73.5, 68.5, 67.2, 67.1, 62.1, 58.7, 29.8, 28.3, 14.2 ppm.

IR (neat): $\tilde{\nu}$ = 3723, 2955, 2912, 2876, 1731, 1653, 1506, 1454, 1417, 1370, 1338, 1308, 1269, 1255, 1222, 1153, 1136, 1083, 1051, 1017, 979, 846, 741 cm⁻¹.

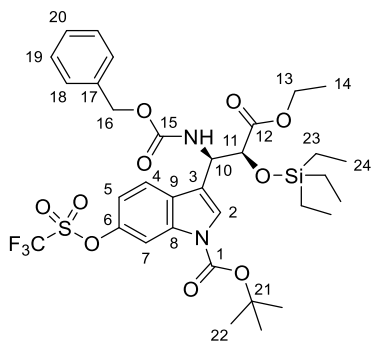
HRMS (ESI): *m/z* calculated for C₁₀H₁₉NNaO₅⁺ ([M+Na]⁺): 505.1945; found: 505.1960.

5.4.5. *tert*-Butyl 3-((5*R*,6*S*)-6-(ethoxycarbonyl)-8,8-diethyl-3-oxo-1-phenyl-2,7-dioxa-4-aza-8-siladecan-5-yl)-6-(((trifluoromethyl)sulfonyl)oxy)-1*H*-indole-1-carboxylate (**110**)



A 10 mL Schlenk flask was charged with tryptophan **104** (73.5 mg, 117 μmol , 1.00 eq.) and dry CH₂Cl₂ (4.0 mL). The solution was cooled to -78 °C and DIPEA (46.7 μL , 268 μmol , 2.30 eq.), followed by TESOTf (44.8 μL , 198 μmol , 1.70 eq.) were added subsequently. The solution was stirred for 150 min at -78 °C and

treated with sat. aq. NH_4Cl -sol. (4 mL). The reaction mixture was allowed to warm up to room temperature, the phases were separated and the aqueous phase was extracted with CH_2Cl_2 (3 x 15 mL). The combined organic phases were dried over Na_2SO_4 , filtered and the solvent was removed under reduced pressure. The crude product was purified by column chromatography (SiO_2 , *c*-hexane/EtOAc 19:1 \rightarrow 9:1) to give silyl ether **110** (108 mg, 0.171 mmol, 53%) as a colorless oil.



$R_f = 0.50$ (*c*-hexane/EtOAc = 4:1).

$^1\text{H NMR}$ (600 MHz, CDCl_3) $\delta = 8.15$ (s, 1H, H7), 7.69 (d, $J = 8.7$ Hz, 1H, H4 or H5), 7.61 (s, 1H, H2), 7.34 (q, $J = 6.4, 5.3$ Hz, 5H, H18+H19+H20), 7.17 (dd, $J = 8.7, 2.3$ Hz, 1H, H4 or H5), 5.76 (d, $J = 9.1$ Hz, 1H, NH), 5.48 (d, $J = 9.0$ Hz, 1H, H11), 5.09 (s, 2H, H16), 4.52 (s, 1H, H10), 4.22 (qq, $J = 7.4, 3.5$ Hz, 2H, H13), 1.66 (s, 9H, H22), 1.27 (t, $J = 7.2$ Hz, 3H, H14), 0.78 (t, $J = 8.0$ Hz, 9H, H24), 0.43 (dhept, $J = 31.0, 7.9$ Hz, 6H, H23) ppm.

$^{19}\text{F NMR}$ (376 MHz, CDCl_3) $\delta = -72.54$ ppm.

$^{13}\text{C NMR}$ (151 MHz, CDCl_3) $\delta = 171.2$ (1C, C12), 155.8 (1C, C15), 149.0 (1C, C1), 147.1 (1C, C6), 136.3 (1C, C_q), 135.3 (1C, C_q), 128.7 (1C, C_q), 128.4 (1C, C_q), 125.8 (1C, C2), 120.5 (1C, C4 or C5), 120.0 (C_q), 119.4, 117.9, 116.3 (1C, C4 or C5), 109.3 (1C, C7), 85.0 (1C, C21), 73.7 (1C, C10), 67.3 (1C, C16), 61.8 (1C, C13), 51.3 (1C, C11), 29.9, 28.2 (3C, C22), 14.3 (1C, C14), 6.6 (3C, C24) 4.6 (3C, C23) ppm.

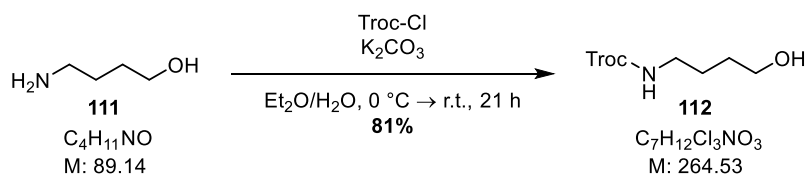
IR (neat): $\tilde{\nu} = 2957, 2937, 2913, 2879, 1739, 1499, 1472, 1445, 1423, 1371, 1330, 1245, 1211, 1143, 924, 743$ cm^{-1} .

$[\alpha]_D^{23}$ ($c = 1.18, \text{CHCl}_3$) = +6.48.

HRMS (ESI): m/z calculated for $\text{C}_{33}\text{H}_{43}\text{F}_3\text{N}_2\text{NaO}_{10}\text{SSi}^+$ ($[\text{M}+\text{Na}]^+$): 767.2252; found: 767.2242.

5.5. Synthesis of Boc- Δ Lys(Troc)-OMe (72)

5.5.1. 2,2,2-Trichloroethyl (4-hydroxybutyl)carbamate (**112**)



A 25 mL flask was charged with aq. NaOH-sol. (2 M, 11.8 mL, 23.6 mmol, 1.05 eq.) and cooled to 0 °C. 4-Aminobutanol (**111**, 2.00 g, 22.4 mmol, 1.00 eq.) was added dropwise over 5 min, followed by syringe pump addition of TrocCl (3.4 mL, 24.7 mmol, 1.10 eq.) over 1 h. The reaction mixture was allowed to warm up to room temperature and stirred for 21 h. The reaction mixture was extracted with EtOAc (50 mL), acidified with 1 M HCl to pH = 1 and extracted again with EtOAc (3 x 50 mL). The combined organic phases were washed with brine (50 mL), dried over Na₂SO₄, filtered and the solvent was removed under reduced pressure. The crude product was purified by column chromatography (SiO₂, *i*-hexane/EtOAc 1:2) to give carbamate **112** (4.82 g, 18.2 mmol, 81%) as a colorless oil.

R_f = 0.4 (*c*-hexane/EtOAc = 1:2).

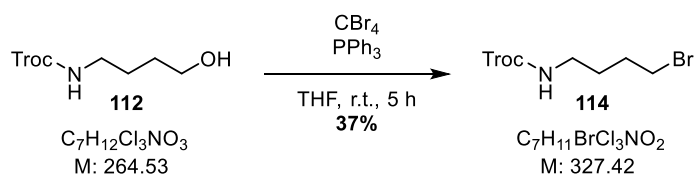
¹H NMR (500 MHz, CDCl₃) δ = 5.25 (s, 1H), 4.72 (s, 2H), 3.69 (t, *J* = 5.9 Hz, 2H), 3.28 (q, *J* = 6.5 Hz, 2H), 1.79 (s, 1H), 1.71 – 1.56 (m, 4H) ppm.

¹³C NMR (126 MHz, CDCl₃) δ = 154.9, 95.8, 74.6, 62.4, 41.1, 29.7, 26.5 ppm.

IR (neat): $\tilde{\nu}$ = 3330, 2937, 2874, 1713, 1539, 1454, 1407, 1372, 1248, 1145, 1038, 810, 723 cm⁻¹.

HRMS (ESI): *m/z* calculated for C₇H₁₂Cl₃NNaO₃⁺ ([M+Na]⁺): 285.9775; found: 285.9831.

5.5.2. 2,2,2-Trichloroethyl (4-bromobutyl)carbamate (**114**)



A 100 mL Schlenk flask was charged with alcohol **112** (2.00 g, 7.56 mmol, 1.00 eq.) in THF (75 mL). PPh₃ (1.12 g, 14.4 mmol, 1.90 eq.) was added and the solution was stirred at room temperature for 30 min. CBr₄ (1.82 g, 14.4 mmol, 1.90 eq.) was added and stirring was continued for 5 h. The solvent was removed under reduced pressure and the crude product was purified by column chromatography (SiO₂, *i*-hexane/EtOAc 7:1) affording bromide **114** (0.926 g, 2.83 mmol, 37%) as a colorless volatile liquid.

R_f = 0.5 (*c*-hexane/EtOAc = 4:1).

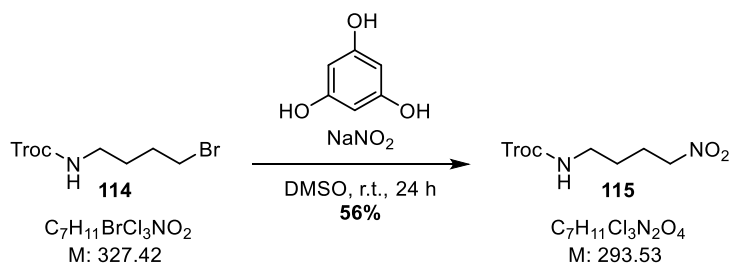
¹H NMR (500 MHz, CDCl₃) δ = 5.05 (s, 1H), 4.73 (s, 2H), 3.44 (t, *J* = 6.6 Hz, 2H), 3.29 (td, *J* = 7.0, 6.1 Hz, 2H), 1.92 (ddt, *J* = 9.5, 8.0, 6.4 Hz, 2H), 1.78 – 1.66 (m, 2H) ppm.

¹³C NMR (126 MHz, CDCl₃) δ = 154.8, 95.7, 74.6, 40.5, 33.1, 29.8, 28.6 ppm.

IR (neat): $\tilde{\nu}$ = 3339, 2946, 2864, 1714, 1521, 1446, 1405, 1365, 1236, 1140, 1093, 1051, 950, 873, 818, 768, 723 cm^{-1} .

HRMS (ESI): m/z calculated for $\text{C}_7\text{H}_{11}\text{BrCl}_3\text{KNO}_2^+$ ($[\text{M}+\text{K}]^+$): 363.8670; found: 363.8716.

5.5.3. 2,2,2-Trichloroethyl (4-nitrobutyl)carbamate (**115**)



A 25 mL Schlenk flask was charged with phloroglucinol (0.392 g, 3.11 mmol, 1.10 eq.), NaNO_2 (0.390 g, 5.66 mmol, 2.00 eq.) and dry DMSO (10 mL). Bromide **114** (0.926 g, 2.83 mmol, 1.00 eq.) was added and the reaction mixture was stirred for 24 h at room temperature. The solution was treated with brine (100 mL), extracted with Et_2O (4 x 50 mL) and the combined organic phases were dried over Na_2SO_4 , filtered and the solvent was removed under reduced pressure. The crude product was purified by column chromatography (SiO_2 , *i*-hexane/ EtOAc 3:1) to give nitro compound **115** (0.467 g, 1.59 mmol, 56%) as a colorless oil.

R_f = 0.3 (*c*-hexane/ EtOAc = 4:1).

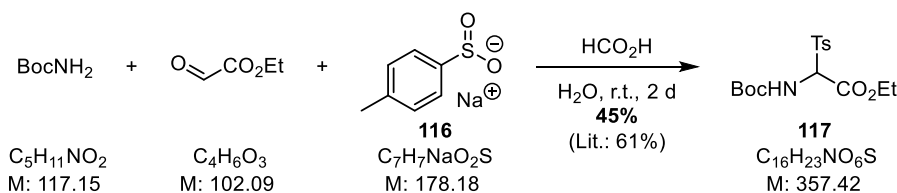
$^1\text{H NMR}$ (500 MHz, CDCl_3) δ = 5.16 (s, 1H), 4.73 (s, 2H), 4.44 (t, J = 6.9 Hz, 2H), 3.31 (q, J = 6.7 Hz, 2H), 2.13 – 2.01 (m, 2H), 1.66 (dq, J = 10.1, 7.0 Hz, 2H).ppm.

$^{13}\text{C NMR}$ (126 MHz, CDCl_3) δ = 154.9, 95.7, 75.1, 74.7, 40.3, 26.8, 24.5 ppm.

IR (neat): $\tilde{\nu}$ = 3373, 2954, 2930, 2850, 2156, 1991, m 1715, 1550, 1456, 1432, 1378, 1235, 1142, 912, 816, 723 cm^{-1} .

HRMS (ESI): m/z calculated for $\text{C}_7\text{H}_{11}\text{Cl}_3\text{N}_2\text{NaO}_4^+$ ($[\text{M}+\text{Na}]^+$): 314.9677; found: 314.9681.

5.5.4. Ethyl α -N-Boc- α -tosylglycinate (**117**)



According to a procedure reported by KINOSHITA *et al.*, a 10 mL flask was charged with freshly distilled ethyl glyoxylate (1.74 g, 17.1 mmol, 2.00 eq.), *tert*-butyl carbamate (1.00 g, 8.54 mmol, 1.00 eq.) and sodium *p*-toluene sulfinate (**116**, 6.77 g, 38.0 mmol, 4.45 eq.). Aq. Formic acid ($w=50\%$, 5 mL) was added and the mixture was stirred at room temperature for 2 d. The reaction mixture was poured into ice water and the colorless precipitate was filtered, washed with water and dried in a vacuum desiccator for 5 d over P_2O_5 affording tosylglycinate **117** (1.37 g, 3.83 mmol, 45%) as a colorless solid.

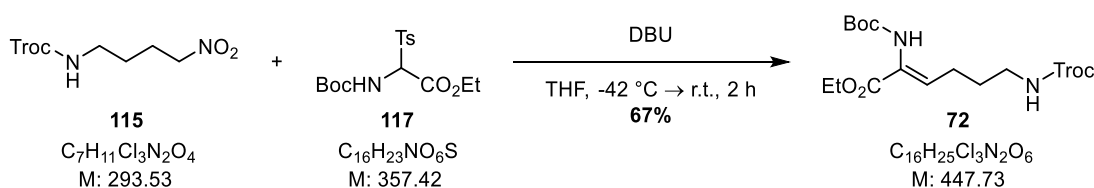
R_f = 0.1 (c-hexane/EtOAc = 4:1).

$^1\text{H NMR}$ (600 MHz, CDCl_3) δ = 7.83 (dd, J = 17.3, 8.1 Hz, 2H), 7.36 (d, J = 8.1 Hz, 2H), 5.81 (dd, J = 14.6, 10.0 Hz, 1H), 5.61 (dd, J = 37.0, 10.0 Hz, 1H), 4.34 (qd, J = 7.1, 1.9 Hz, 2H), 2.44 (s, 3H), 1.41 – 1.21 (m, 12H) ppm.

$^{13}\text{C NMR}$ (151 MHz, CDCl_3) δ = 163.5, 153.5, 145.8, 133.8, 129.9, 129.8, 81.7, 73.6, 63.6, 28.1, 21.8, 14.1 ppm.

The analytical data of compound **117** is in agreement with the literature.^[40]

5.5.5. Ethyl α -N-Boc- ϵ -N'-Troc-(Z)- α,β -didehydrolysinate (**72**)



A 50 mL Schlenk flask was charged with nitrocompound **115** (474 mg, 1.62 mmol, 1.10 eq.) and dry DBU (0.46 mL, 3.08 mmol, 2.10 eq.) in dry THF (20 mL). The solution was stirred for 10 min at room temperature, cooled to -42 °C and tosylate **117** (525 mg, 1.47 mmol, 1.00 eq.) in dry THF (5 mL) was added over 1 h using a syringe pump. The cooling bath was removed and stirring was continued for 1 h. The solvent was removed under reduced pressure and the residue was partitioned between water (50 mL) and EtOAc (50 mL). The phases were separated and the aqueous phase was extracted with EtOAc (2 x 30 mL). The combined organic phases were washed with brine (50 mL), dried over Na_2SO_4 , filtered over a silica plug (3 cm) and the solvent was removed under reduced pressure. The crude product was purified by column chromatography (SiO_2 , c-hexane/EtOAc 4:1) to give dehydrolysine **72** (443 mg, 0.989 mmol, 67%) as a colorless oil.

R_f = 0.2 (c-hexane/EtOAc = 4:1).

$^1\text{H NMR}$ (600 MHz, CDCl_3) δ = 6.53 (t, J = 7.5 Hz, 1H), 6.13 (s, 1H), 5.66 (s, 1H), 4.72 (s, 2H), 4.23 (q, J = 7.1 Hz, 2H), 3.27 (q, J = 6.2 Hz, 2H), 2.30 (q, J = 7.2 Hz, 2H), 1.76 (p, J = 6.8 Hz, 2H), 1.48 (s, 9H), 1.31 (t, J = 7.1 Hz, 3H) ppm.

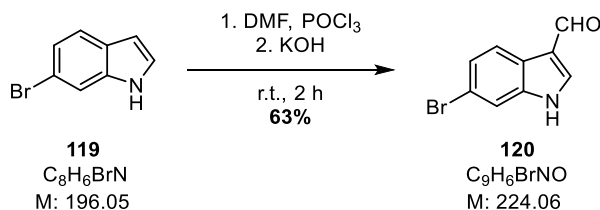
$^{13}\text{C NMR}$ (126 MHz, CDCl_3) δ = 164.9, 154.9, 153.7, 135.7, 126.5, 95.9, 80.9, 74.6, 61.7, 60.5, 40.4, 28.4, 25.5, 14.3 ppm.

IR (neat): $\tilde{\nu}$ = 3334, 2979, 2936, 2871, 1704, 1660, 1515, 1447, 1423, 1392, 1367, 1332, 1243, 1154, 1047, 923, 857, 815, 768, 724 cm^{-1} .

HRMS (ESI): m/z calculated for $\text{C}_{16}\text{H}_{25}\text{Cl}_3\text{N}_2\text{NaO}_6^+$ ($[\text{M}+\text{Na}]^+$): 469.0670; found: 469.0703.

5.6. C6-Indole Bond Formation via HECK Reaction

5.6.1. 6-Bromo-1*H*-indole-3-carbaldehyde (**120**)



A 250 mL Schlenk-flask was charged with dry DMF (50 mL) and cooled to 0 °C. Freshly distilled POCl₃ (4.6 mL, 49.5 mmol, 1.70 eq.) was added dropwise over 30 min and the solution was stirred at 0 °C. In a second Schlenk-flask 6-bromoindole (**119**, 5.71 g, 29.1 mmol, 1.00 eq.) was dissolved in dry DMF (30 mL) and was added dropwise over 1 h to the reaction mixture (the temperature should not rise above 10 °C!). After addition, the mixture was allowed to warm up to room temperature and stirred for 1 h. The solution was poured into 400 mL ice-water and the green suspension was treated dropwise with 10% NaOH-sol. (80 mL) until the solution was alkaline (pH = 14). The suspension was vigorously stirred and heated rapidly to reflux in a preheated oil bath for 30 min. The dark residue was removed by hot filtration and the filtrate was rapidly cooled to 0 °C. The precipitated orange solid was filtered, washed extensively with water, and dried under reduced pressure to give spectroscopically pure carbaldehyde **120** (4.10 g, 18.3 mmol, 63%) as an orange solid.

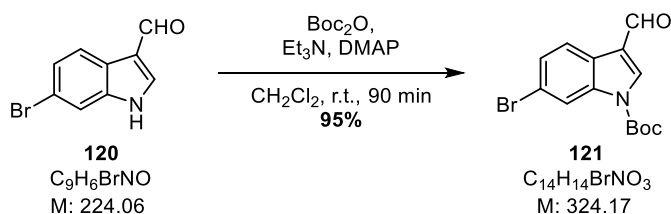
$R_f = 0.4$ (EtOAc).

¹H NMR (600 MHz, MeOD-*d*₄) $\delta = 9.90$ (s, 1H), 8.10 (s, 1H), 8.06 (d, $J = 8.4$ Hz, 1H), 7.65 (d, $J = 1.7$ Hz, 1H), 7.35 (dd, $J = 8.4, 1.7$ Hz, 1H) ppm.

¹³C NMR (151 MHz, CDCl₃) $\delta = 187.3, 140.0, 139.7, 126.7, 124.6, 123.7, 120.0, 118.1, 116.1$. ppm.

The analytical data of compound **120** is in agreement with the literature.^[197]

5.6.2. *tert*-Butyl 6-bromo-3-formyl-1*H*-indole-1-carboxylate (**121**)



A 10 mL Schlenk flask was charged with carbaldehyde **120** (0.500 g, 2.23 mmol, 1.00 eq.) and dry CH₂Cl₂ (1.7 mL). Dry Et₃N (0.62 mL, 4.46 mmol, 2.00 eq.) and Boc₂O (0.536 g, 2.46 mmol, 1.10 eq.) were added carefully, followed by addition of DMAP (54.5 mg, 0.446 mmol, 0.20 eq.). The solution was stirred for 90 min at room temperature, filtered through a plug of SiO₂ and the solvent was removed under reduced pressure.

The crude product was purified by column chromatography (SiO₂, c-hexane/EtOAc 19:1 → 9:1) affording *N*-protected indole **121** (0.686 g, 2.12 mmol, 95%) as a pale yellow solid.

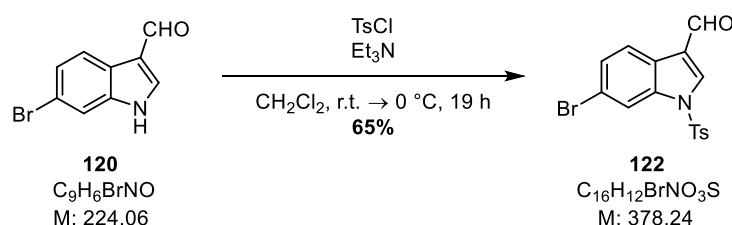
R_f = 0.6 (c-hexane/EtOAc = 2:1).

¹H NMR (600 MHz, CDCl₃) δ = 10.07 (s, 1H), 8.40 – 8.34 (m, 1H), 8.19 (s, 1H), 8.15 (d, *J* = 8.4 Hz, 1H), 7.49 (dd, *J* = 8.4, 1.7 Hz, 1H), 1.71 (s, 10H). ppm.

¹³C NMR (151 MHz, CDCl₃) δ = 185.6, 148.5, 136.7, 136.6, 128.1, 125.1, 123.4, 121.4, 120.0, 118.6, 86.4, 28.2 ppm.

The analytical data of compound **121** is in agreement with the literature.^[197]

5.6.3. 6-Bromo-1-tosyl-1*H*-indole-3-carbaldehyde (**122**)



A 100 mL Schlenk flask was charged with carbaldehyde **120** (3.00 g, 13.4 mmol, 1.00 eq.) in dry CH₂Cl₂ (35 mL). The solution was cooled to 0 °C, Et₃N (3.7 mL, 26.8 mmol, 2.00 eq.) and TsCl (2.55 g, 13.4 mmol, 1.00 eq.) were added. The solution was allowed to warm up to room temperature and stirred for 19 h. The reaction mixture was treated with 10% citric acid (50 mL) and stirred at room temperature for 30 min. The phases were separated and the aqueous phase was extracted once with CH₂Cl₂ (30 mL). The combined organic phases were washed with sat. aq. NaHCO₃-sol. (50 mL), brine (50 mL), dried over MgSO₄, filtered and the solvent was removed under reduced pressure. The crude product was recrystallized from CHCl₃/*n*-hexane to obtain protected indole **122** (3.28 g, 8.67 mmol, 65%) as orange crystals.

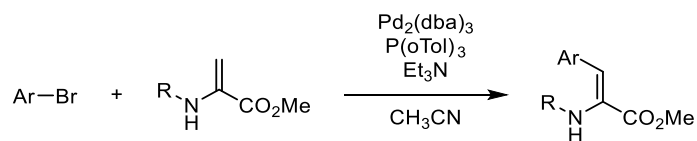
R_f = 0.4 (c-hexane/EtOAc = 4:1).

¹H NMR (600 MHz, CDCl₃) δ = 10.06 (s, 1H), 8.19 (s, 1H), 8.13 (dd, *J* = 1.7, 0.5 Hz, 1H), 8.11 (d, *J* = 8.3 Hz, 1H), 7.86 – 7.83 (m, 2H), 7.47 (dd, *J* = 8.4, 1.7 Hz, 1H), 7.35 – 7.31 (m, 2H), 2.40 (s, 3H) ppm.

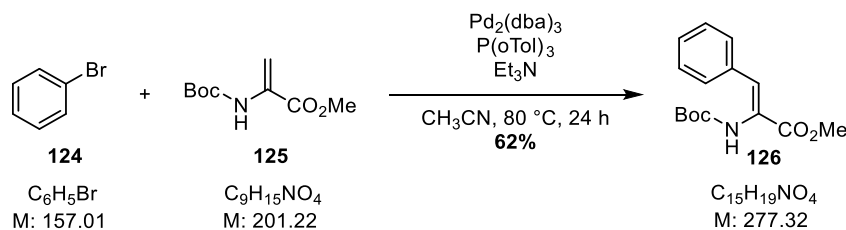
¹³C NMR (151 MHz, CDCl₃) δ = 185.1, 146.7, 136.4, 135.9, 134.2, 130.6, 128.6, 127.4, 125.2, 123.9, 122.1, 120.2, 116.5, 21.8 ppm.

The analytical data of compound **122** is in agreement with the literature.^[198]

5.6.4. General Procedure for the HECK-Reaction with Dehydroalanine Derivatives (GP2)



A Schlenk-flask was charged with $\text{Pd}_2(\text{dba})_3$ (0.05 eq.) and $\text{P}(\text{oTol})_3$ (0.20 eq.). Dehydroalanine substrate (1.00 eq.), aryl bromide (1.00-3.00 eq.), and Et_3N (0.91 mL, 6.65 mmol, 3.00 eq.) in dry, degassed CH_3CN (0.1 M) were added and the solution was heated to 80 °C. The reaction mixture was allowed to cool down to room temperature and treated with sat. aq. NH_4Cl -sol. (10 mL). The phases were separated, the aqueous phase was extracted with EtOAc (3 x 5 mL/mmol), the combined organic phases were washed with brine (10 mL/mmol), dried over Na_2SO_4 , filtered and the solvent was removed under reduced pressure. The crude product was purified by column chromatography.

5.6.5. Methyl *N*-Boc-(*Z*)- α,β -didehydrophenylalaninate (**126**)

Compound **126** was prepared according to **GP2** starting from $\text{Boc-}\Delta\text{Ala-OMe}$ (**125**, 0.439 g, 2.18 mmol, 1.00 eq.), bromobenzene (**124**, 0.69 mL, 6.65 mmol, 3.00 eq.), $\text{Pd}_2(\text{dba})_3$ (99.8 mg, 0.109 mmol, 0.05 eq.), $\text{P}(\text{oTol})_3$ (132 mg, 0.436 mmol, 0.20 eq.), Et_3N (0.91 mL, 6.65 mmol, 3.00 eq.), and 11 mL CH_3CN . After 24 h, full conversion was observed. The crude product was purified by column chromatography (SiO_2 , *c*-hexane/ EtOAc = 10:1) to afford (*Z*)- $\text{Boc-}\Delta\text{Phe-OMe}$ **126** (0.374 g, 1.35 mmol, 62%) as a colorless resin.

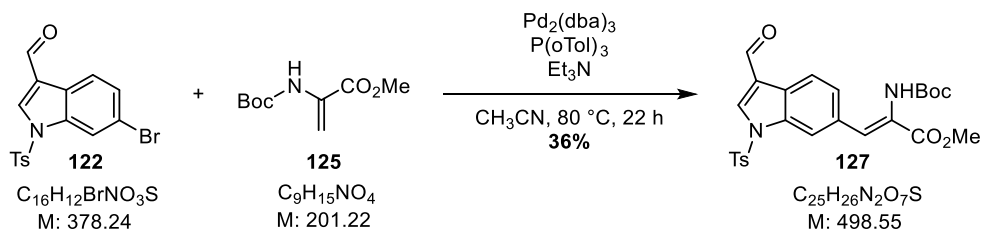
R_f = 0.3 (*n*-pentane/ EtOAc = 5:1).

$^1\text{H NMR}$ (500 MHz, CDCl_3) δ = 7.54 (d, J = 7.5 Hz, 2H), 7.40 – 7.34 (m, 2H), 7.33 – 7.30 (m, 1H), 7.25 (s, 1H), 6.18 (s, 1H), 3.86 (s, 3H), 1.40 (s, 9H) ppm.

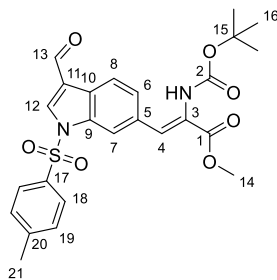
$^{13}\text{C NMR}$ (151 MHz, CDCl_3) δ = 166.2, 152.8, 134.3, 130.2, 129.8, 129.3, 128.7, 124.7, 81.1, 52.7, 28.2 ppm.

The analytical data of compound **126** is in agreement with the literature.^[49]

5.6.6. Methyl (Z)-2-((tert-butoxycarbonyl)amino)-3-(3-formyl-1-tosyl-1H-indol-6-yl)acrylate (127)



Compound **127** was prepared according to **GP2** starting from Boc- Δ Ala-OMe (**125**, 13.1 mg, 65.0 μmol , 1.30 eq.), bromoindole **122** (18.9 mg, 50.0 μmol , 1.00 eq.), $\text{Pd}_2(\text{dba})_3$ (2.29 mg, 2.50 μmol , 0.05 eq.), $\text{P}(\text{oTol})_3$ (3.04 mg, 10.0 μmol , 0.20 eq.), Et_3N (20.9 μL , 150 μmol , 3.00 eq.), and 0.5 mL CH_3CN . After 22 h, 62% conversion was observed. The crude product was purified by column chromatography (SiO_2 , *c*-hexane/EtOAc = 9:1 \rightarrow 3:1) to afford **127** (8.92 mg, 17.9 μmol , 36%, 46% brsm) as a colorless solid. Starting material **122** (4.02 mg; 10.6 μmol ; 21%) was reisolated.



$R_f = 0.6$ (*c*-hexane/EtOAc = 2:1).

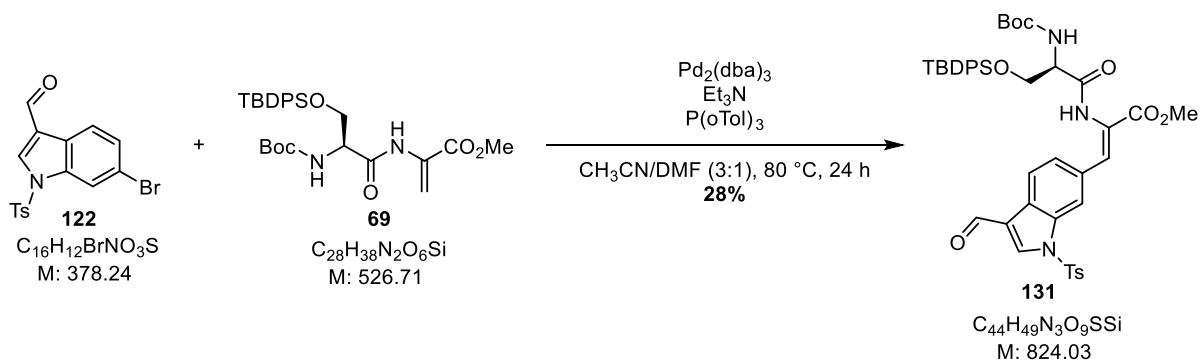
$^1\text{H NMR}$ (500 MHz, CDCl_3) δ = 10.08 (s, 1H, H13), 8.25 (s, 1H, H12), 8.21 (d, 3J = 8.3 Hz, 1H, H8), 8.19 (s, 1H, H7), 7.87 (d, 3J = 8.4 Hz, 2H, H18), 7.55 (d, 3J = 8.3 Hz, 1H, H6), 7.37 (s, 1H, H4), 7.33 (d, 3J = 8.1 Hz, 2H, H19), 7.29 (s, 1H, -NH), 3.89 (s, 3H, H14), 2.39 (s, 3H, H21), 1.43 (s, 9H, H16) ppm.

$^{13}\text{C NMR}$ (126 MHz, CDCl_3) δ = 185.5 (C13), 166.3 (C1), 153.4 (C2), 146.7 (C20), 137.5 (C12), 135.6 (C10), 134.5 (C17), 132.6 (C5), 132.2 (C), 130.8 (C19), 130.4 (C4), 127.7 (C18), 127.1 (C11), 127.0 (C6), 122.7 (C5), 122.4 (C8), 115.0 (C7), 81.7 (C15), 53.1 (C14), 28.5 (C16), 22.0 (C21) ppm.

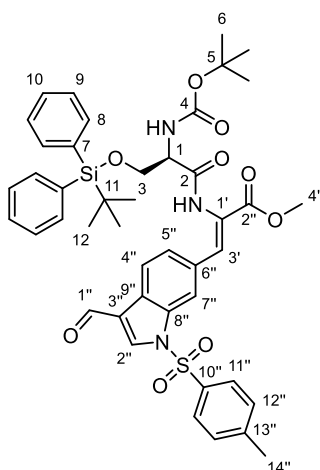
IR (neat): $\tilde{\nu}$ = 3324, 3123, 2979, 2967, 1715, 1679, 1595, 1537, 1491, 1435, 1381, 1331, 1236, 1176, 1102, 986 cm^{-1} .

HRMS (ESI): m/z calculated for $\text{C}_{25}\text{H}_{26}\text{N}_2\text{NaO}_7\text{S}^+$ ($[\text{M}+\text{Na}]^+$): 521.1353; found: 521.1359.

5.6.7. Methyl (*R,Z*)-2-(2-((*tert*-butoxycarbonyl)amino)-3-((*tert*-butyldiphenylsilyloxy)propanamido)-3-(3-formyl-1-tosyl-1*H*-indol-6-yl)acrylate (**131**)



Compound **131** was prepared according to **GP2** starting from Boc-Ser(TBDPS)- Δ Ala-OMe (**69**, 150 mg, 0.285 mmol, 1.10 eq.), bromoindole **122** (97.7 mg, 0.258 mmol, 1.00 eq.), $Pd_2(dba)_3$ (23.7 mg, 25.8 μ mol, 0.05 eq.), $P(oTol)_3$ (31.6 mg, 0.104 mmol, 0.20 eq.), Et_3N (0.11 mL, 0.794 mmol, 3.1 eq.), 2.6 mL CH_3CN and 0.8 mL DMF. After 24 h, full conversion was observed. The crude product was purified by column chromatography (SiO_2 , c -hexane/ $EtOAc$ = 9:1 \rightarrow 2:1) to afford **131** (60.2 mg; 73.1 μ mol; 28%) as a yellow oil.



R_f = 0.40 (c -hexane/ $EtOAc$ = 2:1).

1H NMR (700 MHz, $CDCl_3$) δ = 10.06 (s, 1H), 8.42 (s, 1H), 8.22 (s, 1H), 8.16 (d, J = 8.3 Hz, 1H), 8.10 (s, 1H), 7.86 – 7.81 (m, 2H), 7.64 (ddd, J = 18.4, 8.0, 1.5 Hz, 4H), 7.59 (s, 1H), 7.50 (d, J = 8.4 Hz, 1H), 7.47 – 7.30 (m, 6H), 7.28 (d, J = 8.3 Hz, 2H), 5.36 (s, 1H), 4.52 (q, J = 6.3 Hz, 1H), 4.18 – 4.05 (m, 1H), 3.92 (dd, J = 10.4, 6.5 Hz, 1H), 3.84 (s, 3H), 2.36 (s, 3H), 1.41 (s, 9H), 1.01 (s, 9H).

^{13}C NMR (151 MHz, $CDCl_3$) δ = 185.1 (C1''), 169.5 (C2), 165.5 (C2''), 155.9 (C4), 146.6 (C10''), 135.7 (C10a), 135.6 (C8a), 135.4 (C9a), 132.8 (C7), 132.6 (C3'), 132.5 (C7), 132.2 (C7''), 132.0 (C6''), 130.6 (C13''), 130.1 (C12''), 128.1 (C10b), 128.01 (C8b), 127.99 (C9b), 127.4 (C11''), 127.1 (C9''), 126.8 (C5''), 125.6 (C1'), 122.6 (C4''), 122.3 (C3''), 115.1 (C2''), 80.5 (C5), 63.5 (C3), 56.2 (C1), 52.9 (C4'), 29.8 (C11), 28.4 (C6), 26.9 (C12), 21.8 (C14'').

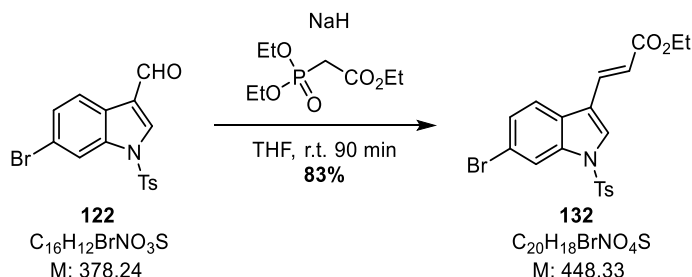
IR (neat): $\tilde{\nu}$ = 3017, 2928, 1722, 1682, 1488, 1366, 1232, 1112, 752 cm^{-1} .

$[\alpha]_D^{23}$ (c = 1.07, $CHCl_3$) = -13.01 .

HRMS (ESI): m/z calculated for $C_{44}H_{49}KN_3O_9SSi^+$ ($[M+K]^+$): 862.2591; found: 862.2521.

When the amide NH was irradiated, 0.7%, 0.9% and 1.8% of NOE were observed for the H4'', H5'' and H1, respectively.

5.6.8. 6-Bromo-1-tosyl-1H-indole-3-carbaldehyde (**122**)



A 100 mL Schlenk-flask was charged with sodium hydride (60% in mineral oil, 396 mg, 9.91 mmol, 1.50 eq.) and dry THF (33 mL). The suspension was cooled to 0 °C and triethylphosphonoacetate (2.0 mL, 9.91 mmol, 1.50 eq.) was added dropwise. The mixture was stirred for 15 min at room temperature, at which point 6-indole **122** (2.50 g, 6.61 mmol, 1.00 eq.) in dry THF (13 mL) was added. After 90 min full conversion of the starting material was observed and the dark red solution was treated with sat. aq. NH_4Cl -sol. (50 mL). The mixture was stirred for 5 min at room temperature and extracted with Et_2O (3 x 70 mL). The combined organic phases were washed with brine (70 mL), dried over $MgSO_4$, filtered and the solvent was removed under reduced pressure. The orange crude product was recrystallized from $CHCl_3/nHex$ to receive the ester **132** (1.45 g, 3.23 mmol, 49%) as colorless crystals. A second fraction (1.01 g, 2.26 mmol, 34%) was obtained by column chromatography of the mother liquor (SiO_2 , $cHex/EtOAc$ 20:1 → 10:1) as a colorless solid.

R_f = 0.5 (c -hexane/ $EtOAc$ = 4:1).

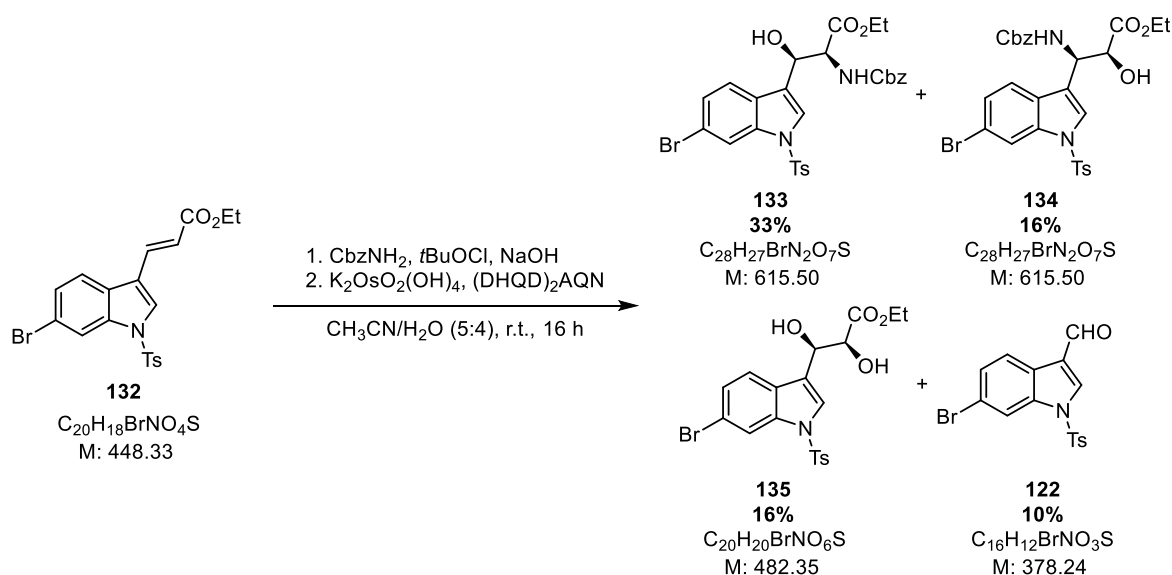
1H NMR (600 MHz, $CDCl_3$) δ = 8.18 (d, J = 1.7 Hz, 1H), 7.79 (dd, J = 6.7, 1.7 Hz, 3H), 7.73 (d, J = 16.2 Hz, 1H), 7.64 (d, J = 8.5 Hz, 1H), 7.43 (dd, J = 8.5, 1.7 Hz, 1H), 7.28 (d, J = 8.1 Hz, 2H), 6.46 (d, J = 16.2 Hz, 1H), 4.27 (q, J = 7.1 Hz, 2H), 2.37 (s, 3H), 1.34 (t, J = 7.1 Hz, 3H) ppm.

^{13}C NMR (126 MHz, $CDCl_3$) δ = 167.0, 146.0, 136.3, 135.1, 134.6, 130.4, 128.6, 127.6, 127.1, 126.9, 121.9, 119.4, 119.0, 118.1, 117.0, 60.8, 21.8, 14.5 ppm.

IR (neat): $\tilde{\nu}$ = 3109, 2986, 2935, 2903, 1707, 1637, 1597, 1565, 1536, 1493, 1461, 1419, 1371, 1323, 1300, 1275, 1173, 1135, 1103, 1087, 1034, 972, 805, 751 cm^{-1} .

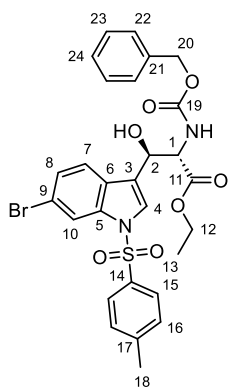
HRMS (ESI): m/z calculated for $C_{20}H_{19}BrNO_4S^+$ ($[M+H]^+$): 448.0213; found: 448.0230.

5.6.9. Ethyl (2S,3R)-2-(((benzyloxy)carbonyl)amino)-3-(6-bromo-1-tosyl-1H-indol-3-yl)-3-hydroxypropanoate (**133**)



Caution! The reaction is oxygen- and light sensitive, therefore all solutions, incl. aq. NaOH-sol. (0.40 M) and CH₃CN were degassed by three FPT cycles freshly before use. Additionally, the stoichiometry has to be very precise, e.g. excess/substoichiometric base has a negative impact on the reaction, measurements using calibrated equipment (**calibrated** Eppendorf syringes or graduated pipettes, instead of syringes) is encouraged.

A 100 mL Schlenk flask was charged with benzyl carbamate (1.15 g, 7.61 mmol, 3.10 eq.), aq. NaOH-sol. (0.40 M, 17.0 mL, 6.80 mmol, 2.78 eq.) in dry CH₃CN (15 mL) and cooled to 0 °C. Freshly prepared *t*BuOCl (purity determined by redox titration >96%, 0.832 mL, 7.36 mmol, 3.00 eq.) was added dropwise over 2 min, the reaction was allowed to warm up to room temperature and stirred for 30 min. The ligand, (DHQD)₂AQN (126 mg, 0.147 mmol, 0.06 eq.) dissolved in CH₃CN (3.5 mL) was added in one portion, followed by addition of the starting material **132** (1.10 g, 2.45 mmol, 1.00 eq.), dissolved in CH₃CN (5 mL). Subsequent addition of potassium osmate dihydrate (54.2 mg, 0.147 mmol, 0.06 eq.) dissolved in aq. NaOH-sol. (0.40 M, 1.6 mL, 0.64 mmol, 0.26 eq.) results in a pale green suspension. The reaction mixture was stirred under light exclusion for 16 h and treated with NaHSO₃ (1.00 g). Acetonitrile was removed under reduced pressure and the aqueous phase was extracted with EtOAc (3 x 50 mL). The combined organic phases were washed with water (50 mL), sat. aq. NH₄Cl-sol. (50 mL), sat. aq. NaHCO₃-sol. (5%, 50 mL), brine (50 mL), dried over MgSO₄, filtered and the solvent was removed under reduced pressure. The crude product was purified by column chromatography (SiO₂, *c*-hexane/EtOAc 9:1 → 1:1) to give benzylalcohol **133** (505 mg, 0.821 mmol, 33%) as a colorless solid. Additionally, protected benzylamine **134** (243 mg, 0.395 mmol, 16%), diol **135** (190 mg, 0.394 mmol, 16%) and aldehyde **122** (88.5 mg, 0.234 mmol, 10%) were isolated as side products.



$R_f = 0.29$ (c-hexane/EtOAc = 2:1).

$^1\text{H NMR}$ (600 MHz, CDCl_3) $\delta = 8.13$ (d, $J = 1.7$ Hz, 1H, H10), 7.72 (d, $J = 8.0$ Hz, 2H, H15), 7.59 (s, 1H, H4), 7.46 (d, $J = 8.4$ Hz, 1H, H8), 7.34 (dt, $J = 20.5, 8.4$ Hz, 5H, H22-24), 7.27 (s, 1H, H7), 7.20 (d, $J = 8.0$ Hz, 2H, H16), 5.62 (d, $J = 9.0$ Hz, 1H, C1-NH), 5.43 (d, $J = 3.2$ Hz, 1H, H2), 5.07 – 4.96 (m, 2H, H20), 4.75 – 4.65 (m, 1H, H1), 4.27 – 4.10 (m, 2H, H12), 2.89 (s, 1H, C2-OH), 2.31 (s, 3H, H18), 1.20 (t, $J = 7.1$ Hz, 3H, H13) ppm.

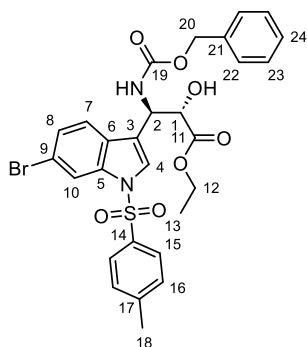
$^{13}\text{C NMR}$ (151 MHz, CDCl_3) $\delta = 170.4$ (C11), 156.5 (C19), 145.5 (C17), 135.9 (C21), 135.0 (C17), 130.2 (C15), 128.7, 128.4, 128.1, 127.5, 127.0, 126.9, 124.5, 121.3, 118.9, 116.9, 68.6 (C2), 67.4 (C20), 62.3, 58.7 (C1), 27.1, 21.7, 14.2 (C13) ppm.

IR (neat): $\tilde{\nu} = 3447, 3101, 3057, 2970, 2925, 1733, 1598, 1553, 1455, 1420, 1371, 1265, 1215, 1189, 1172, 1133, 1096, 1085, 1041, 980, 900, 865, 811, 735, 702$ cm^{-1} .

$[\alpha]_D^{26}$ ($c = 0.625$, CHCl_3) = -21.98 .

HRMS (ESI): m/z calculated for $\text{C}_{28}\text{H}_{27}\text{BrN}_2\text{NaO}_7\text{S}^+$ ($[\text{M}+\text{Na}]^+$): 637.0615; found: 637.0554.

Ethyl (2S,3R)-3-(((benzyloxy)carbonyl)amino)-3-(6-bromo-1-tosyl-1H-indol-3-yl)-2-hydroxypropanoate (134)



$R_f = 0.38$ (c-hexane/EtOAc = 2:1).

$^1\text{H NMR}$ (500 MHz, CDCl_3) $\delta = 8.60$ (s, 1H, H10), 8.23 (d, $J = 8.5$ Hz, 1H, H8), 8.13 (s, 1H, H4), 7.78 (d, $J = 8.0$ Hz, 2H, H15), 7.50 – 7.44 (m, 1H, H7), 7.39 – 7.28 (m, 5H, H22, H23, H24), 7.23 – 7.16 (m, 2H, H16), 5.20 (s, 2H, H20), 5.14 – 4.93 (m, 4H, H1, H2, OH, NH), 4.13 (d, $J = 6.8$ Hz, 2H, H12), 2.34 (s, 3H, H18), 1.01 (t, $J = 7.1$ Hz, 3H, H13) ppm.

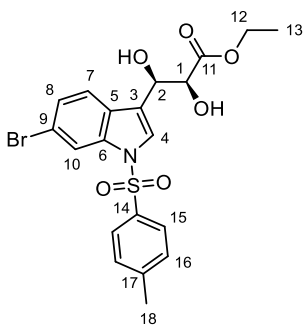
$^{13}\text{C NMR}$ (126 MHz, CDCl_3) $\delta = 166.7$ (C19), 154.7 (C11), 150.7, 146.5 (C14), 135.8 (C21), 135.1 (C17), 134.2, 133.5 (C10), 130.5 (C16), 128.8, 128.7, 128.6 (C7), 128.4, 128.0, 127.3 (C15), 124.6 (C8), 116.3 (C4), 74.5 (C2), 68.0 (C20), 67.4 (C1), 64.1, 21.8 (C18), 13.7 (C13). ppm.

IR (neat): $\tilde{\nu}$ = 3409, 3146, 3066, 3019, 2969, 1805, 1726, 1686, 1598, 1484, 1455, 1417, 1386, 1261, 1215, 1192, 1180, 1149, 1090, 1027, 972, 930, 822, 746 cm^{-1} .

$[\alpha]_{\text{D}}^{23}$ ($c = 0.770$, CHCl_3) = +14.56.

HRMS (ESI): m/z calculated for $\text{C}_{28}\text{H}_{27}\text{BrN}_2\text{NaO}_7\text{S}^+$ ($[\text{M}+\text{Na}]^+$): 637.0615; found: 637.0634.

Ethyl (2S,3R)-3-(6-bromo-1-tosyl-1H-indol-3-yl)-2,3-dihydroxypropanoate (**135**)



$R_f = 0.13$ (c -hexane/EtOAc = 2:1).

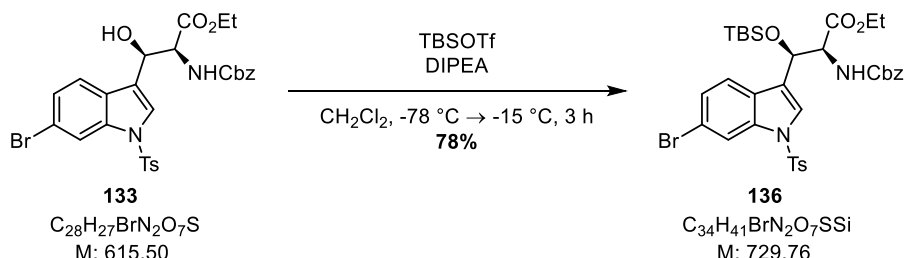
$^1\text{H NMR}$ (600 MHz, CDCl_3) δ = 8.14 (d, $J = 1.7$ Hz, 1H, H10), 7.79 – 7.72 (m, 2H, H15), 7.66 (d, $J = 1.0$ Hz, 1H, H4), 7.49 (d, $J = 8.4$ Hz, 1H, H8), 7.33 (dd, $J = 8.4, 1.7$ Hz, 1H, H7), 7.24 – 7.21 (m, 2H, H16), 5.18 (d, $J = 2.8$ Hz, 1H, H2), 4.45 (d, $J = 2.8$ Hz, 1H, H1), 4.24 (qq, $J = 10.8, 7.2$ Hz, 2H, H12), 3.53 (s, 1H, C1-OH), 3.05 (s, 1H, C2-OH), 2.34 (s, 3H, H18), 1.24 (t, $J = 7.1$ Hz, 3H, H13) ppm.

$^{13}\text{C NMR}$ (151 MHz, CDCl_3) δ = 172.6 (C11), 145.5 (C14), 135.8 (C6/C9), 135.0 (C17), 130.2 (C15), 128.1 (C5), 127.0 (C15), 126.8 (C7), 124.8 (C4), 121.5 (C8), 121.5 (C3), 118.8 (C6/C9), 116.8 (C10), 73.5 (C1), 68.4 (C2), 62.6 (C12), 14.2 (C13) ppm.

IR (neat): $\tilde{\nu}$ = 3422, 3100, 3065, 2979, 2925, 2871, 1730, 1598, 1496, 1455, 1420, 1370, 1265, 1172, 1134, 1095, 1085, 1042, 981, 864, 811, 735 cm^{-1} .

HRMS (ESI): m/z calculated for $\text{C}_{20}\text{H}_{20}\text{BrNNaO}_6\text{S}^+$ ($[\text{M}+\text{Na}]^+$): 504.0087; found: 504.0082.

5.6.10. Ethyl (2S,3R)-2-(((benzyloxy)carbonyl)amino)-3-(6-bromo-1-tosyl-1H-indol-3-yl)-3-(((tert-butyl)dimethylsilyloxy)propanoate (**136**)



A 5 mL Schlenk tube was charged with alcohol **133** (100 mg, 162 μmol , 1.00 eq.) and dry CH_2Cl_2 (1.6 mL). The solution was cooled to -78 $^\circ\text{C}$, DIPEA (85 μL , 0.487 mmol, 3.00 eq.) and TBSOTf (73 μL , 0.325 mmol, 2.00 eq.) were added and the solution was stirred at -78 $^\circ\text{C}$ for 2 h. The solution was allowed to warm up to -15 $^\circ\text{C}$ and after 1 h, full conversion of starting material **133** was observed. The reaction mixture was

treated with sat. aq. NH_4Cl -sol. (5 mL), the phases were separated and the aqueous phase was extracted with CH_2Cl_2 (3 x 5 mL). The combined organic phases were washed with sat. aq. NH_4Cl -sol. (5 mL), brine (5 mL), dried over Na_2SO_4 , filtered and the solvent was removed under reduced pressure. The crude product was purified by column chromatography (SiO_2 , *c*-hexane/ EtOAc 10:1) to give silyl ether **136** (92.9 mg, 127 μmol , 78%) as a colorless resin.

R_f = 0.6 (*c*-hexane/ EtOAc = 2:1).

$^1\text{H NMR}$ (500 MHz, CDCl_3 , 4:1 mixture of rotamers) δ = 8.18 (s, 0.2H), 8.15 (d, J = 1.7 Hz, 0.8H), 7.74 (d, J = 8.2 Hz, 0.4H), 7.69 (d, J = 8.4 Hz, 1.6H), 7.53 – 7.44 (m, 2H), 7.39 – 7.28 (m, 4H), 7.26 – 7.17 (m, 3.2H), 7.13 (t, J = 7.6 Hz, 0.4H), 6.61 (d, J = 7.5 Hz, 0.4H), 5.56 (d, J = 9.7 Hz, 0.8H), 5.47 (dd, J = 2.5, 0.9 Hz, 0.8H), 5.43 (br s, 0.2H), 5.38 (d, J = 10.0 Hz, 0.2H), 4.96 (d, J = 12.2 Hz, 0.8H), 4.89 (d, J = 12.2 Hz, 0.8H), 4.69 (d, J = 12.3 Hz, 0.2H), 4.54 (dd, J = 9.7, 2.5 Hz, 0.8H), 4.42 (dd, J = 10.2, 1.9 Hz, 0.2H), 4.31 (d, J = 12.3 Hz, 0.2H), 4.25 (dq, J = 10.8, 7.1 Hz, 1H), 4.14 (dq, J = 10.9, 7.2 Hz, 1H), 2.32 (s, 2.4H), 2.28 (s, 0.6H), 1.28 (t, J = 7.2 Hz, 3H), 0.88 (s, 2H), 0.84 (s, 7H), -0.01 – -0.04 (m, 3H), -0.17 (s, 0.6H), -0.23 (s, 2.4H). ppm.

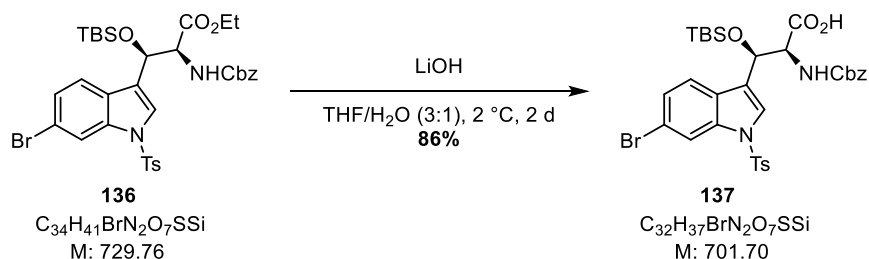
$^{13}\text{C NMR}$ (126 MHz, CDCl_3) δ = 170.1, 156.1, 145.4, 136.2, 136.0, 135.1, 130.2, 130.1, 128.7, 128.4, 128.3, 128.1, 127.4, 126.9, 126.86, 126.8, 125.1, 124.8, 122.6, 121.3, 118.8, 117.0, 69.3, 67.1, 62.0, 59.9, 27.0, 25.7, 21.7, 18.2, 14.2, -4.7, -5.5. ppm.

IR (neat): $\tilde{\nu}$ = 2954, 2927, 2898, 2857, 2359, 1724, 1599, 1507, 1456, 1420, 1373, 1258, 1189, 1173, 1130, 1087, 1058, 1028, 981, 837, 810, 778 cm^{-1} .

$[\alpha]_D^{26}$ (c = 0.625, CHCl_3) = +23.21.

HRMS (ESI): m/z calculated for $\text{C}_{34}\text{H}_{41}\text{BrN}_2\text{NaO}_7\text{SSi}^+$ ($[\text{M}+\text{Na}]^+$): 751.1479; found: 751.1449.

5.6.11. (2*S*,3*R*)-2-(((Benzyloxy)carbonyl)amino)-3-(6-bromo-1-tosyl-1*H*-indol-3-yl)-3-((tert-butyl)dimethylsilyloxy) propanoic acid (**137**)



A 10 mL flask was charged with ester **136** (144 mg, 198 μmol , 1.00 eq.) and a THF/water mixture (3:1, 4 mL). The solution was cooled to 0 °C and LiOH monohydrate (20.0 mg, 477 μmol , 2.41 eq.) was added. The reaction mixture was stirred at 3 °C for 2 d, acidified with aq. HCl -sol. (1 M) to pH = 3, diluted with water (5 mL), and extracted with EtOAc (3 x 15 mL). The combined organic phases were washed with brine (20 mL), dried over Na_2SO_4 , filtered and the solvent was removed under reduced pressure. The crude product was purified by column chromatography (SiO_2 , $\text{CH}_2\text{Cl}_2/\text{MeOH}$ 20:1) to give carboxylic acid **137** (119 mg, 170 μmol , 86%) as a colorless solid.

R_f = 0.5 ($\text{CH}_2\text{Cl}_2/\text{MeOH}$ = 10:1).

¹H NMR (600 MHz, CDCl₃, 3:1 mixture of rotamers) δ = 8.19 (s, 0.25H), 8.15 (s, 0.75H), 7.73 (d, J = 7.9 Hz, 0.5H), 7.69 (d, J = 8.1 Hz, 1.5H), 7.58 (s, 0.25H), 7.52 (s, 0.75H), 7.43 (d, J = 8.4 Hz, 0.75H), 7.40 – 7.28 (m, 4H), 7.25 (d, J = 7.1 Hz, 1.5H), 7.20 (d, J = 8.0 Hz, 2H), 7.14 (t, J = 7.7 Hz, 0.5H), 6.64 (d, J = 7.5 Hz, 0.25H), 6.06 (d, J = 9.6 Hz, 0.25H), 5.62 – 5.54 (m, 1.5H), 5.51 (s, 0.25H), 4.96 (s, 1.5H), 4.74 – 4.66 (m, 0.25H), 4.62 (dd, J = 9.2, 2.6 Hz, 1H), 4.47 (dd, J = 33.3, 10.9 Hz, 0.25H), 2.33 (s, 2.25H), 2.28 (s, 0.75H), 2.19 (s, 1H), 0.94 – 0.81 (m, 9H), 0.03 (s, 2.25H), 0.01 (s, 0.75H), -0.13 – -0.20 (m, 3H). ppm.

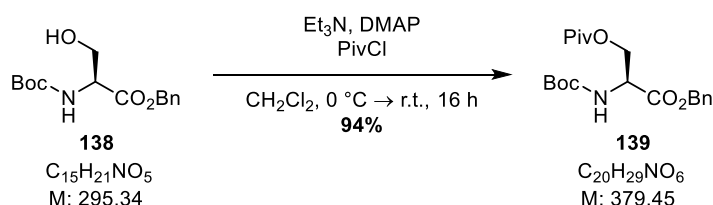
¹³C NMR (151 MHz, CDCl₃) δ = 174.2, 156.2, 145.5, 136.0, 134.9, 130.2, 128.7, 128.5, 128.4, 128.2, 127.4, 127.3, 127.0, 126.94, 126.87, 124.9, 122.1, 121.0, 118.9, 117.1, 68.8, 67.4, 66.0, 59.6, 31.1, 25.8, 21.7, 18.2, 15.3, -4.7, -5.4. ppm.

IR (neat): $\tilde{\nu}$ = 3058, 2984, 2941, 1734, 1479, 1445, 1373, 1266, 1241, 1156, 1045, 848, 734 cm⁻¹.

$[\alpha]_D^{23}$ (c = 0.770, CHCl₃) = +42.12.

HRMS (ESI): m/z calculated for C₃₂H₃₆BrN₂O₇SSi⁺ ([M-H]⁺): 699.1201; found: 699.1199.

5.6.12. Boc-Ser(Piv)-OBn (**139**)



A 50 mL Schlenk flask was charged with Boc-Ser-OBn (**138**, 1.51 g, 5.11 mmol, 1.00 eq.), Et₃N (1.0 mL, 10.2 mmol, 2.00 eq.) DMAP (0.125 g, 1.02 mmol, 0.20 eq.) and dry CH₂Cl₂ (25 mL). The solution was cooled to 0 °C and freshly distilled PivCl (0.76 mL, 6.13 mmol, 1.20 eq.) PivCl was added dropwise over 10 min. The solution was allowed to warm up to room temperature and stirred for 16 h. The reaction mixture was treated with sat. aq. NaHCO₃-sol. (20 mL) and the aqueous phase was extracted with CH₂Cl₂ (3 x 20 mL). The combined organic phases were dried over Na₂SO₄, filtered and the solvent was removed under reduced pressure. The crude product was purified by column chromatography (SiO₂, *c*-hexane/EtOAc 10:1) affording Boc-Ser(Piv)-OBn (**139**, 1.83 g, 4.82 mmol, 94%) as colorless crystals.

R_f = 0.5 (*c*-hexane/EtOAc = 4:1).

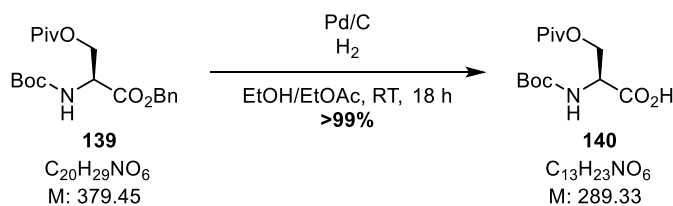
¹H NMR (500 MHz, CDCl₃) δ = 7.40 – 7.29 (m, 5H), 5.27 (d, J = 8.6 Hz, 1H), 5.23 – 5.12 (m, 2H), 4.63 (dt, J = 8.4, 3.7 Hz, 1H), 4.45 (dd, J = 11.2, 4.2 Hz, 1H), 4.31 (dd, J = 11.3, 3.5 Hz, 1H), 1.44 (s, 9H), 1.12 (s, 9H) ppm.

¹³C NMR (126 MHz, CDCl₃) δ = 178.1, 169.9, 155.3, 135.2, 128.8, 128.7, 128.5, 80.5, 67.7, 64.3, 53.4, 38.9, 28.4, 27.2 ppm.

IR (neat): $\tilde{\nu}$ = 3384, 2976, 2365, 1717, 1498, 1460, 1366, 1158 cm⁻¹.

$[\alpha]_D^{25}$ (c = 0.980, CHCl₃) = +6.211.

HRMS (ESI): m/z calculated for C₂₀H₂₉NNaO₆⁺ ([M+Na]⁺): 402.1887; found: 402.1892.

5.6.13. Boc-Ser(Piv)-OH (**140**)

A 25 mL Schlenk flask was charged with Boc-Ser(Piv)-OBn (**139**, 1.81 g, 4.77 mmol, 1.00 eq.) and Pd/C (w=5%, 250 mg). The flask was evacuated and flushed with an hydrogen atmosphere (1 atm). A EtOH/EtOAc mixture (1:1, 10 mL) was added and the solution was stirred vigorously for 16 h. The solution was filtered through Celite® and the filtrate was concentrated under reduced pressure to obtain Boc-Ser(Piv)-OH (**140**, 1.37 g, 4.73 mmol, 99%) as colorless crystals.

R_f = 0.3 (CH₂Cl₂/MeOH = 10:1).

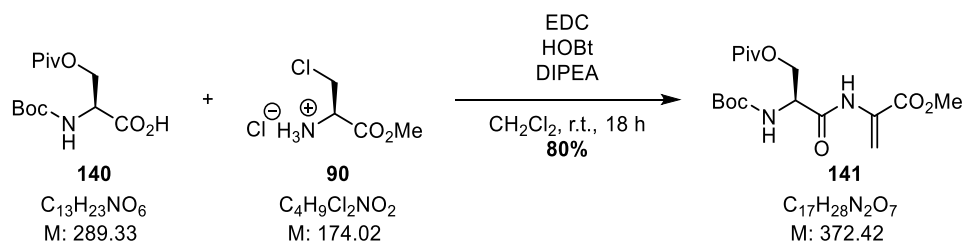
¹H NMR (500 MHz, CDCl₃, 3:1 mixture of rotamers) δ = 10.56 (s, 1H), 6.62 (br s, 0.3H), 5.28 (d, J = 8.4 Hz, 0.7H), 4.64 (dd, J = 8.2, 4.2 Hz, 1H), 4.54 – 4.31 (m, 2H), 1.45 (d, J = 4.8 Hz, 9H), 1.18 (s, 9H). ppm.

¹³C NMR (126 MHz, CDCl₃) δ = 178.3, 174.4, 155.5, 80.8, 64.1, 53.1, 39.0, 28.4, 27.2 ppm.

IR (neat): $\tilde{\nu}$ = 2978, 2929, 1719, 1507, 1456, 1160 cm⁻¹.

[α]_D²⁵ (c = 1.12, CHCl₃) = +19.513.

HRMS (ESI): m/z calculated for C₁₃H₂₃KNO₆⁺ ([M+K]⁺): 328.1157; found: 328.1149.

5.6.14. Boc-Ser(Piv)- Δ Ala-OMe (**141**)

A 25 mL Schlenk tube was charged with Boc-Ser(Piv)-OH (**140**, 300 mg, 1.04 mmol, 1.00 eq.), chloroalanine **90** (235 mg, 1.35 mmol, 1.30 eq.), HOBt (210 mg, 1.56 mmol, 1.50 eq.), dry CH₂Cl₂ (10 mL) and was cooled to 0 °C. EDC-HCl (417 mg, 2.18 mmol, 2.10 eq.) was added, followed by the dropwise addition of DIPEA (0.82 mL, 4.67 mmol, 4.50 eq.). The solution was allowed to warm up to room temperature and stirring was continued for 18 h. The reaction mixture was treated with aq. HCl-sol. (1 M, 15 mL), stirred for 10 min, the phases were separated and the aqueous phase was extracted with CH₂Cl₂ (3 x 15 mL). The combined organic phases were washed with sat. aq. NaHCO₃-sol. (2 x 15 mL), dried over MgSO₄, filtered and the solvent was removed under reduced pressure. The crude product was purified by column chromatography (SiO₂, c-hexane/EtOAc 9:1 → 6:1) affording Boc-Ser(Piv)- Δ Ala-OMe (**141**, 309 mg, 0.830 mmol, 80%) as a colorless solid.

R_f = 0.4 (c-hexane/EtOAc = 4:1).

$^1\text{H NMR}$ (500 MHz, CDCl_3) δ = 8.49 (s, 1H), 6.61 (s, 1H), 5.93 (d, J = 1.5 Hz, 1H), 5.32 (s, 1H), 4.48 (dd, J = 11.2, 5.5 Hz, 2H), 4.36 – 4.22 (m, 1H), 3.84 (s, 3H), 1.46 (s, 9H), 1.17 (s, 9H) ppm.

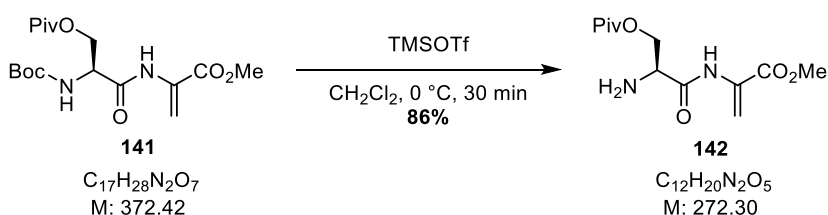
$^{13}\text{C NMR}$ (126 MHz, CDCl_3) δ = 178.5, 168.2, 164.2, 155.6, 130.6, 109.8, 81.1, 63.8, 55.0, 53.2, 39.0, 28.4, 27.2 ppm.

IR (neat): $\tilde{\nu}$ = 2967, 2922, 2850, 1731, 1634, 1523, 1162, 771 cm^{-1} .

$[\alpha]_{\text{D}}^{25}$ (c = 1.15, CHCl_3) = -13.772.

HRMS (ESI): m/z calculated for $\text{C}_{17}\text{H}_{28}\text{N}_2\text{NaO}_7^+$ ($[\text{M}+\text{Na}]^+$): 395.1789; found: 395.1783.

5.6.15. H-Ser(Piv)- Δ Ala-OMe (**142**)

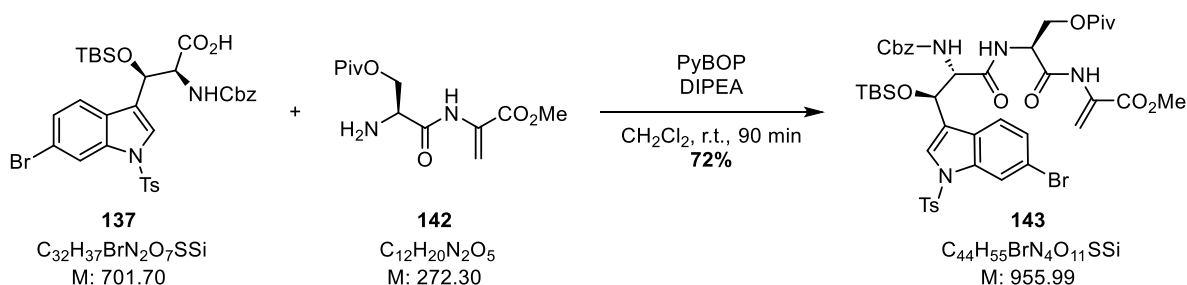


A 5 mL flask was charged with dipeptide **141** (188 mg, 505 μmol , 1.00 eq.) in CH_2Cl_2 (5.0 mL) and cooled to $0\text{ }^\circ\text{C}$. TMSOTf (101 μL , 555 μmol , 1.10 eq.) was added and the solution was stirred for 30 min. The reaction mixture was treated with sat. aq. NaHCO_3 -sol. (5 mL), stirred for 10 min and the aqueous phase was extracted with CH_2Cl_2 (3 x 10 mL). The combined organic phases were dried over K_2CO_3 , filtered and the solvent was removed under reduced pressure to give primary amine **142** (118 mg, 434 μmol , 86%) as a colorless oil.

$^1\text{H NMR}$ (500 MHz, CDCl_3) δ = 9.86 (br s, 1H), 6.65 (s, 1H), 5.92 (d, J = 1.7 Hz, 1H), 4.48 – 4.32 (m, 2H), 3.86 (s, 3H), 3.72 (dd, J = 5.7, 3.7 Hz, 1H), 1.71 (s, 2H), 1.19 (s, 9H) ppm.

HRMS (ESI): m/z calculated for $\text{C}_{12}\text{H}_{20}\text{N}_2\text{NaO}_5^+$ ($[\text{M}+\text{Na}]^+$): 295.1264; found: 295.1284.

5.6.16. Methyl (5*R*,6*S*,9*S*)-5-(6-bromo-1-tosyl-1*H*-indol-3-yl)-6-((*tert*-butoxycarbonyl)amino)-2,2,3,3-tetramethyl-12-methylene-7,10-dioxo-9-((pivaloyloxy)methyl)-4-oxa-8,11-diaza-3-silatridecan-13-oate (**143**)



A 3 mL Schlenk tube was charged with amine **142** (23.9 mg, 87.7 μmol , 1.23 eq.) and dry CH_2Cl_2 (0.72 mL). PyBOP (37.1 mg, 71.3 μmol , 1.00 eq.), indole **137** (50.0 mg, 71.3 μmol , 1.00 eq.) and DIPEA (24.2 μL , 143 μmol , 2.00 eq.) were added in succession and the solution was stirred for 90 min at room temperature.

The reaction mixture was treated with sat. aq. NH_4Cl -sol. (5 mL) and diluted with CH_2Cl_2 (5 mL). The phases were separated and the aqueous phase was extracted with CH_2Cl_2 (3 x 5 mL). The combined organic phases were washed with half-sat. aq. citric acid (10 mL), sat. aq. NaHCO_3 -sol. (10 mL), dried over Na_2SO_4 , filtered and the solvent was removed under reduced pressure. The crude product was purified by column chromatography (SiO_2 , *c*-hexane/*EtOAc* 9:1 \rightarrow 4:1) to give tripeptide **143** (49.2 mg, 51.5 μmol , 72%) as a colorless solid.

$R_f = 0.2$ (*c*-hexane/*EtOAc* = 4:1).

$^1\text{H NMR}$ (600 MHz, CDCl_3) $\delta = 8.26$ (s, 1H), 8.11 (s, 1H), 7.76 – 7.68 (m, 1H), 7.63 (d, $J = 8.0$ Hz, 2H), 7.52 (d, $J = 0.9$ Hz, 1H), 7.41 – 7.30 (m, 5H), 7.27 (d, $J = 8.4$ Hz, 1H), 7.19 (d, $J = 7.9$ Hz, 3H), 6.69 (s, 1H), 5.99 (s, 1H), 5.67 (d, $J = 6.9$ Hz, 1H), 5.57 (d, $J = 3.5$ Hz, 1H), 5.16 – 5.01 (m, 2H), 4.73 (q, $J = 6.1$ Hz, 1H), 4.51 (dd, $J = 7.1, 3.6$ Hz, 1H), 4.40 (dd, $J = 10.7, 4.5$ Hz, 1H), 4.20 (dd, $J = 11.3, 5.8$ Hz, 1H), 3.82 (s, 3H), 2.33 (s, 3H), 1.17 (s, 9H), 0.90 (s, 9H), 0.07 (s, 3H), -0.08 (s, 3H) ppm.

$^{13}\text{C NMR}$ (151 MHz, CDCl_3) $\delta = 178.3, 169.0, 167.1, 164.1, 156.2, 145.4, 136.1, 135.9, 135.1, 130.6, 130.1, 128.8, 128.5, 128.3, 127.7, 126.9, 126.8, 125.2, 122.0, 121.1, 118.8, 117.0, 110.6, 68.0, 67.4, 63.9, 60.2, 53.2, 39.0, 27.2, 25.9, 21.7, 18.3, -4.8, -5.3$ ppm.

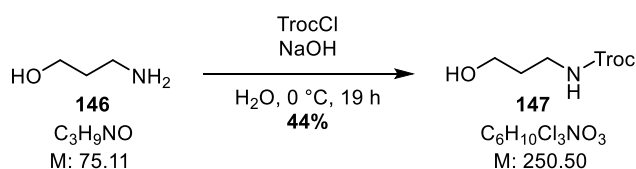
IR (neat): $\tilde{\nu} = 3358, 3309, 2955, 2929, 2857, 1731, 1699, 1666, 1599, 1521, 1377, 1323, 1173, 1136, 1088, 975, 840, 811, 783$ cm^{-1} .

$[\alpha]_{\text{D}}^{23}$ ($c = 0.615, \text{CHCl}_3$) = -82.68.

HRMS (ESI): m/z calculated for $\text{C}_{44}\text{H}_{55}\text{BrN}_4\text{NaO}_{11}\text{SSi}^+$ ($[\text{M}+\text{Na}]^+$): 977.2433; found: 977.2484.

5.7. Installation of the Lysine Side Chain

5.7.1. 2,2,2-Trichloroethyl (3-hydroxypropyl)carbamate (**147**)



A 100 mL flask was charged with NaHCO_3 (2.23 g, 26.6 mmol, 2.00 eq.) in H_2O (20 mL) and Et_2O (20 mL). The biphasic mixture was cooled to 0 $^\circ\text{C}$ and 3-amino-1-propanol (**146**, 1.00 mL, 13.3 mmol, 1.00 eq.) was added dropwise over 5 min. The mixture was stirred for 30 min at 0 $^\circ\text{C}$ and Troc-Cl (2.0 mL, 14.6 mmol, 1.10 eq.) was added gradually over 1 h using a syringe pump. The mixture was allowed to warm up to room temperature and stirred for 19 h. The phases were separated, the aqueous phase was extracted once with *EtOAc* (50 mL), acidified to pH = 3 using 1 M HCl and extracted with *EtOAc* (3 x 50 mL). The combined organic phases were washed with brine (100 mL), dried over Na_2SO_4 , filtered and the solvent was removed under reduced pressure. The crude product was purified by column chromatography (SiO_2 , *c*-hexane/*EtOAc* 4:1) to give carbamate **147** (1.46 g, 5.83 mmol, 44%) as a colorless oil.

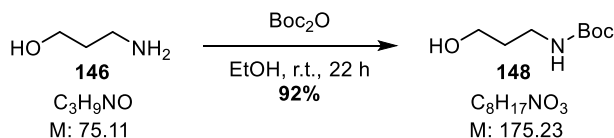
$R_f = 0.7$ (*c*-hexane/*EtOAc* = 1:2).

$^1\text{H NMR}$ (500 MHz, CDCl_3) δ = 5.32 (s, 2H), 4.74 (s, 2H), 4.25 (t, J = 6.0 Hz, 2H), 3.37 (q, J = 6.5 Hz, 2H), 1.95 (p, J = 6.4 Hz, 2H) ppm.

$^{13}\text{C NMR}$ (126 MHz, CDCl_3) δ = 155.6, 95.7, 74.7, 60.0, 38.4, 32.4 ppm.

The analytical data of compound **147** is in agreement with the literature.^[199]

5.7.2. *tert*-Butyl (3-hydroxypropyl)carbamate (**148**)



According to a procedure by CREWS *et al.*^[200], a 500 mL flask equipped with a dropping funnel was charged with 3-amino-1-propanol (**146**, 5.00 g, 66.6 mmol, 1.00 eq.) and EtOH (100 mL). The solution was cooled to 0 °C and Boc_2O (14.5 g, 66.6 mmol, 1.00 eq.) in EtOH (50 mL) was added dropwise to the solution. The reaction mixture was allowed to warm up to room temperature and stirred for 22 h. The solvent was removed under reduced pressure and the residue was partitioned between CH_2Cl_2 (60 mL) and H_2O (60 mL). The phases were separated, the aqueous phase was extracted with CH_2Cl_2 (3 x 50 mL). The combined organic phases were washed brine (100 mL), dried over Na_2SO_4 , filtered and the solvent was removed under reduced pressure to provide carbamate **148** (10.7 g, 61.3 mmol, 92%) as a colorless oil.

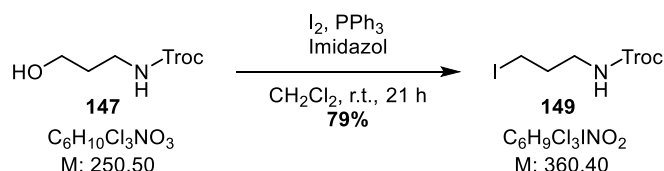
R_f = 0.2 (c-hexane/ EtOAc = 2:1).

$^1\text{H NMR}$ (500 MHz, CDCl_3) δ = 4.82 (s, 1H), 3.65 (q, J = 5.9 Hz, 2H), 3.28 (q, J = 6.3 Hz, 2H), 3.09 (t, J = 6.4 Hz, 1H), 1.65 (p, J = 5.8 Hz, 2H), 1.43 (s, 9H) ppm.

$^{13}\text{C NMR}$ (126 MHz, CDCl_3) δ = 157.3, 79.7, 59.3, 37.0, 33.0, 28.5 ppm.

The analytical data of compound **148** is in agreement with the literature.^[201]

5.7.3. 2,2,2-Trichloroethyl (3-iodopropyl)carbamate (**149**)



A 25 mL Schlenk flask was charged with PPh_3 (0.628 g, 2.40 mmol, 1.20 eq.) and imidazole (163 mg, 2.40 mmol, 1.20 eq.) in dry CH_2Cl_2 (14 mL). The solution was cooled to 0 °C and I_2 (0.608 g, 2.40 mmol, 1.20 eq.) was added. The reaction mixture was allowed to warm up to room temperature and stirred for 30 min. Alcohol **147** (0.500 g, 2.00 mmol, 1.00 eq.) was dissolved in dry CH_2Cl_2 (2.0 mL) and added dropwise

to the reaction mixture. The solution was stirred for 21 h, the suspension was filtered through a glass frit, washed with H₂O (50 mL) and sat. aq. Na₂S₂O₃ (50 mL), dried over Na₂SO₄, filtered and the solvent was removed under reduced pressure. The crude product was purified by column chromatography (SiO₂, *c*-hexane/EtOAc 10:1) to give iodide **149** (0.678 g, 1.88 mmol, 79%) as a colorless liquid.

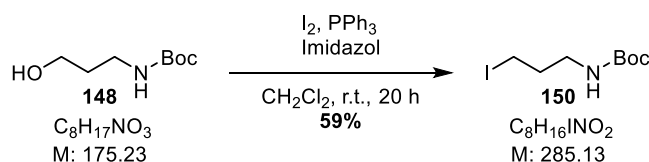
$R_f = 0.3$ (*c*-hexane/EtOAc = 10:1).

¹H NMR (400 MHz, CDCl₃) $\delta = 5.15$ (s, 1H), 4.72 (s, 2H), 3.35 (q, $J = 6.5$ Hz, 2H), 3.20 (t, $J = 6.8$ Hz, 2H), 2.06 (p, $J = 6.7$ Hz, 2H) ppm.

¹³C NMR (101 MHz, CDCl₃) $\delta = 154.7, 76.2, 74.6, 73.1, 41.7, 33.0$ ppm.

IR (neat): $\tilde{\nu} = 3344, 2977, 2930, 1687, 1519, 1454, 1391, 1365, 1270, 1250, 1168, 1069, 1038, 1022, 968, 867, 778$ cm⁻¹.

5.7.4. *tert*-Butyl (3-iodopropyl)carbamate (**150**)



A 25 mL Schlenk flask was charged with PPh₃ (2.84 g, 10.8 mmol, 1.20 eq.) and imidazole (0.737 g, 10.8 mmol, 1.20 eq.) in dry CH₂Cl₂ (55 mL). The solution was cooled to 0 °C and I₂ (2.75 g, 10.8 mmol, 1.20 eq.) was added. The reaction mixture was allowed to warm up to room temperature and stirred for 15 min. Alcohol **148** (1.58 g, 9.03 mmol, 1.00 eq.) was dissolved in dry CH₂Cl₂ (10 mL) and added dropwise to the reaction mixture. The solution was stirred for 20 h, the suspension was filtered through a glass frit, washed with H₂O (50 mL) and sat. aq. Na₂S₂O₃ (2 x 50 mL), dried over Na₂SO₄, filtered and the solvent was removed under reduced pressure. The crude product was purified by column chromatography (SiO₂, *c*-hexane/EtOAc 10:1) to give iodide **150** (1.52 g, 5.35 mmol, 59%) as a colorless liquid.

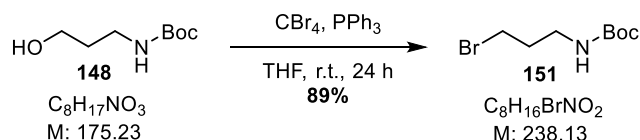
$R_f = 0.6$ (*c*-hexane/EtOAc = 10:1).

¹H NMR (500 MHz, CDCl₃) $\delta = 4.67$ (s, 1H), 3.27 – 3.13 (m, 4H), 2.01 (p, $J = 6.7$ Hz, 2H), 1.44 (s, 9H) ppm.

¹³C NMR (126 MHz, CDCl₃) $\delta = 156.1, 79.6, 60.5, 41.1, 40.6, 33.5, 28.5$ ppm.

The analytical data of compound **150** is in agreement with the literature.^[202]

5.7.5. *tert*-Butyl (3-bromopropyl)carbamate (**151**)



According to a procedure by OHKANDA *et al.*^[203], a 250 mL Schlenk flask was charged with 3-(Boc-amino)-1-propanol (**148**, 1.56 g, 8.90 mmol, 1.00 eq.) in dry THF (100 mL). Triphenylphosphine (4.42 g, 16.9 mmol,

1.90 eq.) and carbon tetrabromide (5.59 g, 16.9 mmol, 1.90 eq.) were added and the reaction mixture was stirred for 24 h at room temperature. The solvent was removed under reduced pressure and the residue was taken up in Et₂O (50 mL), filtered through Celite and the solvent of the filtrate was removed under reduced pressure. The crude product was purified by column chromatography (SiO₂, *n*-pentane/EtOAc 3:1) to give bromide **151** (1.88 g, 7.89 mmol, 89%) as colorless crystals.

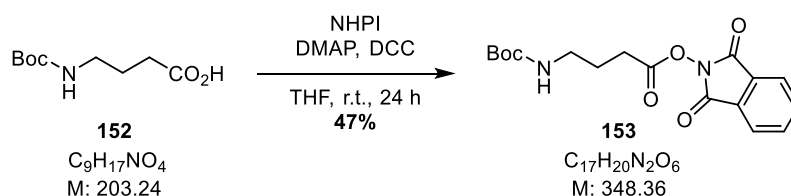
R_f = 0.5 (*c*-hexane/EtOAc = 3:1).

¹H NMR (500 MHz, CDCl₃) δ = 4.66 (s, 1H), 3.44 (t, *J* = 6.5 Hz, 2H), 3.27 (q, *J* = 6.5 Hz, 2H), 2.05 (t, *J* = 6.8 Hz, 2H), 1.44 (s, 9H) ppm.

¹³C NMR (126 MHz, CDCl₃) δ = 156.1, 79.6, 39.1, 32.8, 31.0, 28.5 ppm.

The analytical data of compound **151** is in agreement with the literature.^[203]

5.7.6. 1,3-Dioxoisindolin-2-yl 4-((*tert*-butoxycarbonyl)amino)butanoate (**153**)



A 100 mL Schlenk flask was charged with Boc-GABA-OH (**152**, 2.50 g, 12.3 mmol, 1.00 eq.), NHPI (2.61 g, 16.0 mmol, 1.30 eq.), DCC (3.05 g, 14.8 mmol, 1.20 eq.), DMAP (0.15 g, 1.23 mmol, 0.10 eq.) and dry THF (39 mL). The reaction mixture was stirred for 24 h at room temperature and the solvent was removed under reduced pressure. The crude product was recrystallized from CHCl₃/*c*-hexane to receive NHPI-ester **153** (2.03 g, 5.82 mmol, 47%) as colorless crystals.

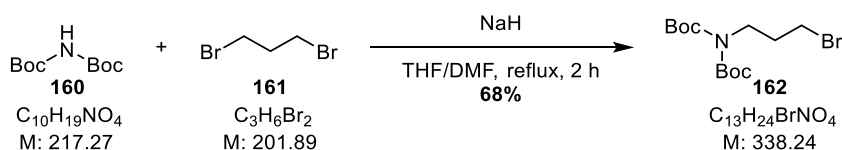
R_f = 0.6 (*c*-hexane/EtOAc = 2:1).

¹H NMR (500 MHz, CDCl₃) δ = 7.89 (dd, *J* = 5.5, 3.1 Hz, 2H), 7.80 (dd, *J* = 5.5, 3.1 Hz, 2H), 4.75 (s, 1H), 3.27 (q, *J* = 6.6 Hz, 2H), 2.72 (t, *J* = 7.3 Hz, 2H), 1.99 (p, *J* = 7.1 Hz, 2H), 1.44 (s, 9H) ppm.

¹³C NMR (126 MHz, CDCl₃) δ = 169.4, 162.1, 156.3, 134.9, 129.0, 124.1, 79.6, 39.5, 33.8, 28.5, 25.3 ppm.

The analytical data of compound **153** is in agreement with the literature.^[204]

5.7.7. *tert*-Butyl (3-bromopropyl)(*tert*-butoxycarbonyl)carbamate (**162**)



A 100 mL two-necked flask equipped with a reflux condenser, was charged with di-*tert*-butyliminodiacrylate (1.00 g, 4.60 mmol, 1.00 eq.) and THF/DMF (3:1, 40 mL). NaH (60% dispersion in mineral oil, 193 mg, 4.8 mmol, 1.05 eq.) was added and the reaction mixture was heated to reflux for 2 h. 1,3-dibromopropane (2.1 mL, 20.7 mmol, 4.50 eq.) was added and the mixture was heated to reflux for additional 2 h. The mixture was diluted with 70 mL Et₂O and cooled to 0 °C. The mixture was carefully treated with H₂O (30 mL), the phases were separated and the organic phase was washed with H₂O (2 x 50 mL), dried over MgSO₄, filtered and the solvent was removed under reduced pressure. The crude product was purified by column chromatography (SiO₂, *n*-pentane/EtOAc 50:1 → 1:1) to give bromide **162** (1.05 g, 3.10 mmol, 68%) as a colorless crystals.

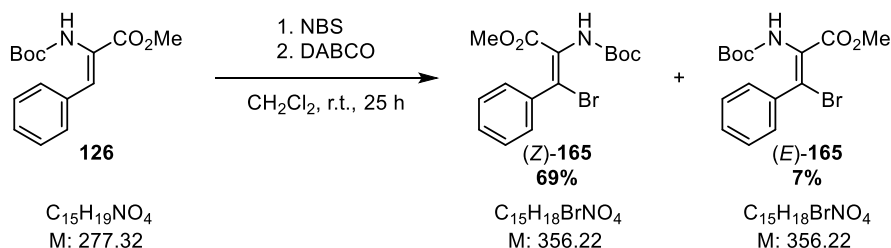
$R_f = 0.7$ (*c*-hexane/EtOAc = 1:1).

¹H NMR (500 MHz, CDCl₃) $\delta = 3.75 - 3.69$ (m, 2H), 3.40 (t, $J = 6.7$ Hz, 2H), 2.15 (p, $J = 6.8$ Hz, 2H), 1.51 (s, 18H) ppm.

¹³C NMR (126 MHz, CDCl₃) $\delta = 152.6, 82.7, 45.4, 32.3, 30.6, 28.2$ ppm.

The analytical data of compound **162** is in agreement with the literature.^[205]

5.7.8. Methyl 3-bromo-2-((*tert*-butoxycarbonyl)amino)-3-phenylacrylate (**165**)



A 25 mL Schlenk flask was charged with (*Z*)-Boc- Δ Phe-OMe (**126**, 0.342 g, 1.23 mmol, 1.00 eq.) and dry CH₂Cl₂ (12 mL). NBS (0.229 g, 1.29 mmol, 1.05 eq.) was added and the solution was stirred for 30 min at room temperature. DABCO (0.144 g, 1.29 mmol, 1.05 eq.) was added and the solution was stirred for 25 h. The reaction mixture was diluted with 20 mL CH₂Cl₂ and washed with H₂O (3 x 20 mL) and brine (20 mL). The organic phase was dried over MgSO₄, filtered and the solvent was removed under reduced pressure. The crude product was purified by column chromatography (SiO₂, *c*-hexane/EtOAc 19:1) to give bromides (*Z*)-**165** (0.301 g, 0.845 mmol, 69%) and (*E*)-**165** (31.3 mg, 87.9 μ mol, 7%) as colorless solids.

(*Z*)-**165**

$R_f = 0.5$ (*c*-hexane/EtOAc = 4:1).

¹H NMR (500 MHz, CDCl₃) $\delta = 7.55 - 7.30$ (m, 5H), 6.56 (s, 1H), 3.53 (s, 3H), 1.49 (s, 9H) ppm.

¹³C NMR (176 MHz, CDCl₃) $\delta = 163.7, 152.1, 137.6, 129.5, 129.3, 129.1, 128.4, 114.1, 82.3, 52.6, 28.3$ ppm.

(*E*)-**165**

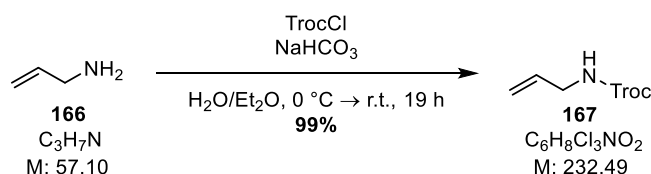
$R_f = 0.3$ (c-hexane/EtOAc = 4:1).

$^1\text{H NMR}$ (600 MHz, CDCl_3) $\delta = 7.50 - 7.39$ (m, 4H), 7.36 (td, $J = 6.3, 2.4$ Hz, 1H), 6.09 (s, 1H), 3.92 (s, 3H), 1.42 (s, 9H) ppm.

$^{13}\text{C NMR}$ (151 MHz, CDCl_3) $\delta = 164.7, 151.7, 136.7, 129.6, 129.2, 129.1, 128.7, 110.4, 81.7, 52.7, 28.2$ ppm.

The analytical data of compounds (Z)-**165** and (E)-**165** are in agreement with the literature.^[60]

5.7.9. 2,2,2-Trichloroethyl allylcarbamate (**167**)



A 100 mL was charged with NaHCO_3 (0.481 g, 5.72 mmol, 1.30 eq.), H_2O (4.3 mL) and Et_2O (4.3 mL). The solution was cooled to $0\text{ }^\circ\text{C}$ and allyl amine (**166**, 0.32 mL, 4.30 mmol, 1.00 eq.) was added dropwise. The solution was stirred for 30 min and TrocCl (0.60 mL, 4.30 mmol, 1.00 eq.) in Et_2O (4.3 mL) was added dropwise over 10 min. The solution was allowed to warm up to room temperature and stirred for 19 h. The phases were separated and the aqueous phase was extracted with Et_2O (2 x 20 mL). The combined organic phases were washed with brine (20 mL), dried over MgSO_4 , filtered and the solvent was removed under reduced pressure. The spectroscopically pure allyl carbamate **167** (0.993 g, 4.27 mmol, 99%) was obtained as colorless crystals.

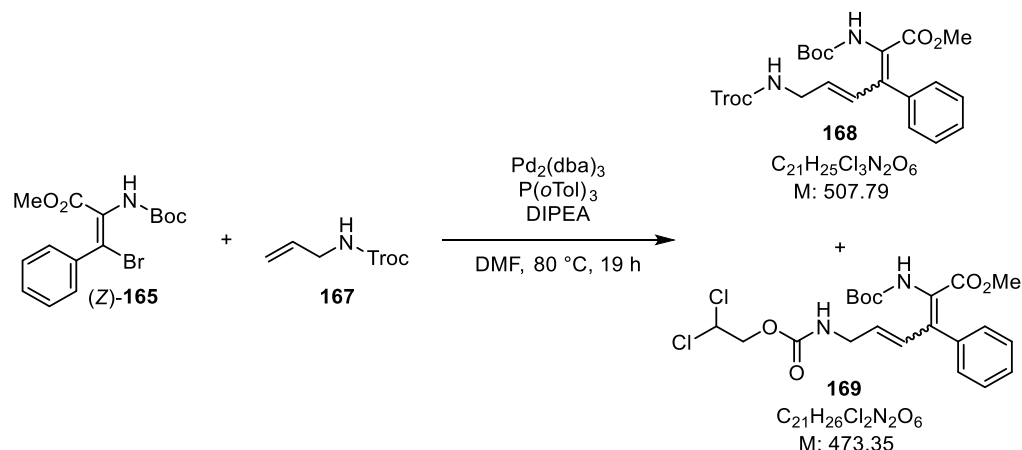
$R_f = 0.6$ (c-hexane/EtOAc = 4:1).

$^1\text{H NMR}$ (600 MHz, CDCl_3) $\delta = 5.87$ (ddt, $J = 17.2, 10.6, 5.5$ Hz, 1H), 5.24 (dq, $J = 17.1, 1.5$ Hz, 1H), 5.18 (dq, $J = 10.3, 1.4$ Hz, 1H), 5.07 (s, 1H), 4.75 (s, 2H), 3.87 (tt, $J = 5.8, 1.6$ Hz, 2H) ppm.

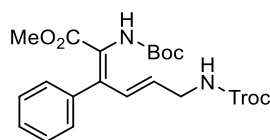
$^{13}\text{C NMR}$ (176 MHz, CDCl_3) $\delta = 154.4, 133.8, 116.6, 95.6, 74.6, 43.6$ ppm.

The analytical data of compound **167** is in agreement with the literature.^[206]

5.7.10. Methyl 2-((*tert*-butoxycarbonyl)amino)-3-phenyl-6-(((2,2,2-trichloroethoxy)carbonyl)amino)hexa-2,4-dienoate (**168**)



A 6 mL PTFE-lined vial was charged with bromide (*Z*)-**165** (80.0 mg, 0.225 mmol, 1.00 eq.), Troc-allyl amine (**167**, 78.3 mg, 0.337 mmol, $\text{Pd}_2(\text{dba})_3$ (20.6 mg, 22.5 μmol , 0.10 eq.), $\text{P}(\text{oTol})_3$ (27.3 mg, 89.8 μmol , 0.40 eq.) and dry, degassed DMF (2.3 mL). DIPEA (115 μL , 0.674 mmol, 3.00 eq.) was added, the vial was flushed with argon and the mixture was heated to 80 °C for 19 h. The reaction mixture was treated with sat. aq. NH_4Cl -sol. (5 mL), stirred for 30 min at room temperature and extracted with EtOAc (3 x 10 mL). The combined organic phases were washed with sat. aq. NH_4Cl -sol. (10 mL), H_2O (10 mL) and brine (10 mL), dried over MgSO_4 , filtered and the solvent was removed under reduced pressure. The crude product was purified by column chromatography (SiO_2 , *c*-hexane/EtOAc 24:1 \rightarrow 3:1) followed by a subsequent isocratic column chromatography (SiO_2 , *n*-hexane/EtOAc 4:1) to afford olefinated product **168** (14.9 mg, 29.3 μmol , 13%, d.r.: 3:1 (*E,E*)/(*Z,E*)) and dechlorinated product (*E,E*)-**169** (15.2 mg, 32.1 μmol , 14%) as colorless oils.



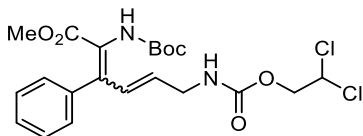
$R_f = 0.2$ (*c*-hexane/EtOAc = 4:1).

$^1\text{H NMR}$ (500 MHz, CDCl_3) $\delta = 7.35 - 7.29$ (m, 3H), 7.12 (dd, $J = 7.3, 2.1$ Hz, 2H), 6.72 (s, 1H), 6.27 (s, 0.7H, (*Z,E*)-**168**), 6.16 (s, 0.3H, (*E,E*)-**168**), 5.46 (dt, $J = 15.5, 5.7$ Hz, 1H), 5.10 (s, 1H), 4.73 (s, 2H), 3.95 (td, $J = 6.0, 1.7$ Hz, 2H), 3.83 (s, 0.7H, (*E,E*)-**168**), 3.41 (s, 2.3H, (*Z,E*)-**168**), 1.49 (s, 9H) ppm.

$^{13}\text{C NMR}$ (176 MHz, CDCl_3) $\delta = 165.8, 164.6, 154.5, 153.2, 137.2, 134.9, 131.4, 129.4, 129.1, 128.2, 128.0, 105.3, 95.7, 74.7, 53.0, 51.9, 43.3, 28.4, 28.3$ ppm.

IR (neat): $\tilde{\nu} = 3338, 2931, 2846, 2172, 2132, 2029, 1721, 1507, 1480, 1453, 1436, 1332, 1243, 1155, 1066, 920, 907, 786, 724$ cm^{-1} .

HRMS (ESI): m/z calculated for $\text{C}_{21}\text{H}_{25}\text{Cl}_3\text{N}_2\text{NaO}_6^+$ ($[\text{M}+\text{Na}]^+$): 529.0671; found: 529.0716.

Methyl 2-((*tert*-butoxycarbonyl)amino)-6-(((2,2-dichloroethoxy)carbonyl)amino)-3-phenylhexa-2,4-dienoate (169)

$R_f = 0.2$ (c-hexane/EtOAc = 4:1).

$^1\text{H NMR}$ (500 MHz, CDCl_3) $\delta = 7.45 - 7.30$ (m, 3H), 7.17 – 7.06 (m, 2H), 6.68 (d, $J = 16.0$ Hz, 1H), 6.28 (d, $J = 12.5$ Hz, 1H), 5.84 (t, $J = 6.0$ Hz, 1H), 5.45 (dt, $J = 15.3, 5.8$ Hz, 1H), 4.97 (s, 1H), 4.41 (d, $J = 6.0$ Hz, 2H), 3.92 (td, $J = 5.9, 1.6$ Hz, 2H), 3.41 (s, 3H), 1.55 – 1.37 (m, 9H) ppm.

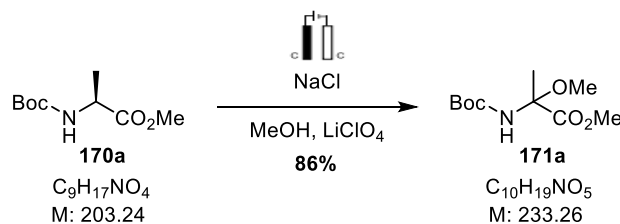
$^{13}\text{C NMR}$ (176 MHz, CDCl_3) $\delta = 165.9, 165.8, 164.6, 154.5, 153.2, 137.2, 134.9, 131.4, 129.4, 129.1, 128.2, 128.0, 105.3, 95.7, 74.7, 60.5, 53.0, 51.9, 43.3, 28.4, 28.3$ ppm.

IR (neat): $\tilde{\nu} = 3359, 2952, 2921, 2850, 2153, 1717, 1596, 1484, 1340, 1247, 1158, 1065, 983, 913, 783, 732, 706$ cm^{-1} .

HRMS (ESI): m/z calculated for $\text{C}_{21}\text{H}_{26}\text{Cl}_2\text{N}_2\text{NaO}_6^+$ ($[\text{M}+\text{Na}]^+$): 495.1060; found: 495.1132.

5.8. Electrosynthesis of Protected Dehydroamino Acids

5.8.1. Procedure for the Decagram-scale Synthesis of Methyl *N*-Boc- α -methoxyalaninate (**171a**)



A 400 mL glass-beaker was charged with Boc-Ala-OMe (**170a**, 17.3 g, 85.0 mmol, 1.00 eq.), NaCl (2.98 g, 51.0 mmol, 0.60 eq.), LiClO₄ (3.01 g, 0.1 M), MeOH (283 mL, 0.3 M) and a stir bar. 6 graphite electrodes (8.2 mm diameter) were inserted to the reaction vessel, using a 3D printed PLA-holder and connected in parallel and alternating polarity (5 mm interelectrode gap between each rods, total electrode area covered by solution 70 cm²). The reaction vessel was placed into a bowl water at room temperature and stirred. A constant current (500 mA, cell voltage: 3.0-4.2 V typically) was passed through the solution and the conversion was monitored *via* GC-MS. After 13 h (3.0 F/mol), the polarity of the electrodes was switched and the reaction continued for 22 h (total current passed: 7.6 F/mol), after which full conversion of the starting material was observed. The solvent was evaporated and the residue was treated with water (200 mL) and EtOAc (200 mL). The phases were separated and the aqueous phase was extracted with EtOAc (2 x 100 mL). The combined organic phases were washed with 200 mL brine, dried over MgSO₄ and the solvent was removed under reduced pressure to obtain spectroscopically pure methoxylated product **171a** (17.1 g, 73.3 mmol, 86%) without further purification.

5.8.2. Decagram-scale SHONO-type Oxidation using a 6-Electrode Setup

5.8.3. Setup of the Reaction



Figure 5.1: From left to right: 1) Electrode configuration using 8.2 mm graphite rods in a 3D-printed PLA-Holder (STL-File in the attachments); 2) Reaction setup with lab power supply and 400 mL glass beaker 3) Close-up of the reaction solution.

After the reaction

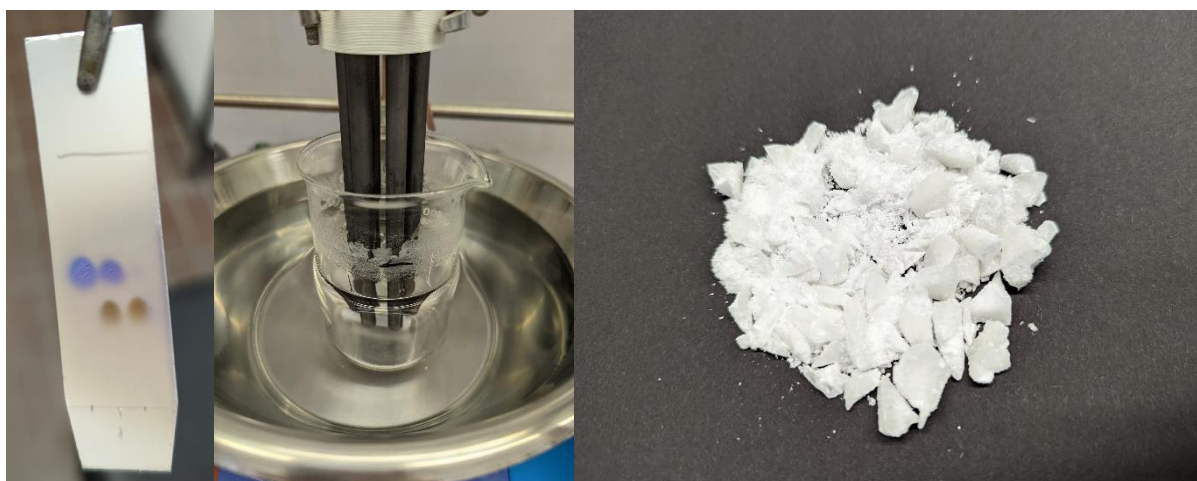
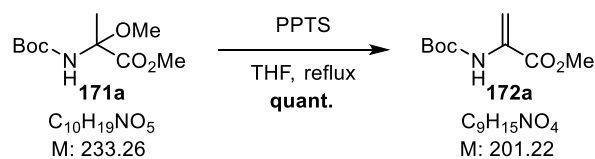
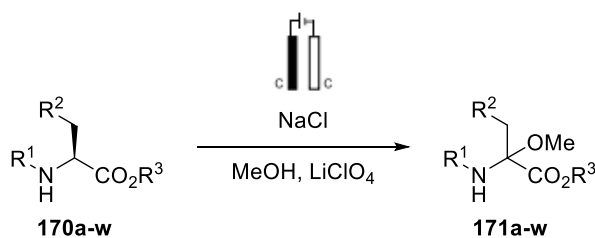


Figure 5.2: From left to right: 1) TLC (SiO₂, c-hexane/EtOAc = 2:1, anisaldehyde stain) after full conversion; 2) Reaction vessel after reaction 3) Isolated product 171a.

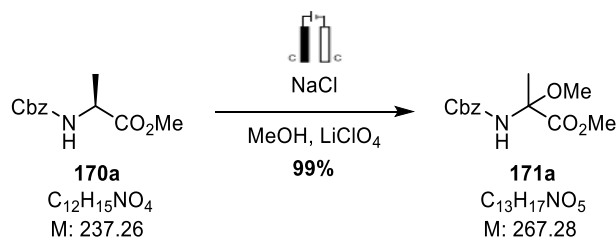
5.8.4. Decagram-scale Synthesis of Methyl *N*-Boc- α,β -didehydroalaninate (**172a**)

A two-necked 500 mL flask equipped with a reflux condenser was charged with Methyl *N*-Boc- α -methoxyalaninate (**171a**, 16.4 g, 70.3 mmol, 1.00 eq.) and 350 mL dry THF. PPTS (4.79 g, 21.1 mmol, 0.30 eq.) was added and the solution was heated to reflux in an oil bath. After 5 h, full conversion was observed. The solution was cooled to 0 °C and the precipitate was filtered to reisolate PPTS (3.72 g, 16.3 mmol, 77%). The filtrate was concentrated to 50 mL and treated with sat. aq. NaHCO₃-sol. (200 mL). The aqueous phase was extracted with EtOAc (3 x 100 mL), the combined organic phases were washed with brine (300 mL), dried over MgSO₄ and the solvent was removed under reduced pressure to obtain Methyl *N*-Boc- α,β -didehydroalaninate (**172a**, 14.3 g, 71.1 mmol, >99%) as a colorless oil.

5.8.5. General Procedure for the gram-scale SHONO-type Oxidation (GP3)



A 50 mL test tube (25 x 150 mm) was charged with the substrate **170a-w** (4.00 mmol, 1.00 eq.), NaCl (140 mg, 2.40 mmol, 0.60 eq.), LiClO₄ (142 mg, 0.1 M), 14 mL MeOH (0.3 M) and a stir bar (4.5 x 15 mm). The reaction mixture was stirred (500 rpm) until all solids were dissolved and graphite electrodes (8.2 mm diameter, 5 mm electrode gap) were placed into the container. A constant current (50 mA, cell voltage: 3.0-4.2 V typically) was passed through the solution and the conversion was monitored *via* GC-MS or NMR by taking aliquots. After the conversion was complete or no further conversion was detected, the solvent was removed under reduced pressure. The crude product was dissolved in EtOAc (10 mL) and filtered over a silica plug (3 cm). The solvent was removed under reduced pressure.

5.8.6. Methyl α -N-Boc- α -methoxyalaninate (**171a**)

Compound **171a** was prepared according to **GP3** starting from **170a** (813 mg, 4.00 mmol, 1.00 eq.) and MeOH (14 mL). After 4.0 F/mol, full conversion was observed via GC-MS and the title compound (**2a**, 929 mg, 3.98 mmol; 99%) was obtained as colorless crystals. The product was spectroscopically pure without further purification.

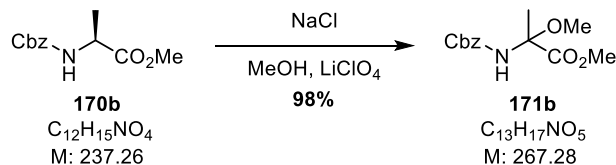
$R_f = 0.2$ (*c*-hexane/EtOAc = 4:1).

$^1\text{H NMR}$ (500 MHz, CDCl_3) $\delta = 5.65$ (s, 1H), 3.83 (s, 3H), 3.26 (s, 3H), 1.72 (s, 3H), 1.45 (s, 9H) ppm.

$^{13}\text{C NMR}$ (126 MHz, CDCl_3) δ 171.3, 153.6, 85.2, 80.5, 53.1, 51.2, 28.4, 23.5 ppm.

IR (neat): $\tilde{\nu} = 3356, 2975, 2954, 2926, 2850, 1720, 1507, 1455, 1367, 1294, 1248, 1214, 1162, 1068, 979, 868, 808, 771 \text{ cm}^{-1}$.

HRMS (ESI): m/z calculated for $\text{C}_{10}\text{H}_{19}\text{NNaO}_5^+$ ($[\text{M}+\text{Na}]^+$): 256.1155; found: 256.1160.

5.8.7. Methyl α -N-Cbz- α -methoxyalaninate (**171b**)

Compound **171b** was prepared according to **GP3** starting from **170b** (949 mg, 4.00 mmol, 1.00 eq.) and 14 mL MeOH. After 4.0 F/mol, full conversion was observed *via* GC-MS and the title compound (**2b**, 1.05 g, 3.91 mmol; 98%) was obtained as colorless solid. The product was spectroscopically pure without further purification.

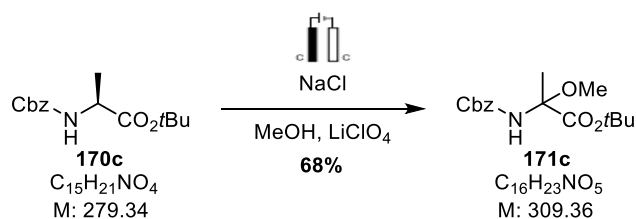
$R_f = 0.15$ (*c*-hexane/EtOAc = 4:1).

$^1\text{H NMR}$ (600 MHz, CDCl_3) $\delta = 7.39 - 7.34$ (m, 4H), 7.35 - 7.30 (m, 1H), 6.05 (s, 1H), 5.12 (s, 2H), 3.81 (s, 3H), 3.25 (s, 3H), 1.76 (s, 3H) ppm.

$^{13}\text{C NMR}$ (151 MHz, CDCl_3) $\delta = 171.4, 154.3, 136.1, 128.7, 128.4, 128.3, 85.5, 67.2, 53.5, 51.2, 23.0$ ppm.

IR (neat): $\tilde{\nu} = 3324, 3033, 3000, 2851, 1730, 1520, 1454, 1377, 1322, 1295, 1248, 1144, 1124, 1067, 977, 952, 876, 783, 740 \text{ cm}^{-1}$.

HRMS (ESI): m/z calculated for $\text{C}_{13}\text{H}_{17}\text{NNaO}_5^+$ ($[\text{M}+\text{Na}]^+$): 290.0999; found: 290.0989.

5.8.8. *tert*-Butyl α -*N*-Cbz- α -methoxyalaninate (**171c**)

Compound **171c** was prepared according to **GP3** starting from **170c** (1.12 g, 4.00 mmol, 1.00 eq.) and 14 mL MeOH. After 5.0 F/mol, full conversion was observed *via* GC-MS. Column chromatography of the crude product (SiO₂, *c*-hexane/EtOAc 6:1) afforded the title compound (**2c**, 0.840 g, 2.72 mmol; 68%) as a colorless viscous oil.

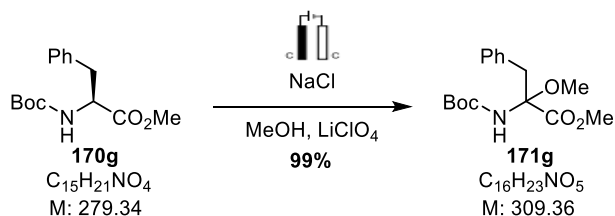
R_f = 0.5 (*c*-hexane/EtOAc = 4:1).

¹H NMR (600 MHz, CDCl₃) δ = 7.50 – 7.34 (m, 4H), 7.33 – 7.28 (m, 1H), 6.13 (s, 1H), 5.19 – 5.06 (m, 2H), 3.20 (s, 3H), 1.76 (s, 3H), 1.49 (s, 9H) ppm.

¹³C NMR (151 MHz, CDCl₃) δ = 169.6, 154.0, 136.4, 128.7, 128.3, 128.2, 85.7, 83.4, 66.7, 51.2, 27.9, 23.2 ppm.

IR (neat): $\tilde{\nu}$ = 3410, 3031, 2979, 1739, 1704, 1637, 1510, 1480, 1455, 1370, 1330, 1257, 1194, 1159, 1066, 967, 892, 847, 808 cm⁻¹.

HRMS (ESI): m/z calculated for C₁₆H₂₃NNaO₅⁺ ([M+Na]⁺): 332.1468; found: 332.1489.

5.8.9. Methyl α -*N*-Boc- α -methoxyphenylalaninate (**171g**)

Compound **171g** was prepared according to **GP3** starting from **170g** (2.23 g, 7.98 mmol, 1.00 eq.) and 27 mL MeOH. After passing 4.9 F/mol, full conversion was observed *via* GC-MS and the title compound (**171g**, 2.44 g, 7.88 mmol; 99%) was obtained as colorless resin. The product was spectroscopically pure without further purification.

R_f = 0.6 (*c*-hexane/EtOAc = 1:1).

¹H NMR (500 MHz, CDCl₃) δ = 7.30 – 7.22 (m, 3H), 7.16 – 7.10 (m, 2H), 5.68 (s, 1H), 3.96 – 3.83 (m, 1H), 3.81 (s, 3H), 3.25 (s, 3H), 3.19 (d, J = 13.5 Hz, 1H), 1.49 (s, 9H) ppm.

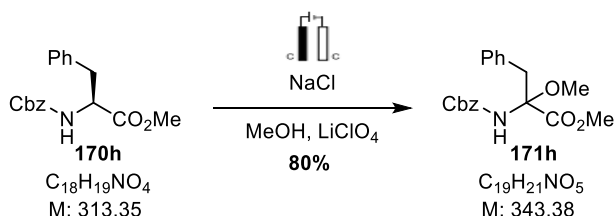
¹³C NMR (151 MHz, CDCl₃) δ = 170.4, 153.6, 134.8, 130.2, 128.5, 127.4, 89.0, 80.3, 53.0, 51.6, 41.3, 28.4, 28.2 ppm.

IR (neat): $\tilde{\nu}$ = 3427, 3344, 2975, 2952, 2835, 1725, 1492, 1455, 1367, 1319, 1299, 1282, 1242, 1205, 1159, 1086, 1076, 1016, 888, 868, 824, 739 cm⁻¹.

HRMS (ESI): m/z calculated for C₁₆H₂₃NNaO₅⁺ ([M+Na]⁺): 332.1468; found: 332.1455.

The analytical data of compound **2e** is in agreement with the literature.^[152]

5.8.10. Methyl α -N-Cbz- α -methoxyphenylalaninate (**171h**)



Compound **171h** was prepared according to **GP3** starting from **170h** (1.25 g, 4.00 mmol, 1.00 eq.) and 14 mL MeOH. After passing 6.1 F/mol, full conversion was observed *via* GC-MS. Column chromatography of the crude product (SiO₂, *c*-hexane/EtOAc 3:1) afforded the title compound (**171h**, 1.09 g, 3.19 mmol; 80%) as colorless solid.

R_f = 0.5 (*c*-hexane/EtOAc = 2:1).

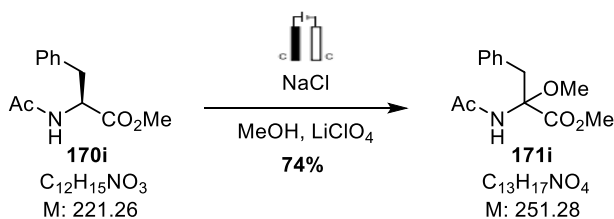
¹H NMR (600 MHz, CDCl₃) δ 7.43 – 7.32 (m, 5H), 7.23 – 7.16 (m, 3H), 7.03 (d, J = 6.7 Hz, 2H), 5.95 (s, 1H), 5.23 (d, J = 12.1 Hz, 1H), 5.11 (d, J = 12.5 Hz, 1H), 3.88 (d, J = 12.9 Hz, 1H), 3.80 (s, 3H), 3.23 (s, 3H), 3.21 (d, J = 13.6 Hz, 1H) ppm.

¹³C NMR (151 MHz, CDCl₃) δ 170.1, 154.0, 136.3, 134.4, 130.1, 128.7, 128.5, 128.5, 128.4, 127.4, 89.3, 66.9, 53.2, 51.7, 41.2 ppm.

IR (neat): $\tilde{\nu}$ = 3412, 3032, 2954, 2927, 2850, 1729, 1495, 1455, 1319, 1281, 1199, 1155, 1074, 1021, 830, 740 cm⁻¹.

HRMS (ESI): m/z calculated for C₁₉H₂₁NNaO₅⁺ ([M+Na]⁺): 366.1312; found: 366.1302.

5.8.11. Methyl α -N-Ac- α -methoxyphenylalaninate (**171i**)



Compound **171i** was prepared according to **GP3** starting from **170i** (0.885 g, 4.00 mmol, 1.00 eq.) and 14 mL MeOH. After passing 4.0 F/mol, full conversion was observed *via* GC-MS and the title compound (**171i**, 0.747 g, 2.97 mmol; 74%) was obtained as colorless resin. The product was spectroscopically pure without further purification.

R_f = 0.8 (*c*-hexane/EtOAc = 2:1).

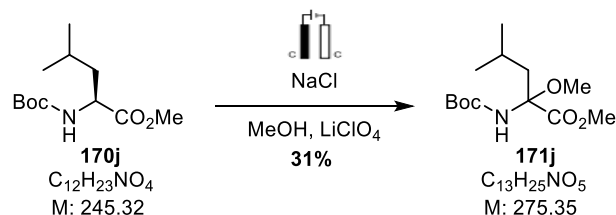
$^1\text{H NMR}$ (600 MHz, CDCl_3) δ = 7.30 – 7.23 (m, 3H), 7.13 – 7.09 (m, 2H), 6.63 (s, 1H), 3.81 (s, 3H), 3.79 (d, J = 13.7 Hz, 1H), 3.27 (s, 3H), 3.25 (d, J = 13.8 Hz, 1H), 2.05 (s, 3H) ppm.

$^{13}\text{C NMR}$ (151 MHz, CDCl_3) δ = 170.6, 170.4, 134.3, 130.1, 128.5, 127.5, 88.6, 53.2, 51.8, 40.6, 23.9 ppm.

IR (neat): $\tilde{\nu}$ = 3314, 3062, 3032, 2950, 2839, 2249, 1744, 1669, 1531, 1496, 1455, 1437, 1371, 1335, 1286, 1263, 1206, 1110, 1085, 1067, 1030, 974, 955, 913, 862, 830, 813, 786 cm^{-1} .

HRMS (ESI): m/z calculated for $\text{C}_{13}\text{H}_{17}\text{NNaO}_4^+$ ($[\text{M}+\text{Na}]^+$): 274.1050; found: 274.1041.

5.8.12. Methyl α -N-Boc- α -methoxyleucinate (**171j**)



Compound **171j** was prepared according to **GP3** starting from **170j** (0.981 g, 4.00 mmol, 1.00 eq.) and 14 mL MeOH. After passing 8.0 F/mol, 41% conversion was observed *via* GC-MS and did not progress any further. Column chromatography of the crude product (SiO_2 , n -pentane/ Et_2O 10:1 \rightarrow 5:1) afforded the title compound (**171j**, 0.339 g, 1.23 mmol; 31%; 56% brsm) as colorless oil. Starting material **170j** was reisolated (0.438 g; 1.79 mmol; 45%).

R_f = 0.4 (n -pentane/ Et_2O = 5:1).

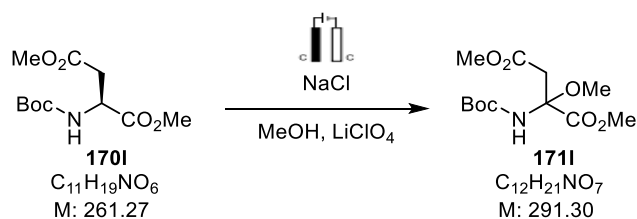
$^1\text{H NMR}$ (600 MHz, CDCl_3) δ = 5.78 (s, 1H), 3.81 (s, 3H), 3.19 (s, 3H), 1.80 (dd, J = 14.0, 6.7 Hz, 1H), 1.64 – 1.54 (m, 2H), 1.45 (s, 9H), 0.91 (d, J = 6.7 Hz, 3H), 0.85 (d, J = 6.7 Hz, 3H) ppm.

$^{13}\text{C NMR}$ (151 MHz, CDCl_3) δ = 171.4, 153.3, 87.8, 80.2, 53.0, 50.7, 43.6, 28.3, 24.3, 23.4, 23.3 ppm.

IR (neat): $\tilde{\nu}$ = 3362, 2961, 2930, 2874, 2850, 1725, 1599, 1499, 1453, 1439, 1390, 1366, 1250, 1165, 1055, 1020, 747 cm^{-1} .

HRMS (ESI): m/z calculated for $\text{C}_{13}\text{H}_{25}\text{NNaO}_5^+$ ($[\text{M}+\text{Na}]^+$): 298.1625; found: 298.1618.

The analytical data of compound 2h is in agreement with the literature.^[152]

5.8.13. Dimethyl *N*-Boc- α -methoxyaspartate (**171l**)

Compound **171l** was prepared according to **GP3** starting from **170l** (1.05 g, 4.00 mmol, 1.00 eq.) and 14 mL MeOH. After 9.6 F/mol, the conversion didn't progress any further and the flow of current was stopped. The crude product was purified by column chromatography (SiO_2 , *n*-pentane/EtOAc 4:1 \rightarrow 3:1) and the title compound (**171l**, 187 mg, 0.641 mmol; 16%, 23% brsm) was obtained as a colorless solid. Starting material **170l** (0.317 g; 1.21 mmol; 30%) was reisolated.

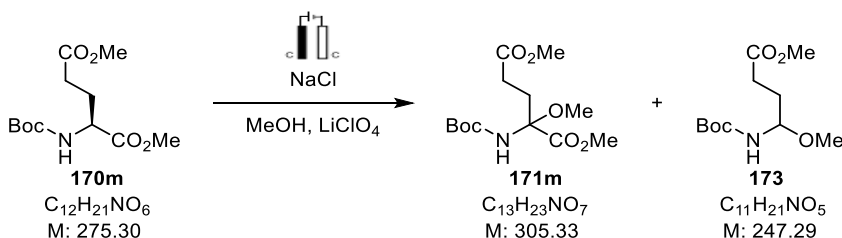
$R_f = 0.5$ (*c*-hexane/EtOAc 2:1).

$^1\text{H NMR}$ (600 MHz, CDCl_3) $\delta = 6.33$ (s, 1H), 3.84 (s, 3H), 3.67 (s, 3H), 3.35 (s, 1H), 3.23 (s, 3H), 3.05 (d, $J = 16.0$ Hz, 1H), 1.45 (s, 9H) ppm.

$^{13}\text{C NMR}$ (176 MHz, CDCl_3) $\delta = 170.2, 169.3, 153.6, 85.1, 80.6, 53.4, 52.0, 51.2, 40.3, 28.3$ ppm.

IR (neat): $\tilde{\nu} = 3017, 2954, 2853, 1740, 1738, 1491, 1438, 1366, 1303, 1217, 1157, 1077, 1046, 1024, 755$ cm^{-1} .

HRMS (ESI): m/z calculated for $\text{C}_{12}\text{H}_{21}\text{NNaO}_7^+$ ($[\text{M}+\text{Na}]^+$): 314.1210; found: 314.1224.

5.8.14. Dimethyl *N*-Boc- α -methoxyglutamate (**171m**)

Compound **171m** was prepared according to **GP3** starting from **170m** (1.05 g, 4.00 mmol, 1.00 eq.) and 14 mL MeOH. After 7.7 F/mol, the conversion didn't progress any further and the flow of current was stopped. The crude product was purified by column chromatography (SiO_2 , *c*-hexane/EtOAc 3:1) and the title compound (**171m**, 241 mg, 0.799 mmol; 20%, 33% brsm) was obtained as colorless oil. Additionally, compound **173** (74.4 mg, 0.301 mmol, 8%, 13% brsm) was isolated as colorless oil and remaining starting material **170m** (0.448 g; 1.63 mmol; 41%) was recovered.

$R_f = 0.3$ (*c*-hexane/EtOAc = 2:1).

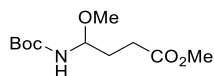
$^1\text{H NMR}$ (500 MHz, CDCl_3) $\delta = 5.84$ (s, 1H), 3.82 (s, 3H), 3.67 (s, 3H), 3.26 (s, 3H), 2.60 – 2.49 (m, 1H), 2.38 – 2.29 (m, 3H), 1.45 (s, 9H) ppm.

$^{13}\text{C NMR}$ (151 MHz, CDCl_3) $\delta = 173.2, 170.3, 153.5, 86.9, 53.1, 51.9, 51.2, 31.1, 28.6, 28.4, 28.3, 27.8$ ppm.

IR (neat): $\tilde{\nu} = 3355, 3328, 1737, 1721, 1515, 1441, 1366, 1216, 1167, 1051, 935, 890, 855$ cm^{-1} .

HRMS (ESI): m/z calculated for $C_{13}H_{23}NNaO_7^+$ ($[M+Na]^+$): 328.1367; found: 328.1357.

Methyl 4-(*N*-Boc)-4-methoxybutanoate (**173**)



R_f = 0.5 (c-hexane/EtOAc = 2:1).

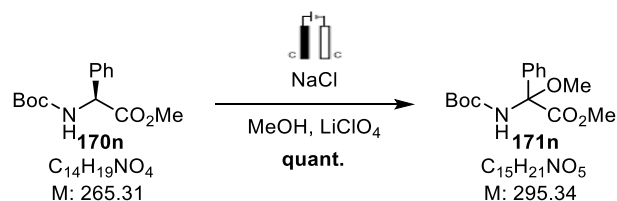
1H NMR (500 MHz, $CDCl_3$) δ 4.93 (d, J = 10.3 Hz, 1H), 4.84 (dt, J = 10.3, 6.3 Hz, 1H), 3.68 (s, 3H), 3.33 (s, 3H), 2.51 – 2.32 (m, 2H), 2.00 – 1.84 (m, 2H), 1.45 (s, 9H) ppm.

^{13}C NMR (151 MHz, $CDCl_3$) δ = 173.7, 155.5, 82.3, 79.9, 55.5, 51.8, 30.7, 29.8, 28.4 ppm.

IR (neat): $\tilde{\nu}$ = 3362, 2979, 2953, 2851, 1718, 1509, 1437, 1367, 1310, 1242, 1156, 1092, 1053, 981, 920, 875, 823 cm^{-1} .

HRMS (ESI): m/z calculated for $C_{11}H_{21}NNaO_5^+$ ($[M+Na]^+$): 270.1312; found: 270.1308.

5.8.15. Methyl *N*-Boc- α -methoxyphenylglycinate (**171n**)



Compound **171n** was prepared according to **GP3** starting from **170n** (1.06 g, 4.00 mmol, 1.00 eq.) and 14 mL MeOH. After passing 4.9 F/mol (100 mA), full conversion was observed via GC-MS and the title compound (**171n**, 1.19 g*, 4.00 mmol; quant.) was obtained as colorless solid. The product was spectroscopically pure without further purification.

R_f = 0.5 (c-hexane/EtOAc = 2:1).

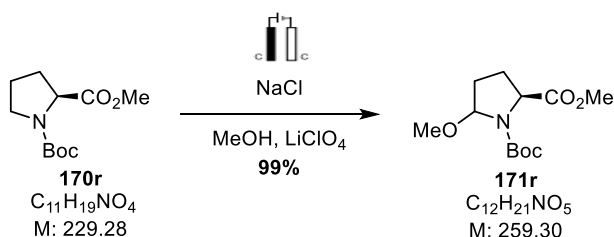
1H NMR (500 MHz, $CDCl_3$) δ = 7.64 – 7.55 (m, 2H), 7.41 – 7.32 (m, 3H), 6.26 (s, 1H), 3.71 (s, 3H), 3.34 (s, 3H), 1.38 (s, 9H) ppm.

^{13}C NMR (151 MHz, $CDCl_3$) δ = 170.6, 153.6, 137.5, 129.0, 128.7, 126.2, 87.9, 81.1, 53.7, 51.0, 28.2 ppm

IR (neat): $\tilde{\nu}$ = 2979, 2937, 1719, 1483, 1450, 1366, 1275, 1162, 1097, 1073, 1013, 874, 727 cm^{-1} .

HRMS (ESI): m/z calculated for $C_{15}H_{21}NNaO_5^+$ ($[M+Na]^+$): 318.1312; found: 318.1310.

*The mass is slightly higher than expected due to unremovable traces of solvent.

5.8.16. Methyl *N*-Boc- δ -methoxyprolinate (**171r**)

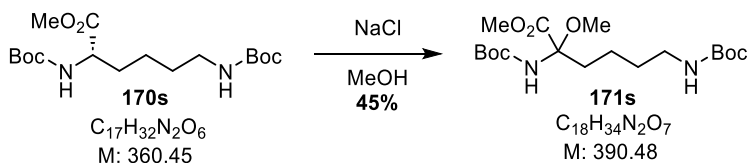
Compound **171r** was prepared according to **GP3** starting from **170r** (0.917 g, 4.00 mmol, 1.00 eq.) and 14 mL MeOH. After passing 16 F/mol (100 mA), full conversion was observed via GC-MS and the title compound (**171r**, 1.03 g, 3.97 mmol, 99%, *d.r.* = 1:1 *trans/cis*) was obtained as colorless oil. The product was spectroscopically pure without further purification.

R_f = 0.4 (*c*-hexane/EtOAc = 4:1).

$^1\text{H NMR}$ (500 MHz, CDCl_3 , mixture of diastereomers and rotamers) δ = 5.33 – 5.12 (m, 1H), 4.41 – 4.20 (m, 1H), 3.81 – 3.70 (m, 3H), 3.46 – 3.35 (m, 3H), 2.55 – 2.24 (m, 1H), 2.22 – 1.72 (m, 3H), 1.54 – 1.36 (m, 9H) ppm.

$^{13}\text{C NMR}$ (151 MHz, CDCl_3) δ = 173.4, 173.1, 154.2, 89.4, 89.3, 88.6, 88.5, 80.9, 80.7, 59.7, 59.3, 59.0, 58.8, 56.3, 56.0, 55.5, 55.1, 52.2, 52.1, 52.1, 33.0, 32.3, 31.2, 30.2, 28.4, 28.4, 28.2, 28.1, 28.1, 27.2 ppm.

The analytical data of compound **171r** is in agreement with the literature.^[207]

5.8.17. Methyl α -*N*-Boc- ϵ -*N'*-Boc- α -methoxylysinate (**171s**)

Compound **171s** was prepared according to **GP3** without the addition of LiClO_4 starting from **170s** (1.44 g, 4.00 mmol, 1.00 eq.) and 14 mL MeOH. After 10 F/mol, the conversion didn't progress any further and the flow of current was stopped. The crude product was purified by column chromatography (SiO_2 , *c*-hexane/EtOAc 3:1) and the title compound (**171s**, 0.701 g, 1.79 mmol; 45%, 63% brsm) was obtained as colorless resin. The starting material **170s** (0.400 g; 1.11 mmol; 28%) was recovered.

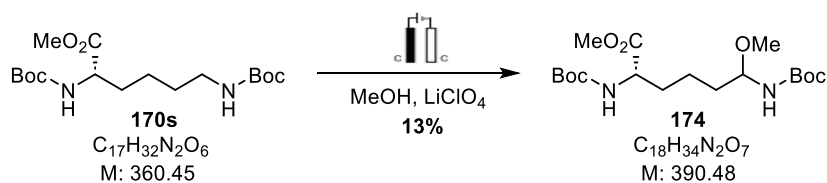
R_f = 0.3 (*c*-hexane/EtOAc = 2:1).

$^1\text{H NMR}$ (500 MHz, CDCl_3) δ = 5.73 (s, 1H), 4.56 (s, 1H), 3.82 (s, 3H), 3.23 (s, 3H), 3.16 – 3.04 (m, 2H), 2.40 (s, 1H), 1.88 (ddd, J = 13.6, 11.6, 5.1 Hz, 1H), 1.45 (s, 18H), 1.43 (s, 19H), 1.34 – 1.12 (m, 3H) ppm.

$^{13}\text{C NMR}$ (126 MHz, CDCl_3) δ = 170.8, 156.1, 153.6, 88.0, 80.4, 79.2, 53.1, 51.1, 40.1, 35.1, 29.7, 28.5, 28.4, 28.3, 20.9 ppm.

IR (neat): $\tilde{\nu}$ = 3439, 3379, 2976, 2933, 2871, 1709, 1491, 1454, 1392, 1366, 1293, 1274, 1245, 1162, 1058, 1007, 896, 878, 775 cm^{-1} .

HRMS (ESI): m/z calculated for $\text{C}_{18}\text{H}_{34}\text{N}_2\text{NaO}_7$ ($[\text{M}+\text{Na}]^+$): 413.2259; found: 413.2255.

5.8.18. Methyl α -N-Boc- ϵ -N'-Boc- ϵ -methoxylysinate (**174**)

Compound **174** was prepared according to **GP3** without the addition of NaCl starting from **170s** (1.44 g, 4.00 mmol, 1.00 eq.) and 14 mL MeOH. After 10.4 F/mol, the conversion didn't progress any further and the flow of current was stopped. The crude product was purified by column chromatography (SiO₂, *c*-hexane/EtOAc = 5:1 → 2:1) and the title compound (**174**, 98.0 mg, 0.251 mmol; 13%, d.r.: ~1:1) was obtained as colorless resin.

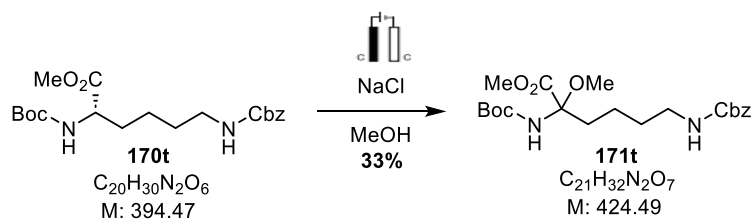
R_f = 0.4 (*c*-hexane/EtOAc = 2:1).

¹H NMR (500 MHz, CDCl₃) δ = 5.08 (d, *J* = 7.5 Hz, 1H), 4.87 (d, *J* = 10.5 Hz, 1H), 4.79 (dt, *J* = 10.3, 5.9, 1H), 4.34 – 4.24 (m, 1H), 3.74 (s, 3H), 3.33 (s, 3H), 1.81 (dq, *J* = 15.9, 6.0, 5.4 Hz, 1H), 1.65 (tt, *J* = 16.0, 6.2 Hz, 2H), 1.51 – 1.39 (m, 21H) ppm.

¹³C NMR (126 MHz, CDCl₃) δ = 173.4, 155.6, 82.7, 80.0, 79.4, 55.4, 53.34 (a-CH_{dia-1}), 53.24 (a-CH_{dia-2}), 52.4, 35.2, 35.1, 32.49, 32.48, 28.43, 28.40, 28.3, 28.0, 27.0, 20.9 ppm.

IR (neat): $\tilde{\nu}$ = 3363, 2977, 2934, 1698, 1499, 1455, 1391, 1365, 1250, 1163, 1092, 1066, 988, 877, 753 cm⁻¹.

HRMS (ESI): *m/z* calculated for C₁₈H₃₄N₂NaO₇⁺ ([M+Na]⁺): 413.2259; found: 413.2243.

5.8.19. Methyl α -N-Boc- ϵ -N'-Cbz- α -methoxylysinate (**171t**)

Compound **171t** was prepared according to **GP3** without the addition of LiClO₄ starting from **170t** (1.58 g, 4.00 mmol, 1.00 eq.) and 14.0 mL MeOH. After 9.3 F/mol, the conversion didn't progress any further and the flow of current was stopped. The crude product was purified by column chromatography (SiO₂, *c*-hexane/EtOAc = 2:1) and the title compound (**171t**, 560 mg, 1.32 mmol; 33%; 59% brsm) was obtained as colorless resin. The starting material **170t** (0.691 g; 1.75 mmol; 44%) was recovered.

R_f = 0.2 (*c*-hexane/EtOAc = 2:1).

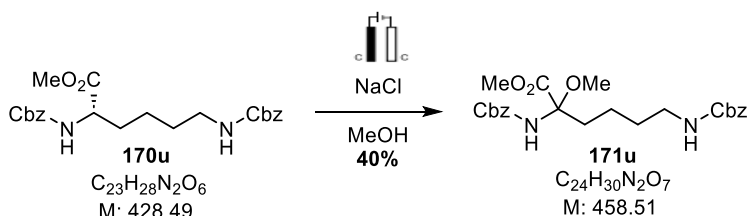
¹H NMR (600 MHz, CDCl₃) δ = 7.35 (d, *J* = 5.9 Hz, 4H), 7.33 – 7.29 (m, 1H), 5.74 (s, 1H), 5.08 (s, 2H), 4.83 (s, 1H), 3.80 (s, 3H), 3.23 (s, 3H), 3.21 – 3.13 (m, 2H), 2.41 (s, 1H), 1.88 (ddd, *J* = 13.4, 11.6, 5.1 Hz, 1H), 1.56 – 1.46 (m, 2H), 1.46 – 1.41 (m, 9H), 1.31 – 1.14 (m, 2H) ppm.

^{13}C NMR (151 MHz, CDCl_3) δ = 170.7, 156.5, 153.6, 136.7, 128.6, 128.24, 128.21, 88.0, 80.5, 66.7, 53.2, 51.1, 40.5, 35.0, 29.5, 28.3, 20.8 ppm.

IR (neat): $\tilde{\nu}$ = 3342, 2971, 2932, 2871, 1702, 1519, 1455, 1366, 1247, 1157, 1004, 752 cm^{-1} .

HRMS (ESI): m/z calculated for $\text{C}_{21}\text{H}_{32}\text{N}_2\text{NaO}_7^+$ ($[\text{M}+\text{Na}]^+$): 447.2102; found: 447.2115.

5.8.20. Methyl α -*N*-Cbz- ϵ -*N'*-Cbz- α -methoxylysinate (**171u**)



Compound **171u** was prepared according to **GP3** without the addition of LiClO_4 starting from **170u** (1.53 g, 3.57 mmol, 1.00 eq.) and 12 mL MeOH. After 9.4 F/mol, the conversion didn't progress any further and the flow of current was stopped. The crude product was purified by column chromatography (SiO_2 , *c*-hexane/EtOAc = 2:1 \rightarrow 1:1) and the title compound (**171u**, 655 mg, 1.43 mmol; 40%; 45% brsm) was obtained as colorless resin. The starting material **170u** (180 mg; 0.419 mmol; 12%) was recovered.

R_f = 0.16 (*c*-hexane/EtOAc = 2:1).

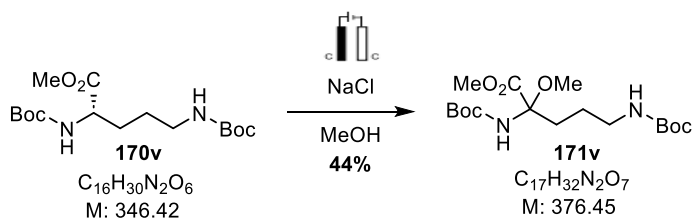
^1H NMR (600 MHz, CDCl_3) δ = 7.40 – 7.26 (m, 10H), 6.18 – 5.98 (m, 1H), 5.18 – 5.02 (m, 4H), 4.79 (s, 1H), 3.80 (s, 3H), 3.20 (s, 3H), 3.19 – 3.10 (m, 2H), 2.49 (s, 1H), 1.92 (td, J = 13.0, 4.9 Hz, 1H), 1.48 (dt, J = 20.3, 6.7 Hz, 2H), 1.30 – 1.08 (m, 2H) ppm.

^{13}C NMR (151 MHz, CDCl_3) δ = 170.6, 156.6, 154.0, 136.7, 136.2, 128.7, 128.6, 128.4, 128.3, 128.2, 88.4, 67.0, 66.8, 53.3, 51.3, 40.5, 34.8, 29.4, 20.8 ppm.

IR (neat): $\tilde{\nu}$ = 3418, 3336, 3033, 2948, 2870, 2853, 1699, 1521, 1455, 1374, 1323, 1233, 1136, 1089, 1067, 1011, 914, 738 cm^{-1} .

HRMS (ESI): m/z calculated for $\text{C}_{24}\text{H}_{30}\text{N}_2\text{NaO}_7^+$ ($[\text{M}+\text{Na}]^+$): 481.1946; found: 481.1972.

5.8.21. Methyl α -*N*-Boc- δ -*N'*-Boc- α -methoxyornithate (**171v**)



Compound **171v** was prepared according to **GP3** without the addition of LiClO_4 starting from **170v** (1.39 g, 4.00 mmol, 1.00 eq.) and 14 mL MeOH. After 11.9 F/mol, the conversion didn't progress any further and the flow of current was stopped. The crude product was purified by column chromatography (SiO_2 , *c*-hexane/EtOAc = 3:1 \rightarrow 2:1) and the title compound (**171v**, 666 mg, 1.77 mmol; 44%; 53% brsm) was obtained as a crystalline solid. The starting material **170v** (0.236 g; 0.681 mmol; 17%) was recovered.

$R_f = 0.3$ (c-hexane/EtOAc = 2:1).

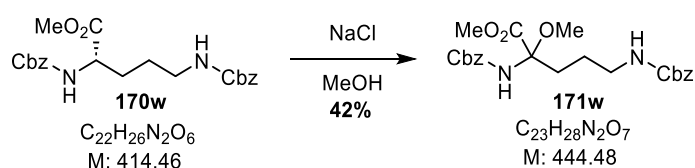
$^1\text{H NMR}$ (500 MHz, CDCl_3) $\delta = 5.77$ (s, 1H), 4.68 (s, 1H), 3.82 (s, 3H), 3.24 (s, 3H), 3.15 – 3.06 (m, 2H), 2.37 (s, 1H), 1.93 (ddd, $J = 13.7, 10.4, 6.1$ Hz, 1H), 1.60 – 1.34 (m, 20H) ppm.

$^{13}\text{C NMR}$ (126 MHz, CDCl_3) $\delta = 250.6, 170.5, 156.0, 153.5, 87.7, 80.4, 79.1, 53.0, 51.0, 40.0, 32.9, 28.4, 28.3, 24.3$ ppm.

IR (neat): $\tilde{\nu} = 3364, 3004, 2978, 2935, 1694, 1512, 1454, 1391, 1366, 1322, 1276, 1247, 1161, 1065, 1004, 871, 753$ cm^{-1} .

HRMS (ESI): m/z calculated for $\text{C}_{17}\text{H}_{32}\text{N}_2\text{NaO}_7^+$ ($[\text{M}+\text{Na}]^+$): 399.2102; found: 399.2119.

5.8.22. Methyl α -N-Cbz- δ -N'-Cbz- α -methoxyornithate (**171w**)



Compound **171w** was prepared according to **GP3** without the addition of LiClO_4 starting from **170w** (1.658 g, 4.00 mmol, 1.00 eq.) and 14 mL MeOH. After 8.7 F/mol, the conversion didn't progress any further and the flow of current was stopped. The crude product was purified by column chromatography (SiO_2 , c-hexane/EtOAc = 1:1) and the title compound (**171w**, 743 mg, 1.67 mmol; 42%, 50% brsm) was obtained as a colorless resin. The starting material **170w** (266 mg; 0.266 mmol; 12%) was recovered.

$R_f = 0.3$ (c-hexane/EtOAc = 1:1).

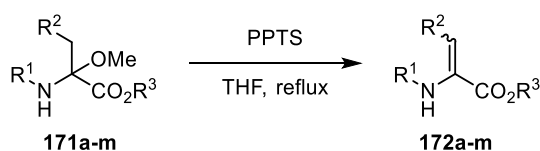
$^1\text{H NMR}$ (600 MHz, CDCl_3) $\delta = 7.41 - 7.27$ (m, 10H), 6.05 (s, 1H), 5.16 – 5.03 (m, 4H), 4.79 (s, 1H), 3.79 (s, 3H), 3.20 (s, 3H), 3.15 (q, $J = 6.6$ Hz, 2H), 2.46 (s, 1H), 1.97 (dt, $J = 13.7, 7.6$ Hz, 1H), 1.39 (p, $J = 7.3$ Hz, 2H) ppm.

$^{13}\text{C NMR}$ (151 MHz, CDCl_3) $\delta = 170.4, 156.4, 153.9, 136.7, 136.1, 128.8, 128.7, 128.6, 128.5, 128.4, 128.3, 128.2, 88.2, 67.1, 66.7, 53.4, 51.3, 40.6, 32.6, 27.5, 24.3$ ppm.

IR (neat): $\tilde{\nu} = 3330, 3060, 3033, 2950, 1704, 1523, 1455, 1328, 1244, 1137, 1090, 1025, 778, 740$ cm^{-1} .

HRMS (ESI): m/z calculated for $\text{C}_{23}\text{H}_{28}\text{N}_2\text{NaO}_7^+$ ($[\text{M}+\text{Na}]^+$): 467.1789; found: 467.1802.

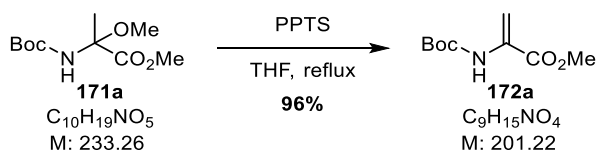
5.8.23. General Procedure for the acid-catalyzed Elimination (**GP4**)



A two-necked flask equipped with a reflux condenser was charged with the methoxylated compound **171a-m** (1.00 eq.) in dry THF (0.1-0.3 M) and PPTS (0.20-0.50 eq.). The reaction mixture was heated to reflux in an oil bath until full conversion was observed. The solution was allowed to cool down to room temperature and treated sat. aq. NaHCO_3 -sol. (20 mL/mmol). The aqueous phase was extracted three times with EtOAc

(5 mL/mmol), the combined organic phases were washed with brine (10 mL/mmol), dried over MgSO₄, filtered and the solvent was removed under reduced pressure.

5.8.24. Methyl *N*-Boc- α,β -didehydroalaninate (**172a**)



Compound **172a** was prepared according to **GP4** starting from **171a** (0.100 g, 0.429 mmol, 1.00 eq.), PPTS (32.3 mg, 0.129 mmol, 0.30 eq.) and 5 mL THF. After 4 h, full conversion was observed and the title compound (**172a**, 83.0 mg, 0.413 mmol; 96%) was obtained as colorless oil. The product was spectroscopically pure without further purification.

R_f = 0.4 (c-hexane/EtOAc = 15:1).

¹H NMR (500 MHz, CDCl₃) δ = 6.99 (s, 1H), 6.12 (s, 1H), 5.68 (d, J = 1.5 Hz, 1H), 3.79 (s, 3H), 1.45 (s, 9H) ppm.

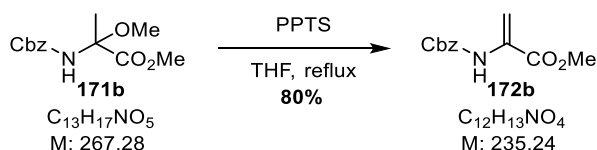
¹³C NMR (126 MHz, CDCl₃) δ = 164.5, 152.6, 131.4, 105.2, 80.7, 52.9, 28.3 ppm.

IR (neat): $\tilde{\nu}$ = 3423, 2978, 2930, 2853, 1717, 1633, 1509, 1441, 1392, 1368, 1326, 1245, 1202, 1158, 1067, 999, 965, 884, 845, 807, 776, 714 cm⁻¹.

HRMS (ESI): m/z calculated for C₉H₁₅NNaO₄⁺ ([M+Na]⁺): 224.0893; found: 224.0891.

The analytical data of compound **172a** is in agreement with the literature.^[36]

5.8.25. Methyl *N*-Cbz- α,β -didehydroalaninate (**172b**)



Compound **172b** was prepared according to **GP4** starting from **171b** (0.874 g, 3.27 mmol, 1.00 eq.), PPTS (0.164 g, 0.654 mmol, 0.20 eq.) and 16 mL THF. After 18 h, full conversion was observed and the title compound (**172b**, 0.618 g, 2.63 mmol; 80%) was obtained as colorless oil. The product was spectroscopically pure without further purification.

R_f = 0.7 (c-hexane/EtOAc = 2:1).

¹H NMR (600 MHz, CDCl₃) δ = 7.40 – 7.37 (m, 3H), 7.37 – 7.32 (m, 1H), 7.26 – 7.22 (m, 1H), 6.25 (s, 1H), 5.79 (d, J = 1.5 Hz, 1H), 5.16 (s, 2H), 3.83 (s, 3H).

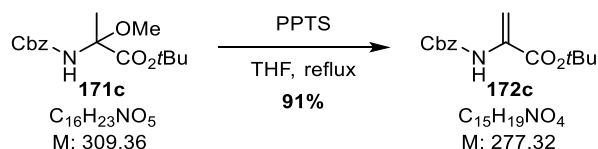
¹³C NMR (151 MHz, CDCl₃) δ 164.3, 153.3, 136.0, 131.1, 128.8, 128.5, 128.4, 106.2, 67.2, 53.1 ppm.

IR (neat): $\tilde{\nu}$ = 3028, 3004, 2954, 2925, 2852, 1738, 1717, 1636, 1519, 1440, 1375, 1323, 1217, 1201, 1066, 897, 805, 749 cm^{-1} .

HRMS (ESI): m/z calculated for $\text{C}_{12}\text{H}_{13}\text{NNaO}_4^+$ ($[\text{M}+\text{Na}]^+$): 258.0737; found: 258.0742.

The analytical data of compound **172b** is in agreement with the literature.^[36]

5.8.26. *tert*-Butyl *N*-Cbz- α,β -didehydroalaninate (**172c**)



Compound **172c** was prepared according to **GP4** starting from **171c** (0.336 g, 1.09 mmol, 1.00 eq.), PPTS (74.0 mg, 0.326 mmol, 0.30 eq.) and 6 mL THF. After 5 h, full conversion was observed and the title compound (**172c**, 0.274 g, 0.988 mmol; 91%) was obtained as colorless oil. The product was spectroscopically pure without further purification.

R_f = 0.7 (*c*-hexane/EtOAc = 4:1).

¹H NMR (700 MHz, CDCl_3) δ = 7.43 – 7.39 (m, 4H), 7.39 – 7.34 (m, 1H), 7.31 – 7.27 (m, 1H), 6.19 (s, 1H), 5.73 (d, J = 1.5 Hz, 1H), 5.19 (s, 2H), 1.54 (s, 9H) ppm.

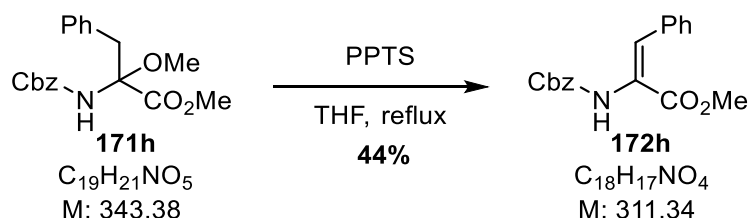
¹³C NMR (176 MHz, CDCl_3) δ = 162.9, 153.3, 136.1, 132.3, 128.7, 128.4, 128.3, 105.0, 82.9, 67.0, 28.0 ppm.

IR (neat): $\tilde{\nu}$ = 3410, 3065, 3033, 2979, 2933, 1738, 1703, 1637, 1509, 1456, 1370, 1330, 1223, 1193, 1158, 967, 892, 847, 807, 767 cm^{-1} .

HRMS (ESI): m/z calculated for $\text{C}_{15}\text{H}_{19}\text{NNaO}_4^+$ ($[\text{M}+\text{Na}]^+$): 300.1206; found: 300.1210.

The analytical data of compound **4c** is in agreement with the literature.^[208]

5.8.27. Methyl *N*-Cbz-(*E*)- α,β -didehydrophenylalaninate (**172h**)



Compound **172h** was prepared according to **GP4** starting from **171h** (100 mg, 0.291 mmol, 1.00 eq.), PPTS (22.0 mg, 87.4 μmol , 0.30 eq.) and 3 mL THF. After 17 h, full conversion was observed. The crude product was purified by column chromatography (SiO_2 , *c*-hexane/EtOAc = 9:1) and the title compound (**172h**, 39.9 mg, 0.128 mmol; 44%, *E/Z* = 97/3) was obtained as colorless oil.

$R_f = 0.4$ (c-hexane/EtOAc = 4:1).

$^1\text{H NMR}$ (600 MHz, CDCl_3) $\delta = 7.63$ (s, 1H), 7.41 – 7.36 (m, 4H), 7.36 – 7.31 (m, 1H), 7.30 (t, $J = 7.3$ Hz, 2H), 7.23 (t, $J = 7.4$ Hz, 3H), 7.01 (s, 1H), 5.17 (s, 2H), 3.61 (s, 3H) ppm.

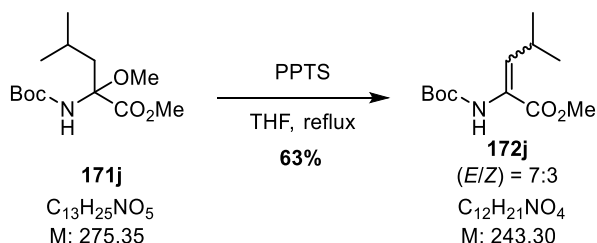
$^{13}\text{C NMR}$ (151 MHz, CDCl_3) $\delta = 165.0, 153.6, 135.9, 135.5, 128.8, 128.7, 128.5, 128.4, 128.0, 127.6, 125.7, 124.6, 67.4, 52.4$ ppm.

IR (neat): $\tilde{\nu} = 3319, 3062, 3031, 2952, 2924, 2853, 1793, 1706, 1637, 1516, 1495, 1455, 1437, 1380, 1310, 1218, 1167, 1049, 1028, 918, 751$ cm^{-1} .

HRMS (ESI): m/z calculated for $\text{C}_{18}\text{H}_{17}\text{NNaO}_4^+$ ($[\text{M}+\text{Na}]^+$): 334.1050; found: 334.1038.

The analytical data of the (*E*)-isomer **172h** is in agreement with the literature.^[209]

5.8.28. Methyl *N*-Boc-(*E/Z*)- α,β -didehydroleucinate (**172j**)



Compound **172j** was prepared according to **GP4** starting from **171j** (0.470 g, 1.71 mmol, 1.00 eq.), PPTS (0.129 g, 0.512 mmol, 0.30 eq.) and 9 mL THF. After 4 h, full conversion was observed. The crude product was purified by column chromatography (SiO_2 , c-hexane/EtOAc = 19:1 \rightarrow 9:1) to afford the (*E*)-isomer *E*-**172j** (0.183 g; 0.752 mmol; 44%) and the (*Z*)-isomer *Z*-**172j** (80.8 mg; 0.332 mmol; 19%) as colorless oils.

Methyl *N*-Boc-(*E*)- α,β -didehydroleucinate (*E*-**172j**)

$R_f = 0.7$ (c-hexane/EtOAc = 4:1).

$^1\text{H NMR}$ (500 MHz, CDCl_3) $\delta = 6.48$ (s, 2H), 3.80 (s, 3H), 3.27 (dp, $J = 10.1, 6.6$ Hz, 1H), 1.45 (s, 9H), 1.04 (d, $J = 6.6$ Hz, 6H) ppm.

$^{13}\text{C NMR}$ (151 MHz, CDCl_3) $\delta = 165.0, 153.4, 137.6, 123.3, 80.3, 52.3, 28.4, 27.5, 23.3$ ppm; **IR** (neat): $\tilde{\nu} = 3420, 3358, 2970, 2931, 2870, 1707, 1645, 1510, 1467, 1437, 1364, 1335, 1246, 1197, 1158, 1046, 1023, 951, 899, 855, 829, 771$ cm^{-1} .

HRMS (ESI): m/z calculated for $\text{C}_{12}\text{H}_{21}\text{NNaO}_4^+$ ($[\text{M}+\text{Na}]^+$): 266.1363; found: 266.1372.

When the γ -proton was irradiated, 1.4% and 0.5% of NOE were observed the olefinic proton and the methylester protons, respectively. No NOE to the *tert*-butyl protons was observed. (2.0 s mixing time)

The analytical data of the (*E*)-isomer *E*-**172j** is in agreement with the literature.^[210]

Methyl *N*-Boc-(*Z*)- α,β -didehydroleucinate (Z-172j**)**

R_f = 0.5 (*c*-hexane/EtOAc = 4:1).

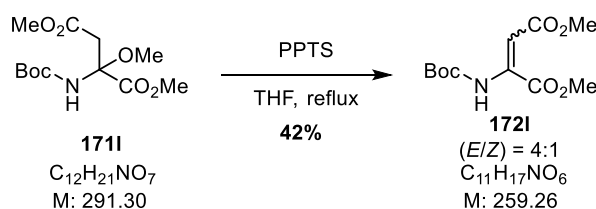
$^1\text{H NMR}$ (500 MHz, CDCl_3) δ = 6.39 (d, $J=10.2$, 1H), 5.78 (s, 1H), 3.77 (s, 3H), 2.70 (dp, $J=10.2$, 6.7, 1H), 1.46 (s, 9H), 1.05 (d, $J = 6.6$ Hz, 6H) ppm.

$^{13}\text{C NMR}$ (176 MHz, CDCl_3) δ = 165.8, 153.9, 144.0, 124.1, 80.5, 52.3, 28.3, 27.6, 21.8 ppm.

IR (neat): $\tilde{\nu}$ = 3346, 2960, 2930, 2871, 1710, 1656, 1496, 1438, 1366, 1314, 1255, 1162, 1050, 1027, 998, 850, 776 cm^{-1} .

HRMS (ESI): m/z calculated for $\text{C}_{12}\text{H}_{21}\text{NO}_4$ ($[\text{M}+\text{Na}]^+$): 266.1363; found: 266.1368.

When the olefinic proton was irradiated, 1.6% of NOE was observed for the methylester protons, respectively. No NOE to the NH proton was observed. (2.0 s mixing time) The analytical data of the (*Z*)-isomer **Z-172j** is in agreement with the literature.^[40]

5.8.29. Dimethyl *N*-Boc-(*E/Z*)- α,β -didehydroaspartate (172l**)**

Compound **172l** was prepared according to **GP4** starting from **171l** (135 mg, 0.463 mmol, 1.00 eq.), PPTS (34.9 mg, 0.139 mmol, 0.30 eq.) and 3 mL THF. After 17 h, full conversion was observed. The crude product was purified by column chromatography (SiO_2 , *c*-hexane/EtOAc = 9:1 \rightarrow 6:1) to afford the (*E*)-isomer **E-172l** (40.4 mg; 156 μmol ; 34%) and the (*Z*)-isomer **Z-172l** (10.1 mg; 39.0 μmol ; 8%) as colorless solids.

Dimethyl *N*-Cbz-(*E*)- α,β -didehydroaspartate (E-172l**)**

R_f = 0.2 (*c*-hexane/EtOAc = 4:1).

$^1\text{H NMR}$ (600 MHz, CDCl_3) δ = 6.84 (s, 1H), 6.30 (s, 1H), 3.89 (s, 3H), 3.71 (s, 3H), 1.47 (s, 9H) ppm.

$^{13}\text{C NMR}$ (126 MHz, CDCl_3) δ = 166.9, 164.3, 151.2, 139.7, 103.2, 82.6, 53.3, 51.9, 28.2 ppm.

IR (neat): $\tilde{\nu}$ = 3299, 2982, 2953, 2850, 1739, 1624, 1528, 1437, 1383, 1370, 1310, 1239, 1140, 1070, 1016, 980, 879, 847, 818, 747 cm^{-1} .

HRMS (ESI): m/z calculated for $\text{C}_{11}\text{H}_{17}\text{NNaO}_6^+$ ($[\text{M}+\text{Na}]^+$): 282.0948; found: 282.0940.

When the NH proton was irradiated, 5.6%, 0.5% and 0.4% of NOE were observed the olefinic proton, the *tert*-butyl When the olefinic proton was irradiated, 4.0%, 0.6% and 0.3% of NOE were observed the NH proton, and the *tert*-butyl

Dimethyl N-Boc-(Z)- α,β -didehydroaspartate (Z-172l)

R_f = 0.5 (c-hexane/EtOAc = 4:1).

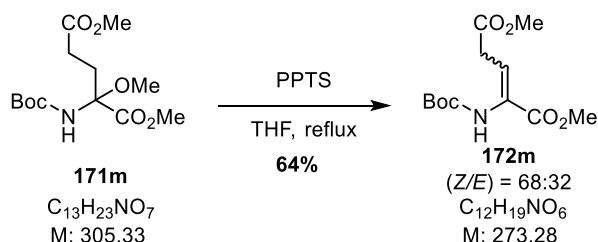
$^1\text{H NMR}$ (600 MHz, CDCl_3) δ = 9.45 (s, 1H), 5.38 (s, 1H), 3.87 (s, 3H), 3.75 (s, 3H), 1.47 (s, 9H) ppm.

$^{13}\text{C NMR}$ (151 MHz, CDCl_3) δ = 168.5, 164.5, 151.3, 145.0, 98.9, 82.7, 53.1, 51.8, 28.1 ppm.

IR (neat): $\tilde{\nu}$ = 3028, 2982, 2954, 2922, 2850, 1738, 1690, 1630, 1479, 1435, 1394, 1370, 1282, 1217, 1146, 1067, 1021, 978, 873, 751 cm^{-1} .

HRMS (ESI): m/z calculated for $\text{C}_{11}\text{H}_{17}\text{NNaO}_6^+$ ($[\text{M}+\text{Na}]^+$): 282.0948; found: 282.0948.

When the NH proton was irradiated, 1.8% of NOE were observed the *tert*-butyl protons. No NOEs for the either methyl ester protons or the olefinic protons were observed. (2.0 s mixing time)

5.8.30. Dimethyl N-Cbz-(Z/E)- α,β -didehydroglutamate (172m)

Compound **172m** was prepared according to **GP4** starting from **171m** (81.0 mg, 0.278 mmol, 1.00 eq.), PPTS (21.0 mg, 83.4 μmol , 0.30 eq.) and 1.5 mL THF. After 6 h, full conversion was observed. Column chromatography (SiO_2 , c-hexane/EtOAc 20:1 \rightarrow 10:1) afforded the *Z*-isomer *Z*-**172m** (22.5 mg, 82.3 μmol ; 30%) and a diastereomeric mixture (*E*-**172m**:*Z*-**172m** 3:2, 25.5 mg, 93.3 μmol ; 34%) as colorless oils.

R_f = 0.31 (c-hexane/EtOAc = 4:1).

$^1\text{H NMR}$ (500 MHz, CDCl_3) δ = 6.74 (t, J = 7.0 Hz, 1H), 6.32 (s, 1H), 3.80 (s, 3H), 3.73 (s, 3H), 3.30 (d, J = 7.0 Hz, 2H), 1.47 (s, 9H) ppm.

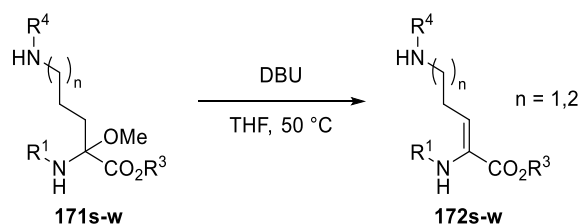
$^{13}\text{C NMR}$ (176 MHz, CDCl_3) δ = 171.1, 165.0, 152.9, 127.6, 125.9, 81.1, 52.7, 52.2, 34.0, 28.3 ppm.

IR (neat): $\tilde{\nu}$ = 3345, 2952, 2917, 2849, 1731, 1715, 1665, 1493, 1467, 1438, 1393, 1367, 1331, 1246, 1159, 1046, 1029, 992, 888, 838, 799, 762 cm^{-1} .

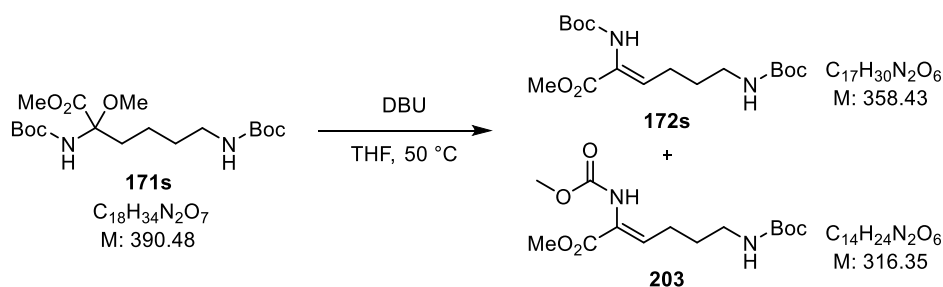
HRMS (ESI): m/z calculated for $\text{C}_{12}\text{H}_{19}\text{NNaO}_6^+$ ($[\text{M}+\text{Na}]^+$): 296.1104; found: 296.1098.

When γ -methylene protons were irradiated, 3.7%, 0.5% and 0.4% of NOE were observed the olefinic proton, the NH proton and the side-chain methylester protons, respectively. No NOE for the α -methyl ester protons was observed. (2.0 s mixing time)

5.8.31. General Procedure for the base-induced Elimination (GP5)



A Schlenk-flask was charged with the methoxylated compound **2l-2p** (1.00 eq.) in dry THF (0.1 M) and DBU (1.3 eq.) was added. The reaction mixture was heated to 50 °C in an oil bath until full conversion was observed. The solution was allowed to cool down to room temperature and partitioned between EtOAc (10 mL/mmol) and sat. aq. NH₄Cl-sol. (10 mL/mmol). The aqueous phase was extracted three times with EtOAc (5 mL/mmol), the combined organic phases were washed with brine (10 mL/mmol), dried over MgSO₄, filtered and the solvent was removed under reduced pressure.

5.8.32. Methyl α -N-Boc- ϵ -N'-Boc-(Z)- α,β -didehydrolysinate (**172s**)

Compound **172s** was prepared according to **GP5** starting from **171s** (91.0 mg, 0.233 mmol, 1.00 eq.), DBU (45 μ L, 0.303 mmol, 1.30 eq.) and 2.0 mL THF. After 38 h, full conversion was observed. Column chromatography (SiO₂, *c*-hexane/EtOAc 6:1 \rightarrow 2:1) afforded the desired product **172s** (36.3 mg, 101 μ mol; 43%) and methylcarbamate **203** (19.6 mg, 62.0 μ mol; 27%) as colorless oil and colorless crystals, respectively.

R_f = 0.4 (*c*-hexane/EtOAc = 2:1).

¹H NMR (500 MHz, CDCl₃) δ = 6.51 (t, J = 7.5 Hz, 1H), 6.29 (s, 1H), 4.88 (s, 1H), 3.77 (s, 3H), 3.13 (q, J = 6.4 Hz, 2H), 2.26 (q, J = 7.3 Hz, 2H), 1.67 (p, J = 6.9 Hz, 2H), 1.46 (d, J = 14.7 Hz, 18H) ppm.

¹³C NMR (151 MHz, CDCl₃) δ = 165.5, 161.2, 156.3, 153.7, 136.2, 80.6, 79.2, 52.4, 39.7, 28.8, 28.5, 28.4, 25.6 ppm.

IR (neat): $\tilde{\nu}$ = 3351, 3004, 2971, 2931, 2868, 1714, 1505, 1438, 1365, 1247, 1163, 1046, 1024, 868, 779, 756 cm⁻¹. HRMS (ESI): m/z calculated for C₁₇H₃₀N₂NaO₆⁺ ([M+Na]⁺): 381.1996; found: 381.1990.

When γ -methylene protons were irradiated, 7.8% and 2.2% of NOE were observed for olefinic proton and the N, respectively

Methyl α -N-Moc- ϵ -N'-Boc-(Z)- α,β -didehydrolysinate (203)

R_f = 0.3 (c-hexane/EtOAc = 2:1).

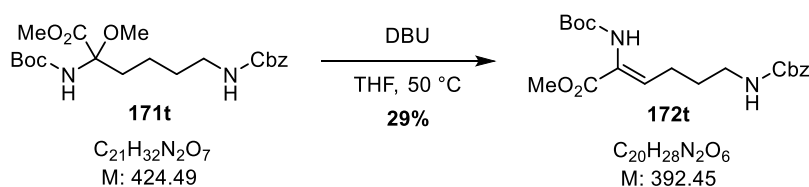
$^1\text{H NMR}$ (500 MHz, CDCl_3) δ = 6.60 (t, J = 7.6 Hz, 1H), 6.49 (s, 1H), 4.76 (s, 1H), 3.78 (s, 3H), 3.72 (s, 3H), 3.13 (q, J = 6.4 Hz, 2H), 2.26 (q, J = 7.3 Hz, 2H), 1.67 (p, J = 6.9 Hz, 2H), 1.44 (s, 9H) ppm.

$^{13}\text{C NMR}$ (151 MHz, CDCl_3) δ = 165.2, 156.4, 155.2, 137.3, 126.2, 79.4, 52.8, 52.6, 39.8, 28.7, 28.5, 25.7 ppm.

IR (neat): $\tilde{\nu}$ = 3348, 2976, 2954, 1711, 1514, 1440, 1366, 1250, 1167, 1060, 777 cm^{-1} .

HRMS (ESI): m/z calculated for $\text{C}_{14}\text{H}_{24}\text{N}_2\text{NaO}_6^+$ ($[\text{M}+\text{Na}]^+$): 339.1526; found: 339.1531.

When γ -methylene protons were irradiated, 1.4% of NOE were observed for the NWhen the olefinic proton was irradiated, 1.2% and 2.3% of NOE were observed for the methyl ester γ -methylene protons, respectively

5.8.33. Methyl α -N-Boc- ϵ -N'-Cbz-(Z)- α,β -didehydrolysinate (172t)

Compound **172t** was prepared according to **GP5** starting from **171t** (53.0 mg, 0.125 mmol, 1.00 eq.), DBU (24 μL , 0.162 mmol, 1.30 eq.) and 1.5 mL THF. After 22 h, full conversion was observed. Column chromatography (SiO_2 , c-hexane/EtOAc 4:1) afforded the desired product **172t** (14.4 mg, 36.7 μmol ; 29%) as a colorless resin.

R_f = 0.3 (c-hexane/EtOAc = 4:1).

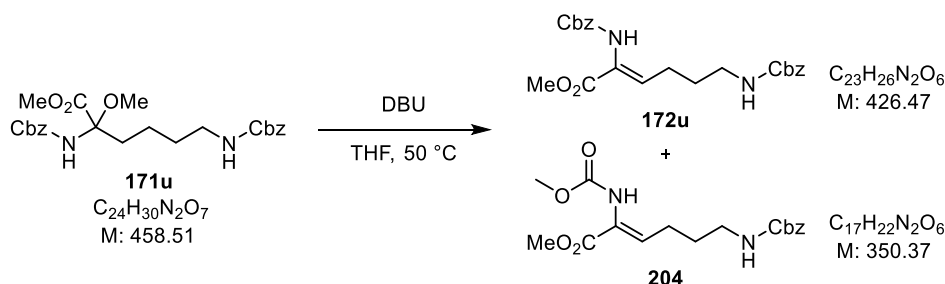
$^1\text{H NMR}$ (600 MHz, CDCl_3) δ = 7.35 (d, J =4.4, 4H), 7.33 – 7.29 (m, 1H), 6.54 (t, J =7.5, 1H), 6.11 (s, 1H), 5.28 – 5.12 (m, 1H), 5.09 (s, 2H), 3.77 (s, 3H), 3.22 (q, J =6.4, 2H), 2.27 (q, J =7.2, 2H), 1.71 (p, J =6.9, 2H), 1.44 (s, 9H) ppm.

$^{13}\text{C NMR}$ (176 MHz, CDCl_3) δ = 165.4, 156.7, 153.7, 136.8, 136.4, 128.6, 128.22, 128.17, 126.2, 80.9, 66.7, 52.5, 40.4, 28.6, 28.4, 28.3, 25.7, 22.5 ppm.

IR (neat): $\tilde{\nu}$ = 3334, 2976, 2952, 2926, 2853, 1699, 1658, 1514, 1455, 1438, 1366, 1247, 1162, 1093, 1047, 1025, 915, 883, 844, 823, 776, 738 cm^{-1} .

HRMS (ESI): m/z calculated for $\text{C}_{20}\text{H}_{28}\text{N}_2\text{NaO}_6^+$ ($[\text{M}+\text{Na}]^+$): 415.1839; found: 415.1874.

When γ -methylene protons were irradiated, 7.5%, 2.1% of NOE were observed for the olefinic and the NWhen the olefinic proton was irradiated, 0.8% of NOE was observed for the methyl ester The analytical data of compound **172t** is in agreement with the literature.^[40]

5.8.34. Methyl α -N-Cbz- ϵ -N'-Cbz-(Z)- α,β -didehydrolysinate (**172u**)

Compound **172u** was prepared according to **GP5** starting from **171u** (200 mg, 0.436 mmol, 1.00 eq.), DBU (85 μ l, 0.567 mmol, 1.30 eq.) and 4.5 mL THF. After 18 h, full conversion was observed. Column chromatography (SiO₂, c-hexane/EtOAc 2:1 \rightarrow 1:1) afforded the desired product **172u** (44.3 mg, 0.104 mmol; 24%) and methylcarbamate **204** (42.7 mg, 42.7 μ mol; 28%) as colorless oils.

R_f = 0.4 (c-hexane/EtOAc = 1:1).

¹H NMR (600 MHz, CDCl₃) δ = 7.39 – 7.27 (m, 10H), 6.60 (t, J = 7.5 Hz, 1H), 6.48 (s, 1H), 5.12 (s, 2H), 5.07 (s, 2H), 3.74 (s, 3H), 3.19 (q, J = 6.2 Hz, 2H), 2.25 (q, J = 7.3 Hz, 2H), 1.68 (p, J = 6.3 Hz, 2H) ppm.

¹³C NMR (151 MHz, CDCl₃) δ = 165.1, 156.7, 154.4, 137.3, 136.7, 136.0, 128.65, 128.60, 128.4, 128.3, 128.2, 126.0, 67.5, 66.7, 52.5, 40.4, 28.5, 25.7 ppm.

IR (neat): $\tilde{\nu}$ = 3320, 3090, 3069, 3031, 2954, 2919, 2850, 1699, 1516, 1455, 1438, 1397, 1246, 1133, 1041, 772, 751 cm⁻¹.

HRMS (ESI): m/z calculated for $C_{23}H_{26}N_2NaO_6^+$ ($[M+Na]^+$): 449.1683; found: 449.1696.

When γ -methylene protons were irradiated, 1.8% and 2.3% of NOE were observed for the N. The analytical data of compound **172u** is in agreement with the literature.^[40]

Methyl α -N-Moc- ϵ -N'-Cbz-(Z)- α,β -didehydrolysinate (**204**)

R_f = 0.3 (c-hexane/EtOAc = 1:1).

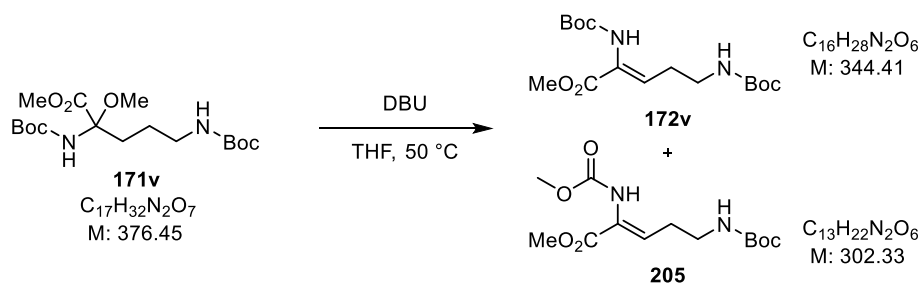
¹H NMR (600 MHz, CDCl₃) δ = 7.40 – 7.28 (m, 5H), 6.61 (t, J = 7.5 Hz, 1H), 6.36 (s, 1H), 5.23 – 5.04 (m, 3H), 3.77 (s, 3H), 3.70 (s, 3H), 3.22 (q, J = 6.5 Hz, 2H), 2.27 (q, J = 7.2 Hz, 2H), 1.71 (p, J = 6.9 Hz, 2H).ppm.

¹³C NMR (176 MHz, CDCl₃) δ = 165.1, 156.7, 155.1, 137.3, 136.8, 128.7, 128.6, 128.2, 126.0, 66.8, 52.9, 52.6, 40.4, 28.5, 25.7 ppm.

IR (neat): $\tilde{\nu}$ = 3338, 2951, 2926, 2857, 1699, 1518, 1455, 1244, 1134, 1056, 751 cm⁻¹.

HRMS (ESI): m/z calculated for $C_{17}H_{22}N_2NaO_6^+$ ($[M+Na]^+$): 373.1370; found: 373.1384.

When γ -methylene protons were irradiated, 2.3% and 0.5% of NOE were observed for the N

5.8.35. Methyl α -N-Boc- δ -N'-Boc-(Z)- α,β -didehydroornithate (**172v**)

Compound **172v** was prepared according to **GP5** starting from **171v** (100 mg, 0.266 mmol, 1.00 eq.), DBU (52 μ L, 0.345 mmol, 1.30 eq.) and 3.0 mL THF. After 18 h, full conversion was observed. Column chromatography (SiO₂, c-hexane/EtOAc 4:1) afforded the desired product **172v** (27.5 mg, 79.8 μ mol; 30%) and methylcarbamate **205** (10.7 mg, 35.3 μ mol; 13%) as colorless oil and colorless crystals, respectively.

R_f = 0.3 (c-hexane/EtOAc = 2:1).

¹H NMR (600 MHz, CDCl₃) δ = 6.52 (t, J =7.5, 1H), 6.17 (s, 1H), 4.97 (s, 1H), 3.78 (s, 3H), 3.28 (q, J =6.4, 2H), 2.42 (q, J =6.9, 2H), 1.47 (s, 9H), 1.44 (s, 9H) ppm.

¹³C NMR (151 MHz, CDCl₃) δ = 165.3, 156.2, 153.5, 133.2, 127.3, 80.9, 79.4, 60.5, 52.5, 39.4, 31.0, 29.1, 28.5, 28.4, 28.4, 28.32, 28.30 ppm.

IR (neat): $\tilde{\nu}$ = 3344, 2977, 2931, 1698, 1506, 1455, 1438, 1391, 1365, 1271, 1248, 1215, 1163, 1094, 1049, 1022, 989, 779 cm⁻¹.

HRMS (ESI): m/z calculated for $C_{16}H_{28}N_2NaO_6^+$ ($[M+Na]^+$): 367.1839; found: 367.1816.

When γ -methylene protons were irradiated, 1.6% of NOE were observed for the NWhen the was irradiated, 1.4% and 2.3% of NOE was observed for the γ -methylene protons

Methyl α -N-Moc- δ -N'-Boc-(Z)- α,β -didehydroornithate (**205**)

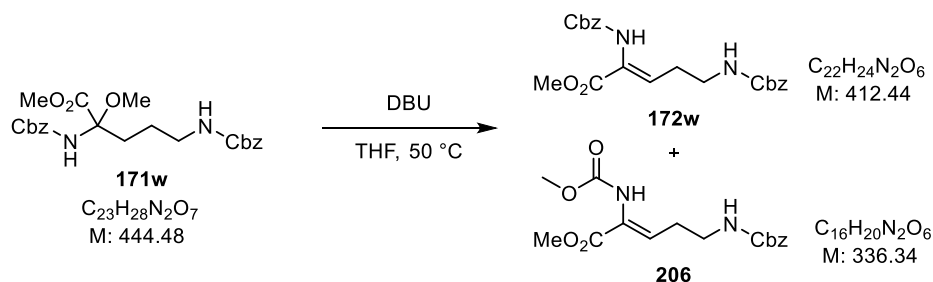
R_f = 0.17 (c-hexane/EtOAc = 2:1).

¹H NMR (600 MHz, CDCl₃) δ = 6.59 (t, J = 7.5 Hz, 1H), 6.32 (s, 1H), 4.90 (s, 1H), 3.79 (s, 3H), 3.73 (s, 3H), 3.29 (q, J = 6.5 Hz, 2H), 2.44 (q, J = 7.0 Hz, 2H), 1.44 (s, 9H) ppm.

¹³C NMR (151 MHz, CDCl₃) δ = 165.0, 156.2, 154.9, 134.1, 126.9, 79.5, 53.0, 52.7, 39.3, 29.1, 28.5 ppm.

IR (neat): $\tilde{\nu}$ = 3348, 2954, 2925, 2853, 1714, 1704, 1506, 1438, 1365, 1245, 1165, 1100, 1055, 986, 862, 778 cm⁻¹.

HRMS (ESI): m/z calculated for $C_{13}H_{22}N_2NaO_6^+$ ($[M+Na]^+$): 325.1370; found: 325.1404.

5.8.36. Methyl α -N-Cbz- ϵ -N'-Cbz-(Z)- α,β -didehydroornithate (**172w**)

Compound **172w** was prepared according to **GP5** starting from **171w** (200 mg, 0.450 mmol, 1.00 eq.), DBU (87 μ l, 0.585 mmol, 1.30 eq.) and 4.5 mL THF. After 18 h, full conversion was observed. Column chromatography (SiO₂, c-hexane/EtOAc 2:1 \rightarrow 1:1) afforded the desired product **172w** (48.9 mg, 0.118 mmol; 26%) and methylcarbamate **203** (47.8 mg, 0.142 mmol; 32%) as colorless oils.

R_f = 0.4 (c-hexane/EtOAc = 1:1); ¹H NMR (600 MHz, CDCl₃) δ = 7.41 – 7.27 (m, 10H), 6.58 (t, J = 7.5 Hz, 1H), 6.37 (s, 1H), 5.13 (s, 2H), 5.10 (s, 2H), 3.76 (s, 3H), 3.36 (q, J = 6.4 Hz, 2H), 2.45 (q, J = 6.9, 2H) ppm.

¹³C NMR (151 MHz, CDCl₃) δ = 164.9, 156.6, 154.3, 136.8, 135.9, 133.9, 128.7, 128.6, 128.5, 128.4, 128.2, 127.0, 67.7, 66.7, 52.7, 39.8, 28.9 ppm.

IR (neat): $\tilde{\nu}$ = 3331, 3066, 3033, 2952, 2920, 2850, 1705, 1519, 1455, 1438, 1398, 1246, 1142, 1097, 1053, 772, 752 cm⁻¹.

HRMS (ESI): m/z calculated for C₂₂H₂₄N₂NaO₆⁺ ([M+Na]⁺): 435.1527; found: 435.1545.

When γ -methylene protons were irradiated, 1.8% of NOE were observed for the NH proton. No NOE for the methyl ester protons was observed. (2.0 s mixing time).

The analytical data of compound Z-**4p** is in agreement with the literature.^[40]

Methyl α -N-Moc- ϵ -N'-Cbz-(Z)- α,β -didehydroornithate (**206**)

R_f = 0.3 (c-hexane/EtOAc = 1:1).

¹H NMR (600 MHz, CDCl₃) δ = 7.37 – 7.28 (m, 5H), 6.58 (t, J = 7.6 Hz, 1H), 6.39 (s, 1H), 5.37 (s, 1H), 5.09 (s, 2H), 3.77 (s, 3H), 3.71 (s, 3H), 3.36 (q, J = 6.3 Hz, 2H), 2.46 (q, J = 7.0 Hz, 2H) ppm.

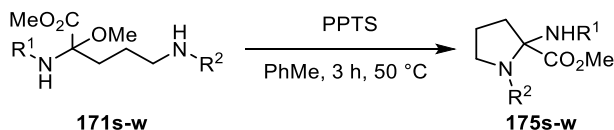
¹³C NMR (151 MHz, CDCl₃) δ = 164.9, 156.6, 154.9, 136.7, 133.9, 129.5, 128.6, 128.1, 127.0, 66.7, 52.9, 52.7, 39.8, 28.8 ppm.

IR (neat): $\tilde{\nu}$ = 3327, 3032, 3001, 2952, 2926, 1700, 1512, 1456, 1439, 1363, 1234, 1216, 1140, 1095, 1056, 774, 751 cm⁻¹.

HRMS (ESI): m/z calculated for C₁₆H₂₀N₂NaO₆⁺ ([M+Na]⁺): 359.1214; found: 359.1216.

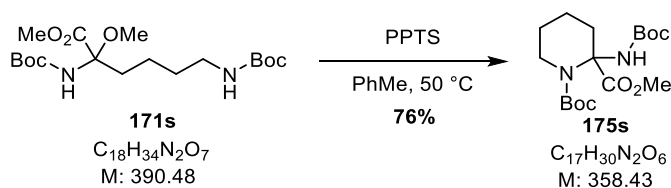
When γ -methylene protons were irradiated, 2.1% of NOE were observed for the NH proton. No NOE for the methyl ester protons was observed. (2.0 s mixing time).

5.8.37. General Procedure for the acid-catalyzed Cyclization of Lysine- and Ornithine-Derivatives (GP6)



A Schlenk-flask was charged with the methoxylated compound **171s-w** (1.00 eq.) in dry toluene (0.1 M) and PPTS (0.3 eq.) was added. The reaction mixture was heated to 50 °C in an oil bath for 3 h. The solution was allowed to cool down to room temperature and partitioned between EtOAc (10 mL/mmol) and sat. aq. NaHCO₃-sol. (10 mL/mmol). The aqueous phase was extracted three times with EtOAc (5 mL/mmol), the combined organic phases were washed with brine (10 mL/mmol), dried over MgSO₄, filtered and the solvent was removed under reduced pressure.

5.8.38. 1-(*tert*-Butyl) 2-methyl 2-((*tert*-butoxycarbonyl)amino)piperidine-1,2-dicarboxylate (**175s**)



Compound **175s** was prepared according to **GP6** starting from **171s** (52.0 mg, 0.133 mmol, 1.00 eq.), PPTS (10.0 mg, 40.0 μmol, 0.30 eq.) and 1.5 mL dry Toluene. After 3 h at 50 °C, full conversion was observed. Column chromatography (SiO₂, *n*-pentane/EtOAc 5:1) afforded the title compound (**175s**, 36.2 mg, 0.101 mmol; 76%) as colorless oil.

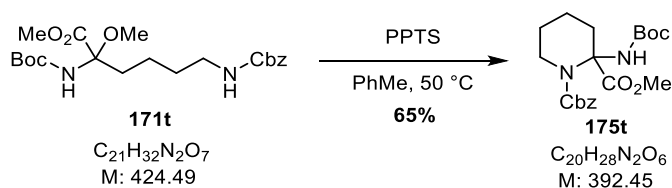
R_f = 0.5 (*c*-hexane/EtOAc = 4:1).

¹H NMR (600 MHz, CDCl₃) δ = 5.87 (s, 1H), 3.87 (dt, *J* = 12.6, 4.7 Hz, 1H), 3.77 (s, 3H), 3.46 (dt, *J* = 13.1, 7.9 Hz, 1H), 2.88 – 2.77 (m, 1H), 1.73 (dddd, *J* = 15.3, 7.6, 5.6, 3.3 Hz, 3H), 1.70 – 1.59 (m, 2H), 1.43 (2s, 18H) ppm.

¹³C NMR (151 MHz, CDCl₃) δ = 172.5, 154.9, 154.3, 81.0, 79.5, 71.9, 53.0, 40.9, 30.5, 29.8, 28.4, 28.3, 28.1, 21.7, 16.8 ppm.

IR (neat): $\tilde{\nu}$ = 3439, 3003, 2976, 2930, 1721, 1489, 1455, 1393, 1365, 1293, 1275, 1242, 1156, 1049, 1007, 896, 877, 849, 774 cm⁻¹.

HRMS (ESI): *m/z* calculated for C₁₇H₃₀N₂NaO₆⁺ ([M+Na]⁺): 381.1996; found: 381.2009.

5.8.39. 1-Benzyl 2-methyl 2-((*tert*-butoxycarbonyl)amino)piperidine-1,2-dicarboxylate (**175t**)

Compound **175t** was prepared according to **GP6** starting from **171t** (110 mg, 0.259 mmol, 1.00 eq.), PPTS (19.5 mg, 77.7 μmol, 0.30 eq.) and 3 mL Toluene. After 3 h at 50 °C, full conversion was observed. Column chromatography (SiO₂, *c*-hexane/EtOAc 19:1 → 4:1) afforded the title compound (**175t**, 66.4 mg, 0.169 mmol; 65%) as colorless oil.

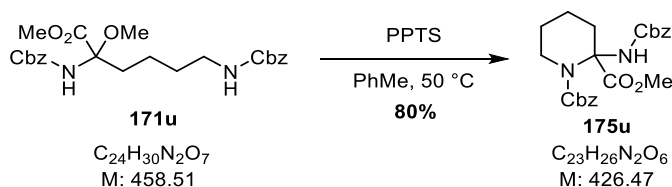
R_f = 0.4 (*c*-hexane/EtOAc = 4:1).

¹H NMR (600 MHz, CDCl₃) δ = 7.42 – 7.28 (m, 5H), 5.87 (s, 1H), 5.18 – 5.07 (m, 2H), 4.06 – 3.94 (m, 1H), 3.66 (s, 3H), 3.59 – 3.49 (m, 1H), 2.93 – 2.81 (m, 1H), 1.84 – 1.61 (m, 5H), 1.42 (s, 9H) ppm.

¹³C NMR (151 MHz, CDCl₃) δ = 171.9, 155.7, 154.3, 136.4, 128.6, 128.2, 128.0, 79.7, 72.2, 67.5, 53.1, 41.3, 30.3, 28.4, 21.7, 16.8 ppm.

IR (neat): $\tilde{\nu}$ = 3436, 3028, 2999, 2970, 2951, 2874, 1718, 1491, 1454, 1408, 1393, 1365, 1344, 1296, 1263, 1232, 1198, 1160, 1134, 1049, 1030, 1005, 908, 891, 825, 770, 732 cm⁻¹.

HRMS (ESI): *m/z* calculated for C₂₀H₂₈N₂NaO₆⁺ ([M+Na]⁺): 415.1839; found: 415.1826.

5.8.40. 1-Benzyl 2-methyl 2-(((benzyloxy)carbonyl)amino)piperidine-1,2-dicarboxylate (**175u**)

Compound **175u** was prepared according to **GP6** starting from **171u** (0.360 g, 0.785 mmol, 1.00 eq.), PPTS (59.2 mg, 0.236 mmol, 0.30 eq.) and 8 mL THF. After 3 h, full conversion was observed. Column chromatography (SiO₂, *c*-hexane/EtOAc 9:1 → 4:1) afforded the title compound (**175u**, 0.268 g, 0.628 mmol; 80%) as colorless resin.

R_f = 0.6 (*c*-hexane/EtOAc = 2:1).

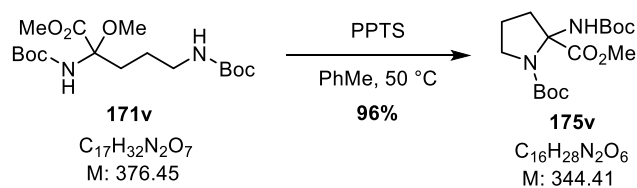
¹H NMR (600 MHz, CDCl₃) δ = 7.39 – 7.27 (m, 10H), 6.20 (s, 1H), 5.14 – 5.08 (m, 3H), 5.03 (d, *J* = 12.3 Hz, 1H), 4.04 – 3.94 (m, 1H), 3.64 (s, 3H), 3.60–3.52 (m, 1H), 2.82 (br t, *J* = 11.8 Hz, 1H), 1.80 (dt, *J* = 14.3, 5.4 Hz, 1H), 1.77 – 1.71 (m, 2H), 1.71 – 1.68 (m, 1H), 1.67 – 1.61 (m, 1H) ppm.

¹³C NMR (151 MHz, CDCl₃) δ = 171.7, 155.7, 154.6, 136.5, 136.3, 128.8, 128.64, 128.60, 128.3, 128.21, 128.16, 128.09, 72.2, 67.6, 66.6, 53.2, 41.3, 30.5, 21.6, 16.8 ppm.

IR (neat): $\tilde{\nu}$ = 3430, 3338, 3062, 3033, 2950, 2870, 1728, 1709, 1497, 1454, 1402, 1341, 1260, 1225, 1194, 1090, 1061, 1046, 1010, 912, 741 cm⁻¹.

HRMS (ESI): *m/z* calculated for C₂₃H₂₆N₂NaO₆⁺ ([M+Na]⁺): 449.1683; found: 449.1666.

5.8.41. 1-(*tert*-Butyl) 2-methyl 2-((*tert*-butoxycarbonyl)amino)pyrrolidine-1,2-dicarboxylate (175v)



Compound **175v** was prepared according to **GP6** starting from **171v** (0.100 g, 0.266 mmol, 1.00 eq.), PPTS (20.0 mg, 79.7 μmol , 0.30 eq.) and 3 mL dry toluene. After 3 h at 50 °C, full conversion was observed. Column chromatography (SiO_2 , *c*-hexane/EtOAc 6:1) afforded the title compound (**175v**, 88.2 mg, 0.256 mmol; 96%) as colorless resin.

R_f = 0.6 (*c*-hexane/EtOAc = 2:1).

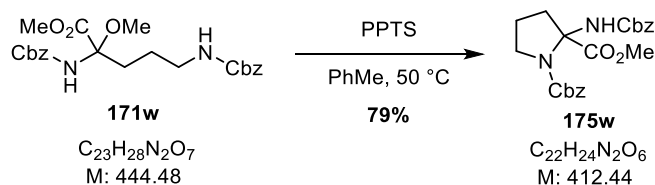
$^1\text{H NMR}$ (500 MHz, CDCl_3 , 1:1 mixture of rotamers) δ = 6.08 (s, 0.5H), 5.93 (s, 0.5H), 3.74 (2s, J = 4.4 Hz, 3H), 3.71 – 3.51 (m, 2H), 2.85 – 2.68 (m, 1H), 2.16 (dtd, J = 13.5, 8.5, 4.6 Hz, 1H), 2.06 (tdd, J = 12.1, 7.3, 4.5 Hz, 1H), 1.94 (dtt, J = 12.7, 8.7, 4.7 Hz, 1H), 1.48 – 1.31 (m, 18H) ppm.

$^{13}\text{C NMR}$ (151 MHz, CDCl_3) δ = 172.5, 172.3, 154.2, 153.7, 153.6, 152.3, 80.6, 80.4, 79.5, 76.4, 75.7, 53.22, 53.17, 47.9, 47.7, 37.5, 36.5, 28.44, 28.36, 28.31, 23.7, 23.0 ppm.

IR (neat): $\tilde{\nu}$ = 3435, 3006, 2977, 2927, 2853, 1749, 1723, 1703, 1491, 1456, 1391, 1366, 1293, 1242, 1157, 1114, 1066, 1002, 929, 882, 753 cm^{-1} .

HRMS (ESI): m/z calculated for $\text{C}_{16}\text{H}_{28}\text{N}_2\text{NaO}_6^+$ ($[\text{M}+\text{Na}]^+$): 367.1839; found: 367.1832.

5.8.42. 1-Benzyl 2-methyl 2-((benzyloxycarbonyl)amino)pyrrolidine-1,2-dicarboxylate (175w)



Compound **175w** was prepared according to **GP6** starting from **171w** (0.387 g, 0.871 mmol, 1.00 eq.), PPTS (65.6 mg, 0.261 mmol, 0.30 eq.) and 3 mL dry THF. After 3 h, full conversion was observed. Column chromatography (SiO_2 , *c*-hexane/EtOAc 5:1 \rightarrow 3:1) afforded the title compound (**175w**, 0.282 g, 0.685 mmol; 79%) as colorless resin.

R_f = 0.3 (*c*-hexane/EtOAc = 4:1).

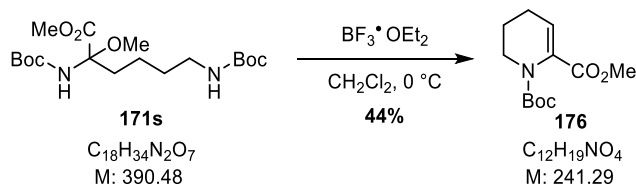
$^1\text{H NMR}$ (600 MHz, CDCl_3 , 2:1 mixture of rotamers) δ = 7.41 – 7.26 (m, 10H), 6.48/6.29 (2s, 1H), 5.27 – 4.92 (m, 4H), 3.76/3.46 (2s, 3H), 3.71 (td, J = 8.9, 4.3 Hz, 1H), 2.89 – 2.75 (m, 1H), 2.29 – 2.13 (m, 2H), 2.02 (dp, J = 12.3, 8.1, 7.7z Hz, 1H) ppm.

$^{13}\text{C NMR}$ (151 MHz, CDCl_3) δ = 171.8, 154.4, 154.2, 153.1, 136.6, 136.4, 136.2, 128.7, 128.63, 128.58, 128.51, 128.4, 128.2, 128.14, 128.05, 127.9, 76.8, 75.8, 67.4, 67.2, 66.6, 53.6, 53.4, 48.6, 47.9, 37.4, 36.5, 23.9, 23.3.

IR (neat): $\tilde{\nu}$ = 3428, 3064, 3032, 2954, 2893, 2850, 1704, 1497, 1454, 1408, 1355, 1290, 1225, 1067, 106, 921, 770, 744 cm^{-1} .

HRMS (ESI): m/z calculated for $\text{C}_{22}\text{H}_{24}\text{N}_2\text{NaO}_6^+$ ($[\text{M}+\text{Na}]^+$): 435.1527; found: 435.1554.

5.8.43. Methyl 2-((*tert*-butoxycarbonyl)amino)-2-methoxypropanoate (**176**)



A 4 mL vial was charged with lysine derivative **171s** (52.0 mg; 0.133 mmol; 1.00 eq.) and 1.5 mL dry CH_2Cl_2 . The solution was cooled to 0 °C and $\text{BF}_3 \cdot \text{OEt}_2$ (5.1 μL , 40.0 μmol , 0.30 eq.) was added. Full conversion was observed after 2 h and the mixture was treated with 2 mL sat. aq. NaHCO_3 -sol.. The reaction mixture was warmed to room temperature and stirring was continued for 30 min. The organic phase was diluted with 5 mL CH_2Cl_2 , washed with brine (5 mL), dried over MgSO_4 , filtered and the solvent was removed under reduce pressure. Column chromatography (SiO_2 , *c*-hexane/*EtOAc* 10:1) afforded compound **176** (20.1 mg, 87 μmol , 65%) as colorless crystals.

R_f = 0.6 (*c*-hexane/*EtOAc* = 2:1).

^1H NMR (600 MHz, CDCl_3) δ = 5.99 (t, J = 3.8 Hz, 1H), 3.78 (s, 3H), 3.63 – 3.55 (m, 2H), 2.23 (td, J = 6.7, 3.9 Hz, 2H), 1.81 (dt, J = 12.1, 6.5 Hz, 2H), 1.44 (s, 9H) ppm.

^{13}C NMR (151 MHz, CDCl_3) δ = 165.8, 153.2, 133.0, 122.1, 83.0, 81.5, 53.1, 52.0, 43.2, 34.8, 29.8, 28.5, 28.3, 28.2, 28.0, 23.1, 22.8 ppm.

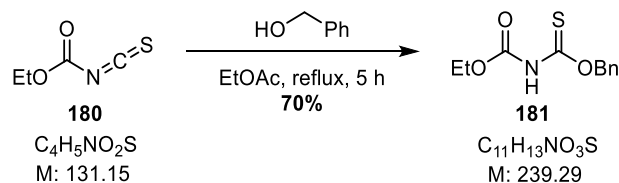
IR (neat): $\tilde{\nu}$ = 2978, 2929, 1733, 1703, 1645, 1453, 1437, 1365, 1338, 1273, 1254, 1230, 1199, 1154, 1120, 1069, 1050, 963, 948, 883, 851, 809, 772, 757 cm^{-1} .

HRMS (ESI): m/z calculated for $\text{C}_{12}\text{H}_{19}\text{NNaO}_4^+$ ($[\text{M}+\text{Na}]^+$): 264.1206; found: 264.1197.

The analytical data of compound **176** is in agreement with the literature.^[211]

5.9. Synthesis of Quisqualic Acid

5.9.1. Ethyl N-[(phenylmethoxy)thioxomethyl]carbamate (**181**)



According to a modified procedure by RENAUT *et al.*,^[177] a heated, two-necked 50 mL flask equipped with a reflux condenser was charged with isothiocyanate **180** (1.50 g, 11.4 mmol, 1.00 eq.) in dry EtOAc (23 mL). Benzylalcohol (1.3 mL, 12.6 mmol, 1.10 eq.) was added dropwise over 10 min and the reaction mixture was heated to reflux for 5 h. The solvent was evaporated under reduced pressure and the residue was taken up in Et₂O (20 mL). After stirring for 2 h at room temperature, the solution was stored at -20 °C overnight. The colorless precipitate was collected by filtration and washed with *n*-hexane. The product was dried at reduced pressure (100 mbar) and spectroscopically pure thionourethane **181** (1.90 g, 7.96 mmol, 70%) was obtained as a colorless solid.

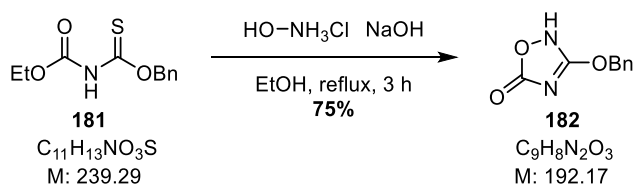
$R_f = 0.3$ (*c*-hexane/EtOAc = 1:1).

¹H NMR (600 MHz, MeOD-*d*₄) $\delta = 7.45$ (dq, $J = 7.8, 2.6$ Hz, 2H), 7.40 – 7.35 (m, 2H), 7.35 – 7.31 (m, 2H), 5.57 (s, 2H), 4.25 – 4.15 (m, 2H), 1.33 – 1.27 (m, 3H) ppm.

¹³C NMR (151 MHz, MeOD-*d*₄) $\delta = 190.2, 152.5, 136.7, 129.5, 129.3, 129.1, 73.6, 63.1, 14.5$ ppm.

The analytical data of compound **181** is in agreement with the literature.^[177]

5.9.2. 3-(Benzyloxy)-1,2,4-oxadiazol-5(2H)-one (**182**)



According to a modified procedure by RENAUT *et al.*,^[177] a heated, two-necked 100 mL flask equipped with a reflux condenser was charged with thionourethane **181** (1.83 g, 7.65 mmol, 1.00 eq.) in dry EtOH (30 mL). Hydroxylamine hydrochloride (0.797 g, 11.5 mmol, 1.50 eq.) was added and the reaction mixture was heated to 45 °C. After 30 min, NaOH (0.489 g, 12.2 mmol, 1.60 eq.) was added and solution was heated to reflux for 3 h. The solvent was evaporated under reduced pressure and water was added to the residue. The solution was adjusted to pH = 12 with 1 M NaOH, extracted with EtOAc (2 x 20 mL) and the organic phases were discarded. The solution was acidified with 1 M HCl to pH = 3, extracted with EtOAc (3 x 20 mL), the combined organic phases were washed with brine (30 mL), dried over MgSO₄, filtered and the solvent was evaporated under reduced pressure. Spectroscopically pure oxadiazolone **182** (1.10 g, 5.73 mmol, 75%) was obtained as a colorless solid.

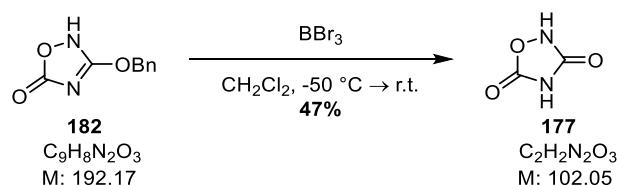
$R_f = 0.4$ (c-hexane/EtOAc = 1:1).

$^1\text{H NMR}$ (600 MHz, CDCl_3) $\delta = 9.70$ (s, 1H), 7.46 – 7.36 (m, 5H), 5.28 (s, 2H) ppm.

$^{13}\text{C NMR}$ (176 MHz, CDCl_3) $\delta = 160.5, 158.9, 133.3, 129.6, 129.0, 129.0, 72.5$ ppm.

The analytical data of compound **182** is in agreement with the literature.^[177]

5.9.3. 1,2,4-Oxadiazolidine-3,5-dione (**177**)



According to a modified procedure by RENAULT *et al.*,^[177] a 50 mL Schlenk flask was charged with starting material **182** (1.00 g, 5.20 mmol, 1.00 eq.) in dry CH_2Cl_2 (24 mL). The solution was cooled to $-50\text{ }^\circ\text{C}$ and BBr_3 (1 M in CH_2Cl_2 , 5.5 mL, 5.50 mmol, 1.06 eq.) was added dropwise over 30 min using a syringe pump. The solution was stirred for 40 min at that temperature and slowly allowed to warm up to room temperature. After 4 h, the solution was poured into an ice-water mixture (50 mL), stirred for 20 min and the phases were separated. The aqueous phase was extracted with Et_2O (4 x 50 mL), the combined organic phases were dried over MgSO_4 , filtered and the solvent was removed under reduced pressure (100 mbar). The residue was recrystallized from $\text{Et}_2\text{O}/n$ -hexane and oxazolidine **177** (0.252 g, 2.47 mmol, 47%) was collected after storage at $-20\text{ }^\circ\text{C}$ for multiple hours as a pale brown solid.

$^1\text{H NMR}$ (700 MHz, $\text{CD}_3\text{CN-}d_3$) $\delta = 9.41$ (br s, 2H) ppm.

$^{13}\text{C NMR}$ (176 MHz, $\text{CD}_3\text{CN-}d_3$) $\delta = 158.9, 154.3$ ppm.

The analytical data of compound **177** is in agreement with the literature.^[177]

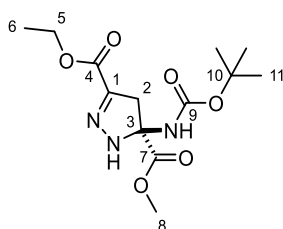
5.10. Synthesis of 2-Pyrazoline Amino Acids

5.10.1. Optimization of Reactions Conditions for the Synthesis of 2-Pyrazoline Amino Acids



6 mL Vials with PTFE-lined screw caps were oven dried and cooled down in a vacuum desiccator. A vial was charged with the catalyst and dry solvent. Boc- Δ Ala-OMe (**125**, 40.2 mg, 0.200 mmol, 1.00 eq.) was weighed in a secured syringe and washed into the reaction solution. EDA (**187**, $w = 87\%$ in CH_2Cl_2 , 18.9 μL , 0.220 mmol, 1.10 eq.) was quickly added using a calibrated transfer pipette (Note: It was important to calibrate the pipette using EDA, not water, as the different density and viscosity introduces significant errors). The vial was flushed with argon and heated to 50 °C in a shaking heating block. After the specified time, the solution was cooled to room temperature, diluted with CHCl_3 (900 μL), and a stock solution of ethylene carbonate (0.5 M in CHCl_3 , 100 μL , 50.0 μmol , 0.25 eq.) was added. The mixture was shaken vigorously for 2 min. An aliquot (500 μL) was taken, the solvent was evaporated under reduced pressure, the residue was taken up in CDCl_3 and the yield was determined by quantitative NMR using the ethylene carbonate signal as an internal standard.

5.10.2. 3-Ethyl 5-methyl 5-((tert-butoxycarbonyl)amino)-4,5-dihydro-1H-pyrazole-3,5-dicarboxylate (**188**)



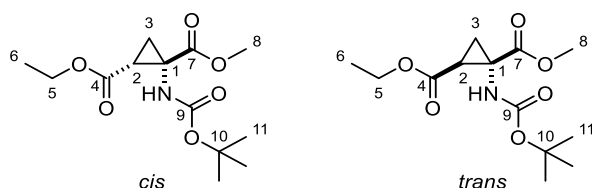
$R_f = 0.3$ (c -hexane/EtOAc = 2:1).

$^1\text{H NMR}$ (500 MHz, CDCl_3) $\delta = 7.44$ (s, 1H, NH), 5.90 (s, 1H, NH), 4.31 (q, $J = 7.1$ Hz, 2H, H5), 3.83 (s, 3H, H8), 3.40 (d, $J = 18.0$ Hz, 1H, H2a), 3.16 (d, $J = 18.0$ Hz, 1H, H2b), 1.43 (s, 9H, H11), 1.35 (t, $J = 7.1$ Hz, 3H, H6) ppm.

$^{13}\text{C NMR}$ (126 MHz, CDCl_3) $\delta = 170.1$ (C7), 161.9 (C4), 154.8 (C9), 140.2 (C1), 81.5 (C3), 79.7 (C10), 61.5 (C5), 53.6 (C8), 42.4 (C2), 28.2 (C11), 14.3 (C6) ppm.

IR (neat): $\tilde{\nu} = 3338, 2981, 2955, 2934, 1707, 1574, 1498, 1456, 1435, 1392, 1369, 1345, 1158, 1132, 1088, 1027, 877, 838, 811, 765$ cm^{-1} .

HRMS (ESI): m/z calculated for $\text{C}_{13}\text{H}_{21}\text{N}_3\text{NaO}_6^+$ ($[\text{M}+\text{Na}]^+$): 338.1323; found: 338.1393.

5.10.3. 2-Ethyl 1-methyl 1-((*tert*-butoxycarbonyl)amino)cyclopropane-1,2-dicarboxylate (**189**)

$R_f = 0.4$ (*c*-hexane/EtOAc = 2:1).

$^1\text{H NMR}$ (600 MHz, CDCl_3) $\delta = 5.15$ (s, 1H, NH_{cis}), 4.15 (dtt, $J = 10.8, 7.1, 3.5$ Hz, 4H, $\text{H5}_{\text{cis}} + \text{H5}_{\text{trans}}$), 3.73 (d, $J = 3.3$ Hz, 3H, H8_{trans}), 3.71 (s, 3H, H8_{cis}), 2.71 (t, $J = 8.2$ Hz, 1H, H2_{cis}), 2.29 (dd, $J = 9.6, 8.0$ Hz, 1H, H2_{trans}), 2.10 (br s, 1H, NH_{cis}), 1.95 (br s, 1H, $\text{H3, H3a}_{\text{trans}}$), 1.83 (ddd, $J = 9.8, 5.9, 3.2$ Hz, 1H, H3a_{cis}), 1.73 (dd, $J = 7.3, 5.0$ Hz, 1H, H3b_{cis}), 1.45 (s, 10H, $\text{H11}_{\text{cis}} + \text{H3b}_{\text{trans}}$), 1.42 (s, 9H, $\text{H11}_{\text{trans}}$), 1.28 (t, $J = 7.1$ Hz, 3H, H6_{trans}), 1.25 (t, $J = 7.1$ Hz, 3H, H6_{cis}) ppm.

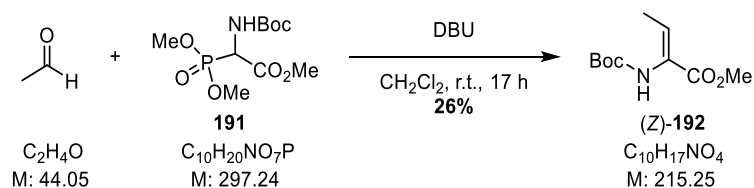
$^{13}\text{C NMR}$ (126 MHz, CDCl_3) $\delta = 171.2$ (C7_{trans}), 170.2 (C7_{cis}), 168.8 (C4_{cis}), 168.2 (C4_{trans}), 155.7 (C9), 80.2 (C10), 61.35 (C1_{trans}), 61.27 (C1_{cis}), 53.0 (C8_{cis}), 52.6 (C8_{trans}), 40.2 (C2_{trans}), 29.1 (C2_{cis}), 28.3 ($\text{C11}_{\text{trans}}$), 28.2 (C11_{cis}), 21.5 (C3_{trans}), 20.8 (C3_{cis}), 14.2 (C6) ppm.

IR (neat): $\tilde{\nu} = 3345, 2980, 2935, 2251, 1704, 1576, 1504, 1435, 1392, 1368, 1341, 1296, 1249, 1212, 1157, 1131, 1080, 1041, 1020, 956, 912, 730$ cm^{-1} .

HRMS (ESI): m/z calculated for $\text{C}_{13}\text{H}_{21}\text{NNaO}_6^+$ ($[\text{M} + \text{Na}]^+$): 310.1262; found: 310.1313.

When β -methine proton (H2) of the *cis*-isomer was irradiated, 0.1% of NOE was observed for the methyl ester protons (H8). No NOE for the NH proton was observed. (2.0 s mixing time)

When β -methine proton (H2) of the *trans*-isomer was irradiated, 6.1% of NOE was observed for the NH proton. No NOE for the methyl ester protons (H8) was observed. (2.0 s mixing time)

5.10.4. Methyl *N*-Boc-(*Z*)- α,β -didehydrobutyrate ((*Z*)-**192**)

A 50 mL Schlenk flask was charged with glycinate **191** (2.00 g, 6.73 mmol, 1.00 eq.), DBU (1.3 mL, 8.41 mmol, 1.25 eq.), dry CH_2Cl_2 (18 mL) and freshly distilled acetaldehyde (0.47 mL, 8.41 mmol, 1.25 eq.). The solution was stirred for 17 h at room temperature and the solvent was removed under reduced pressure. The residue was dissolved in EtOAc (20 mL), washed with H_2O (20 mL), sat. aq. NH_4Cl -sol. (2 x 20 mL), half-sat. aq. NaHCO_3 -sol. (2 x 30 mL), brine (20 mL), dried over Na_2SO_4 , filtered and the solvent was removed under reduced pressure. The crude product was purified by column chromatography (SiO_2 , *c*-hexane/EtOAc 10:1 \rightarrow 7:1) affording (*Z*)-Boc- Δ Abu-OMe ((*Z*)-**192**, 377 mg, 1.75 mmol, 26%) as colorless crystals.

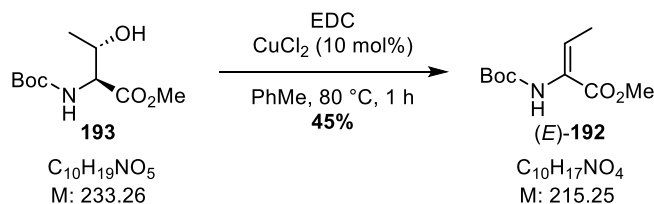
$R_f = 0.2$ (*c*-hexane/EtOAc = 4:1).

$^1\text{H NMR}$ (600 MHz, CDCl_3) $\delta = 6.68$ (q, $J = 7.2$ Hz, 1H), 6.02 (s, 1H), 3.77 (s, 3H), 1.81 (dd, $J = 7.2, 0.8$ Hz, 3H), 1.47 (s, 9H) ppm.

$^{13}\text{C NMR}$ (151 MHz, CDCl_3) $\delta = 165.5, 153.2, 132.2, 126.8, 80.5, 52.4, 28.3, 27.0, 14.4$ ppm.

The analytical data of compound (Z)-**192** is in agreement with the literature.^[183]

5.10.5. Methyl *N*-Boc-(*E*)- α,β -didehydrobutyrate ((*E*)-**192**)



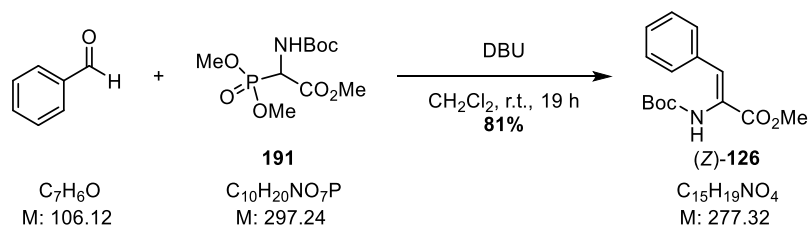
A 100 mL Schlenk flask equipped with a septum was charged with EDC-HCl (0.822 g, 4.29 mmol, 2.00 eq.) in dry toluene (50 mL). A cannula connected to an ammonia gas cylinder and three cannulas for pressure equilibration were pierced through the septum. The solution was treated for 30 min with a constant stream of dry ammonia gas and the precipitated NH_4Cl was filtered into a 100 mL Schlenk flask by inert filtration using a Schlenk-frit. The filtrate was purged with argon for 40 min, testing the exhaust argon for residual ammonia using a wet pH paper still tested positive after the purge but was negative after two FPT cycles. Freshly dehydrated CuCl_2 (28.8 mg, 0.214 mmol, 0.10 eq.) and Boc-Thr-OMe (**193**, 0.500 g, 2.14 mmol, 1.00 eq.) were added and the solution heated to 80 °C for 40 min using a preheated oil bath. The reaction mixture was treated with H_2O (30 mL), the phases were separated and the aqueous phase was extracted with EtOAc (2 x 20 mL). The combined organic phases were washed with aq. citric acid ($w = 5\%$, 30 mL), sat. aq. NaHCO_3 -sol. (30 mL), brine (30 mL), dried over MgSO_4 , filtered and the solvent was evaporated under reduced pressure. The crude product was purified by column chromatography (SiO_2 , *n*-pentane/EtOAc 10:1) affording (*E*)-Boc- Δ Abu-OMe ((*E*)-**192**, 209 mg, 0.971 mmol, 45%) as a colorless solid.

$R_f = 0.4$ (*c*-hexane/EtOAc = 4:1).

$^1\text{H NMR}$ (600 MHz, CDCl_3) $\delta = 6.79$ (s, 1H), 6.57 (s, 1H), 3.83 (s, 3H), 2.06 (d, $J = 7.7$ Hz, 3H), 1.47 (s, 9H) ppm.

$^{13}\text{C NMR}$ (151 MHz, CDCl_3) $\delta = 165.0, 153.6, 125.8, 80.4, 52.2, 28.4, 14.3$ ppm.

The analytical data of compound (*E*)-**192** is in agreement with the literature.^[183]

5.10.6. Methyl *N*-Boc-(*Z*)- α,β -didehydrophenylalaninate ((*Z*)-**126**)

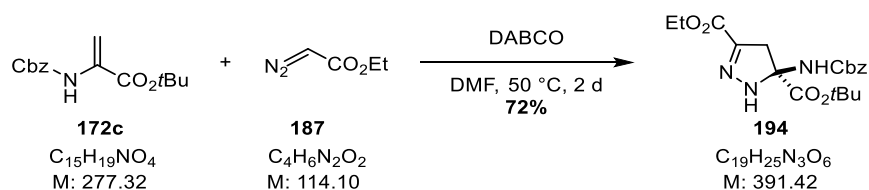
A 50 mL Schlenk flask was charged with glycinate **191** (3.00 g, 10.1 mmol, 1.00 eq.), DBU (1.3 mL, 10.1 mmol, 1.00 eq.), dry CH_2Cl_2 (20 mL) and freshly distilled benzaldehyde (1.0 mL, 10.1 mmol, 1.00 eq.). The solution was stirred for 19 h at room temperature, treated with sulfuric acid (1 M, 50 mL) and the phases were separated. The aqueous phase was extracted with EtOAc (2 x 50 mL) and the combined organic phases were dried over MgSO_4 , filtered and the solvent was removed under reduced pressure. The crude product was purified by column chromatography (SiO_2 , *c*-hexane/EtOAc 10:1) affording (*Z*)-Boc- Δ Phe-OMe ((*Z*)-**126**, 2.27 g, 8.19 mmol, 81%) as a colorless solid.

R_f = 0.4 (*c*-hexane/EtOAc = 4:1).

^1H NMR (500 MHz, CDCl_3) δ = 7.54 (d, J = 7.5 Hz, 2H), 7.39 – 7.34 (m, 2H), 7.34 – 7.28 (m, 1H), 7.25 (s, 1H), 6.18 (s, 1H), 3.86 (s, 3H), 1.39 (s, 9H) ppm.

^{13}C NMR (151 MHz, CDCl_3) δ = 166.4, 155.7, 134.5, 130.4, 130.0, 129.5, 128.9, 120.4, 81.3, 53.0, 28.4 ppm.

The analytical data of compound (*Z*)-**126** is in agreement with the literature.^[212]

5.10.7. 5-(*tert*-Butyl) 3-ethyl 5-(((benzyloxy)carbonyl)amino)-4,5-dihydro-1*H*-pyrazole-3,5-dicarboxylate (**194**)

A 6 mL PTFE-lined screwcap vial was charged with Cbz- Δ Ala-OtBu (**172c**, 112 mg, 0.404 mmol, 1.00 eq.), EDA (**187**, $w = 87\%$ in CH_2Cl_2 , 51.8 μL , 0.606 mmol, 1.50 eq.), DABCO (9.1 mg, 80.8 μmol , 0.20 eq.) and dry DMF (0.81 mL). The vial was flushed with argon and heated to 50 °C in a shaking heating block. After 44 h, the solution was cooled to room temperature, diluted with H_2O (10 mL) and extracted with EtOAc (3 x 10 mL). The combined organic phases were washed with H_2O (10 mL) and brine (10 mL), dried over MgSO_4 , filtered and the solvent was removed under reduced pressure. The crude product was purified by column chromatography (SiO_2 , *c*-hexane/EtOAc 4:1) affording pyrazoline **194** (114 mg, 0.291 mmol, 72%) as a colorless solid.

$R_f = 0.1$ (c-hexane/EtOAc = 4:1).

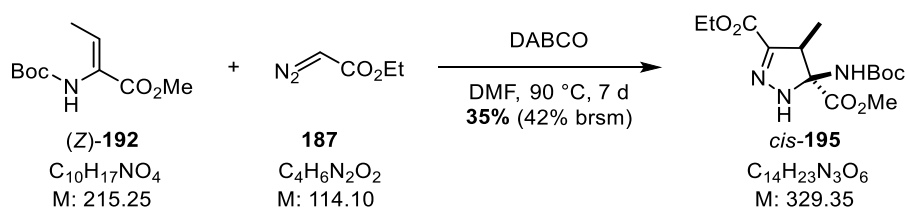
$^1\text{H NMR}$ (600 MHz, CDCl_3) $\delta = 7.39 - 7.29$ (m, 5H), 7.09 (s, 1H), 5.84 (s, 1H), 5.18 - 5.03 (m, 2H), 4.30 (q, $J = 7.1$ Hz, 2H), 3.43 (d, $J = 18.1$ Hz, 1H), 3.13 (d, $J = 18.1$ Hz, 1H), 1.45 (s, 9H), 1.34 (t, $J = 7.1$ Hz, 3H) ppm.

$^{13}\text{C NMR}$ (151 MHz, CDCl_3) $\delta = 168.1, 162.0, 154.9, 140.3, 135.8, 128.7, 128.6, 128.4, 84.2, 79.9, 67.4, 61.6, 42.4, 27.8, 14.3$ ppm.

IR (neat): $\tilde{\nu} = 3341, 2979, 2934, 1709, 1575, 1510, 1455, 1433, 1393, 1370, 1339, 1303, 1253, 1142, 1083, 1027, 912, 842, 747$ cm^{-1} .

HRMS (ESI): m/z calculated for $\text{C}_{19}\text{H}_{25}\text{N}_3\text{NaO}_6^+$ ($[\text{M}+\text{Na}]^+$): 414.1636; found: 414.1732.

5.10.8. 3-Ethyl 5-methyl *cis*-5-((*tert*-butoxycarbonyl)amino)-4-methyl-4,5-dihydro-1*H*-pyrazole-3,5-dicarboxylate (*cis*-**195**)



A 6 mL PTFE-lined screwcap vial was charged with (*Z*)-Boc- Δ Abu-OMe (*(Z)*-**192**, 108 mg, 0.500 mmol, 1.00 eq.), EDA (**187**, $w = 87\%$ in CH_2Cl_2 , 64.2 μL , 0.750 mmol, 1.50 eq.), DABCO (22.4 mg, 200 μmol , 0.40 eq.) and dry DMF (1.3 mL). The vial was flushed with argon and heated to 90 °C in a shaking heating block. After 7 d, the solution was cooled to room temperature, diluted with H_2O (10 mL) and extracted with EtOAc (3 x 10 mL). The combined organic phases were washed with H_2O (10 mL) and brine (10 mL), dried over MgSO_4 , filtered and the solvent was removed under reduced pressure. The crude product was purified by column chromatography (SiO_2 , c-hexane/EtOAc 4:1) affording pyrazoline *cis*-**195** (57.9 mg, 0.176 mmol, 35%, 42% brsm) as a colorless solid. The starting material (*Z*-**192** (16.6 mg, 77.1 μmol , 15%) was recovered.

$R_f = 0.3$ (c-hexane/EtOAc = 2:1).

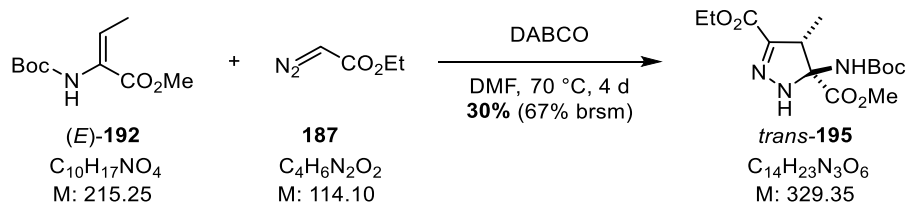
$^1\text{H NMR}$ (600 MHz, CDCl_3) $\delta = 7.28$ (s, 1H), 5.51 (s, 1H), 4.36 - 4.25 (m, 2H), 3.81 (s, 3H), 3.61 (q, $J = 7.4$ Hz, 1H), 1.44 (s, 9H), 1.38 - 1.33 (m, 6H) ppm.

$^{13}\text{C NMR}$ (151 MHz, CDCl_3) $\delta = 170.6, 161.7, 155.1, 144.7, 81.9, 81.5, 61.4, 53.5, 45.8, 28.2, 14.3, 10.3$ ppm.

IR (neat): $\tilde{\nu} = 3332, 2980, 2954, 2934, 1705, 1574, 1498, 1456, 1435, 1393, 1369, 1345, 1244, 1158, 1132, 1085, 1024, 877, 838, 811, 765$ cm^{-1} .

HRMS (ESI): m/z calculated for $\text{C}_{14}\text{H}_{23}\text{N}_3\text{NaO}_6^+$ ($[\text{M}+\text{Na}]^+$): 352.1479; found: 352.1494.

5.10.9. 3-Ethyl 5-methyl *trans*-5-((*tert*-butoxycarbonyl)amino)-4-methyl-4,5-dihydro-1H-pyrazole-3,5-dicarboxylate (*trans*-**195**)



A 6 mL PTFE-lined screwcap vial was charged with (*E*)-Boc- Δ Abu-OMe ((*E*)-**192**, 35.0 mg, 0.163 mmol, 1.00 eq.), EDA (**187**, *w* = 87% in CH_2Cl_2 , 20.9 μL , 0.244 mmol, 1.50 eq.), DABCO (3.66 mg, 32.6 μmol , 0.20 eq.) and dry DMF (0.41 mL). The vial was flushed with argon and heated to 70 $^\circ\text{C}$ in a shaking heating block. After 4 d, the solution was cooled to room temperature, diluted with H_2O (10 mL) and extracted with EtOAc (3 x 10 mL). The combined organic phases were washed with H_2O (10 mL) and brine (10 mL), dried over MgSO_4 , filtered, and the solvent was removed under reduced pressure. The crude product was purified by column chromatography (SiO_2 , *c*-hexane/EtOAc 4:1) affording pyrazoline *trans*-**195** (15.9 mg, 48.3 μmol , 30%, 67% brsm) as a colorless solid. The starting material (*E*)-**192** (14.1 mg, 65.5 μmol , 40%) as well as isomerized starting material (*Z*)-**192** (5.5 mg, 25.5 μmol , 16%) were recovered.

R_f = 0.3 (*c*-hexane/EtOAc = 2:1).

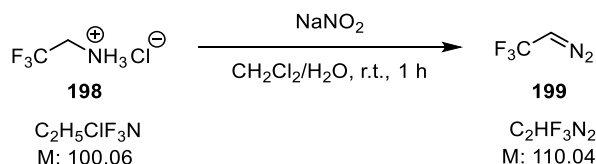
$^1\text{H NMR}$ (600 MHz, CDCl_3) δ = 7.43 (s, 1H), 5.39 (s, 1H), 4.38 – 4.25 (m, 2H), 3.83 (s, 3H), 3.04 (q, J = 7.2 Hz, 1H), 1.43 (s, 9H), 1.36 (t, J = 7.1 Hz, 3H), 1.16 (d, J = 7.2 Hz, 3H) ppm.

$^{13}\text{C NMR}$ (176 MHz, CDCl_3) δ = 168.7, 161.8, 155.2, 143.2, 83.7, 81.8, 61.5, 53.3, 48.8, 29.9, 28.3, 22.8, 14.4, 12.2 ppm.

IR (neat): $\tilde{\nu}$ = 3350, 2955, 2918, 2850, 1737, 1710, 1566, 1506, 1466, 1417, 1377, 1328, 1245, 1216, 1176, 1112, 1066, 1049, 1017, 757 cm^{-1} .

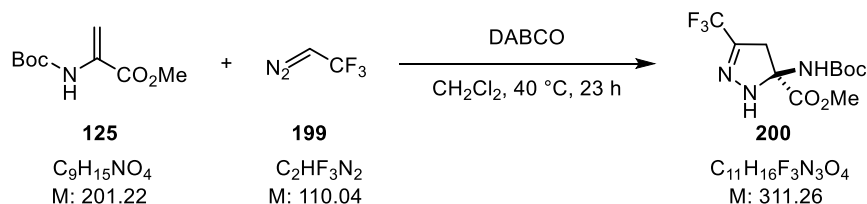
HRMS (ESI): m/z calculated for $\text{C}_{14}\text{H}_{23}\text{N}_3\text{NaO}_6^+$ ($[\text{M}+\text{Na}]^+$): 352.1479; found: 352.1501.

5.10.10. 2-Diazo-1,1,1-trifluoroethane (**199**)



A 10 mL flask was charged 2,2,2-trifluoroethan-1-ammonium chloride (**198**, 0.500 g, 3.69 mmol, 1.00 eq.), sodium nitrite (0.433 g, 6.27 mmol, 1.70 eq.), H_2O (0.50 mL) and CH_2Cl_2 (7.5 mL). The biphasic mixture was stirred vigorously for 1 h and the phases were separated. The organic phase was dried over Na_2SO_4 , filtered, and used immediately for the [2+3] cyclization without further purification.

5.10.11. Methyl 5-((*tert*-butoxycarbonyl)amino)-3-(trifluoromethyl)-4,5-dihydro-1H-pyrazole-5-carboxylate (**200**)



A 6 mL PTFE-lined screwcap vial was charged with Boc- Δ Ala-OMe (**125**, 101 mg, 0.500 mmol, 1.00 eq.) and DABCO (11.2 mg, 0.100 mmol, 0.20 eq.). A freshly prepared solution of 2-Diazo-1,1,1-trifluoroethane (approx. 0.5 M, 3.0 mL, 1.50 mmol, 3.00 eq.) was added, the vial was flushed with argon and heated to 40 °C in a shaking heating block. After 23 h the solution was cooled to room temperature, and all volatiles were removed under reduced pressure. The crude product was purified by column chromatography (SiO₂, *c*-hexane/EtOAc 9:1) affording pyrazoline **200** (143 mg, 0.460 mmol, 92%) as colorless volatile crystals.

R_f = 0.3 (*c*-hexane/EtOAc = 4:1).

¹H NMR (600 MHz, CDCl₃) δ = 6.91 (s, 1H), 5.53 (s, 1H), 3.85 (s, 3H), 3.46 (d, J = 17.9 Hz, 1H), 3.03 (d, J = 17.9 Hz, 1H), 1.44 (s, 9H) ppm.

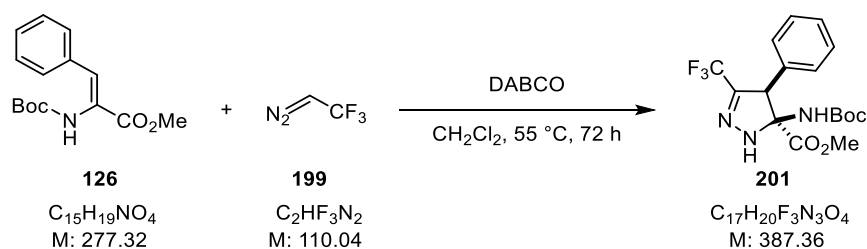
¹⁹F NMR (565 MHz, CDCl₃) δ = -66.62 ppm.

¹³C NMR (176 MHz, CDCl₃) δ = 169.8, 154.5, 139.2 (q, J = 38.2 Hz), 120.1 (q, 269.6 Hz), 81.9, 79.7, 53.9, 41.4, 28.3 ppm.

IR (neat): $\tilde{\nu}$ = 3341, 2983, 2934, 1749, 1715, 1625, 1507, 1438, 1370, 1257, 1193, 1160, 1130, 1092, 1038, 868, 845, 811, 788 cm⁻¹.

HRMS (ESI): m/z calculated for C₁₁H₁₆F₃N₃NaO₄⁺ ([M+Na]⁺): 334.0985; found: 334.0995.

5.10.12. Methyl 5-((*tert*-butoxycarbonyl)amino)-4-phenyl-3-(trifluoromethyl)-4,5-dihydro-1H-pyrazole-5-carboxylate (**201**)



A 6 mL PTFE-lined screwcap vial was charged with (*Z*)-Boc- Δ Phe-OMe ((*Z*)-**126**, 139 mg, 0.500 mmol, 1.00 eq.) and DABCO (11.2 mg, 0.100 mmol, 0.20 eq.). A freshly prepared solution of 2-Diazo-1,1,1-trifluoroethane (approx. 0.5 M, 3.0 mL, 1.50 mmol, 3.00 eq.) was added, the vial was flushed with argon and heated to 55 °C in a shaking heating block. After 72 h the solution was cooled to room temperature, and all volatiles were removed under reduced pressure. The crude product was purified by column chromatography (SiO₂, *c*-hexane/EtOAc 6:1) affording pyrazoline **201** (19.9 mg, 51.4 μ mol, 10%, 30% brsm) as a colorless volatile solid. The starting material (*Z*)-**126** (91.1 mg, 0.329 mmol, 66%) was recovered.

$R_f = 0.3$ (c-hexane/EtOAc = 4:1).

$^1\text{H NMR}$ (600 MHz, CDCl_3) $\delta = 7.48 - 7.38$ (m, 3H), 7.24 - 7.13 (m, 3H), 4.76 (s, 1H), 4.63 (s, 1H), 3.87 (s, 3H), 1.31 (s, 9H) ppm.

$^{19}\text{F NMR}$ (565 MHz, CDCl_3) $\delta = -64.44$ ppm.

$^{13}\text{C NMR}$ (151 MHz, CDCl_3) $\delta = 170.7, 154.9, 143.7$ (q, $J = 37.0$ Hz), 129.9, 129.6, 129.6, 120.1 (q, $J = 271.1$ Hz), 82.0, 81.6, 56.5, 53.9, 29.8, 28.1, 27.0 ppm.

IR (neat): $\tilde{\nu} = 3327, 2982, 2959, 2926, 2850, 1725, 1673, 1620, 1506, 1457, 1426, 1396, 1371, 1301, 1231, 1183, 1164, 1132, 1101, 1061, 896, 867, 831, 793, 778, 744$ cm^{-1} .

HRMS (ESI): m/z calculated for $\text{C}_{17}\text{H}_{20}\text{F}_3\text{N}_3\text{NaO}_4^+$ ($[\text{M}+\text{Na}]^+$): 410.1298; found: 410.1315.

6. References

- [1] Y. Imai, K. J. Meyer, A. Iinishi, Q. Favre-Godal, R. Green, S. Manuse, M. Caboni, M. Mori, S. Niles, M. Ghiglieri, C. Honrao, X. Ma, J. J. Guo, A. Makriyannis, L. Linares-Otoya, N. Böhringer, Z. G. Wuisan, H. Kaur, R. Wu, A. Mateus, A. Typas, M. M. Savitski, J. L. Espinoza, A. O'Rourke, K. E. Nelson, S. Hiller, N. Noinaj, T. F. Schäberle, A. D'Onofrio, K. Lewis, *Nature* **2019**, 576, 459–464.
- [2] J. G. Gerrard, S. McNevin, D. Alfredson, R. Forgan-Smith, N. Fraser, *Emerg. Infect. Dis.* **2003**, 9, 251–254.
- [3] H. M. Wexler, *Clin. Microbiol. Rev.* **2007**, 20, 593–621.
- [4] L. McDonnell, A. Gilkes, M. Ashworth, V. Rowland, T. H. Harries, D. Armstrong, P. White, *Gut Microbes* **2021**, 13, 1870402.
- [5] R. O'Shea, H. E. Moser, *J. Med. Chem.* **2008**, 51, 2871–2878.
- [6] T. Velkov, K. D. Roberts, R. L. Nation, P. E. Thompson, J. Li, *Future Microbiol.* **2013**, 8, 711–724.
- [7] A. Luther, M. Urfer, M. Zahn, M. Müller, S.-Y. Wang, M. Mondal, A. Vitale, J.-B. Hartmann, T. Sharpe, F. L. Monte, H. Kocherla, E. Cline, G. Pessi, P. Rath, S. M. Modaresi, P. Chiquet, S. Stiegeler, C. Verbree, T. Remus, M. Schmitt, C. Kolopp, M.-A. Westwood, N. Desjonquères, E. Brabet, S. Hell, K. Le Poupon, A. Vermeulen, R. Jaisson, V. Rithié, G. Upert, A. Lederer, P. Zbinden, A. Wach, K. Moehle, K. Zerbe, H. H. Locher, F. Bernardini, G. E. Dale, L. Eberl, B. Wollscheid, S. Hiller, J. A. Robinson, D. Obrecht, *Nature* **2019**, 576, 452–458.
- [8] H. Kaur, R. P. Jakob, J. K. Marzinek, R. Green, Y. Imai, J. R. Bolla, E. Agustoni, C. V. Robinson, P. J. Bond, K. Lewis, T. Maier, S. Hiller, *Nature* **2021**, 593, 125–129.
- [9] T. Shono, Y. Matsumura, K. Tsubata, Y. Sugihara, S. Yamane, T. Kanazawa, T. Aoki, *J. Am. Chem. Soc.* **1982**, 104, 6697–6703.
- [10] N. Ritzmann, S. Manioglu, S. Hiller, D. J. Muller, *Structure* **2022**, 30, 350–359.
- [11] S. F. Haysom, J. Machin, J. M. Whitehouse, J. E. Horne, K. Fenn, Y. Ma, H. El Mkami, N. Bohringer, T. F. Schaberle, N. A. Ranson, S. E. Radford, C. Pliotas, *Angew. Chem. Int. Ed.* **2023**, e202218783.
- [12] K. Yokoyama, E. A. Lilla, *Nat. Prod. Rep.* **2018**, 35, 660–694.
- [13] S. J. Booker, C. T. Lloyd, *ACS Bio. & Med. Chem. Au.* **2022**, 2, 538–547.
- [14] S. Guo, S. Wang, S. Ma, Z. Deng, W. Ding, Q. Zhang, *Nature Commun.* **2022**, 13, 2361.
- [15] S. Guo, S. Wang, S. Z. Ma, Z. X. Deng, W. Ding, Q. Zhang, *Nature Commun.* **2022**, 13.
- [16] H. Nguyen, I. D. M. Kresna, N. Boehringer, J. Ruel, E. de la Mora, J. C. Kramer, K. Lewis, Y. Nicolet, T. F. Schäberle, K. Yokoyama, *J. Am. Chem. Soc.* **2022**, 144, 18876–18886.
- [17] S. Gross, F. Panter, D. Pogorevc, C. E. Seyfert, S. Deckarm, C. D. Bader, J. Herrmann, R. Muller, *Chem. Sci.* **2021**, 12, 11882–11893.
- [18] C. E. Seyfert, C. Porten, B. Yuan, S. Deckarm, F. Panter, C. D. Bader, J. Coetzee, F. Deschner, K. Tehrani, P. G. Higgins, H. Seifert, T. C. Marlovits, J. Herrmann, R. Muller, *Angew. Chem. Int. Ed.* **2023**, 62, e202214094.
- [19] Z. G. Wuisan, I. D. M. Kresna, N. Böhringer, K. Lewis, T. F. Schäberle, *Metab. Eng.* **2021**, 66, 123–136.

- [20] M. Nestic, D. B. Ryffel, J. Maturano, M. Shevlin, S. R. Pollack, D. R. Gauthier, P. Trigo-Mouriño, L.-K. Zhang, D. M. Schultz, J. M. McCabe Dunn, L.-C. Campeau, N. R. Patel, D. A. Petrone, D. Sarlah, *J. Am. Chem. Soc.* **2022**, *144*, 14026–14030.
- [21] Y.-C. Lin, F. Schneider, K. J. Eberle, D. Chiodi, H. Nakamura, S. H. Reisberg, J. Chen, M. Saito, P. S. Baran, *J. Am. Chem. Soc.* **2022**, *144*, 14458–14462.
- [22] N. R. Patel, D. Petrone, S. Sarlah, L. C. Campeau, D. Schultz, in *S2.E4: The Total Synthesis of Darobactin A (or is it Davobactin?)*, Spotify Podcast, Pharm To Table Podcast, **2023**. (Accessed: 06.07.2023)
- [23] D. Ryffel, M. Horwitz, in *Synthetic Workshop Videos*, YouTube, **2022**, <https://www.youtube.com/watch?v=xgNyK4cZQUc&t=420s>. (Accessed: 06.07.2023)
- [24] M. Zhao, J. Li, E. Mano, Z. Song, D. M. Tschaen, E. J. J. Grabowski, P. J. Reider, *J. Org. Chem.* **1999**, *64*, 2564–2566.
- [25] N. Schröder, J. Wencel-Delord, F. Glorius, *J. Am. Chem. Soc.* **2012**, *134*, 8298–8301.
- [26] J. W. Bogart, A. A. Bowers, *Org. Biomol. Chem.* **2019**, *17*, 3653–3669.
- [27] D. Siodłak, *Amino Acids* **2015**, *47*, 1–17.
- [28] U. Schmidt, A. Lieberknecht, J. Wild, *Synthesis* **1988**, 1988, 159–172.
- [29] D. Siodłak, B. Rzeszotarska, M. A. Broda, A. E. Kozioł, E. Kołodziejczyk, *Acta Biochim. Pol.* **2004**, *51*, 145–152.
- [30] P. J. Jervis, C. Amorim, T. Pereira, J. A. Martins, P. M. T. Ferreira, *Int. J. Mol. Sci.* **2021**, *22*, 2528.
- [31] M. G. Acker, A. A. Bowers, C. T. Walsh, *J. Am. Chem. Soc.* **2009**, *131*, 17563–17565.
- [32] H. M. Key, S. J. Miller, *J. Am. Chem. Soc.* **2017**, *139*, 15460–15466.
- [33] R. H. de Vries, J. H. Viel, O. P. Kuipers, G. Roelfes, *Angew. Chem. Int. Ed.* **1996**, *60*, 3946–3950.
- [34] R. J. Scamp, E. de Ramon, E. K. Paulson, S. J. Miller, J. A. Ellman, *Angew. Chem. Int. Ed.* **2020**, *59*, 890–895.
- [35] P. M. T. Ferreira, H. L. S. Maia, L. S. Monteiro, J. Sacramento, *J. Chem. Soc., Perkin Trans. 1* **1999**, 3697–3703.
- [36] I. Torrini, G. P. Zecchini, M. P. Paradisi, *Synth. Commun.* **1989**, *19*, 695–703.
- [37] Y. O. You, W. A. van der Donk, *Biochemistry* **2007**, *46*, 5991–6000.
- [38] H. Wang, J. Zhang, M. Xian, *J. Am. Chem. Soc.* **2009**, *131*, 13238–13239.
- [39] J. M. Chalker, S. B. Gunnoo, O. Boutureira, S. C. Gerstberger, M. Fernández-González, G. J. L. Bernardes, L. Griffin, H. Hailu, C. J. Schofield, B. G. Davis, *Chem. Sci.* **2011**, *2*, 1666–1676.
- [40] T. Nagano, H. Kinoshita, *Bull. Chem. Soc. Jpn.* **2000**, *73*, 1605–1613.
- [41] R. Kimura, T. Nagano, H. Kinoshita, *Bull. Chem. Soc. Jpn.* **2002**, *75*, 2517–2525.
- [42] U. Schmidt, A. Lieberknecht, J. Wild, *Synthesis* **1984**, 1984, 53–60.
- [43] Y. Yasuno, M. Hamada, T. Yamada, T. Shinada, Y. Ohfuné, *Eur. J. Org. Chem.* **2013**, 2013, 1884–1888.
- [44] H. Azuma, K. Okano, T. Fukuyama, H. Tokuyama, in *Org. Synth.* **2011**, *88*, 152–161.
- [45] U. Schmidt, E. Öhler, *Angew. Chem. Int. Ed.* **1977**, *16*, 327–328.
- [46] T. Nanjo, T. Oshita, A. Matsumoto, Y. Takemoto, *Chem. Eur. J.* **2022**, *28*, e202201120.
- [47] H. Kohn, K. N. Sawhney, P. Bardel, D. W. Robertson, J. D. Leander, *J. Med. Chem.* **1993**, *36*, 3350–3360.

-
- [48] S. Jin, J. Liebscher, *Synlett* **1999**, 4, 459–461.
- [49] P. M. T. Ferreira, H. L. S. Maia, L. S. Monteiro, J. Sacramento, *J. Chem. Soc., Perkin Trans. 1* **2001**, 3167–3173.
- [50] T. Brandhofer, O. G. Mancheño, *ChemCatChem* **2019**, 11, 3797–3801.
- [51] H. Yin, M. Zheng, H. Chen, S. Wang, Q. Zhou, Q. Zhang, P. Wang, *J Am Chem Soc* **2020**, 142, 14201–14209.
- [52] O. Zhang, J. W. Schubert, *J. Org. Chem.* **2020**, 85, 6225–6232.
- [53] R. C. W. van Lier, A. D. de Bruijn, G. Roelfes, *Chem. Eur. J.* **2021**, 27, 1430–1437.
- [54] A. Rehpenn, A. Walter, G. Storch, *Chem. Sci.* **2022**, 13, 14151–14156.
- [55] M. P. Sibi, Y. Asano, J. B. Sausker, *Angew. Chem. Int. Ed.* **2001**, 40, 1293–1296.
- [56] W. S. Knowles, *J. Chem. Educ.* **1986**, 63, 222.
- [57] L. Panella, A. M. Aleixandre, G. J. Kruidhof, J. Robertus, B. L. Feringa, J. G. De Vries, A. J. Minnaard, *J. Org. Chem.* **2006**, 71, 2026–2036.
- [58] M. Biosca, P. de la Cruz-Sánchez, O. Pàmies, M. Diéguez, *J. Org. Chem.* **2020**, 85, 4730–4739.
- [59] Y. Yasuno, I. Mizutani, Y. Sueuchi, Y. Wakabayashi, N. Yasuo, K. Shimamoto, T. Shinada, *Chem. Eur. J.* **2019**, 25, 5145–5148.
- [60] P. M. Ferreira, L. S. Monteiro, G. Pereira, *Amino Acids* **2010**, 39, 499–513.
- [61] A. S. Abreu, P. M. T. Ferreira, M.-J. R. P. Queiroz, I. C. F. R. Ferreira, R. C. Calhelha, L. M. Estevinho, *Eur. J. Org. Chem.* **2005**, 14, 2951–2957.
- [62] M. J. R. P. Queiroz, A. Begouin, G. Pereira, P. M. T. Ferreira, *Tetrahedron* **2008**, 64, 10714–10720.
- [63] M. J. Burk, J. G. Allen, W. F. Kiesman, K. M. Stoffan, *Tetrahedron Lett.* **1997**, 38, 1309–1312.
- [64] P. J. Harrington, L. S. Hegedus, K. F. McDaniel, *J. Am. Chem. Soc.* **1987**, 109, 433–4338.
- [65] F. Bartoccini, D. M. Cannas, F. Fini, G. Piersanti, *Org. Lett.* **2016**, 18, 2762–2765.
- [66] J. J. Bozell, C. Vogt, J. Gozum, *J. Org. Chem.* **1991**, 56, 2584–2587.
- [67] R. H. de Vries, J. H. Viel, R. Oudshoorn, O. P. Kuipers, G. Roelfes, *Chem. Eur. J.* **2019**, 25, 12698–12702.
- [68] K. Tanaka, M. Takahashi, H. Imase, T. Osaka, K. Noguchi, M. Hirano, *Tetrahedron* **2008**, 64, 6289–6293.
- [69] C. D. Gilmore, K. M. Allan, B. M. Stoltz, *J. Am. Chem. Soc.* **2008**, 130, 1558–1559.
- [70] C. Zhu, N. W. J. Ang, T. H. Meyer, Y. Qiu, L. Ackermann, *ACS Cent. I Sci.* **2021**, 7, 415–431.
- [71] M. C. Leech, K. Lam, *Nat. Rev. Chem.* **2022**, 6, 275–286.
- [72] D. E. Danly, *J. Electrochem. Soc.* **1984**, 131, 435C.
- [73] E. Steckhan, *Angew. Chem. Int. Ed.* **1986**, 25, 683–701.
- [74] E. Steckhan, *Top. Curr. Chem.* **1987**, 142, 1–69.
- [75] E. T. Seo, R. F. Nelson, J. M. Fritsch, L. S. Marcoux, D. W. Leedy, R. N. Adams, *J. Am. Chem. Soc.* **1966**, 88, 3498–3503.
- [76] T. Shono, H. Hamaguchi, Y. Matsumura, *J. Am. Chem. Soc.* **1975**, 97, 4264–4268.
- [77] A. M. Jones, C. E. Banks, *Beilstein J. Org. Chem.* **2014**, 10, 3056–3072.
- [78] J.-i. Yoshida, K. Nishiwaki, *J. Chem. Soc., Dalton Trans.* **1998**, 2589–2596.

- [79] J.-i. Yoshida, S. Suga, *Chem. Eur. J.* **2002**, *8*, 2650–2658.
- [80] J.-i. Yoshida, A. Shimizu, R. Hayashi, *Chem. Rev.* **2018**, *118*, 4702–4730.
- [81] A. Kirste, B. Elsler, G. Schnakenburg, S. R. Waldvogel, *J. Am. Chem. Soc.* **2012**, *134*, 3571–3576.
- [82] X. Dong, J. L. Roeckl, S. R. Waldvogel, B. Morandi, *Science* **2021**, *371*, 507–514.
- [83] J. Luo, T. L. Liu, *Journal of Bioresources and Bioproducts* **2023**, *8*, 1–14.
- [84] M. Klein, S. R. Waldvogel, *Angew. Chem. Int. Ed.* **2022**, *61*, e202204140.
- [85] A. K. Miller, C. C. Hughes, J. J. Kennedy-Smith, S. N. Gradl, D. Trauner, *J. Am. Chem. Soc.* **2006**, *128*, 17057–17062.
- [86] T.-S. Kam, T.-M. Lim, G.-H. Tan, *J. Chem. Soc., Perkin Trans. 1* **2001**, 1594–1604.
- [87] F. Wang, S. S. Stahl, *Acc. Chem. Res.* **2020**, *53*, 561–574.
- [88] S. B. Beil, D. Pollok, S. R. Waldvogel, *Angew. Chem. Int. Ed.* **2021**, *60*, 14750–14759.
- [89] L. F. T. Novaes, J. S. K. Ho, K. Mao, K. Liu, M. Tanwar, M. Neurock, E. Villemure, J. A. Terrett, S. Lin, *J. Am. Chem. Soc.* **2022**, *144*, 1187–1197.
- [90] T. Shono, Y. Matsumura, K. Inoue, *J. Org. Chem.* **1983**, *48*, 1388–1389.
- [91] Y. Lin, L. R. Malins, *J. Am. Chem. Soc.* **2021**, *143*, 11811–11819.
- [92] A. S. Mackay, R. J. Payne, L. R. Malins, *J. Am. Chem. Soc.* **2022**, *144*, 23–41.
- [93] D. Karipal Padinjare Veedu, L. A. Connal, L. R. Malins, *Angew. Chem. Int. Ed.* **2023**, *62*, e202215470.
- [94] F. Wang, M. Rafiee, S. S. Stahl, *Angew. Chem. Int. Ed.* **2018**, *57*, 6686–6690.
- [95] P.-S. Gao, X.-J. Weng, Z.-H. Wang, C. Zheng, B. Sun, Z.-H. Chen, S.-L. You, T.-S. Mei, *Angew. Chem. Int. Ed.* **2020**, *59*, 15254–15259.
- [96] F. Blanco, D. G. Lloyd, L. M. Azofra, I. Alkorta, J. Elguero, *Struct. Chem.* **2013**, *24*, 421–432.
- [97] B. Nehra, S. Rulhania, S. Jaswal, B. Kumar, G. Singh, V. Monga, *Eur. J. Med. Chem.* **2020**, *205*, 112666.
- [98] K. Manna, U. Banik, P. S. Ghosh, M. Das, *Nirma Univ. J. Pharm. Sci.* **2014**, *1*, 37–49.
- [99] B. Dipankar, C. Hirakmoy, B. Asish, C. Abhijit, *Int. Res. J. Pharm. Appl. Sci.* **2011**, *1*, 68–80.
- [100] W. Yang, Y. Hu, Y. S. Yang, F. Zhang, Y. B. Zhang, X. L. Wang, J. F. Tang, W. Q. Zhong, H. L. Zhu, *Bioorg. Med. Chem.* **2013**, *21*, 1050–1063.
- [101] H. H. Wang, K. M. Qiu, H. E. Cui, Y. S. Yang, L. Yin, M. Xing, X. Y. Qiu, L. F. Bai, H. L. Zhu, *Bioorg. Med. Chem.* **2013**, *21*, 448–455.
- [102] P. Rathore, S. Yaseen, S. Ovais, R. Bashir, R. Yaseen, A. D. Hameed, M. Samim, R. Gupta, F. Hussain, K. Javed, *Bioorg. Med. Chem. Lett.* **2014**, *24*, 1685–1691.
- [103] D. Matiadis, M. Sagnou, *Int. J. Mol. Sci.* **2020**, *21*, 5507.
- [104] R. Aggarwal, A. Bansal, I. Rozas, B. Kelly, P. Kaushik, D. Kaushik, *Eur. J. Med. Chem.* **2013**, *70*, 350–357.
- [105] M. A. Ali, M. Shaharyar, A. A. Siddiqui, *Eur. J. Med. Chem.* **2007**, *42*, 268–275.
- [106] Z. A. Kaplancikli, A. Ozdemir, G. Turan-Zitouni, M. D. Altintop, O. D. Can, *Eur. J. Med. Chem.* **2010**, *45*, 4383–4387.
- [107] V. Monga, K. Goyal, M. Steindel, M. Malhotra, D. P. Rajani, S. D. Rajani, *Med. Chem. Res.* **2014**, *23*, 2019–2032.

-
- [108] Z. A. Kaplancikli, G. Turan-Zitouni, A. Ozdemir, O. D. Can, P. Chevallet, *Eur. J. Med. Chem.* **2009**, *44*, 2606–2610.
- [109] U. D. Ozkay, O. D. Can, Z. A. Kaplancikli, *Med. Chem. Res.* **2012**, *21*, 1056–1061.
- [110] J. H. M. Lange, H. H. van Stuivenberg, W. Veerman, H. C. Wals, B. Stork, H. Coolen, A. C. McCreary, T. J. P. Adolfs, C. G. Kruse, *Bioorg. Med. Chem. Lett.* **2005**, *15*, 4794–4798.
- [111] J. H. M. Lange, A. Attali, M. A. W. van der Neut, H. C. Wals, A. Mulder, H. Zilaout, A. Duursma, H. H. M. van Aken, B. J. van Vliet, *Bioorg. Med. Chem. Lett.* **2010**, *20*, 4992–4998.
- [112] J. Tryggvi, *Top 200 Small Molecule Drugs by Retail Sales in 2022*, **2023**.
<https://njardarson.lab.arizona.edu/content/top-pharmaceuticals-poster> (Accessed: 24.07.2023)
- [113] R. H. Wiley, L. C. Behr, R. Fusco, C. H. Jarboe, in *Chem. Heterocycl. Compd.*, Interscience Publishers, New York, **1967**, 81–174.
- [114] A. Lévai, J. Jekó, *Monatsh. Chem.* **2006**, *137*, 339–345.
- [115] D. Matiadis, *Adv. Synth. Catal.* **2023**, *365*, 1934–1969.
- [116] T. Vahedpour, M. Hamzeh-Mivehroud, S. Hemmati, S. Dastmalchi, *ChemistrySelect* **2021**, *6*, 6483–6506.
- [117] A. Lévai, *J. Heterocycl. Chem.* **2002**, *39*, 1–13.
- [118] P. R. Krishna, E. R. Sekhar, F. Mongin, *Tetrahedron Lett.* **2008**, *49*, 6768–6772.
- [119] N. M. Abunada, H. M. Hassaneen, N. G. Kandile, O. A. Miqdad, *Molecules* **2008**, *13*, 1011–1024.
- [120] X. Kou, Q. Shao, C. Ye, G. Yang, W. Zhang, *J. Am. Chem. Soc.* **2018**, *140*, 7587–7597.
- [121] CDC, *CDC. Antibiotic Resistance Threats in the United States, 2019*. Atlanta, GA: U.S. Department of Health and Human Services, CDC; 2019.
- [122] R. P. Loach, O. S. Fenton, K. Amaike, D. S. Siegel, E. Ozkal, M. Movassaghi, *J. Org. Chem.* **2014**, *79*, 11254–11263.
- [123] A. B. Dounay, L. E. Overman, *Chem. Rev.* **2003**, *103*, 2945–2964.
- [124] G. Yang, P. Lindovska, D. Zhu, J. Kim, P. Wang, R.-Y. Tang, M. Movassaghi, J.-Q. Yu, *J. Am. Chem. Soc.* **2014**, *136*, 10807–10813.
- [125] A. El-Faham, F. Albericio, *Chem. Rev.* **2011**, *111*, 6557–6602.
- [126] M. J. Dunn, R. F. Jackson, *Tetrahedron* **1997**, *53*, 13905–13914.
- [127] P. Dumy, M. Keller, D. E. Ryan, B. Rohwedder, T. Wöhr, M. Mutter, *J. Am. Chem. Soc.* **1997**, *119*, 918–925.
- [128] Y. Sato, M. Sodeoka, M. Shibasaki, *Chem. Lett.* **1990**, *19*, 1953–1954.
- [129] M. Shibasaki, M. Sodeoka, *J. Synth. Org. Chem. Jpn.* **1994**, *52*, 956–967.
- [130] C. Moinet, J.-C. Fiaud, *Tetrahedron Lett.* **1995**, *36*, 2051–2052.
- [131] F. Ozawa, Y. Kobatake, A. Kubo, T. Hayashi, *J. Chem. Soc., Chem. Commun.* **1994**, 1323–1324.
- [132] K. Teranishi, S.-i. Nakatsuka, T. Goto, *Synthesis* **1994**, 1018–1020.
- [133] J. A. Bodkin, M. D. McLeod, *J. Chem. Soc., Perkin Trans. 1* **2002**, 2733–2746.
- [134] B. N. Hemric, *Org. Biomol. Chem.* **2021**, *19*, 46–81.
- [135] G. S. B. Tao, K. B. Sharpless, *Tetrahedron Lett.* **1998**, *39*, 2507–2510.
- [136] R. Moreira, M. Diamandas, S. D. Taylor, *J. Org. Chem.* **2019**, *84*, 15476–15485.

- [137] S. Jagtap, *Catalysts* **2017**, *7*, 267.
- [138] D. Boschelli, T. Takemasa, Y. Nishitani, S. Masamune, *Tetrahedron Lett.* **1985**, *26*, 5239–5242.
- [139] J. Jover, J. Cirera, *Dalton Trans.* **2019**, *48*, 15036–15048.
- [140] P. G. M. Wuts, in *Greene's Protective Groups in Organic Synthesis*, 5 ed., John Wiley & Sons, New Jersey, **2014**, 895–1193.
- [141] H.-Q. Cao, H.-N. Liu, Z.-Y. Liu, B. Qiao, F.-G. Zhang, J.-A. Ma, *Org. Lett.* **2020**, *22*, 6414–6419.
- [142] K. Teegardin, J. I. Day, J. Chan, J. Weaver, *Org. Process Res. Dev.* **2016**, *20*, 1156–1163.
- [143] T. Neveselý, M. Wienhold, J. J. Molloy, R. Gilmour, *Chem. Rev.* **2022**, *122*, 2650–2694.
- [144] I. W. Davies, L. Gerena, L. Castonguay, C. H. Senanayake, R. D. Larsen, T. R. Verhoeven, P. J. Reider, *Chem. Comm.* **1996**, 1753–1754.
- [145] S. E. B. D. Rieke, P. M. Hudnall, T. P. Burns, G. S. Poindexter, *Org. Synth.* **1979**, *59*, 85.
- [146] H. Gilman, F. Schulze, *J. Am. Chem. Soc.* **1925**, *47*, 2002–2005.
- [147] D. Kurandina, P. Chuentragool, V. Gevorgyan, *Synthesis* **2019**, *51*, 985–1005.
- [148] R. McCrindle, G. Ferguson, G. J. Arsenault, A. J. McAlees, *J. Chem. Soc., Chem. Commun.* **1983**, 571–572.
- [149] S. Y. W. Lau, N. G. Andersen, B. A. Keay, *Org. Lett.* **2001**, *3*, 181–184.
- [150] Z. Ahmadi, J. S. McIndoe, *Chem. Comm.* **2013**, *49*, 11488–11490.
- [151] N. Tamura, Y. Matsushita, K. Yoshioka, M. Ochiai, *Tetrahedron* **1988**, *44*, 3231–3240.
- [152] H. Poisel, *Chem. Ber.* **1977**, *110*, 942–947.
- [153] R. Spina, E. Colacino, J. Martinez, F. Lamaty, *Chem. Eur. J.* **2013**, *19*, 3817–3821.
- [154] A. Dondoni, D. Perrone, P. Merino, *J. Org. Chem.* **1995**, *60*, 8074.
- [155] Y.-M. Shao, W.-B. Yang, H.-P. Peng, M.-F. Hsu, K.-C. Tsai, T.-H. Kuo, A. H. J. Wang, P.-H. Liang, C.-H. Lin, A.-S. Yang, C.-H. Wong, *ChemBioChem* **2007**, *8*, 1654–1657.
- [156] M. Sinha, V. R. Dola, A. Soni, P. Agarwal, K. Srivastava, W. Haq, S. K. Puri, S. B. Katti, *Bioorg. Med. Chem.* **2014**, *22*, 5950–5960.
- [157] S. Bera, G. Panda, *Org. Biomol. Chem.* **2014**, *12*, 3976–3985.
- [158] Z. Ye, Z. Zhou, N. Ayat, X. Wu, E. Jin, X. Shi, Z.-R. Lu, *Contrast Media Mol. Imaging* **2016**, *11*, 32–40.
- [159] R. S. Pottorf, P. Szeto, *1-Ethyl-3-(3'-dimethylaminopropyl)carbodiimide Hydrochloride*, John Wiley & Sons, Ltd., **2001**, 1.
- [160] P. Fatas, J. Bachl, S. Oehm, A. I. Jimenez, C. Cativiela, D. Diaz Diaz, *Chem. Eur. J.* **2013**, *19*, 8861–8874.
- [161] J. D. McKerrow, J. M. A. Al-Rawi, P. Brooks, *Synth. Commun.* **2010**, *40*, 1161–1179.
- [162] C. D. McCune, M. L. Beio, J. M. Sturdivant, R. de la Salud-Bea, B. M. Darnell, D. B. Berkowitz, *J. Am. Chem. Soc.* **2017**, *139*, 14077–14089.
- [163] N. H. Alvarez, H. v. d. Langemheen, A. J. Brouwer, R. M. J. Liskamp, *Bioorg. Med. Chem.* **2017**, *25*, 5055–5063.
- [164] T. Asakura, M. Kamio, A. Nishioka, *Biopolymers* **1979**, *18*, 467–477.
- [165] I. Tameo, H. Hiroshi, M. Kazuo, M. Muneji, *Bull. Chem. Soc. Jpn.* **1979**, *52*, 826–830.
- [166] T. Tajima, H. Kurihara, T. Fuchigami, *J. Am. Chem. Soc.* **2007**, *129*, 6680–6681.

-
- [167] J.-H. Kruse, P. Biehl, F. H. Schacher, *Macromol. Rapid Commun.* **2019**, *40*, 1800857.
- [168] S. Sakakibara, *Bull. Chem. Soc. Jpn.* **1960**, *33*, 814–818.
- [169] P. P. D. Chuan, F. S.; Chad, T. C., *Sci. Sin.* **1976**, *21*, 691.
- [170] T. Efferth, S. Kahl, K. Paulus, M. Adams, R. Rauh, H. Boechzelt, X. Hao, B. Kaina, R. Bauer, *Mol. Cancer Ther.* **2008**, *7*, 152–161.
- [171] J. M. Henley, K. A. Wilkinson, *Nat. Rev. Neurosci.* **2016**, *17*, 337–350.
- [172] S. R. Platt, *Vet. J.* **2007**, *173*, 278–286.
- [173] W. Zhang, A. Robert, S. B. Vogensen, J. R. Howe, *Biophys. J.* **2006**, *91*, 1336–1346.
- [174] R. Jin, M. Horning, M. L. Mayer, E. Gouaux, *Biochemistry* **2002**, *41*, 15635–15643.
- [175] J. L. Muir, K. J. Page, D. J. S. Sirinathsinghji, T. W. Robbins, B. J. Everitt, *Behav. Brain Res.* **1993**, *57*, 123–131.
- [176] J. W. Lee, O. Furmanski, D. A. Castellanos, L. A. Daniels, A. T. Hama, J. Sagen, *Neurosci. Lett.* **2008**, *439*, 212–215.
- [177] P. Renaut, D. Thomas, F. D. Bellamy, *Synthesis* **1991**, 265–266.
- [178] S. H. McCooey, S. J. Connon, *Angew. Chem. Int. Ed.* **2005**, *44*, 6367–6370.
- [179] B. Vakulya, S. Varga, A. Csámpai, T. Soós, *Org. Lett.* **2005**, *7*, 1967–1969.
- [180] S. J. Connon, *Chem. Comm.* **2008**, 2499–2510.
- [181] G. Bencivenni, P. Galzerano, A. Mazzanti, G. Bartoli, P. Melchiorre, *Proc. Natl. Acad. Sci.* **2010**, *107*, 20642–20647.
- [182] M. N. Grayson, K. N. Houk, *J. Am. Chem. Soc.* **2016**, *138*, 9041–9044.
- [183] H. Sai, T. Ogiku, H. Ohmizu, *Synthesis* **2003**, 201–204.
- [184] S. P. Green, K. M. Wheelhouse, A. D. Payne, J. P. Hallett, P. W. Miller, J. A. Bull, *Org. Process Res. Dev.* **2020**, *24*, 67–84.
- [185] J. D. Clark, A. S. Shah, J. C. Peterson, L. Patelis, R. J. A. Kersten, A. H. Heemskerk, *Thermochim. Acta* **2002**, *386*, 73–79.
- [186] P. Bajaj, G. Sreenilayam, V. Tyagi, R. Fasan, *Angew. Chem. Int. Ed.* **2016**, *55*, 16110–16114.
- [187] G. Maas, *Angew. Chem. Int. Ed.* **2009**, *48*, 8186–8195.
- [188] T. Bug, M. Hartnagel, C. Schlierf, H. Mayr, *Chemistry* **2003**, *9*, 4068–4076.
- [189] L. Li, R. J. Mayer, D. S. Stephenson, P. Mayer, A. R. Ofial, H. Mayr, *Chem. Eur. J.* **2022**, *28*, e202201376.
- [190] K. J. Hock, R. M. Koenigs, *Chem. Eur. J.* **2018**, *24*, 10571–10583.
- [191] D. N. Tran, C. Battilocchio, S.-B. Lou, J. M. Hawkins, S. V. Ley, *Chem. Sci.* **2015**, *6*, 1120–1125.
- [192] W. T. Liu, Jack, B. Wei, M. Lee, M. N. Hopkins, J. Bacsá, S. S. Stahl, H. M. L. Davies, *ACS Catal.* **2021**, *11*, 2676–2683.
- [193] M. I. Javed, M. Brewer, *Org. Lett.* **2007**, *9*, 1789–1792.
- [194] A. Greb, J. S. Poh, S. Greed, C. Battilocchio, P. Pasau, D. C. Blakemore, S. V. Ley, *Angew. Chem. Int. Ed.* **2017**, *56*, 16602–16605.
- [195] Y.-W. Pan, C.-W. Guo, H.-Y. Tu, C.-W. Tsai, W.-C. Cheng, *ACS Comb. Sci.* **2013**, *15*, 425–434.
- [196] T. Menard, A. Laverny, S. E. Denmark, *J. Org. Chem.* **2021**, *86*, 14290–14310.

- [197] D. Schäfer, P. Weiß, J. Ermert, J. Castillo Meleán, F. Zarrad, B. Neumaier, *Eur. J. Org. Chem.* **2016**, 2016, 4621–4628.
- [198] B. Jiang, C.-G. Yang, J. Wang, *J. Org. Chem.* **2001**, 66, 4865–4869.
- [199] M. Shimizu, M. Sodeoka, *Org. Lett.* **2007**, 9, 5231–5234.
- [200] H. S. Tae, T. B. Sundberg, T. K. Neklesa, D. J. Noblin, J. L. Gustafson, A. G. Roth, K. Raina, C. M. Crews, *ChemBioChem* **2012**, 13, 538–541.
- [201] H. Shiozaki, M. Miyahara, K. Otsuka, K. Miyako, A. Honda, Y. Takasaki, S. Takamizawa, H. Tukada, Y. Ishikawa, R. Sakai, M. Oikawa, *Org. Lett.* **2018**, 20, 3403–3407.
- [202] A. R. Ellwood, M. J. Porter, *J. Org. Chem.* **2009**, 74, 7982–7985.
- [203] S. Machida, K. Usuba, M. A. Blaskovich, A. Yano, K. Harada, S. M. Sebti, N. Kato, J. Ohkanda, *Chem. Eur. J.* **2008**, 14, 1392–1401.
- [204] G. L. Lackner, K. W. Quasdorf, G. Pratsch, L. E. Overman, *J. Org. Chem.* **2015**, 80, 6012–6024.
- [205] S. Roy, A. Eastman, G. W. Gribble, *Org. Biomol. Chem.* **2006**, 4, 3228–3234.
- [206] M. Kazuhiro, O. Atsuhiko, N. Katsuhiko, *Bull. Chem. Soc. Jpn.* **1987**, 60, 1021–1026.
- [207] C. Aubry, H. Oulyadi, G. Dutheil, J. Leprince, H. Vaudry, X. Pannecoucke, J.-C. Quirion, *J. Pept. Sci.* **2006**, 12, 154–160.
- [208] P. Strazzolini, M. Scuccato, A. G. Giumanini, *Tetrahedron* **2000**, 56, 3625–3633.
- [209] M. Hamada, T. Shinada, Y. Ohfuné, *Org. Lett.* **2009**, 11, 4664–4667.
- [210] K. Miki, I. Kohki, K. Rumi, K. Hideki, *Bull. Chem. Soc. Jpn.* **2009**, 82, 364–380.
- [211] K. F. W. Hekking, D. C. J. Waalboer, M. A. H. Moelands, F. L. v. Delft, F. P. J. T. Rutjes, *Adv. Synth. Catal.* **2008**, 350, 95–106.
- [212] A. P. Vartak, K. Skoblenick, N. Thomas, R. K. Mishra, R. L. Johnson, *J. Med. Chem.* **2007**, 50, 6725–6729.

7. Appendix

7.1. List of Abbreviations

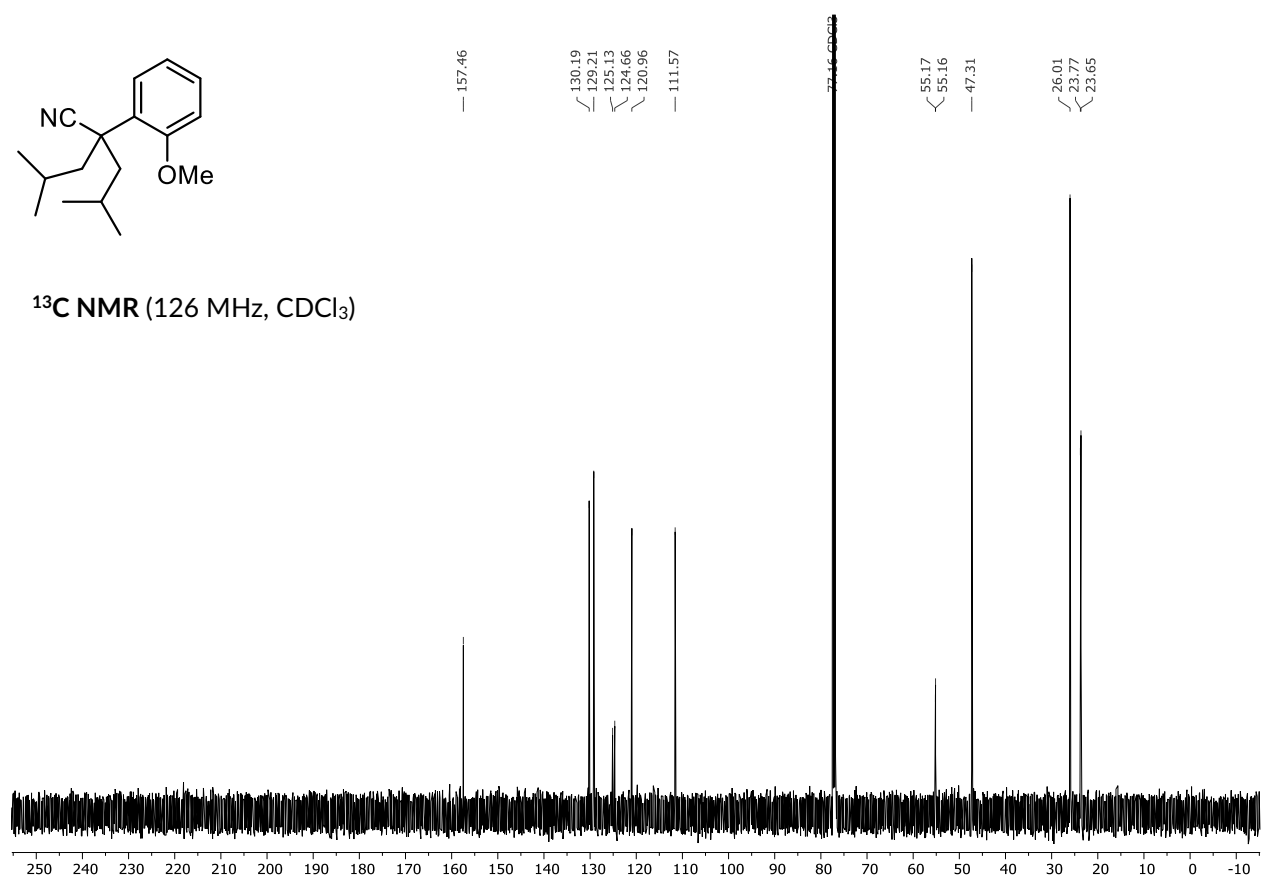
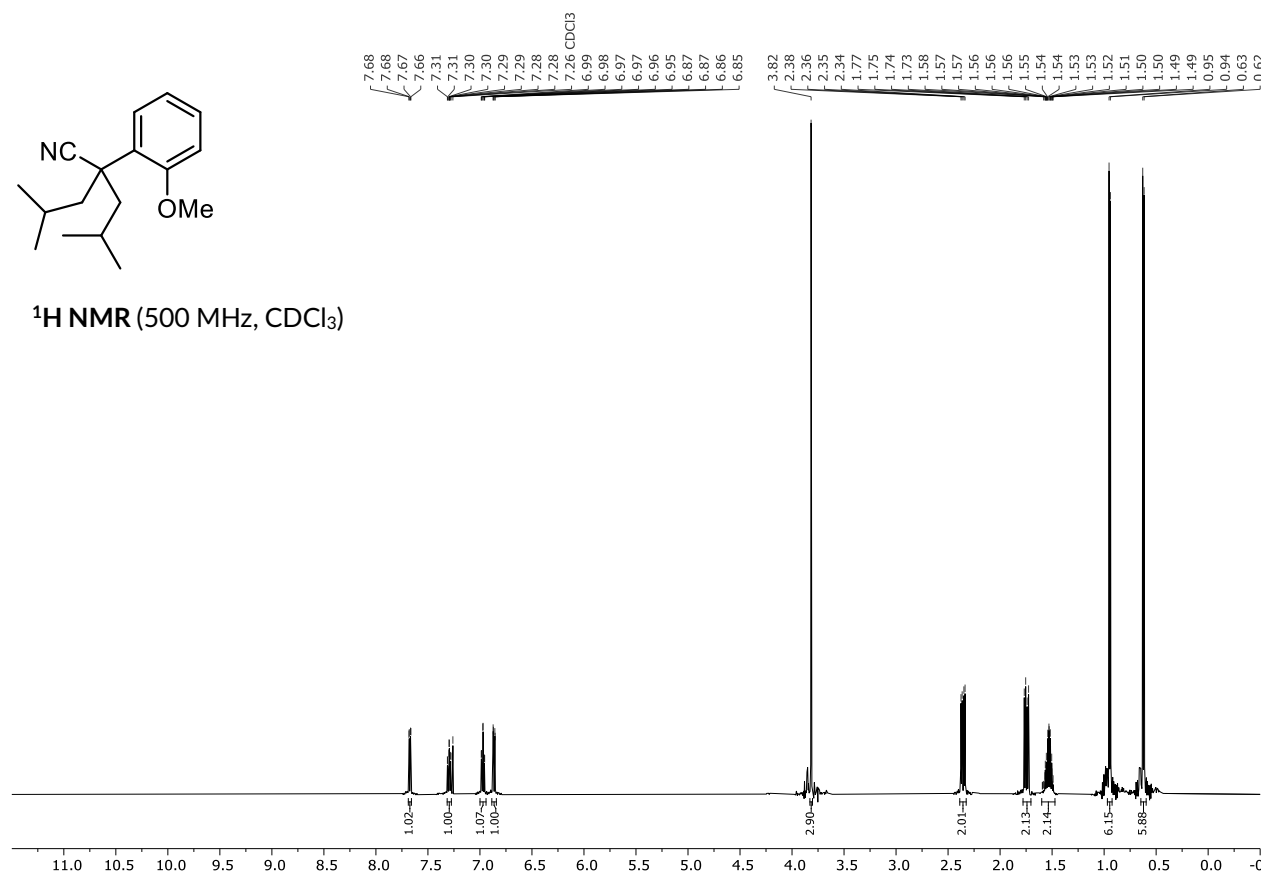
ABCO	quinuclidine	COMU	(1-cyano-2-ethoxy-2-oxoethylidenaminoxy)dimethylamino-morpholino-carbenium hexafluorophosphate
ABNO	9-azabicyclo[3.3.1]nonane <i>N</i> -oxyl	Cp*	1,2,3,4,5-pentamethylcyclopentadiyl
Abu	2-aminobutyric acid	Cy	cyclohexyl
Ac	acetyl	d	day(s)
AIBN	2,2'-azobis(2-methylpropionitrile)	<i>d.r.</i>	diastereomeric ratio
Alk	alkyl	Da	Dalton
ALS	amyotrophic lateral sclerosis	DABCO	1,4-diazabicyclo[2.2.2]octane
AMPA	α -amino-3-hydroxy-5-methylisoxazole-4-propionic acid	dAdo	2'-desoxyadenosine
aq.	aqueous	dba	dibenzylideneacetone
AQN	Anthraquinone-1,4-diyl	DBU	1,8-Diazabicyclo[5.4.0]undec-7-ene
Ar	arene	DCE	1,2-dichloroethane
Asp	asparagine	Decom	decomposition
ATP	adenosine 5'-triphosphate	p.	
ATR	attenuated total reflection	DFT	density-functional theory
BAM	β -barrel assembly machinery	dhAA	α,β -dehydroamino acid
BBN	9-borabicyclo[3.3.1]nonane	DHQ	dihydroquinine
BGC	biosynthetic gene cluster	DHQD	dihydroquinidine
Bn	benzyl	DIPEA	<i>N,N</i> -diisopropylethylamine
Boc	<i>tert</i> -butyloxycarbonyl	DMAP	4-(dimethylamino)pyridine
BOX	bis(oxazoline)	DMF	dimethylformamide
PhBPE	1,2-Bis-2,5-diphenylphospholano)ethane	DMSO	dimethyl sulfoxide
bpy	2,2'-bipyridyl	dppp	1,3-bis(diphenylphosphino)propane
bpz	2,2'-bipyrazine	dtbbpy	4,4'-di- <i>tert</i> -butyl-2,2'-dipyridyl
br	broad	DtBuPF	1,1'-bis(di- <i>tert</i> -butylphosphino)ferrocene
brsm	Based on recovered starting material	<i>EC</i> ₅₀	half maximal effective concentration
BTM	2-phenyl-2,3-dihydroimidazo[2,1- <i>b</i>][1,3]benzothiazole	ECEC	electrochemical-chemical-electrochemical-chemical process
Bu	butyl	EDA	ethyl diazoacetate
Cbz	benzyloxycarbonyl	EDC	<i>N</i> -(3-dimethylaminopropyl)- <i>N'</i> -ethylcarbodiimide
cf.	confer / compare		

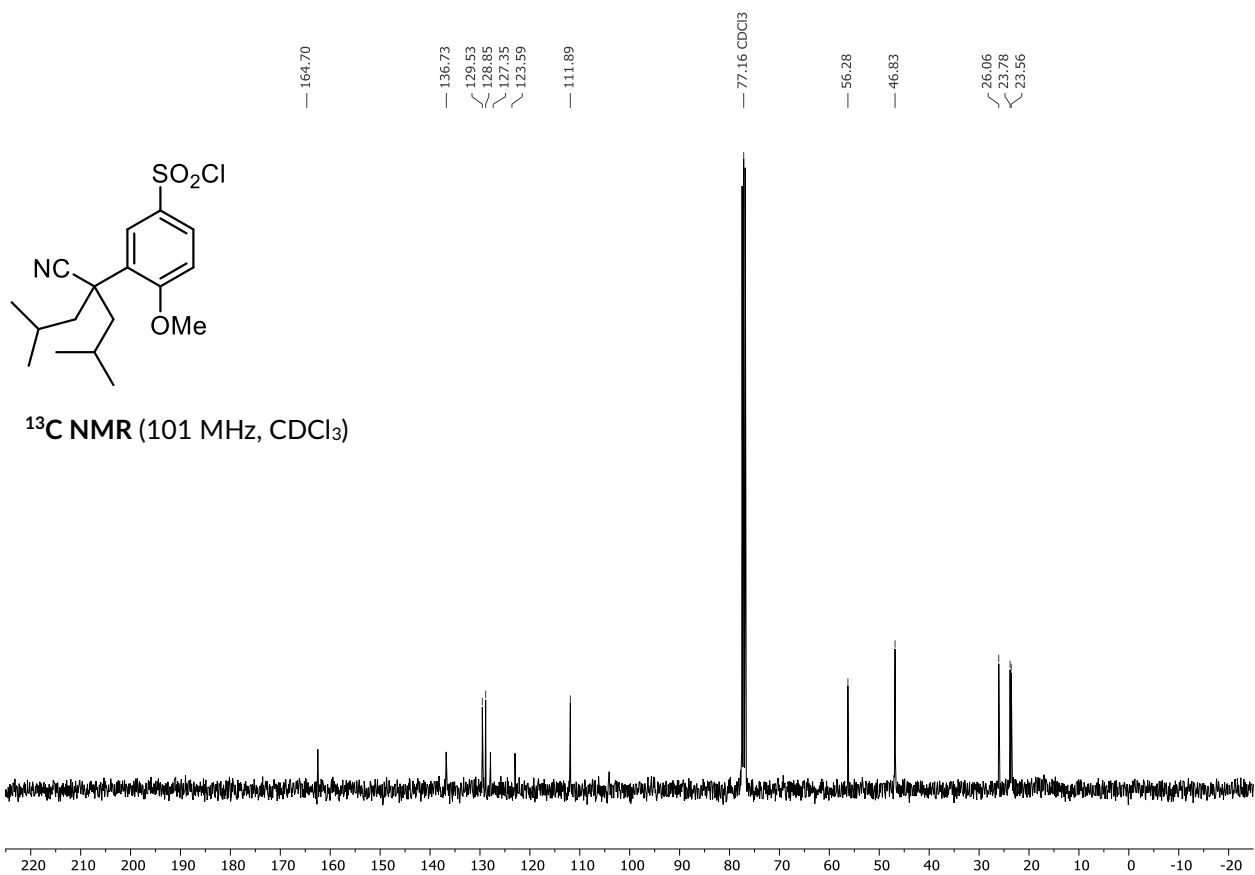
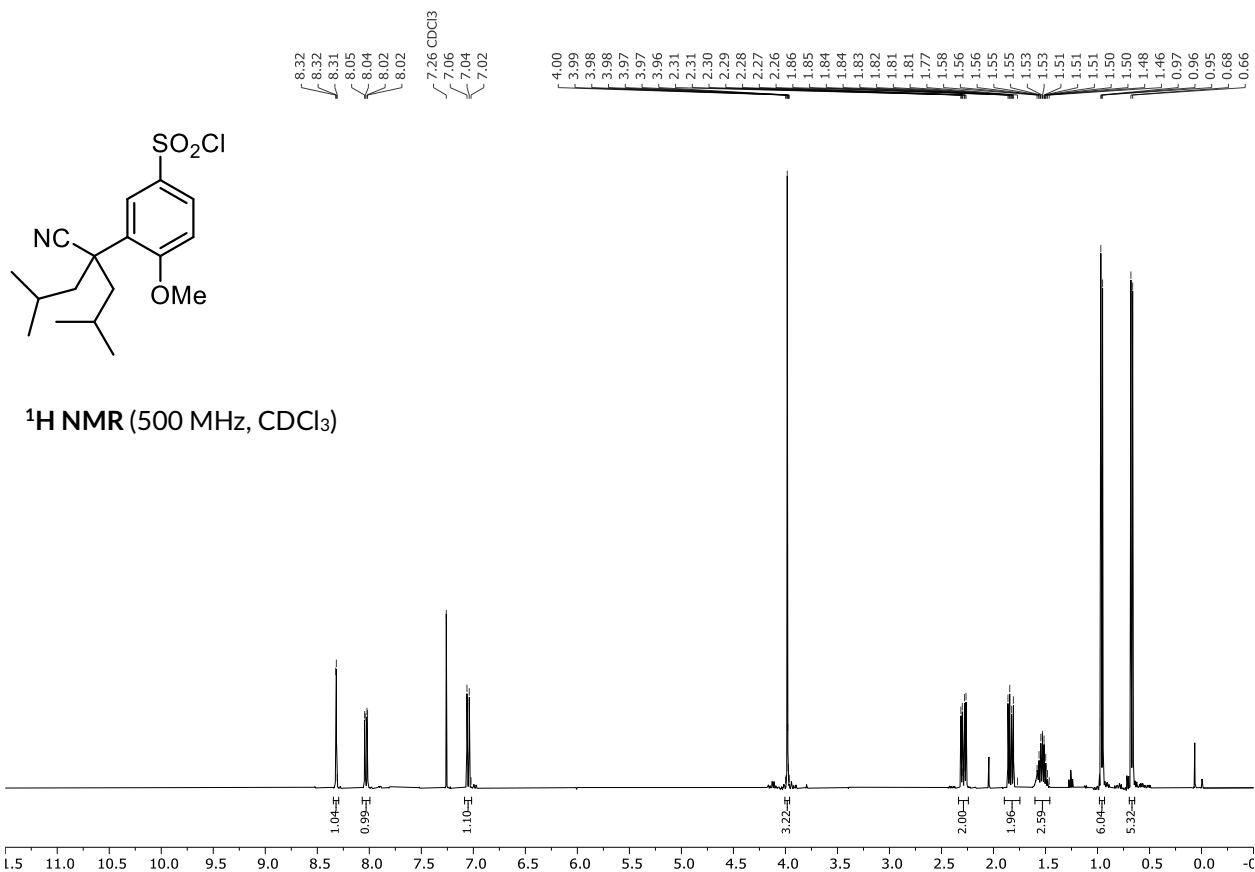
EDG	electron donating group(s)	mCPBA	3-chloroperbenzoic acid
ee	enantiomeric excess	Me	methyl
EEDQ	2-ethoxy-1-ethoxycarbonyl-1,2-dihydroquinoline	Med	mediator
EM	electron microscopy	MIC	minimum inhibitory concentration
$E_p^{1/2}$	half-peak potential	min	minute(s)
eq.	equivalent(s)	Ms	mesyl
ESI	electrospray ionization	nbd	norborna-2,5-diene
Et	ethyl	NBS	<i>N</i> -bromosuccinimide
<i>et al.</i>	<i>et alii</i>	NHPI	<i>N</i> -hydroxyphthalimide
EWG	electron withdrawing group(s)	NHPI	<i>N</i> -hydroxyphthalimide
F	Farad	NIS	<i>N</i> -iodosuccinimide
GABA	4-aminobutanoic acid	NMP	<i>N</i> -methyl-2-pyrrolidone
GC-MS	gas chromatography / mass spectrometry	NMR	nuclear magnetic resonance
Glu	glutamic acid	NOE	nuclear overhauser effect
Gly	glycine	NOESY	nuclear Overhauser enhancement spectroscopy
GOESY	gradient enhanced nuclear Overhauser enhancement spectroscopy	<i>n</i> Pr	<i>n</i> -propyl
GP	general procedure	NSAID	non-steroidal anti-inflammatory drug
h	hours	Nuc	nucleophile
HFIP	1,1,1,3,3,3-hexafluoro isopropanol	OMP	outer membrane protein
HMBC	heteronuclear multiple bond correlation	<i>o</i> Tol	<i>ortho</i> -tolyl
HOAt	1-hydroxy-7-azabenzotriazole	Ox	oxidized form
HOBt	1-hydroxybenzotriazole	p	quintet
HOMO	highest occupied molecular orbital	PCET	proton-coupled electron transfer
HPLC	high-performance liquid chromatography	PG	protecting group
HRMS	high-resolution mass spectrometry	Ph	phenyl
HWE	HORNER-WADSWORTH-EMMONS	PHAL	1,4-phthalazinediyl
IR	infrared spectroscopy	Phe	phenylalanine
L-DOPA	3-(3,4-dihydroxyphenyl)-L-alanine	Phth	phthaloyl
Leu	leucine	Piv	pivaloyl
LUMO	lowest unoccupied molecular orbital	ppm	parts per million
Lys	lysine	PPTS	pyridinium <i>p</i> -toluenesulfonate
m	multiplet	ppy	2-phenylpyridine
		Pro	proline
		PTC	phase transfer catalyst
		PTFE	polytetrafluoroethylene
		PyBOP	benzotriazol-1-yloxytripyrrolidino-phosphonium hexafluorophosphat

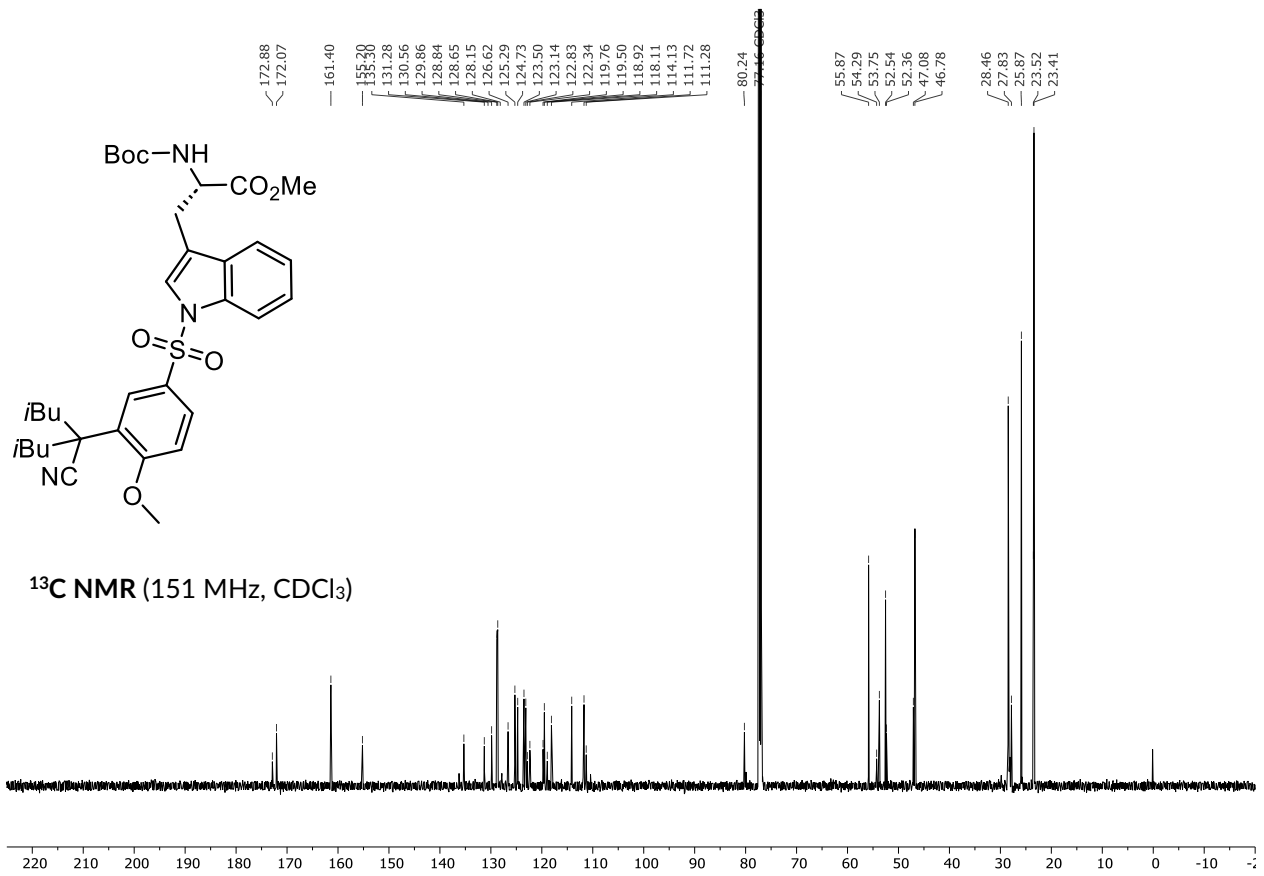
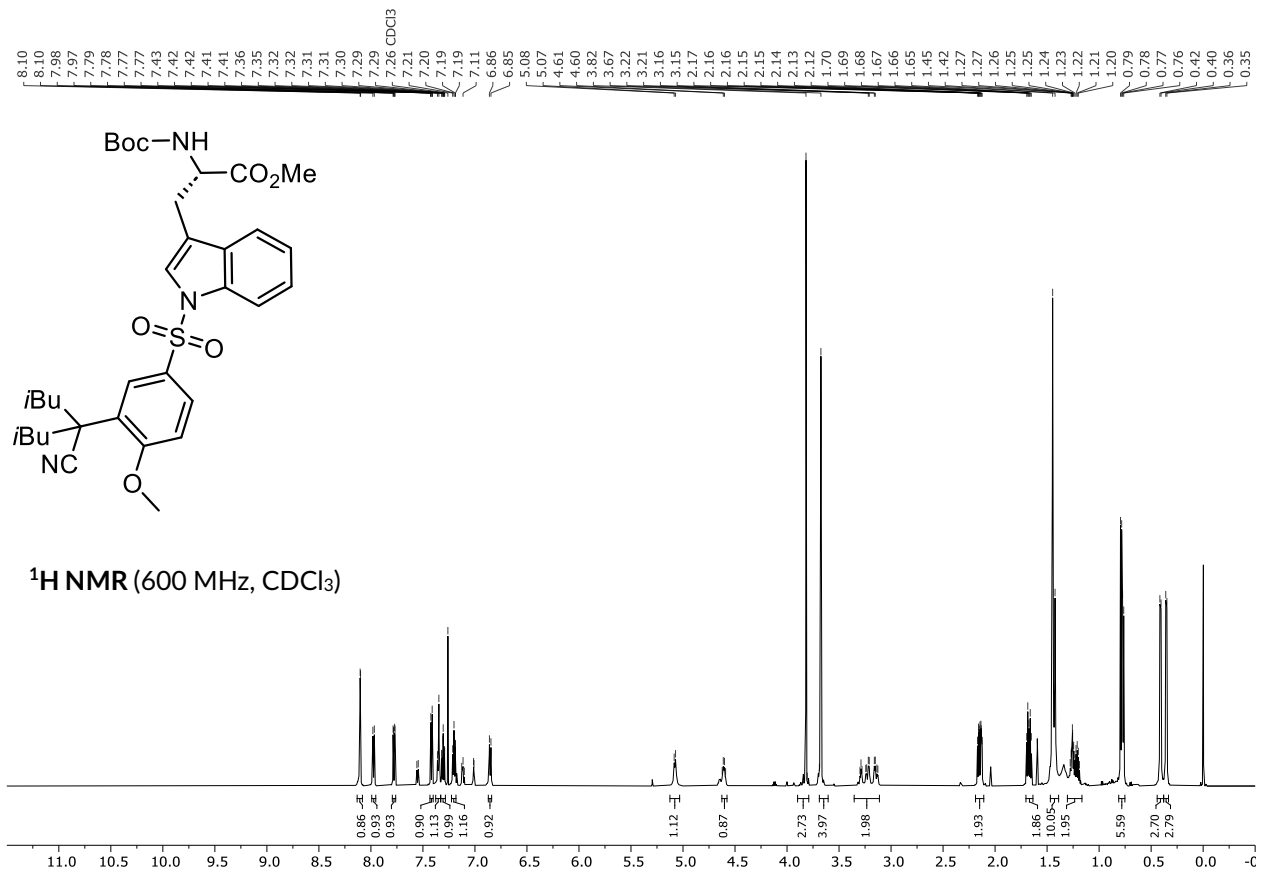
Pyr	2,5-diphenyl-4,6-pyrimidinediyl	TBS	<i>tert</i> -butyldimethylsilyl
quant.	quantitative	Temp	3-(4-cyano-2,6-dimethylheptan-4-yl)-4-methoxybenzene-1-sulfonyl
r.t.	room temperature	TEMPO	2,2,6,6-tetramethylpiperidine 1-oxyl
Red	Reduced form	TES	triethylsilyl
red	reduced form	Tf	triflyl
R_f	retention factor	TFA	trifluoroacetic acid
ROESY	rotating frame Overhauser enhancement spectroscopy	TFE	2,2,2-trifluoroethanol
rSAM	radical S-adenosyl methionine	TG-DSC	thermogravimetry-differential scanning calometry
RVC	reticulated vitreous carbon	THF	tetrahydrofuran
s	singlet	TIPS	triisopropylsilyl
s. m.	starting material	TLC	thin layer chromatography
sat.	saturated	TMG	1,1,3,3-tetramethylguanidine
Ser	serine	TMS	trimethylsilyl/trimethylsilane
SET	single electron transfer	TOF	time-of-flight
S_N	nucleophilic substitution	Troc	2,2,2-trichloroethyloxycarbonyl
S_{NAr}	aromatic nucleophilic substitution	Trp	tryptophan
SOMO	single occupied molecular orbital	Trt	trityl
SPhos	Dicyclohexyl(2',6'-dimethoxy[1,1'-biphenyl]-2-yl)phosphane	Ts	<i>p</i> -toluenesulfonyl
Sub	substrate	Tyr	tyrosine
t	triplet	w%	weight-%
TBAF	tetrabutylammonium fluoride	Xan	xanthyl
TBAT	tetrabutylammonium difluorotriphenylsilicate	XPhos	2-dicyclohexylphosphino-2',4',6'-triisopropylbiphenyl
TBDPS	<i>tert</i> -butyldiphenylchlorosilyl		

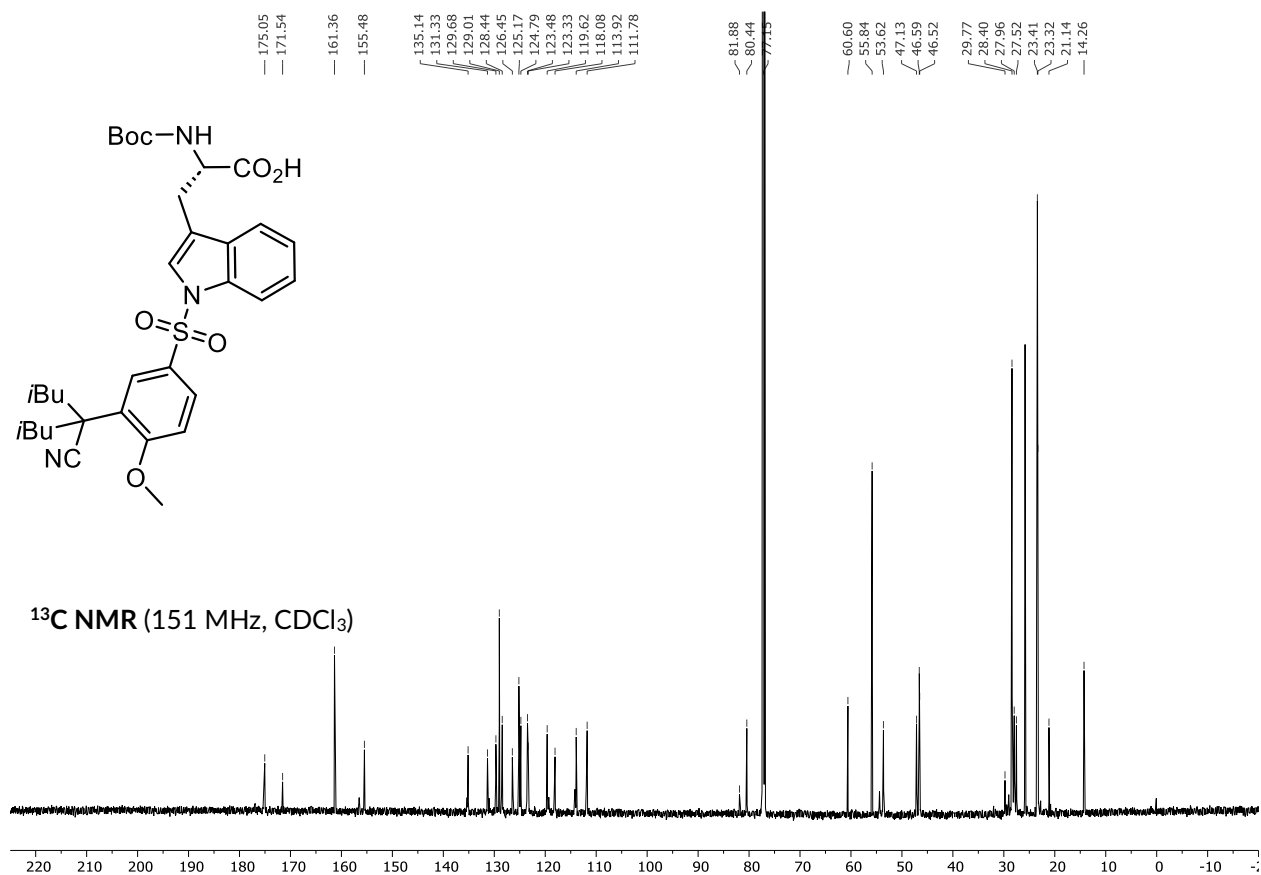
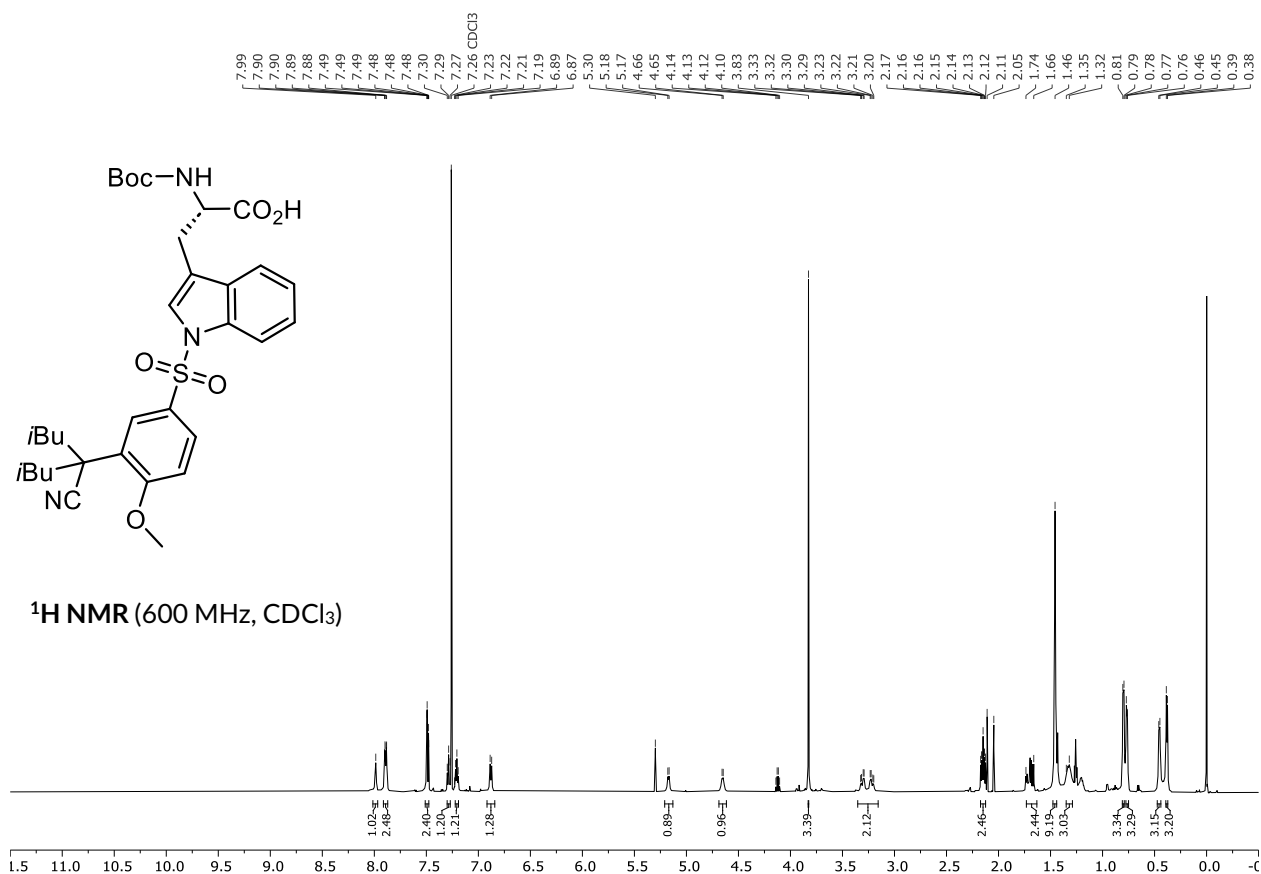
7.2. NMR Spectra

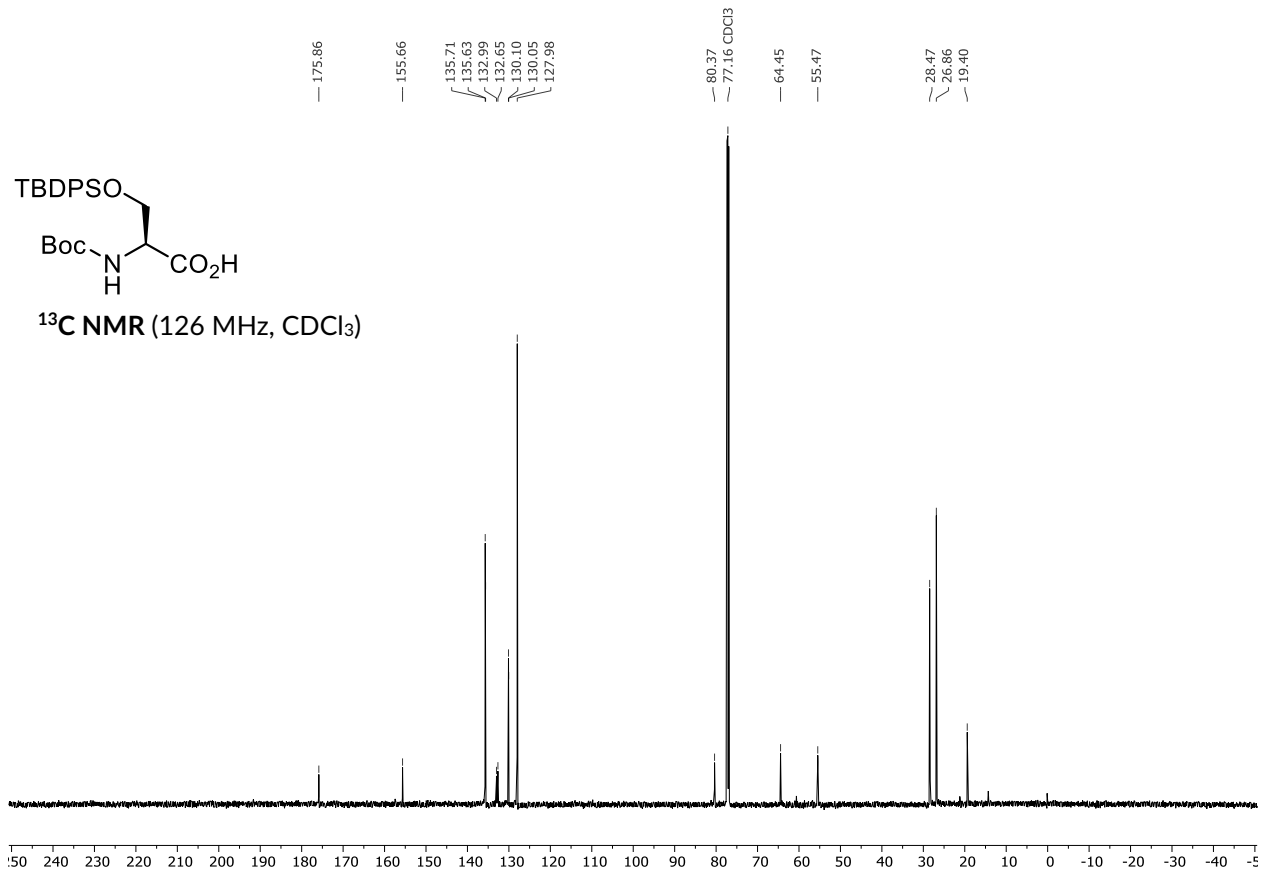
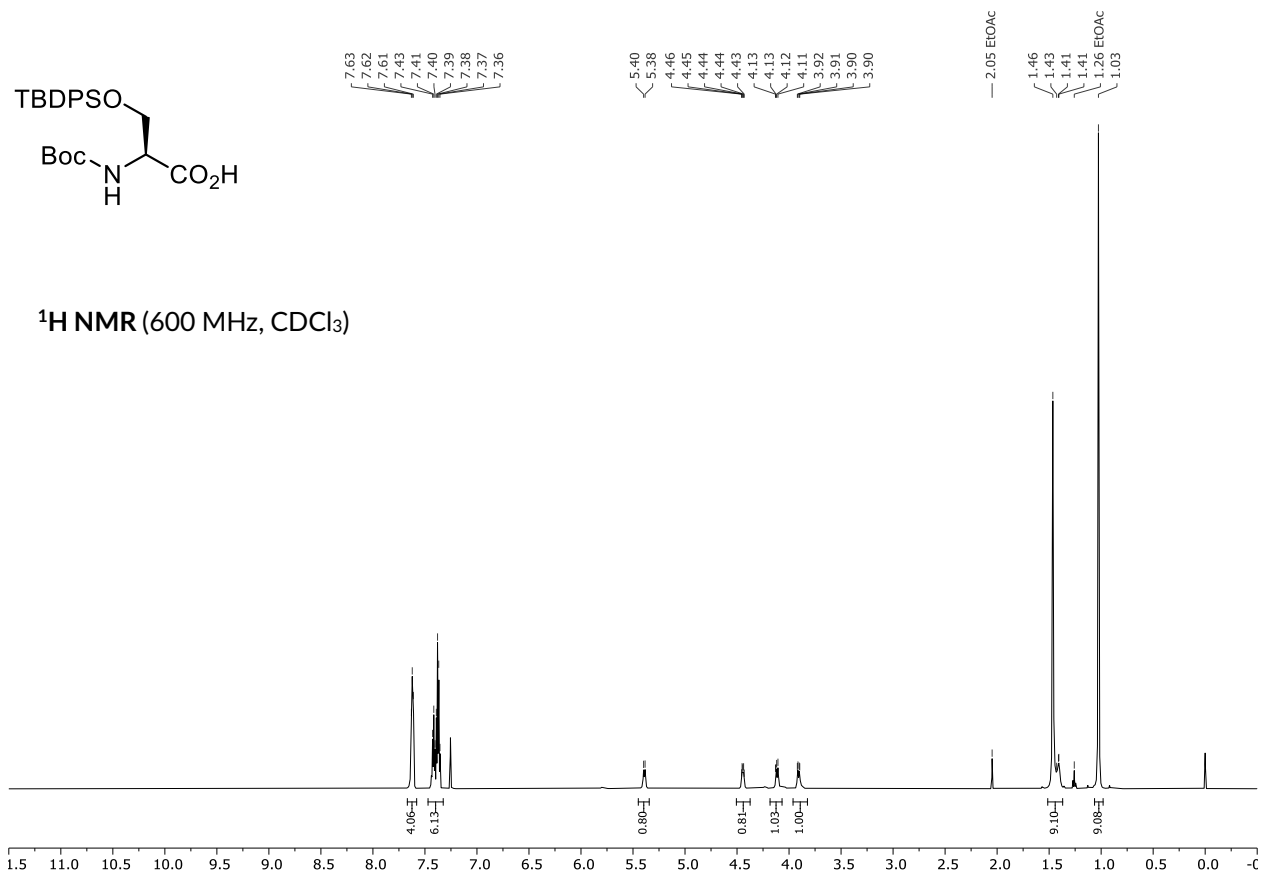
7.2.1. Template-assisted C6-Indole Functionalization of the Eastern Fragment

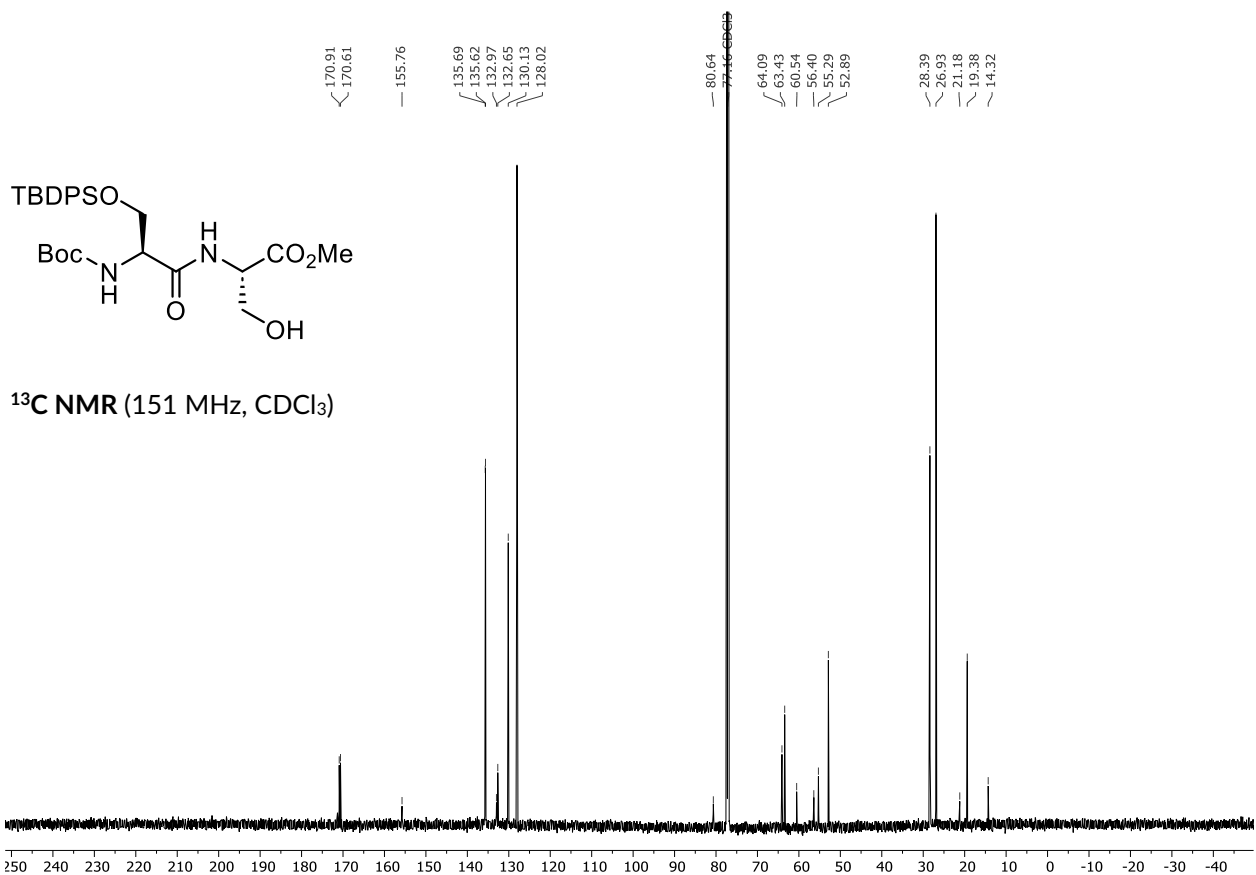
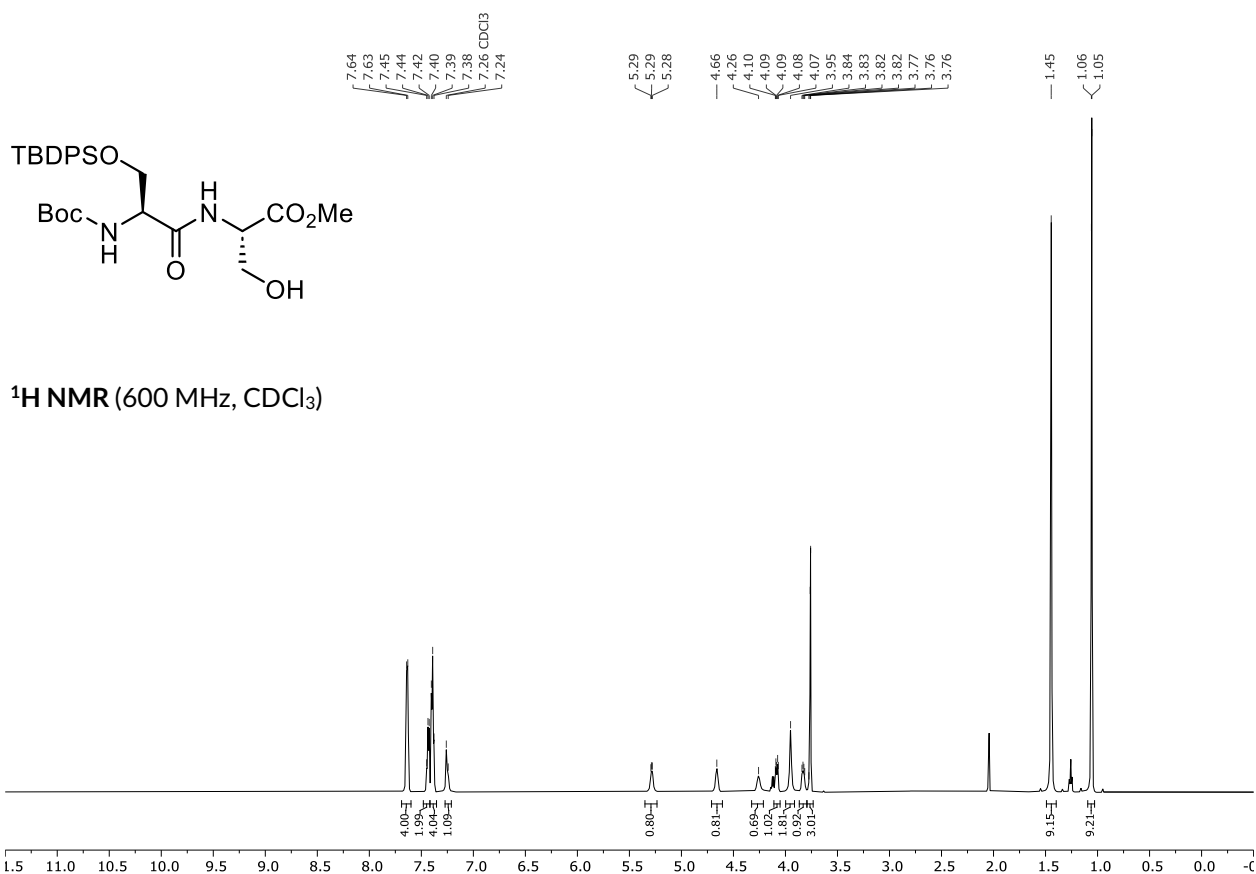


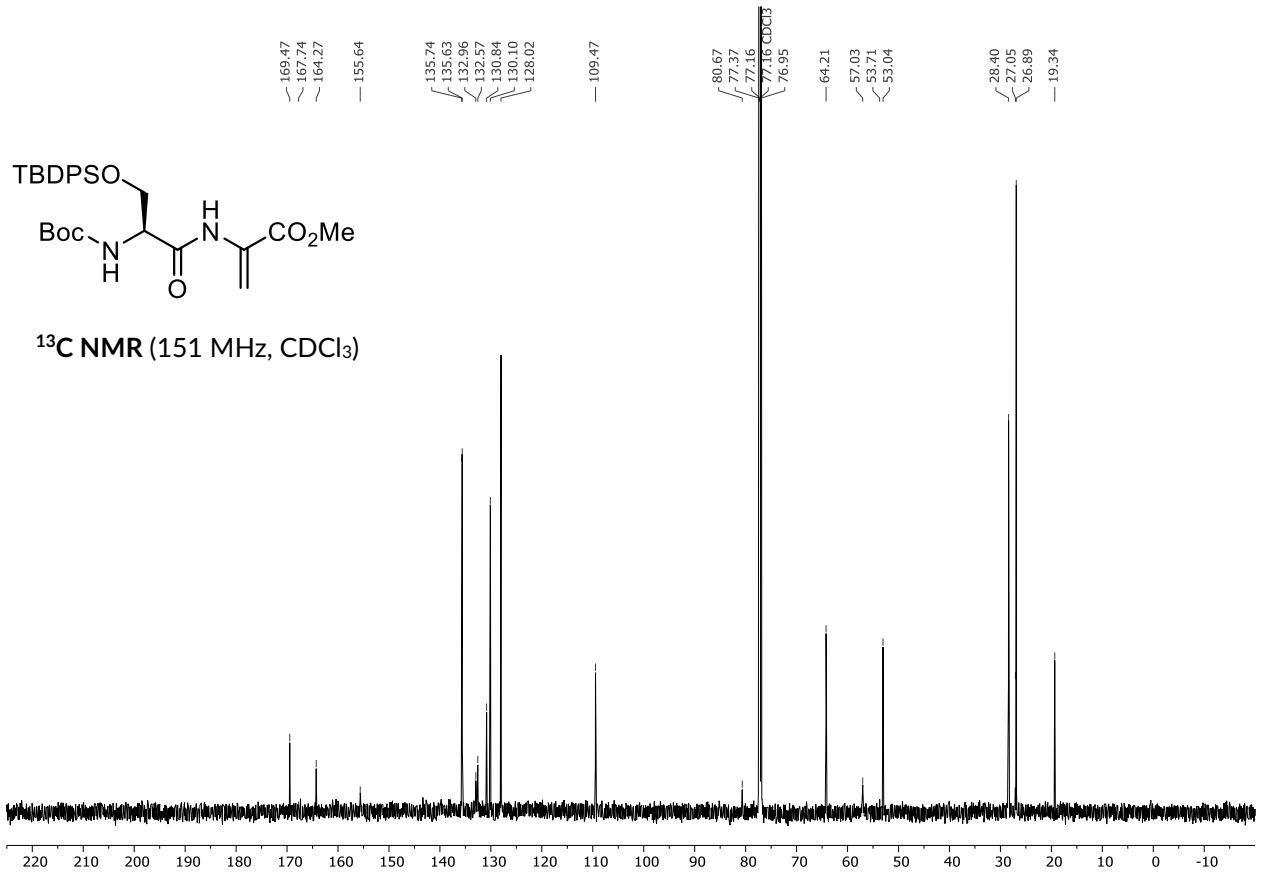
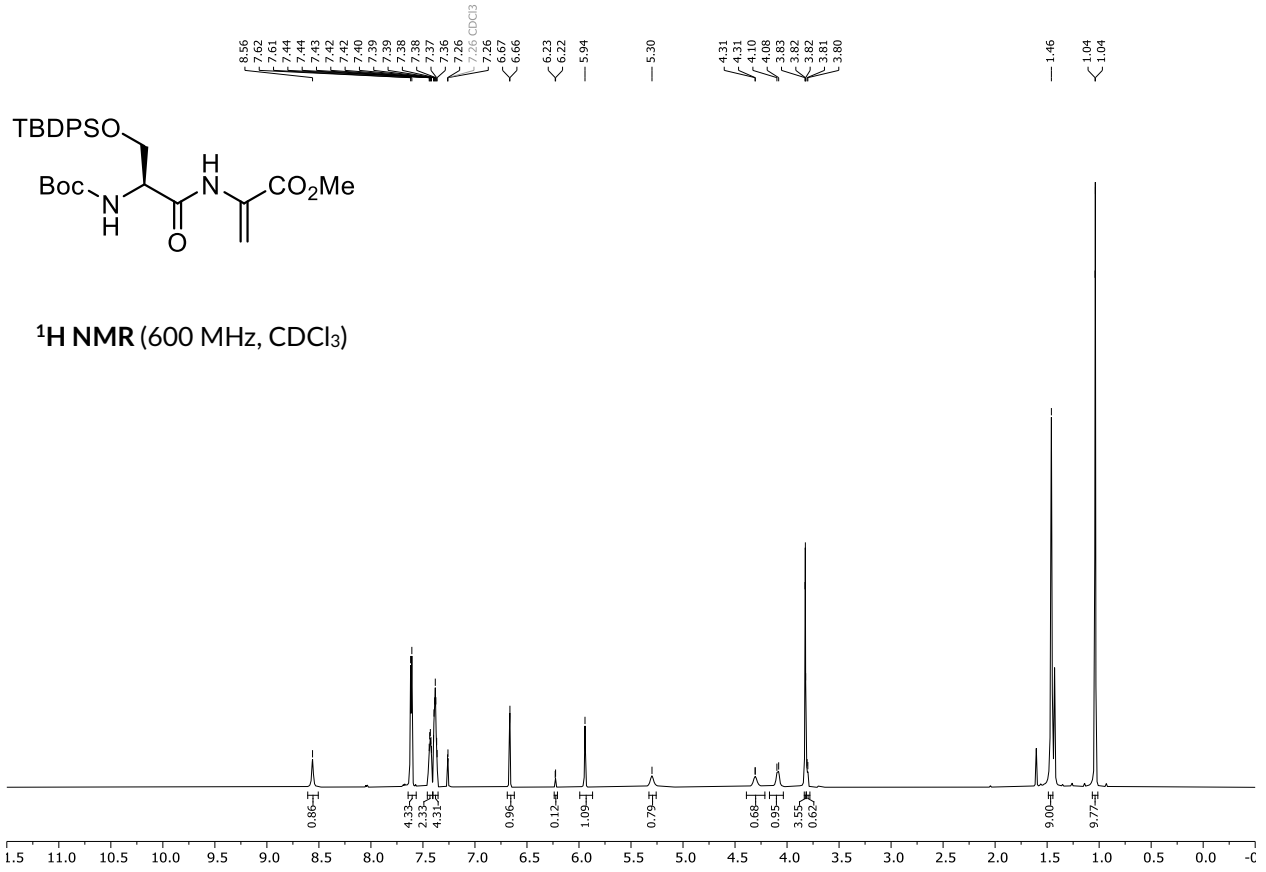


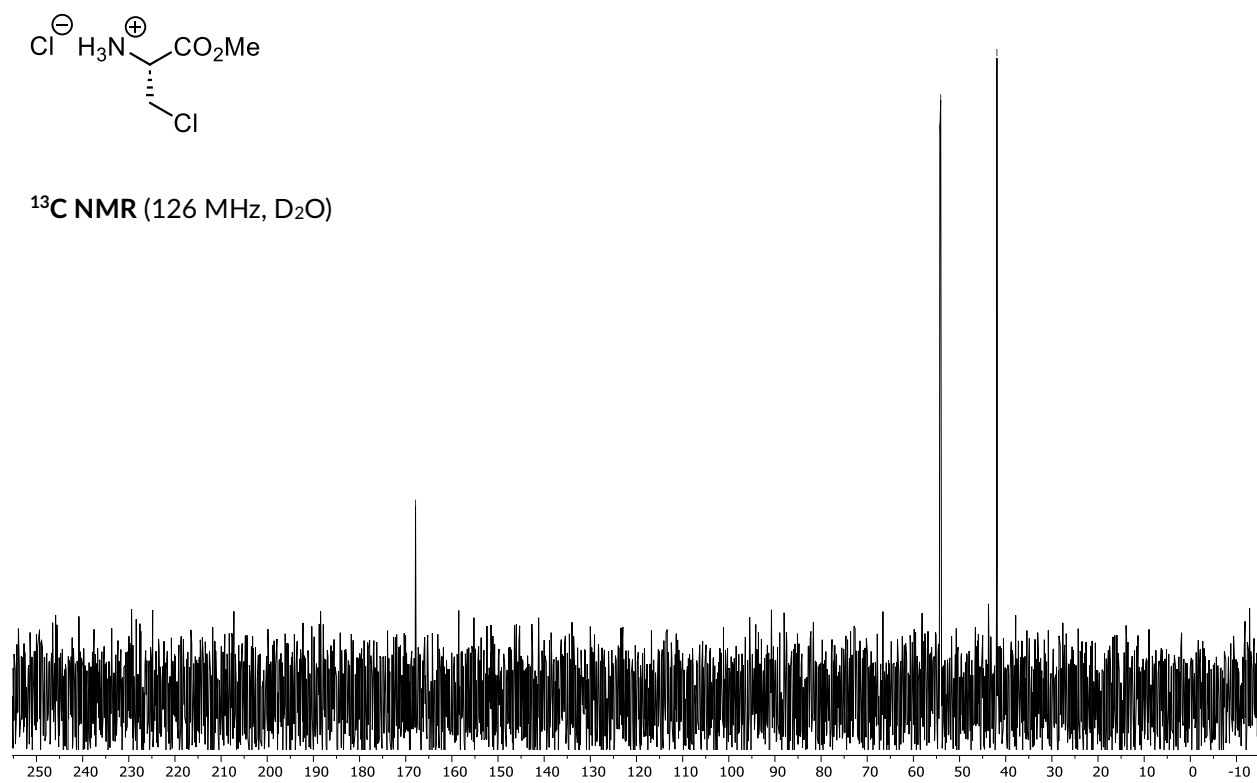
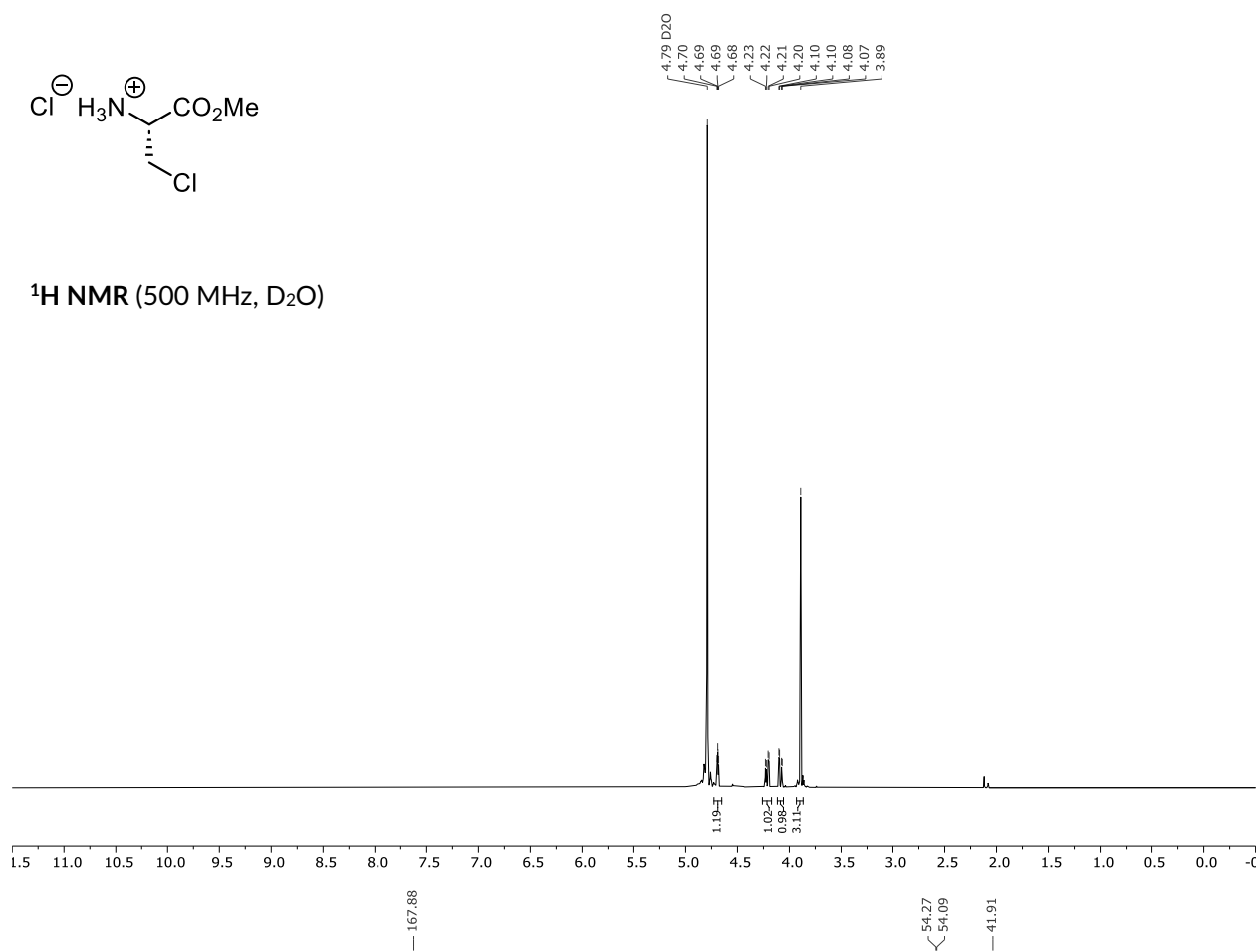


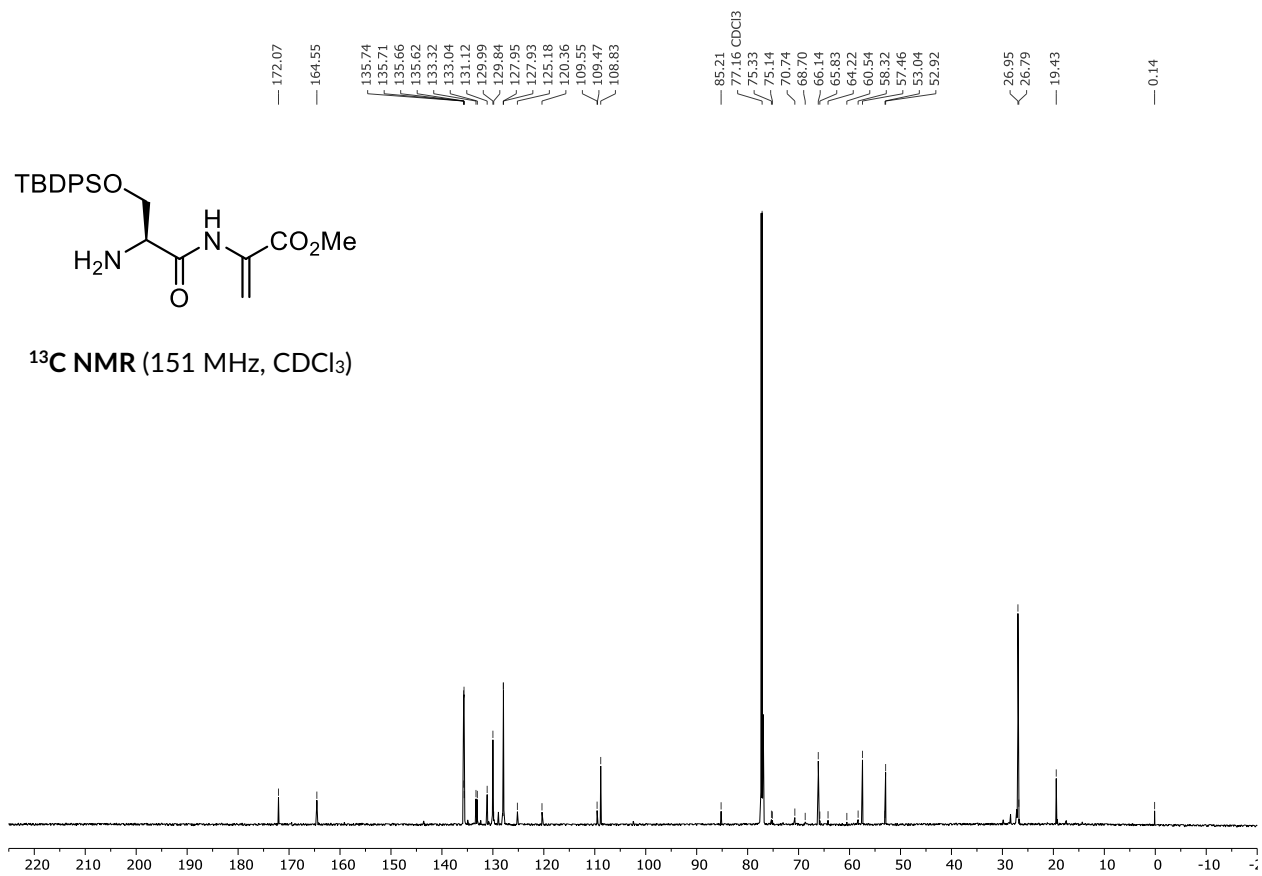
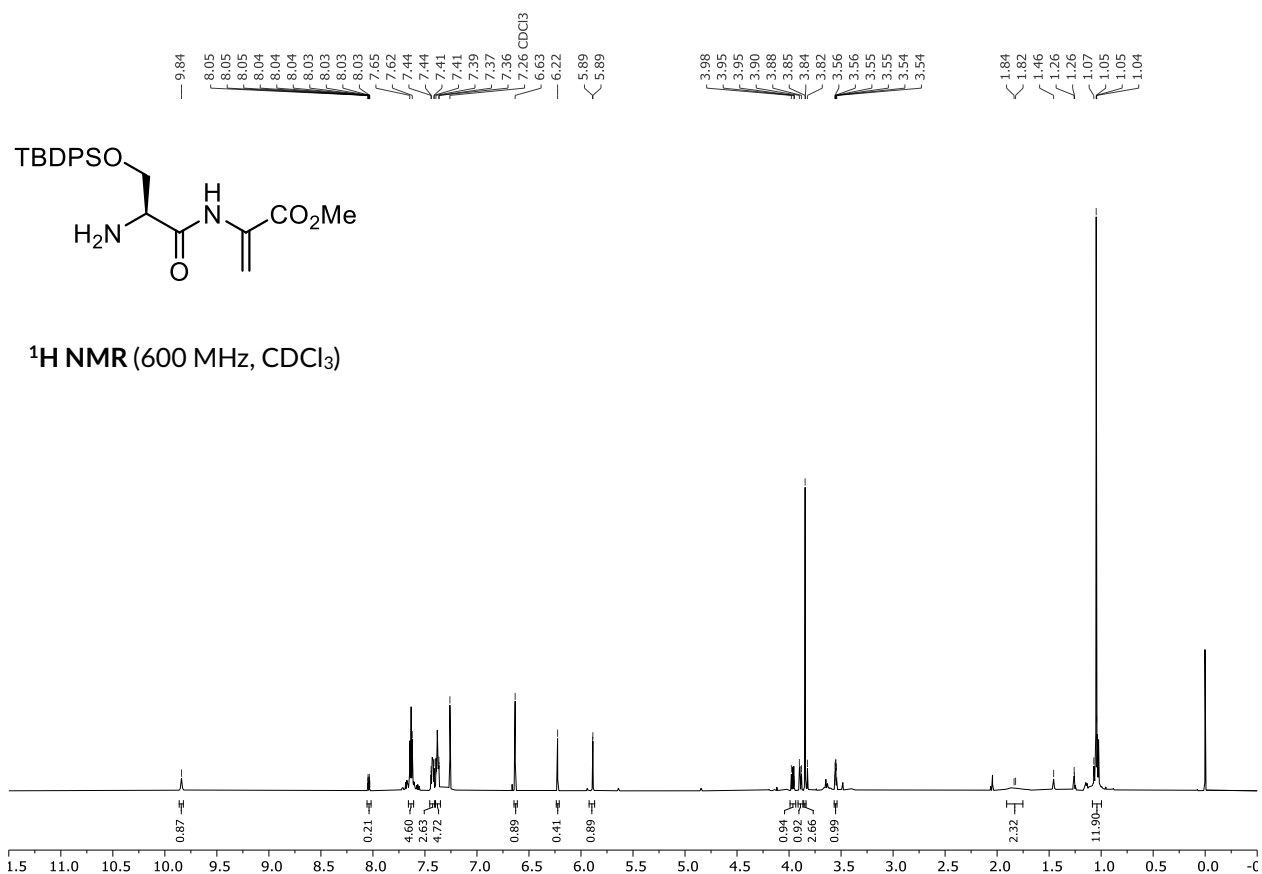


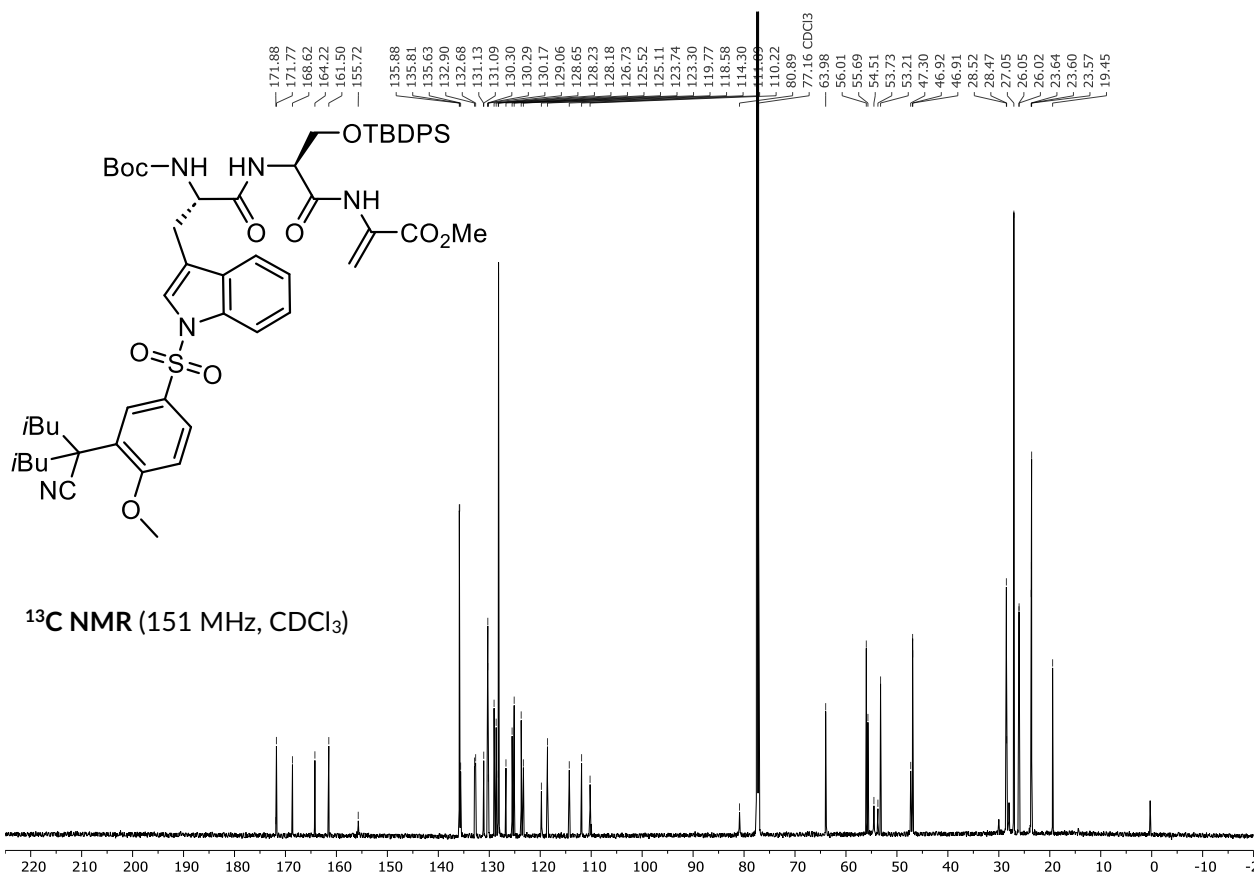
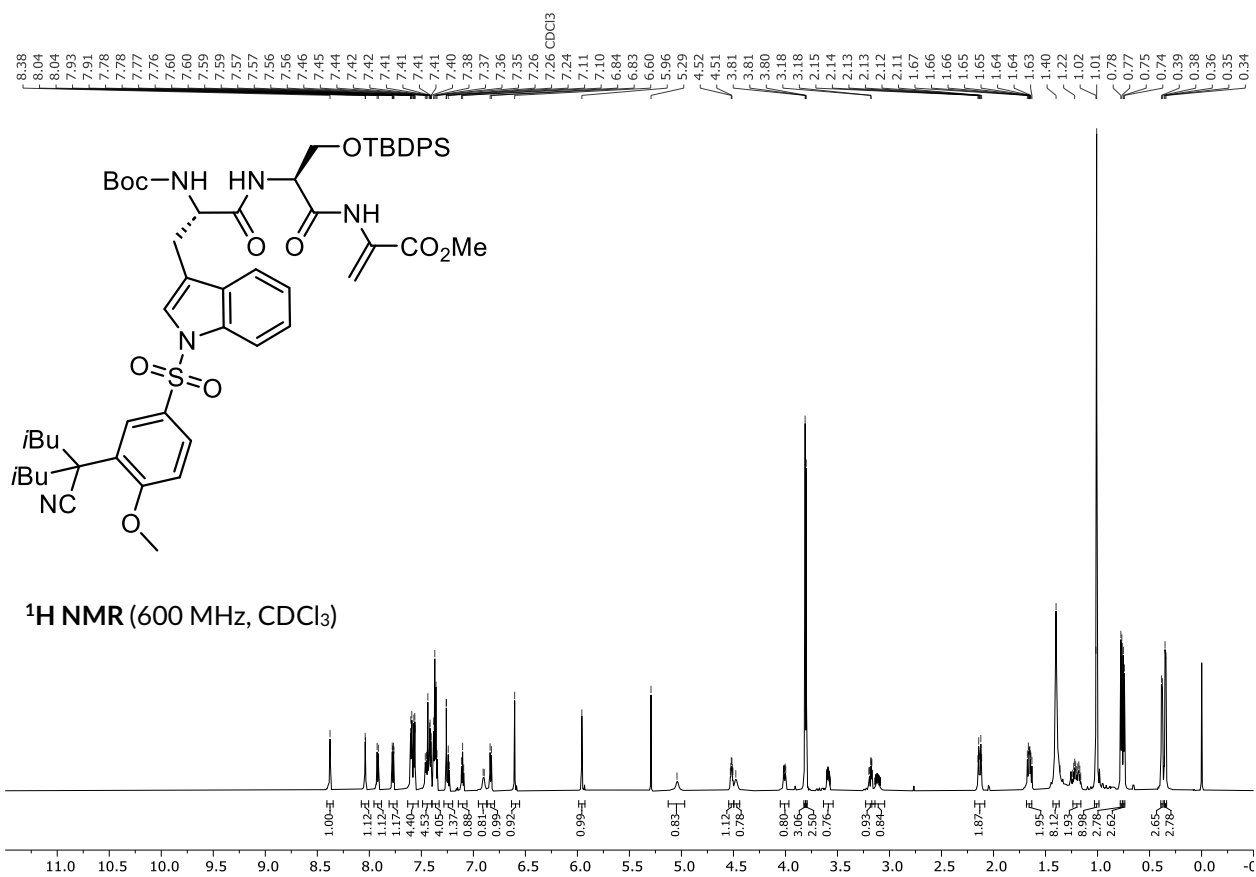




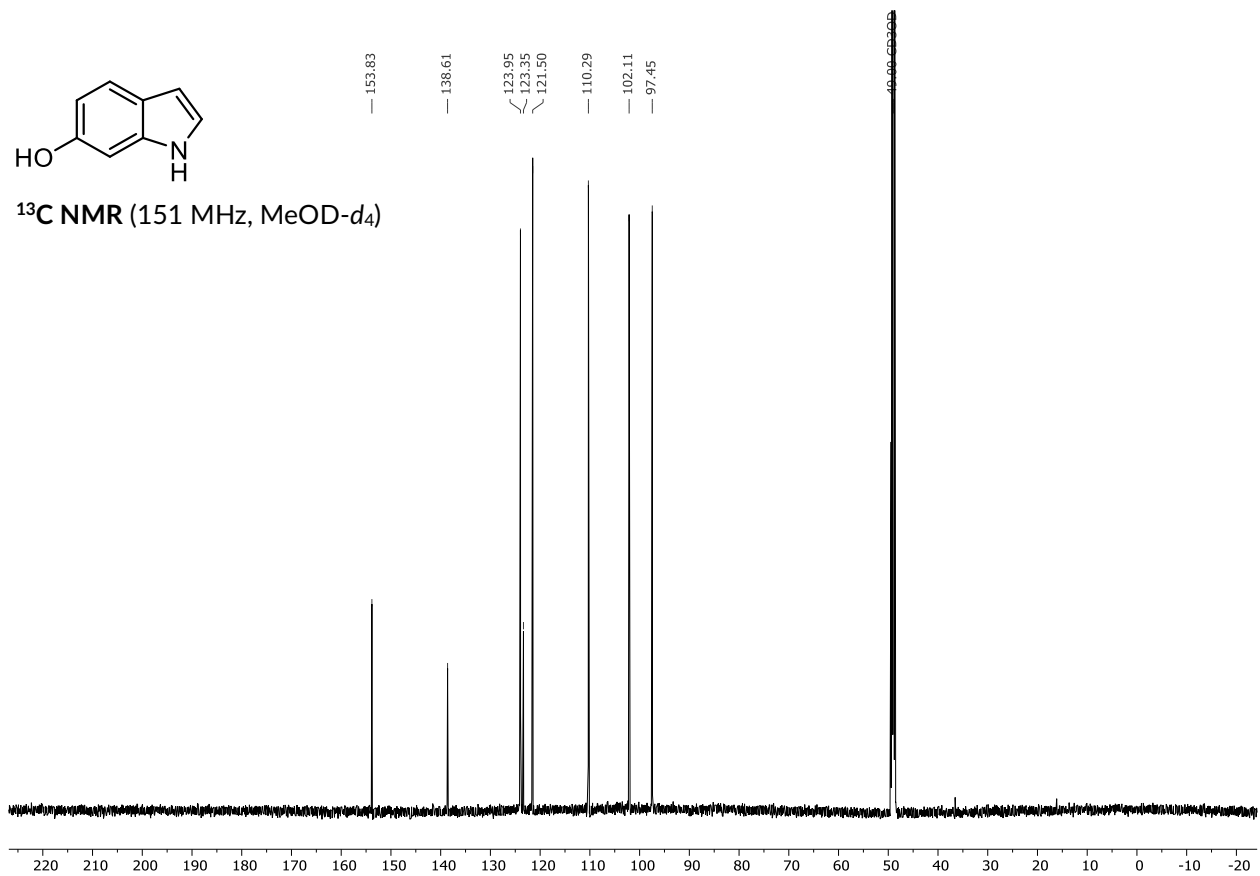
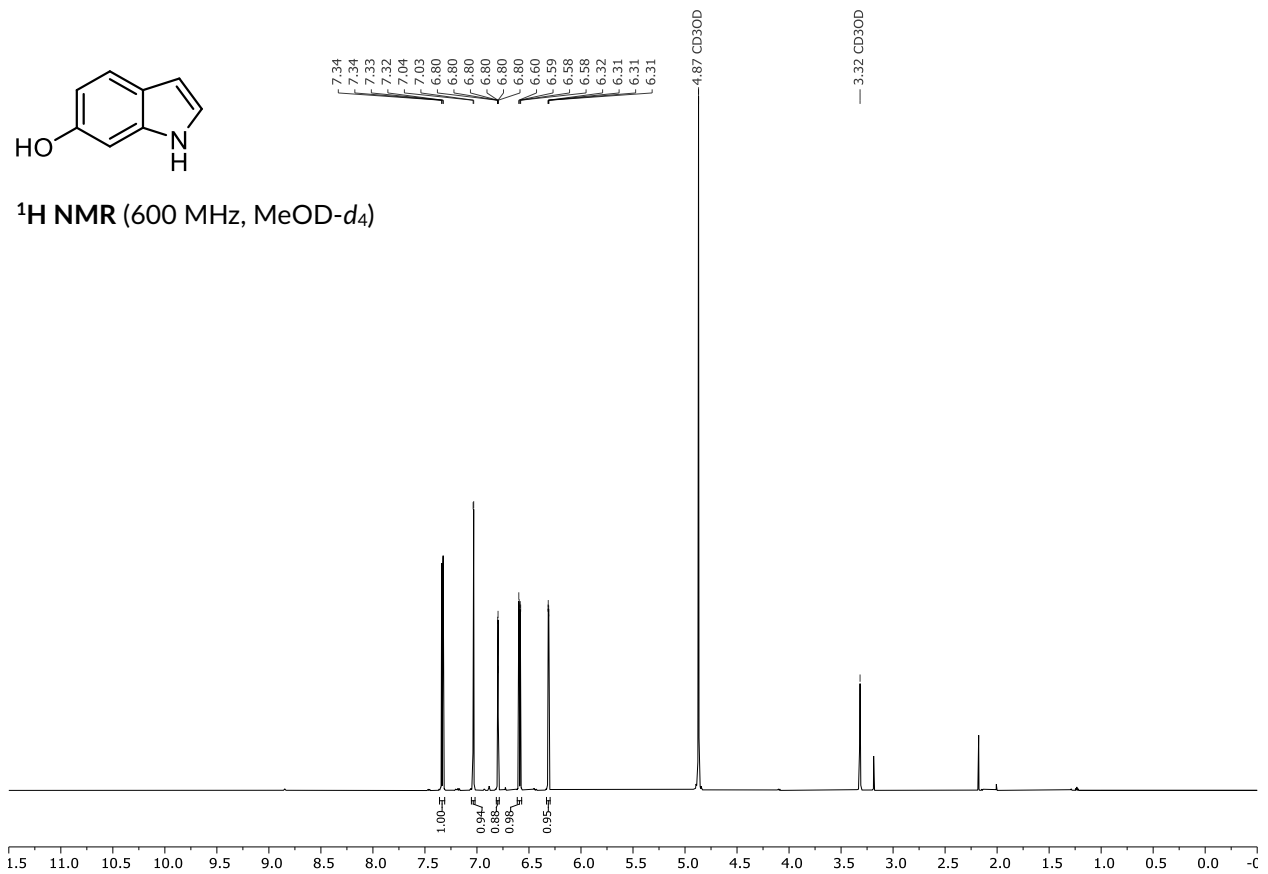


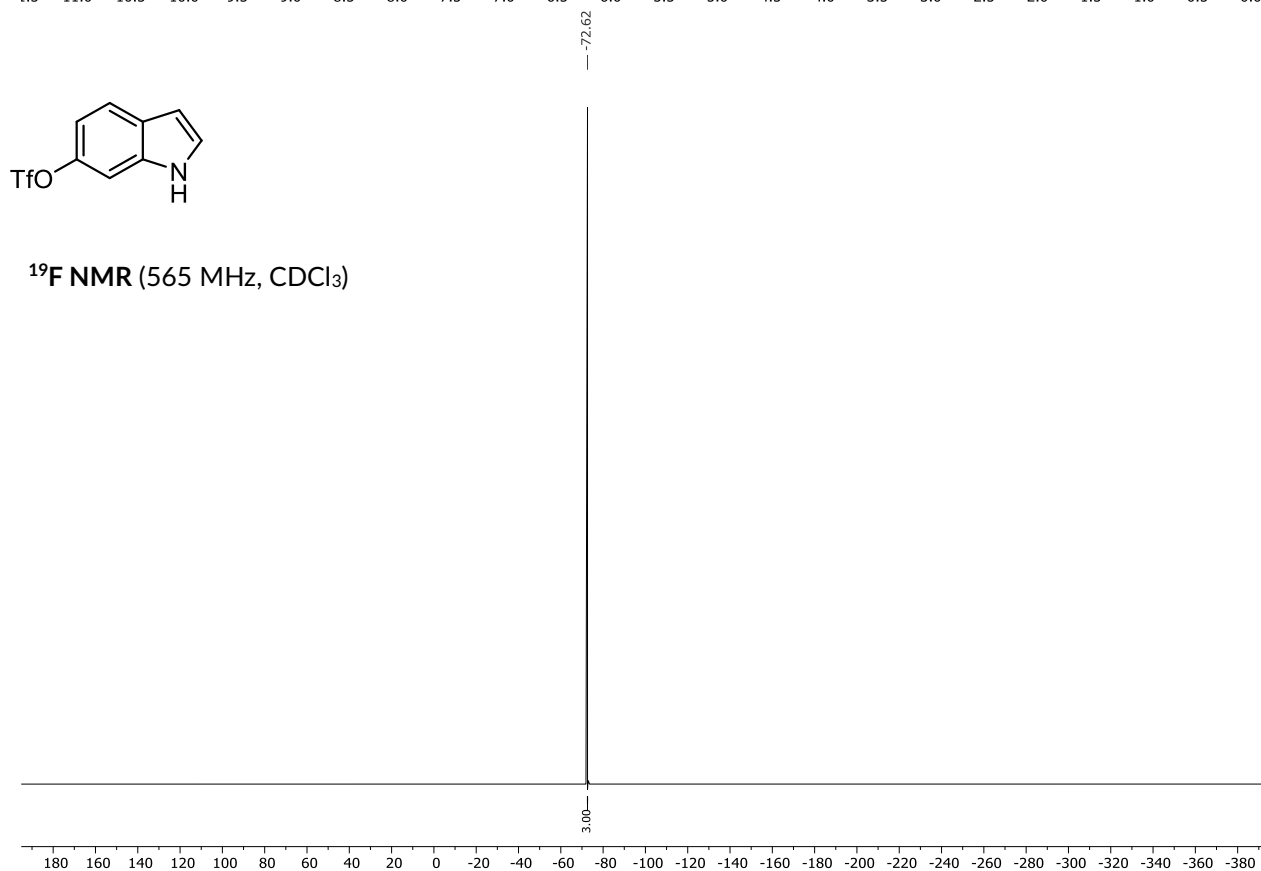
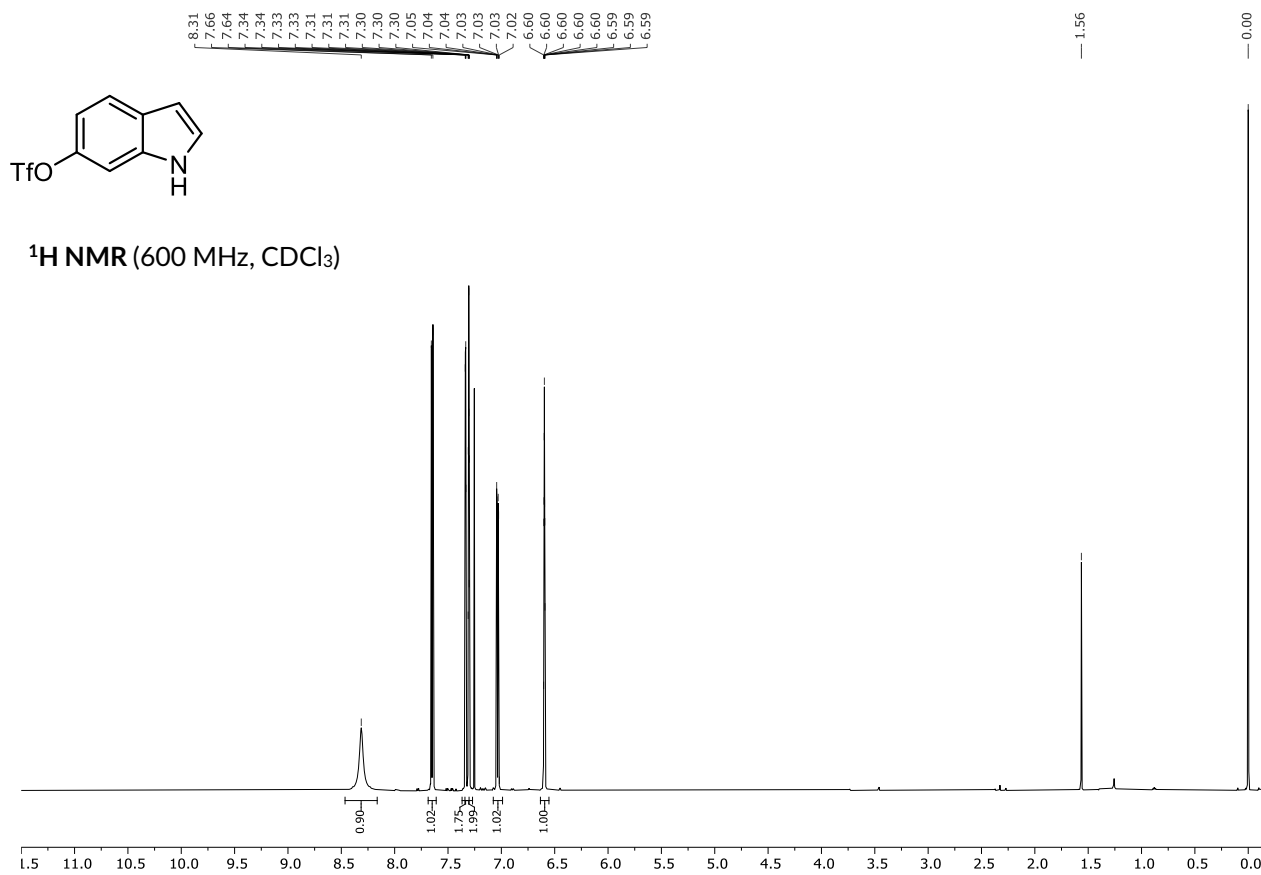


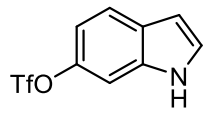




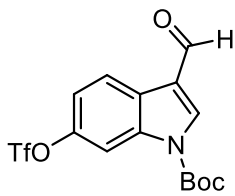
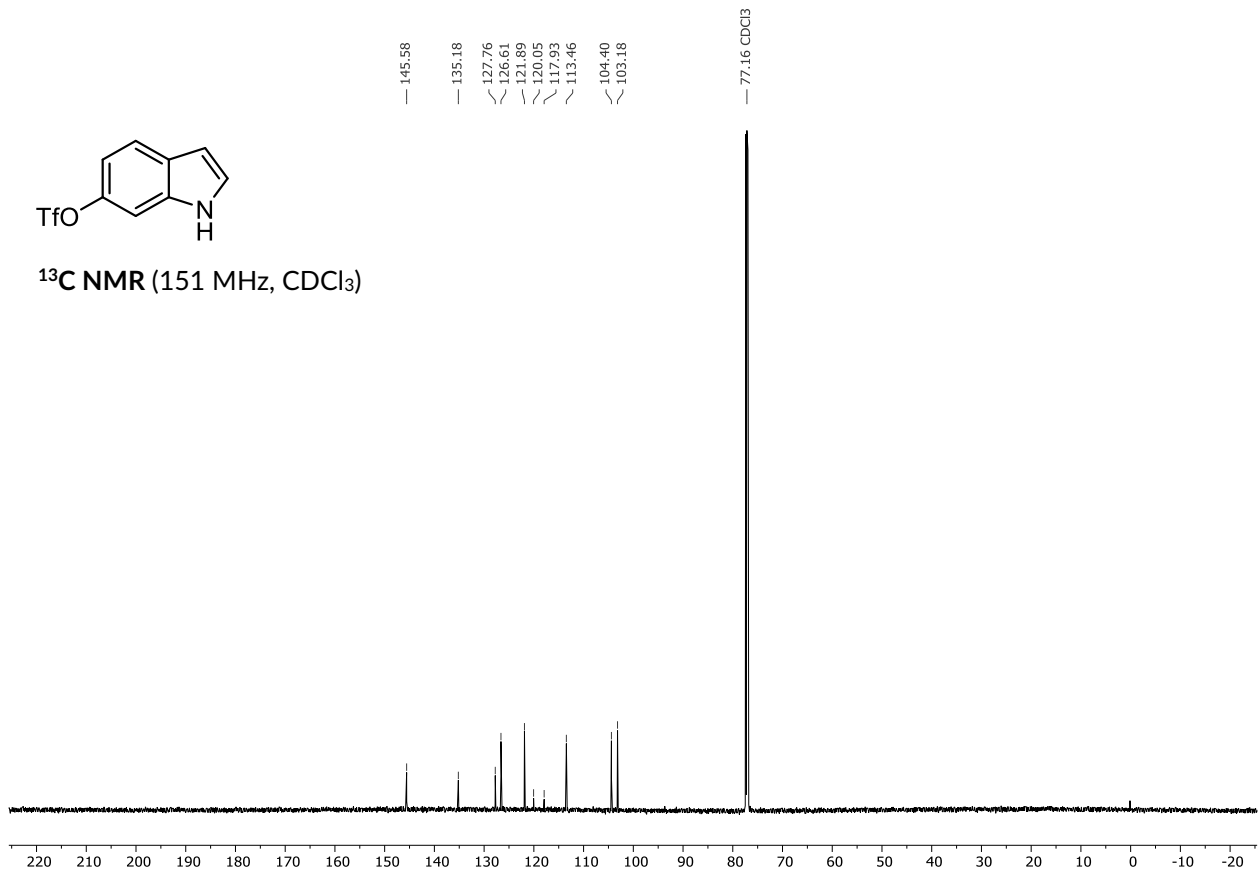
7.2.2. Synthesis of a 6-Triflyl Tryptophan



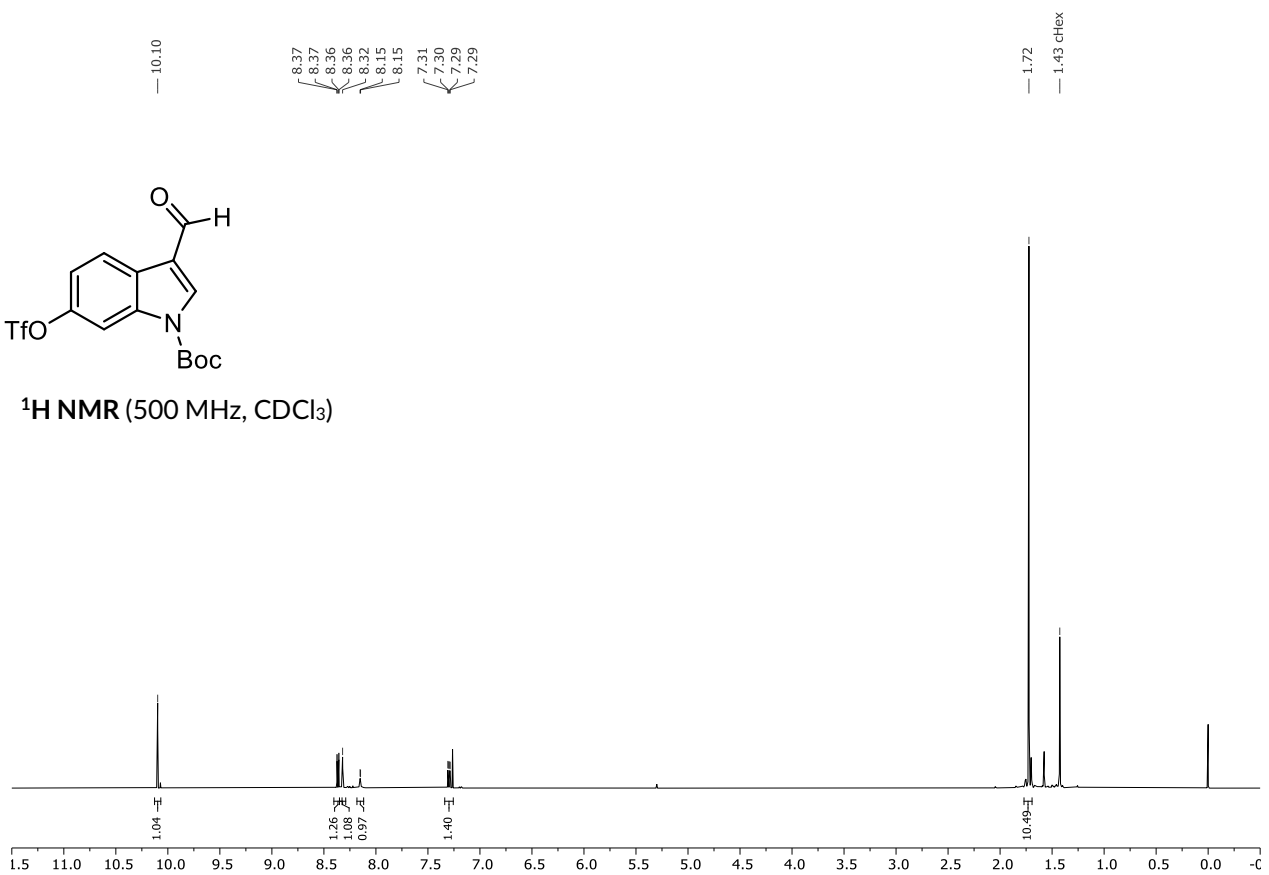


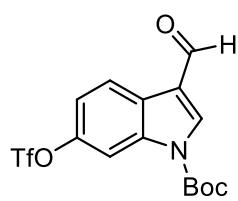
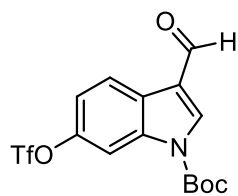
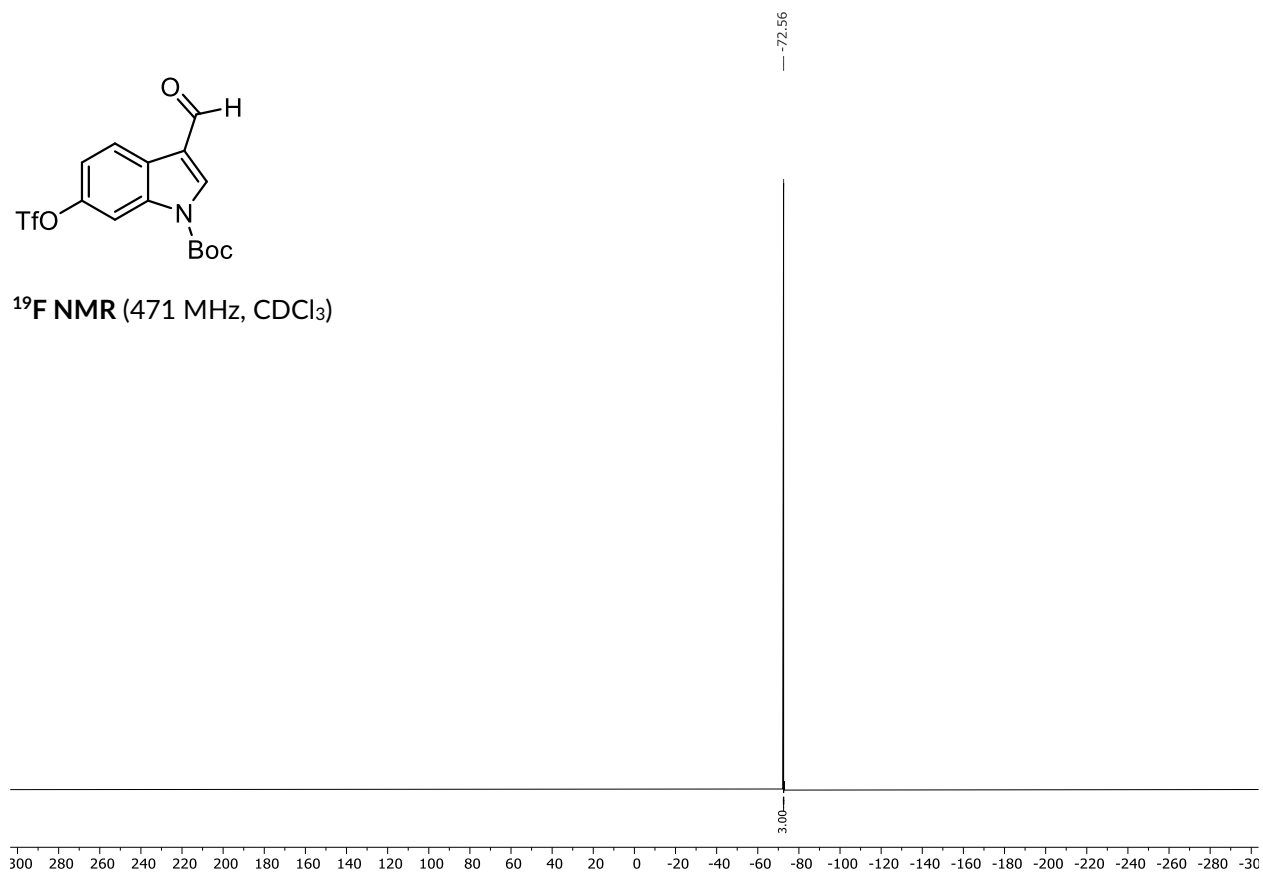
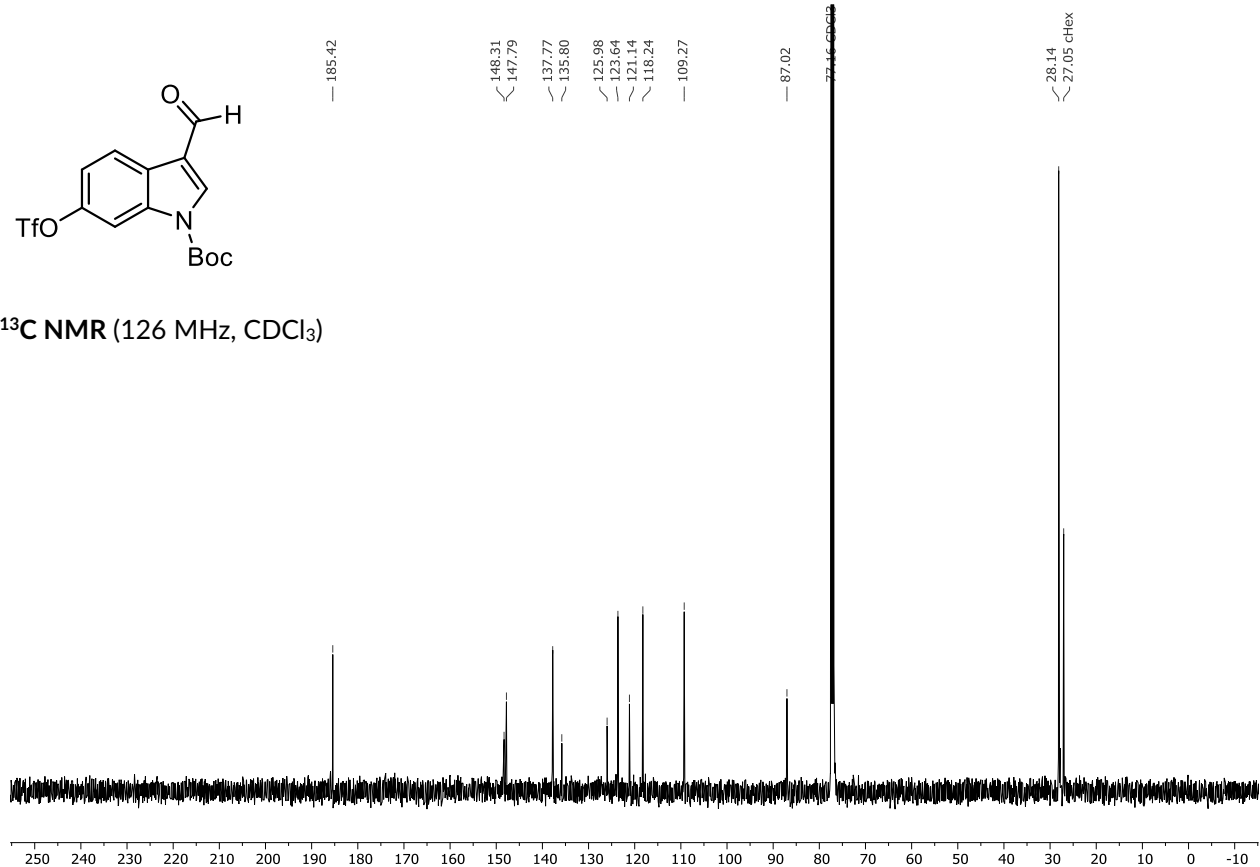


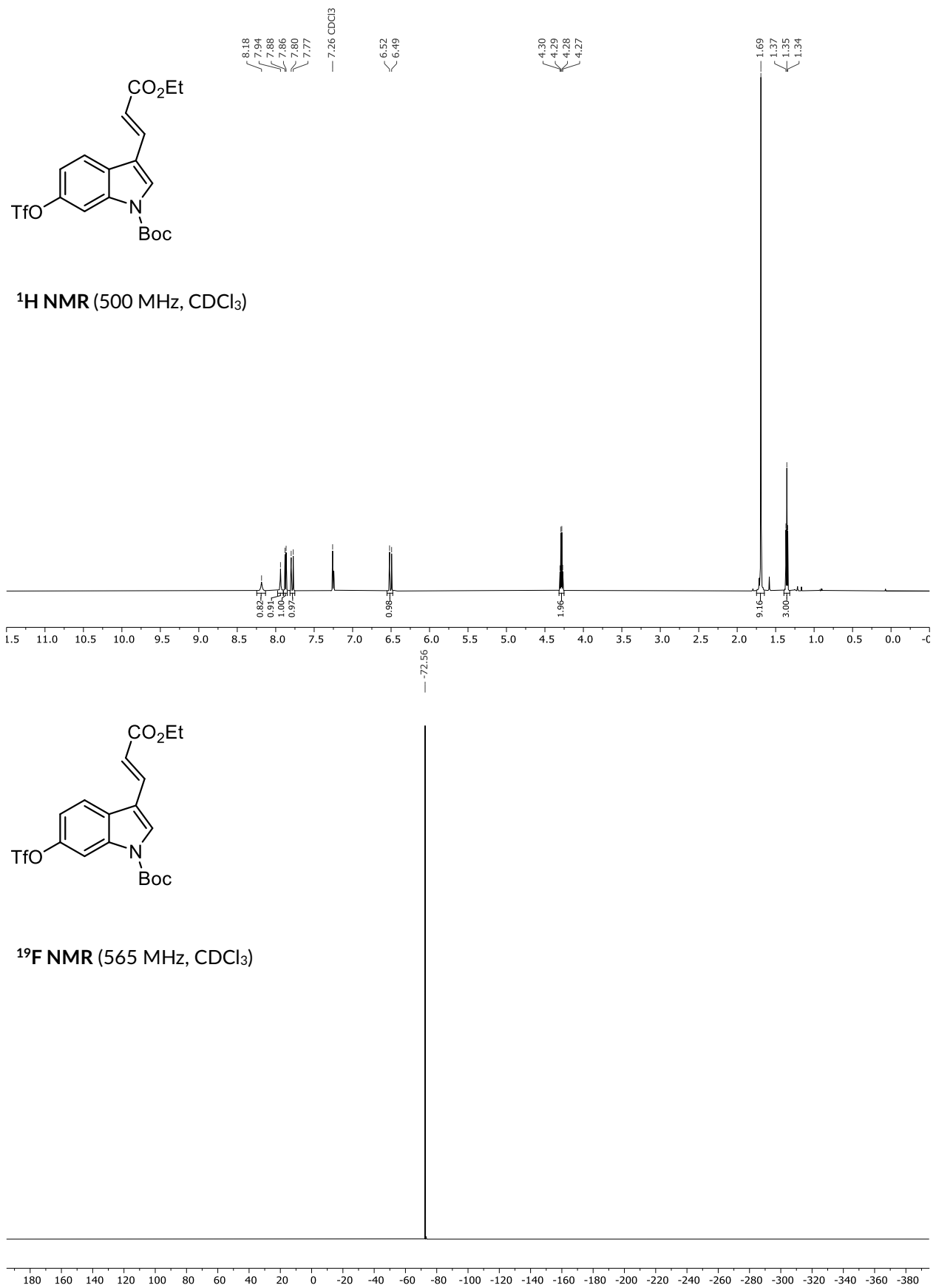
^{13}C NMR (151 MHz, CDCl_3)

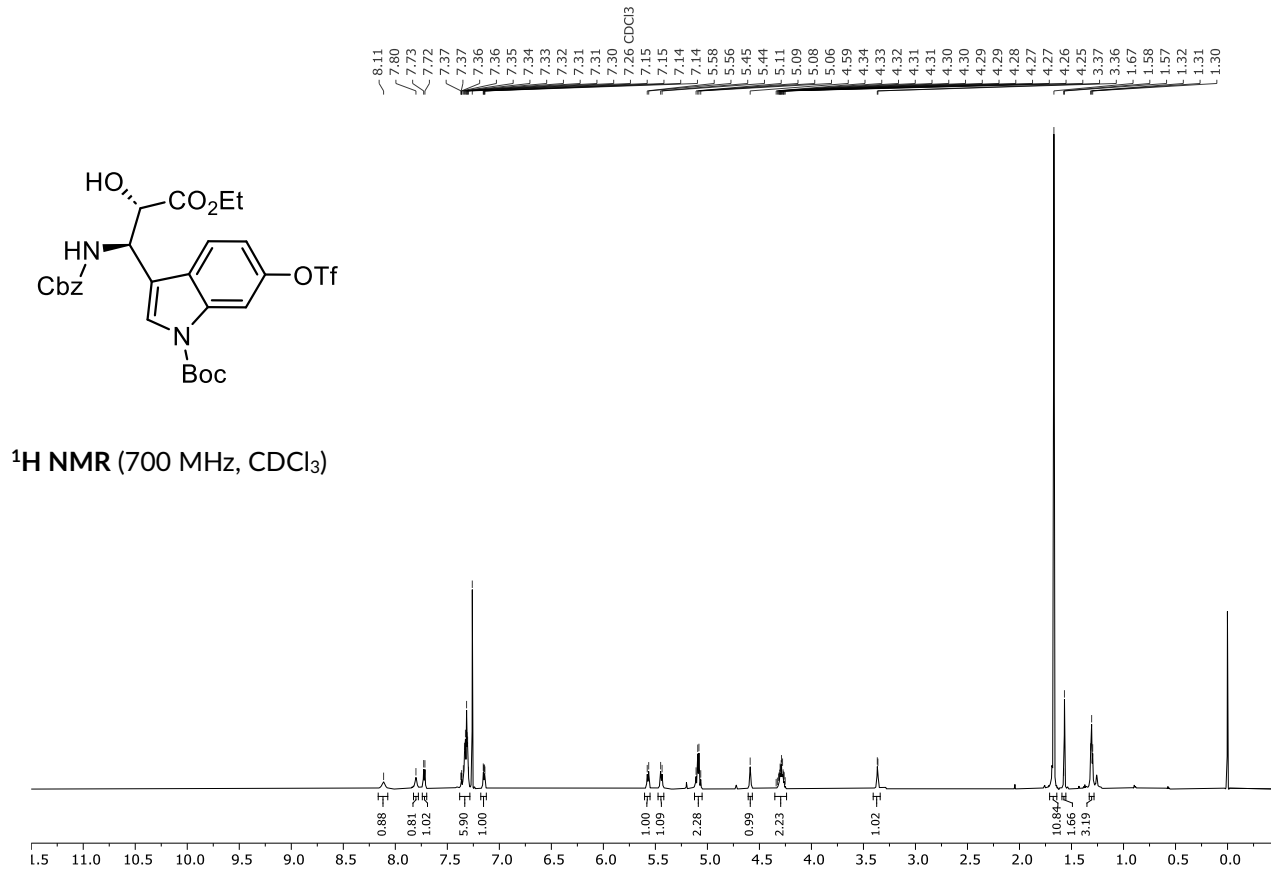
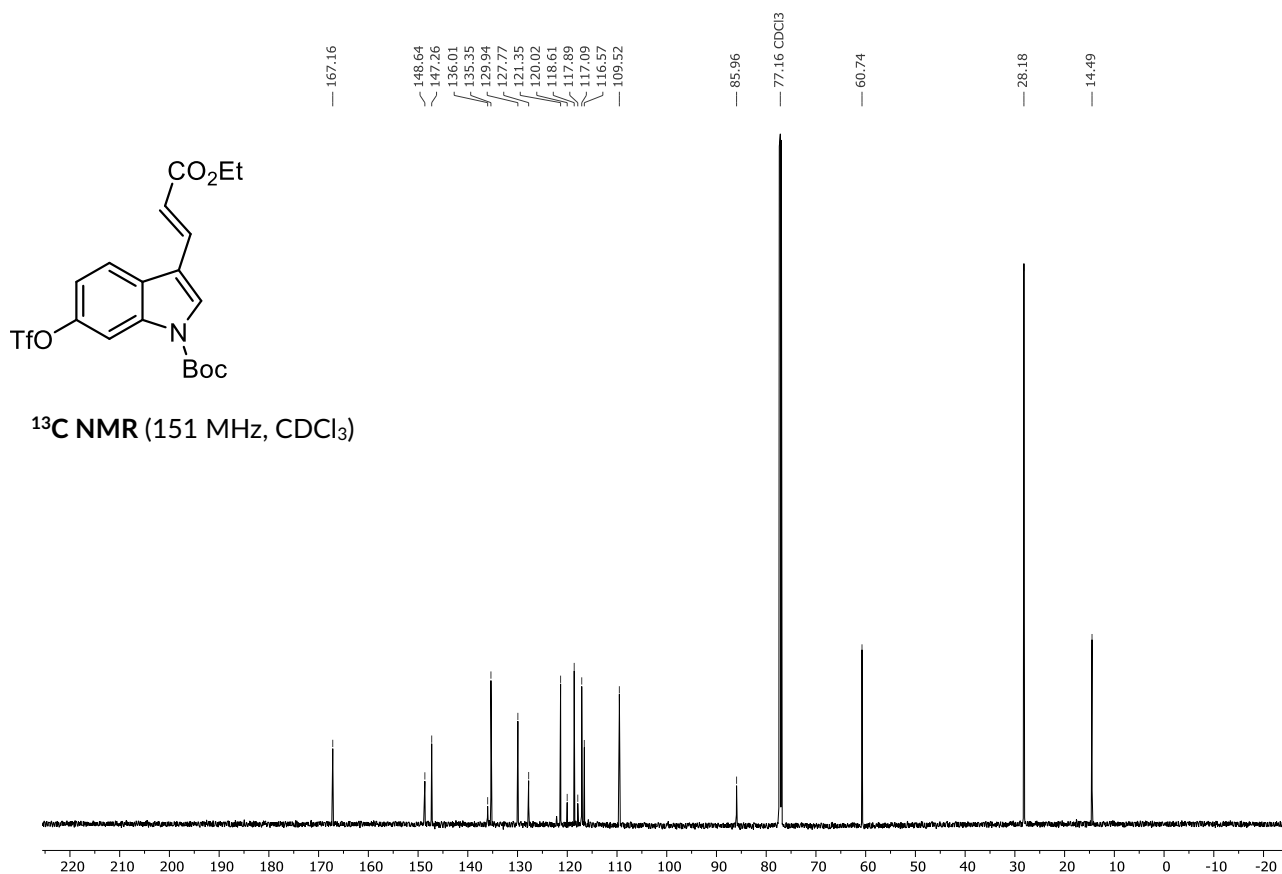


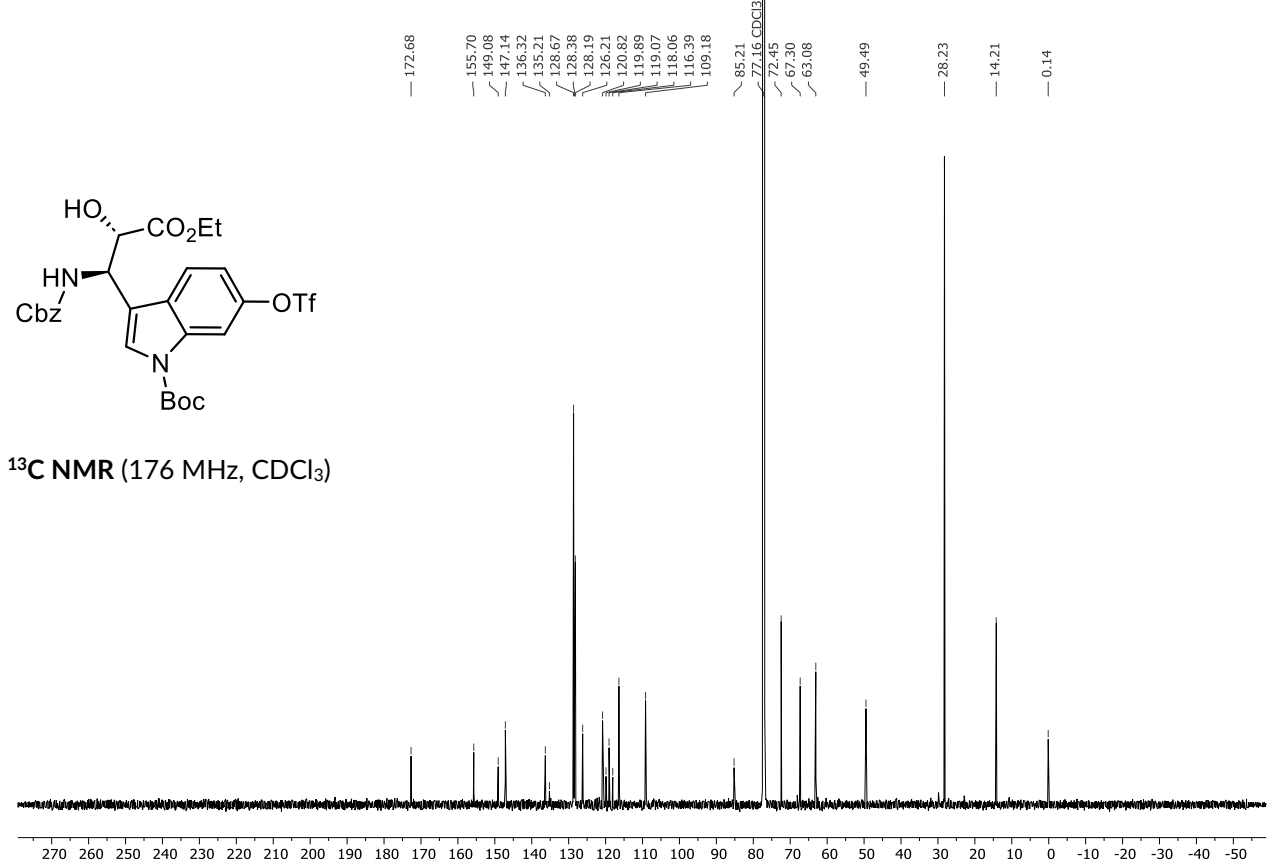
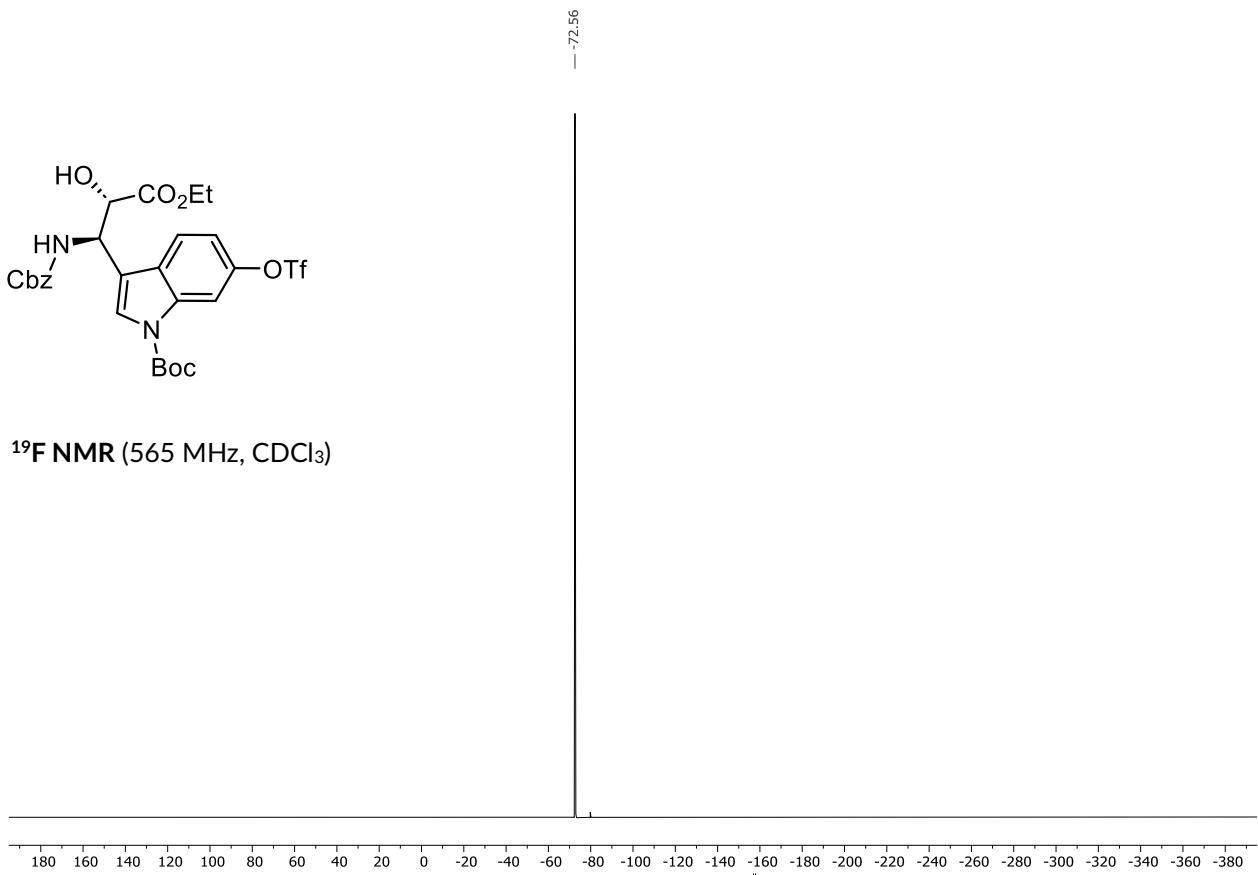
^1H NMR (500 MHz, CDCl_3)

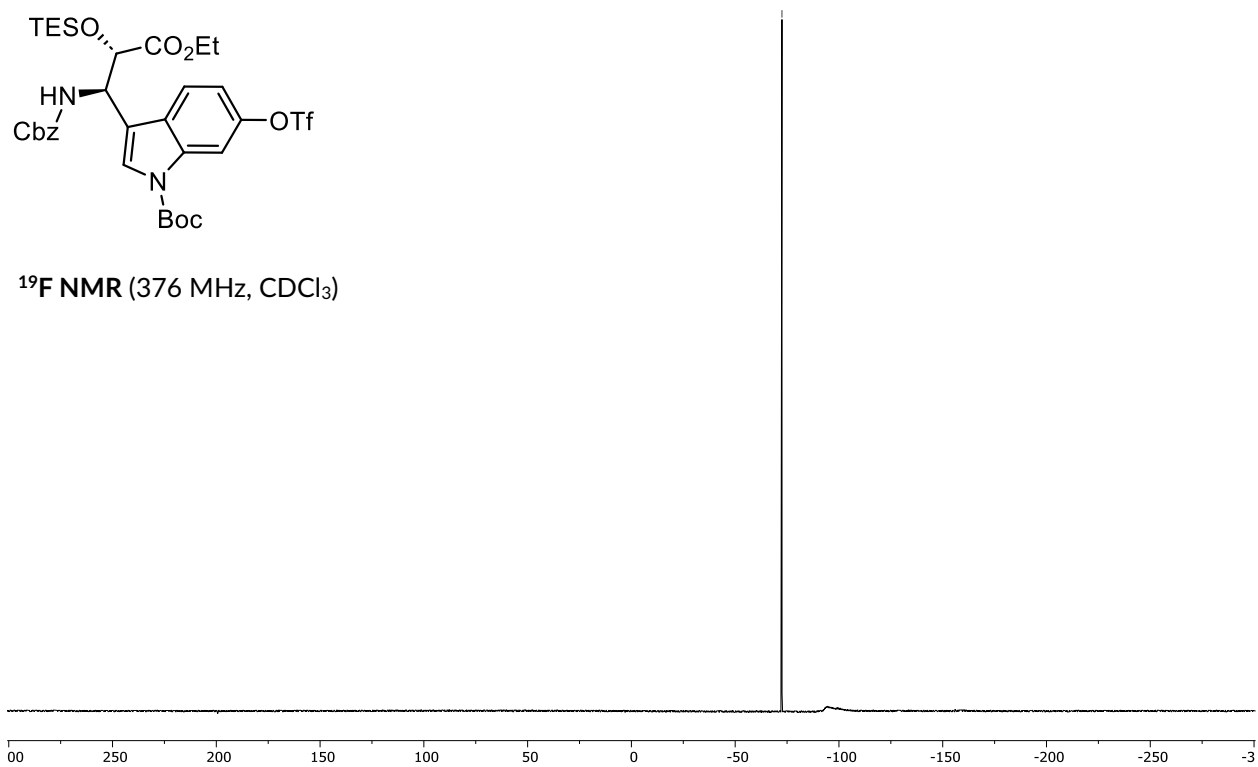
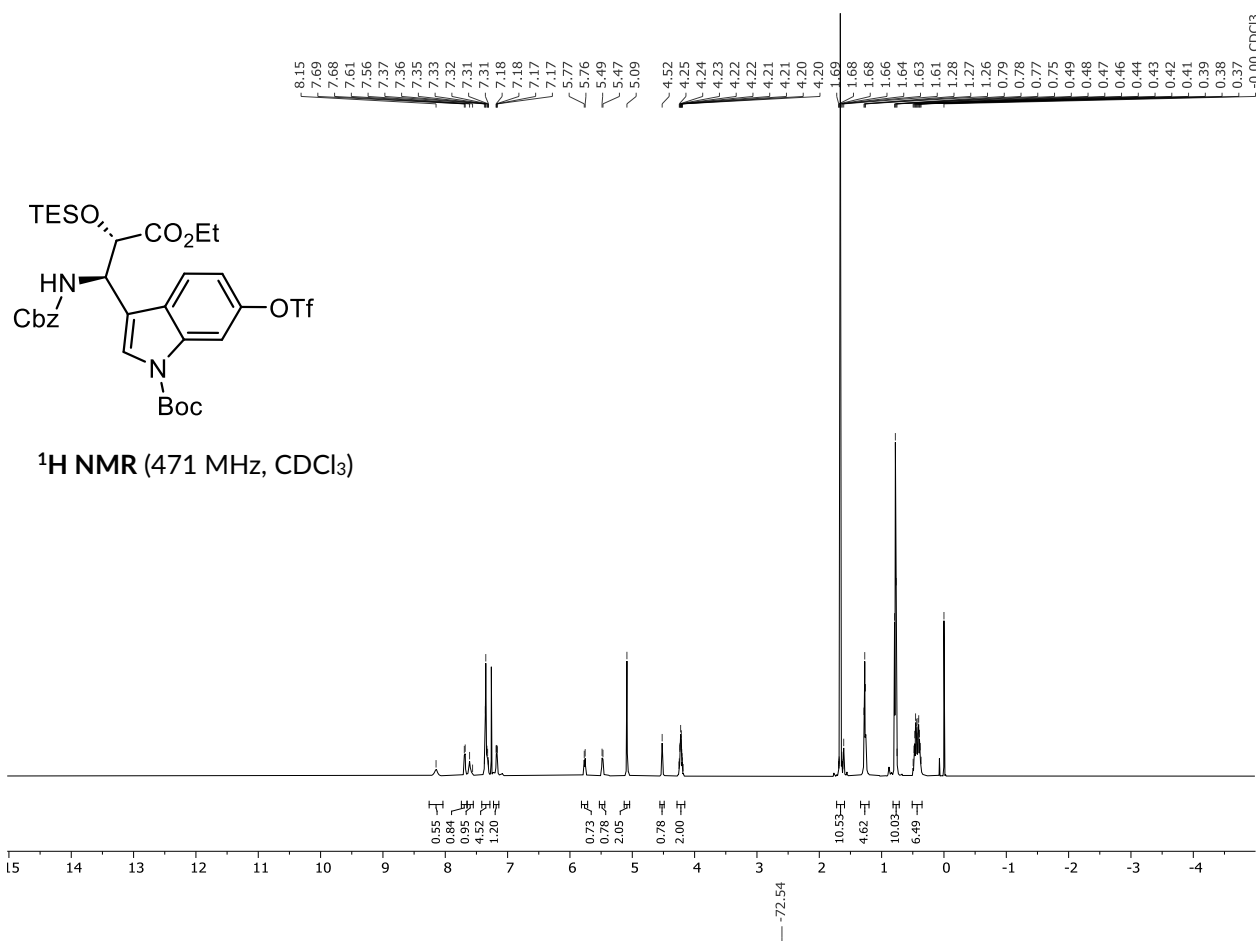


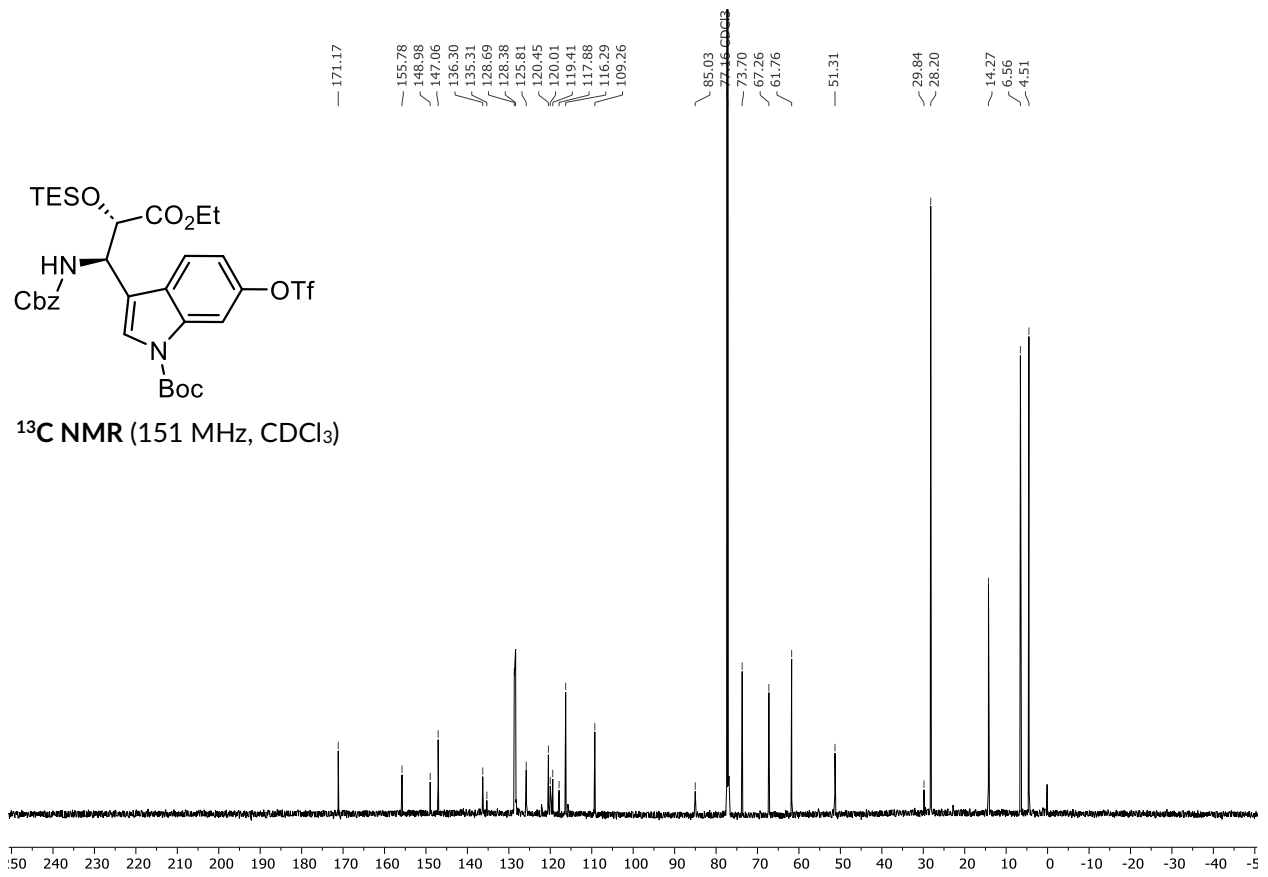
 ^{19}F NMR (471 MHz, CDCl_3) ^{13}C NMR (126 MHz, CDCl_3)



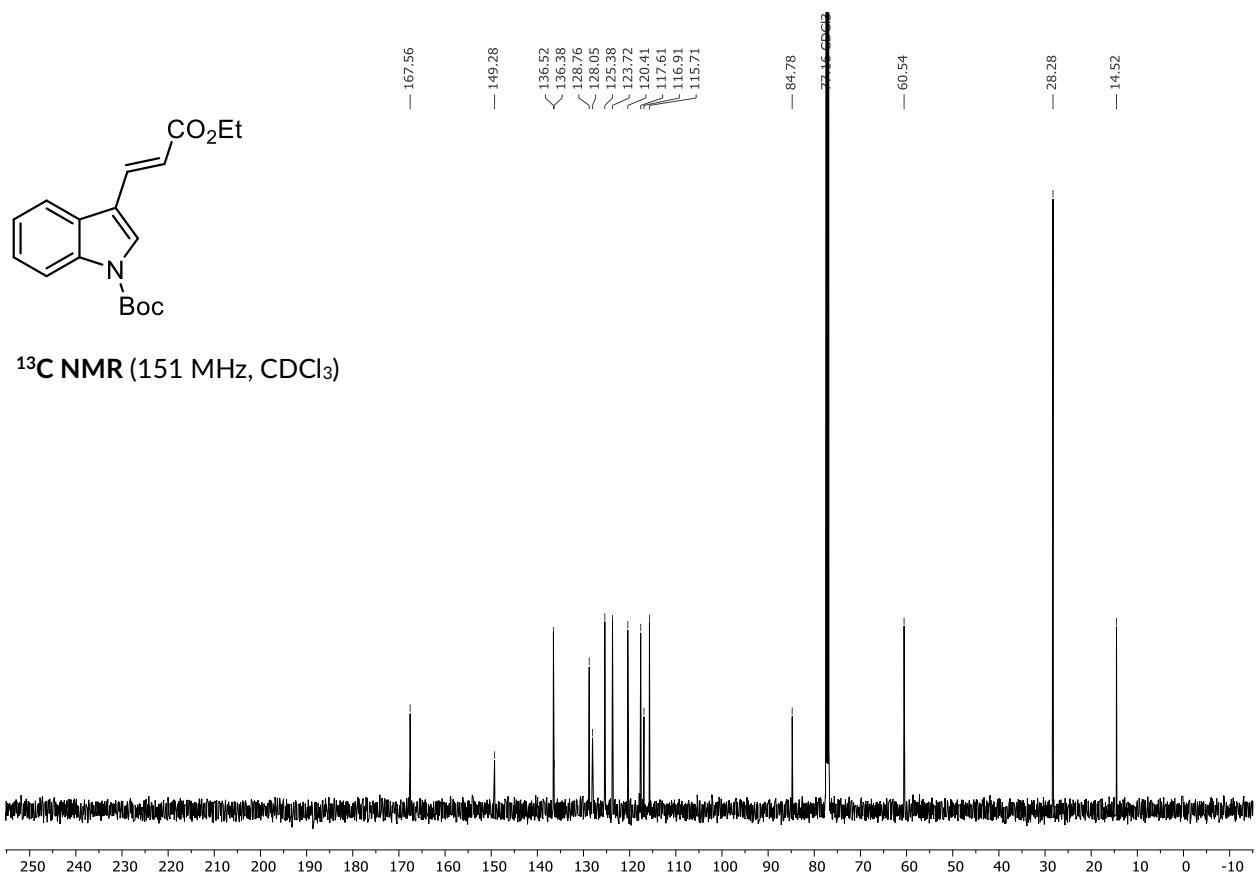
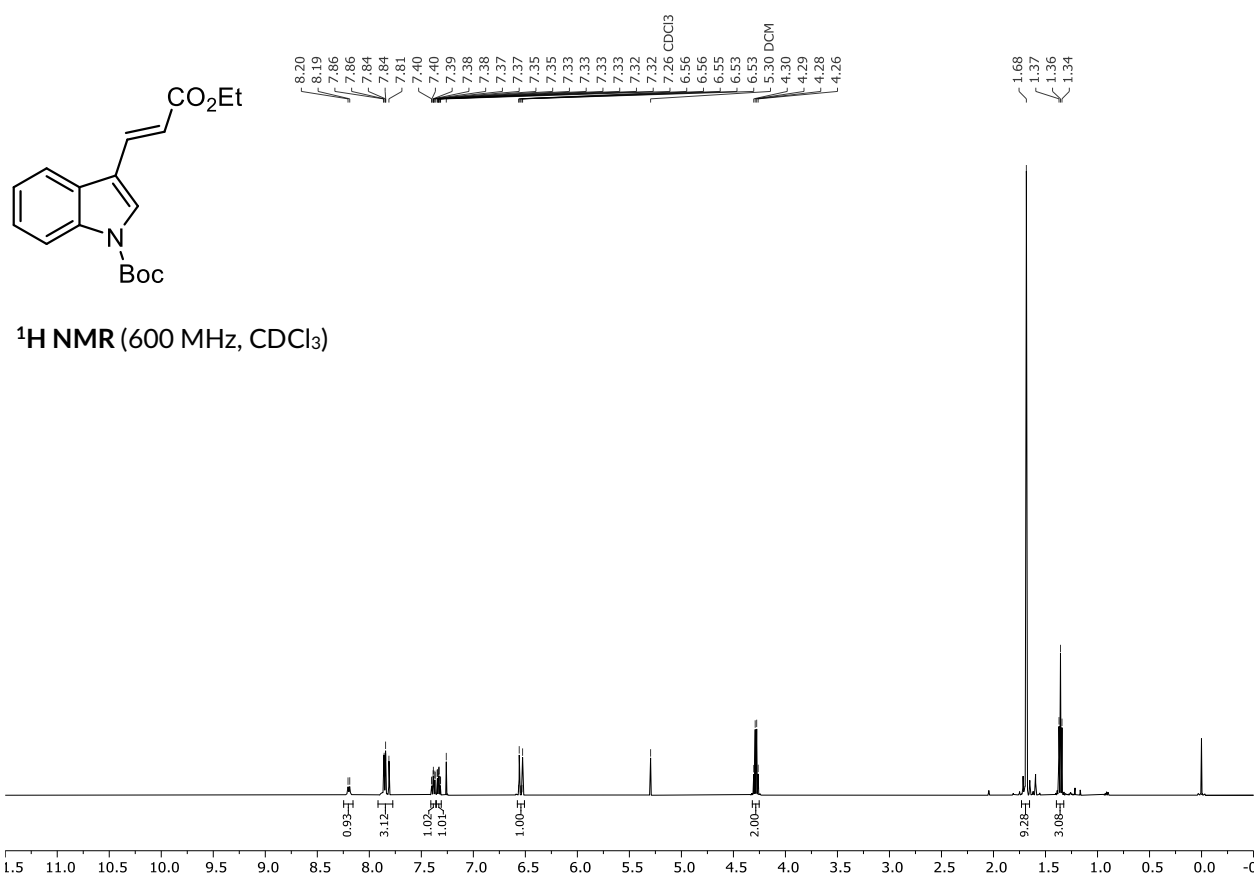


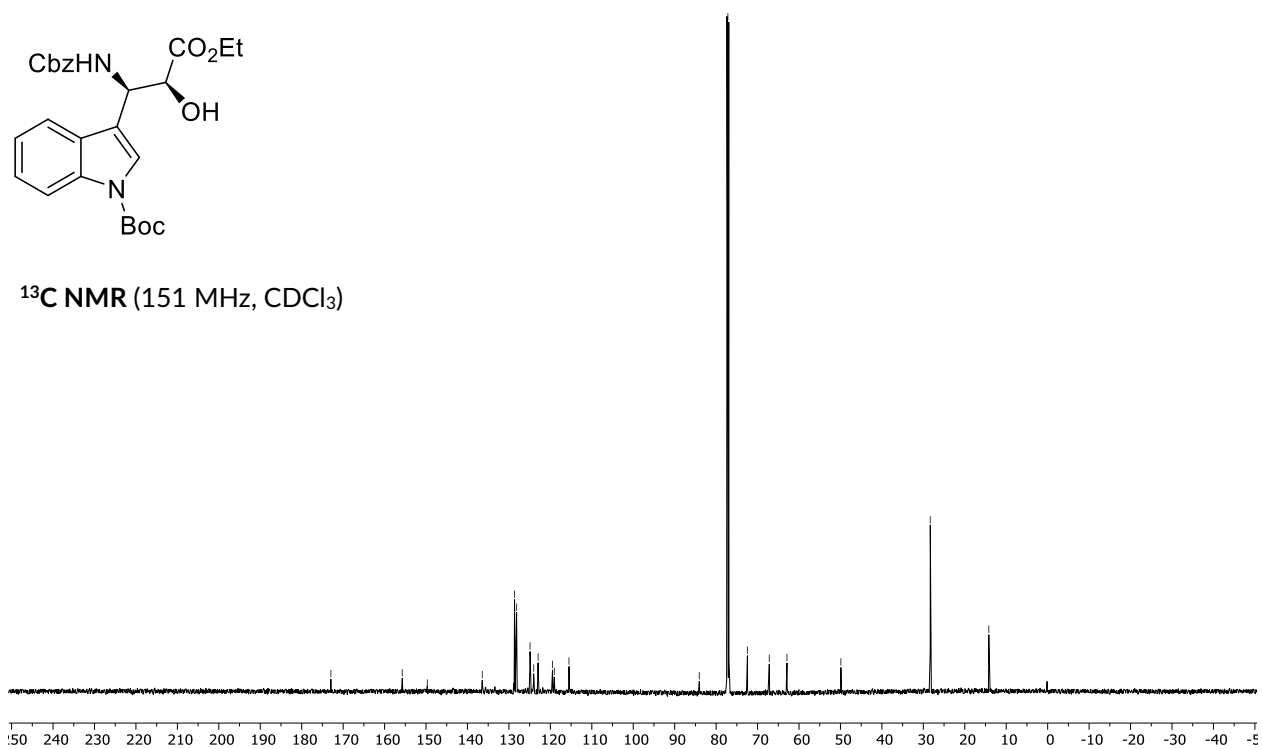
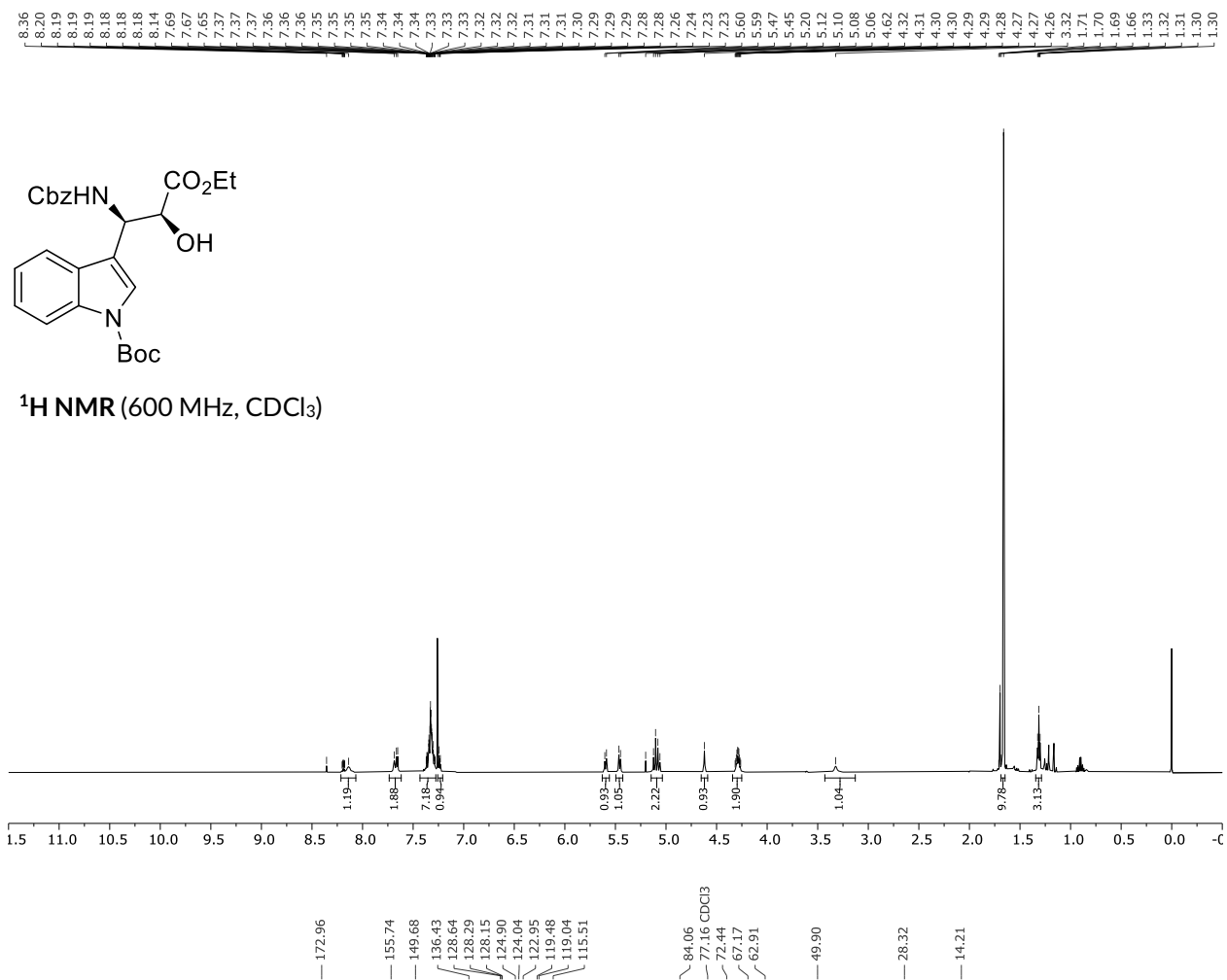


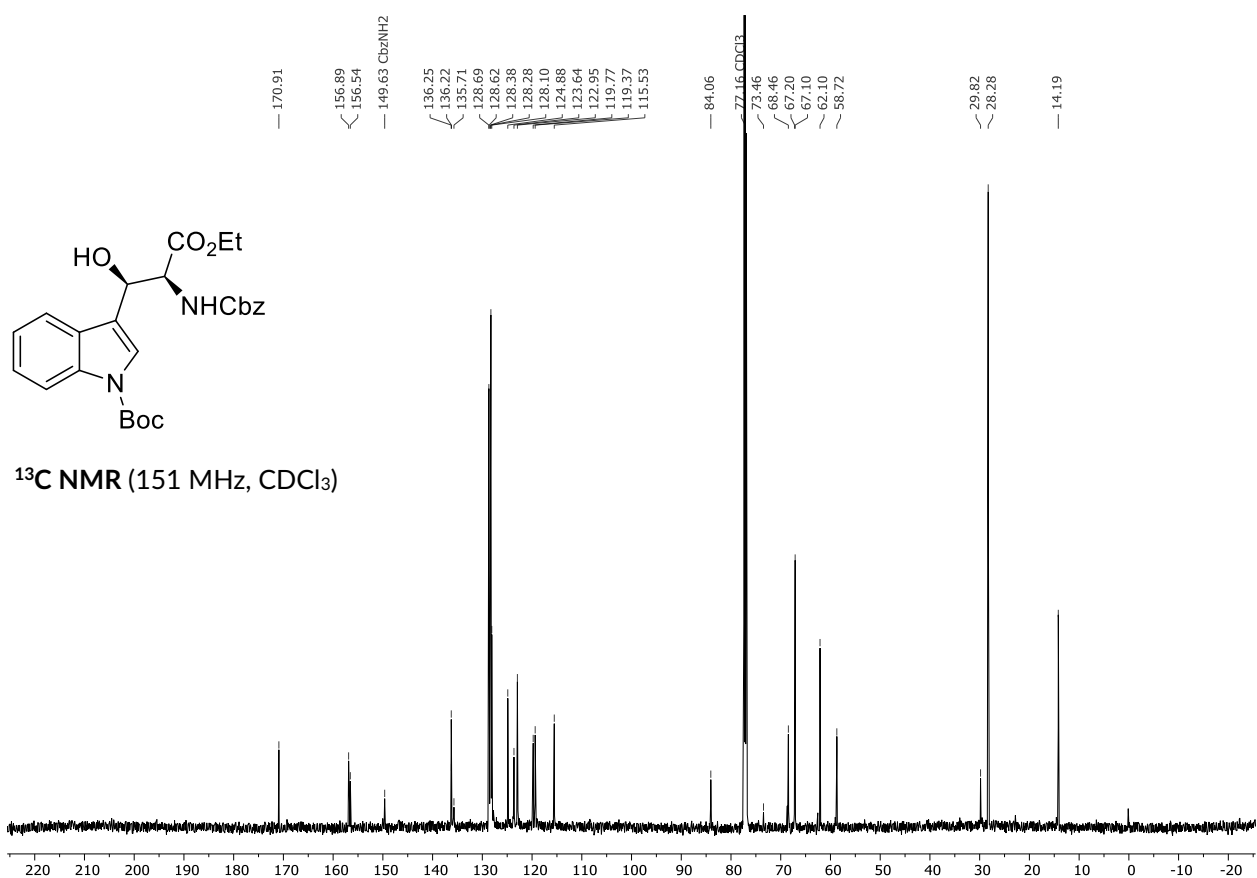
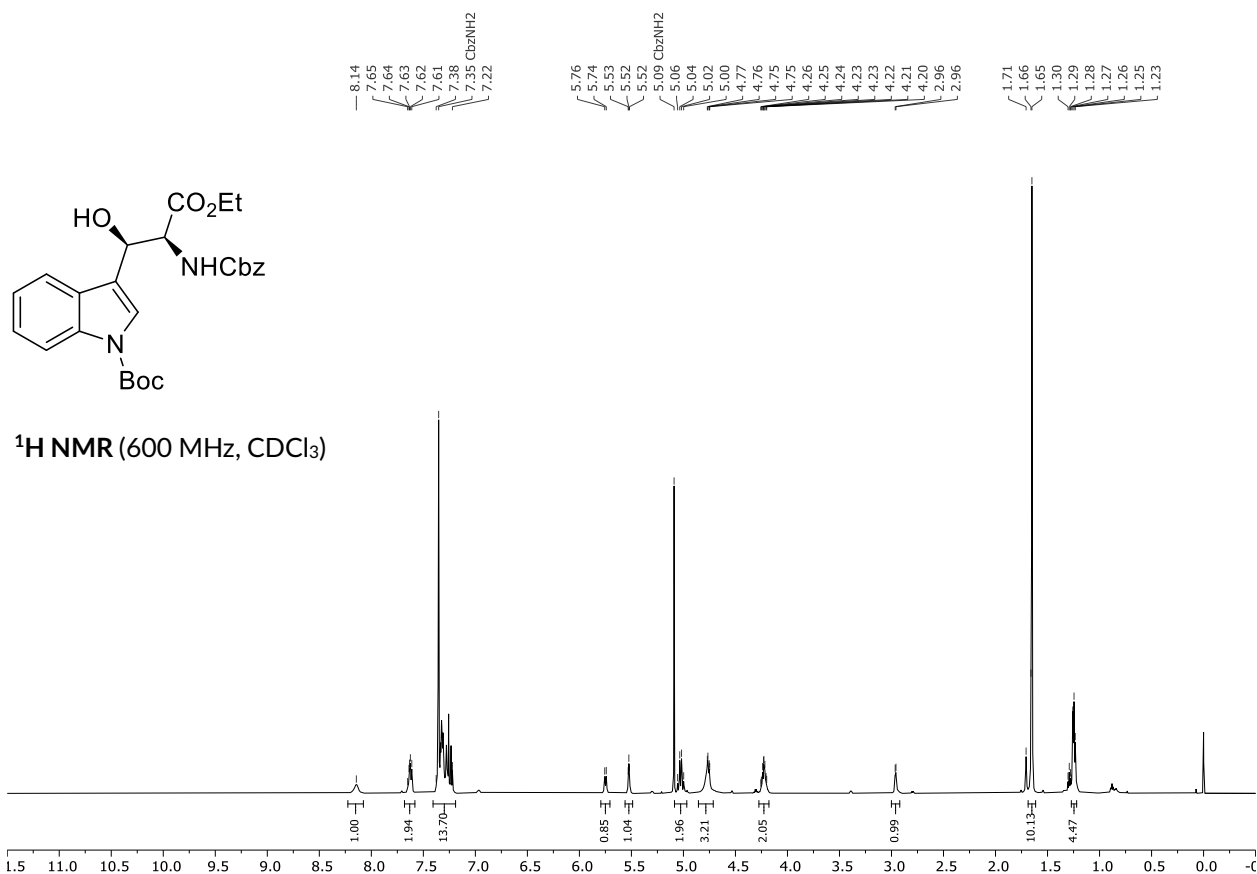


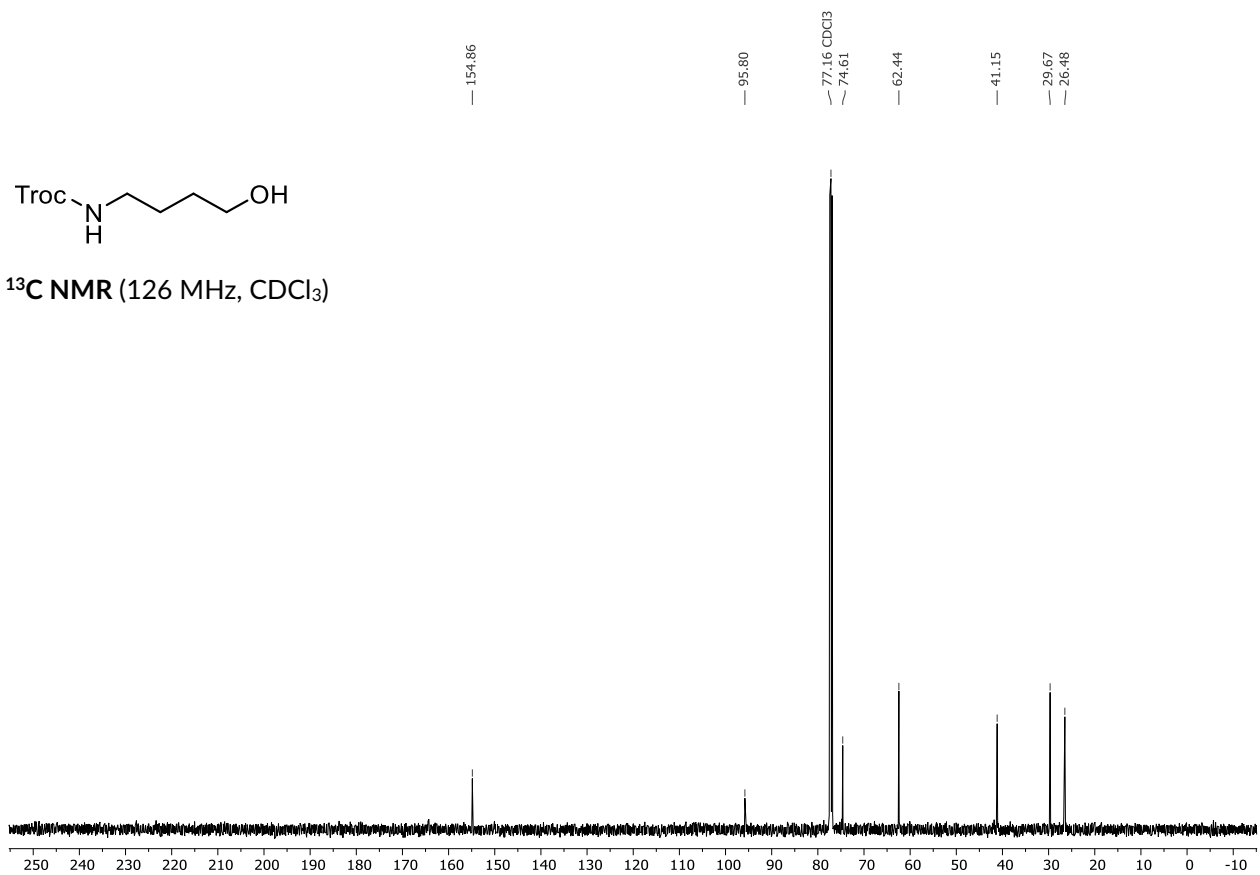
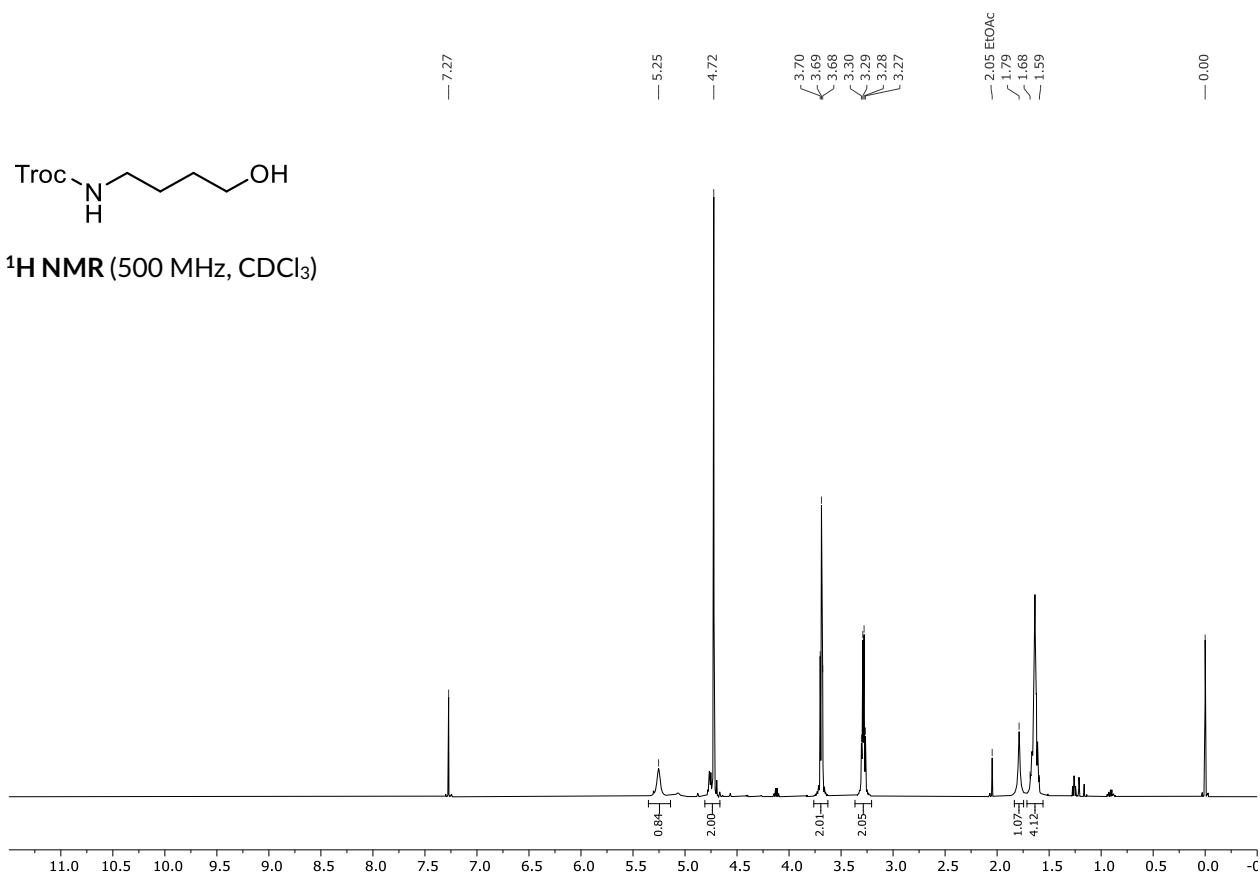


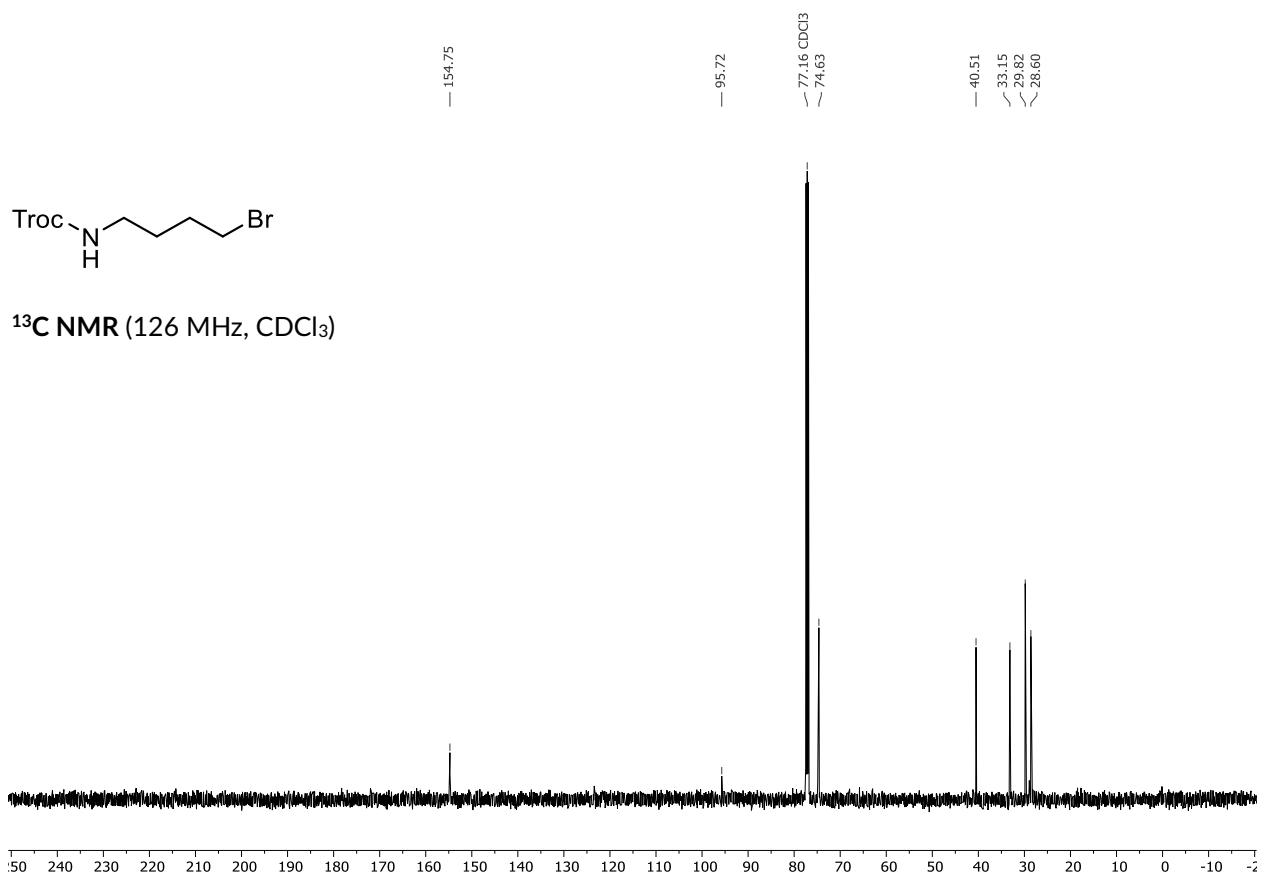
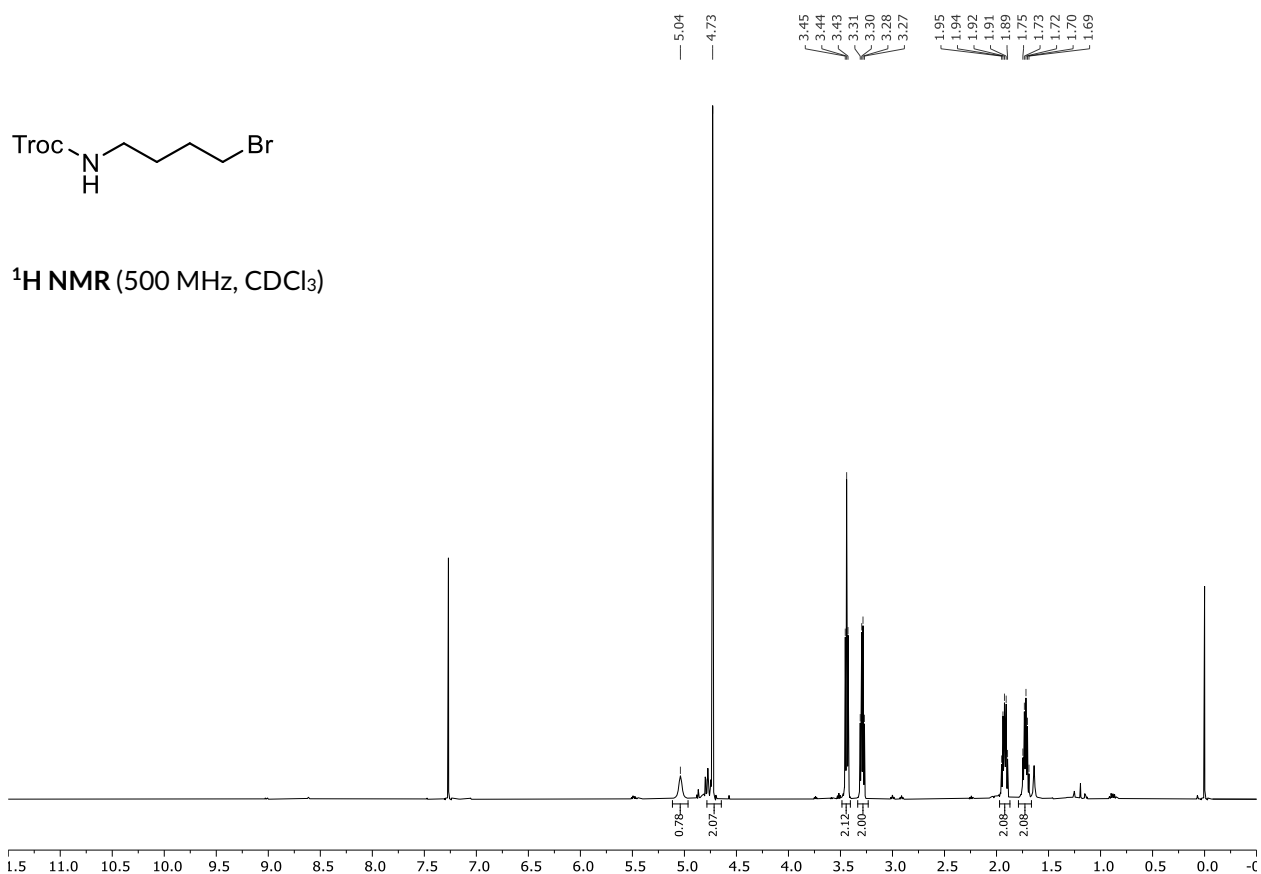
7.2.3. SHARPLESS Asymmetric Aminohydroxylation

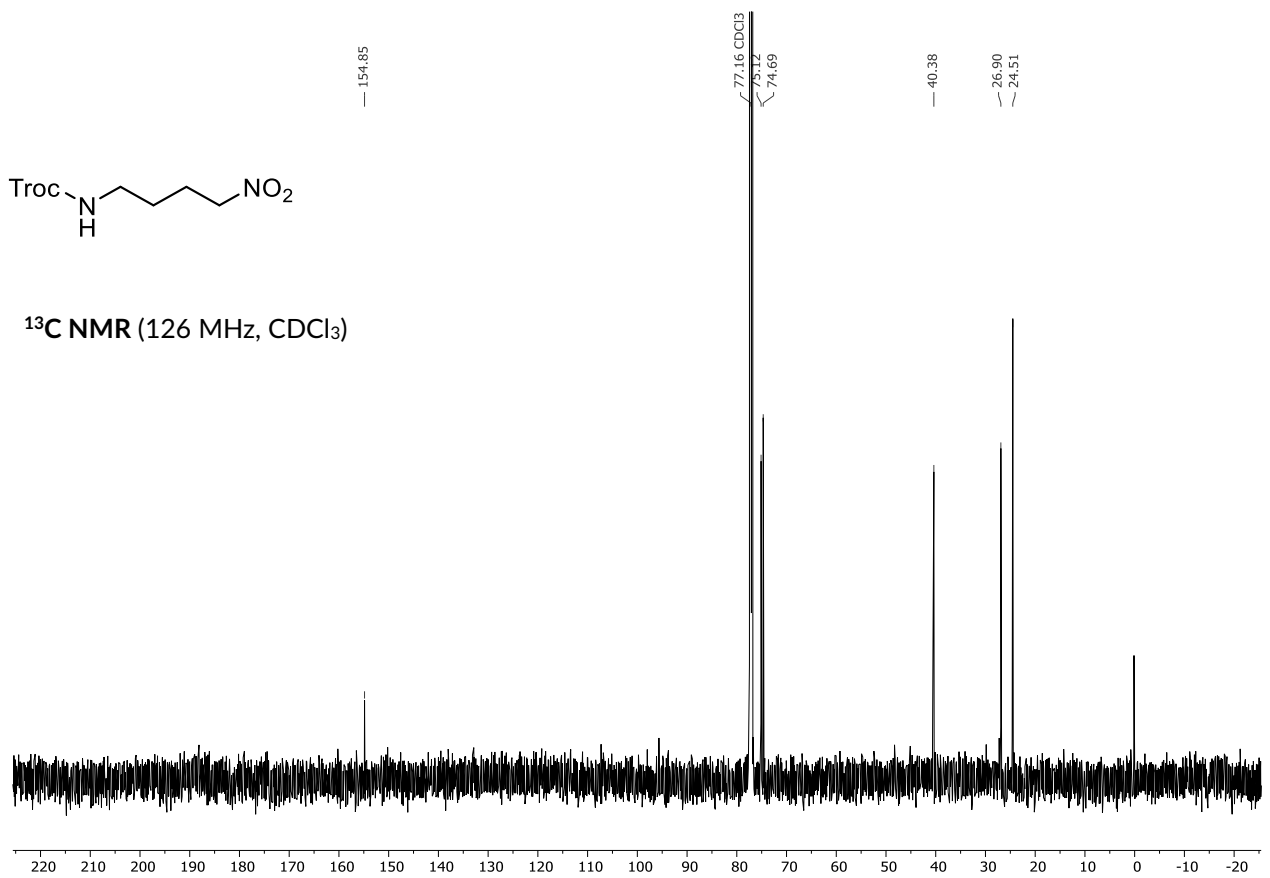
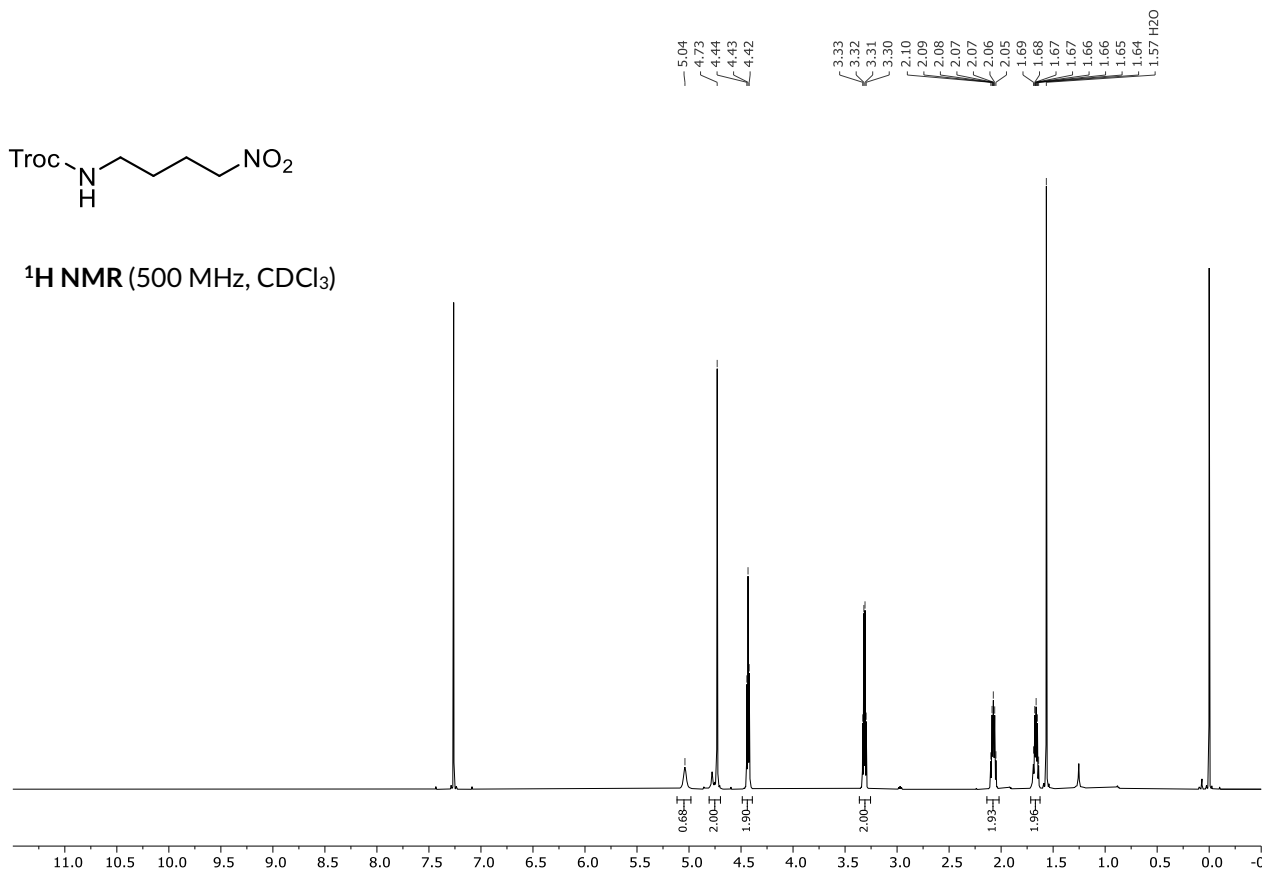


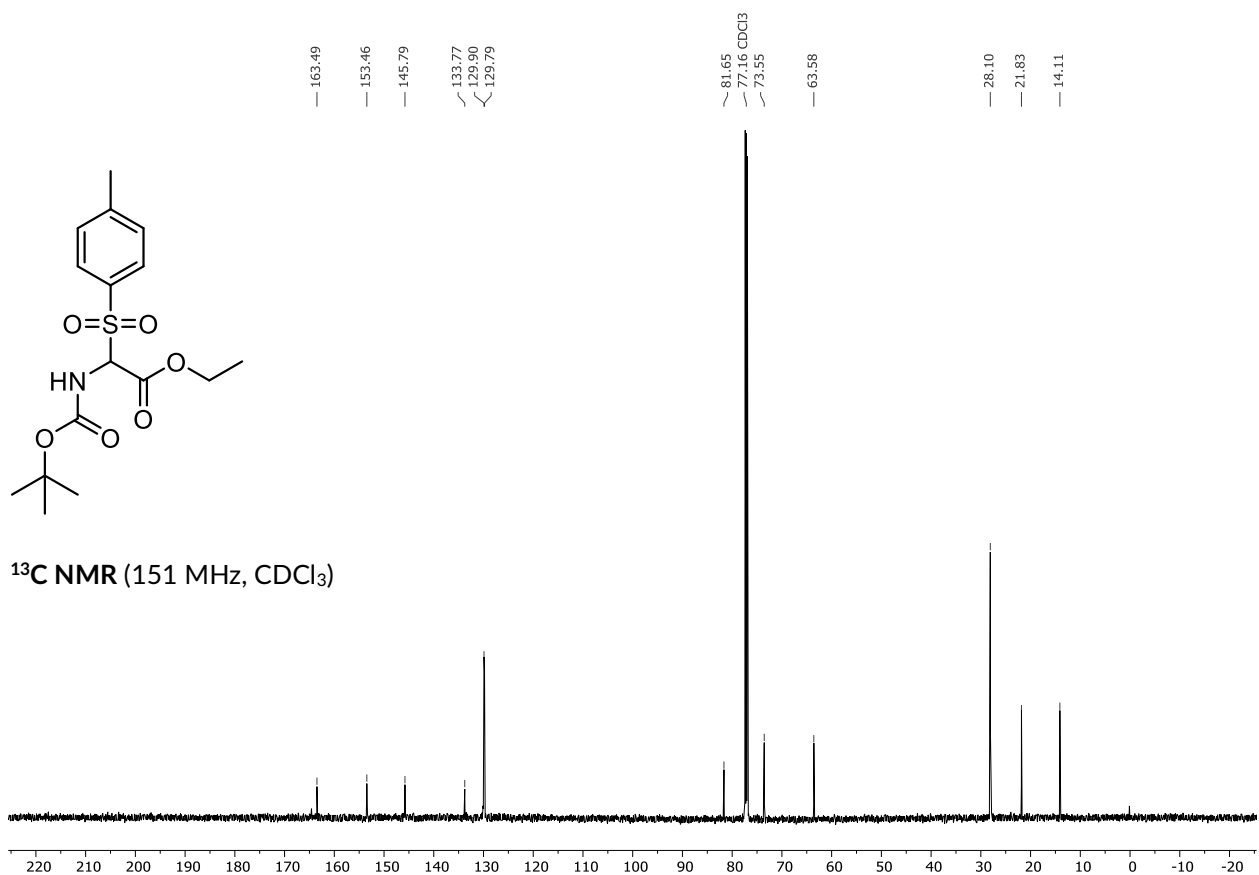
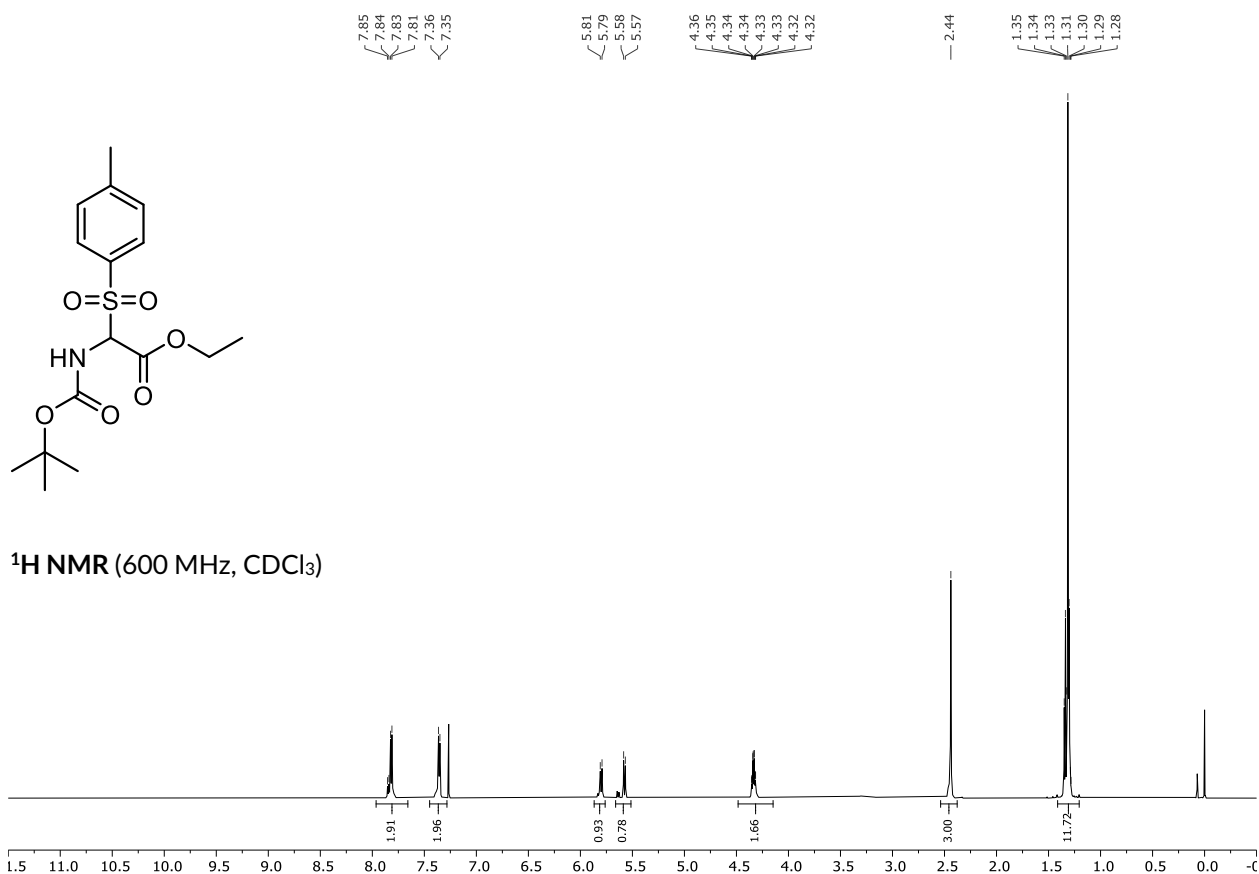


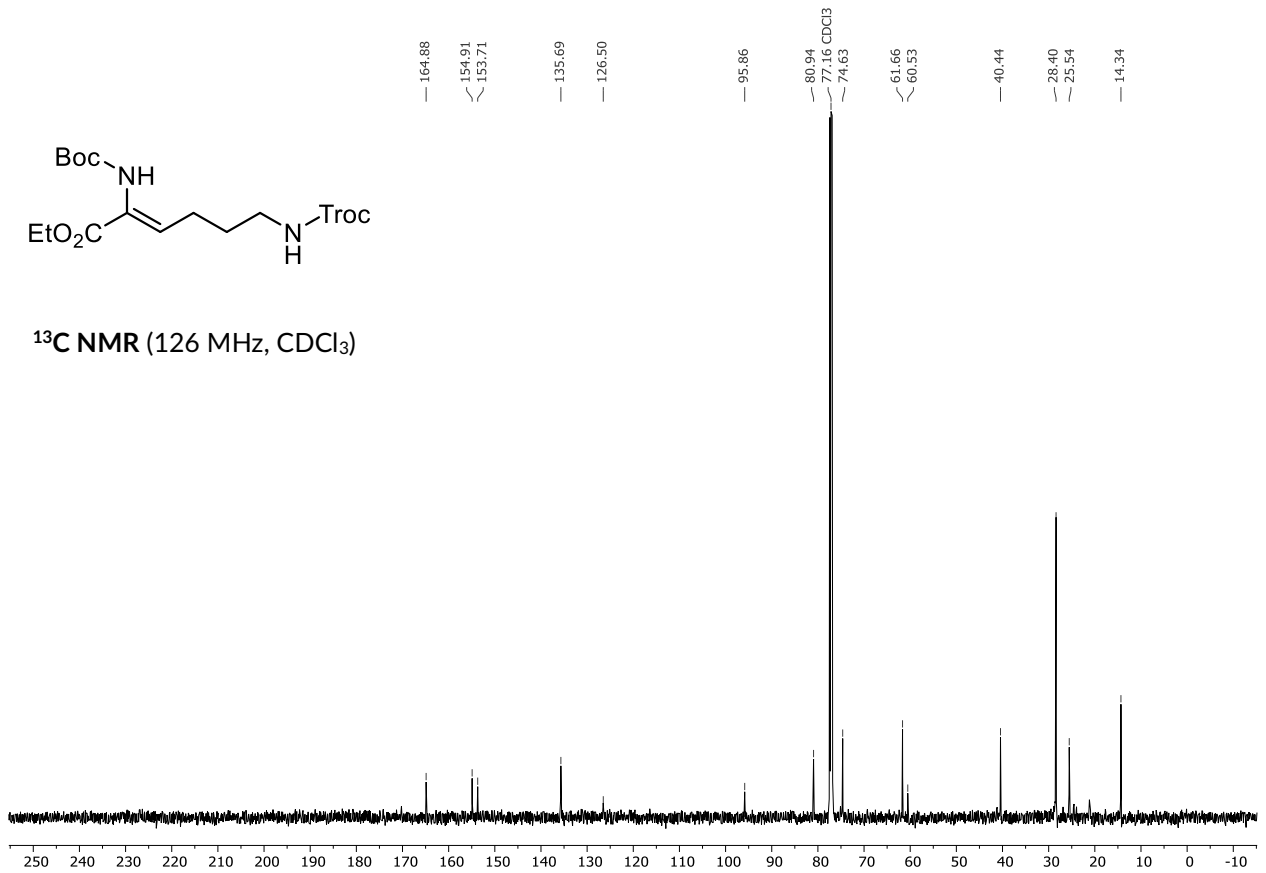
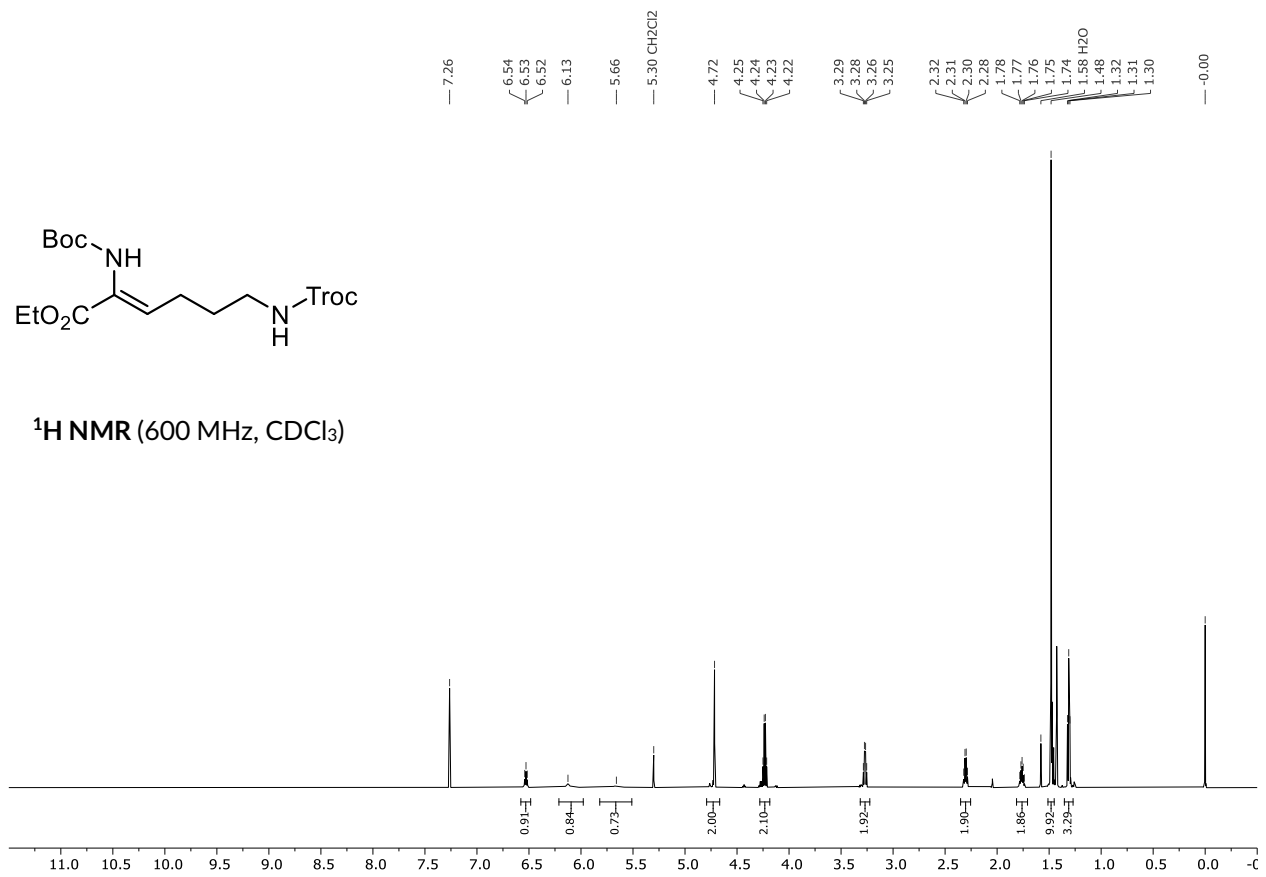


7.2.4. Synthesis of Boc- Δ Lys(Troc)-OMe (72)

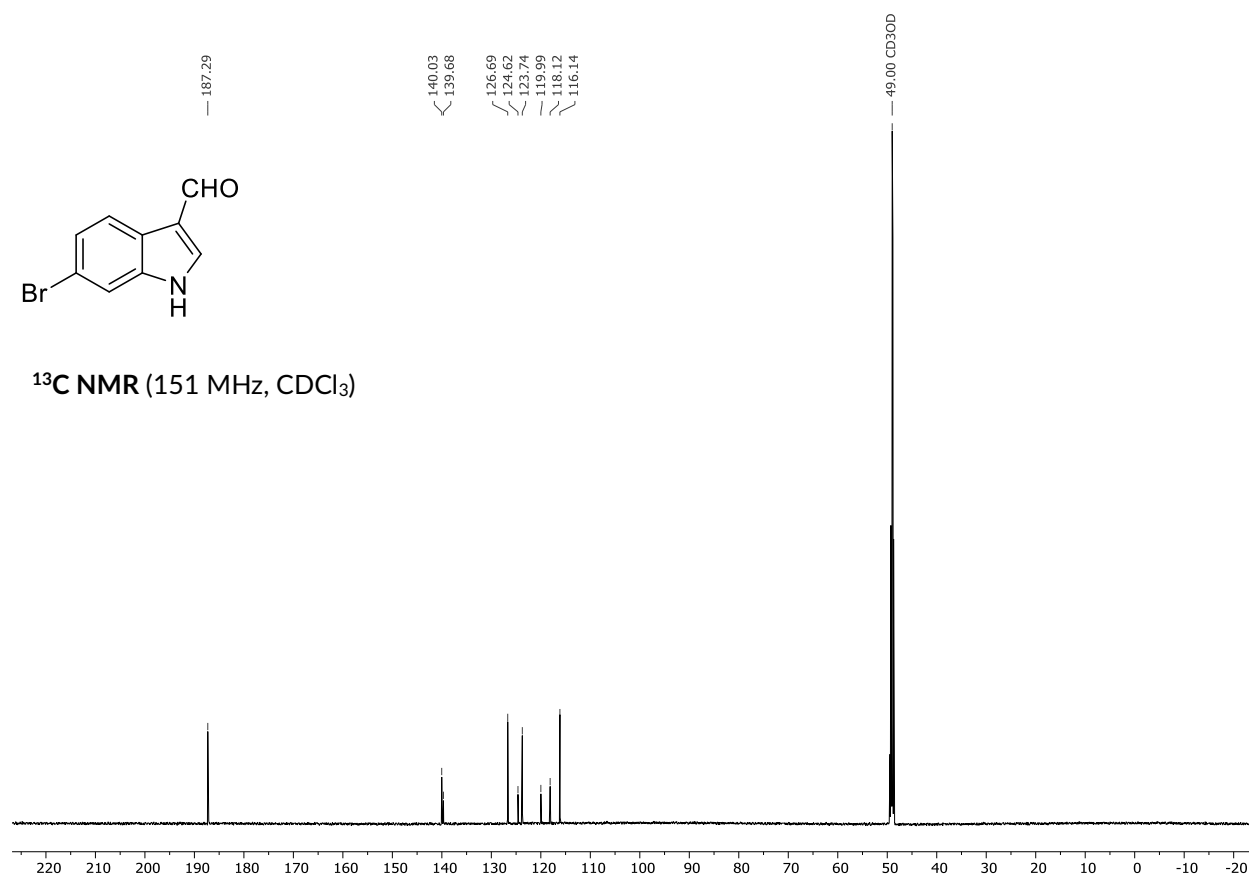
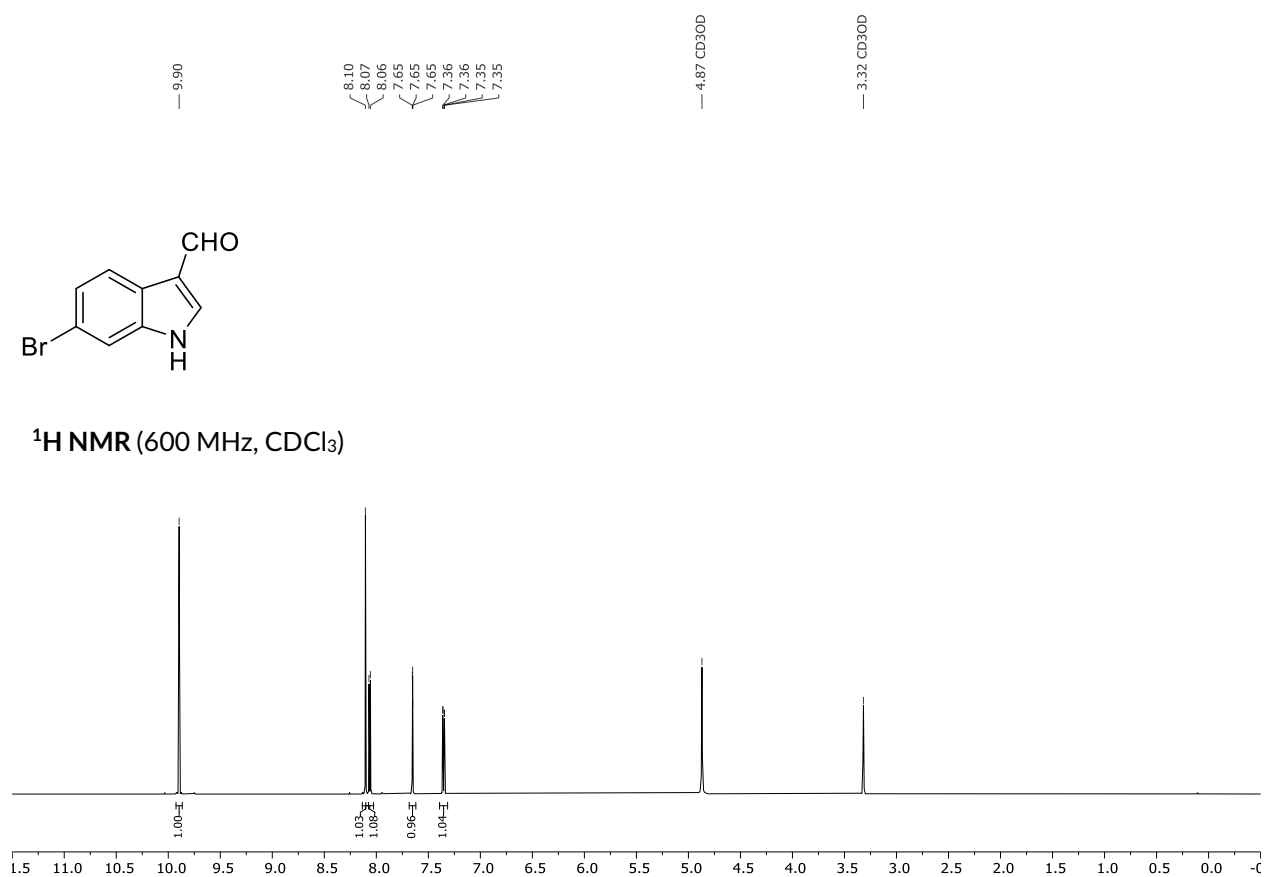


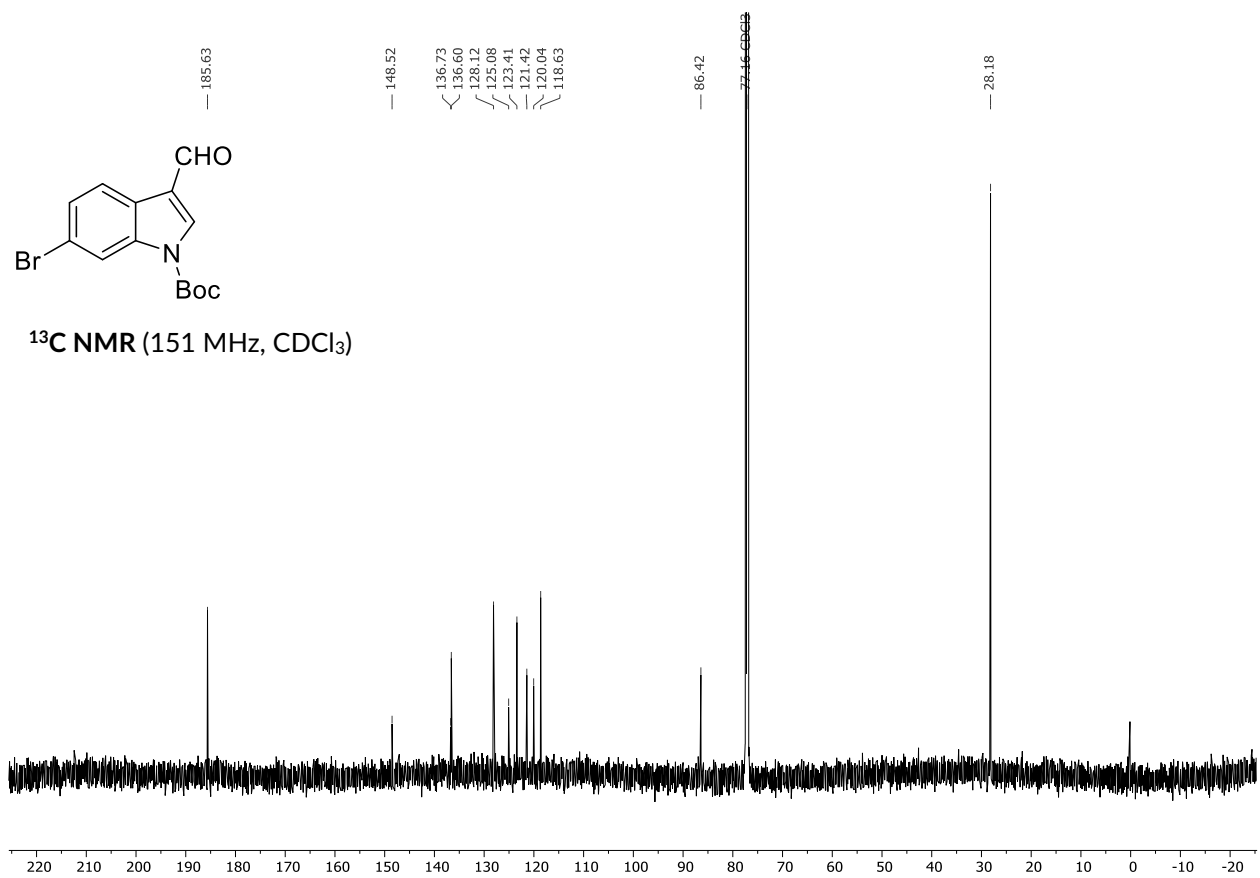
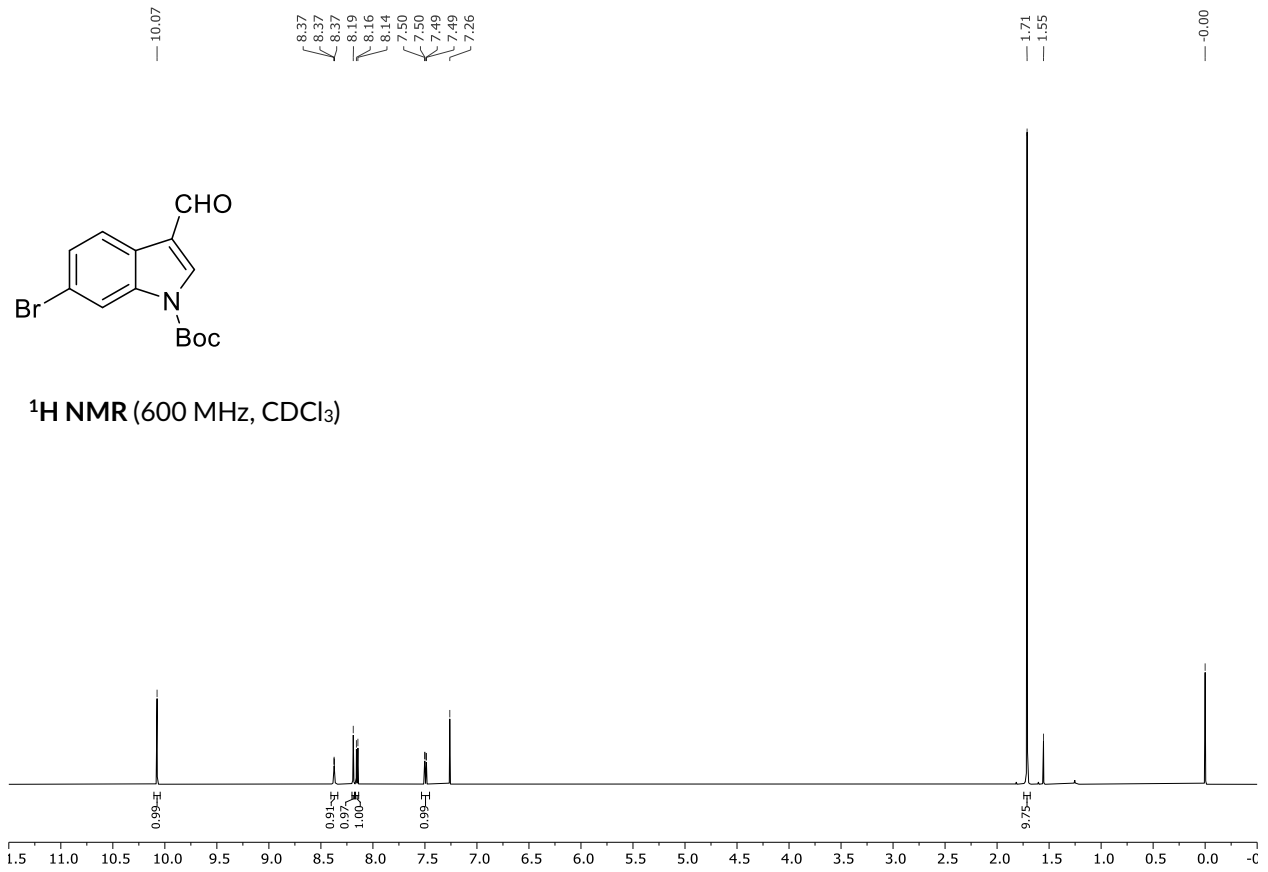


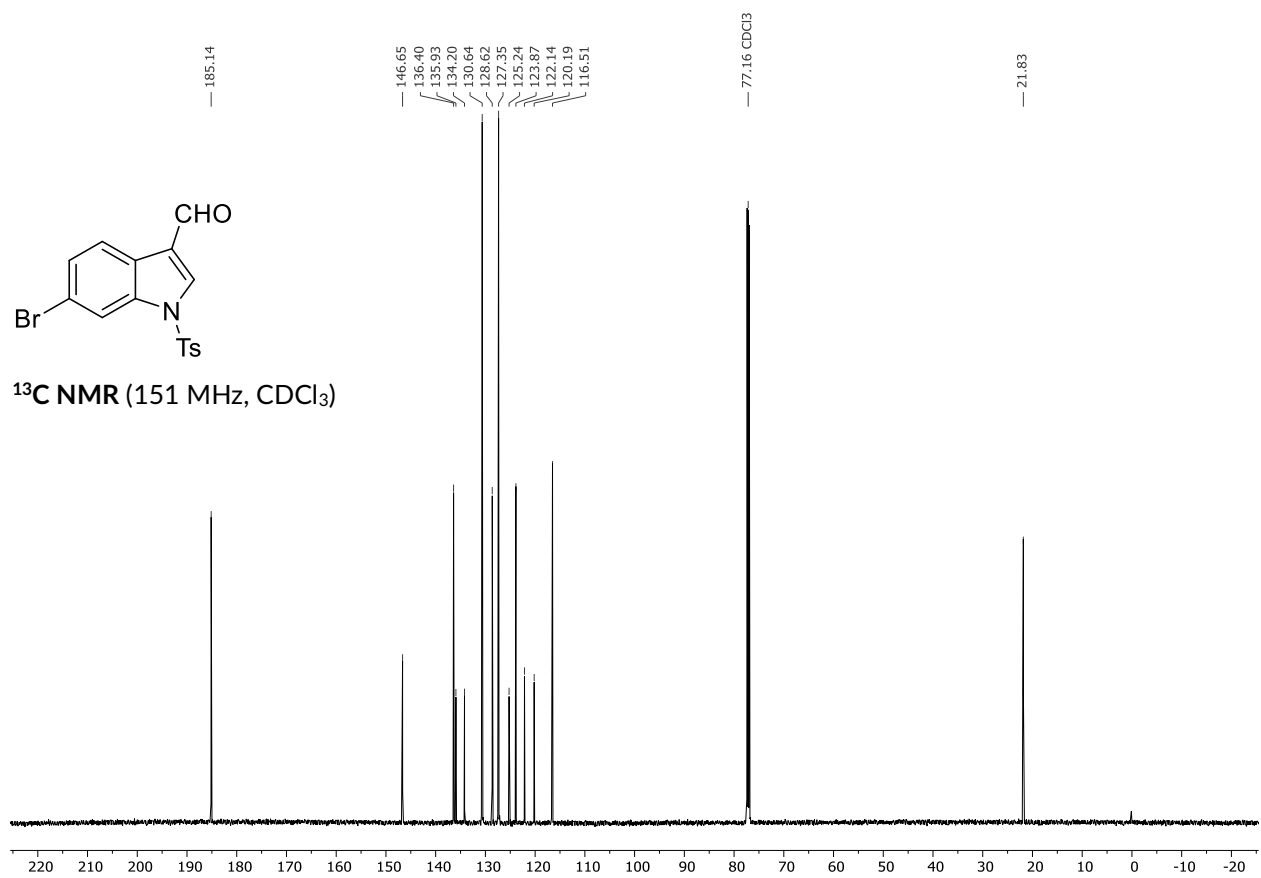
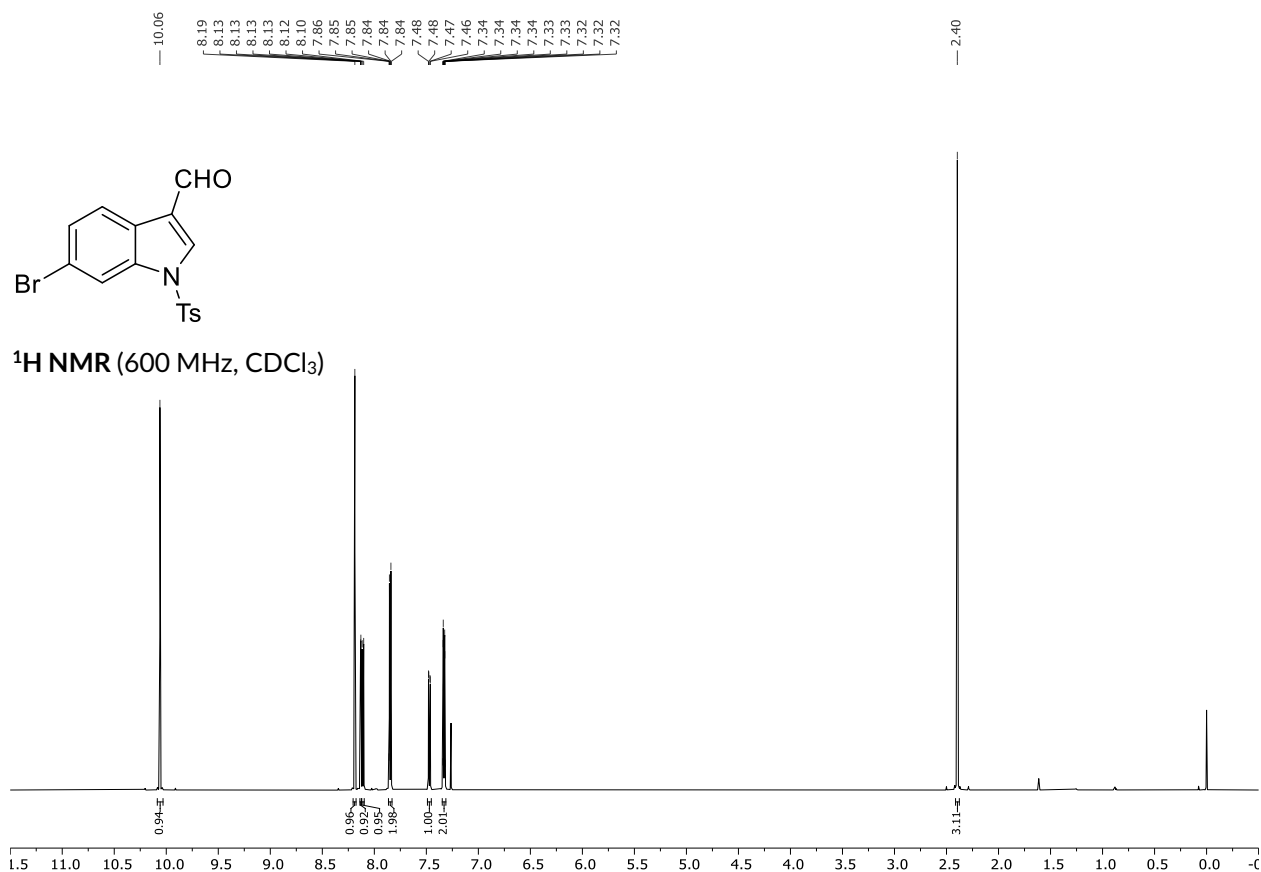


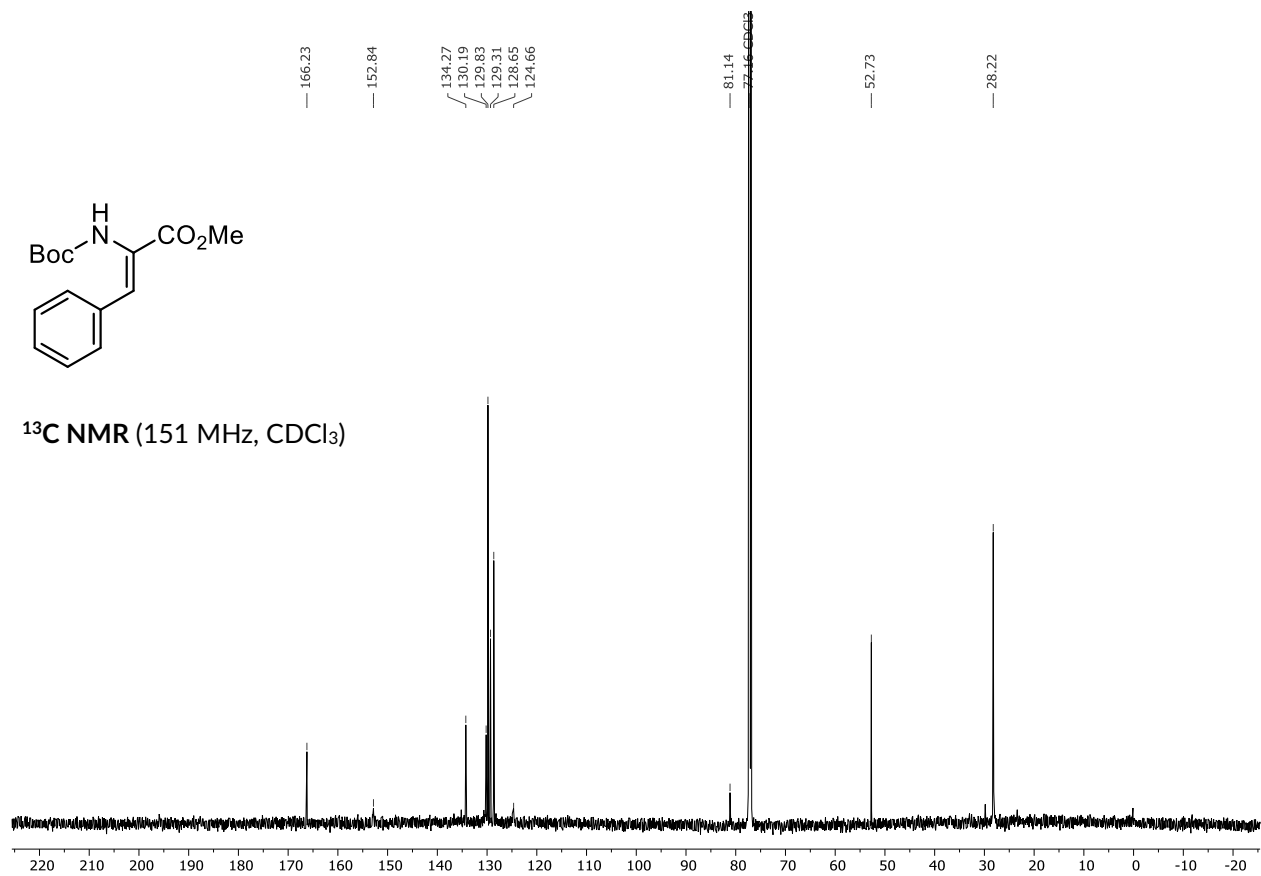
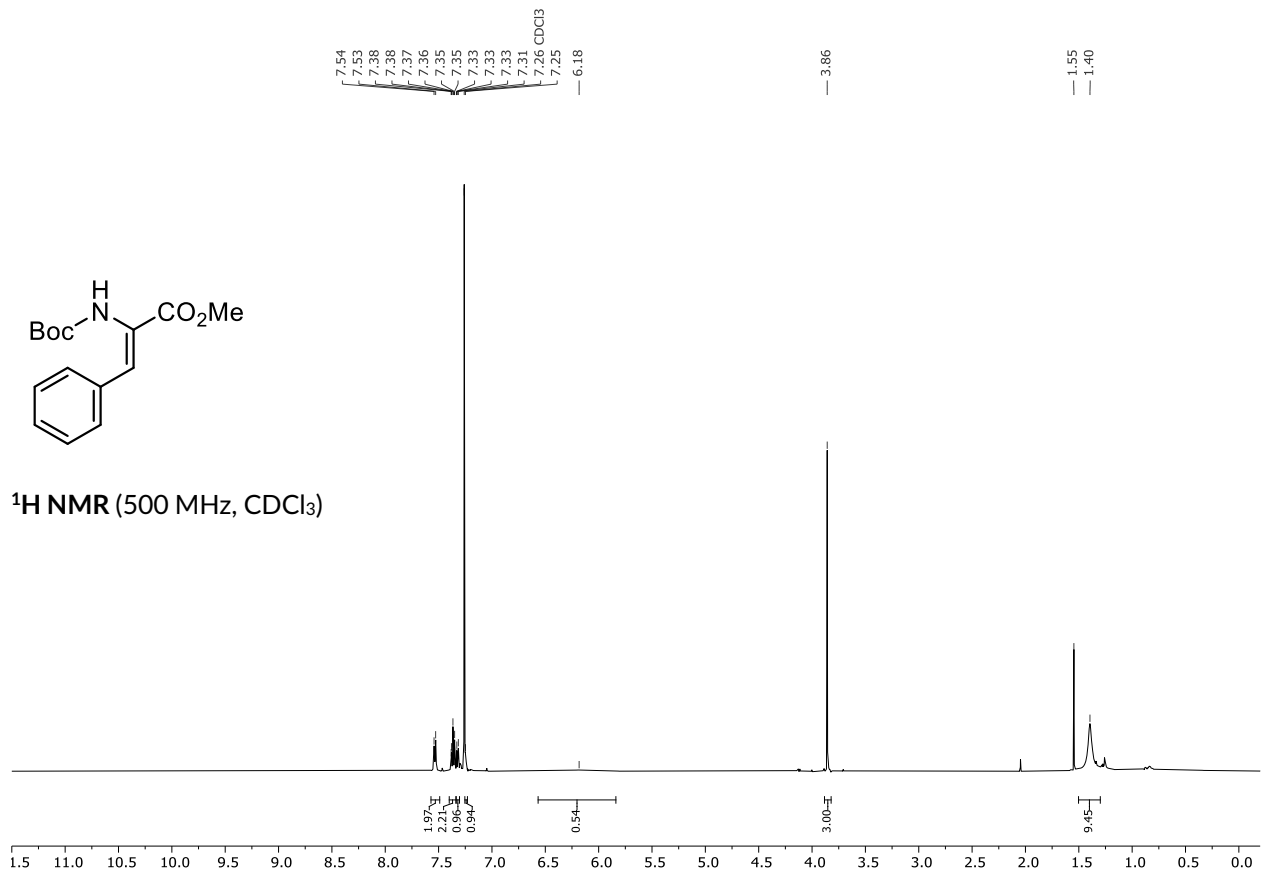


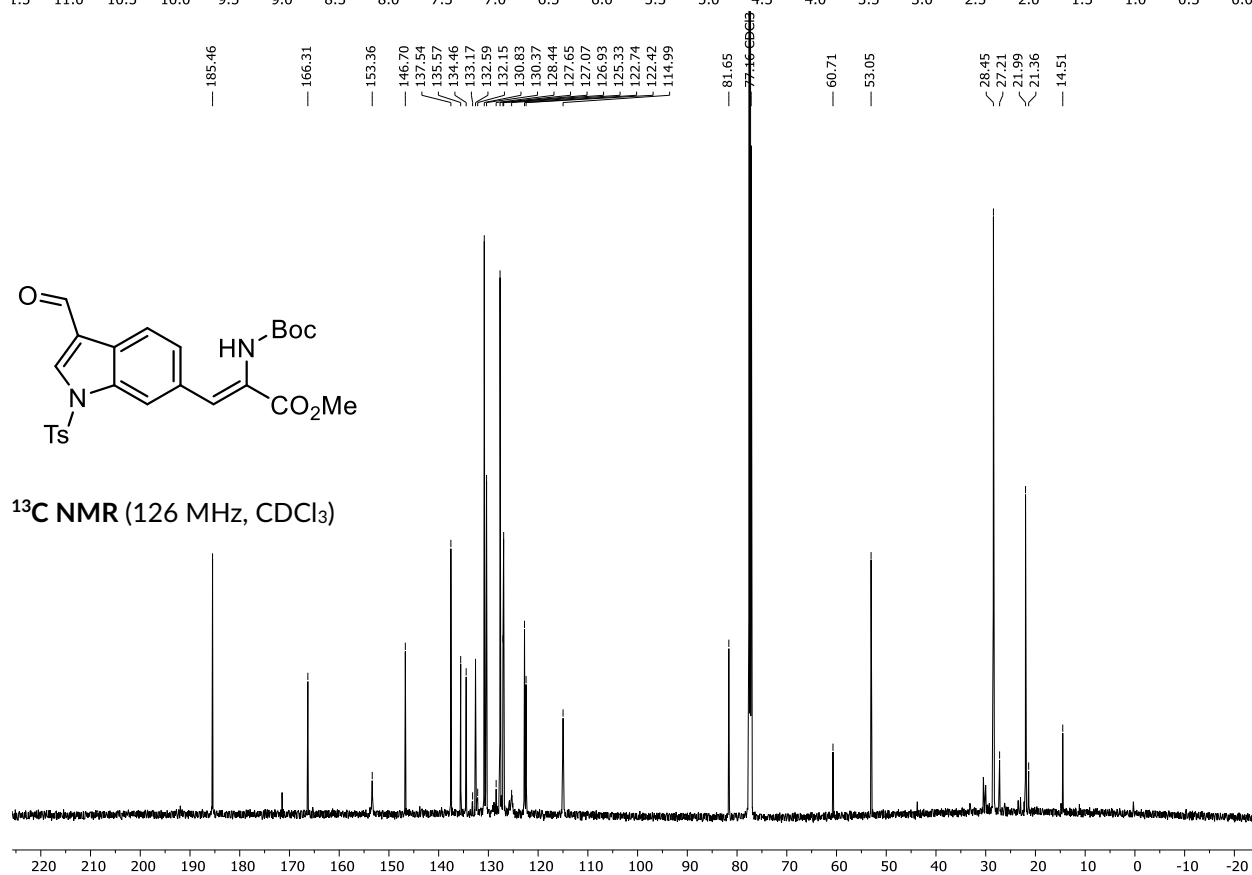
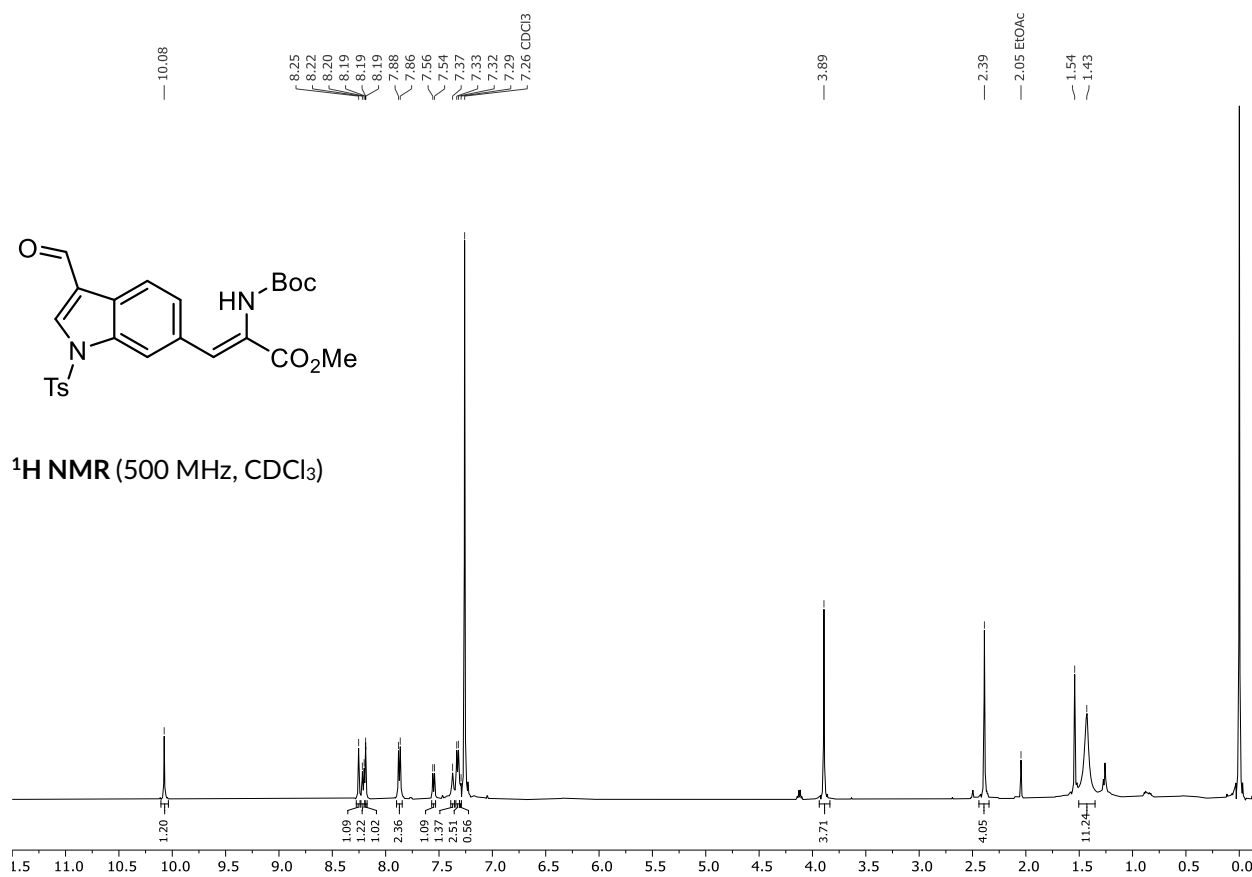
7.2.5. C6-Indole Bond Formation via HECK Reaction

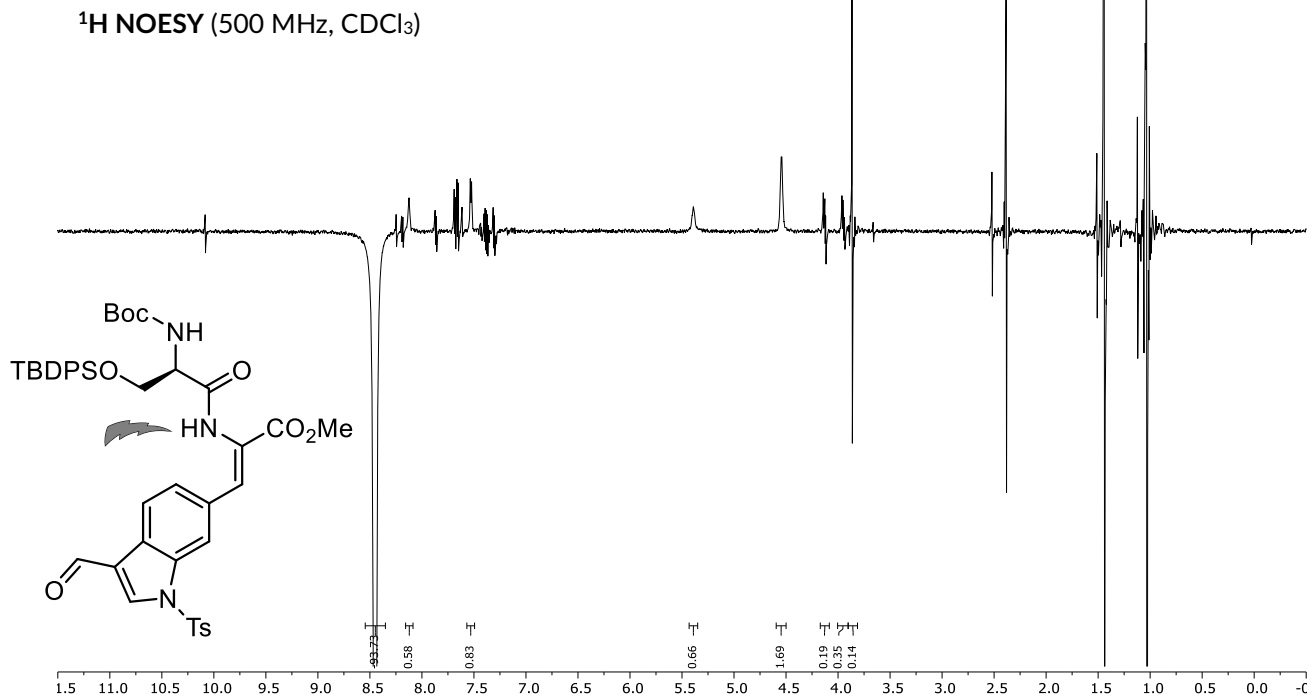
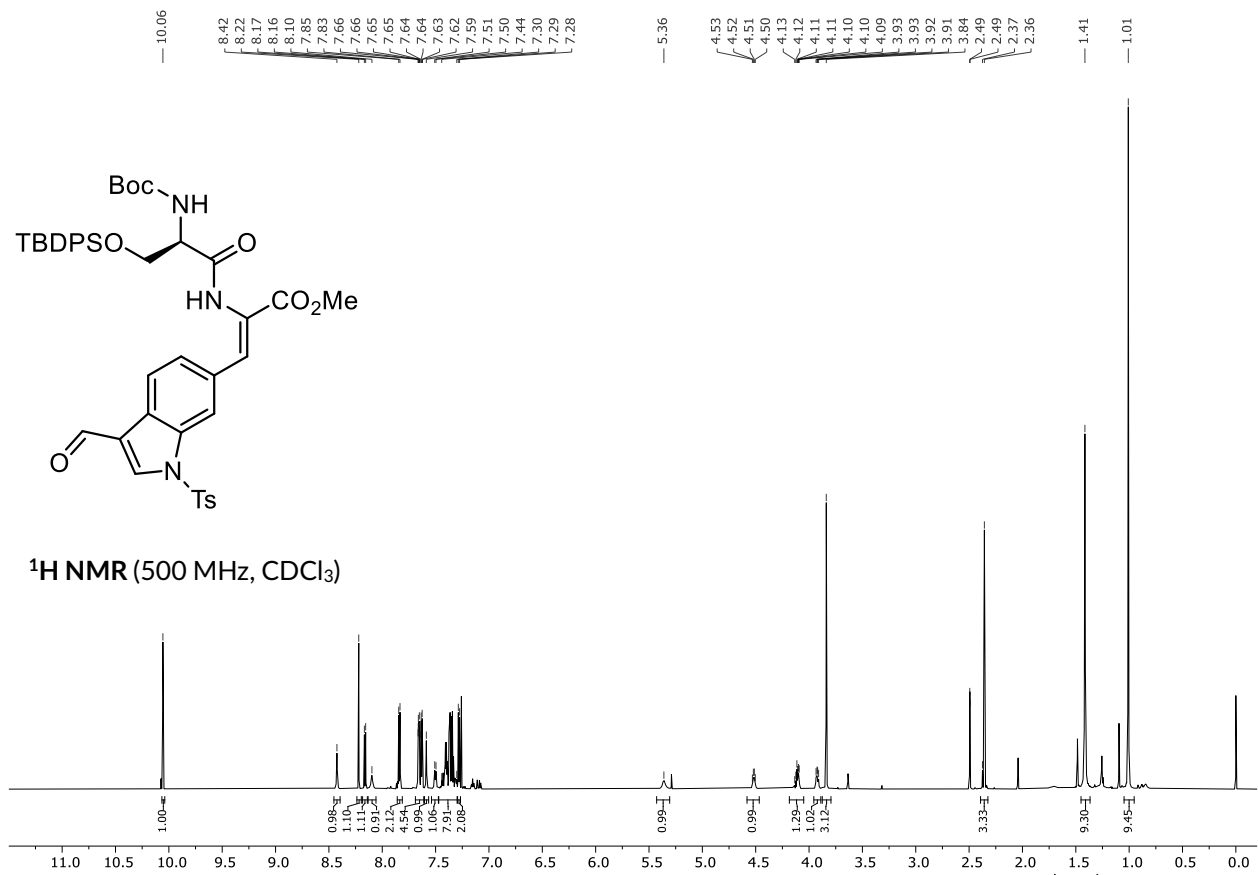


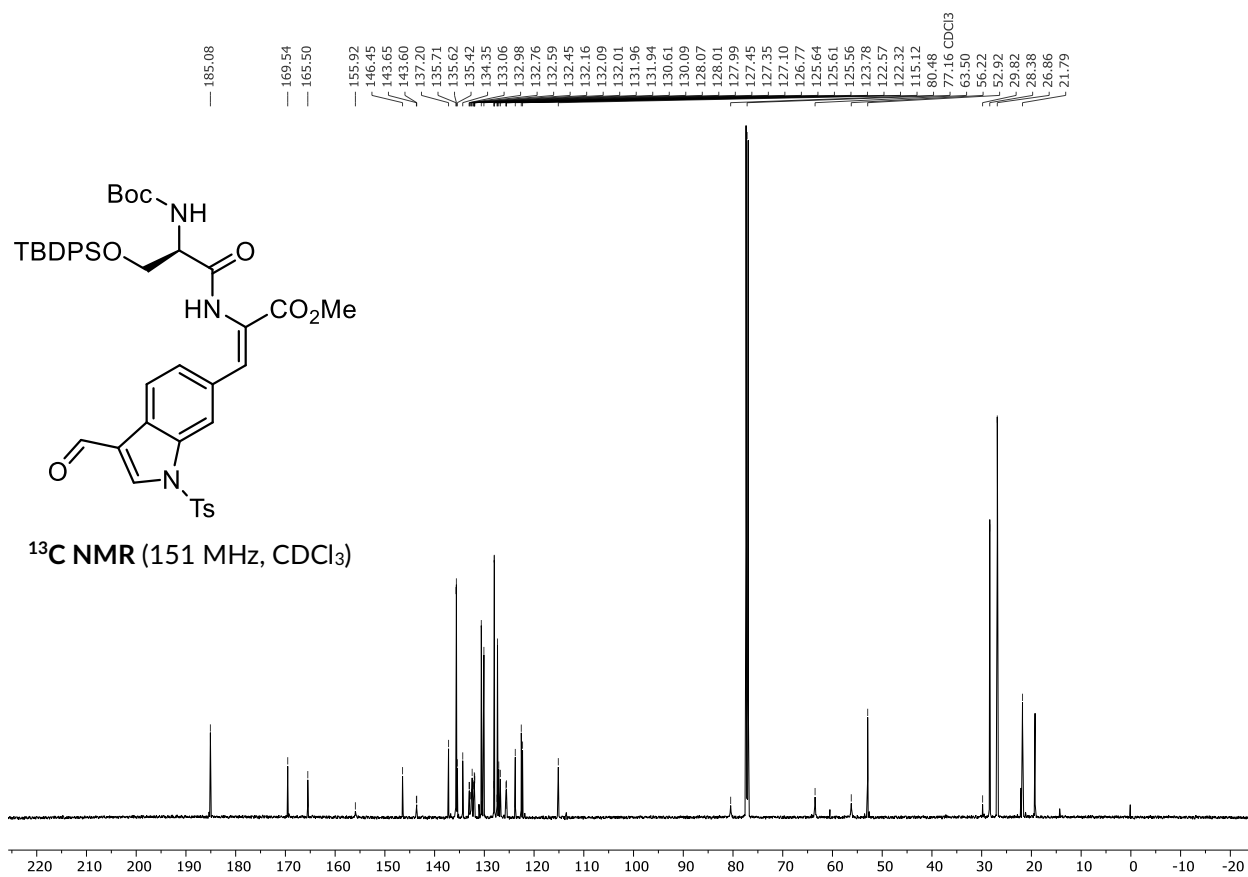


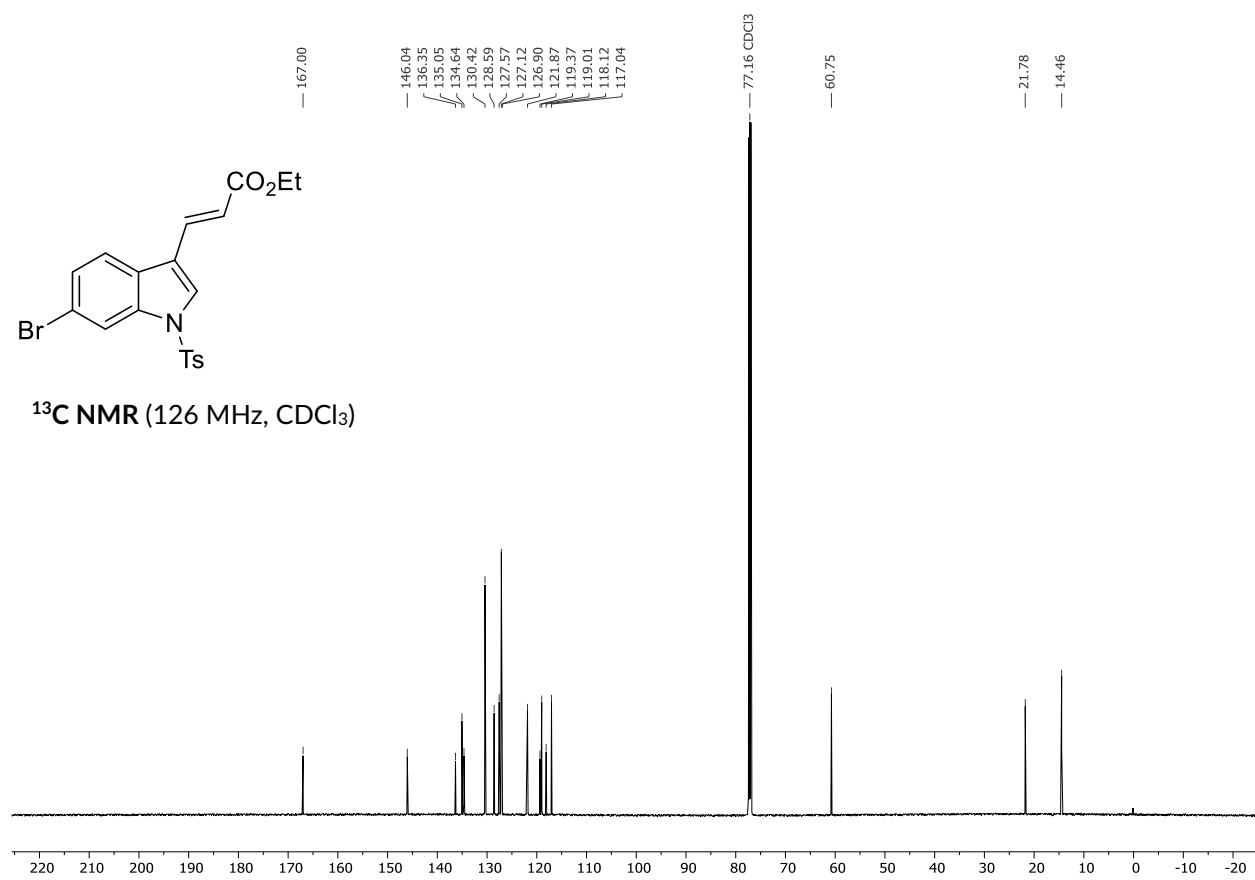
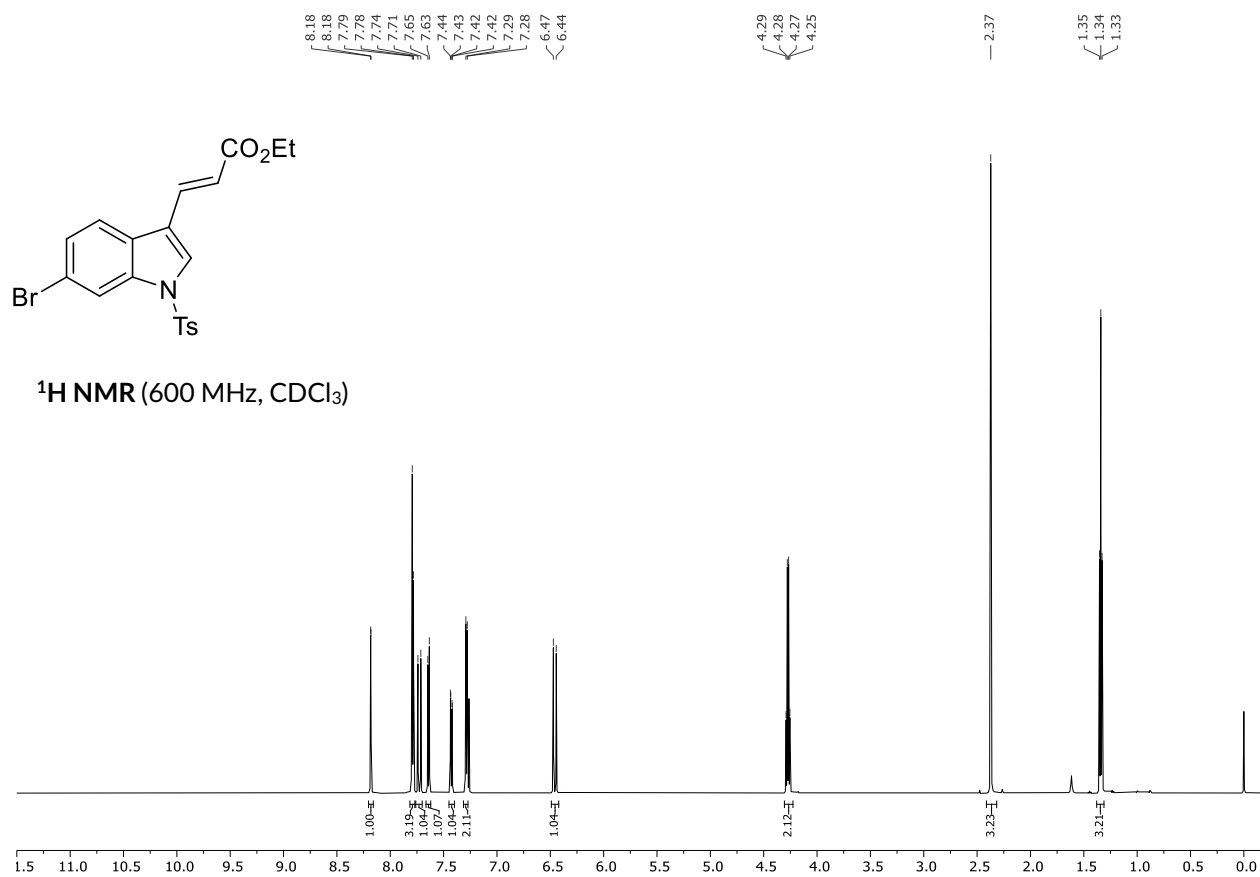


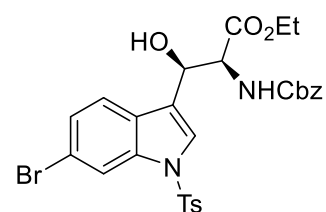
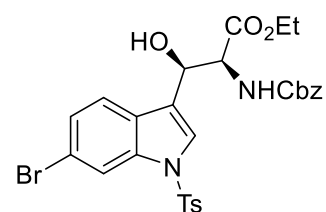
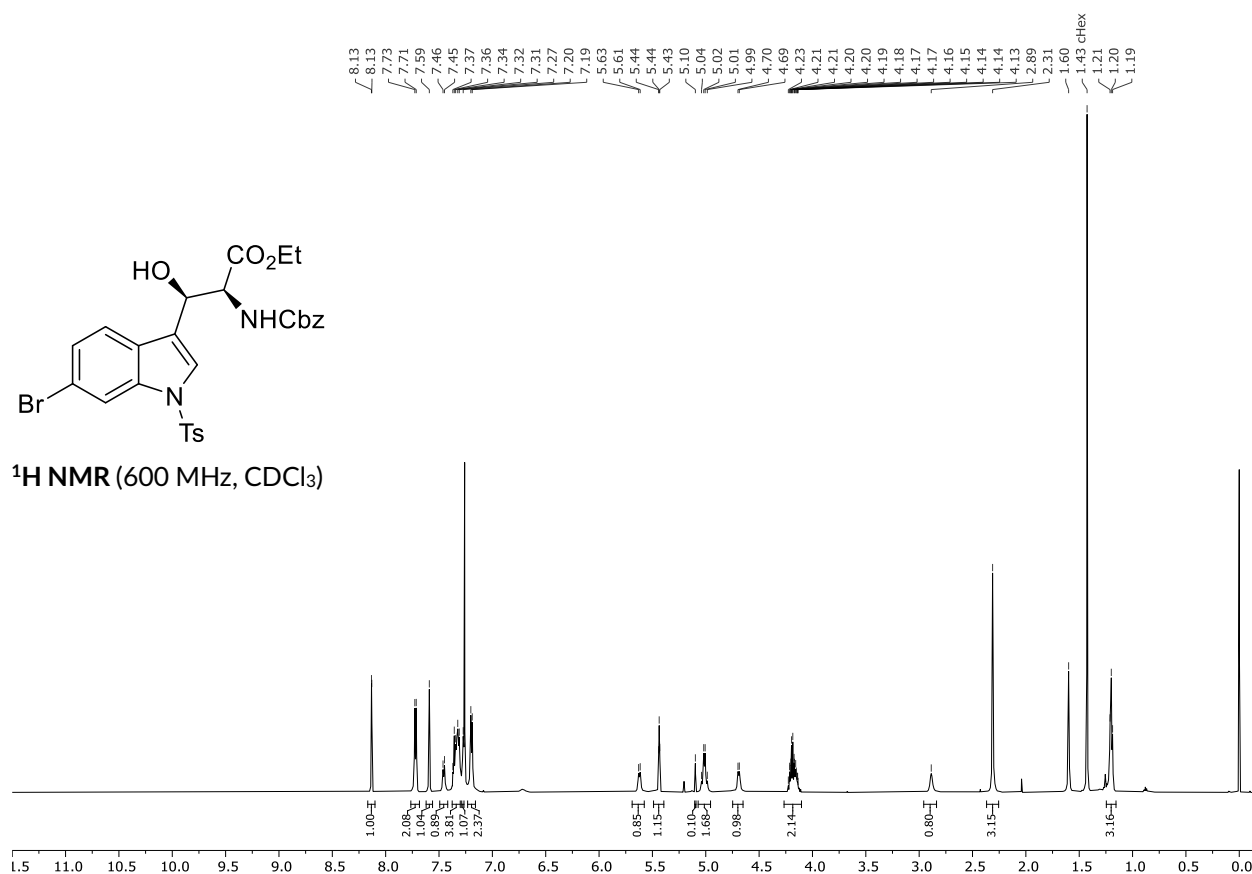
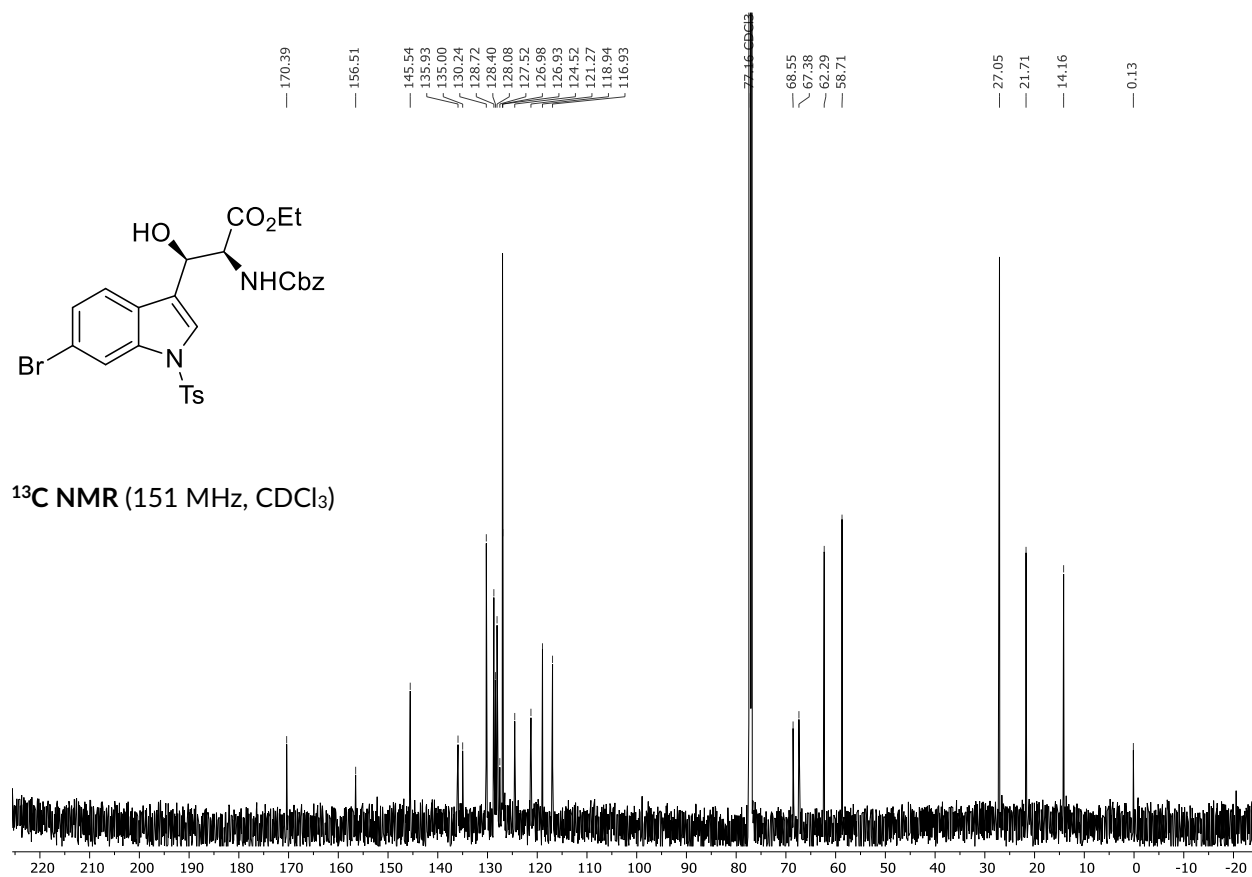


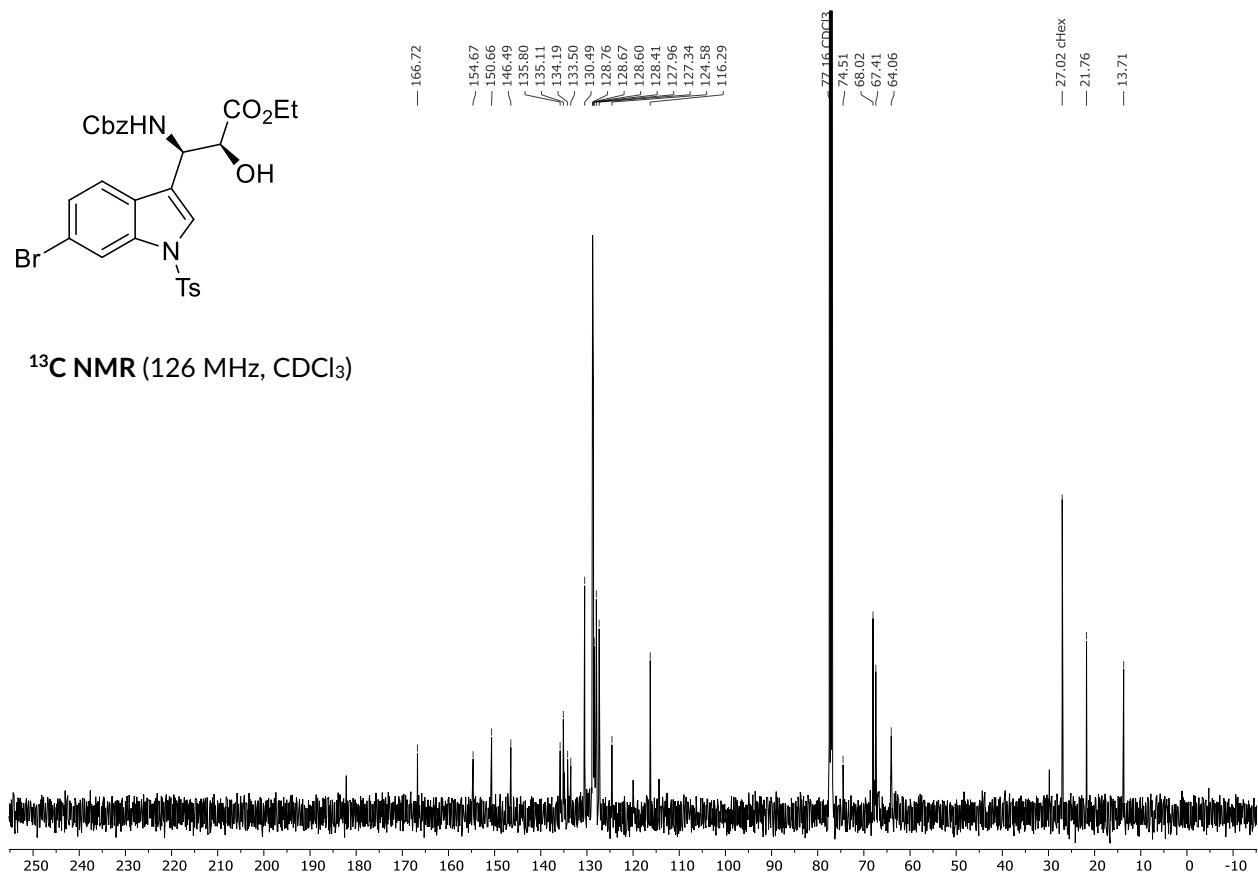
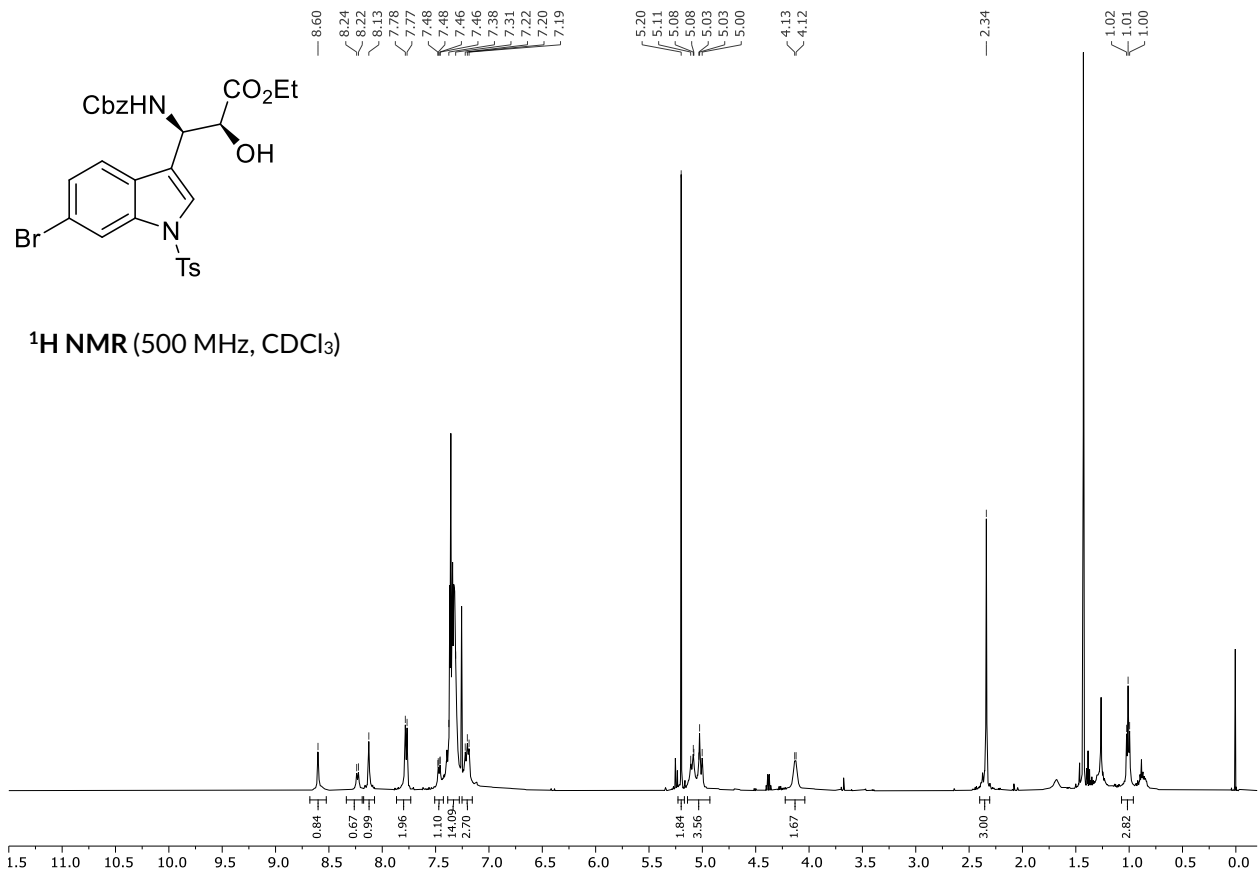


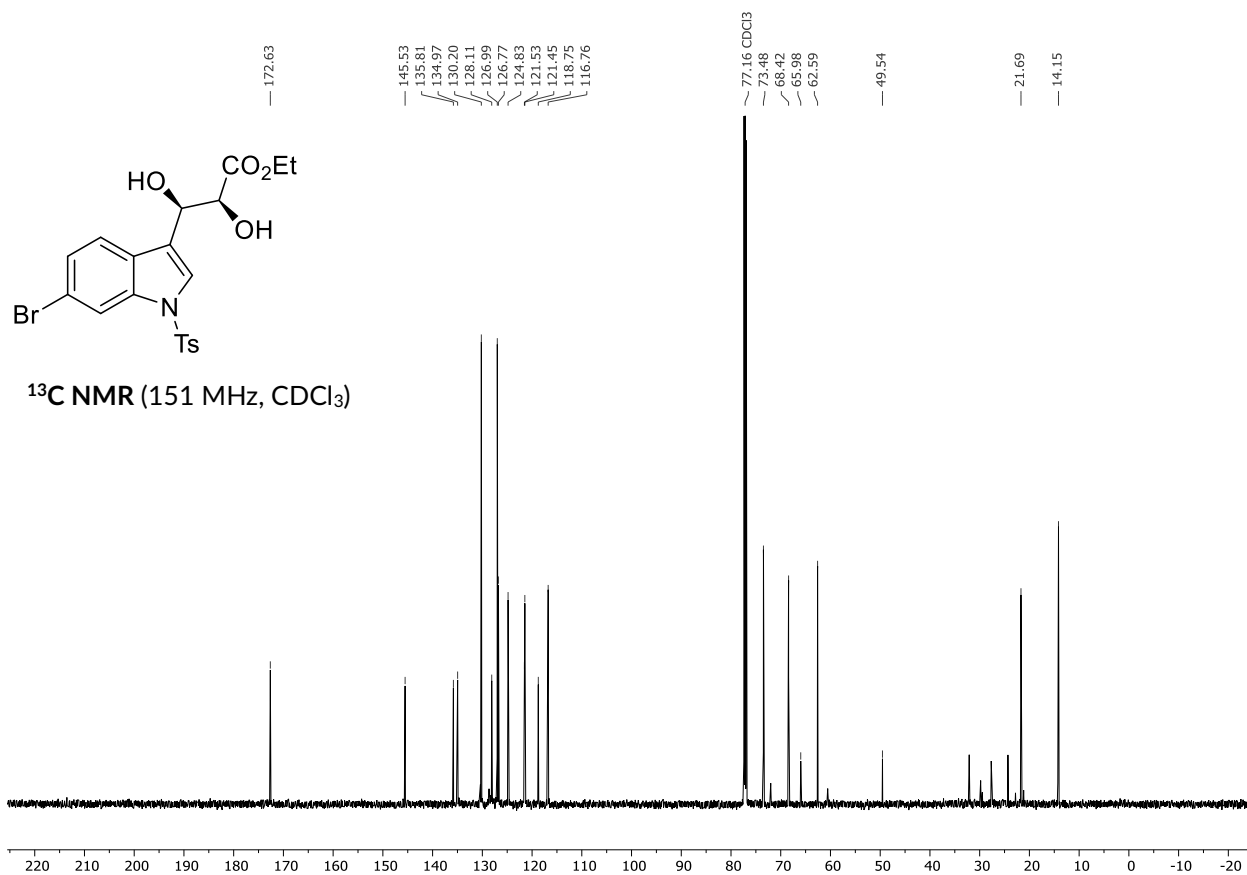
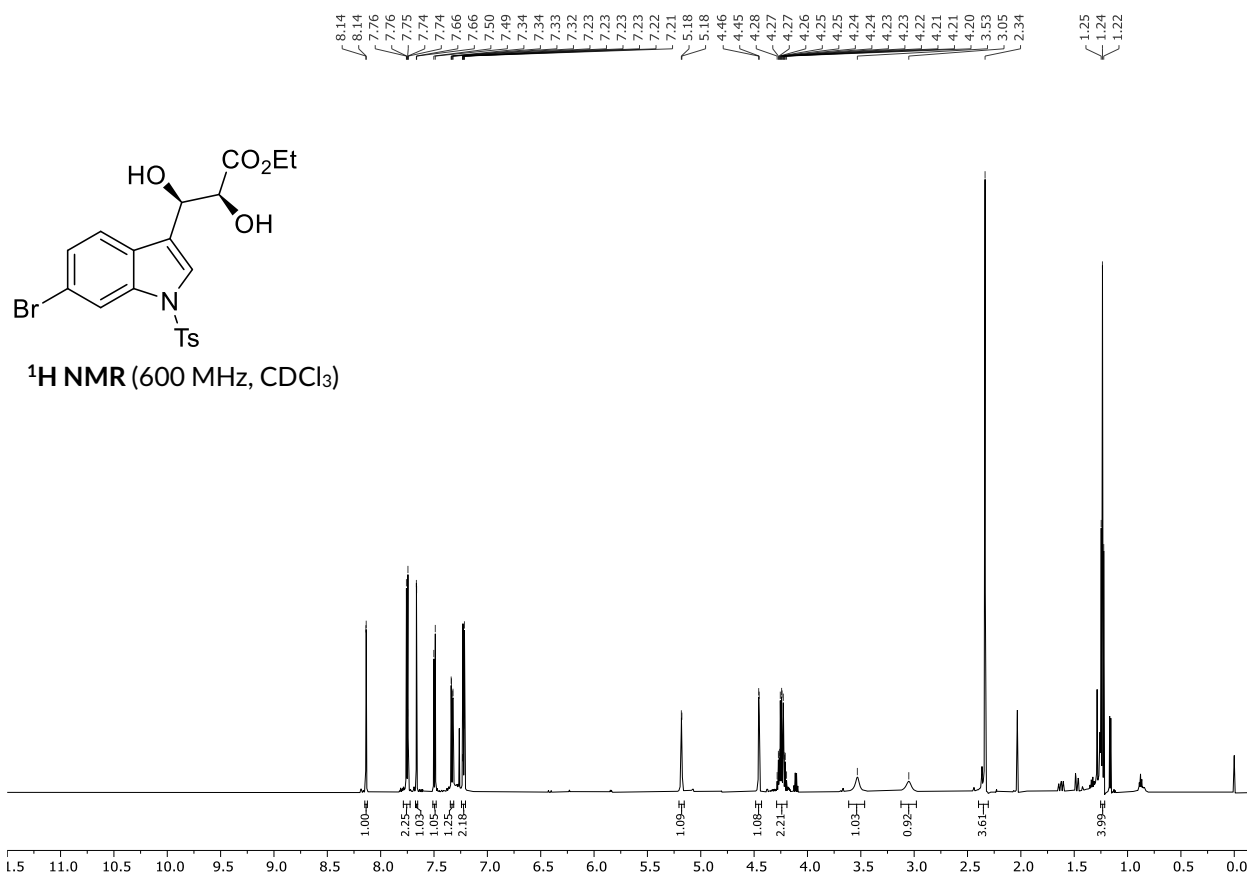


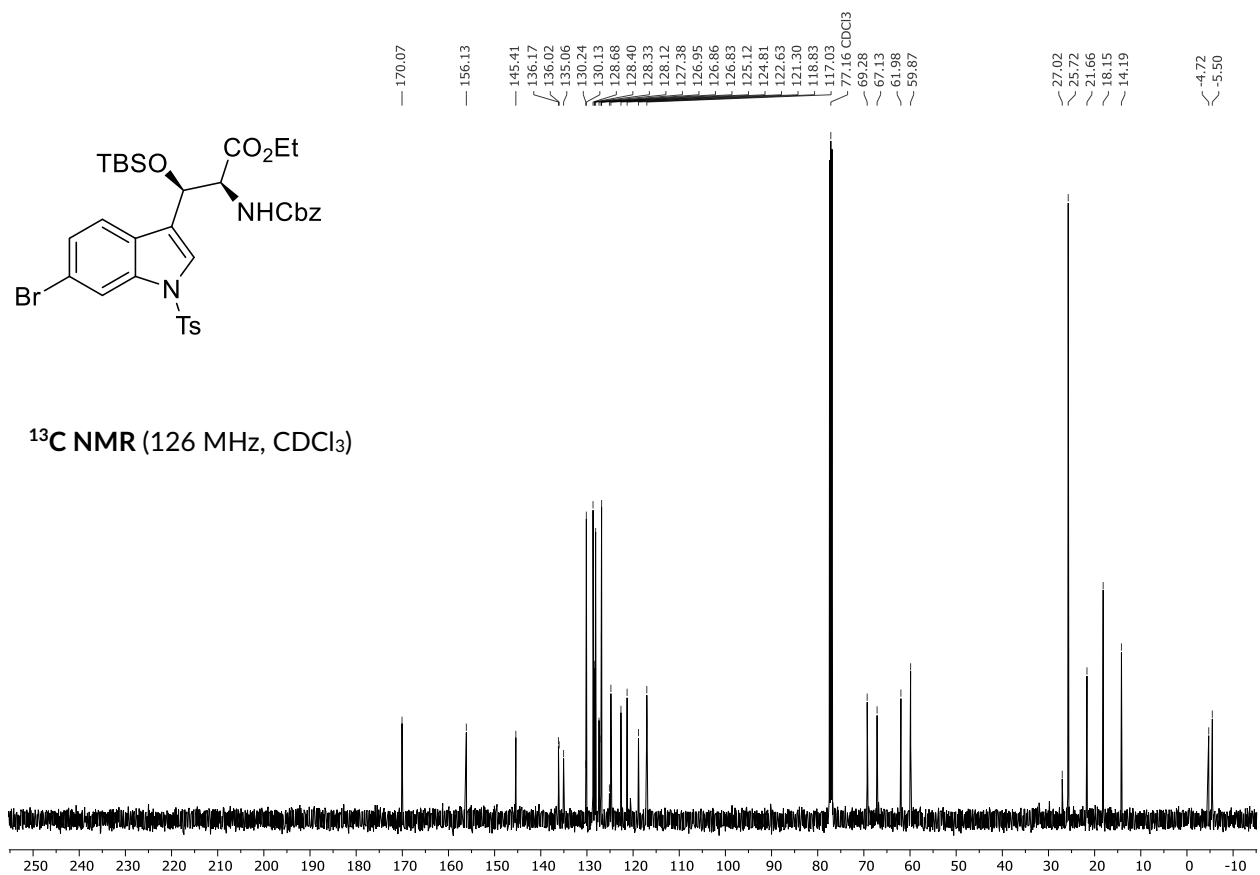
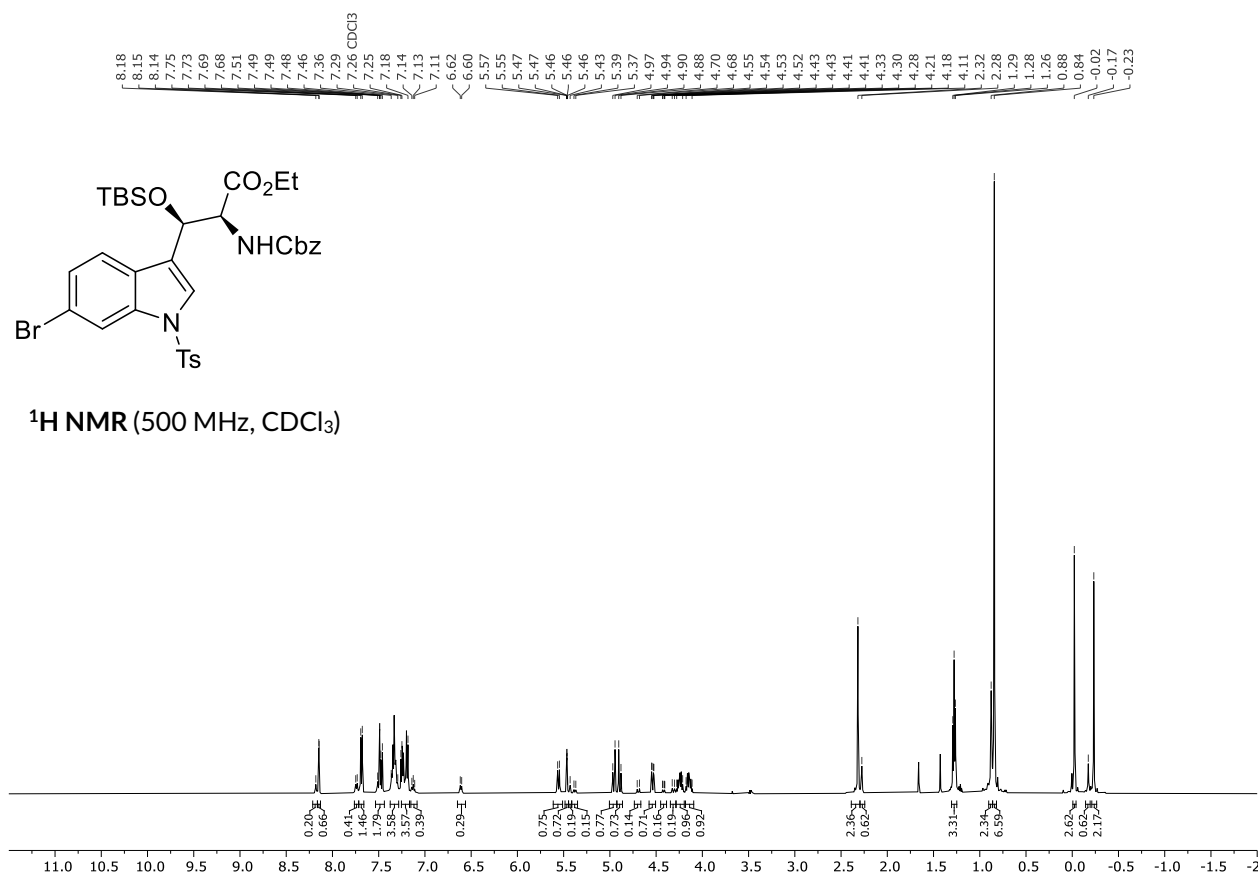


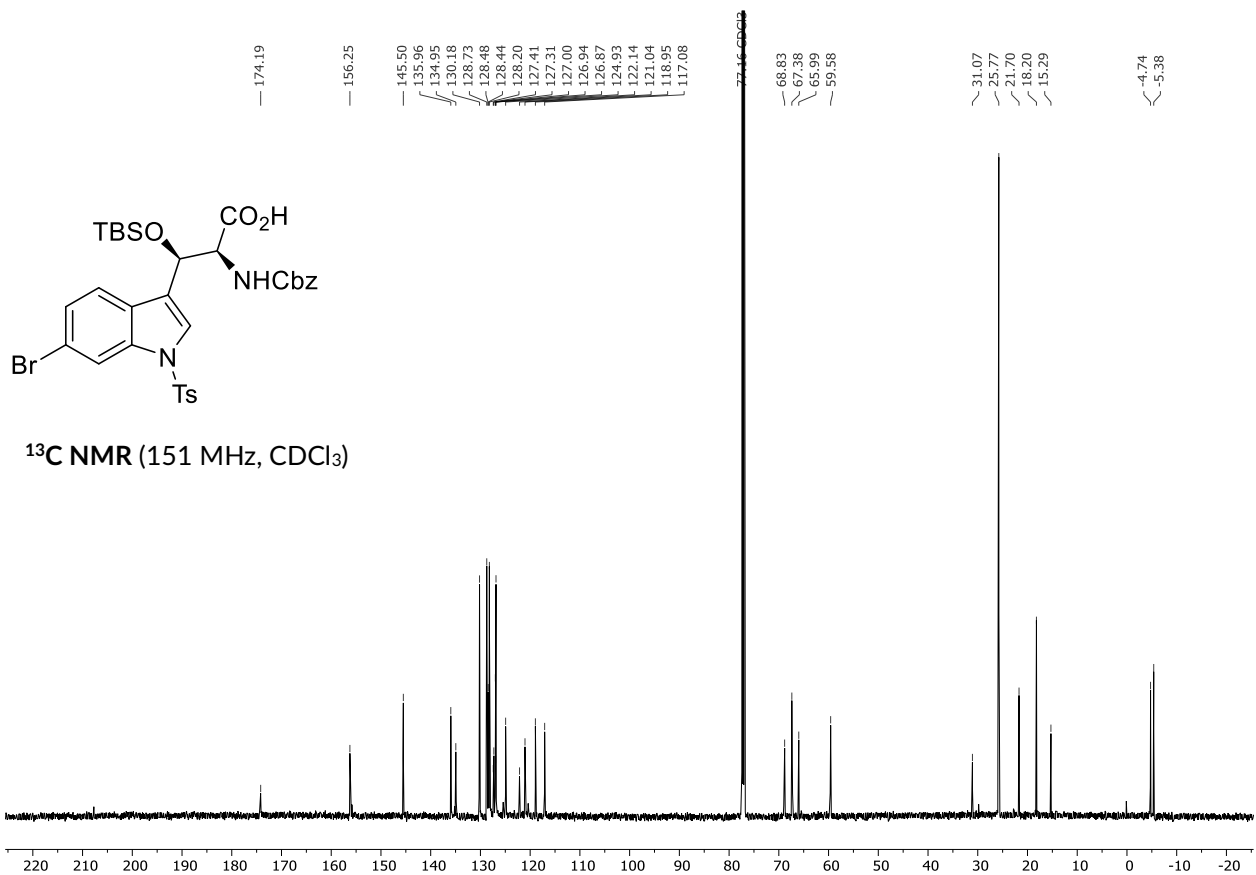
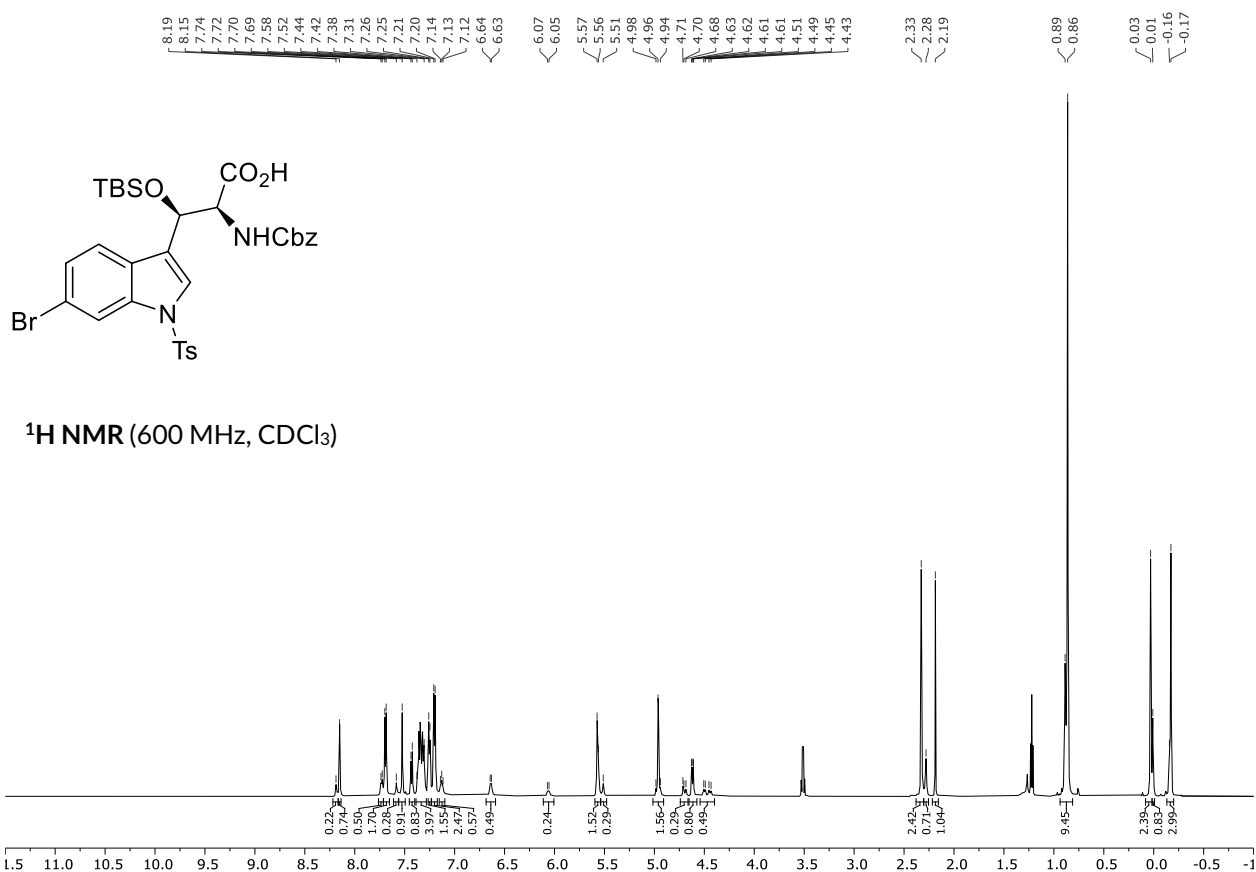


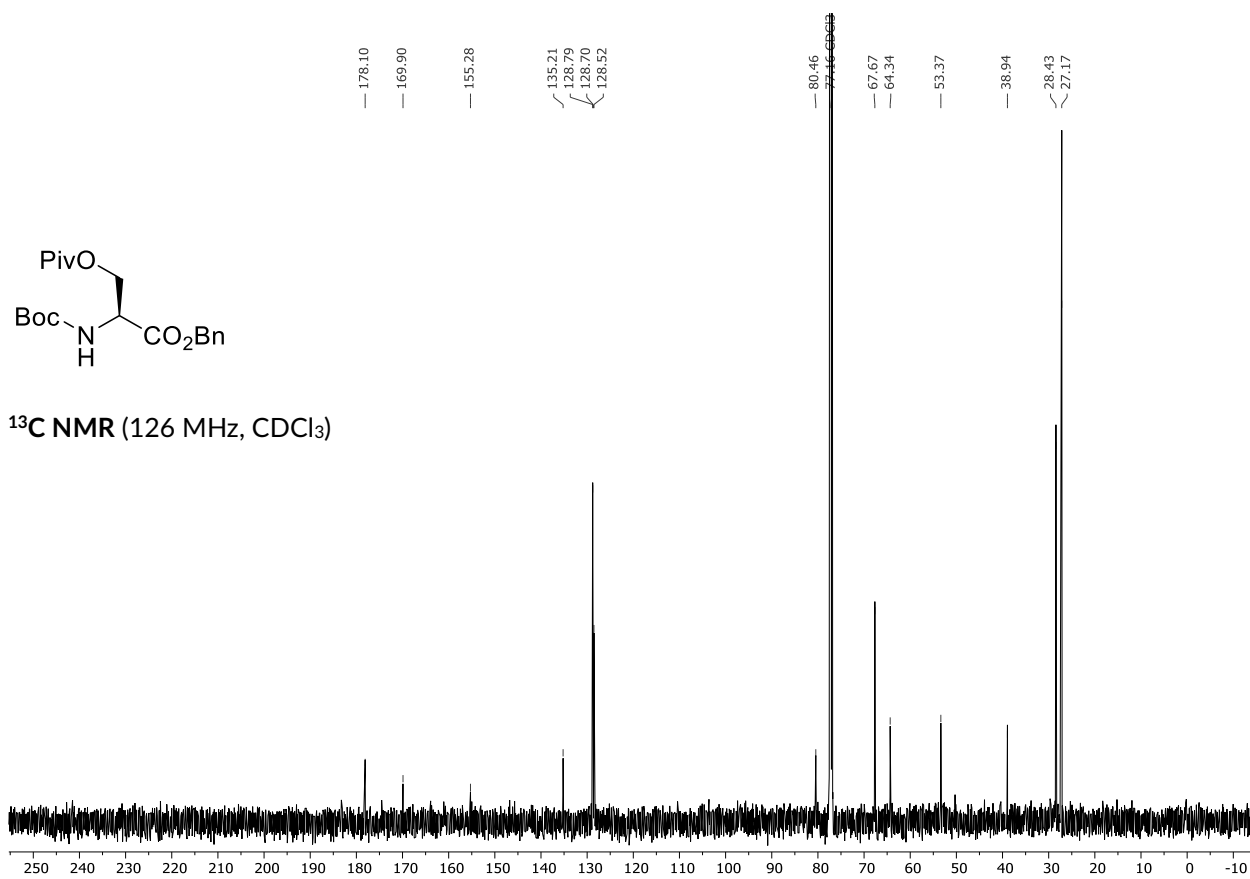
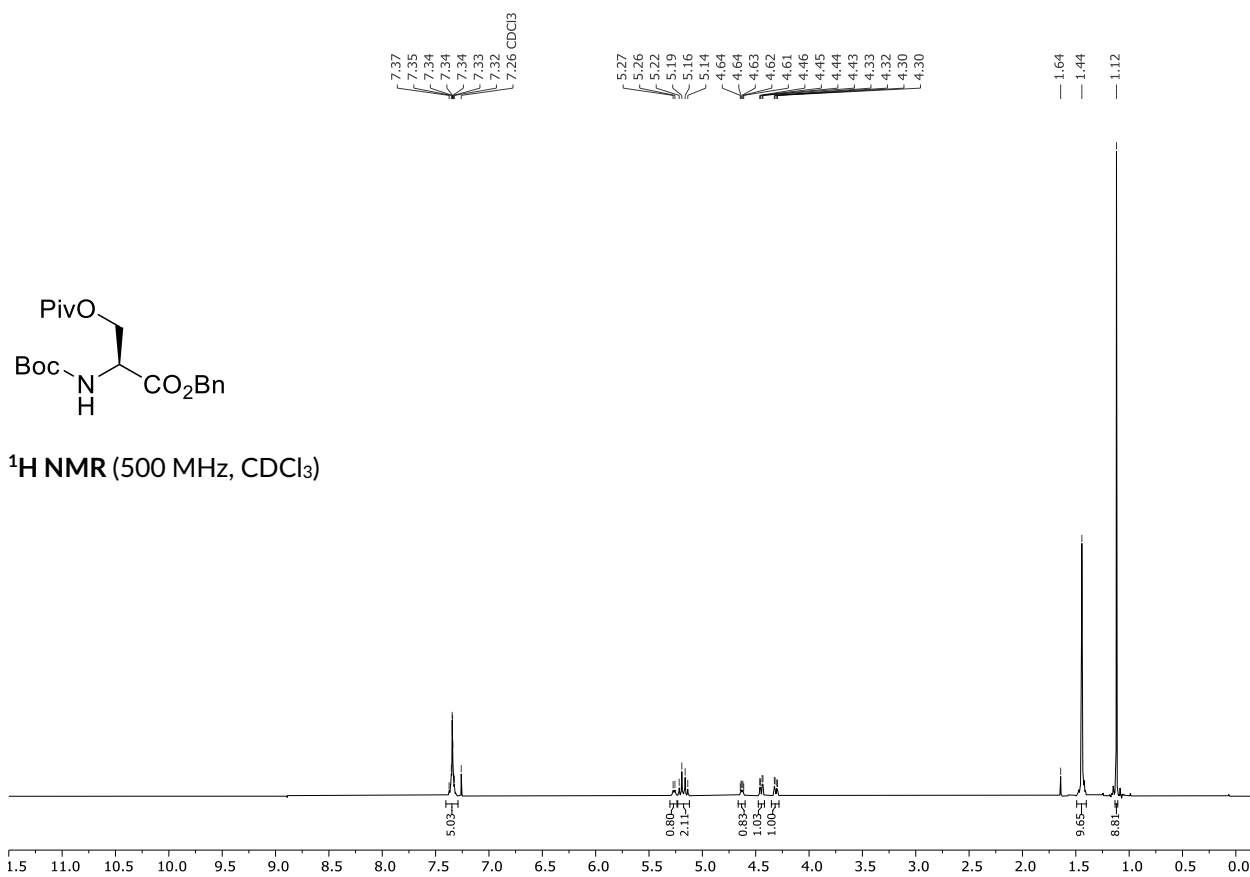
 ^1H NMR (600 MHz, CDCl_3) ^{13}C NMR (151 MHz, CDCl_3)

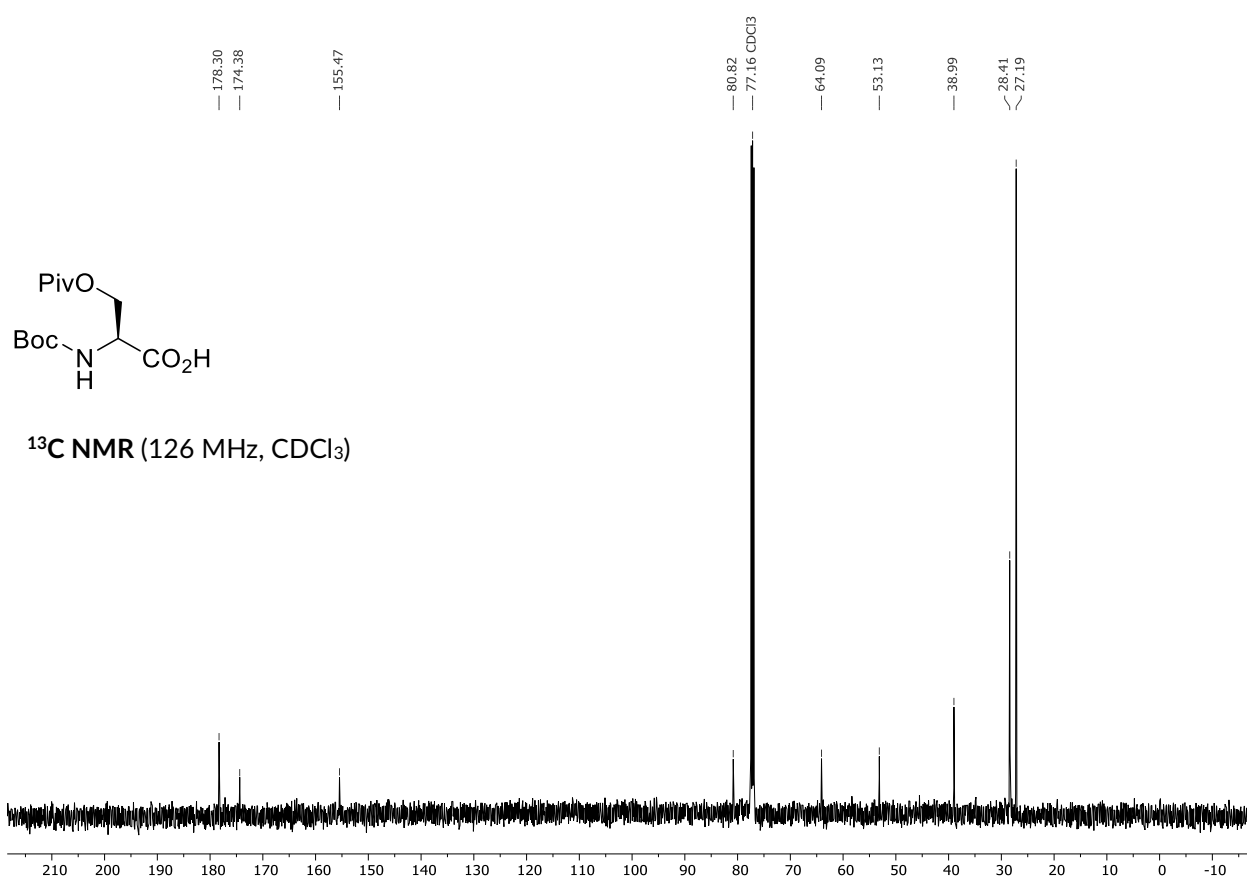
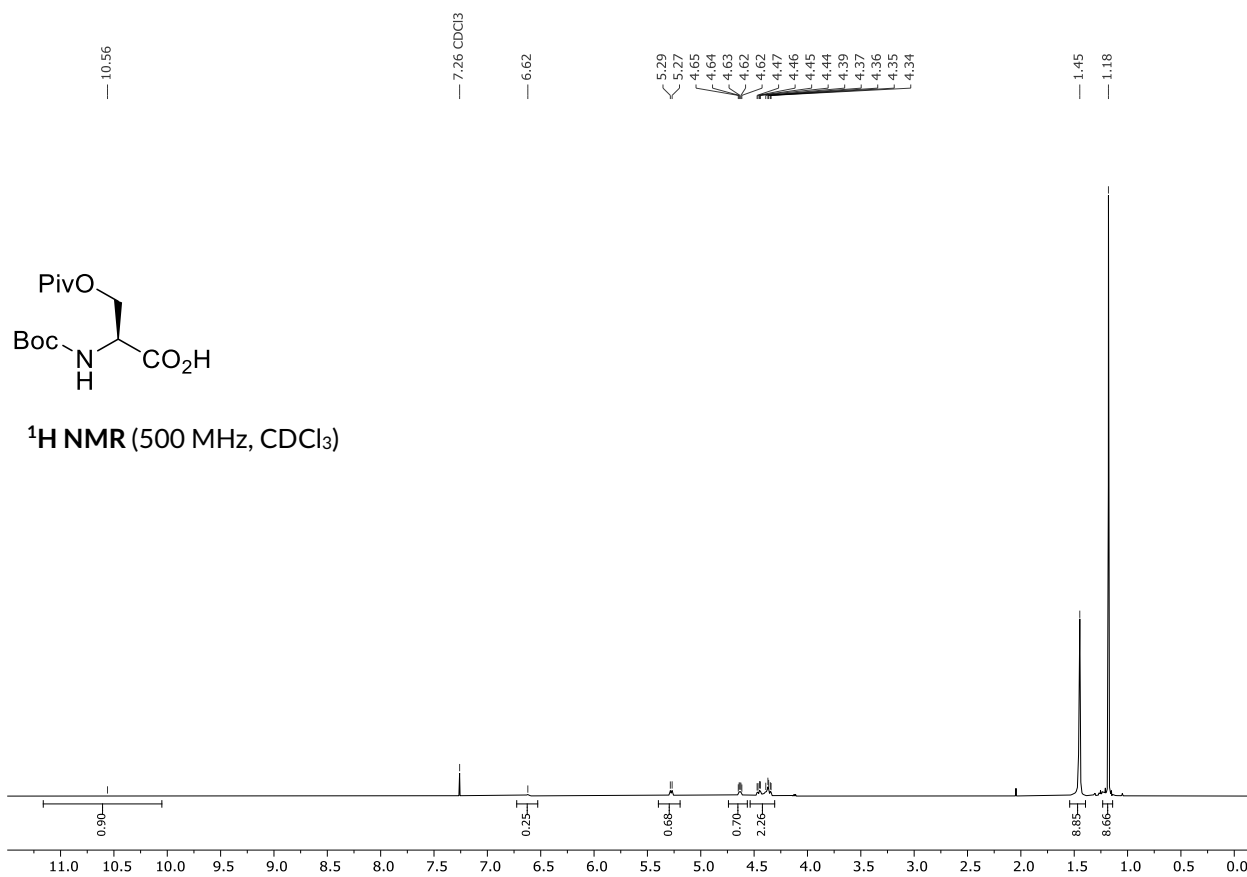


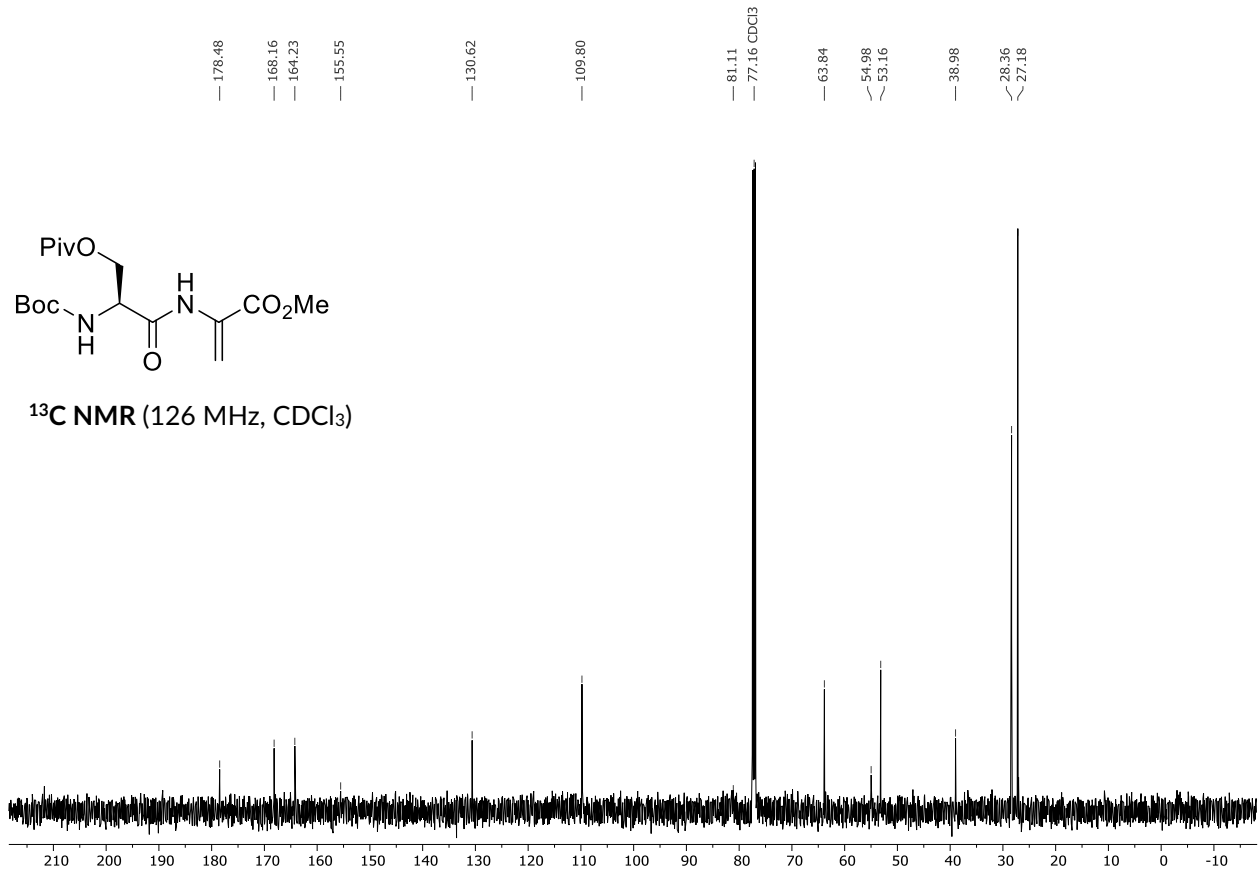
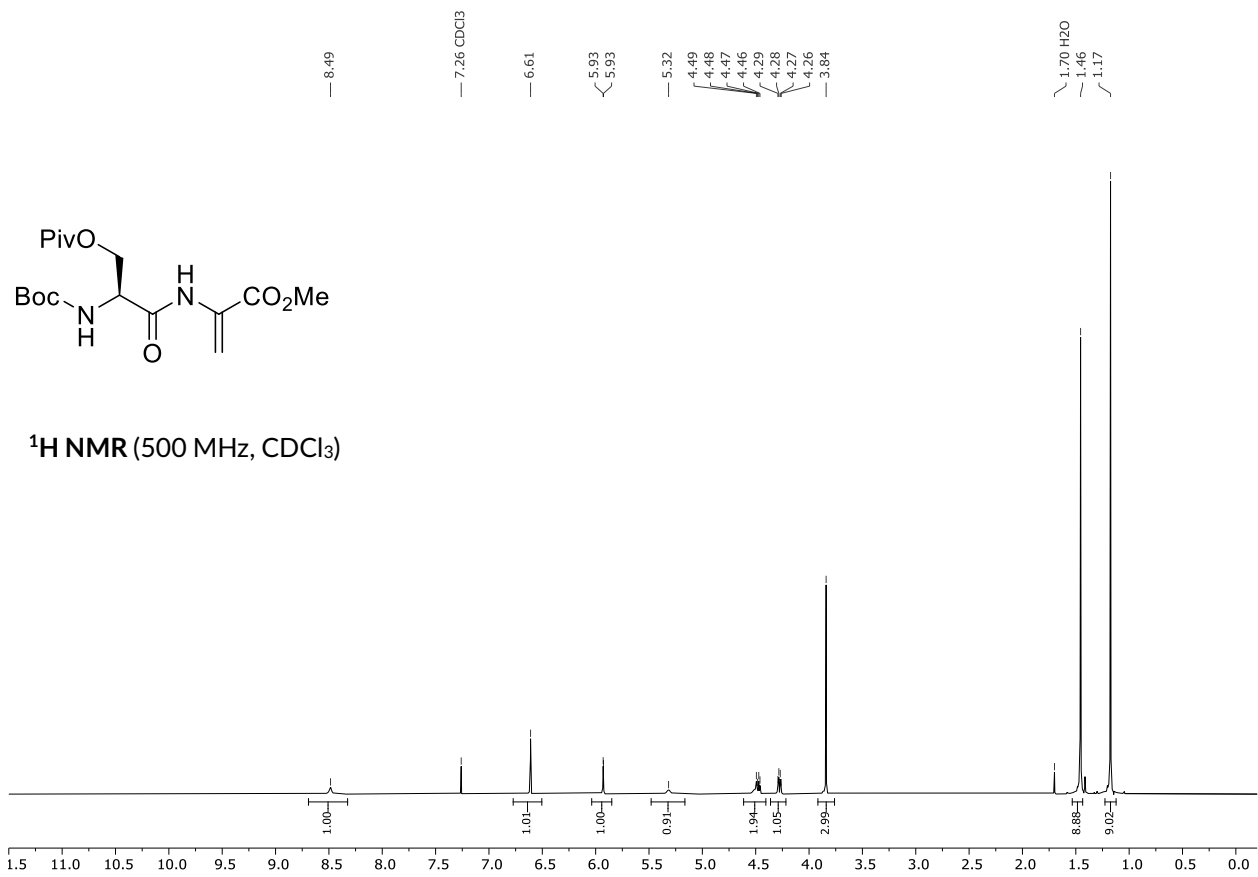


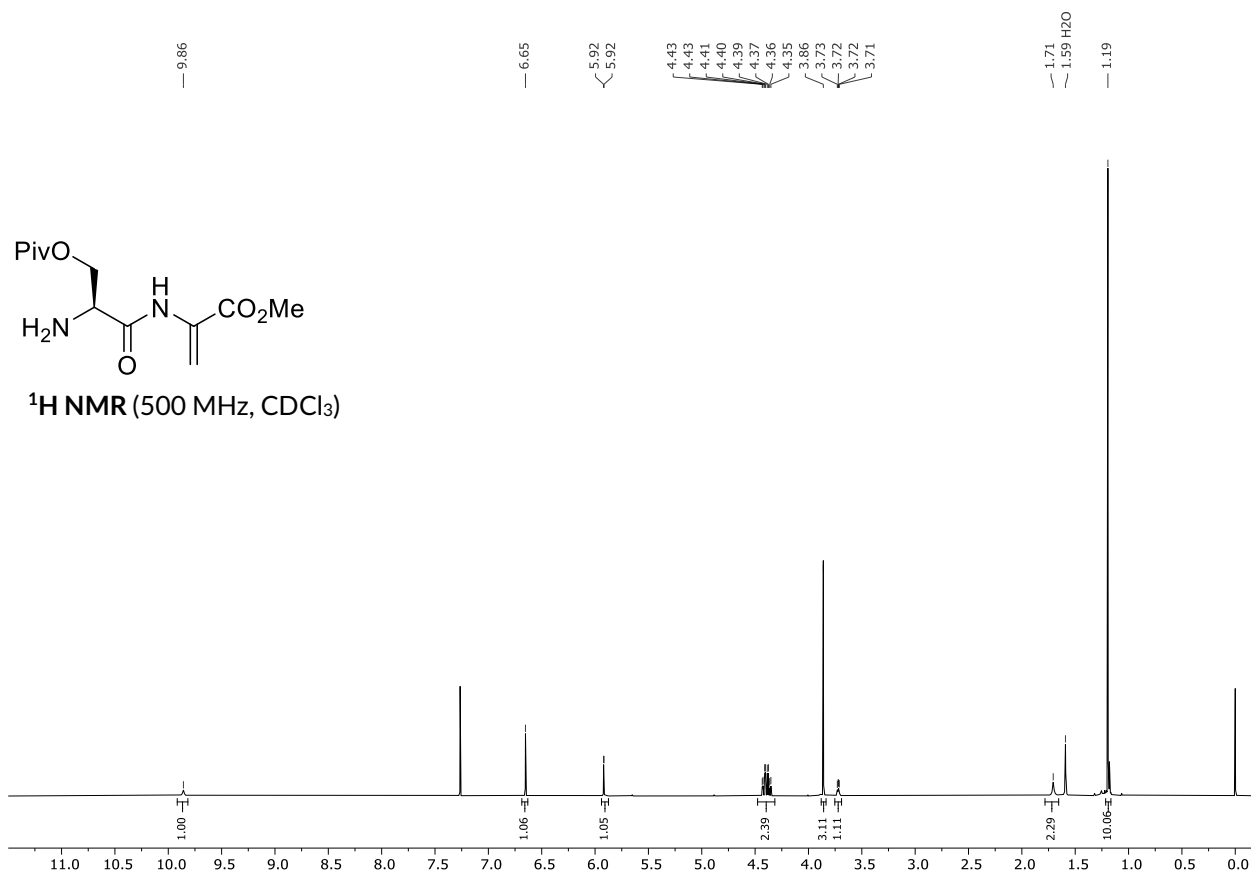


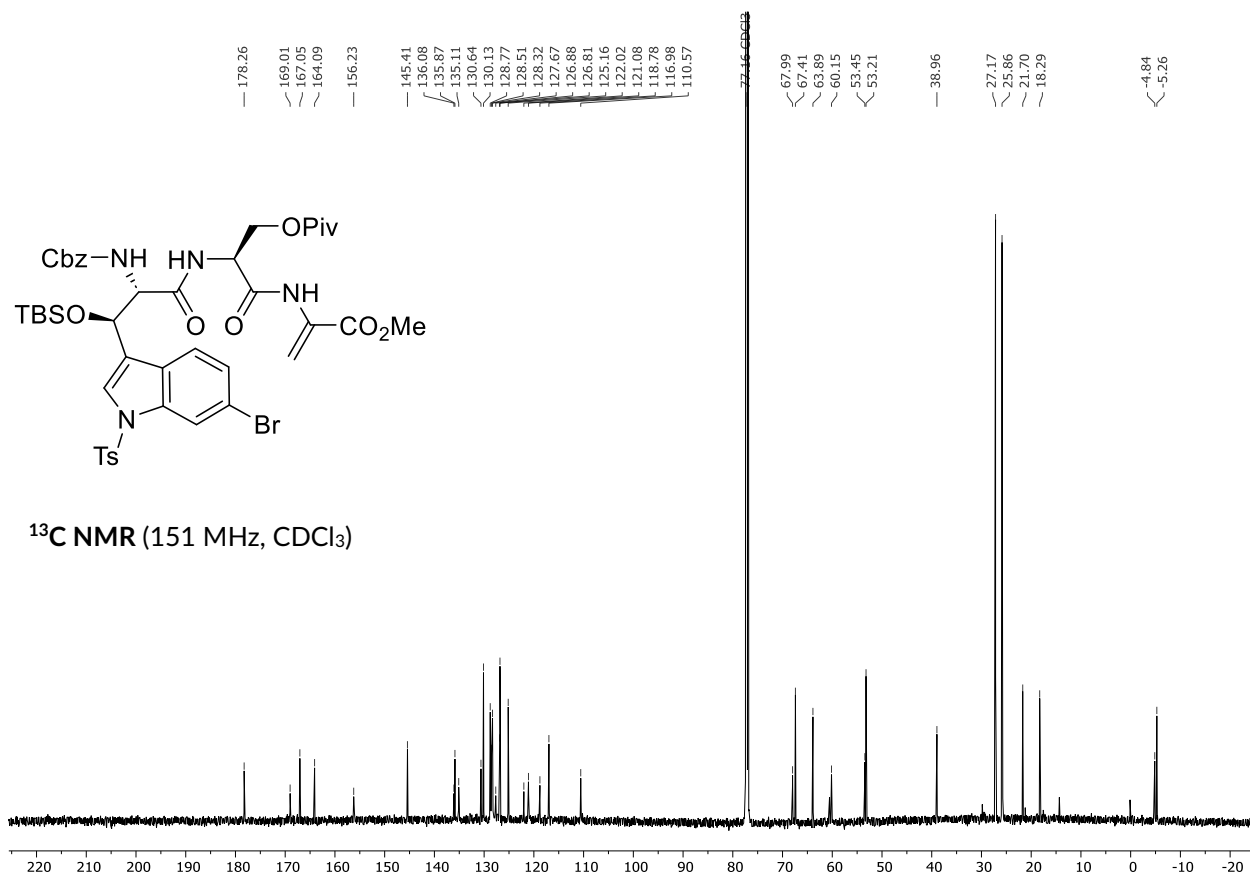
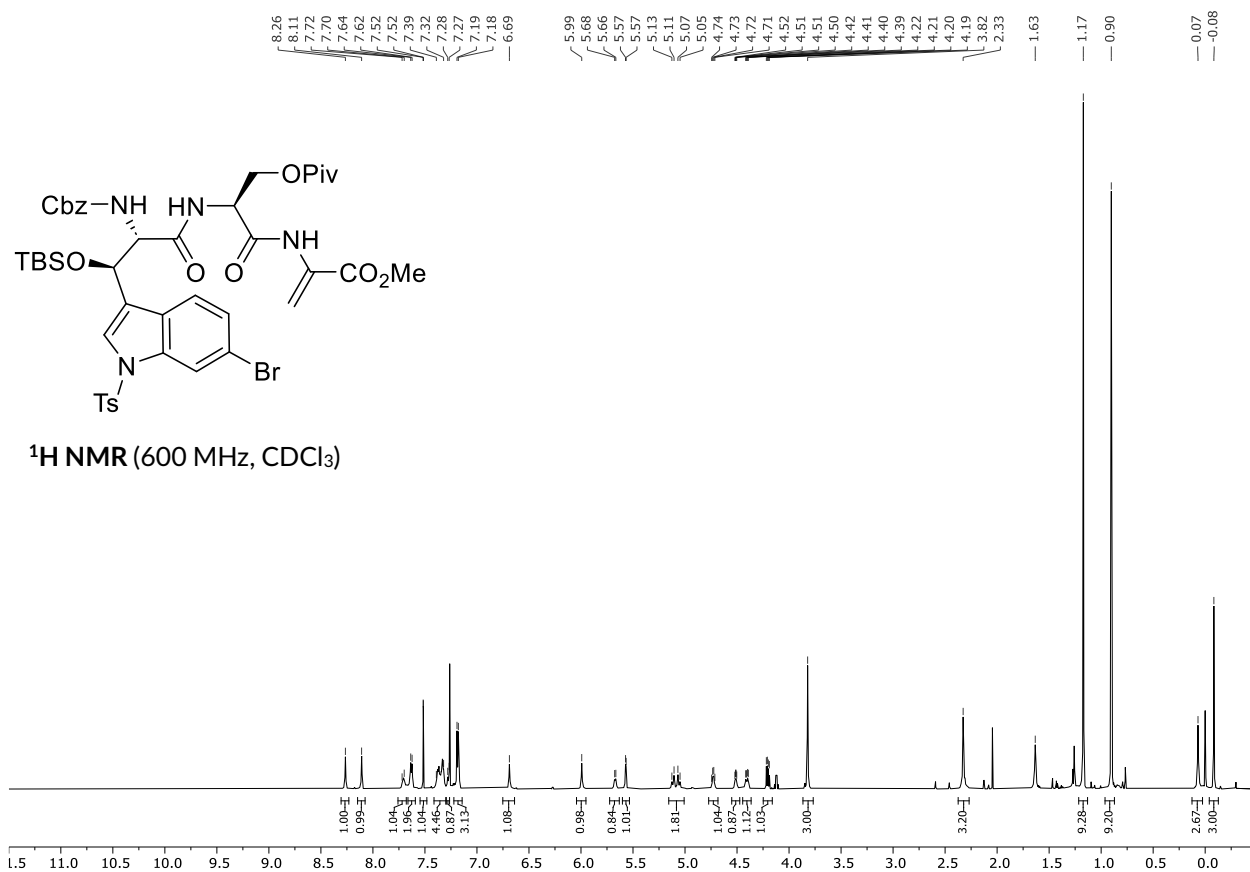




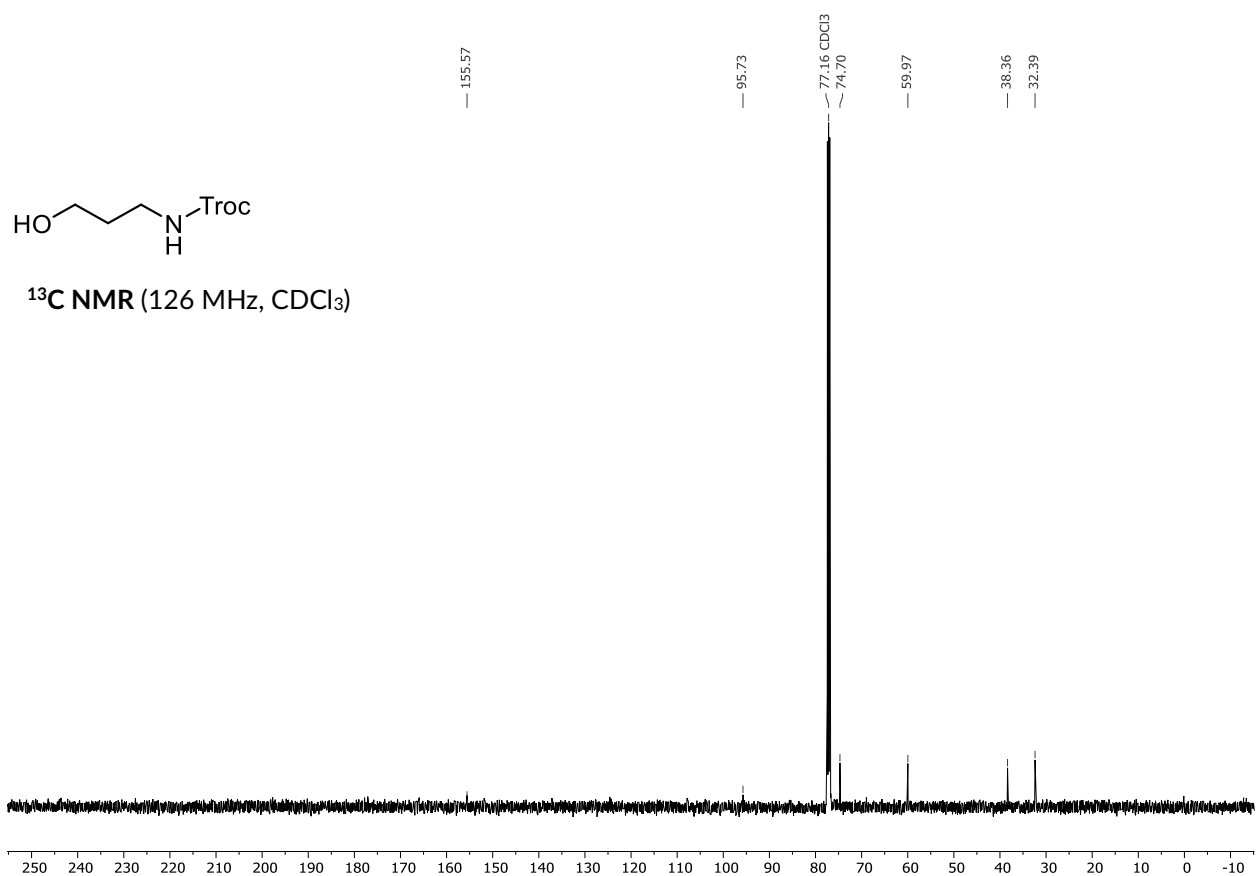
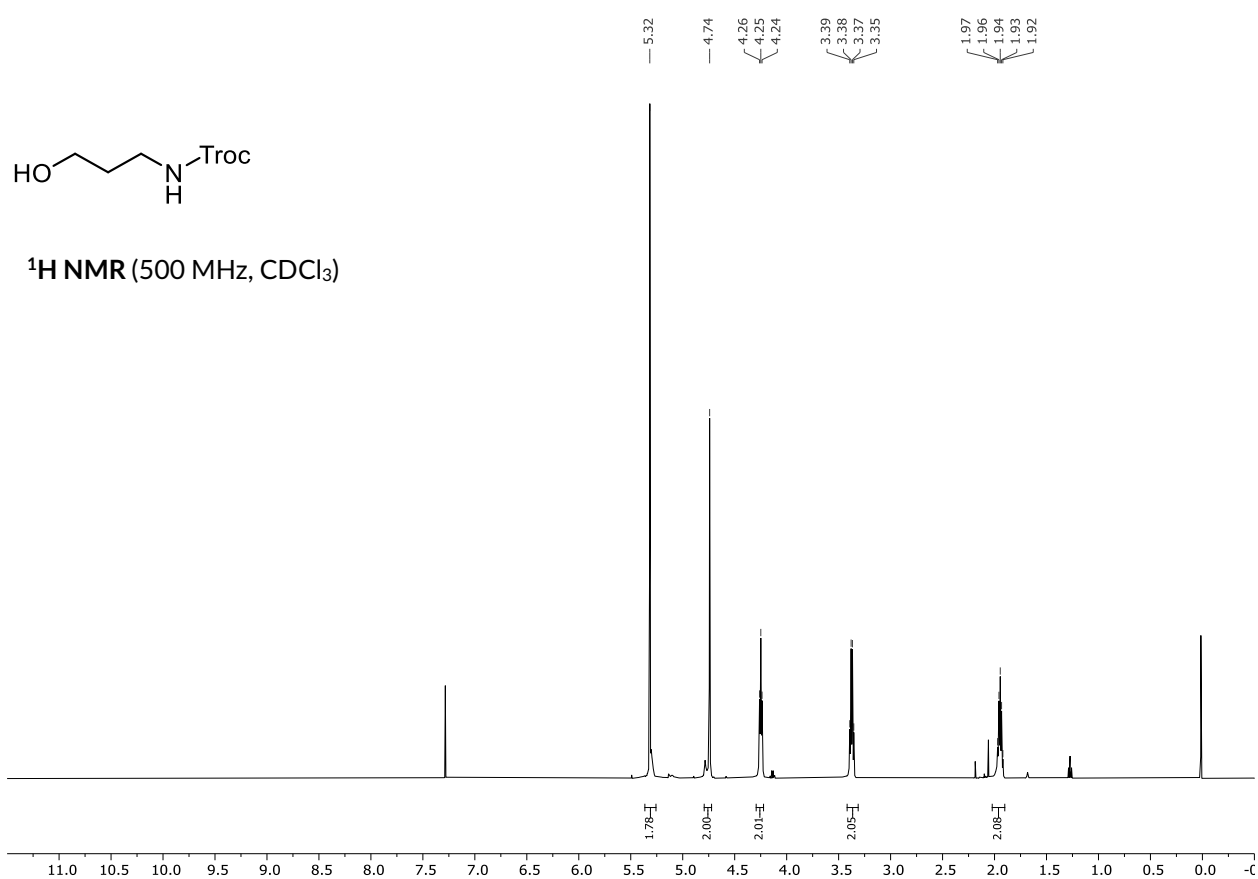


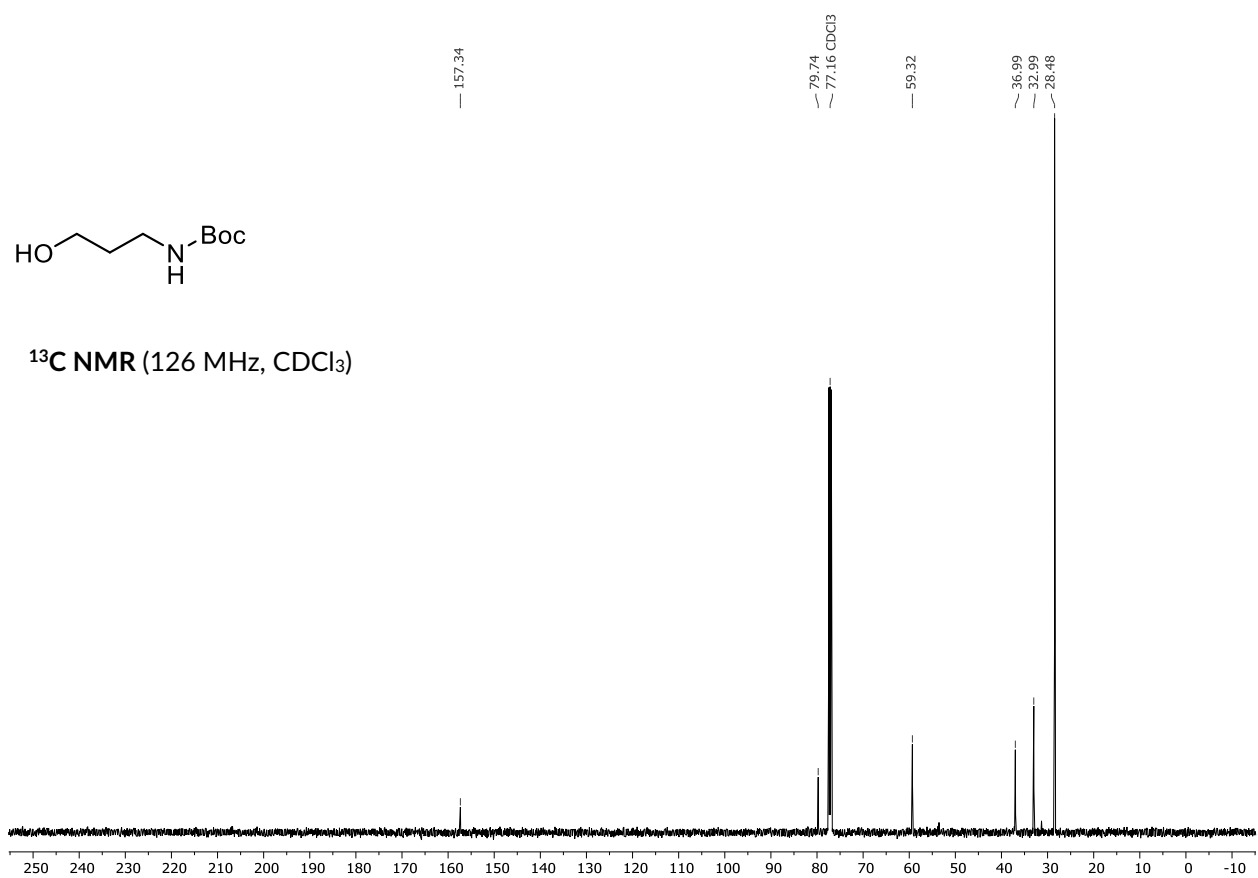
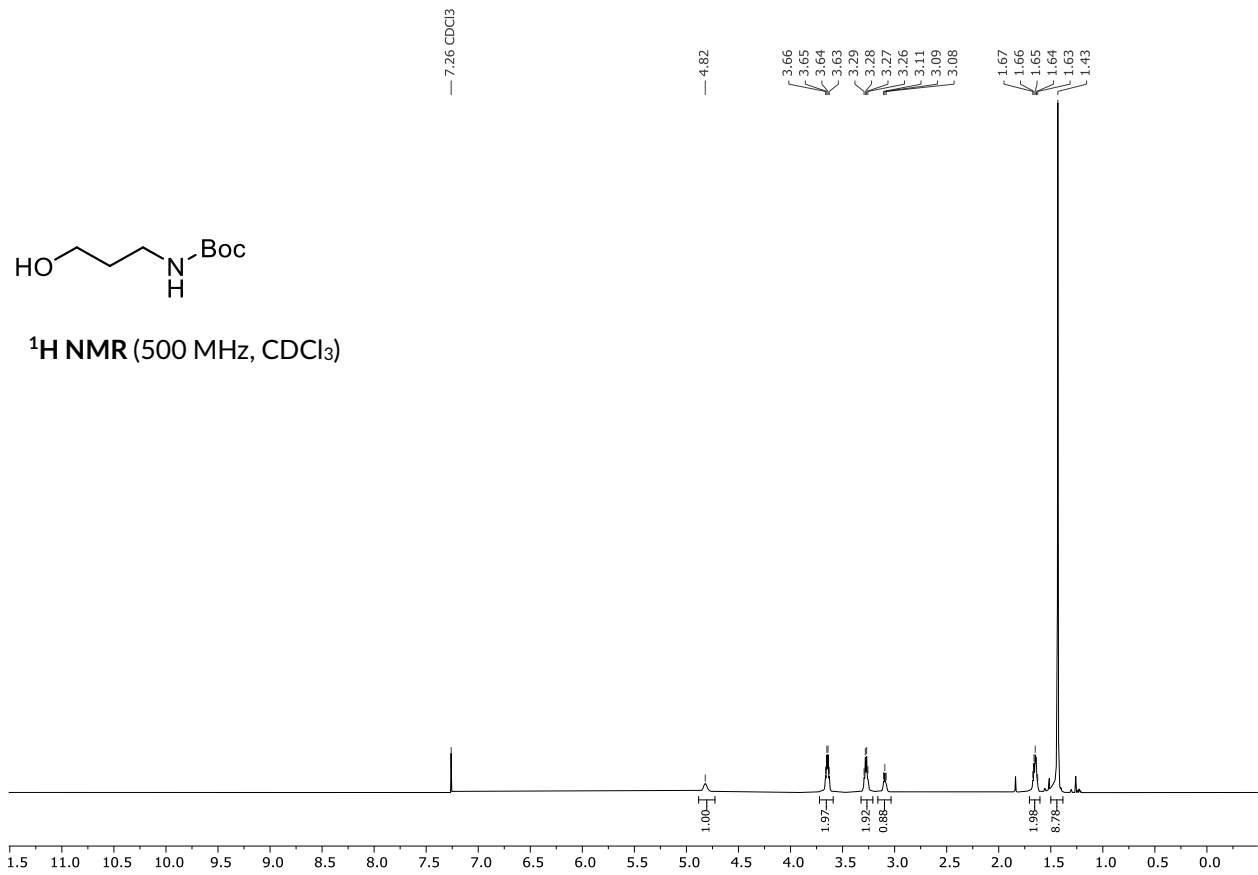


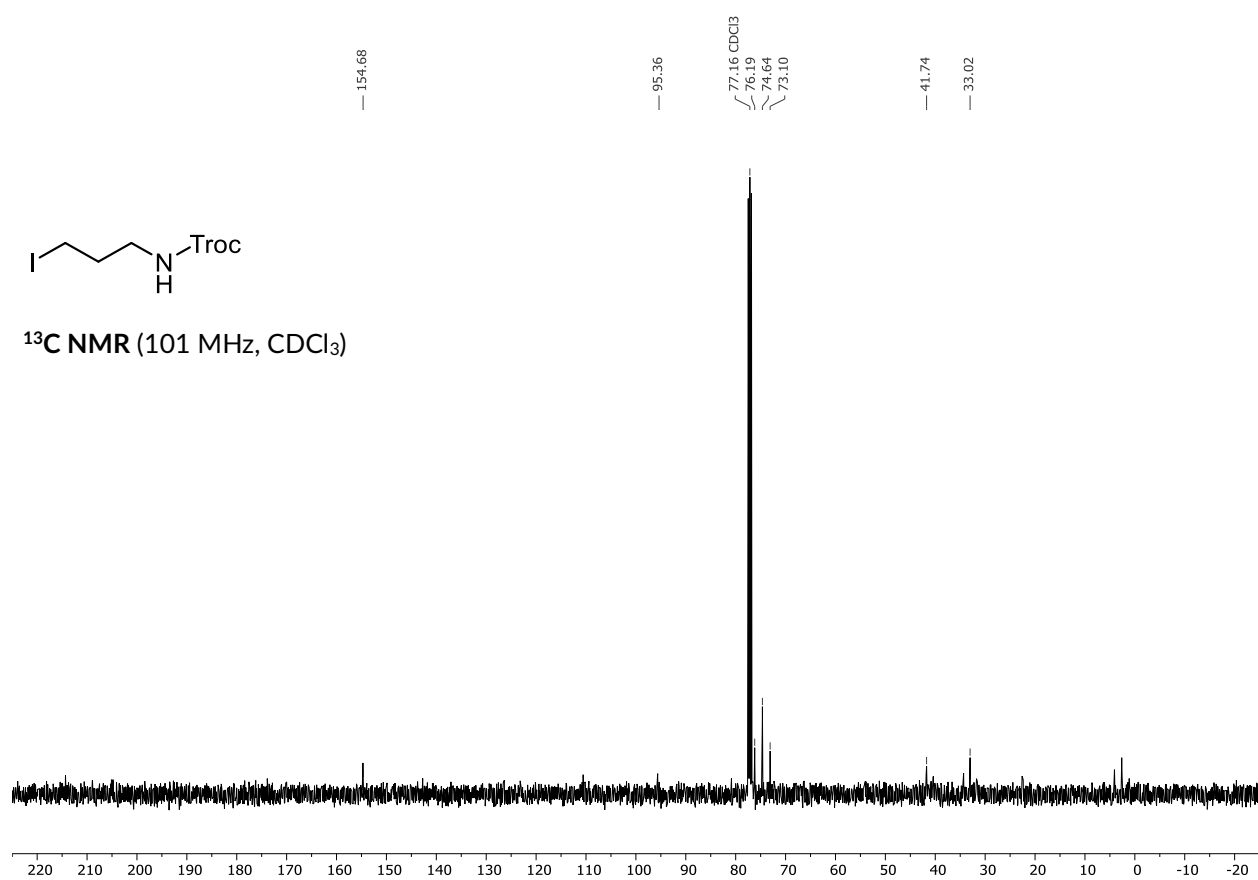
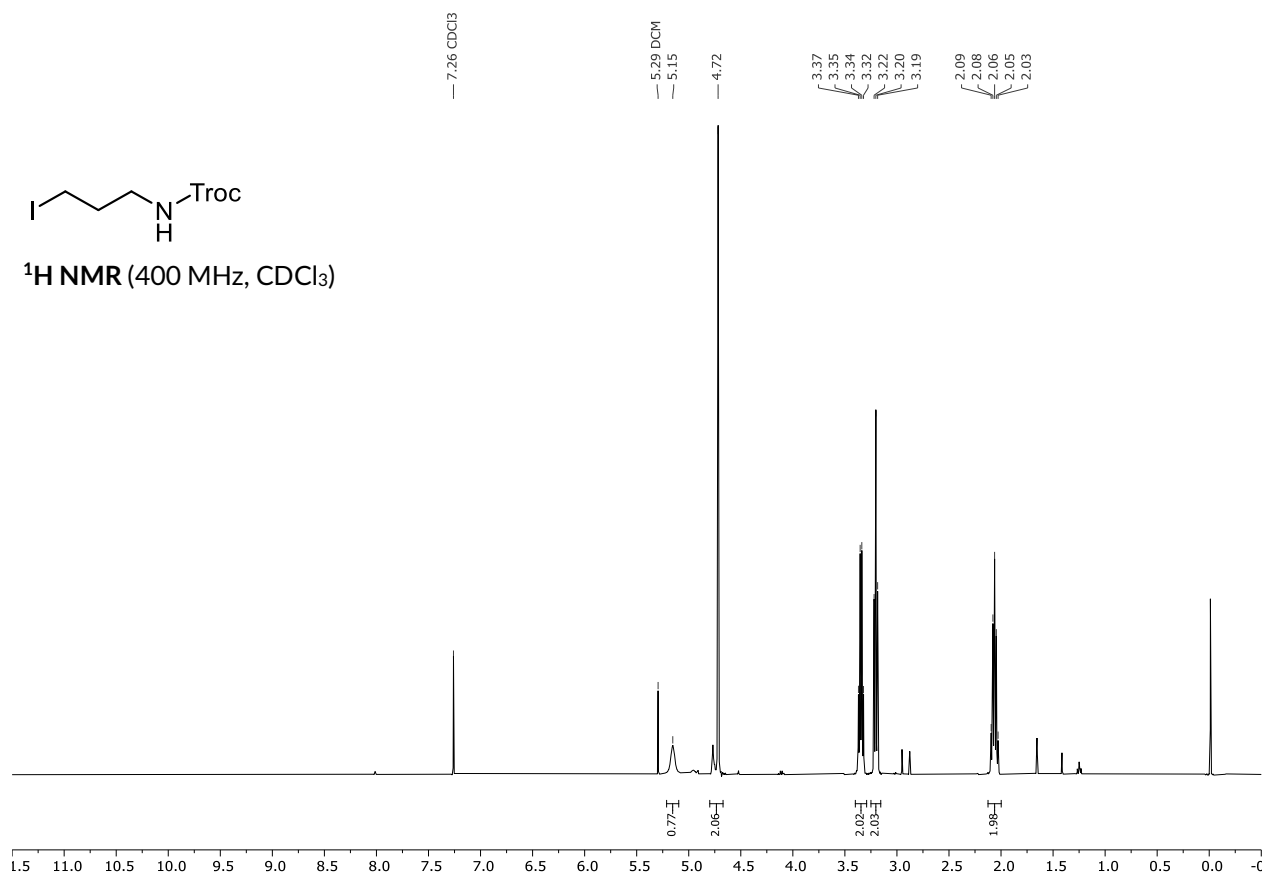


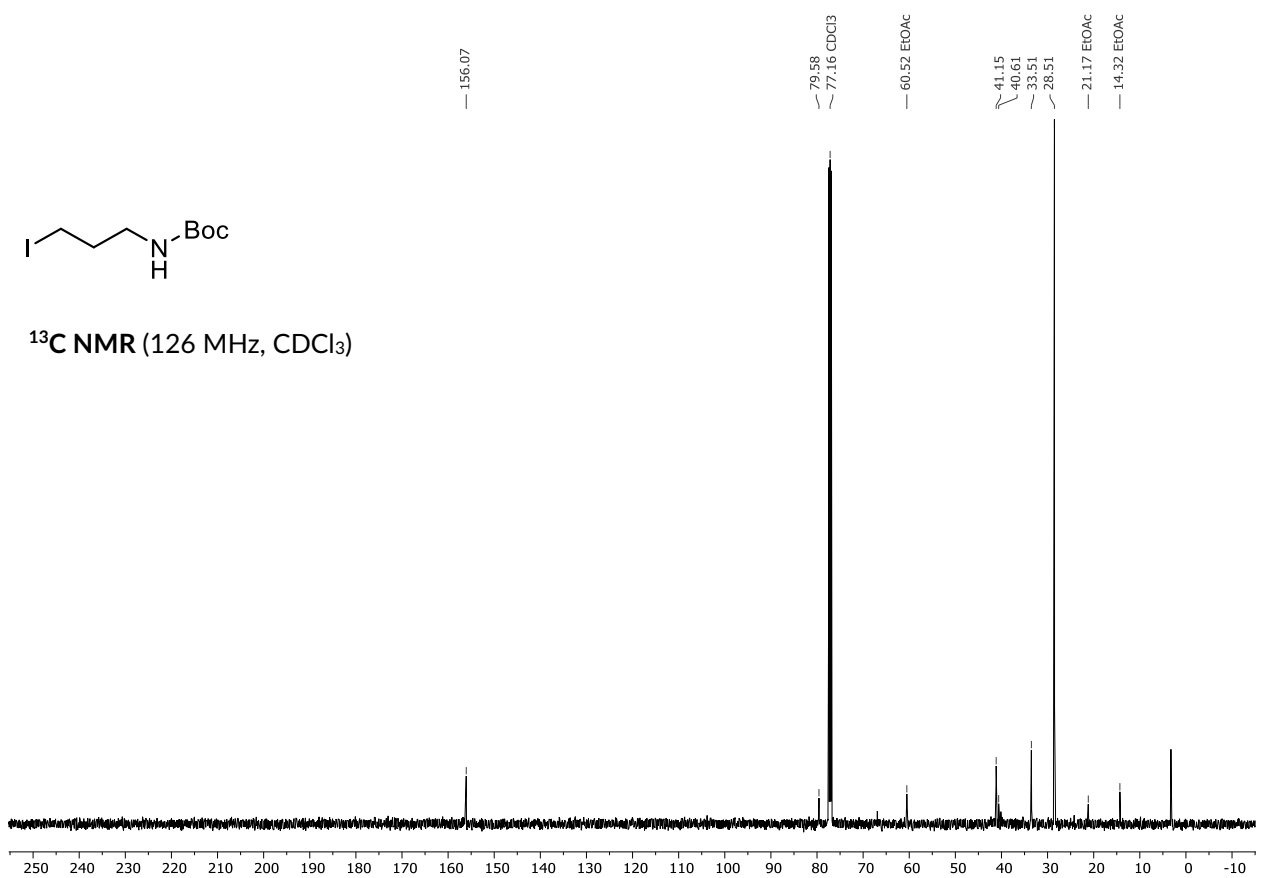
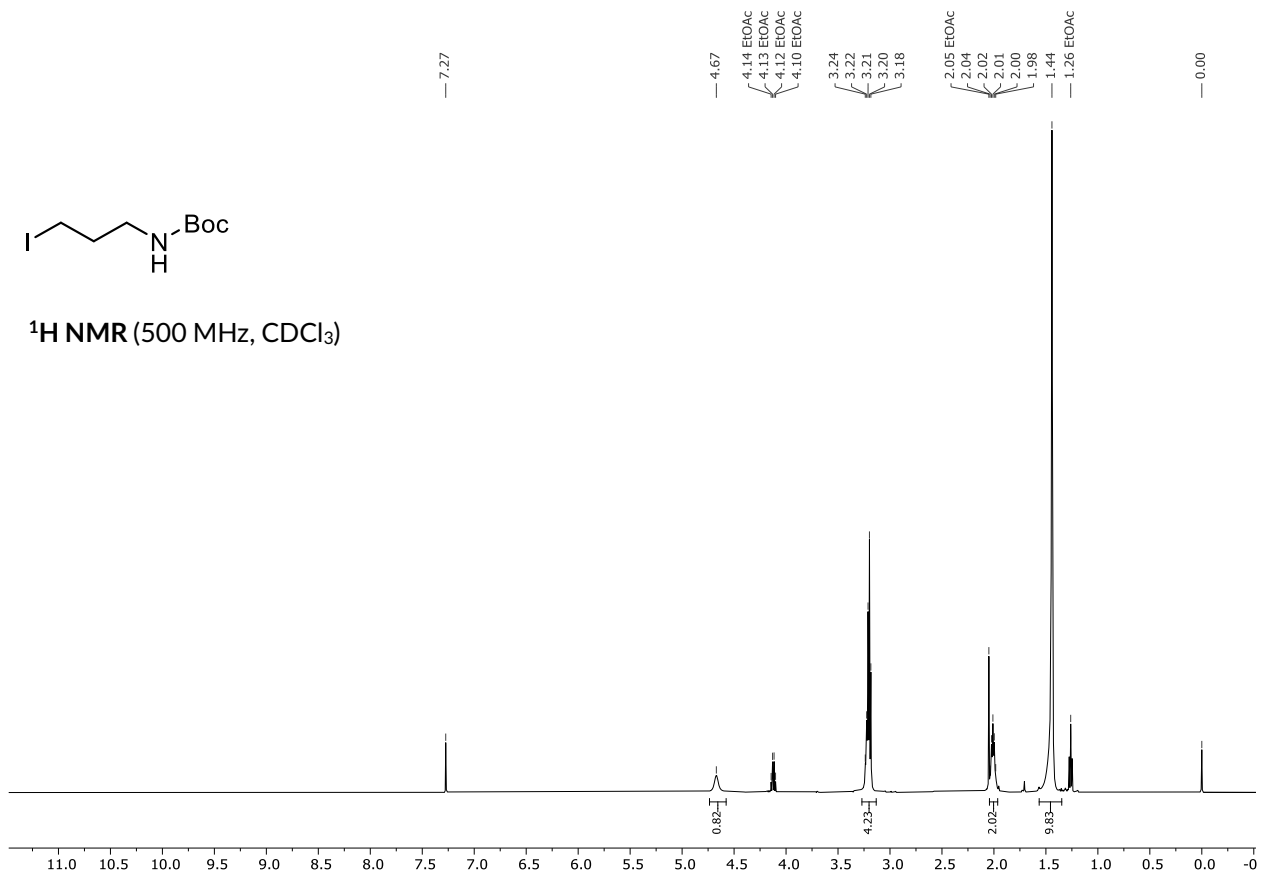


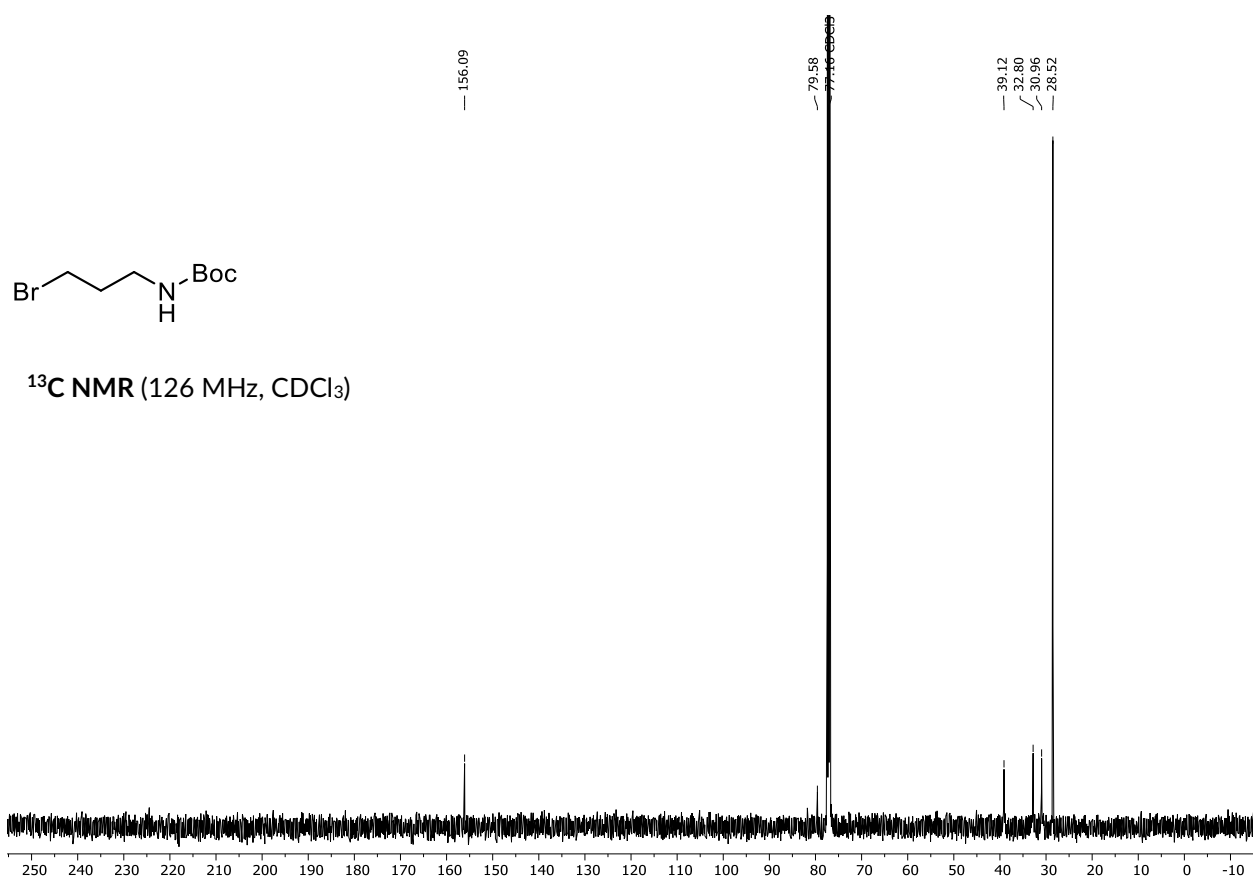
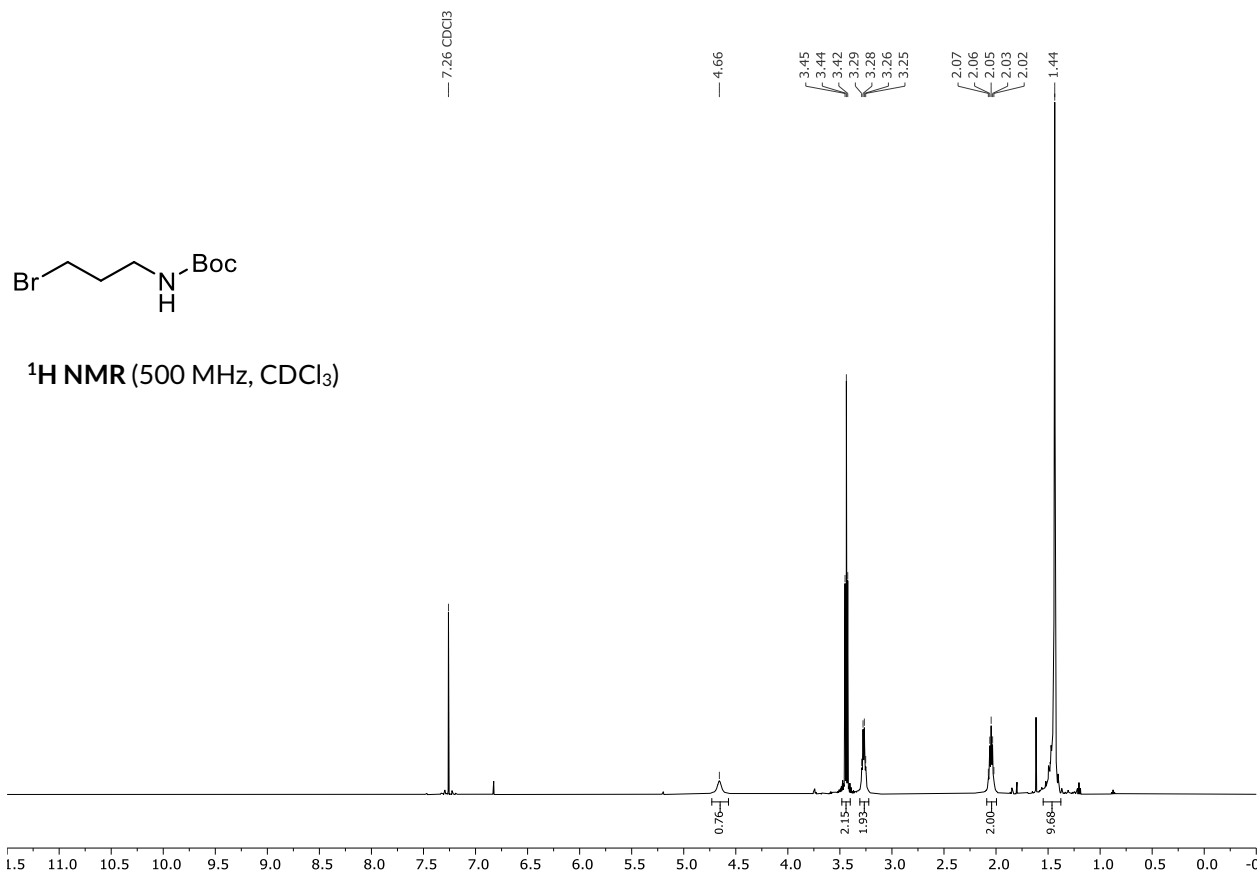
7.2.6. Installation of the Lysine Side Chain

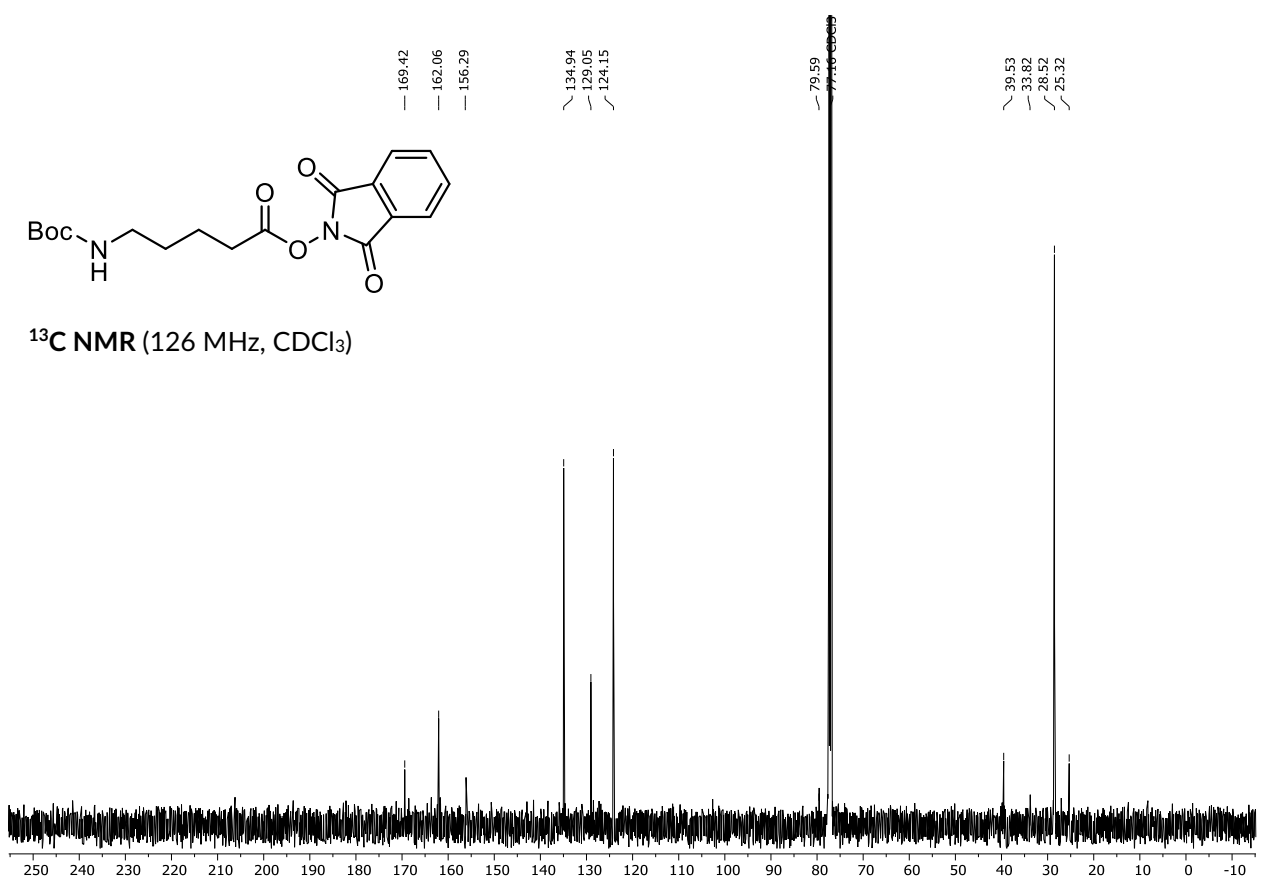
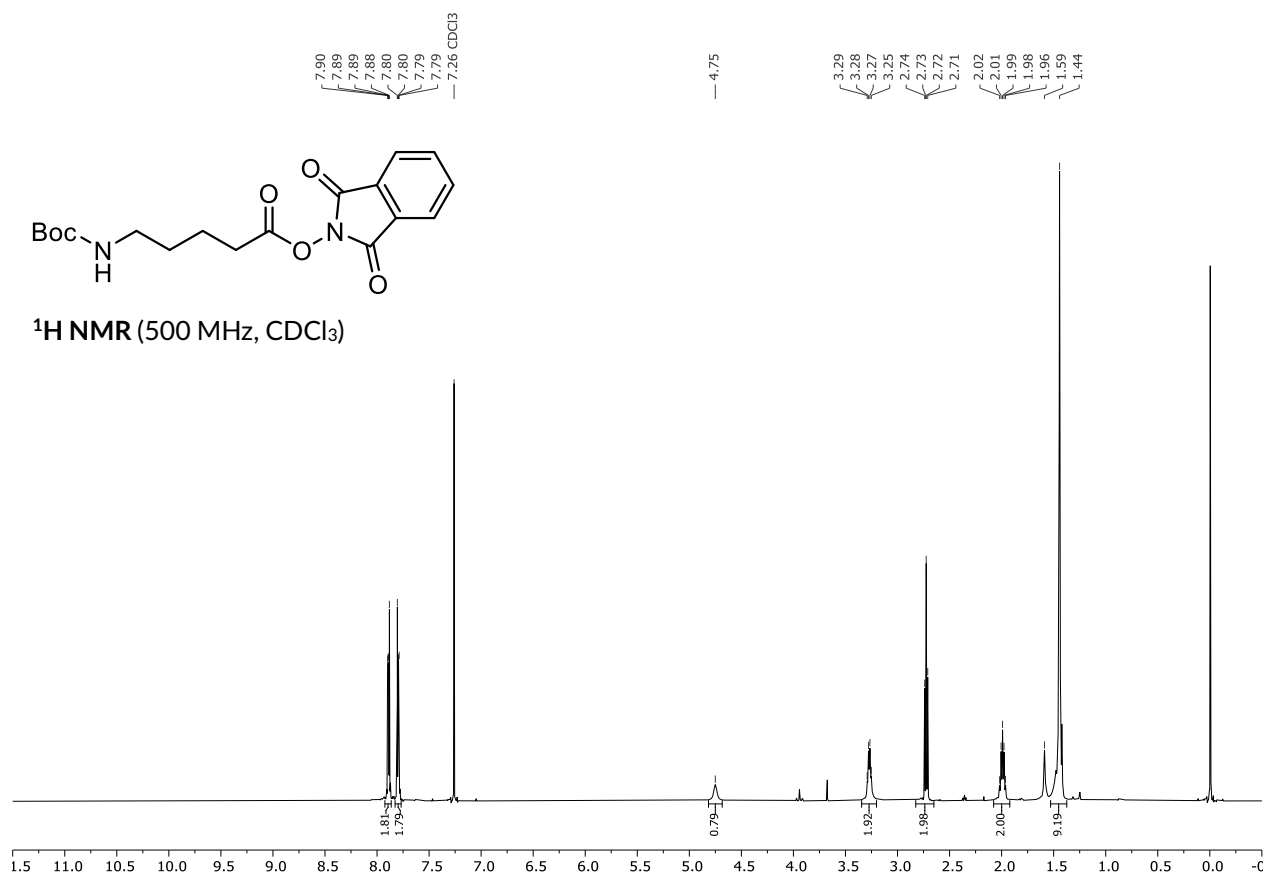


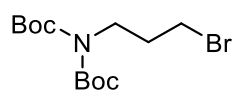




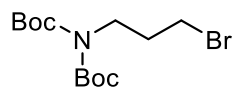
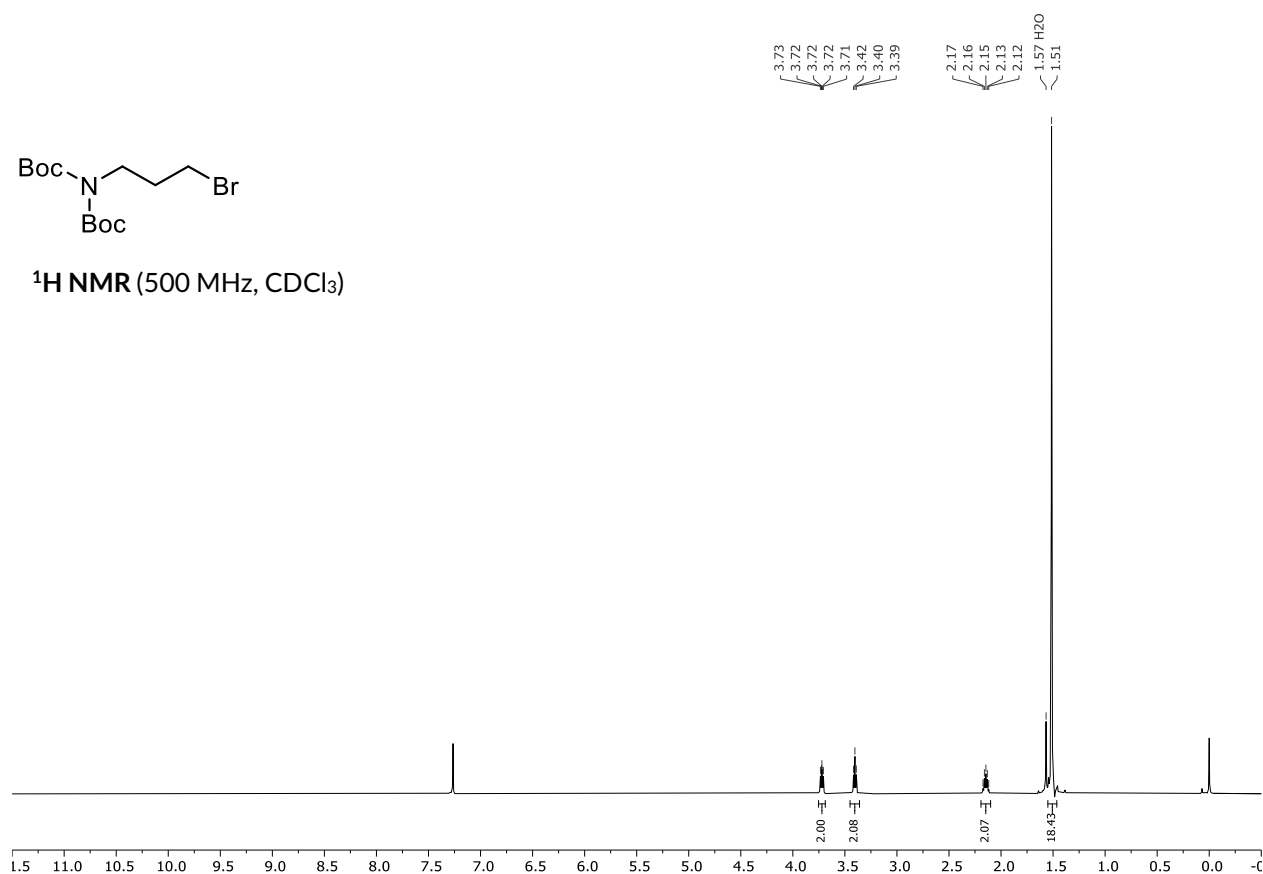




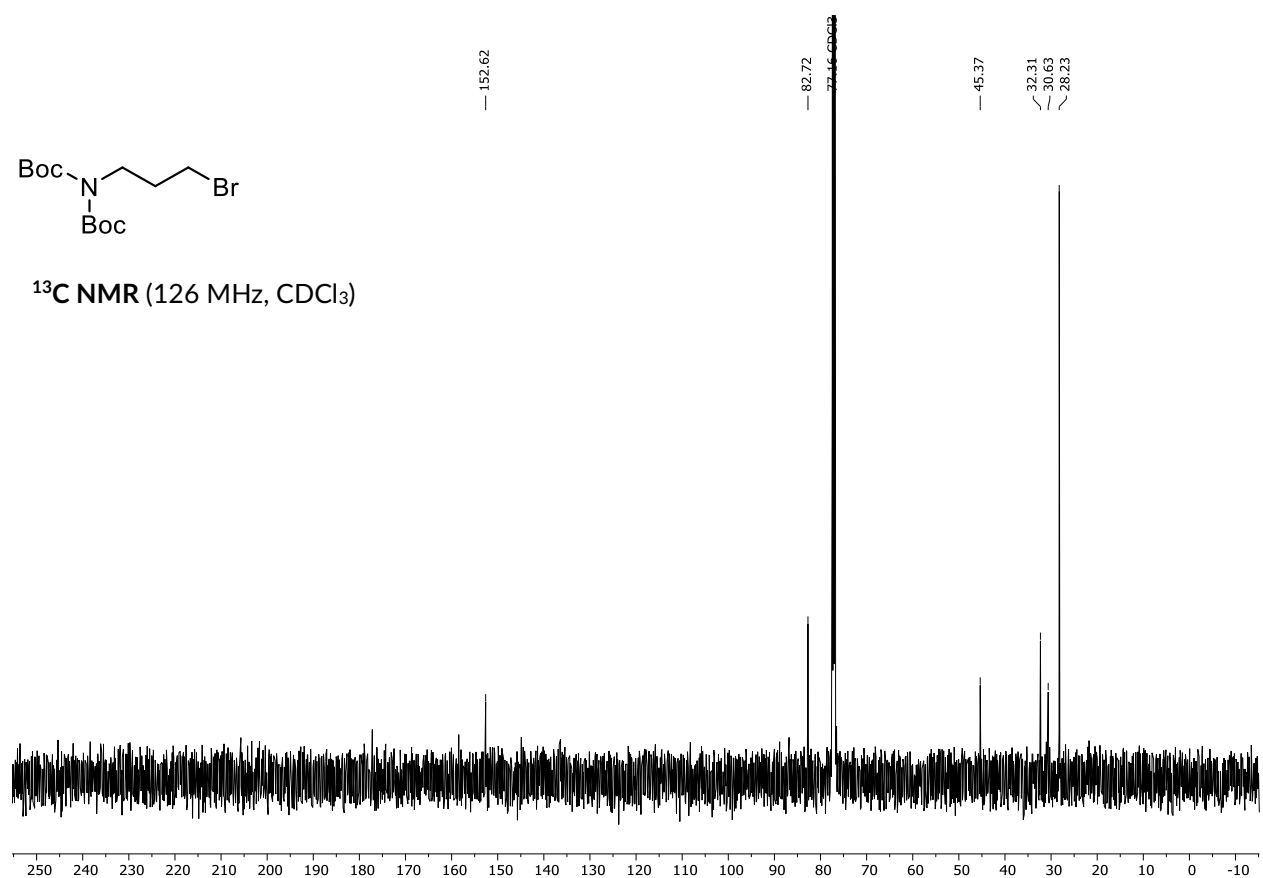


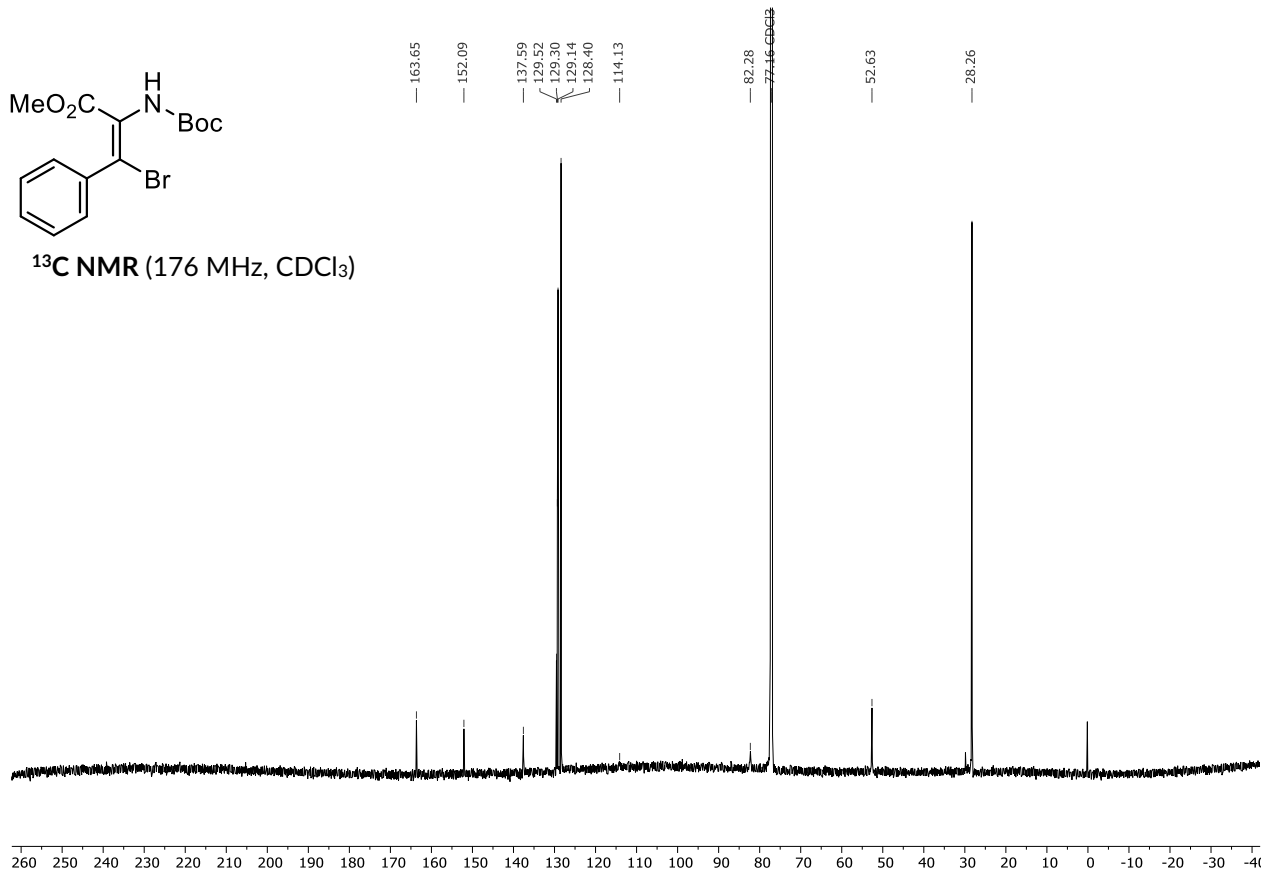
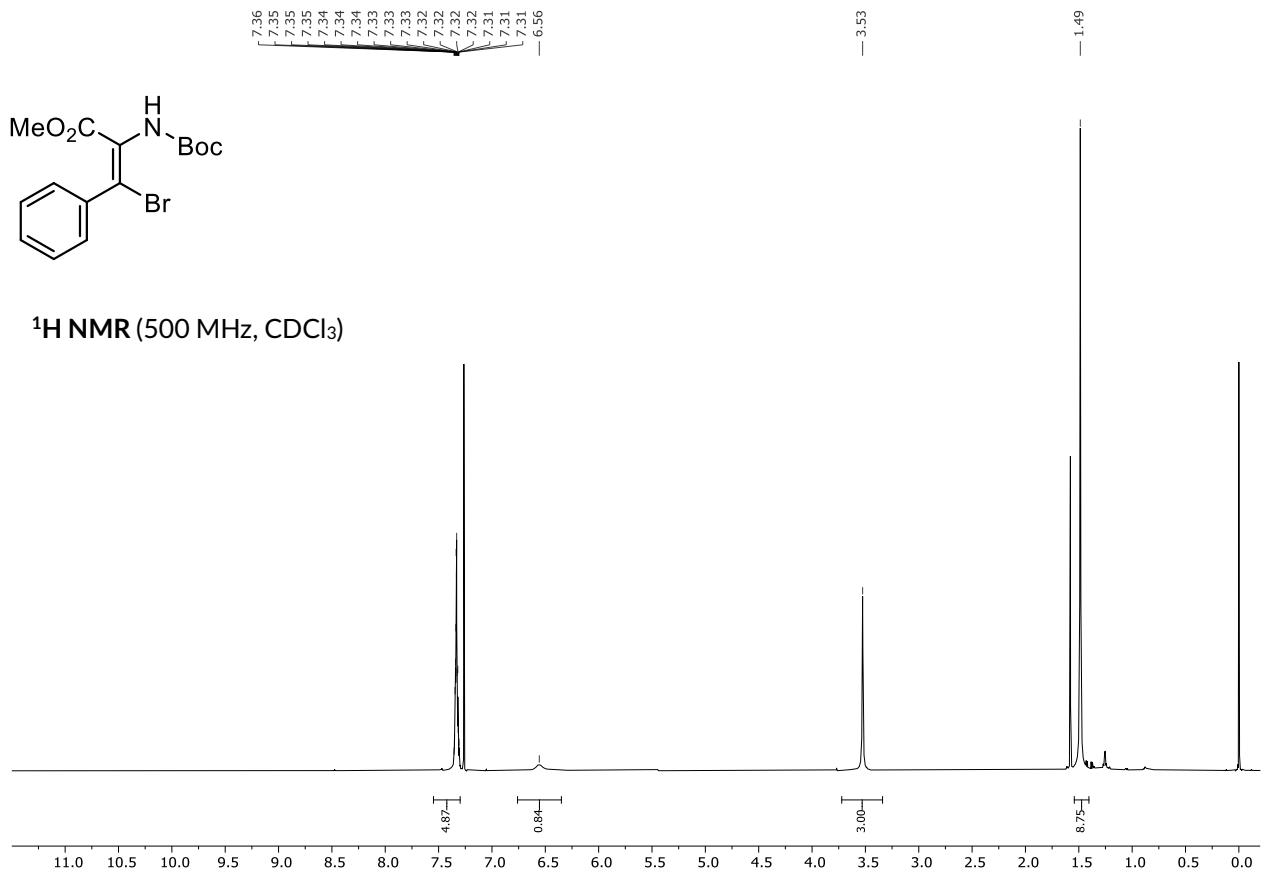


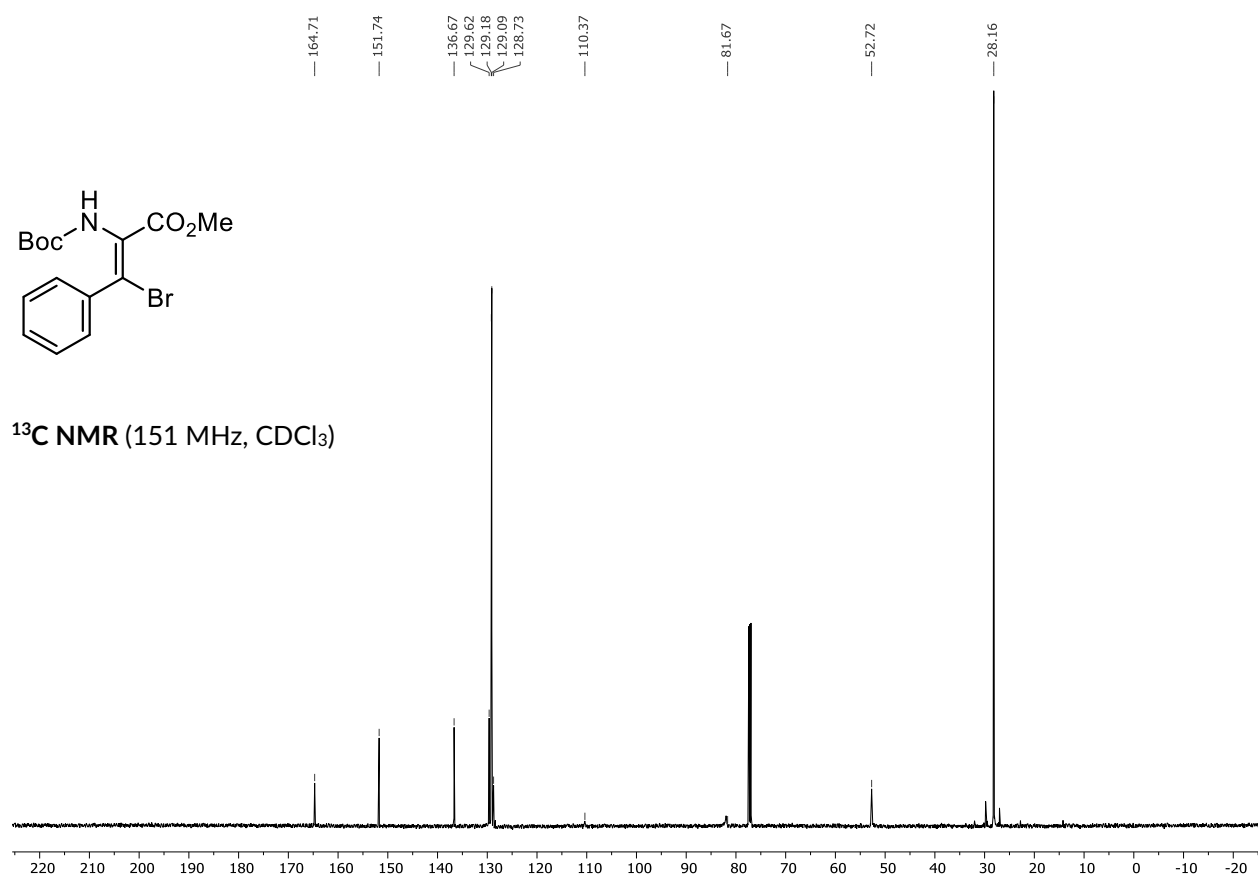
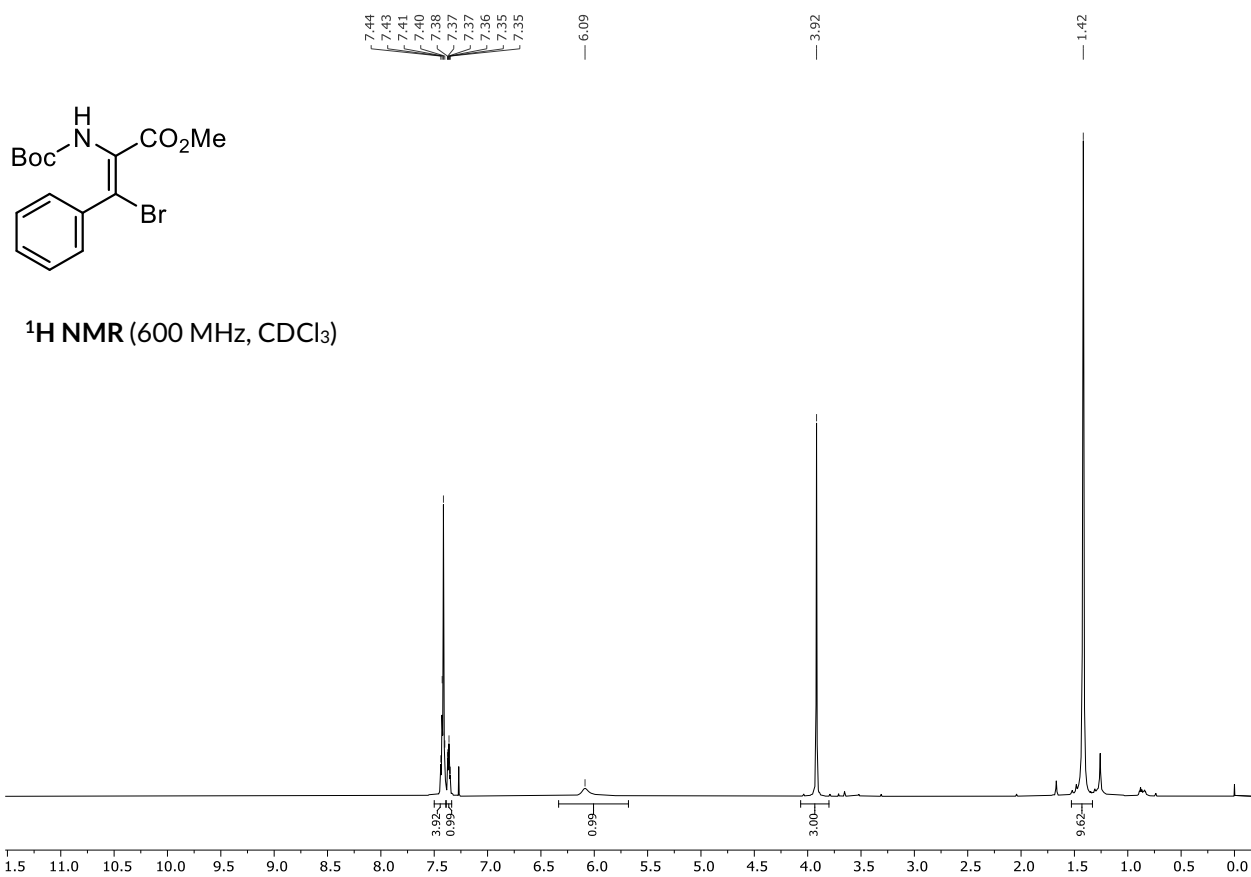
^1H NMR (500 MHz, CDCl_3)

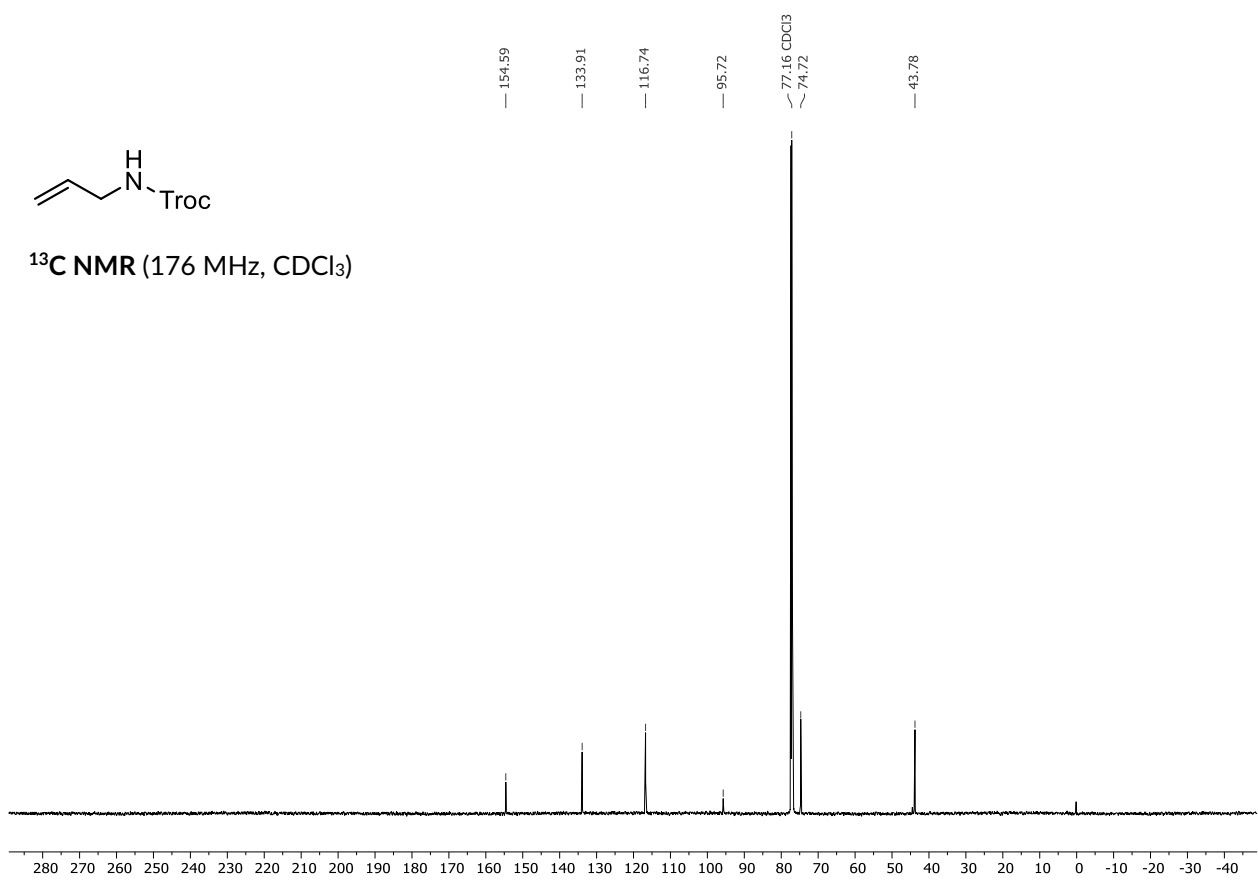
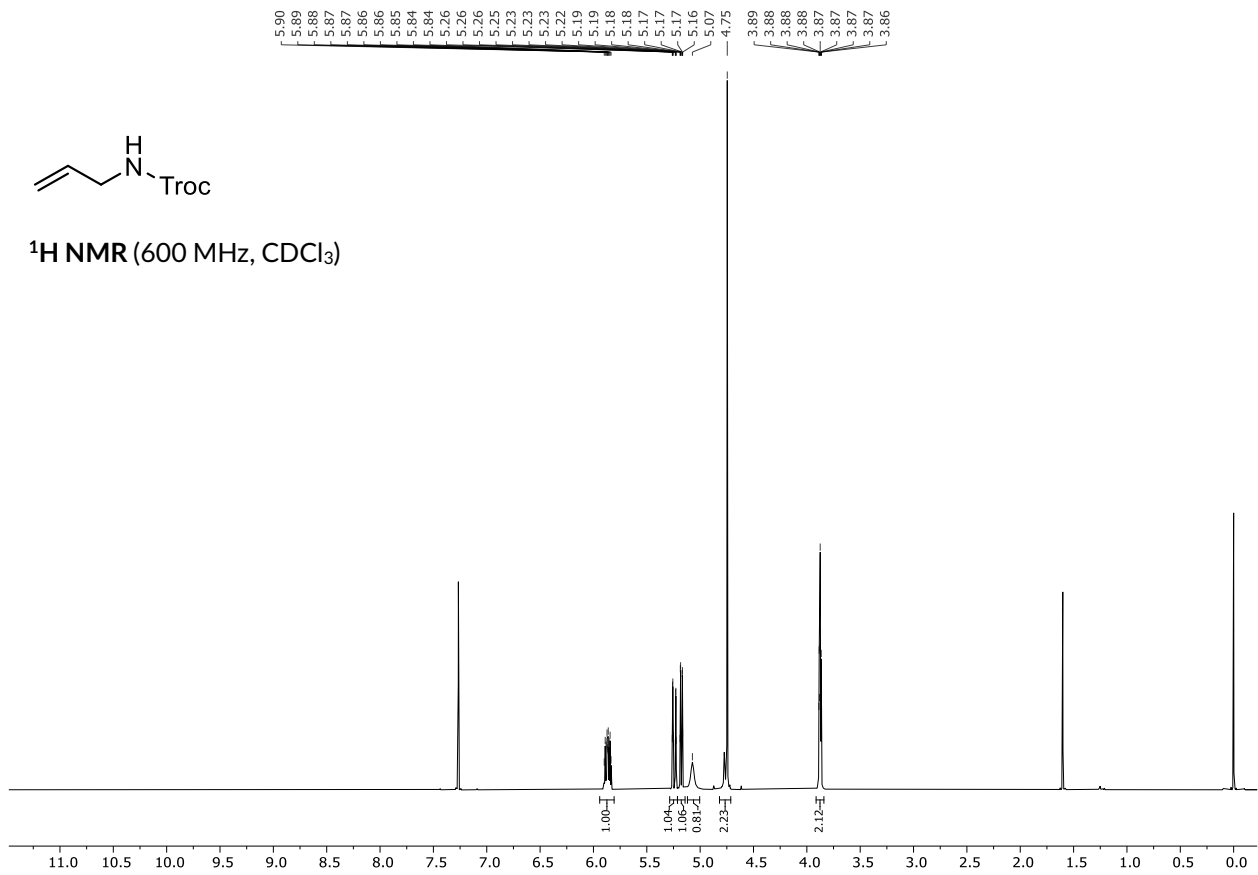


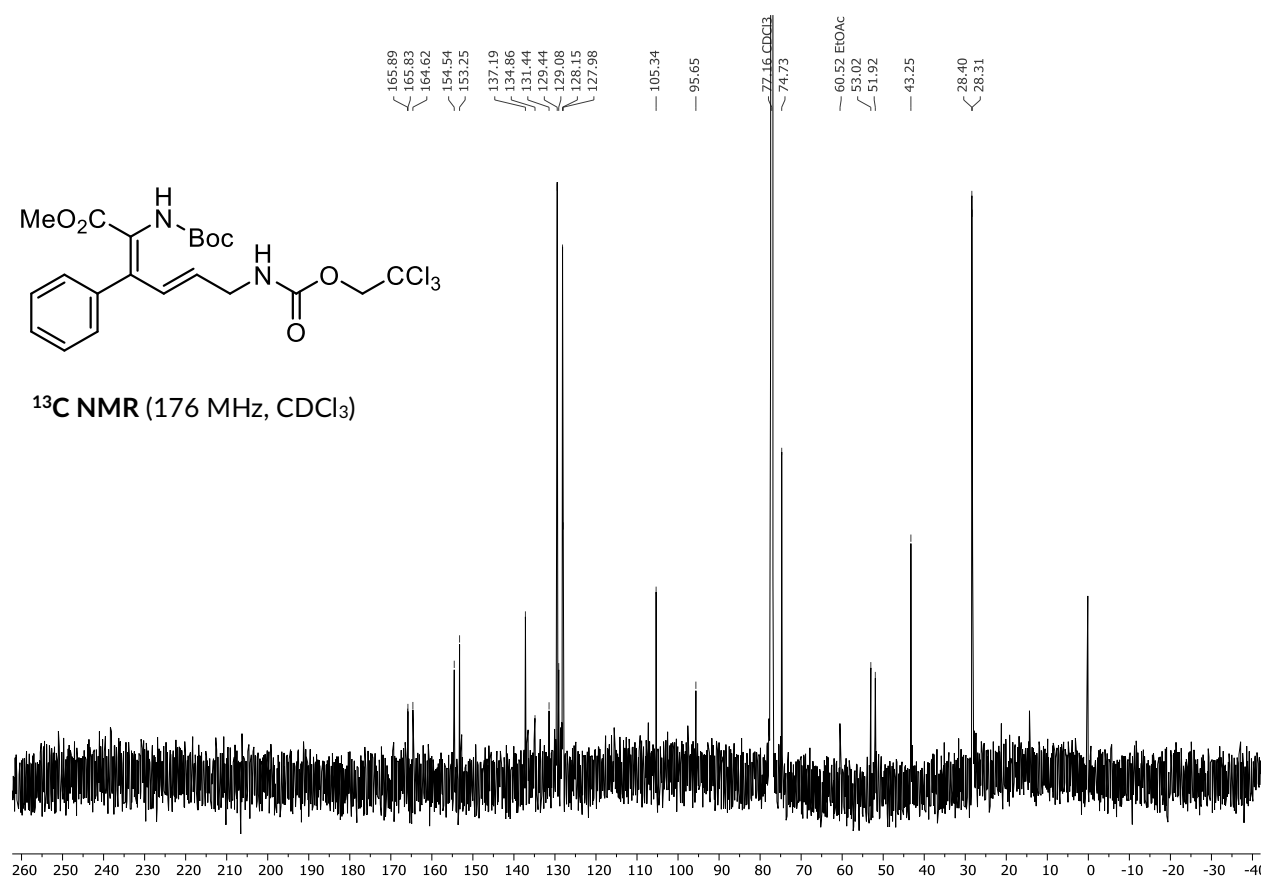
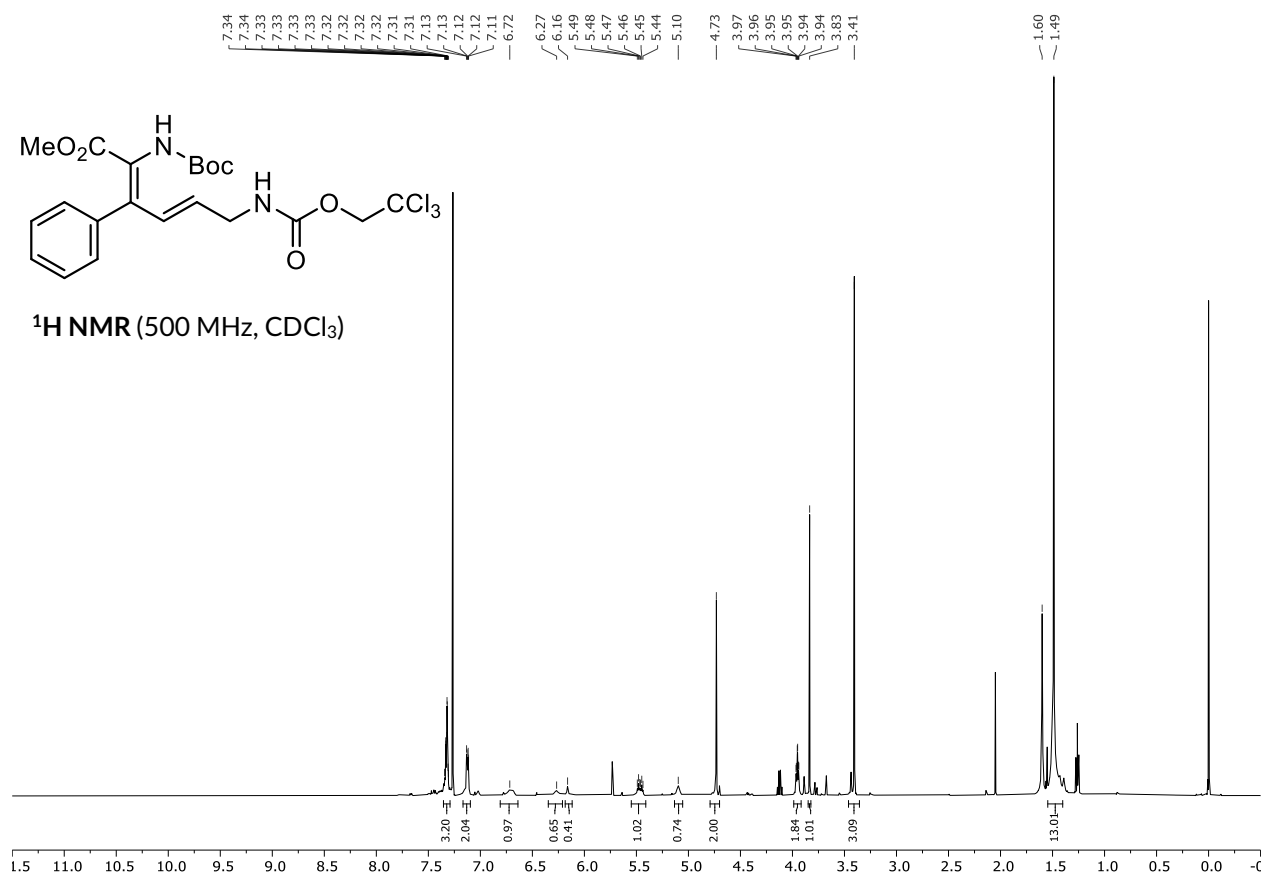
^{13}C NMR (126 MHz, CDCl_3)

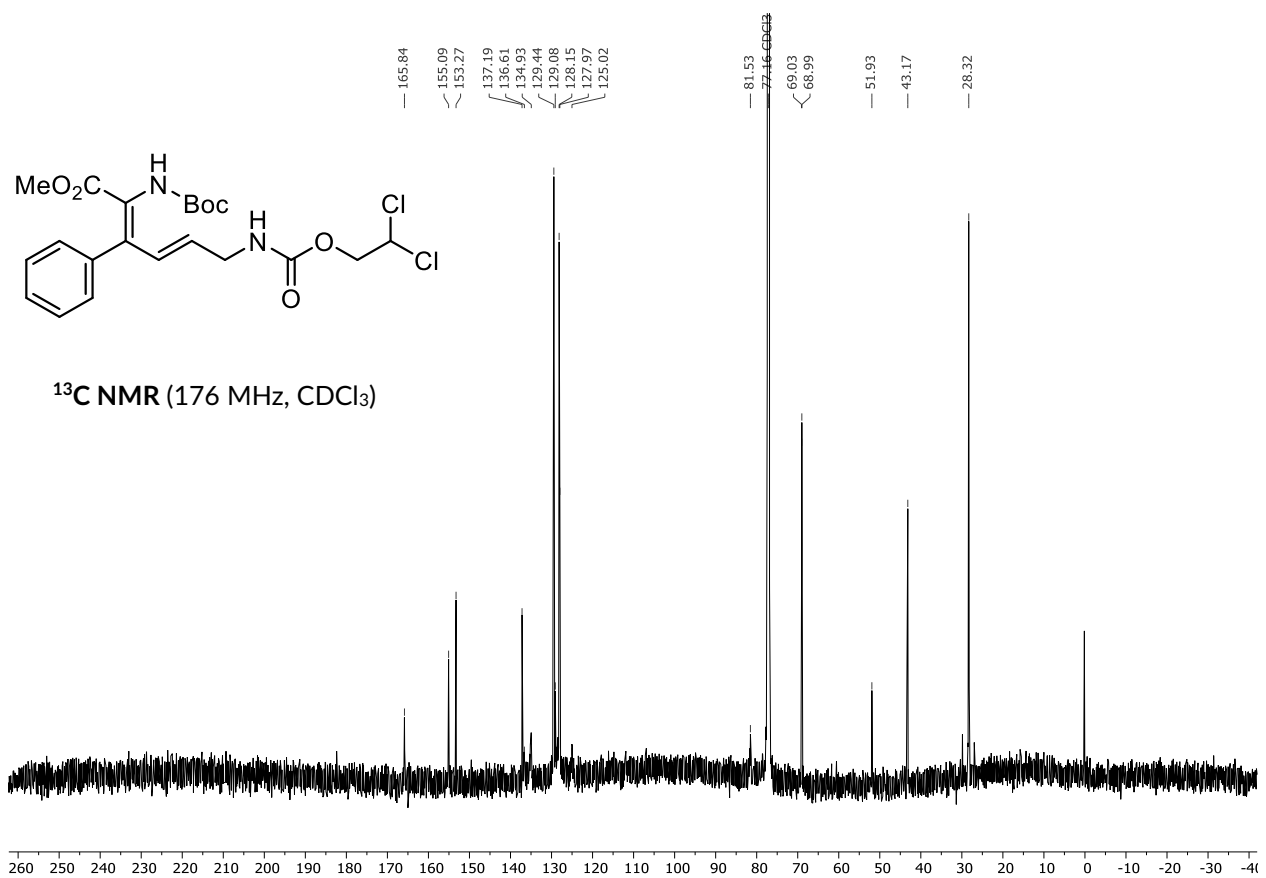
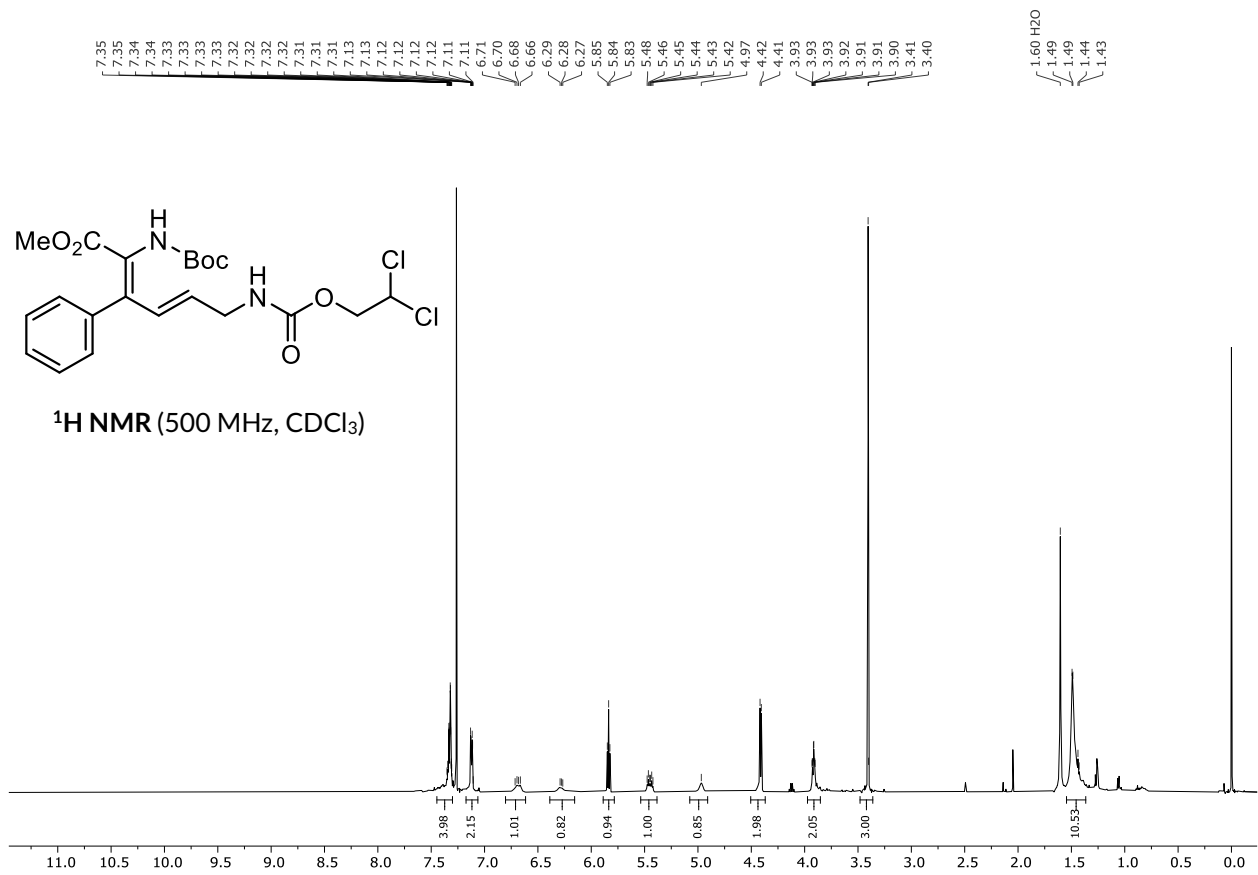




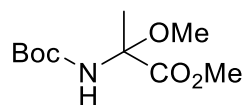
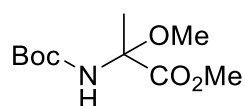
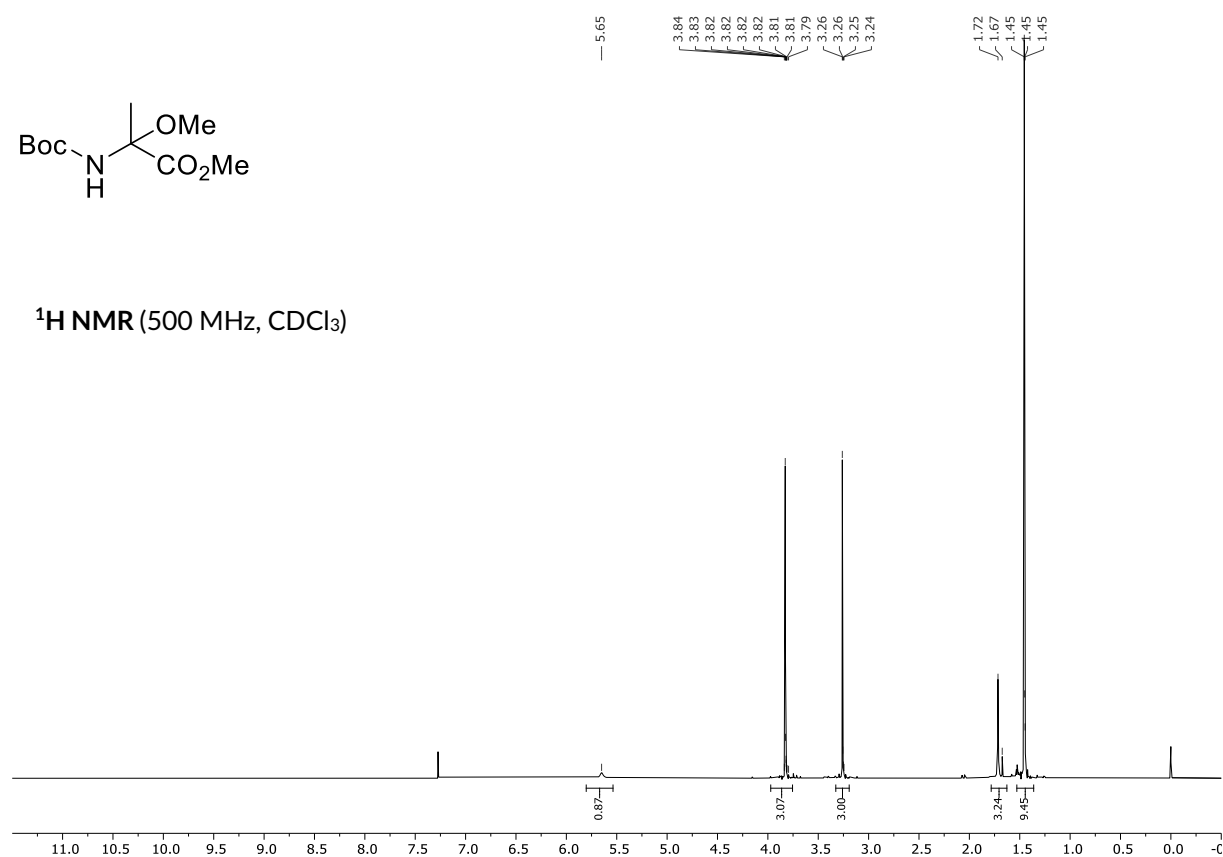
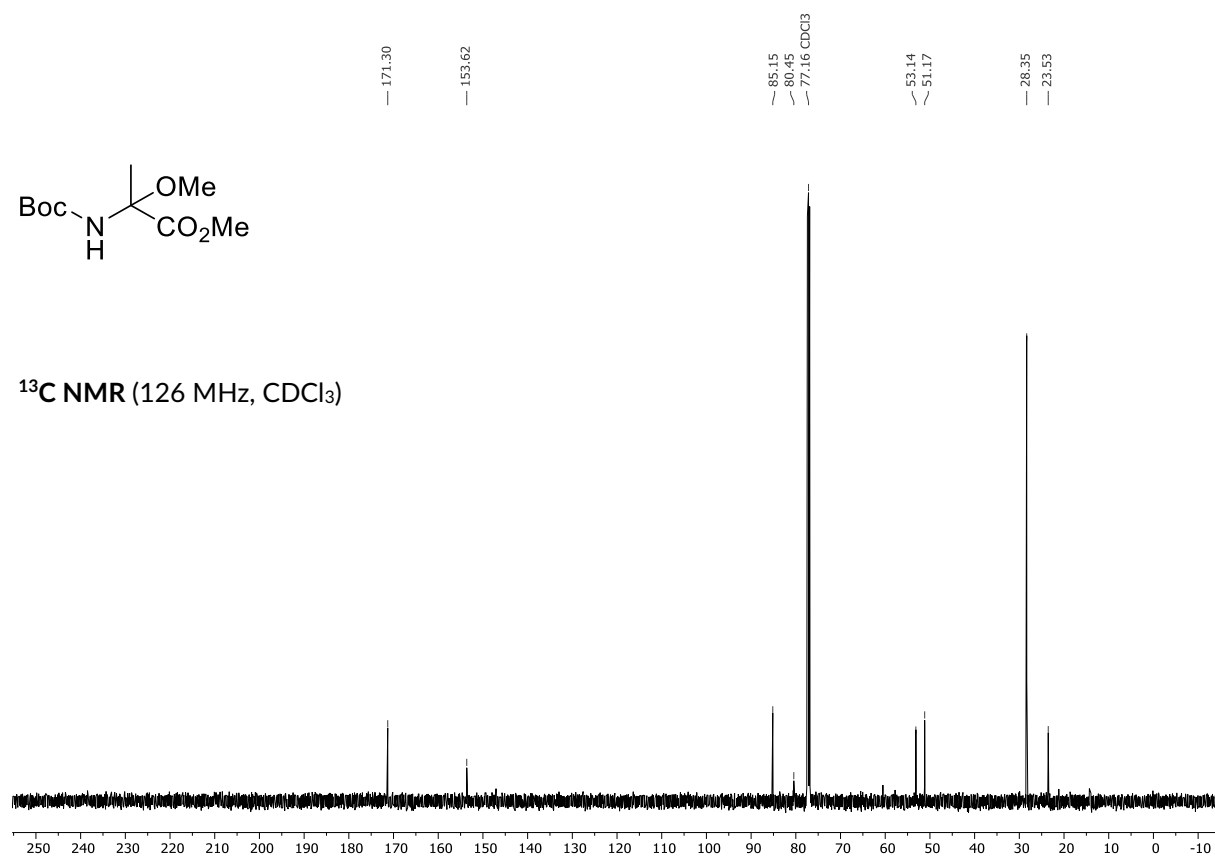


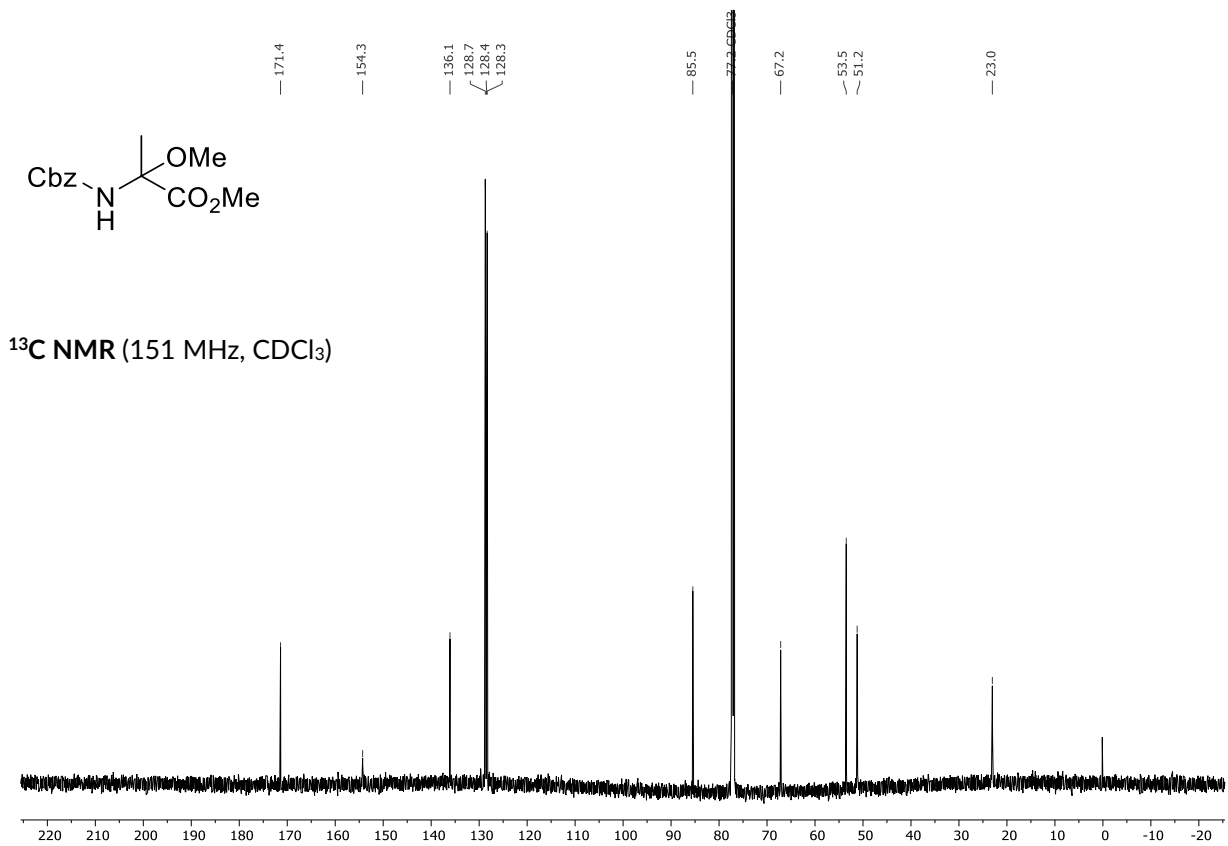
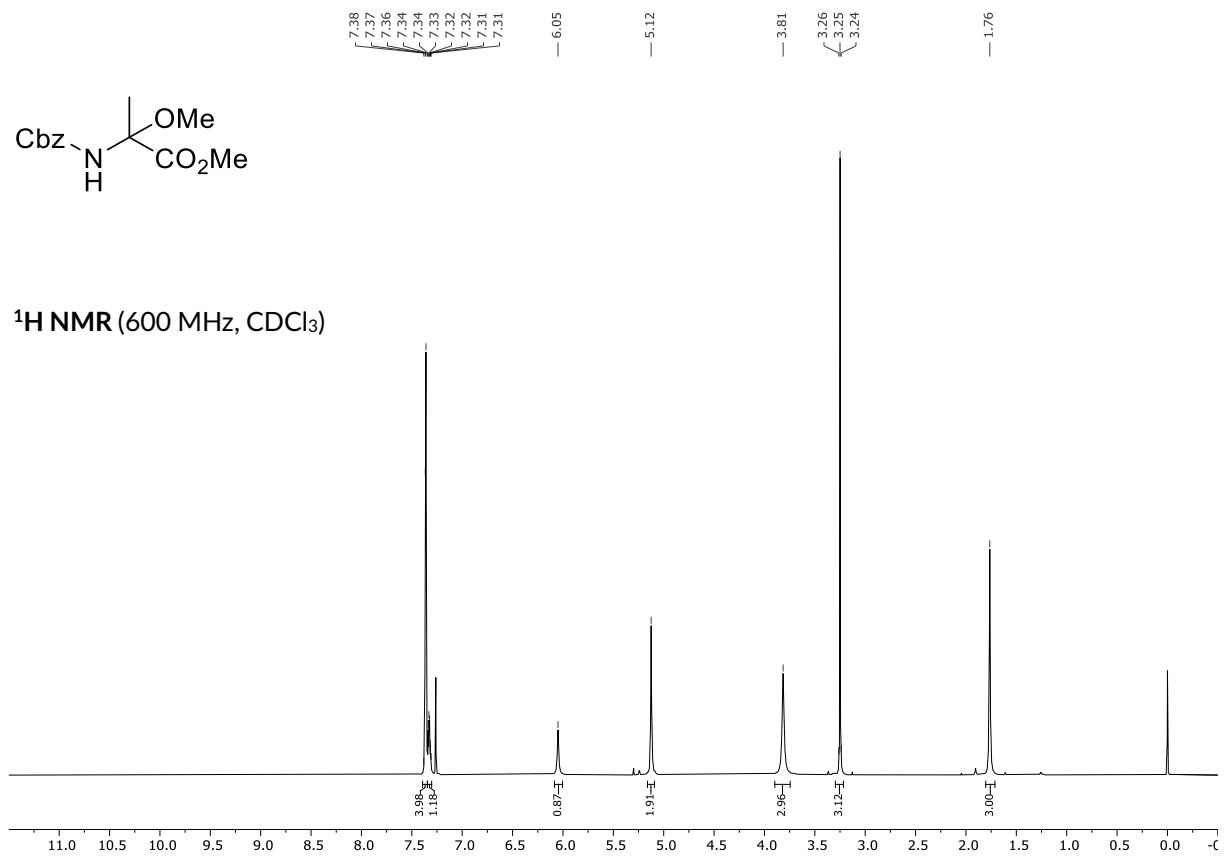


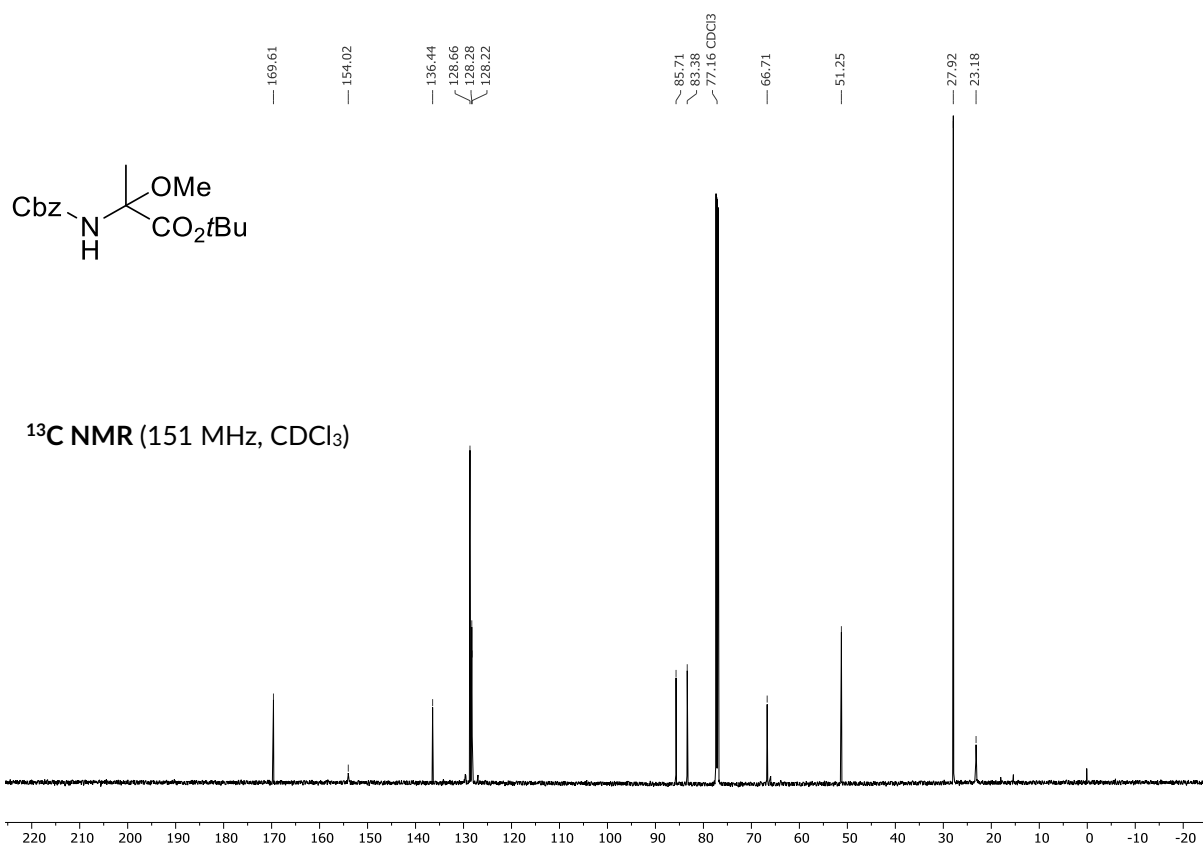
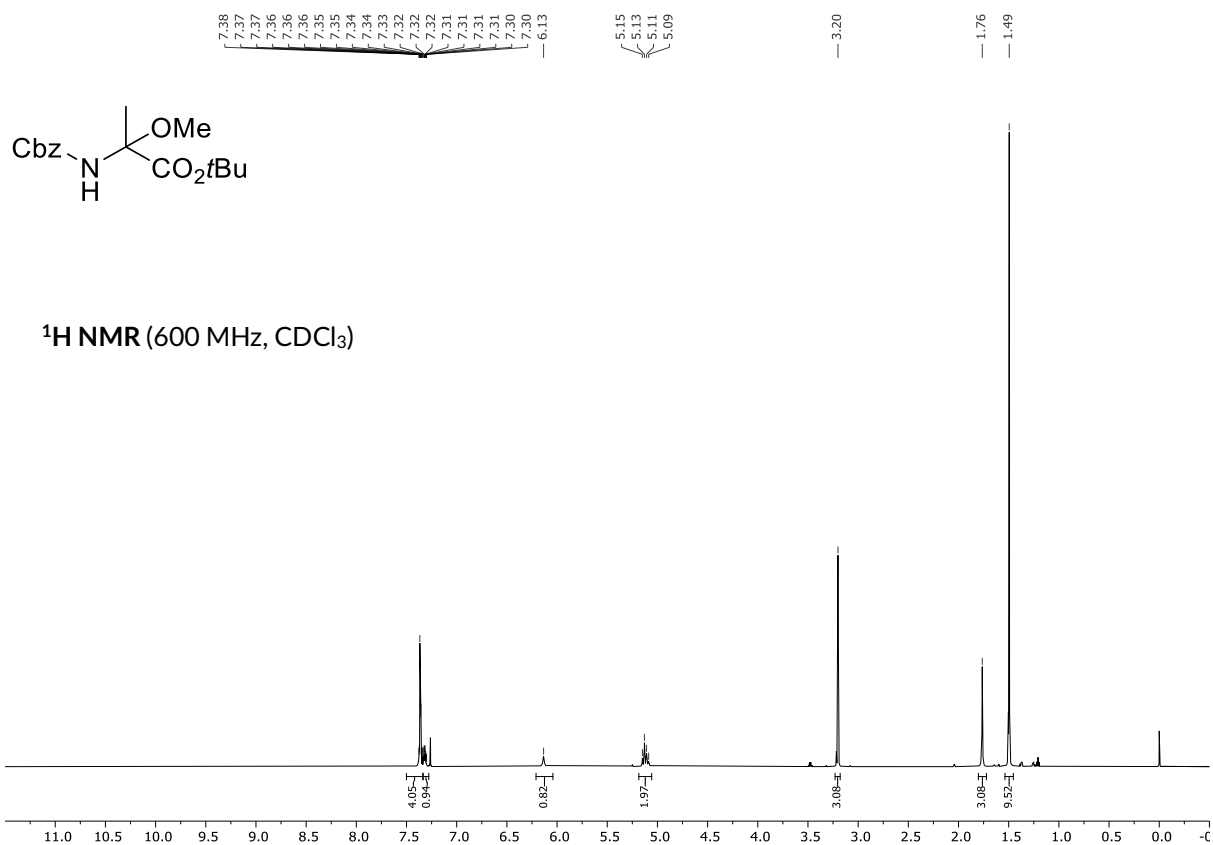


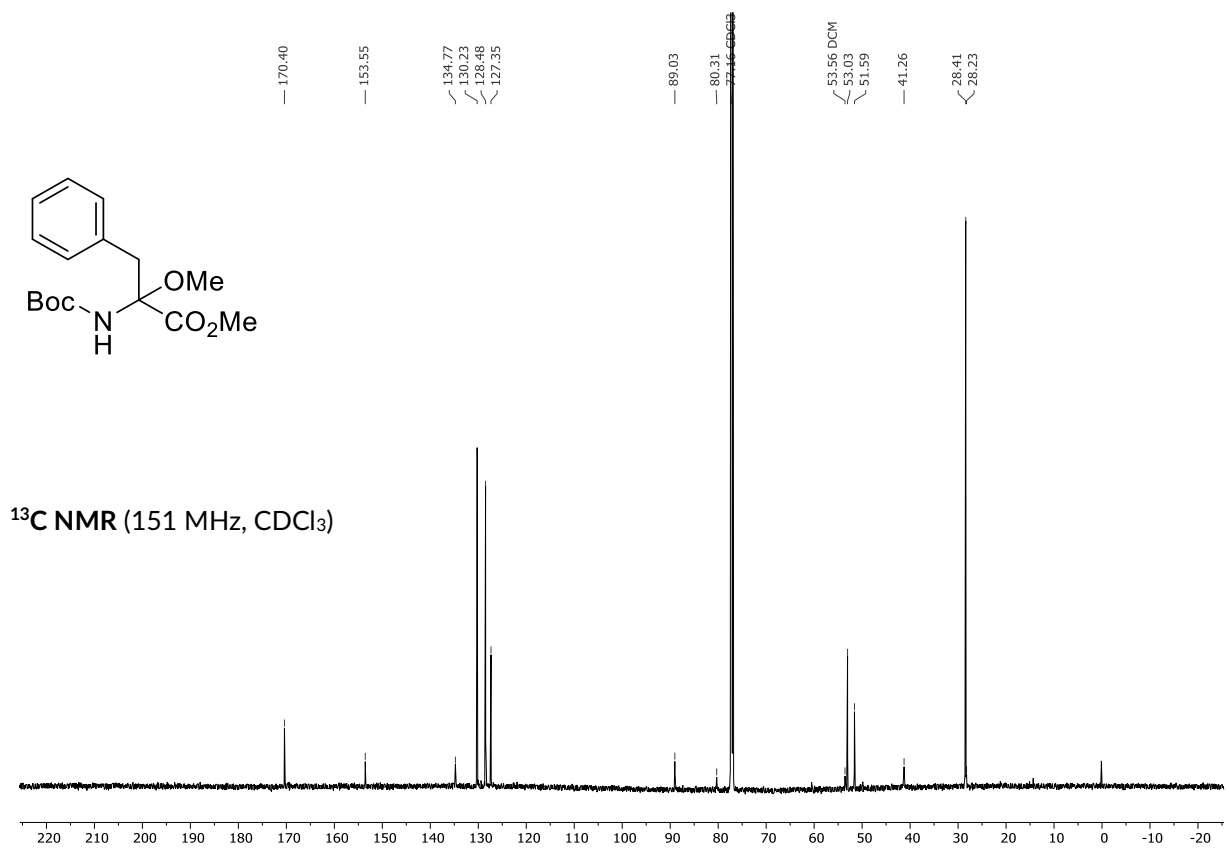
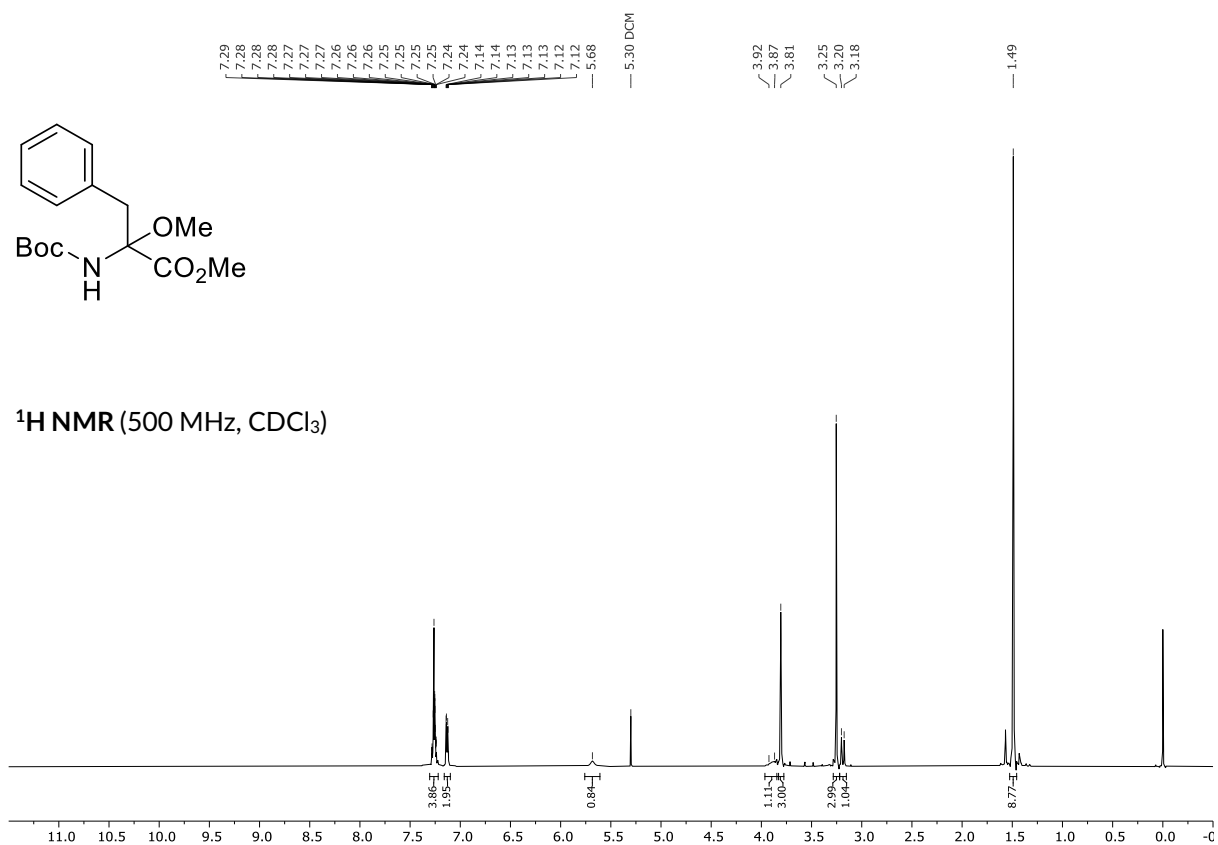


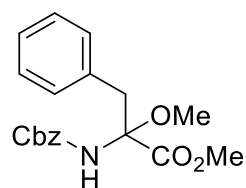
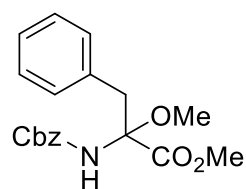
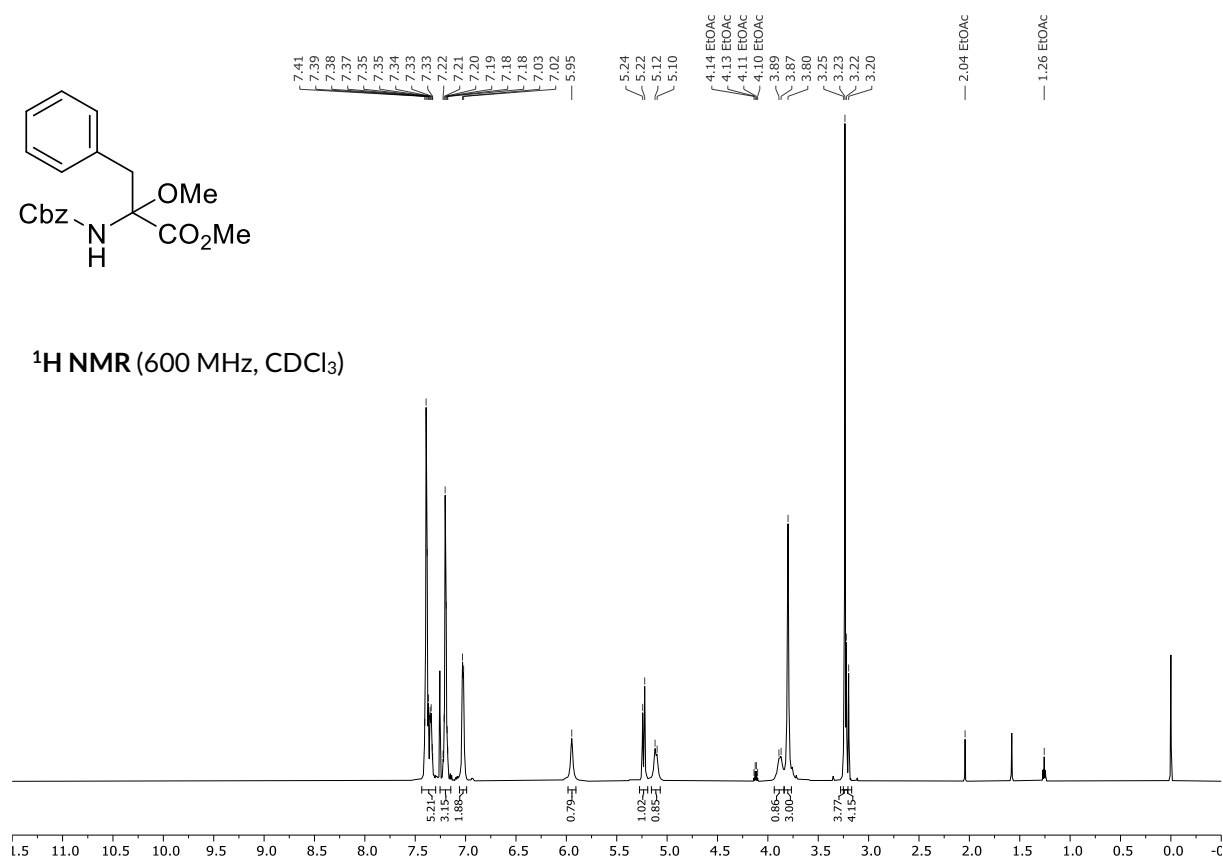
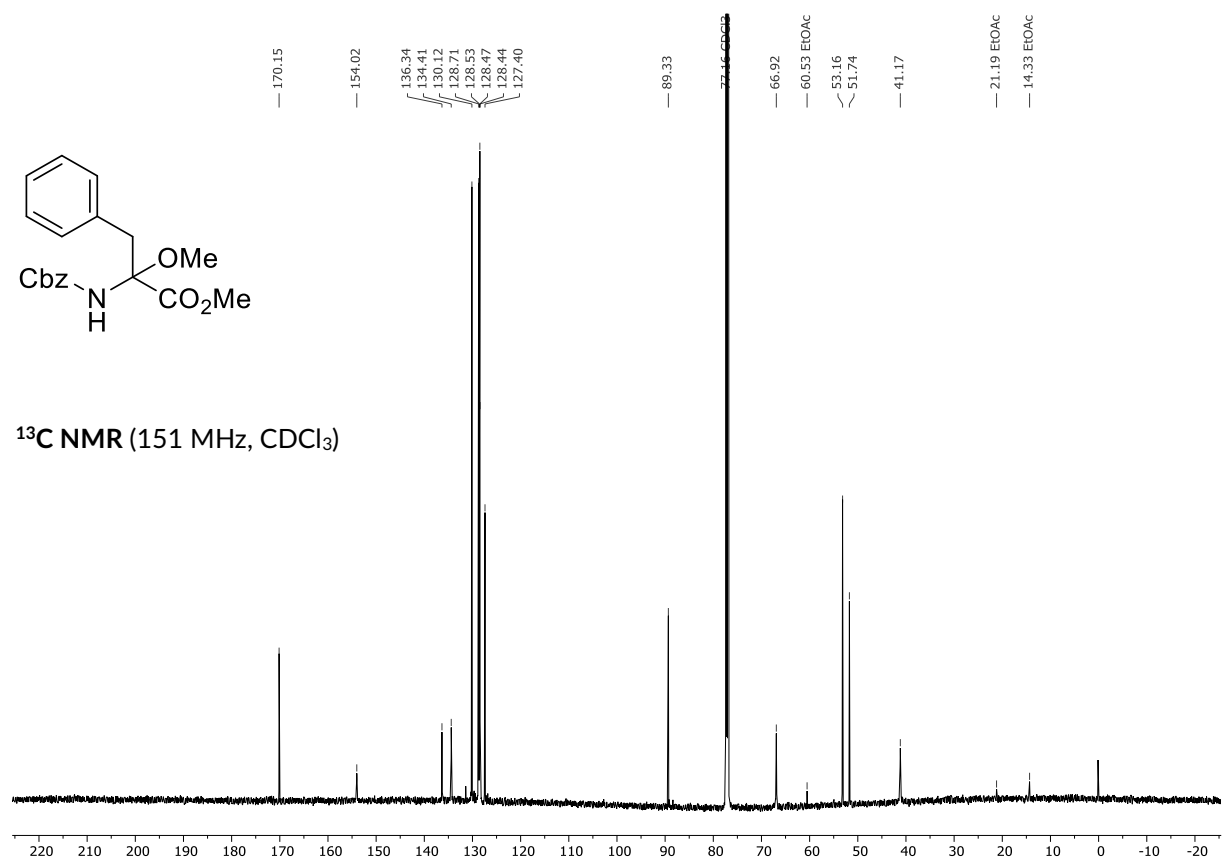
7.2.7. Electrosynthesis of Protected Dehydroamino Acids

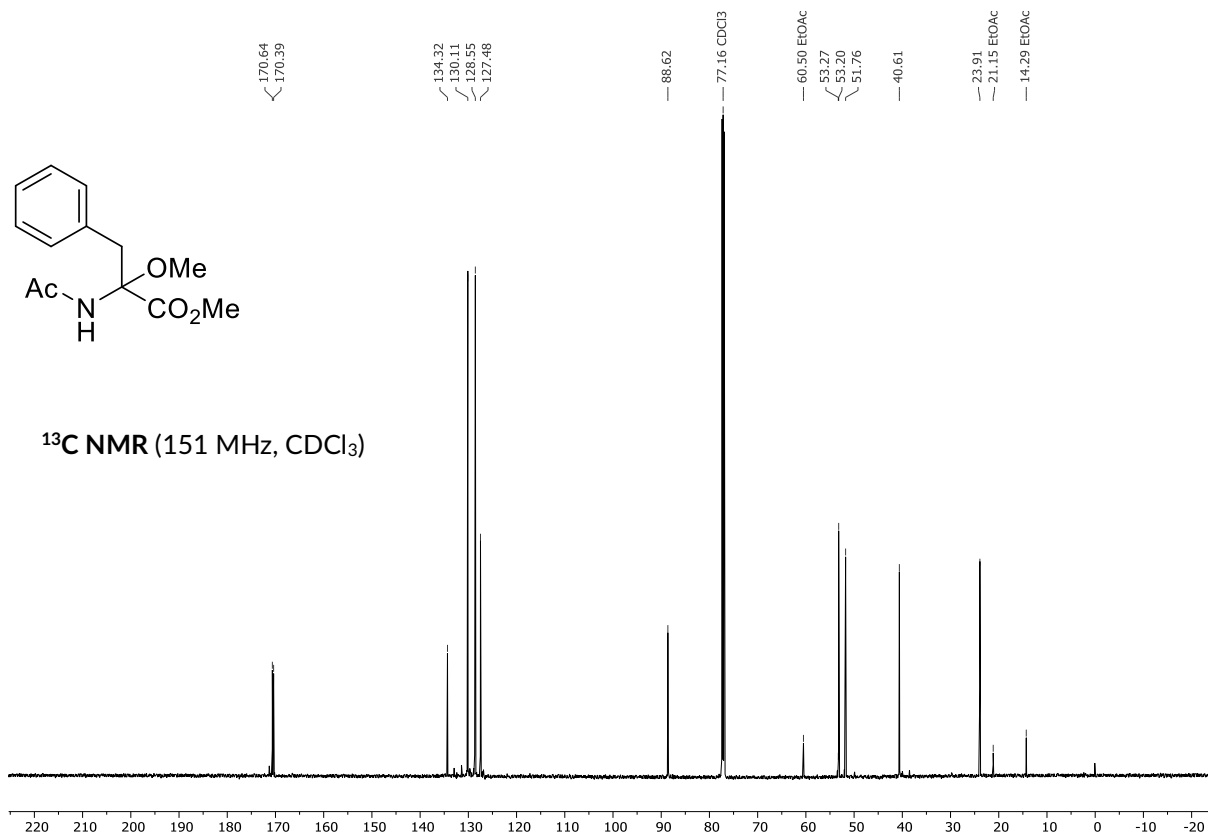
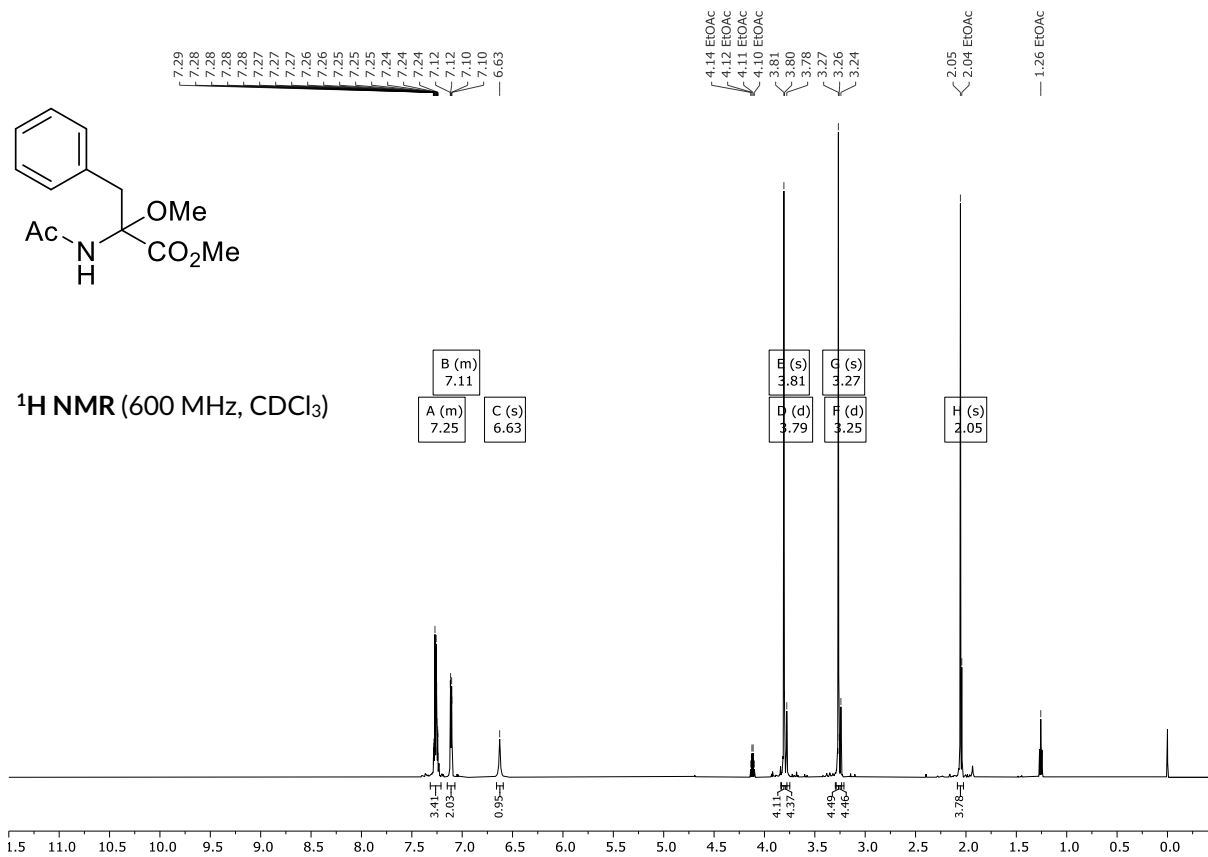
 $^1\text{H NMR}$ (500 MHz, CDCl_3) $^{13}\text{C NMR}$ (126 MHz, CDCl_3)

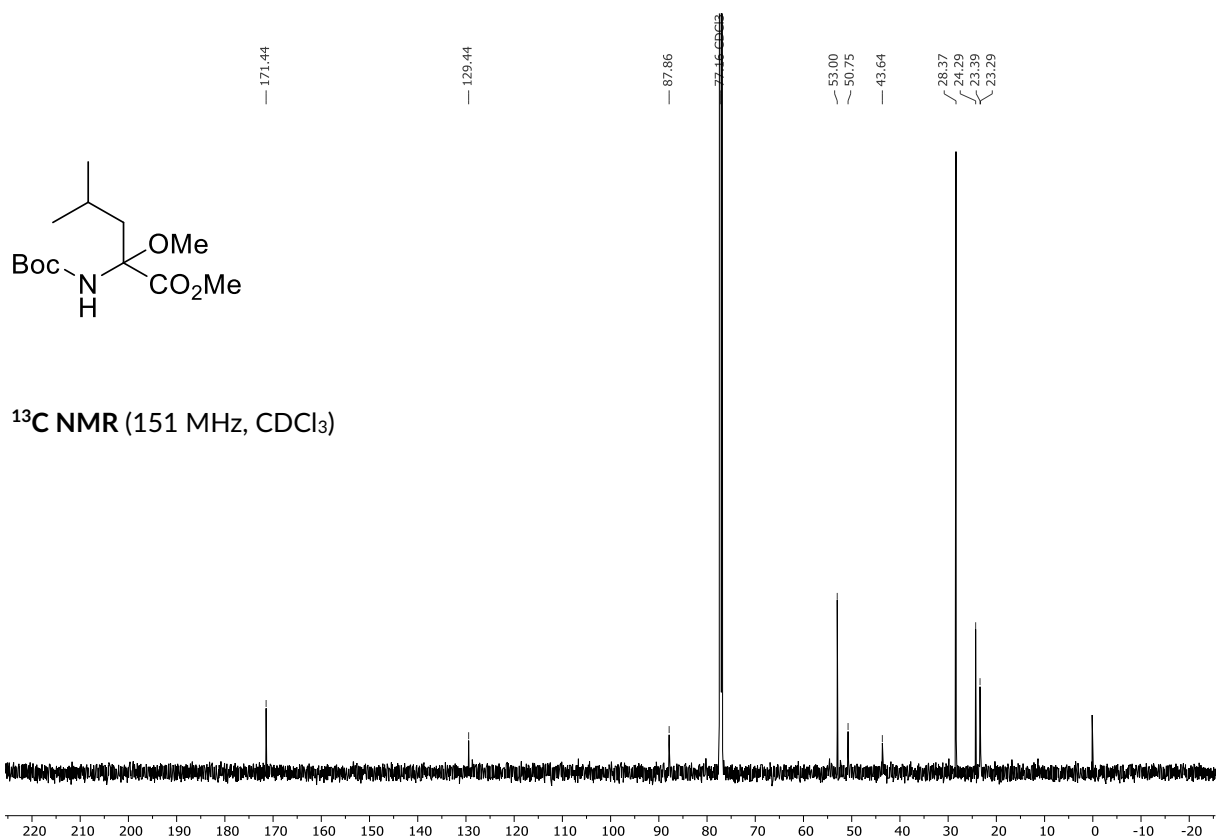
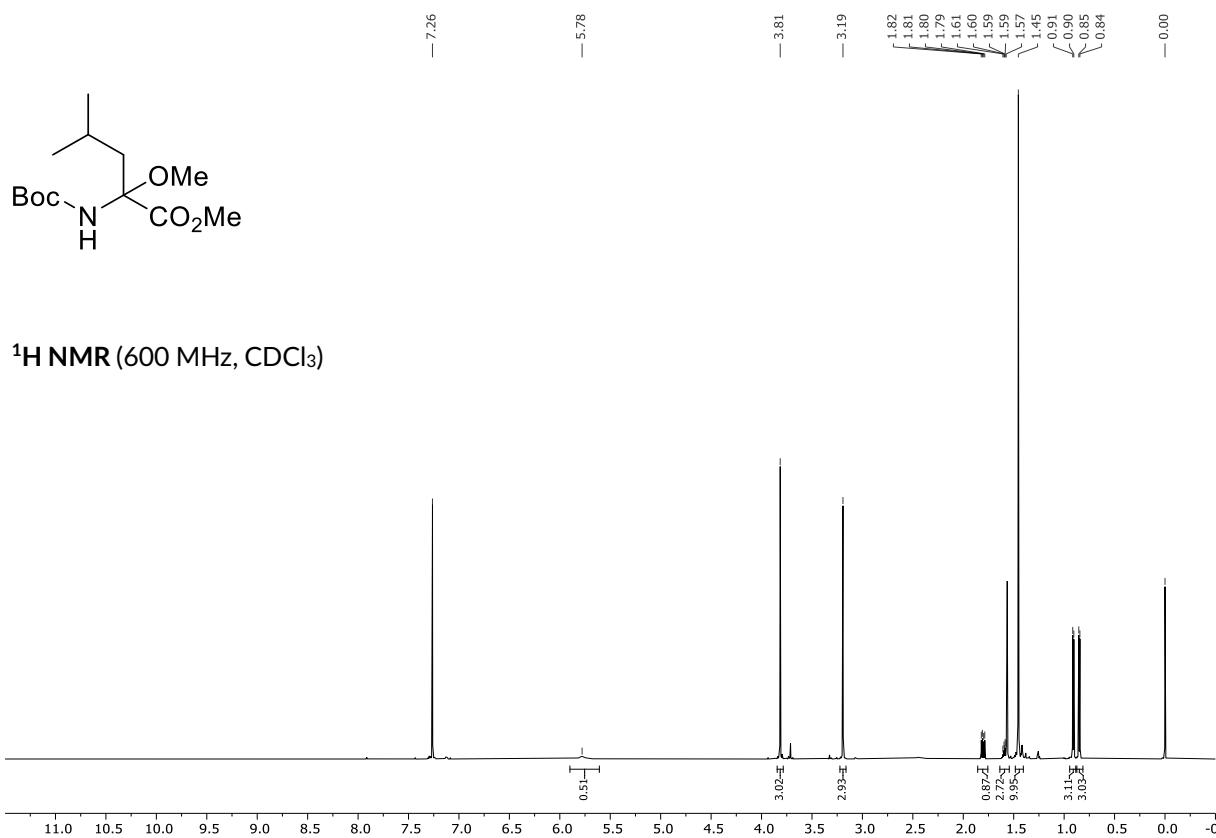


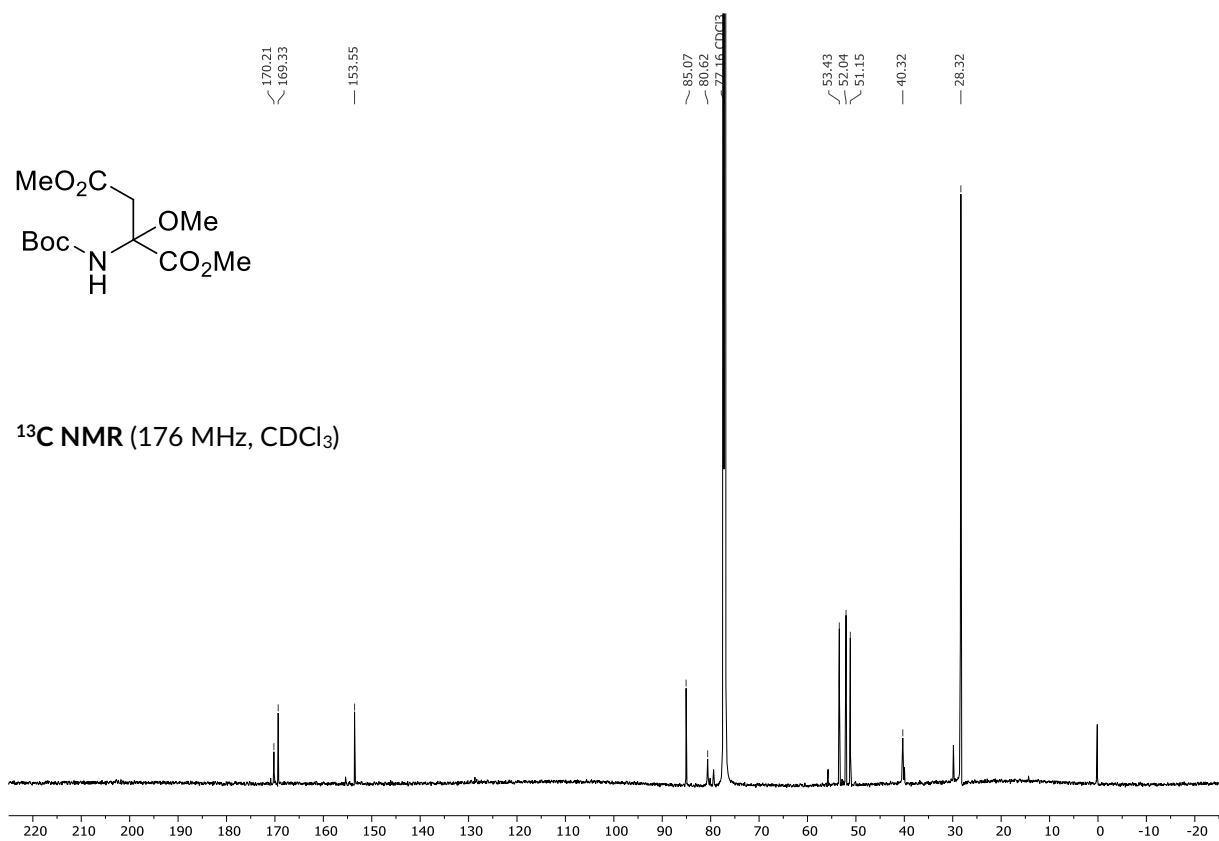
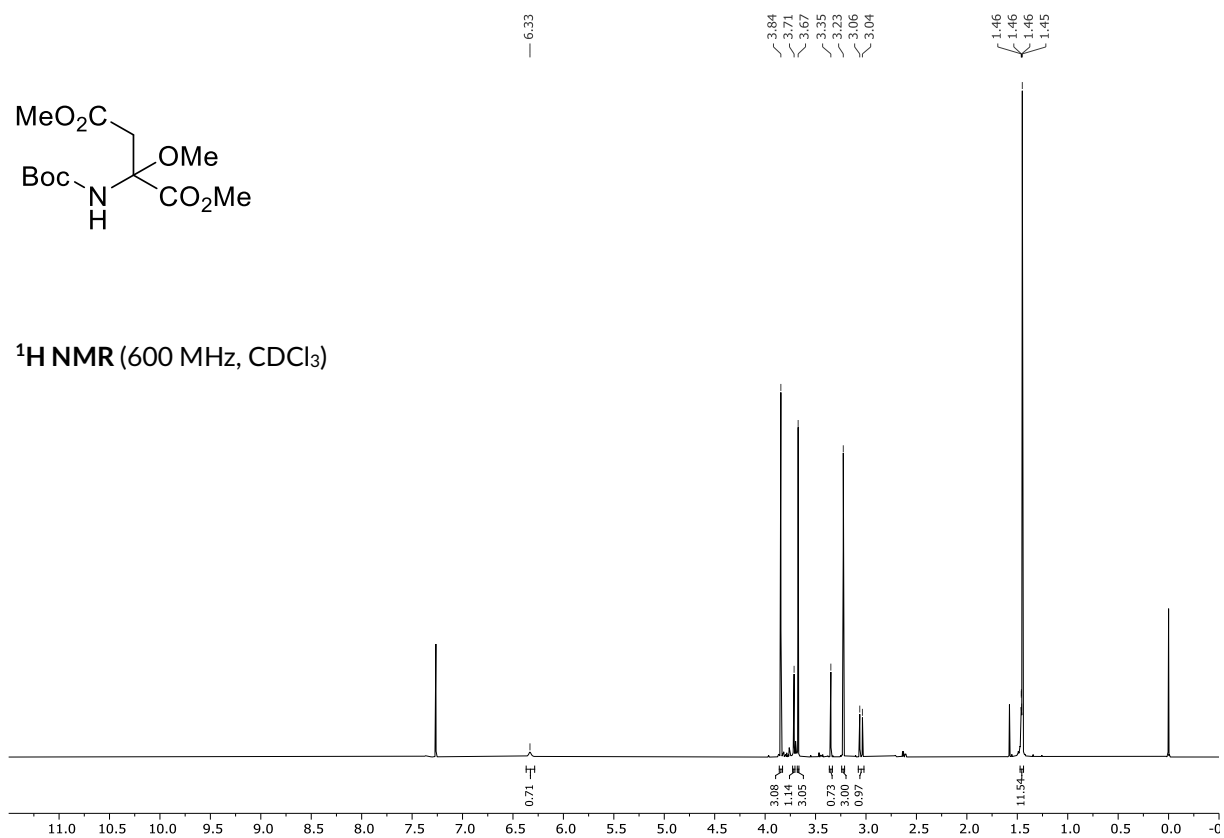


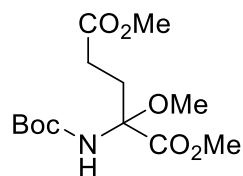


 ^1H NMR (600 MHz, CDCl_3) ^{13}C NMR (151 MHz, CDCl_3)

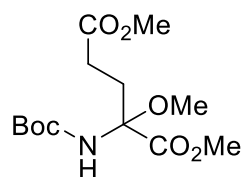
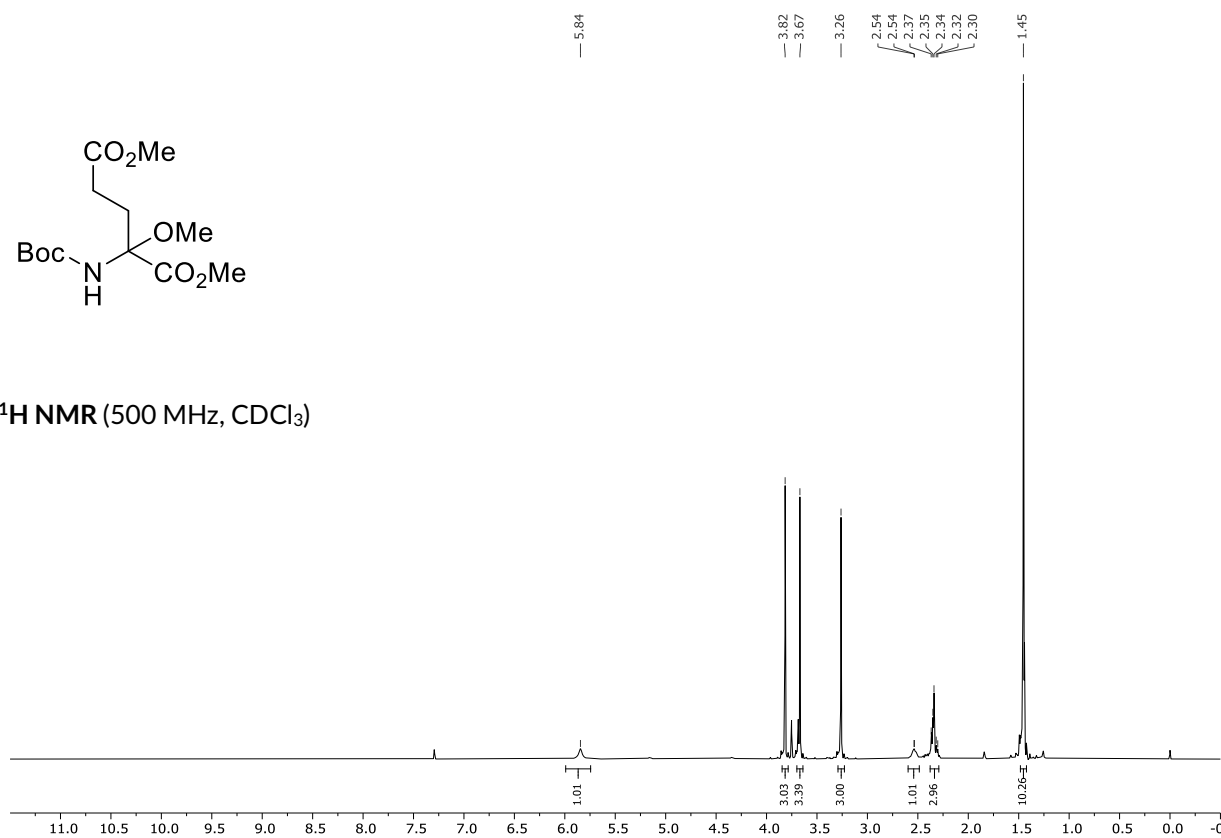




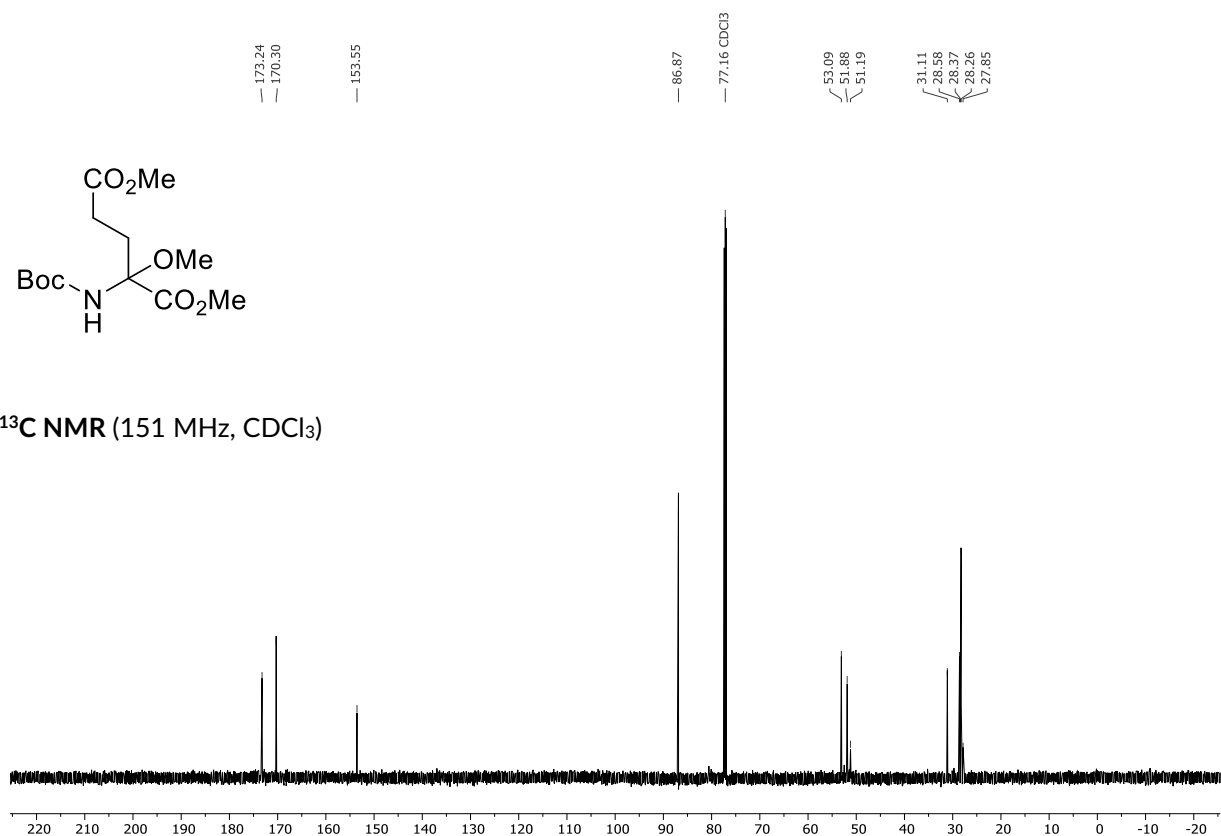


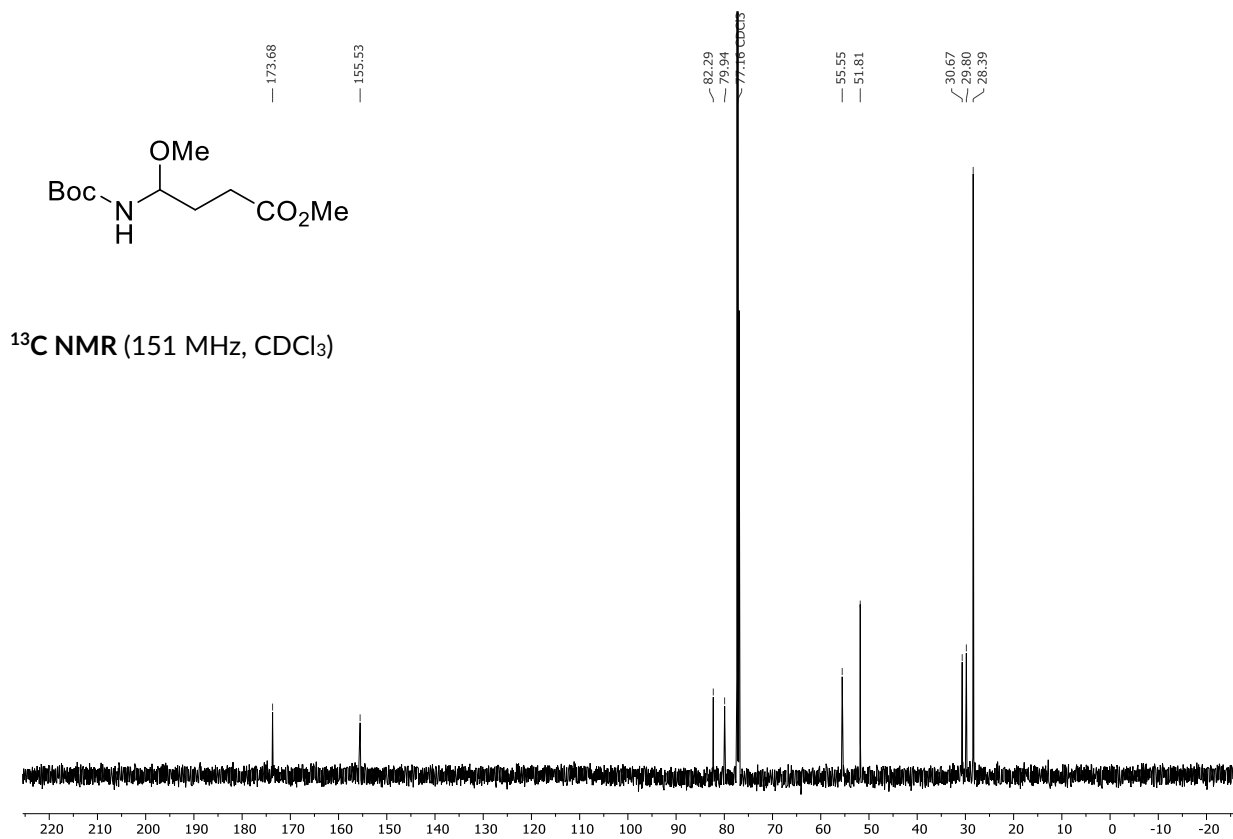
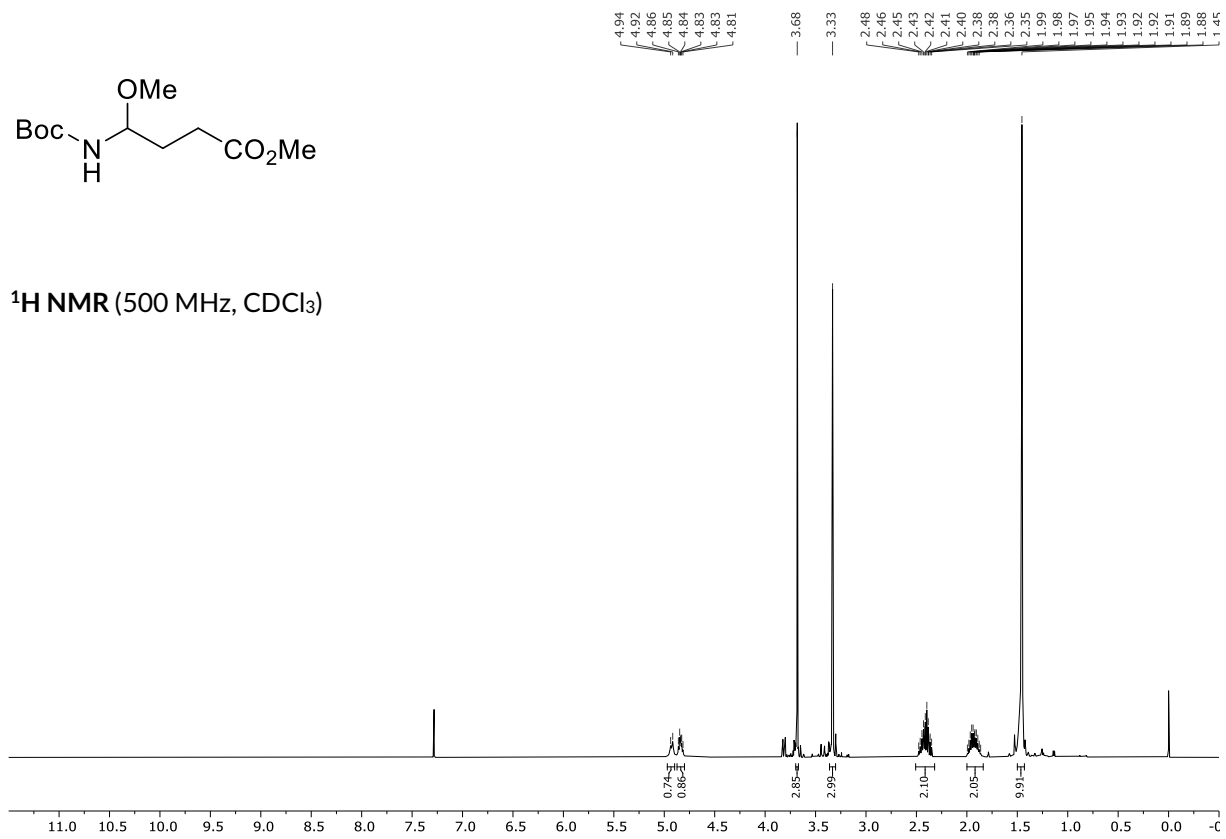


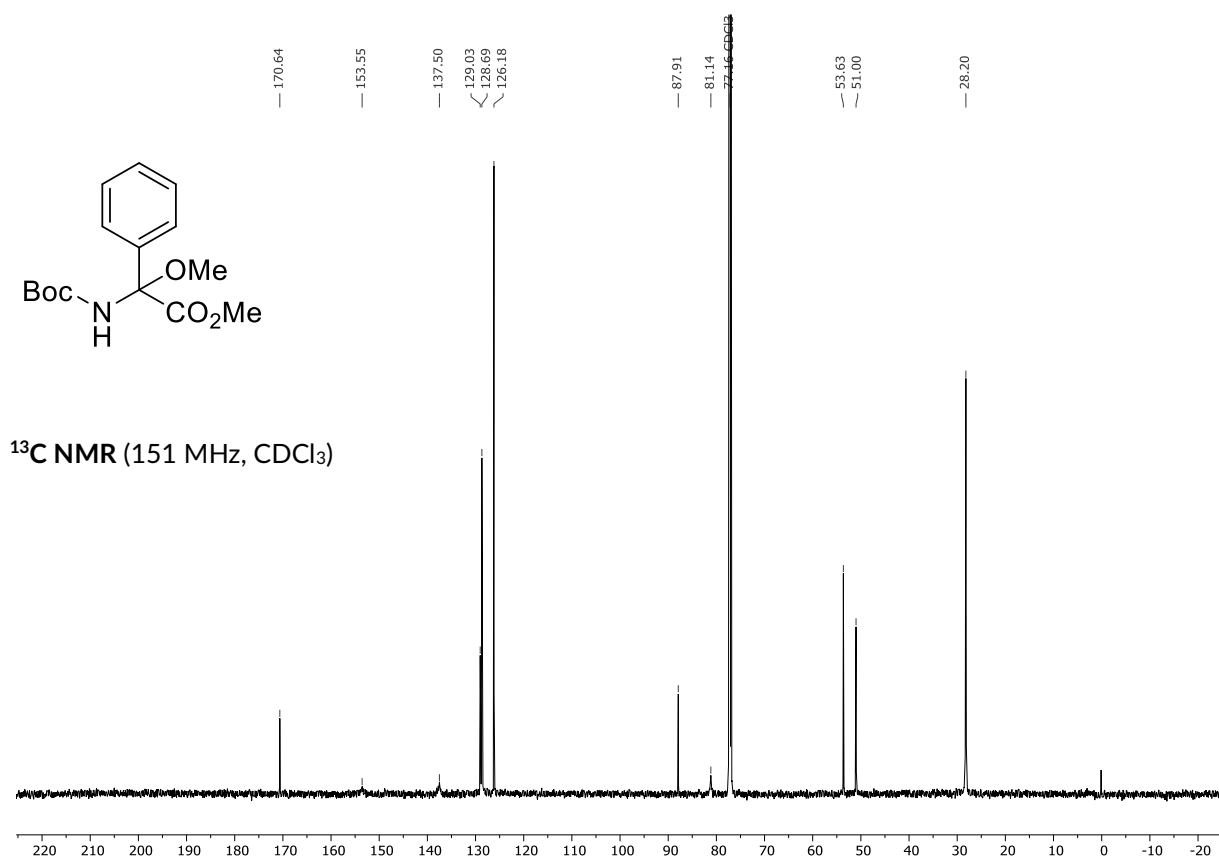
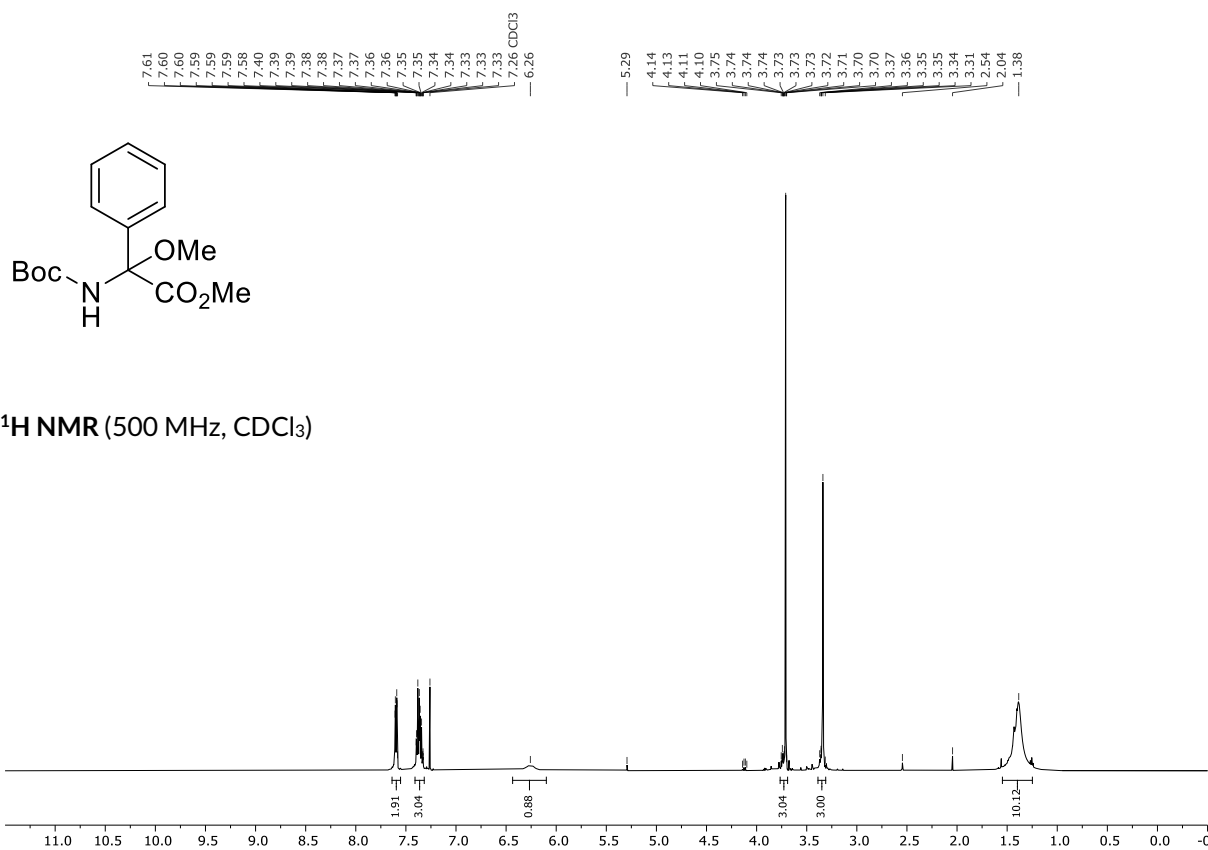
^1H NMR (500 MHz, CDCl_3)

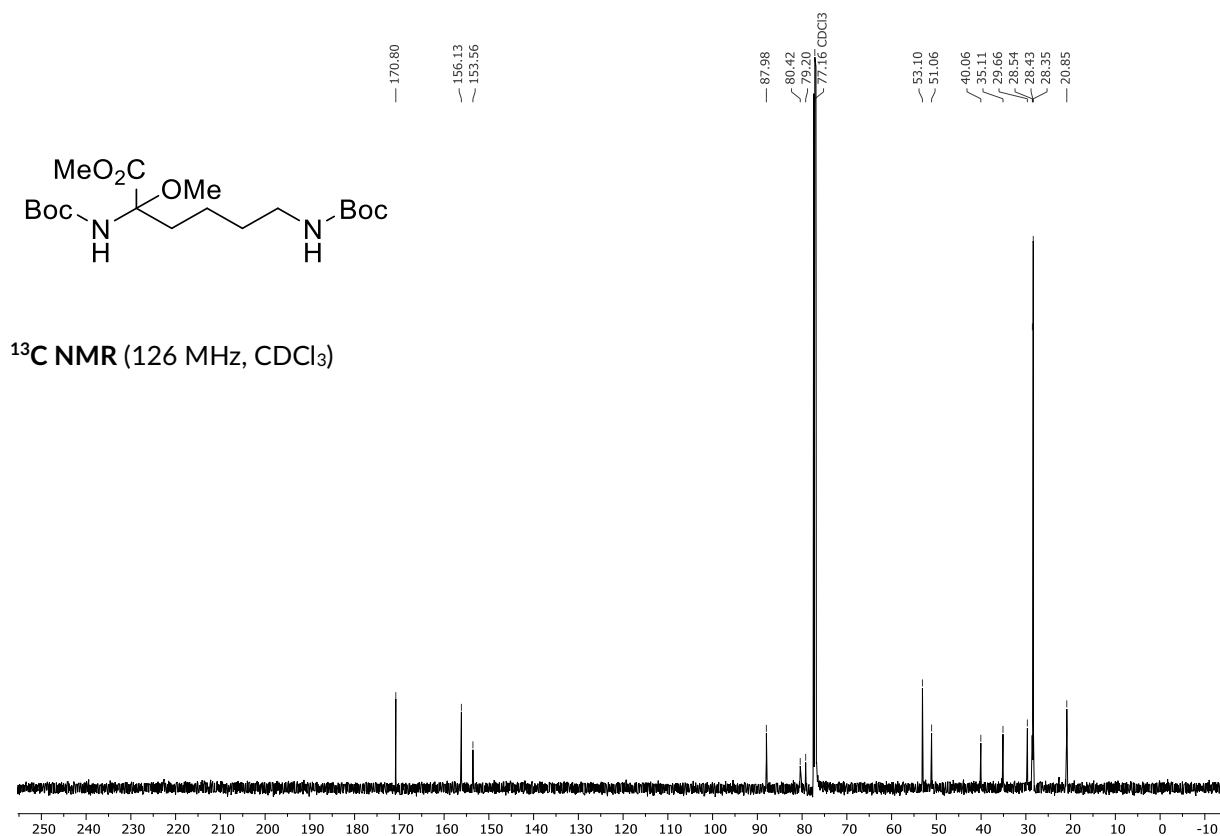
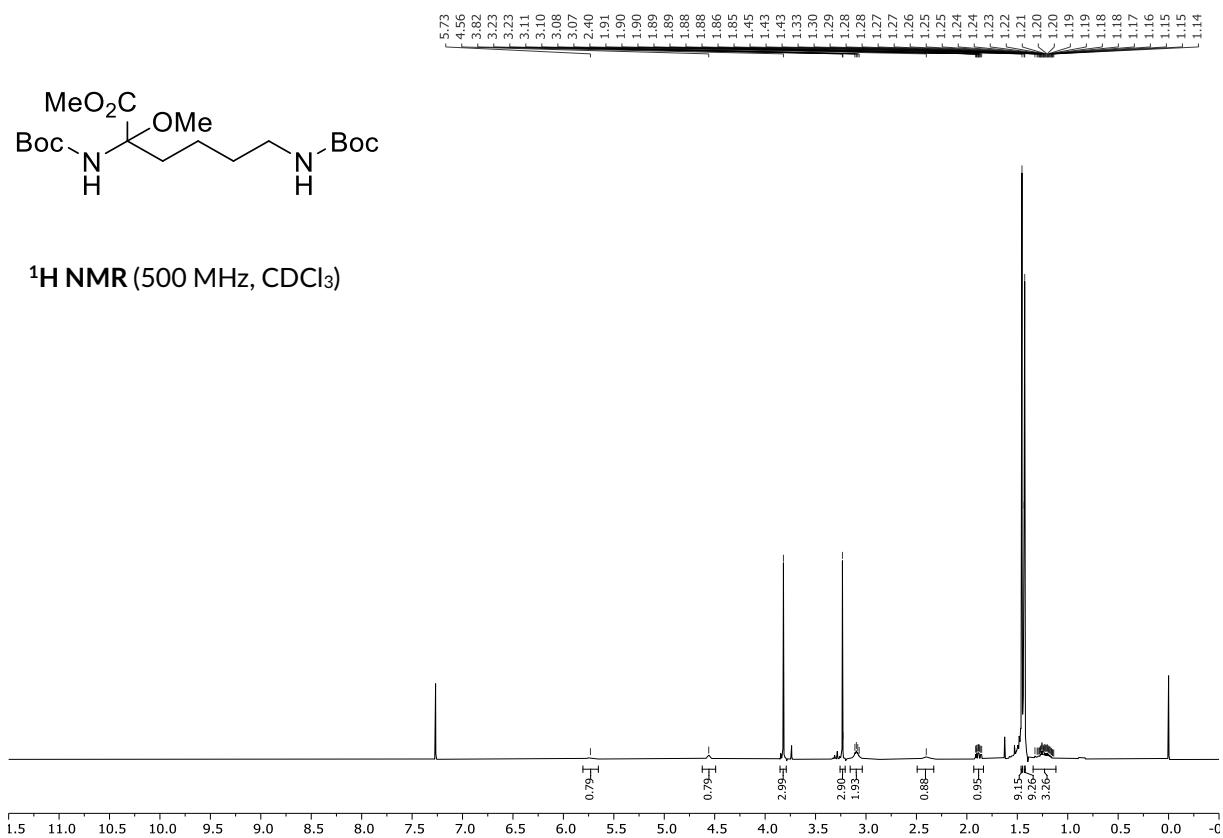


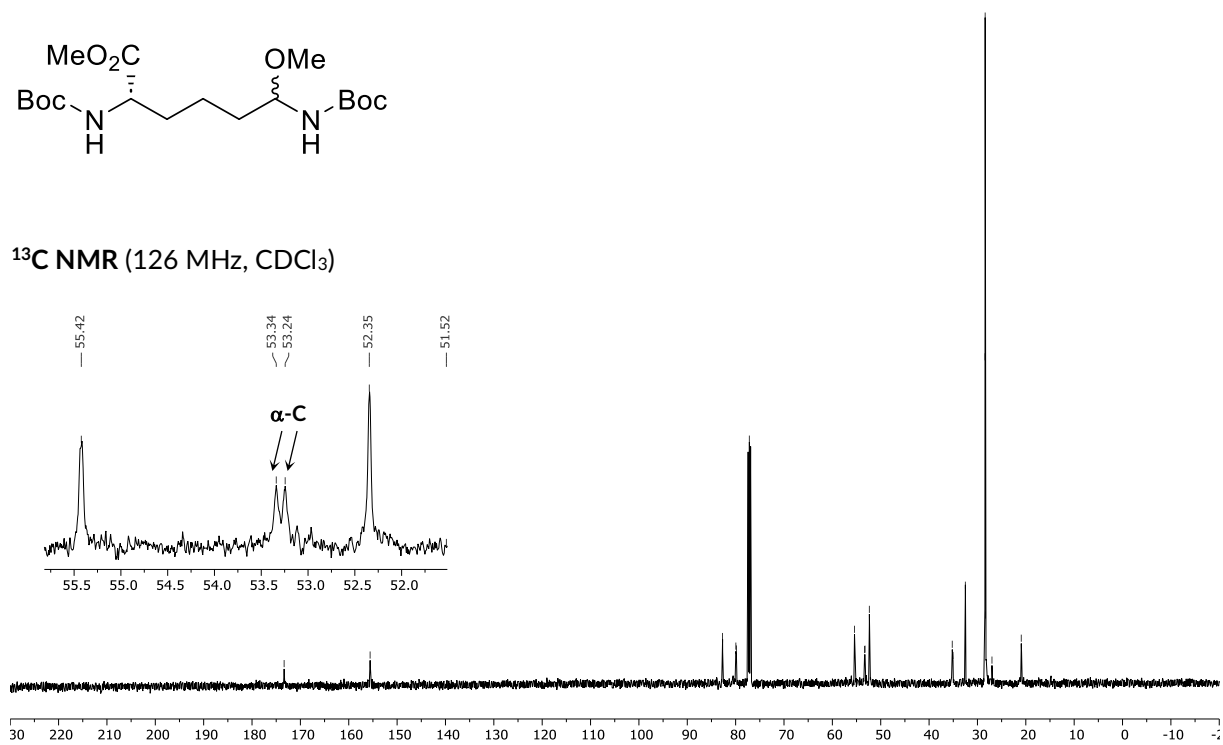
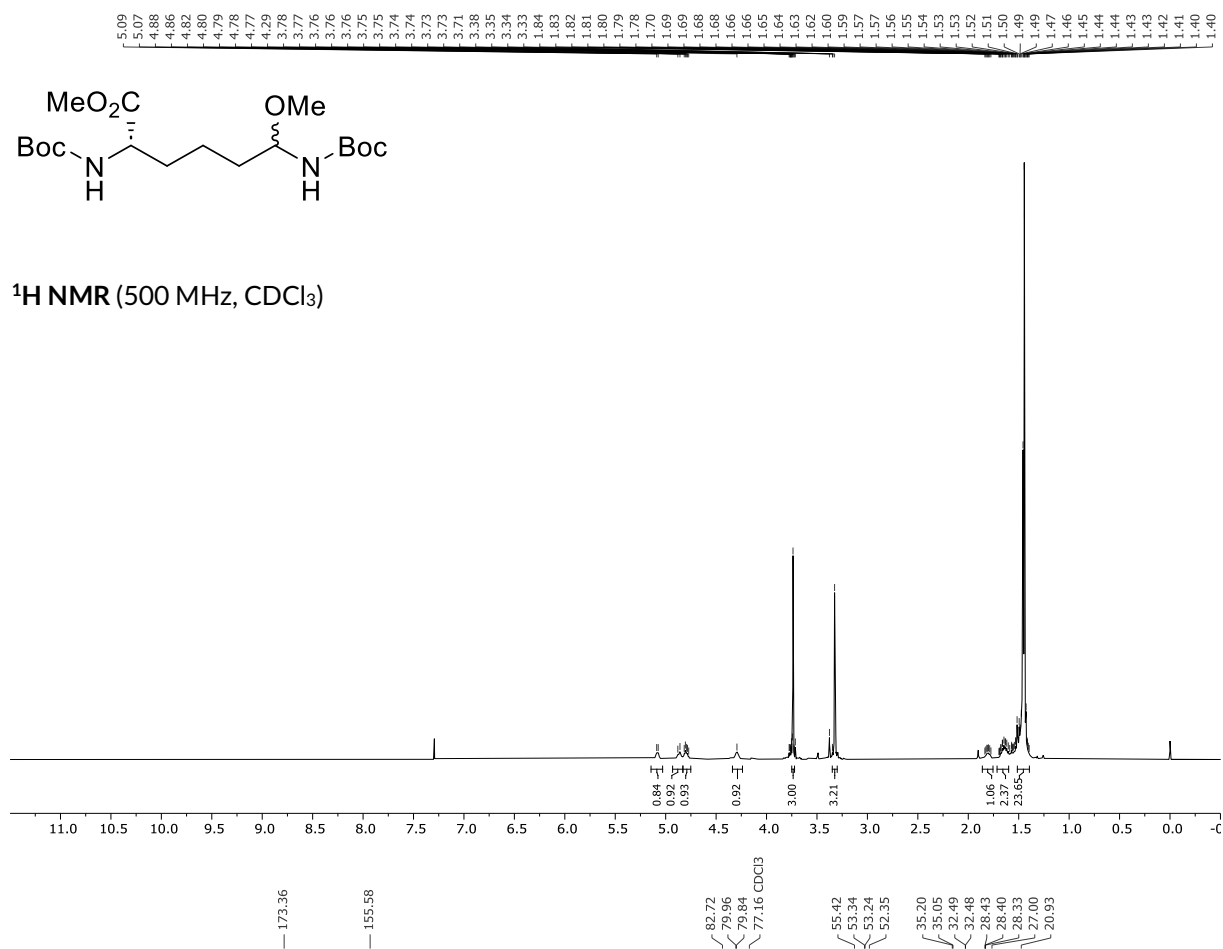
^{13}C NMR (151 MHz, CDCl_3)

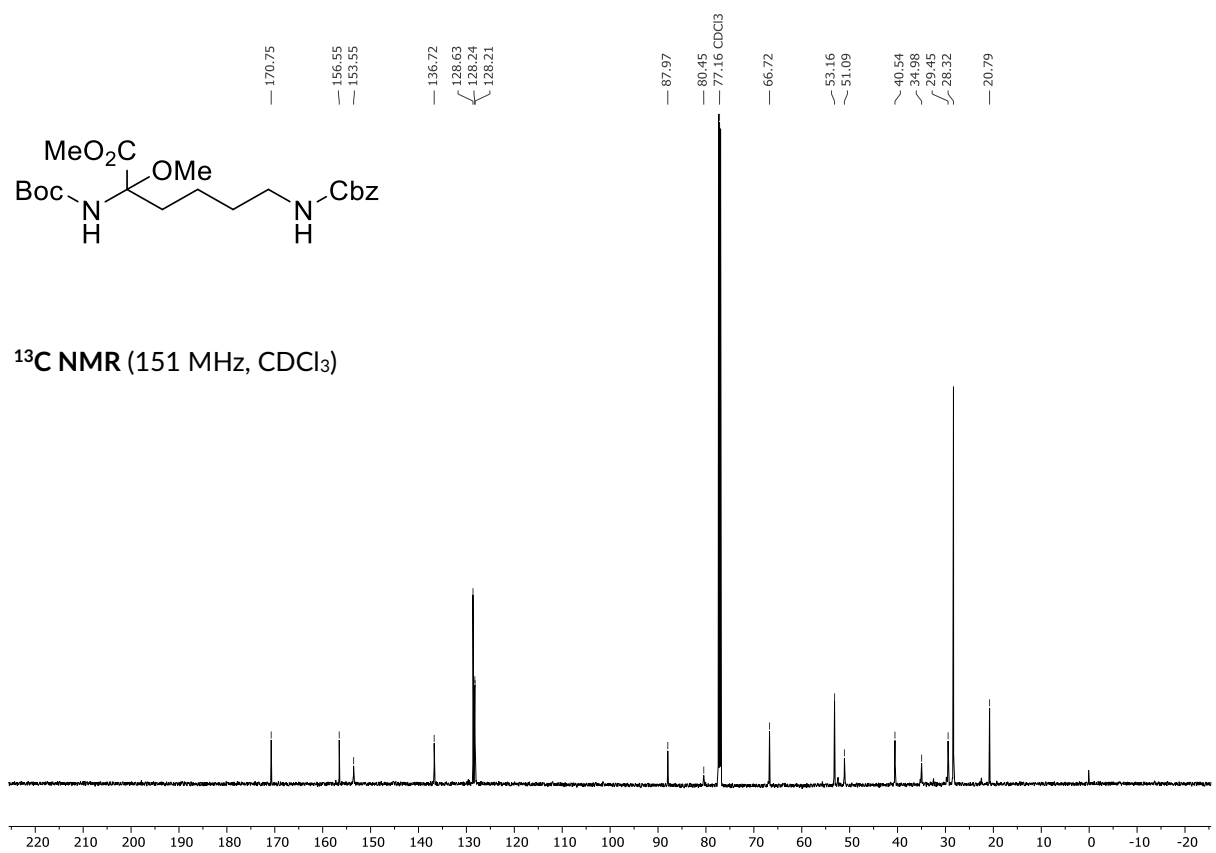
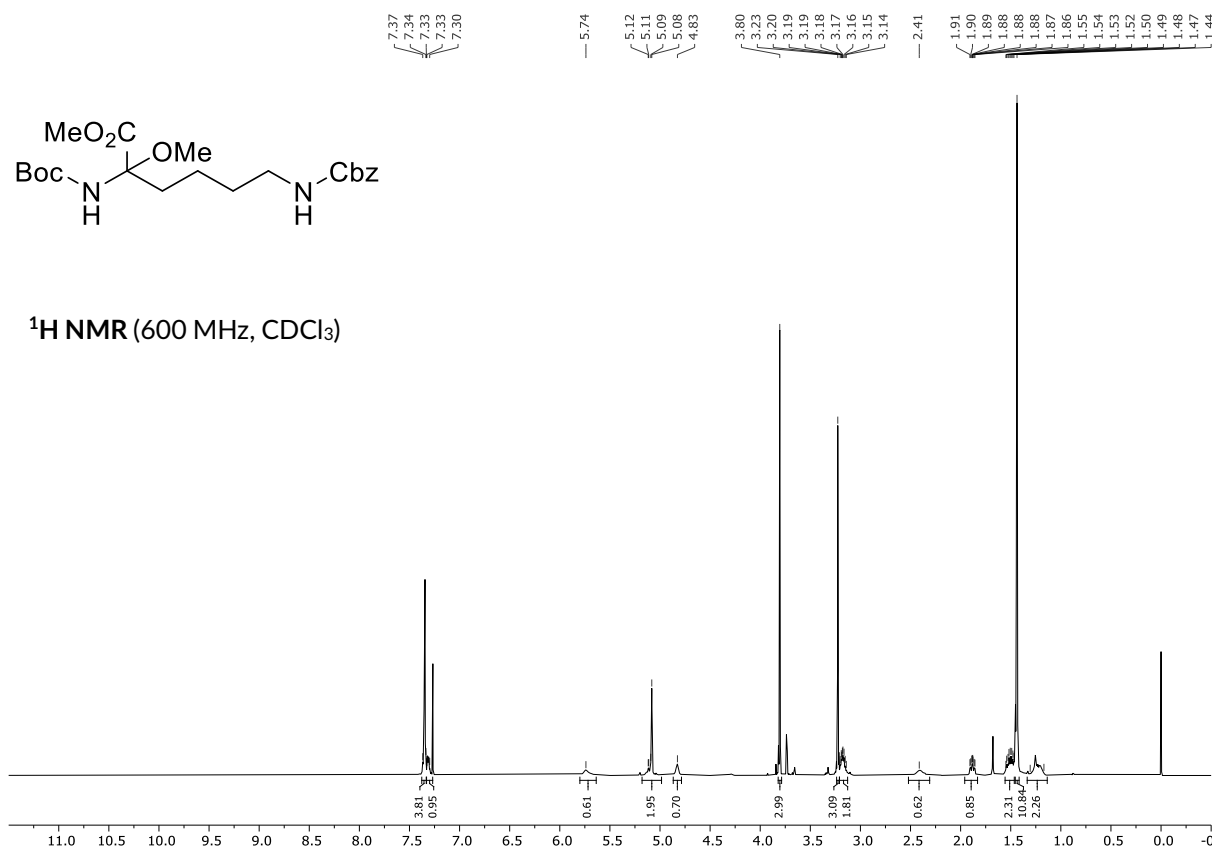


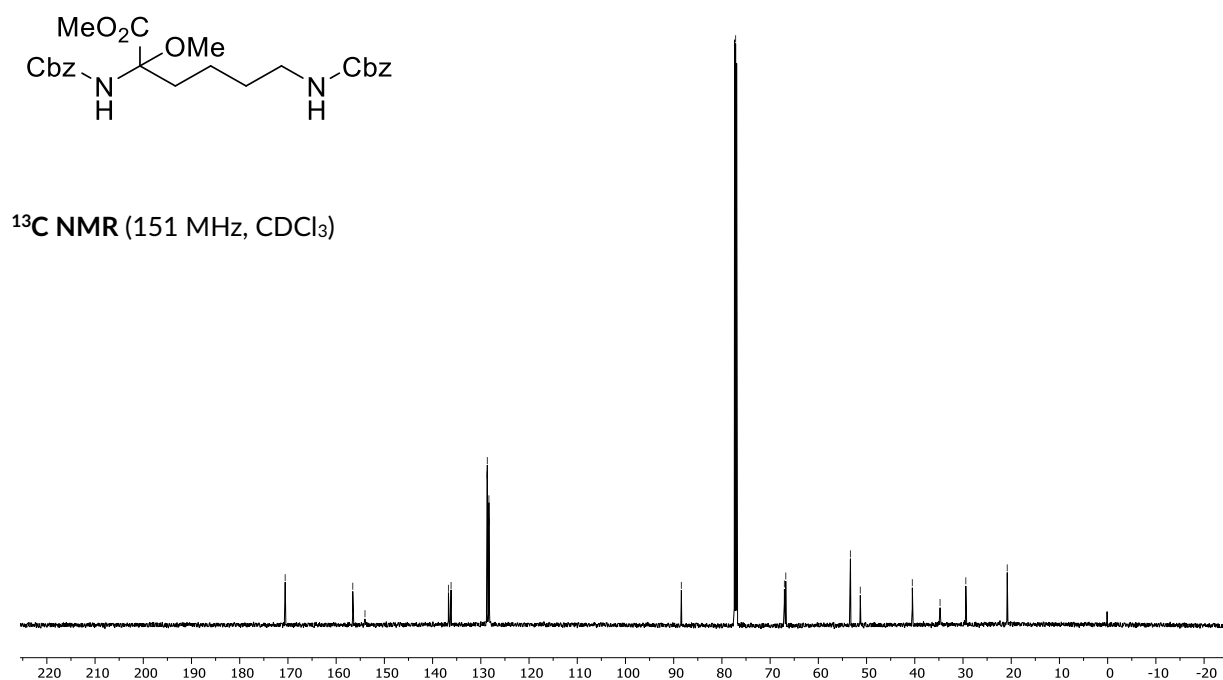
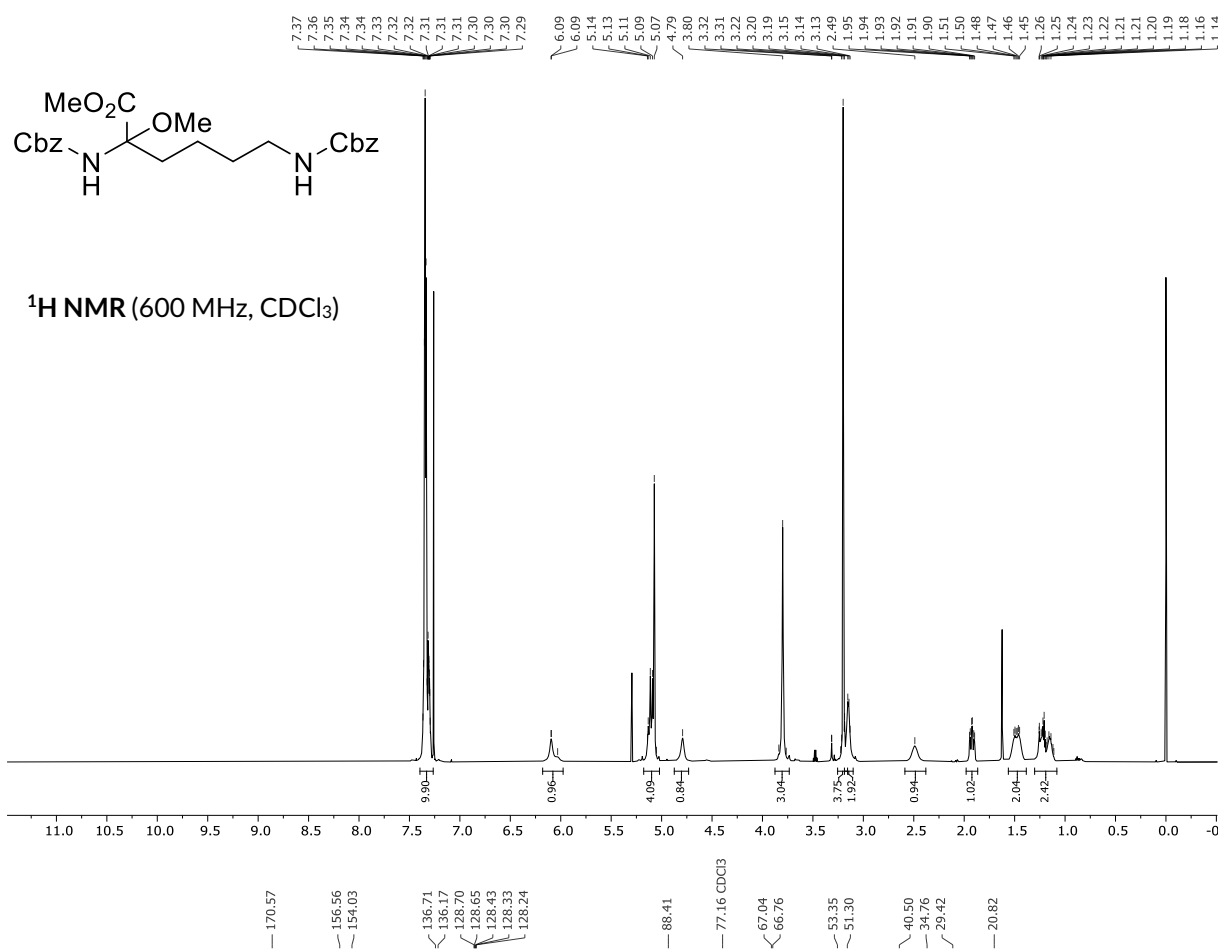


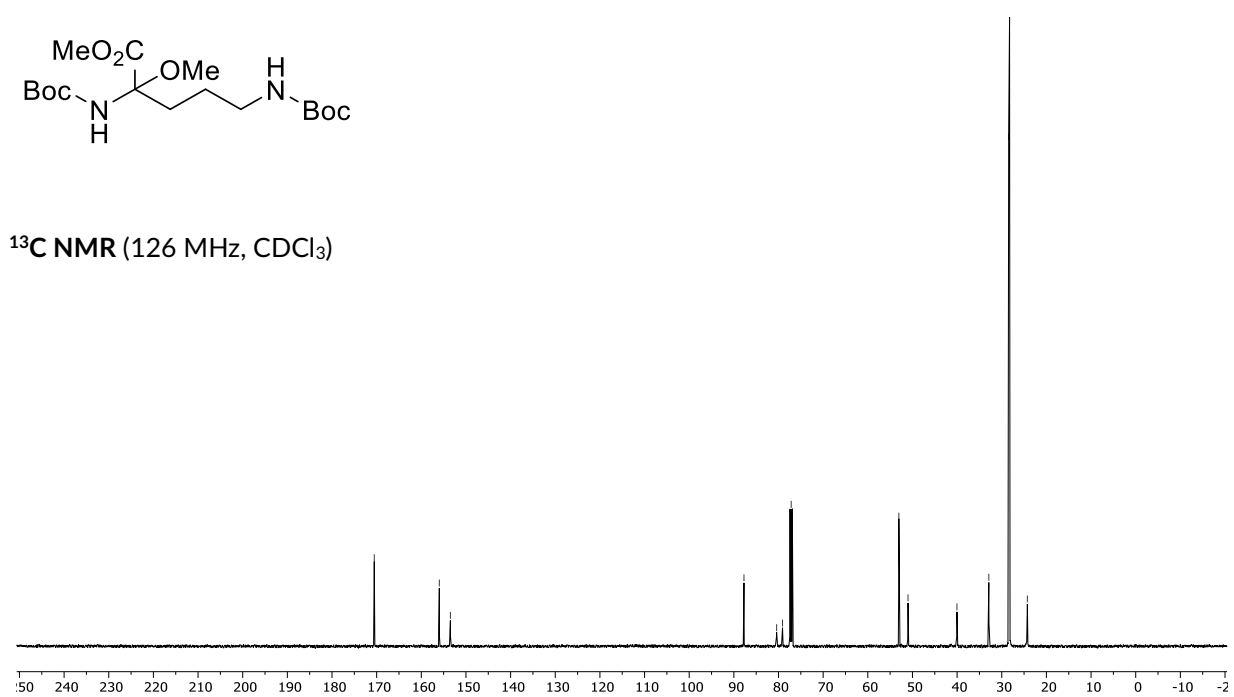
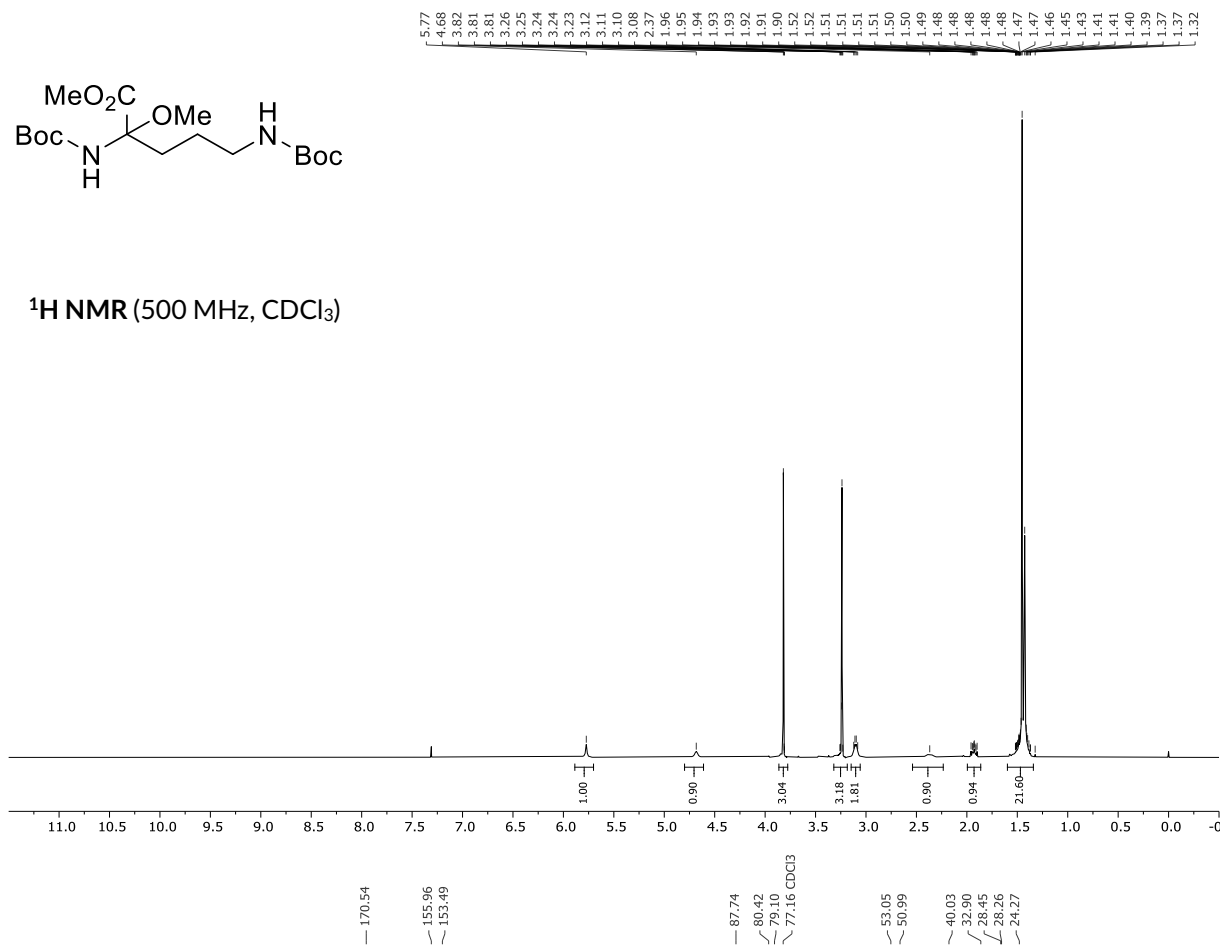


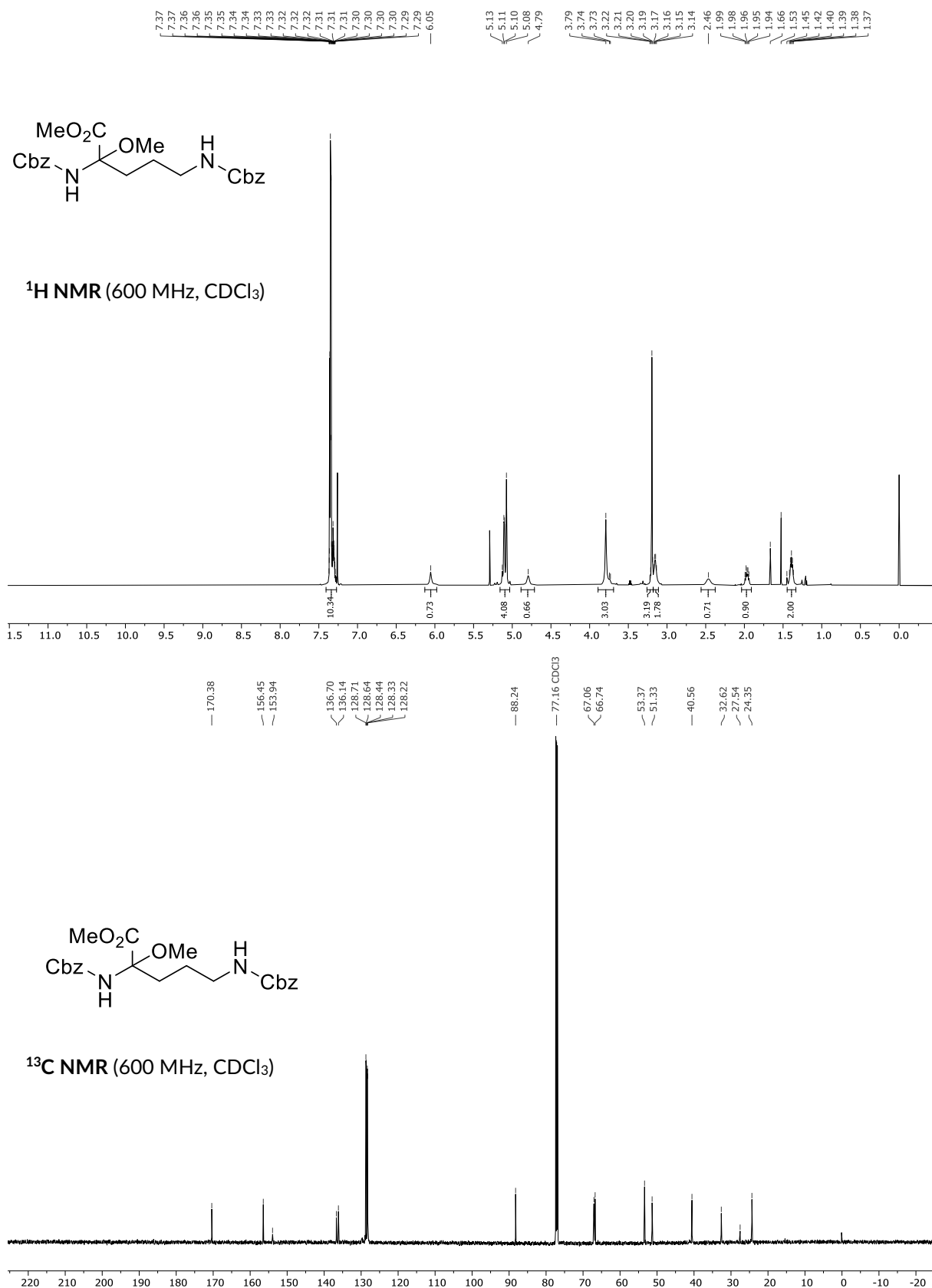


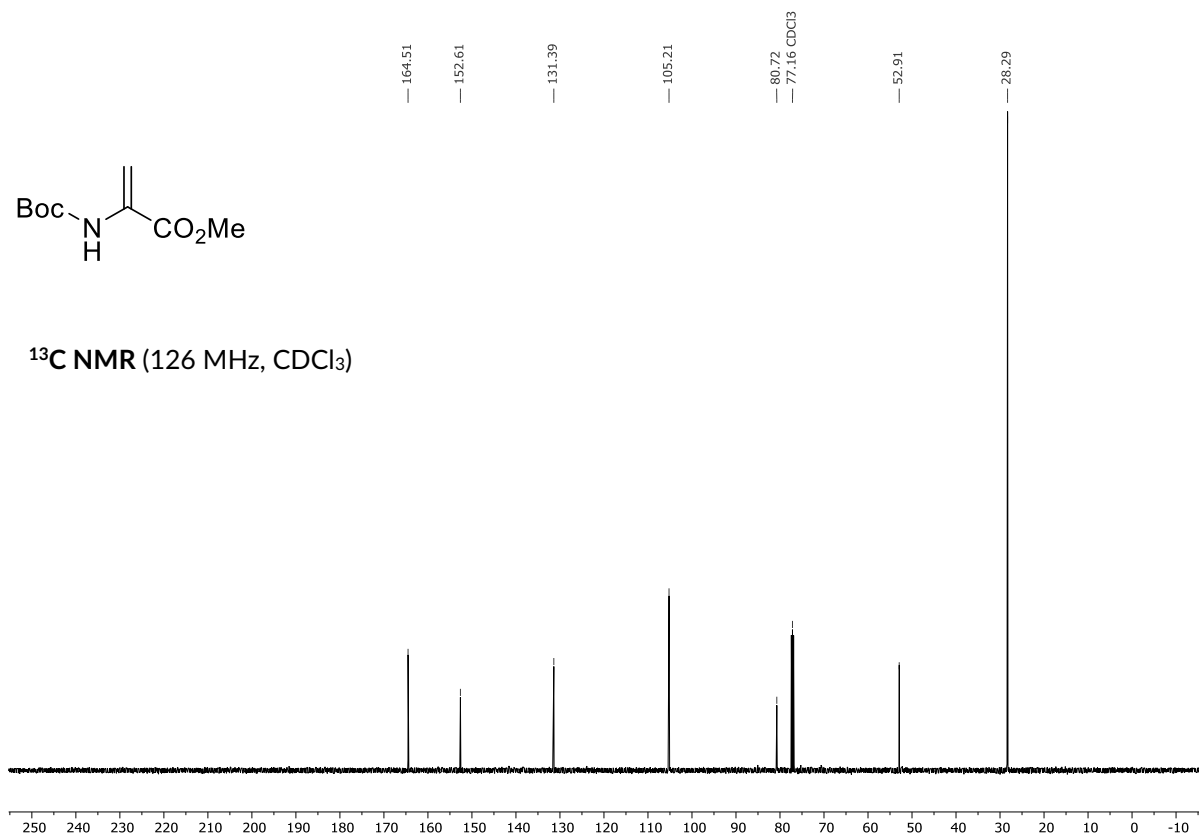
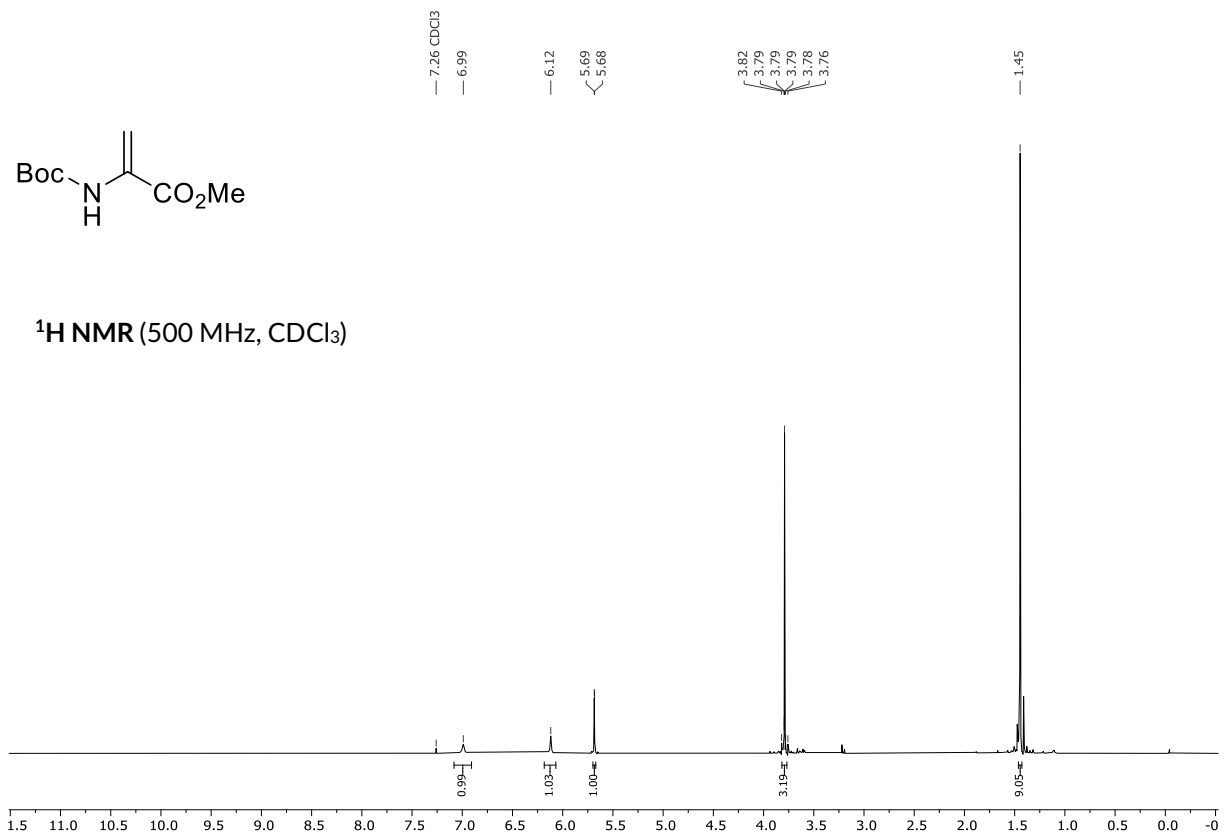


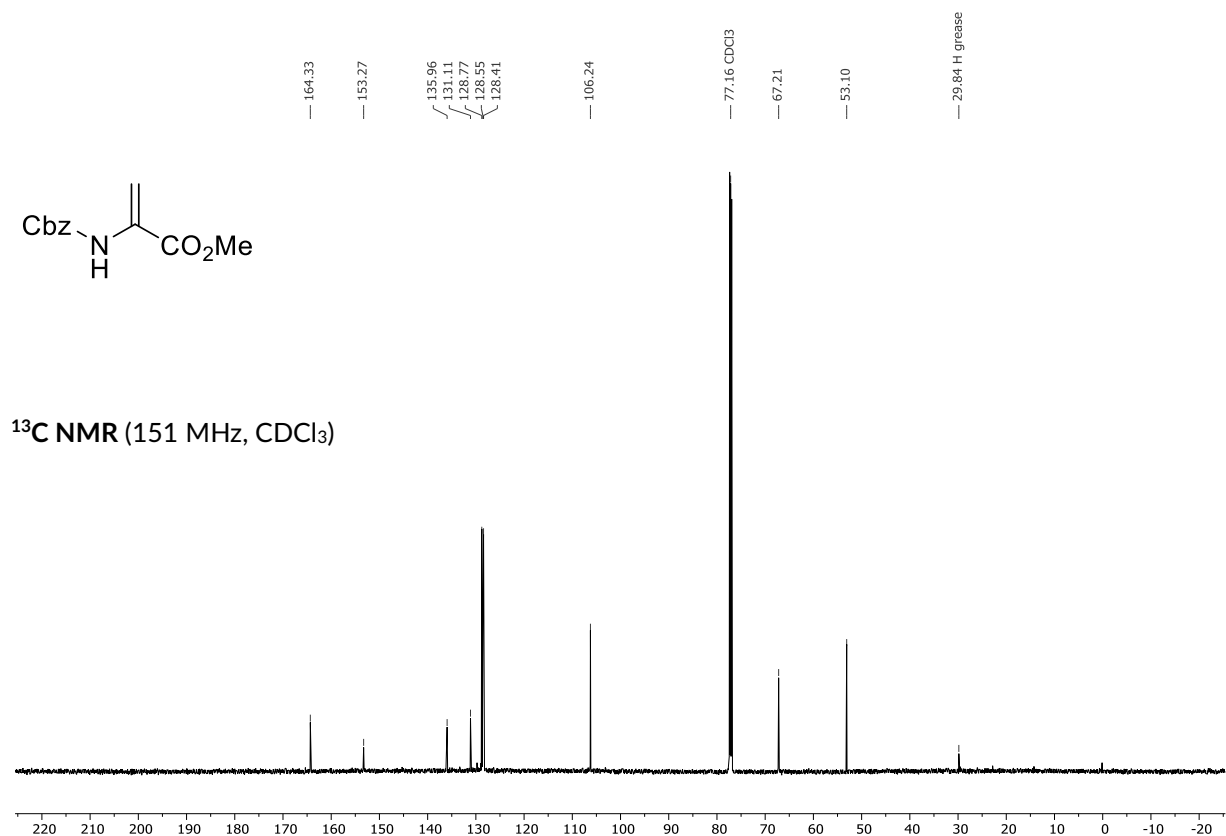
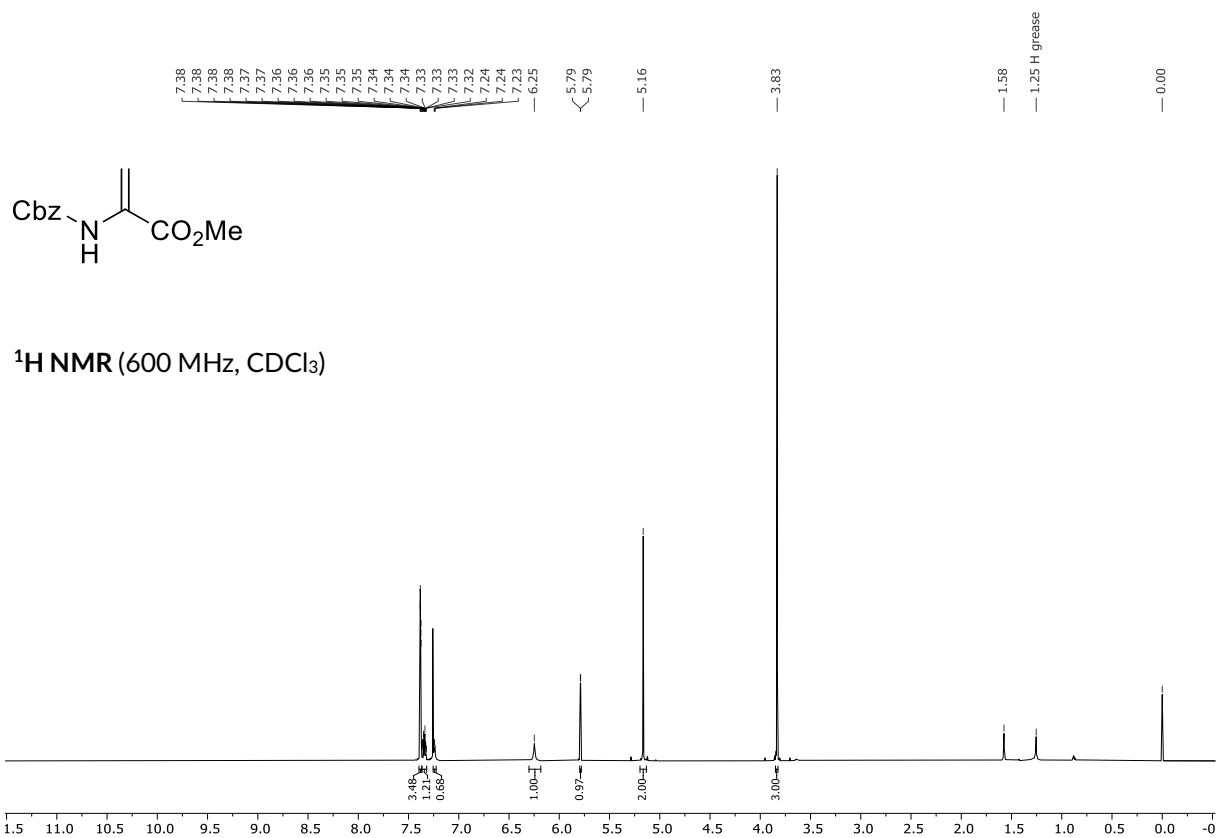


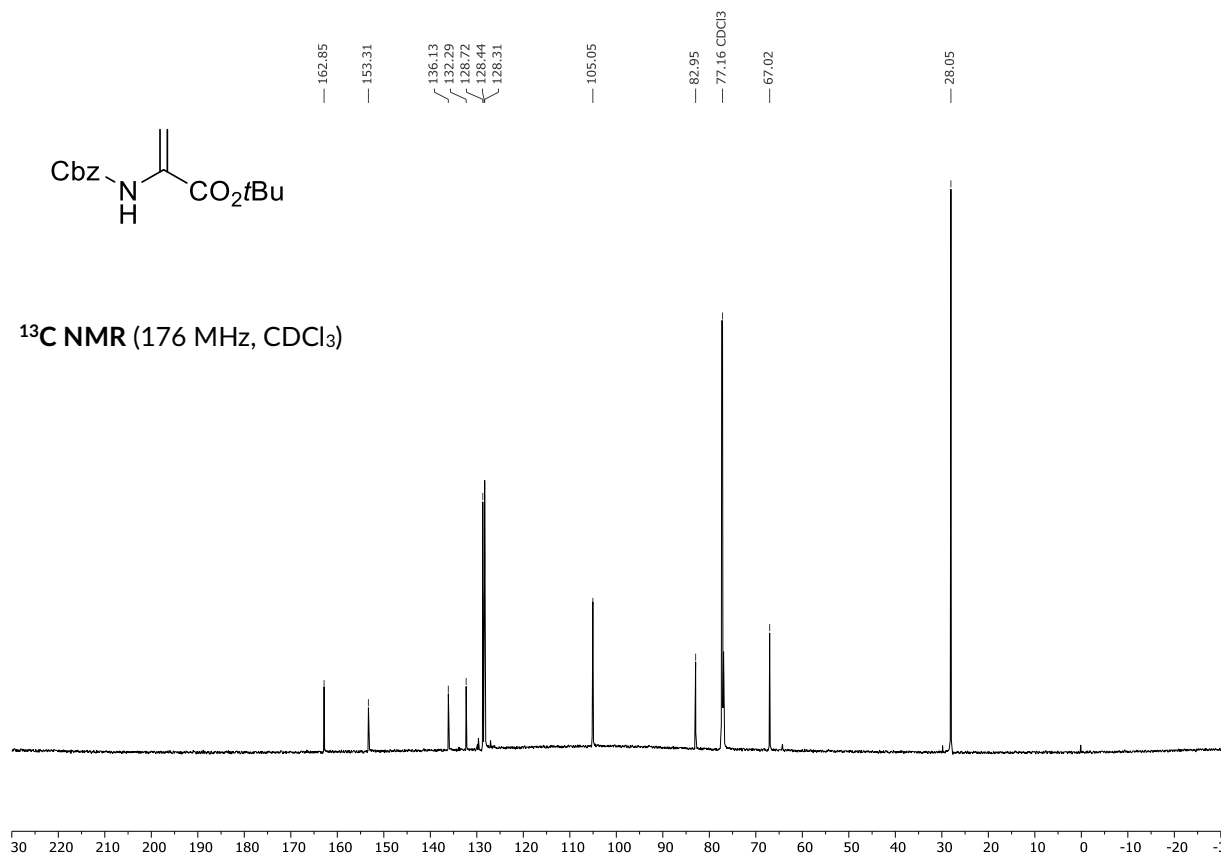
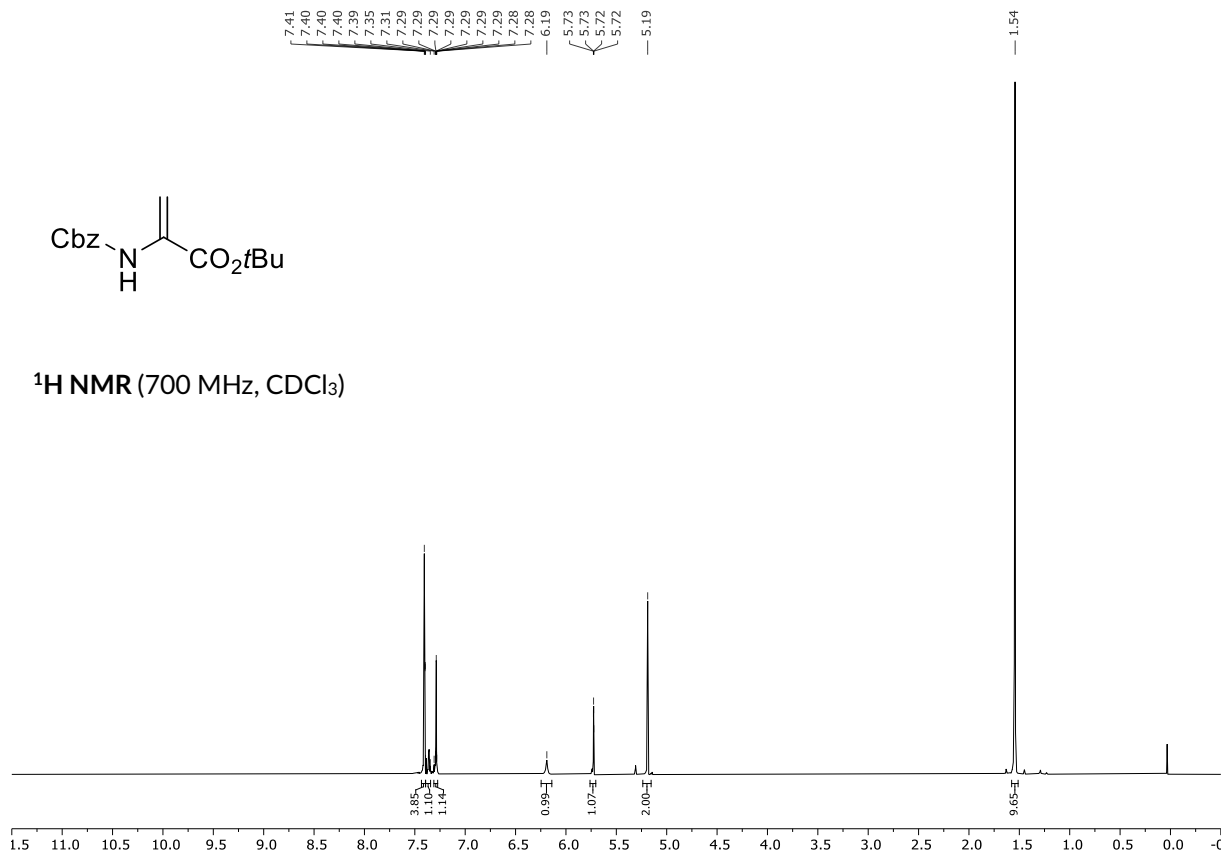


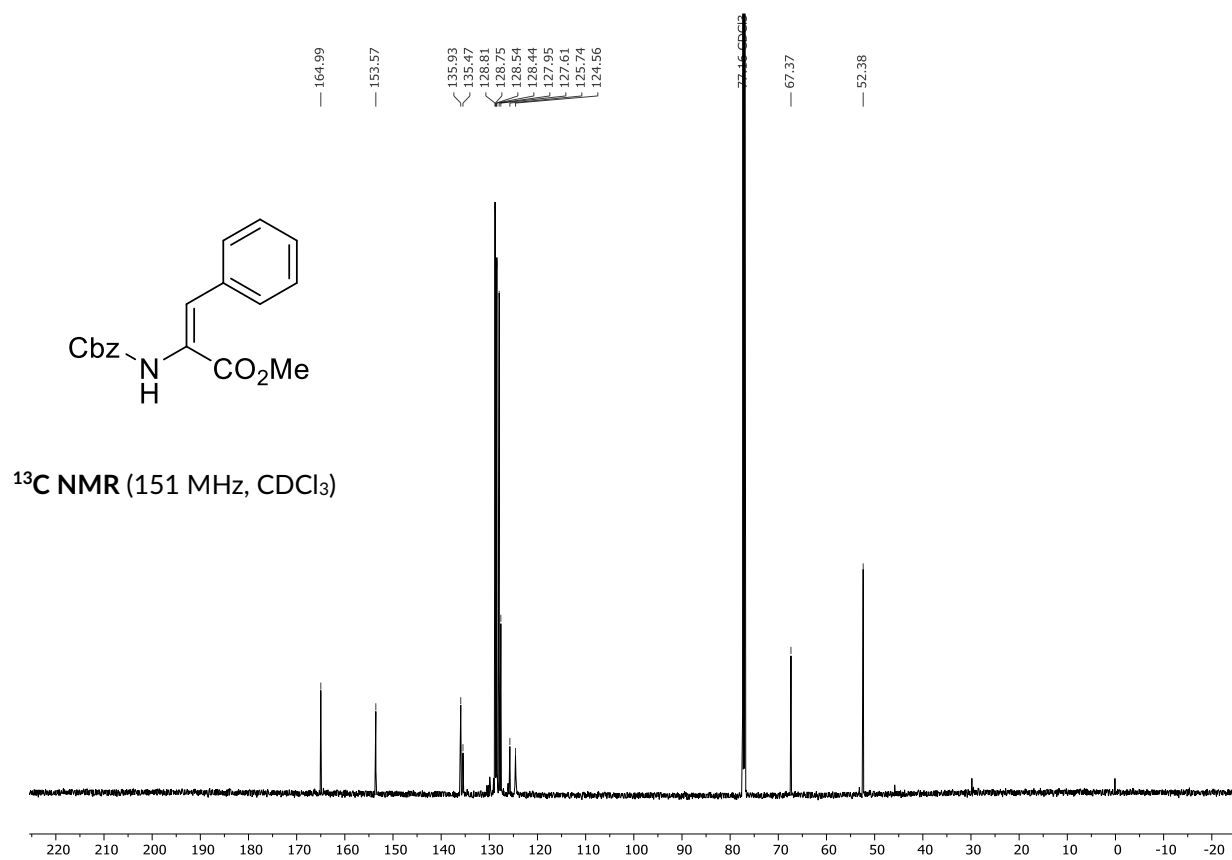
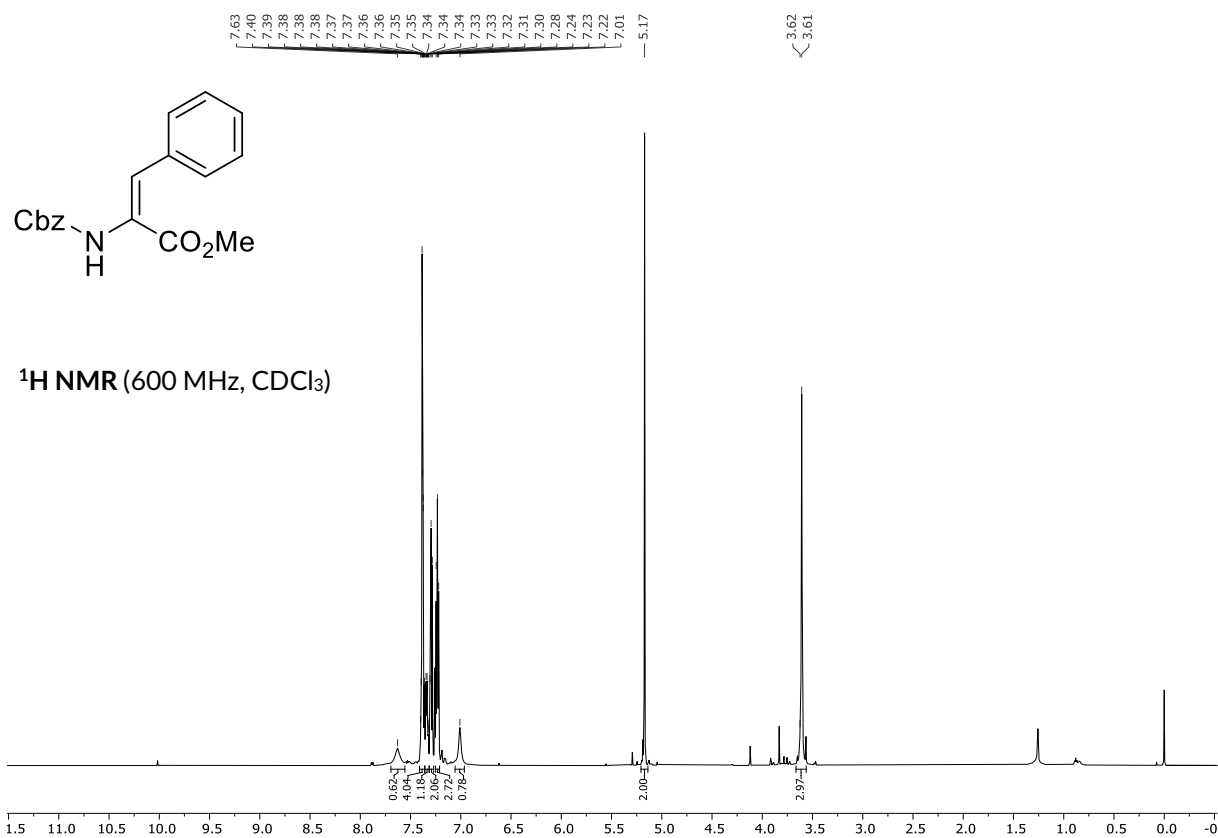


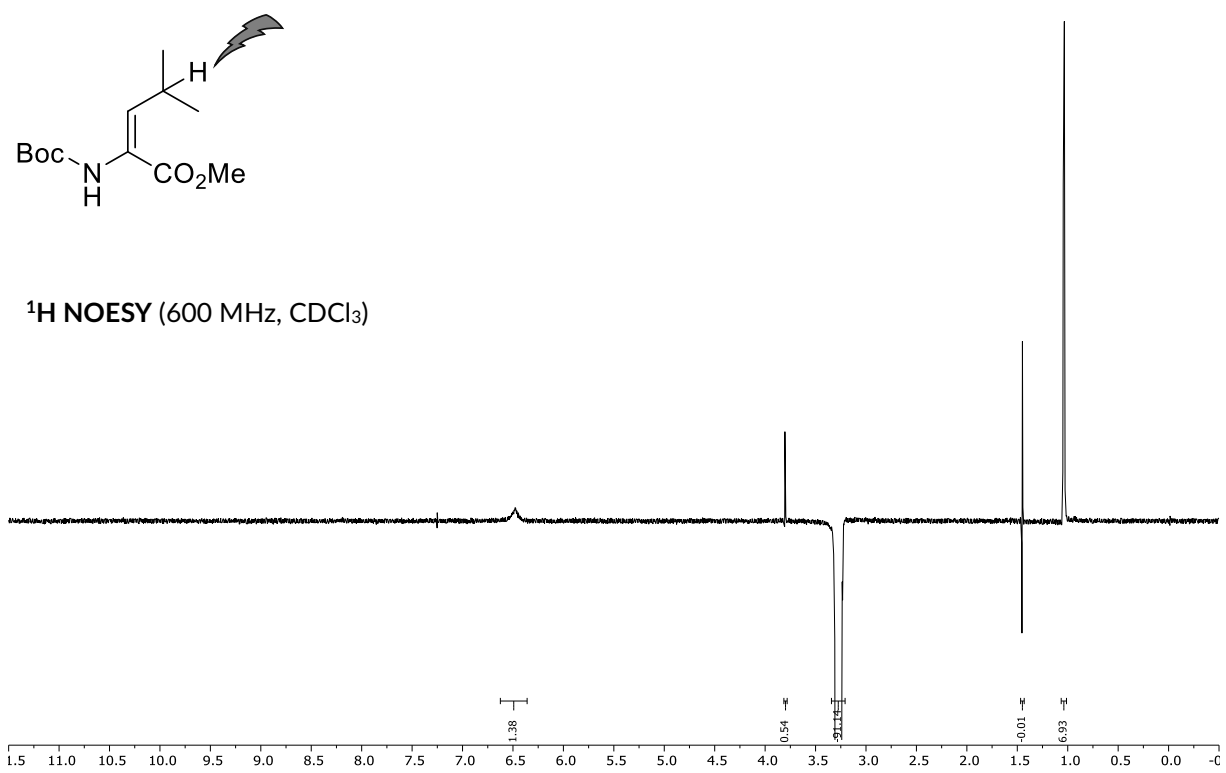
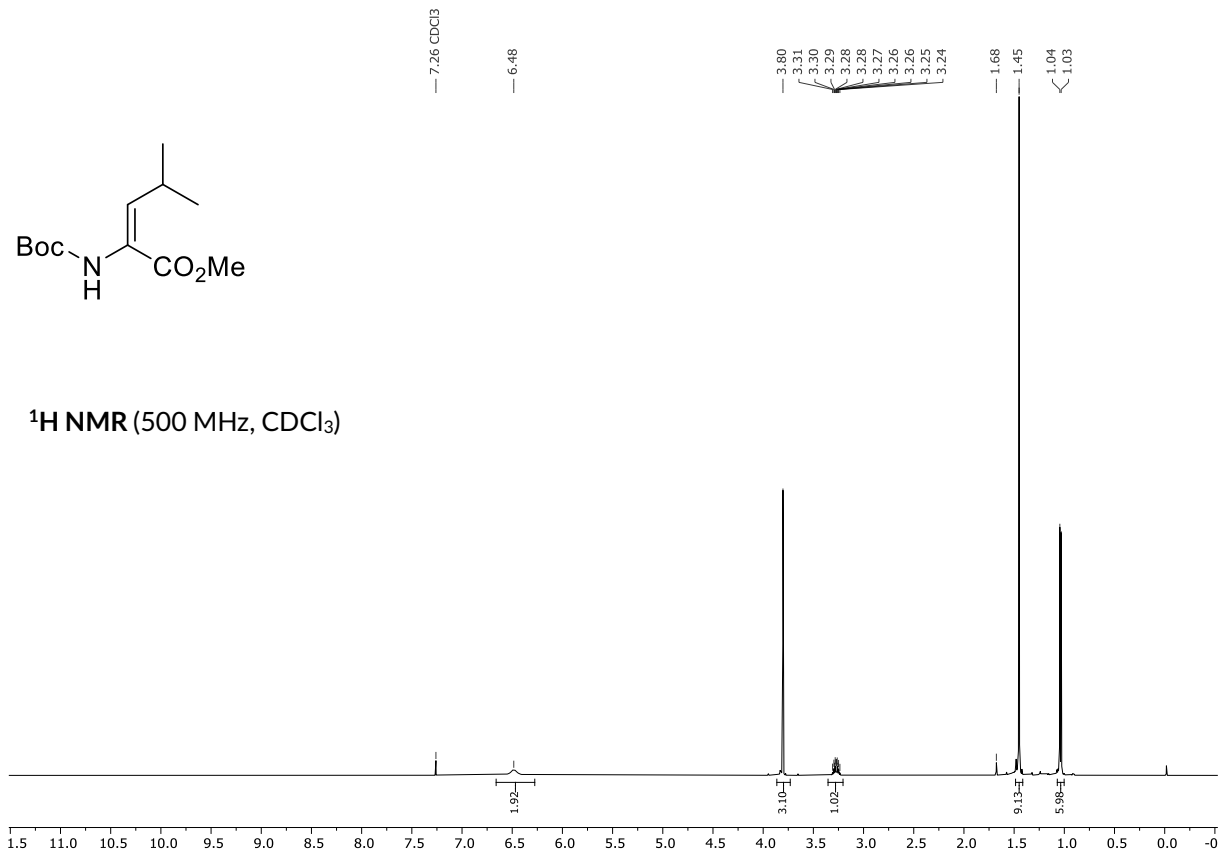


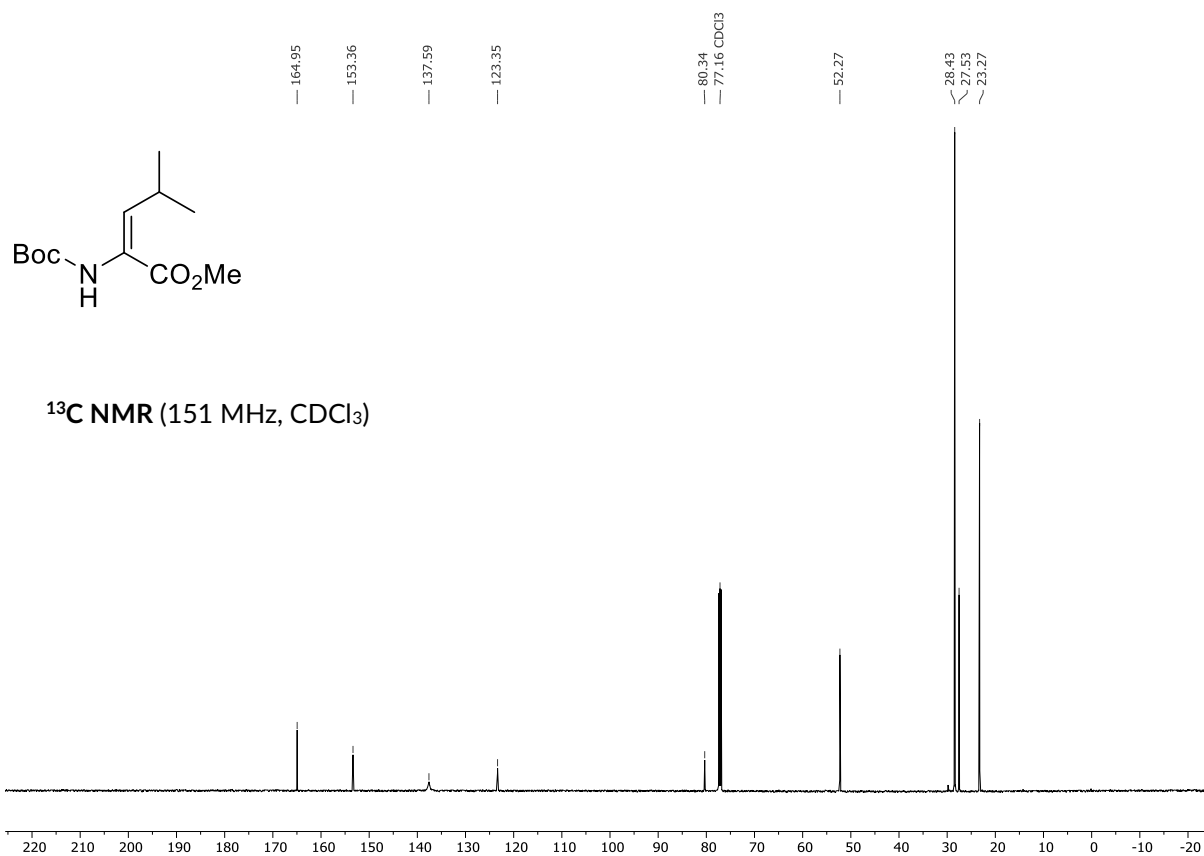


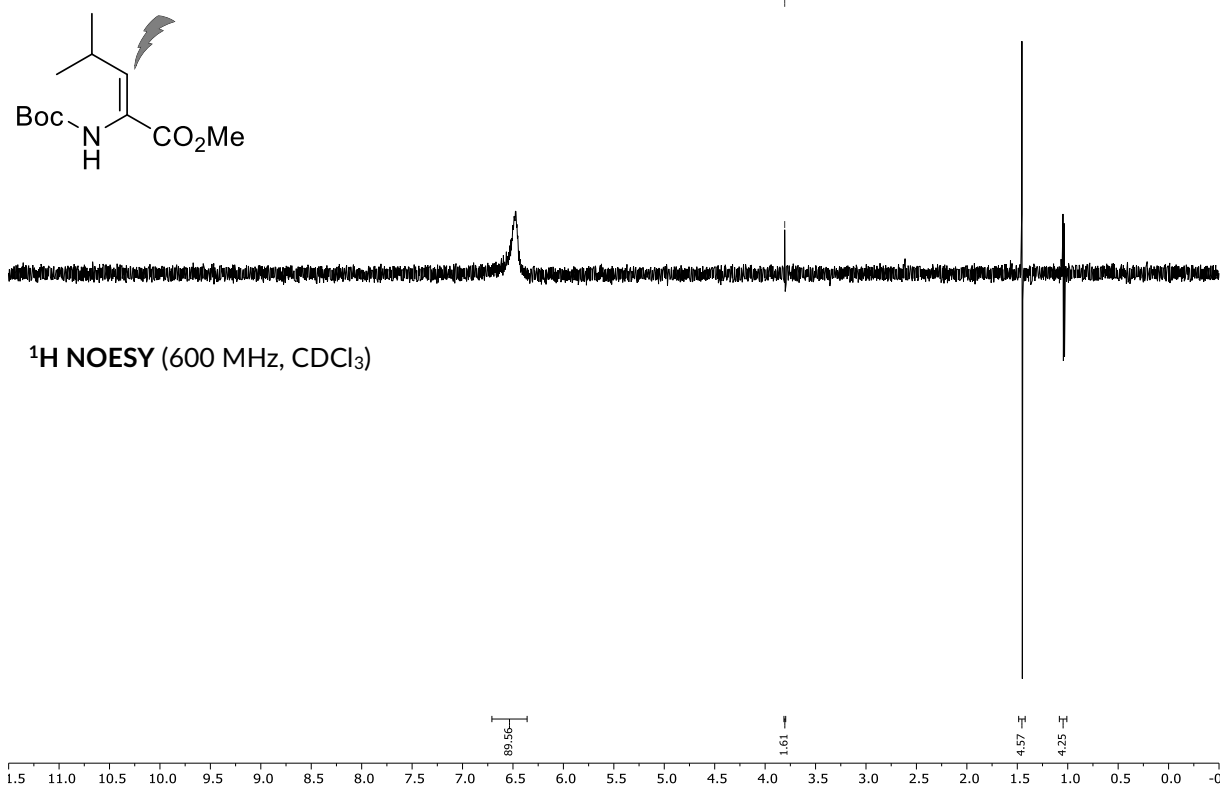
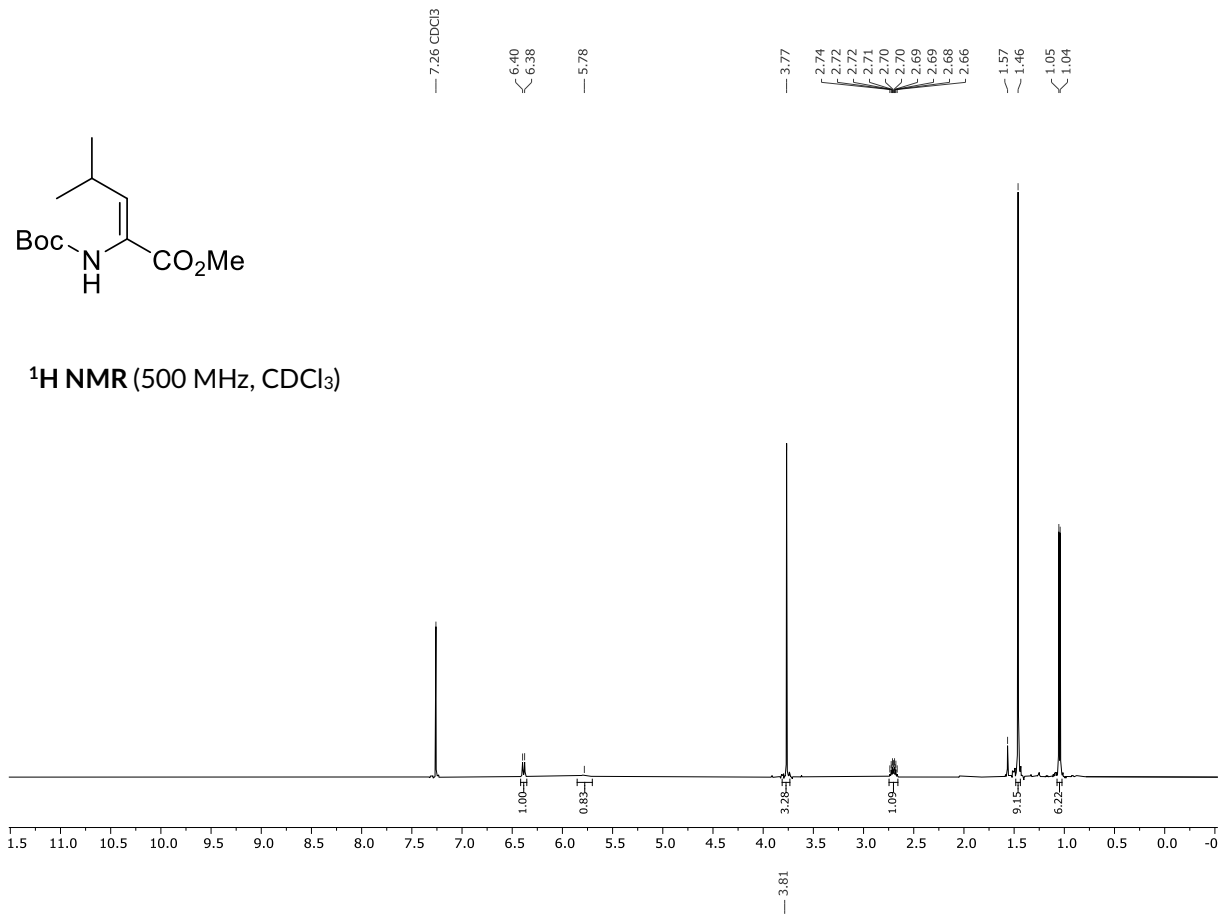


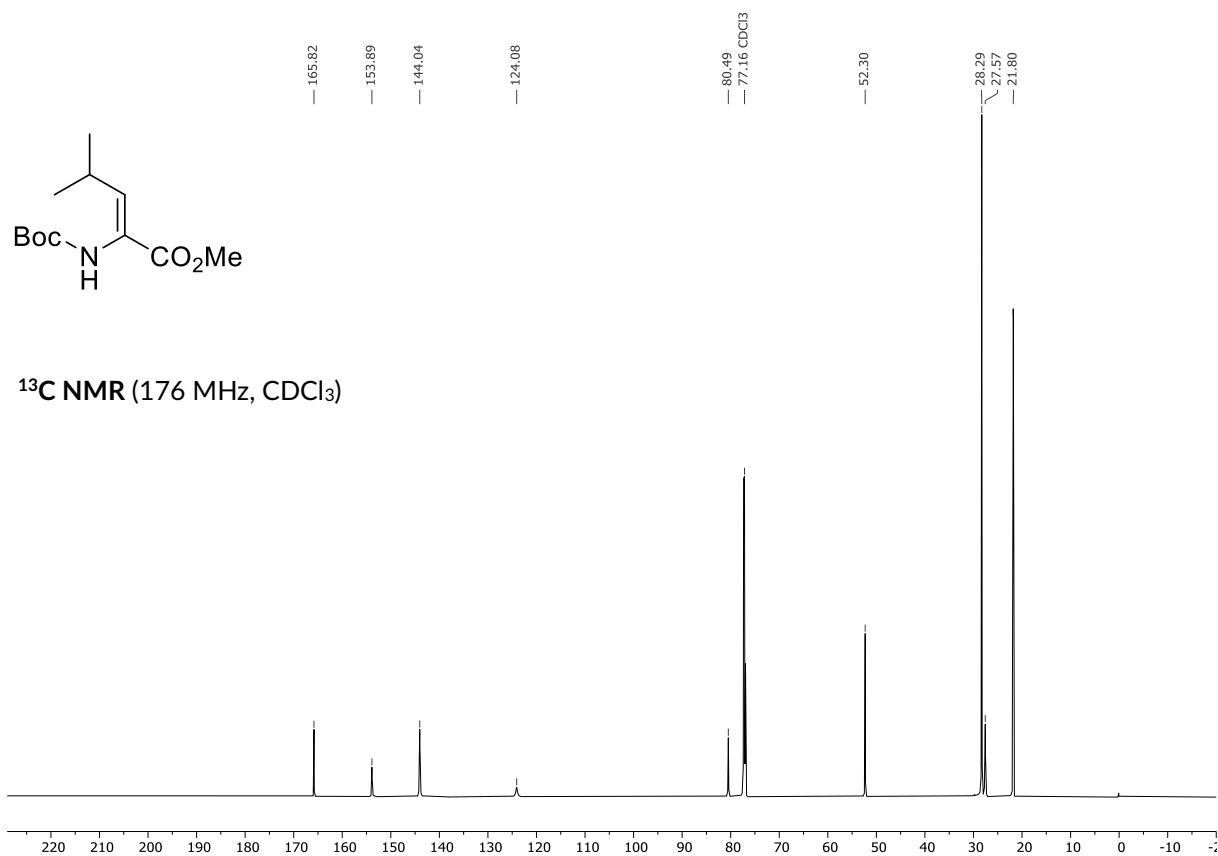


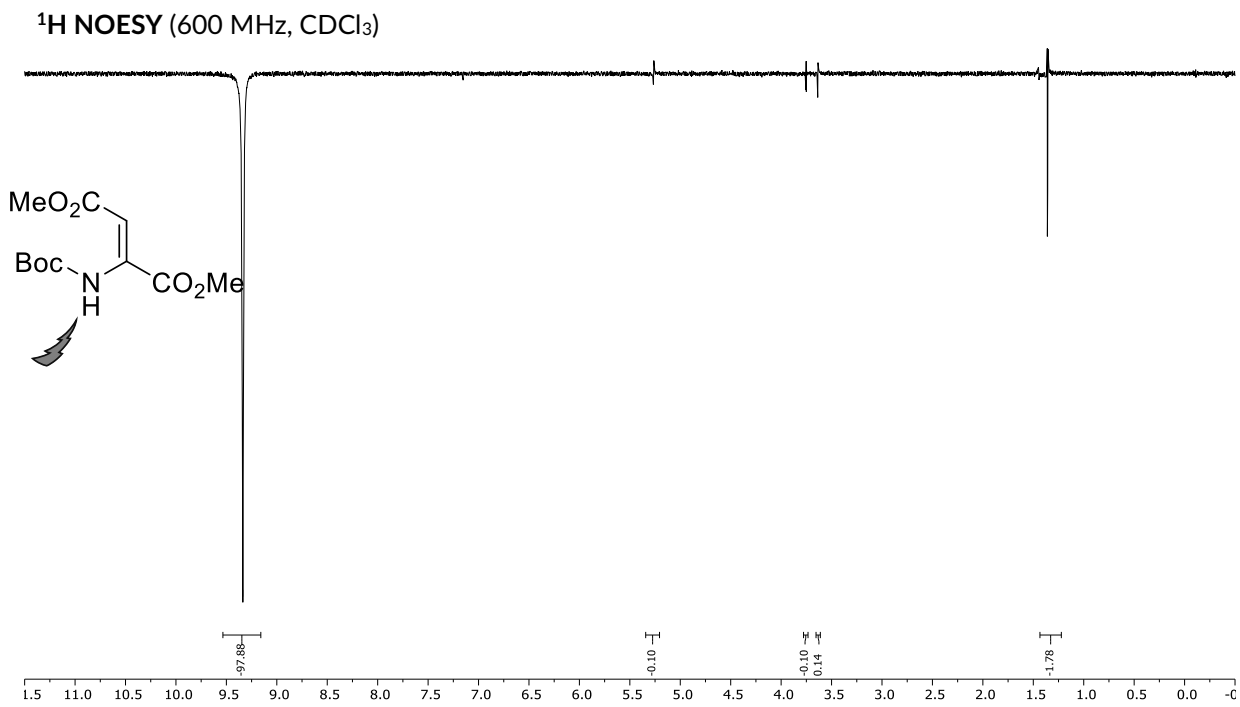
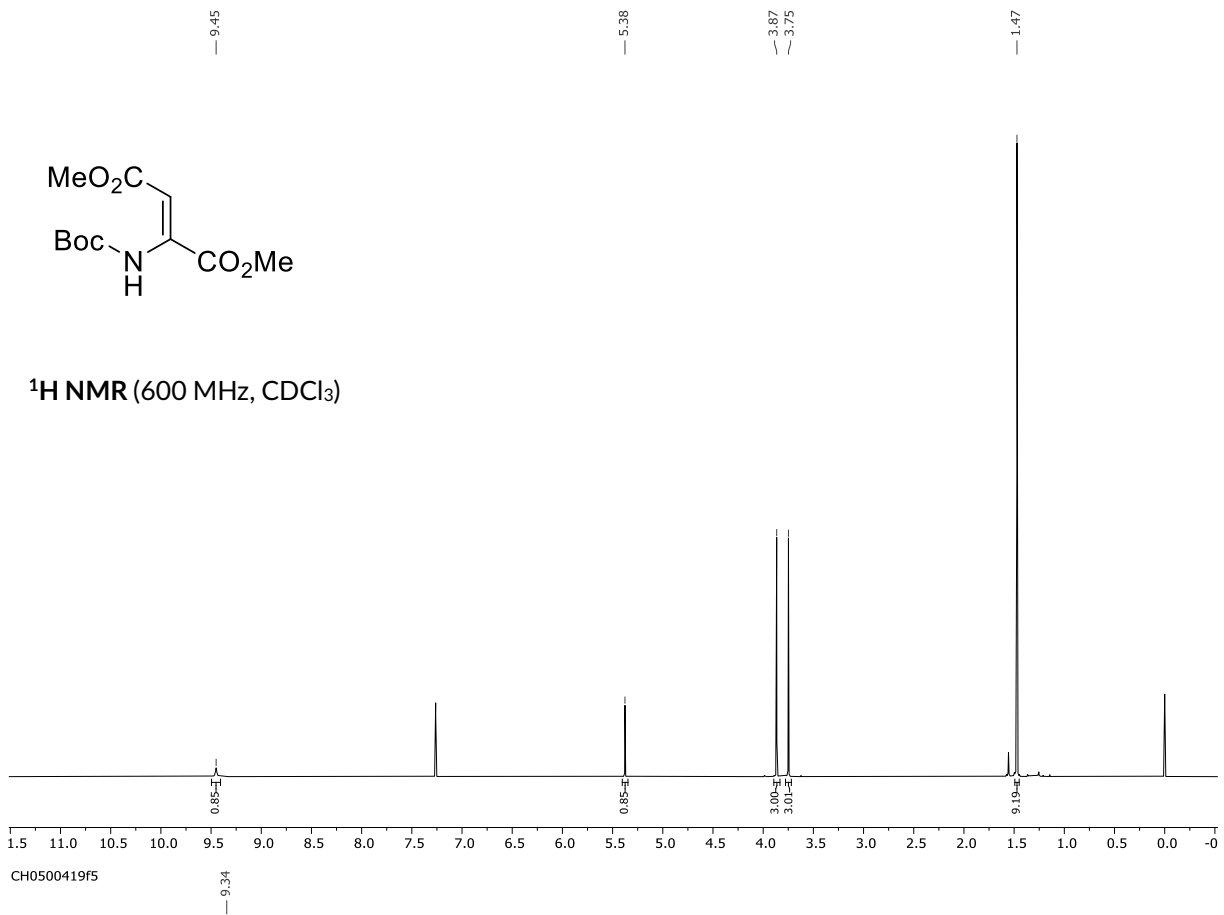


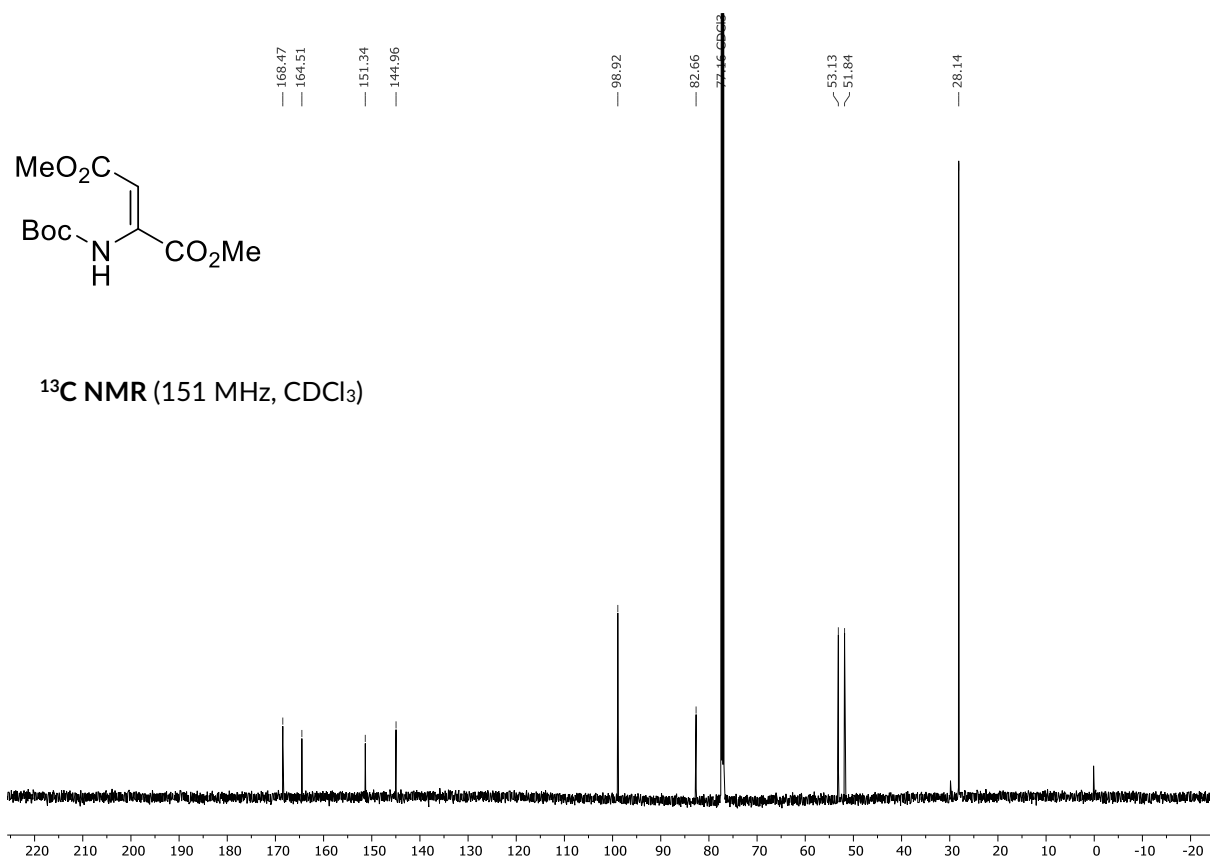


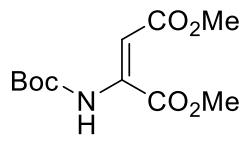




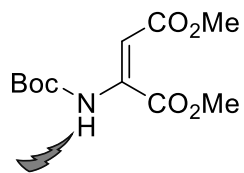
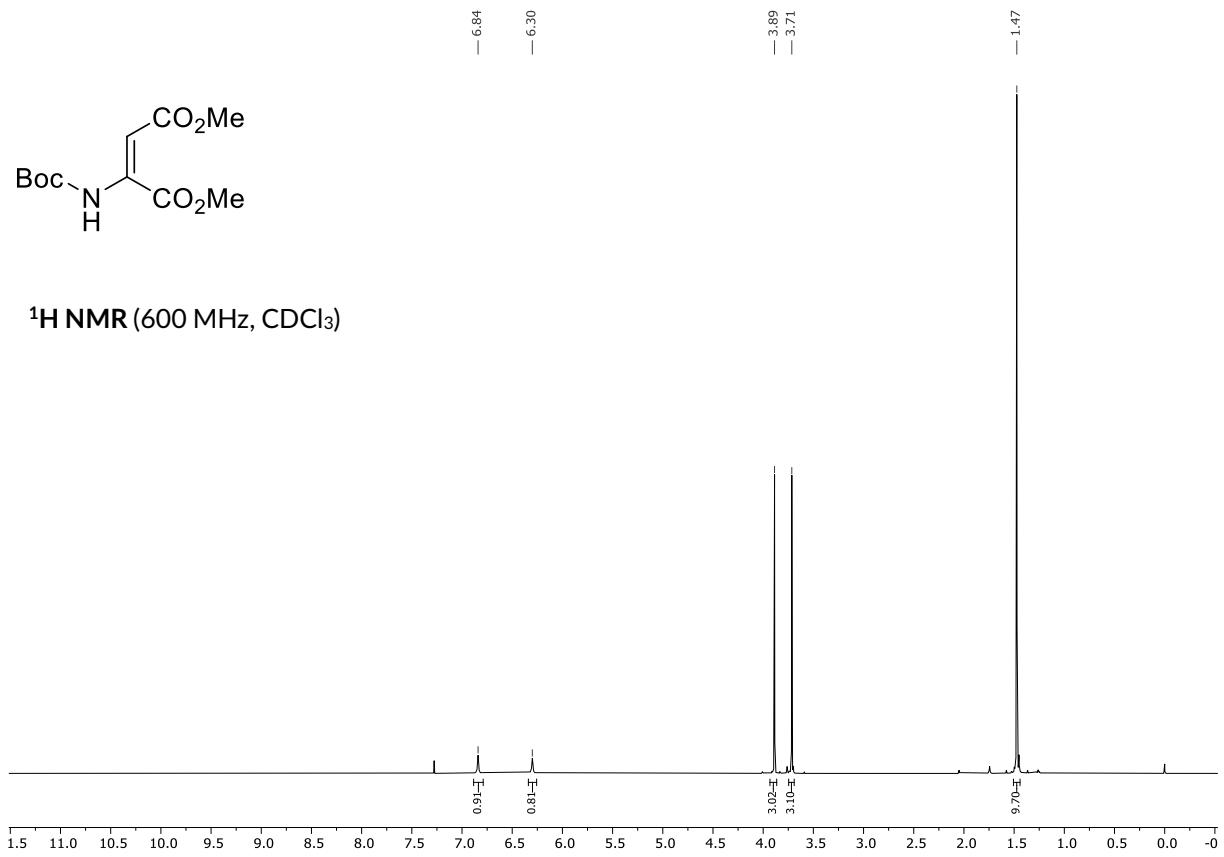




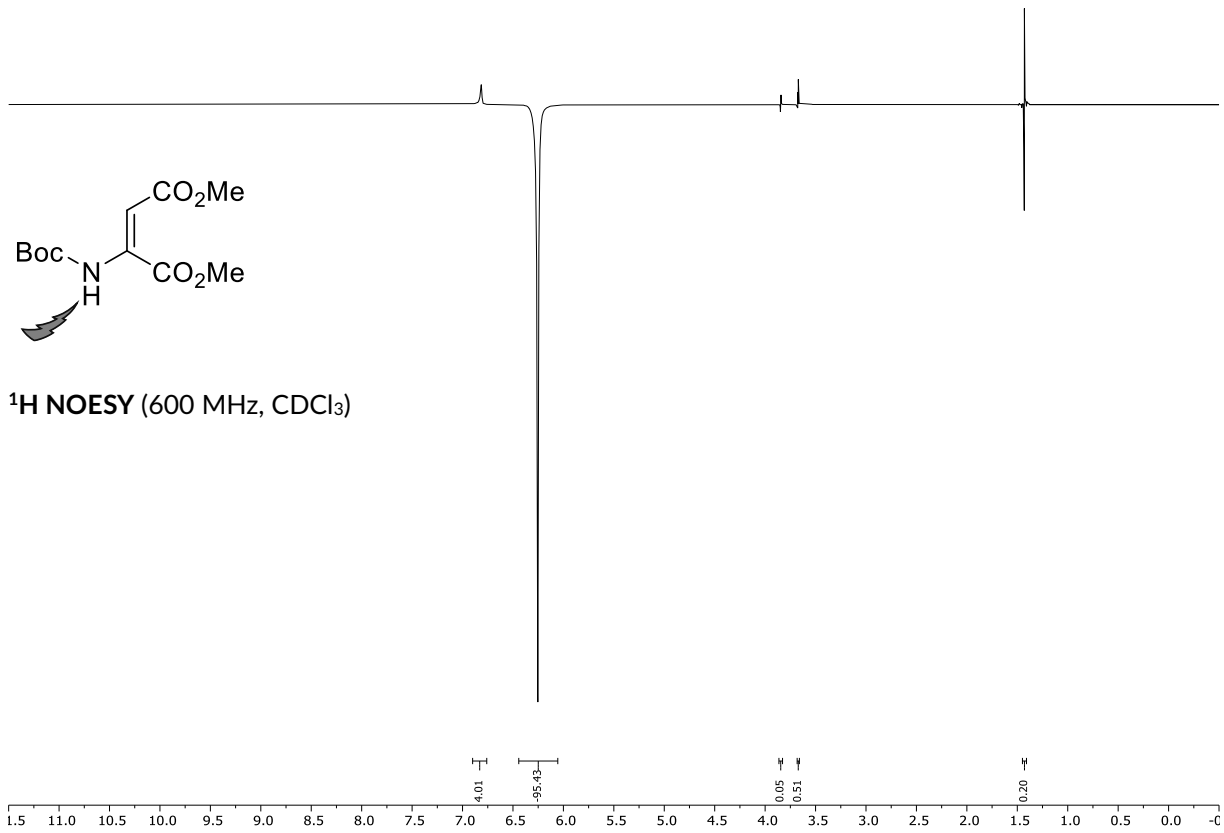


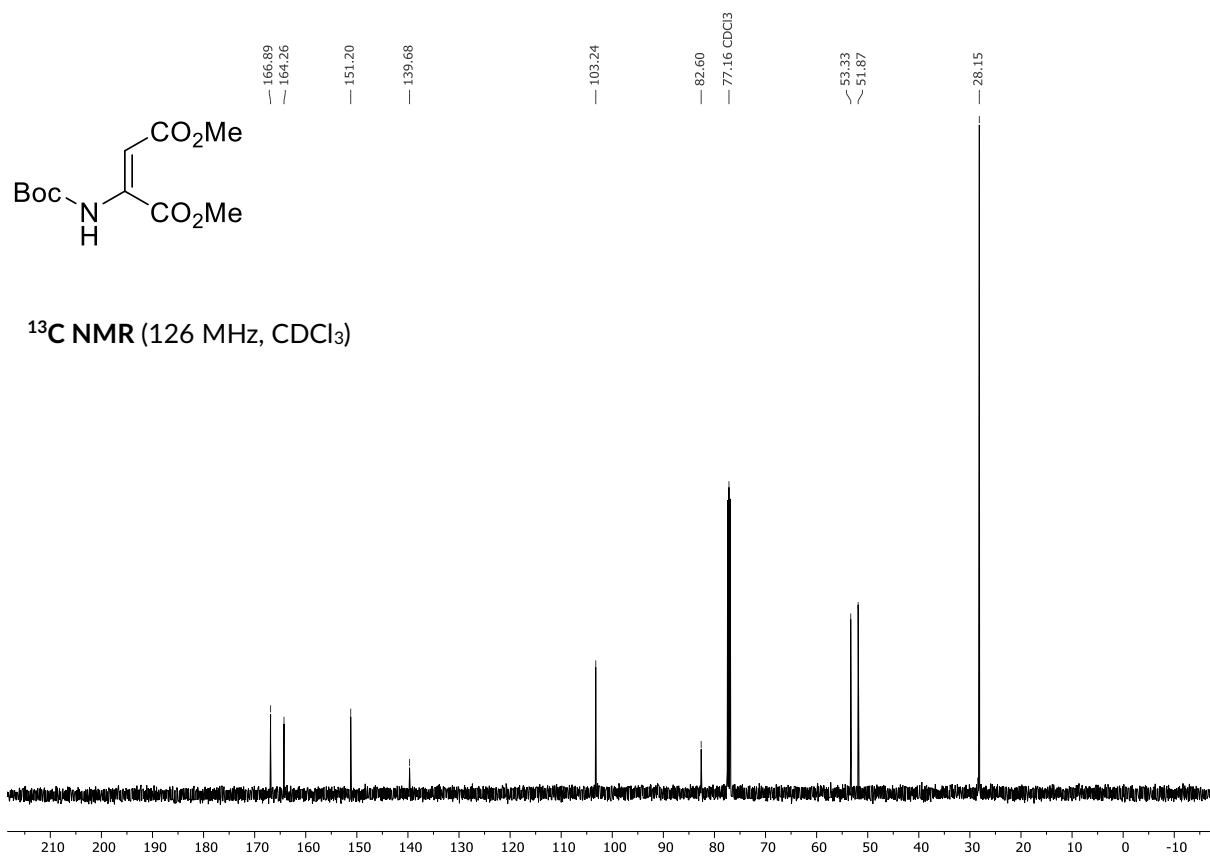


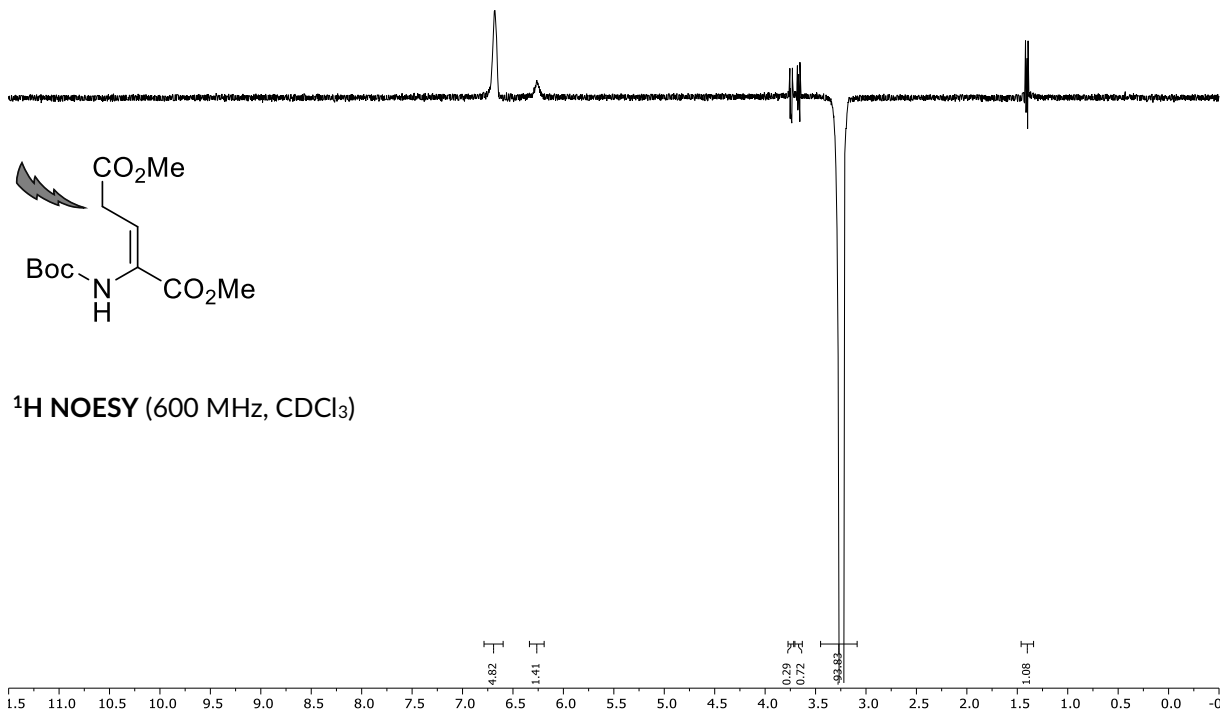
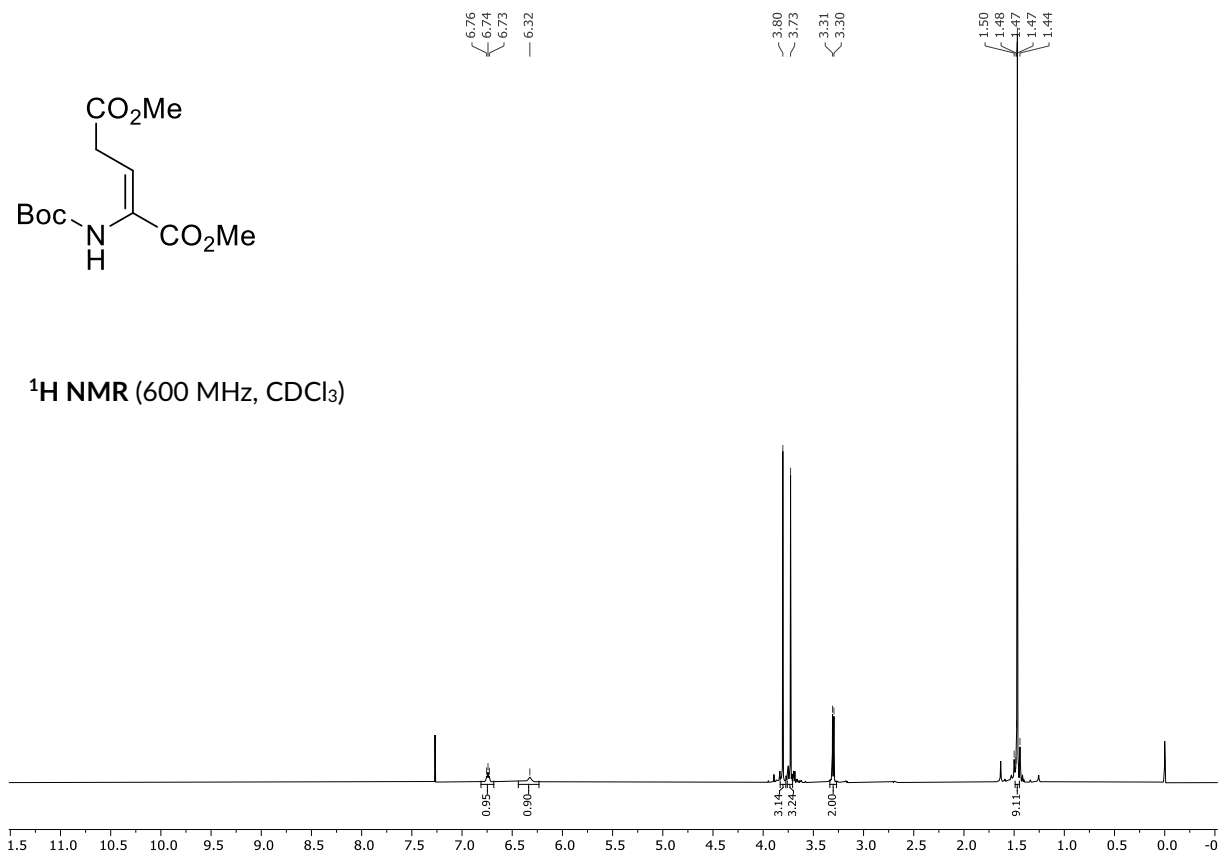
¹H NMR (600 MHz, CDCl₃)

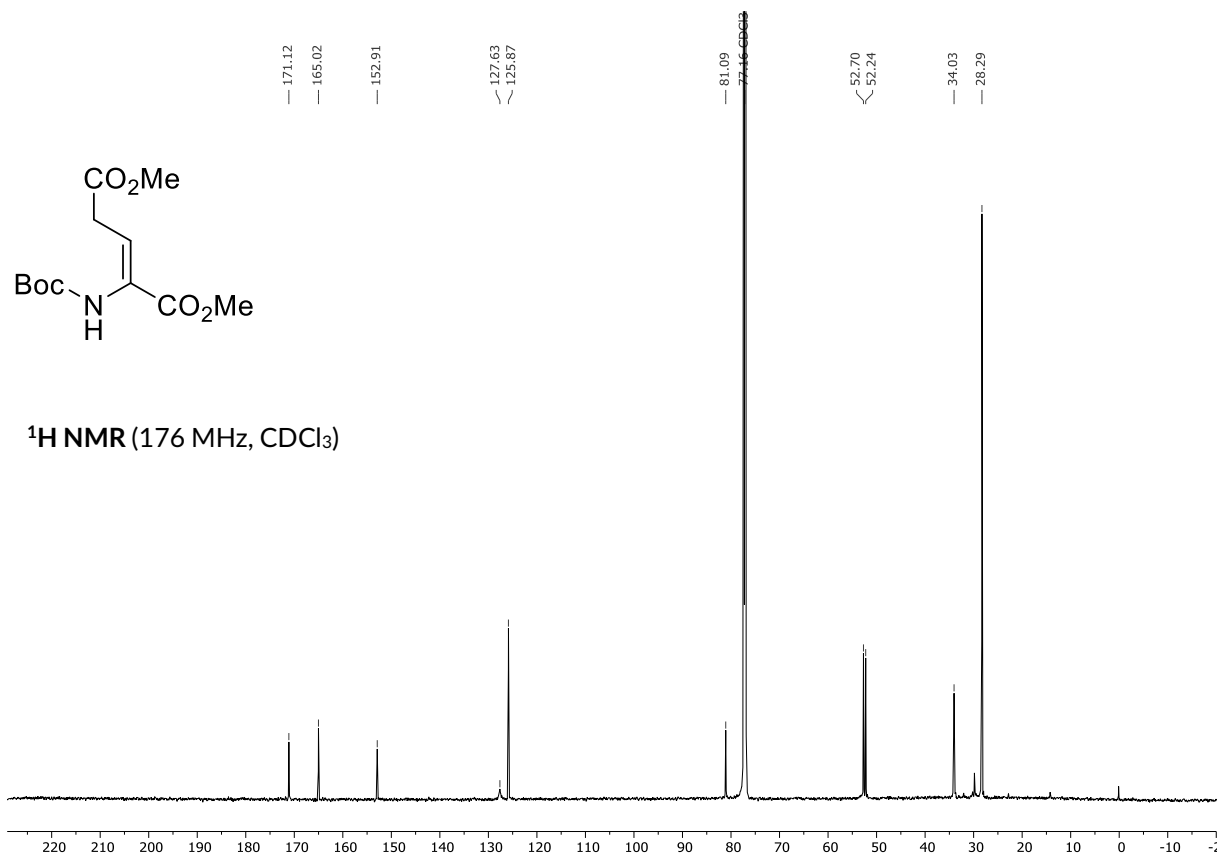


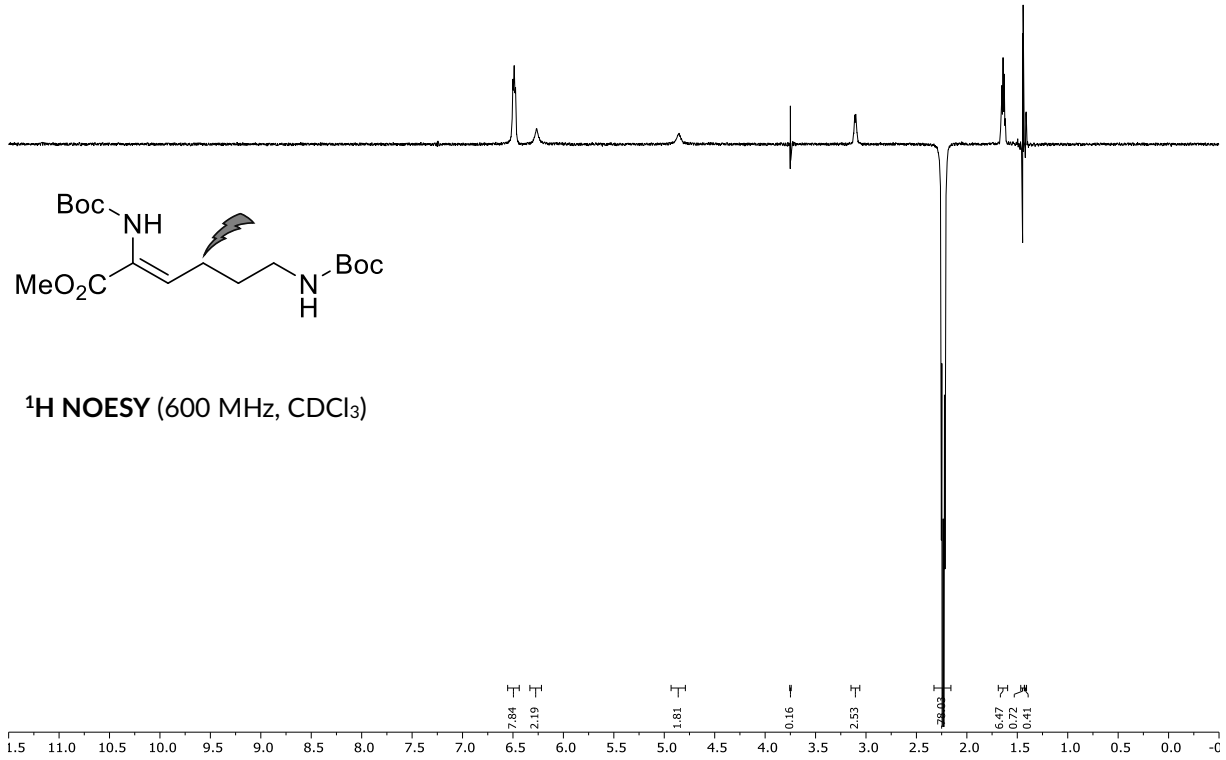
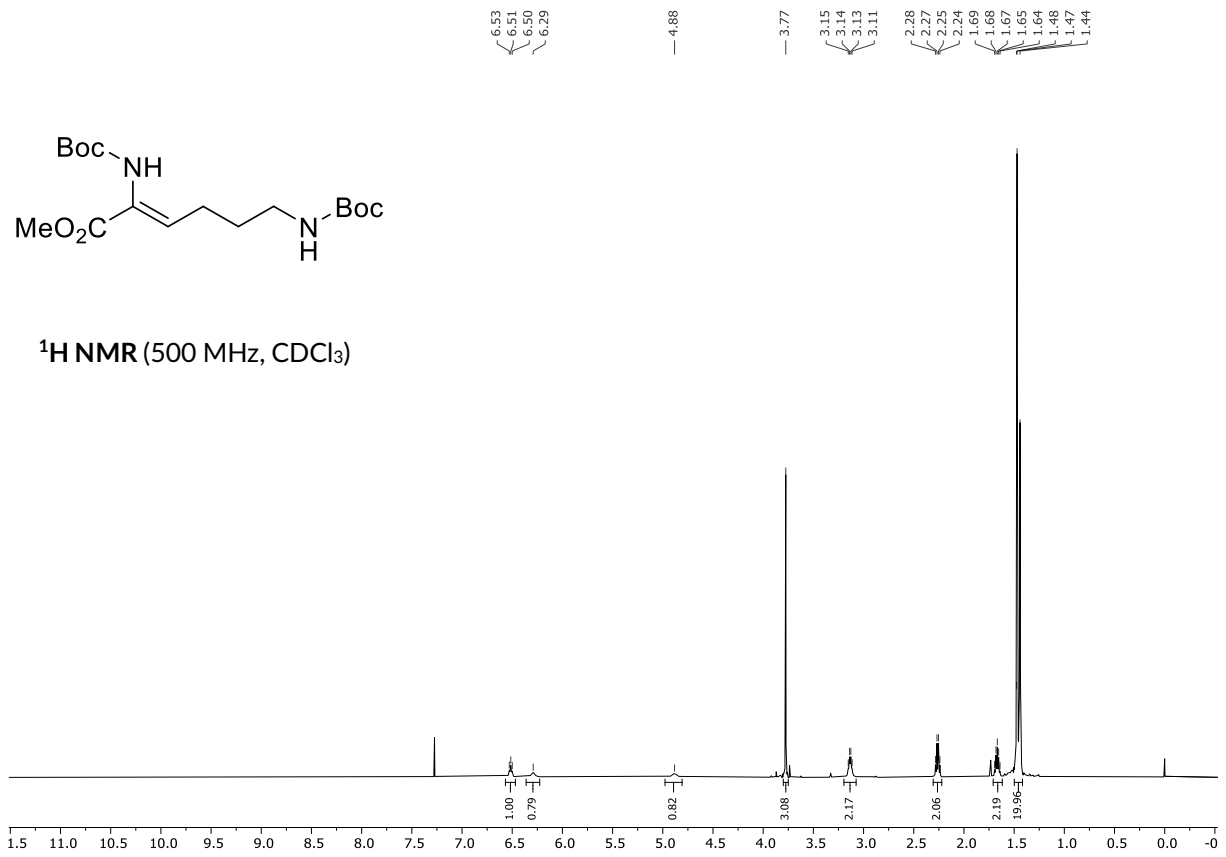
¹H NOESY (600 MHz, CDCl₃)

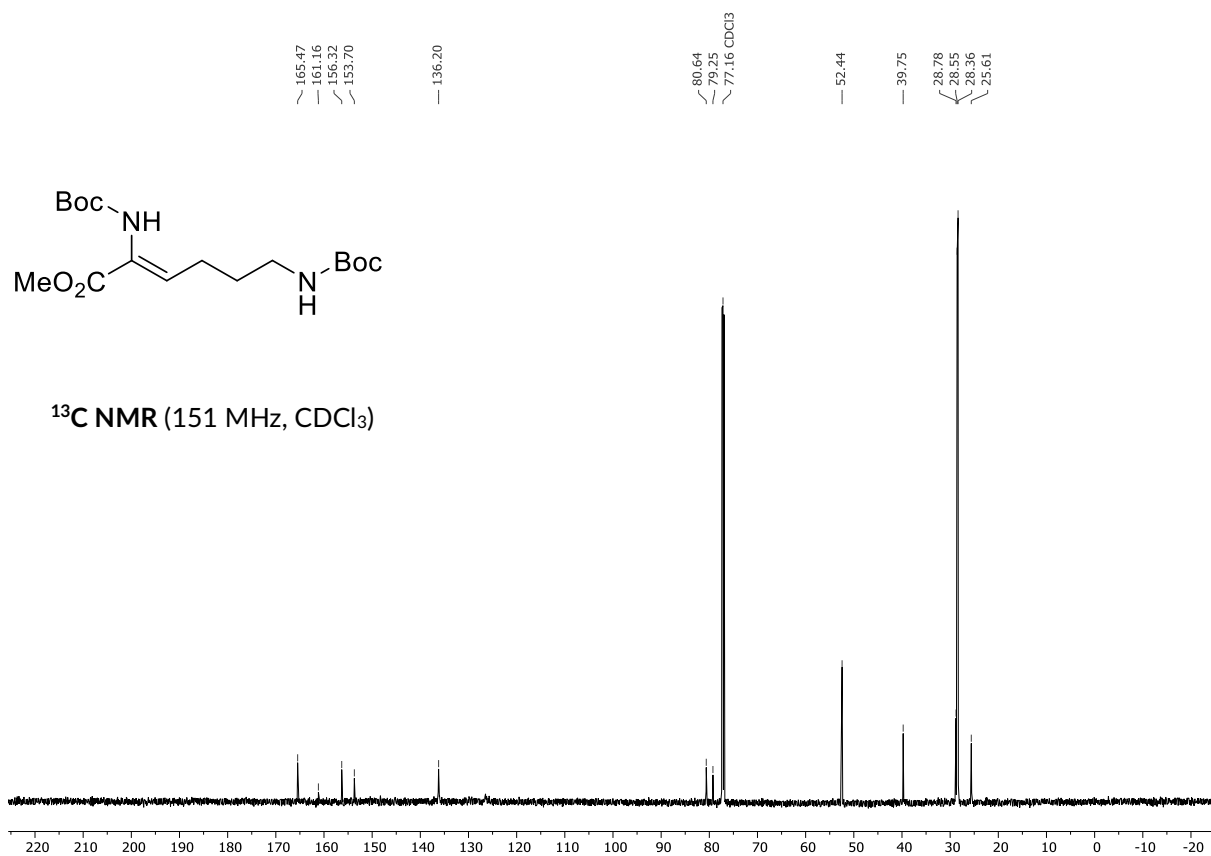


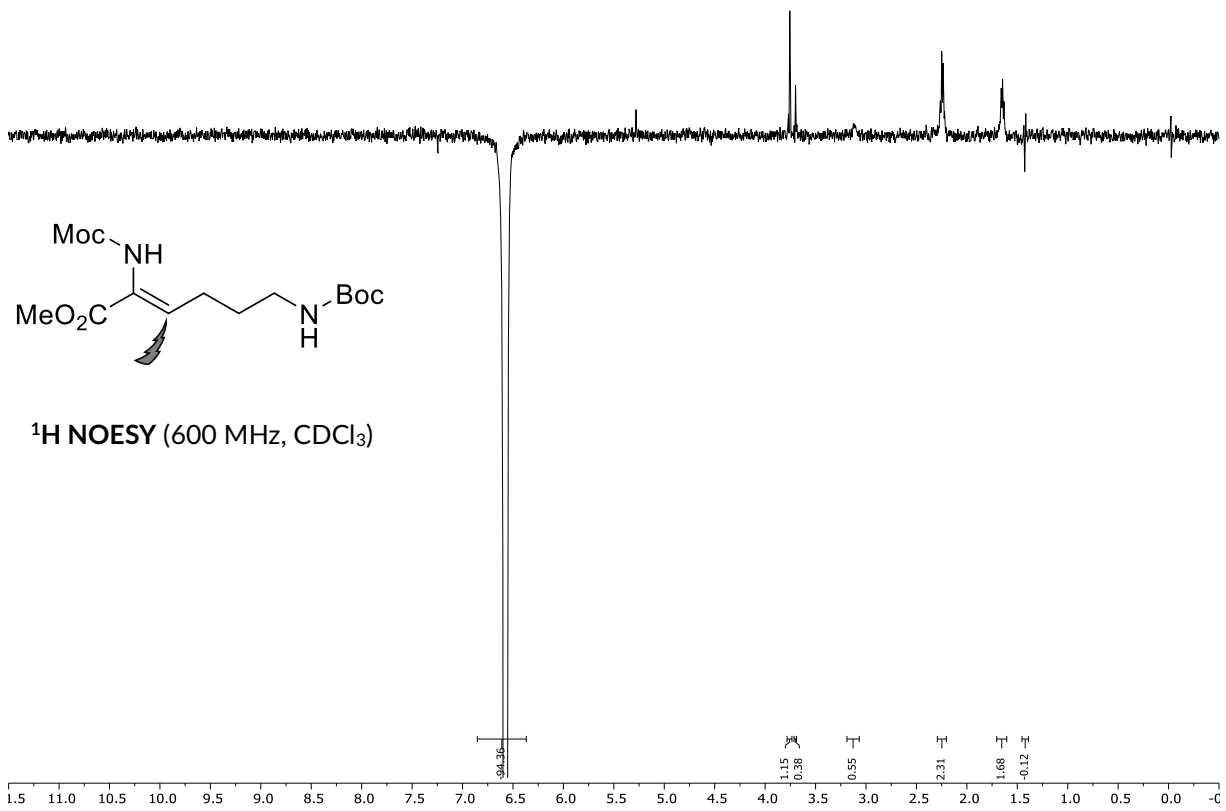
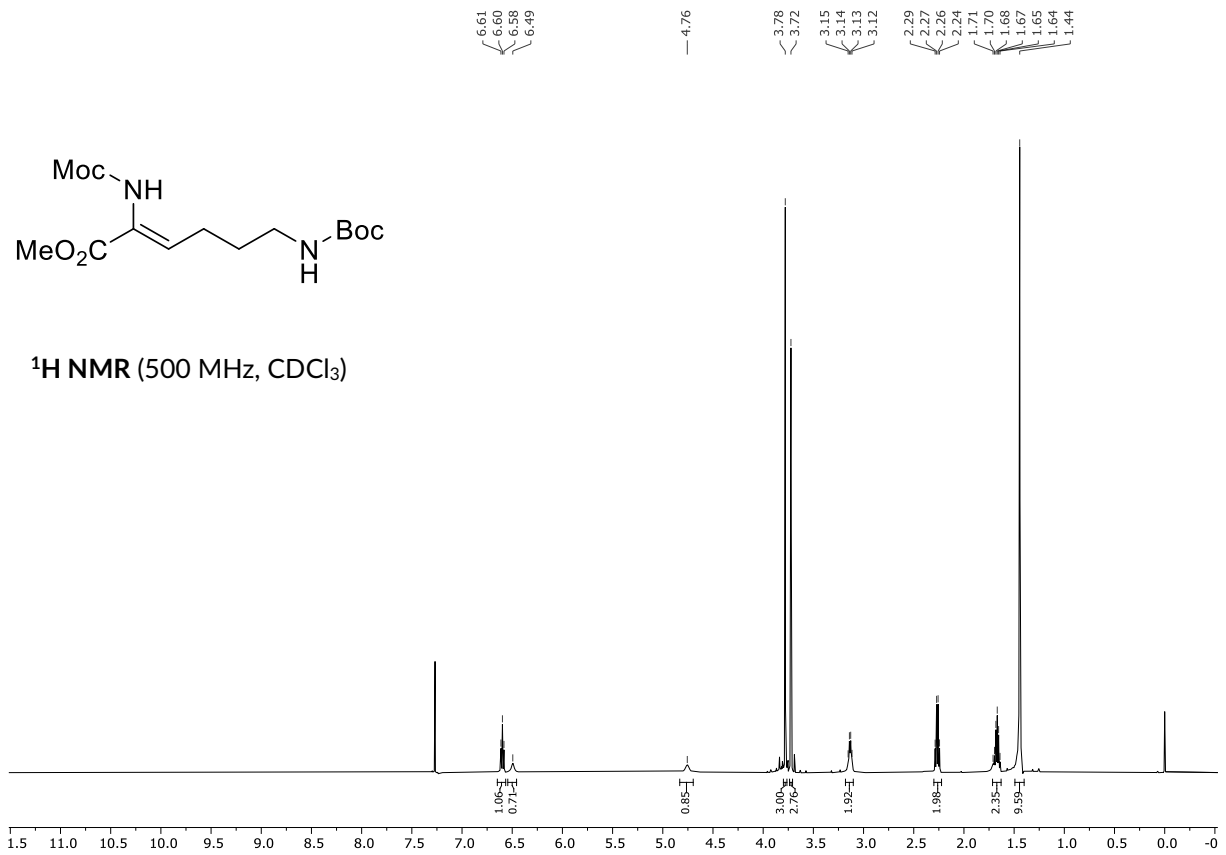


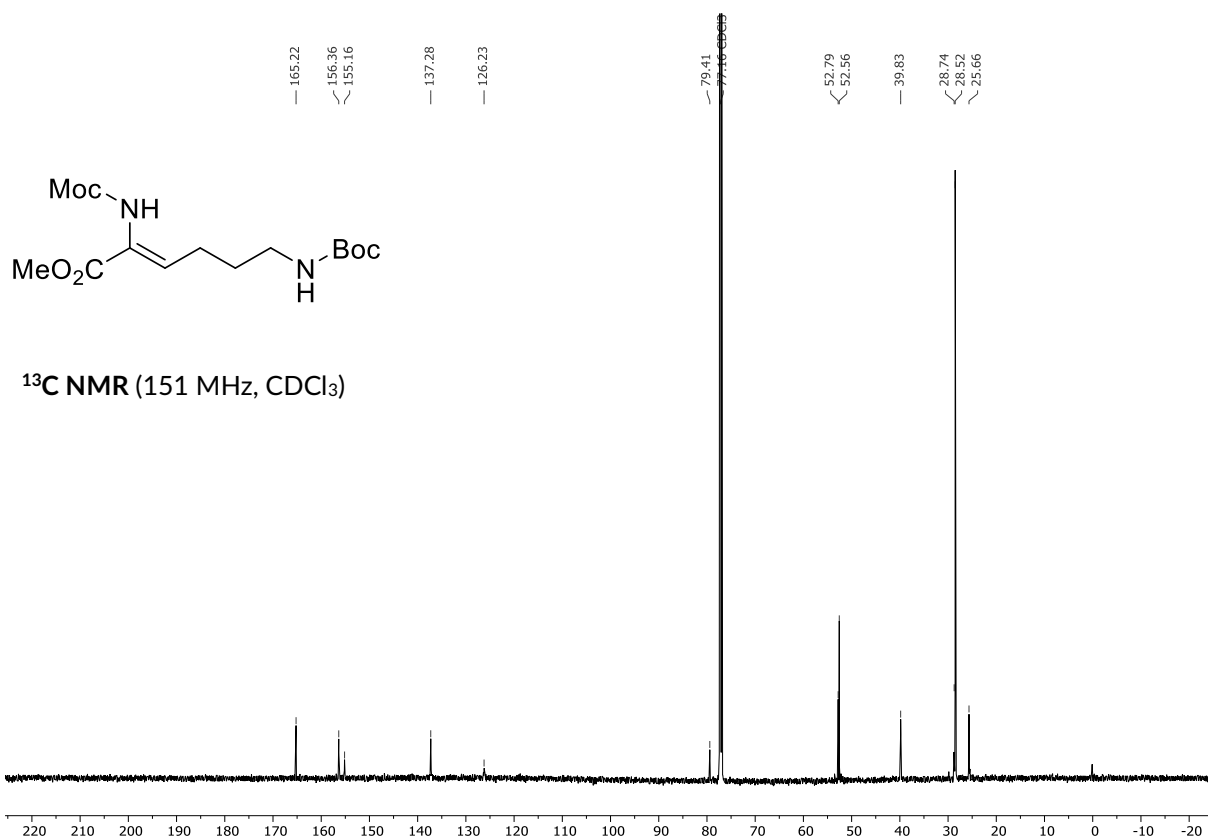
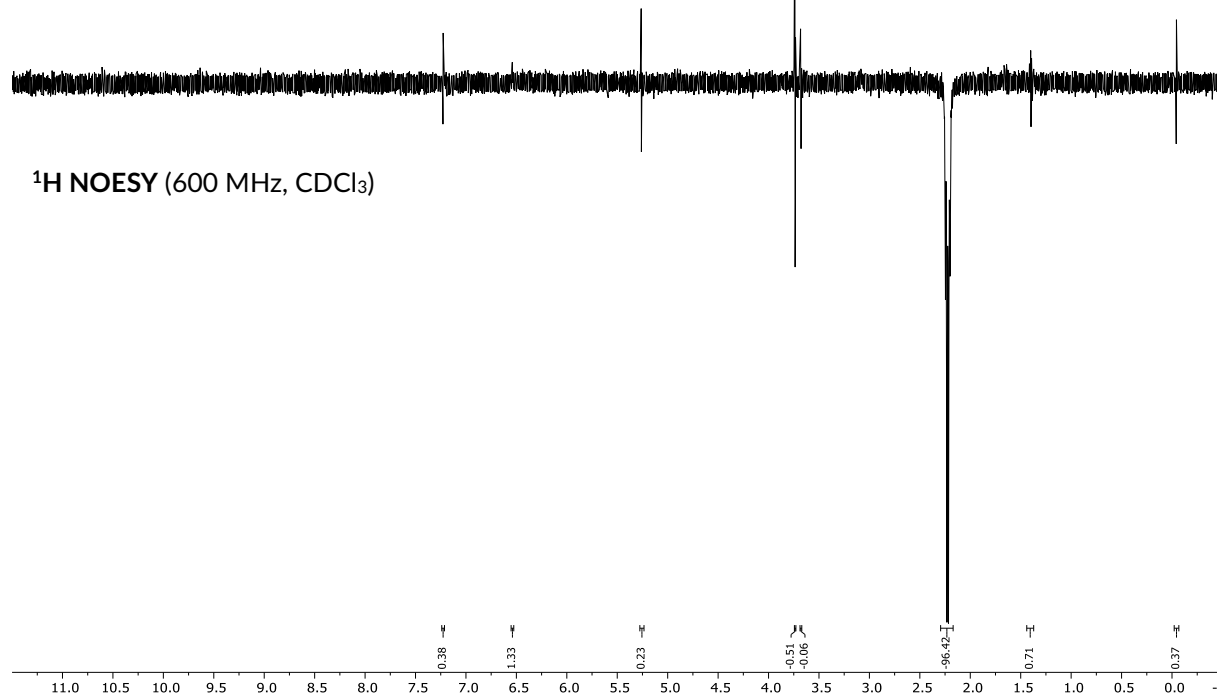
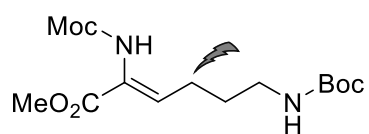


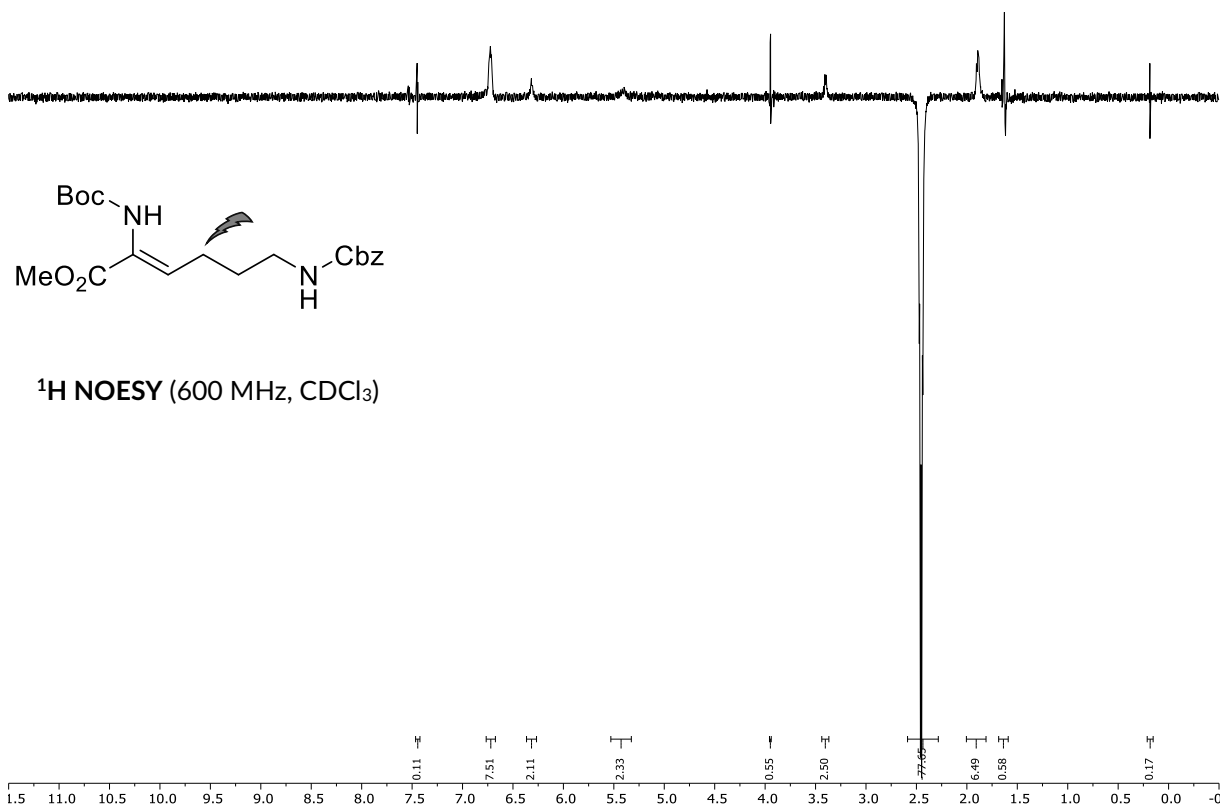
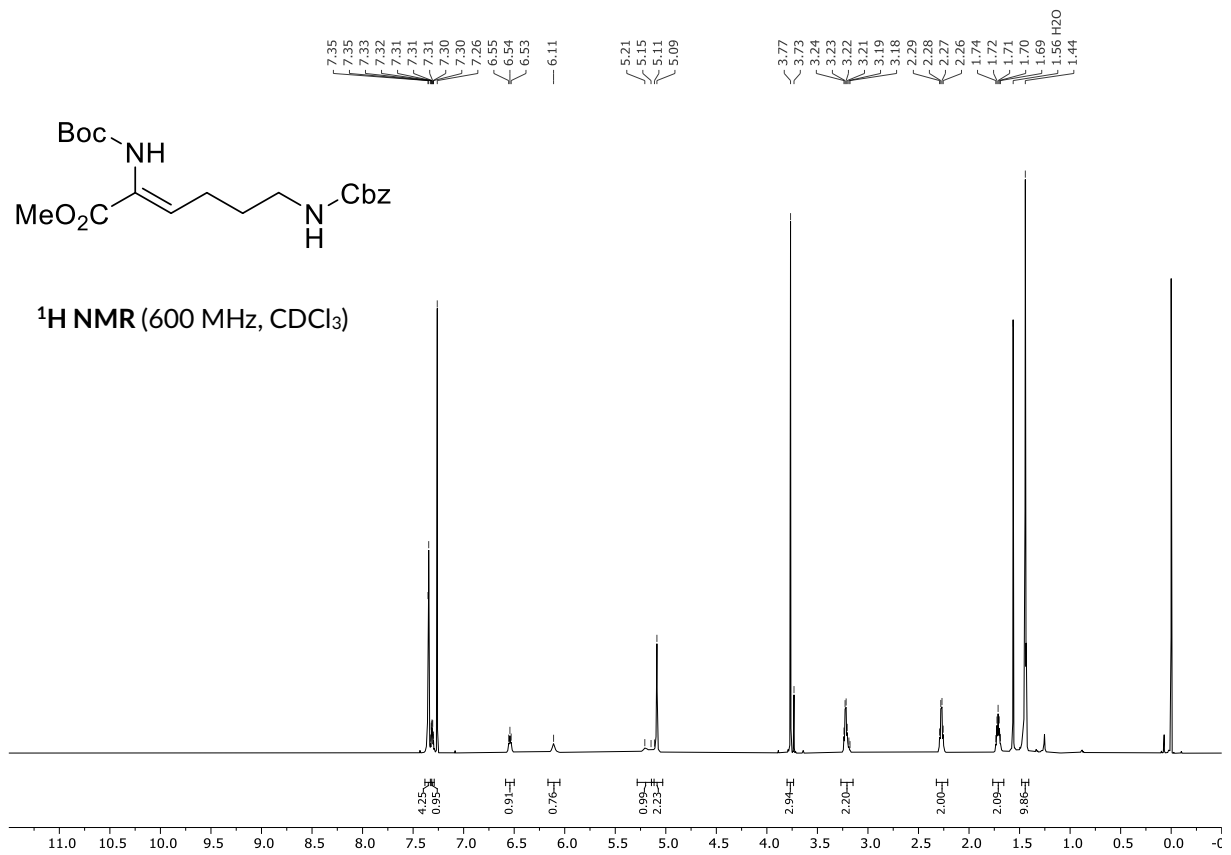




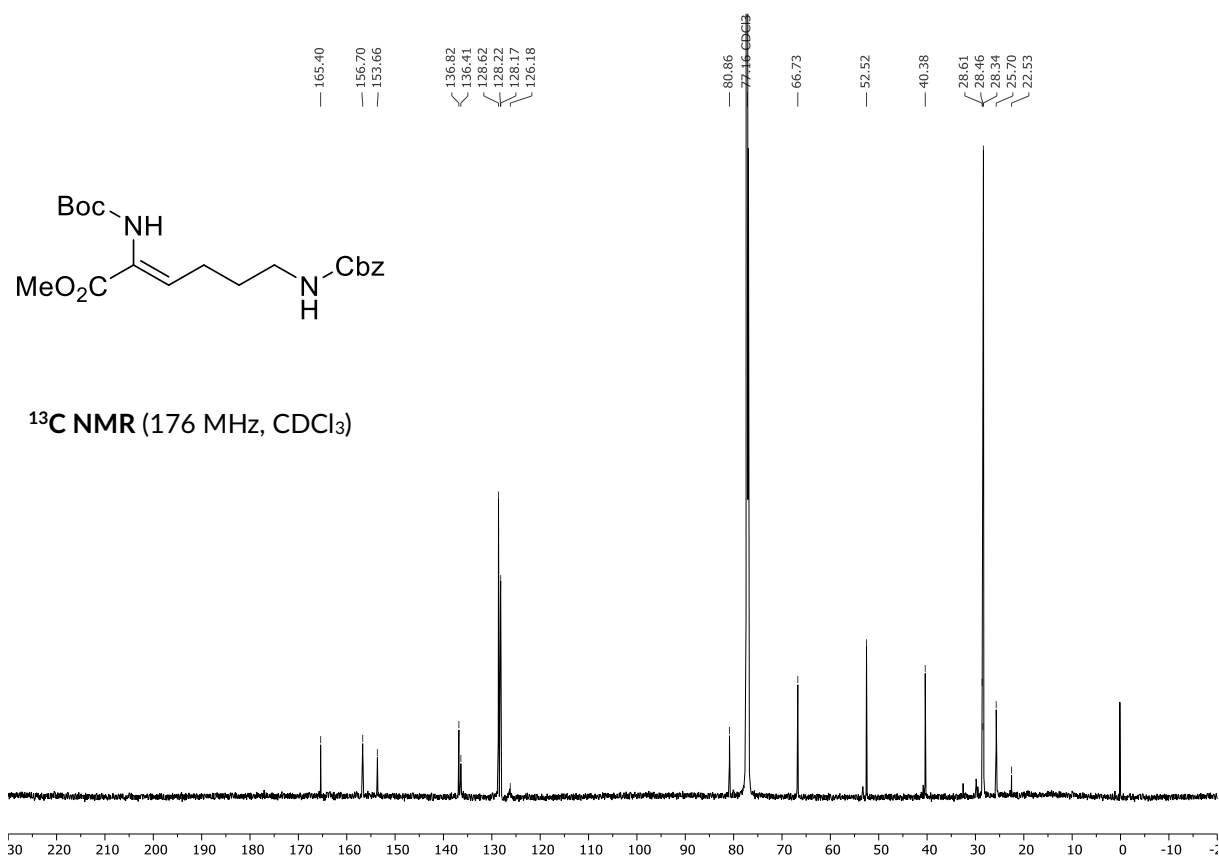
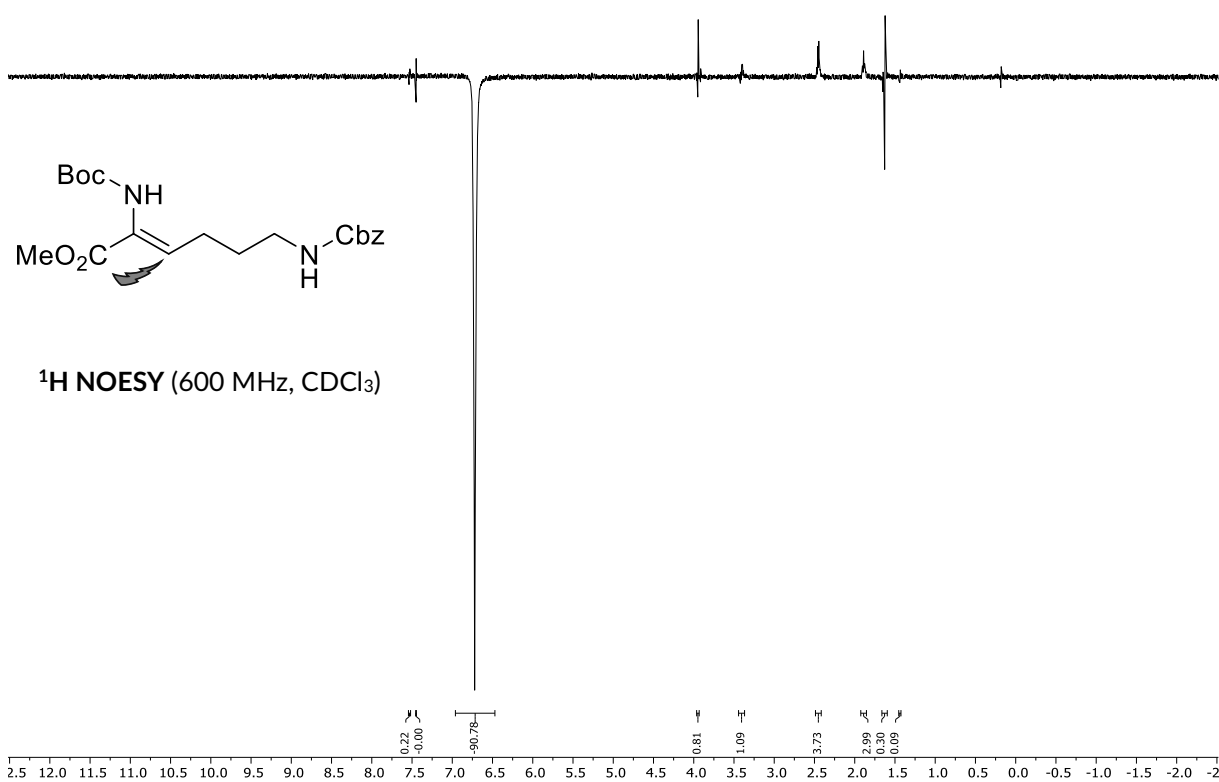


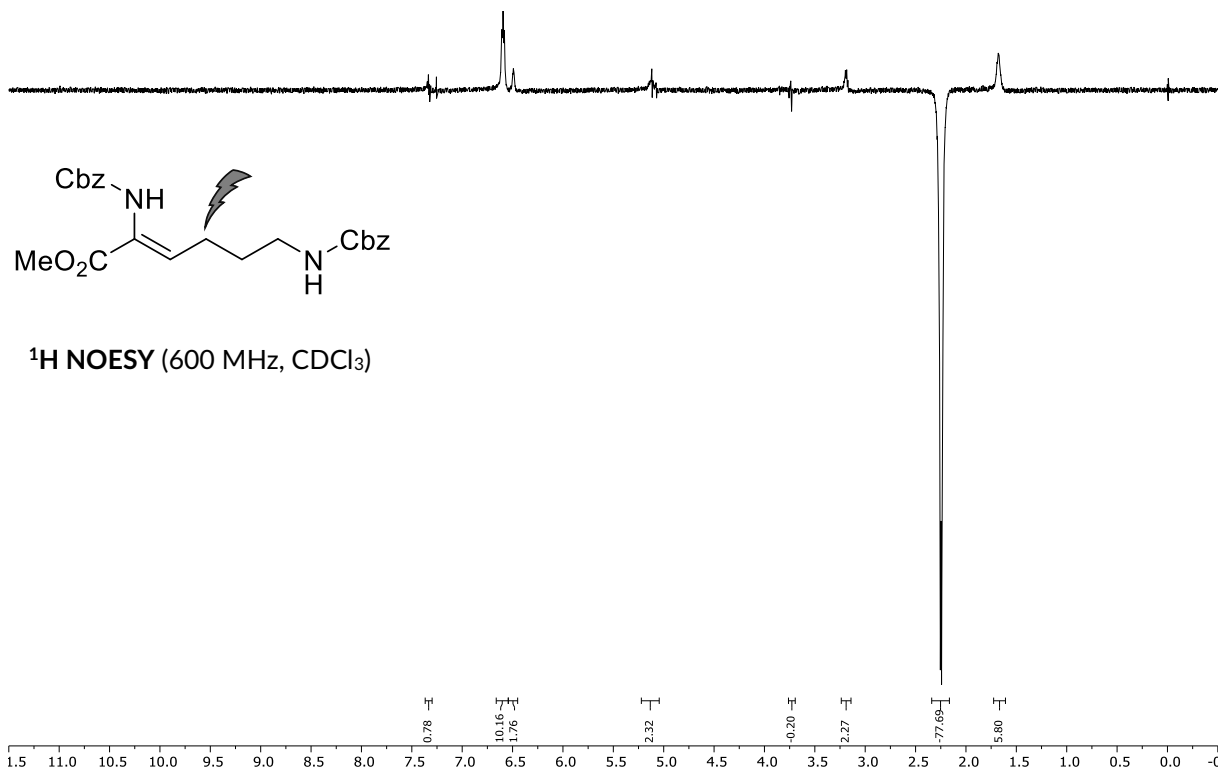
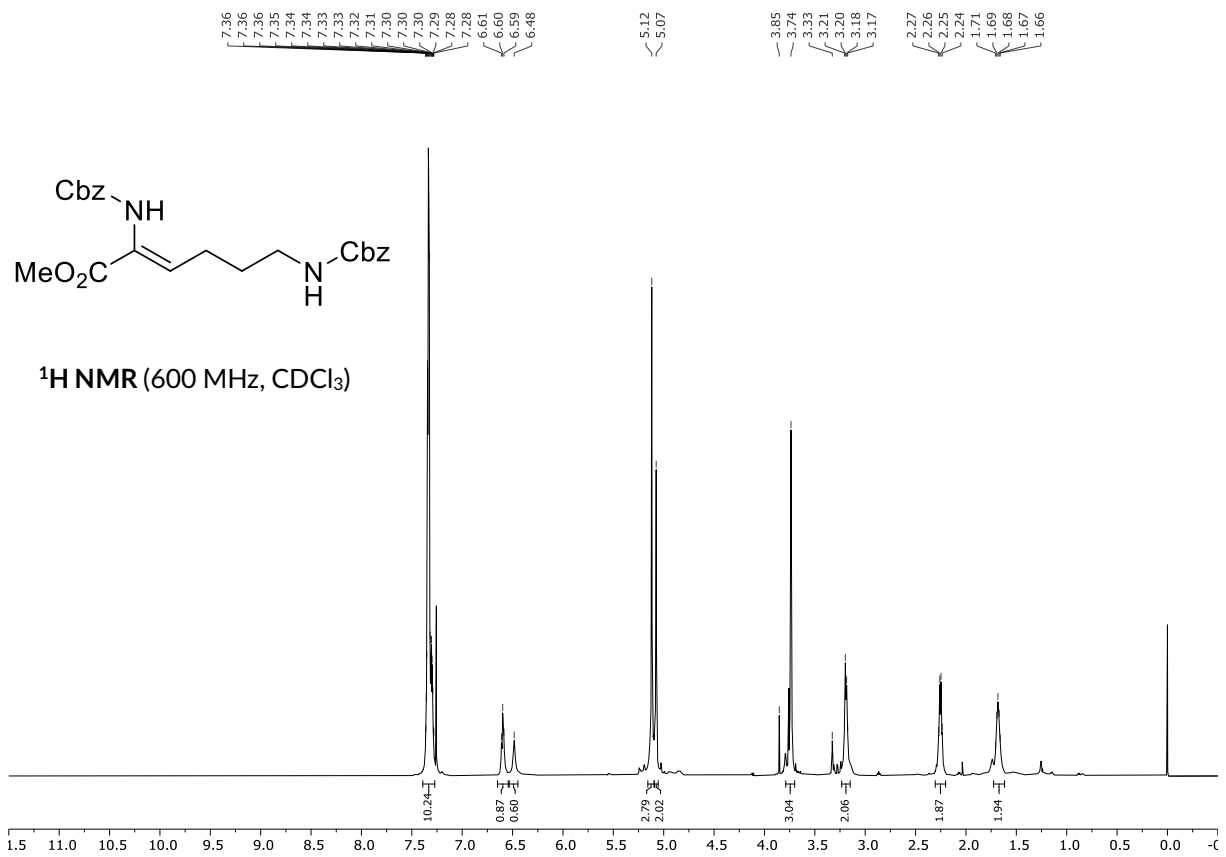


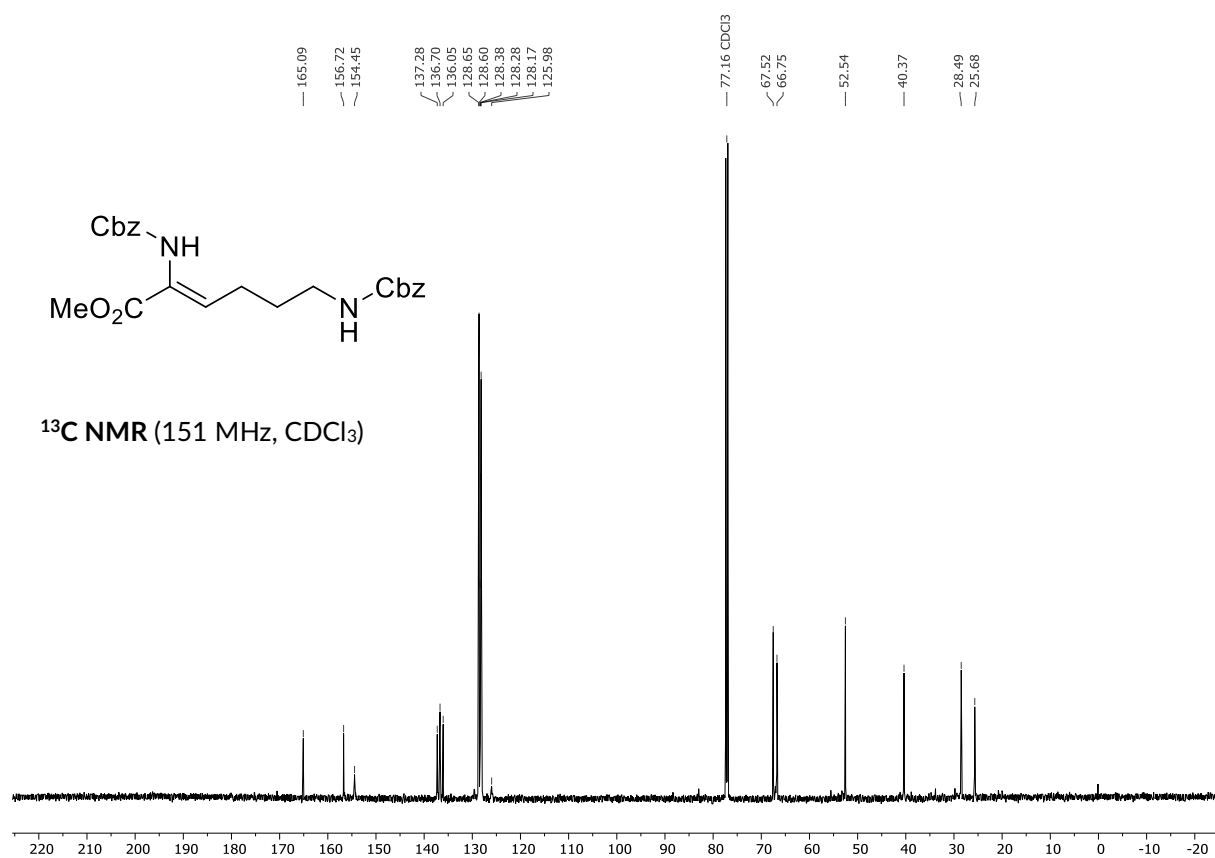


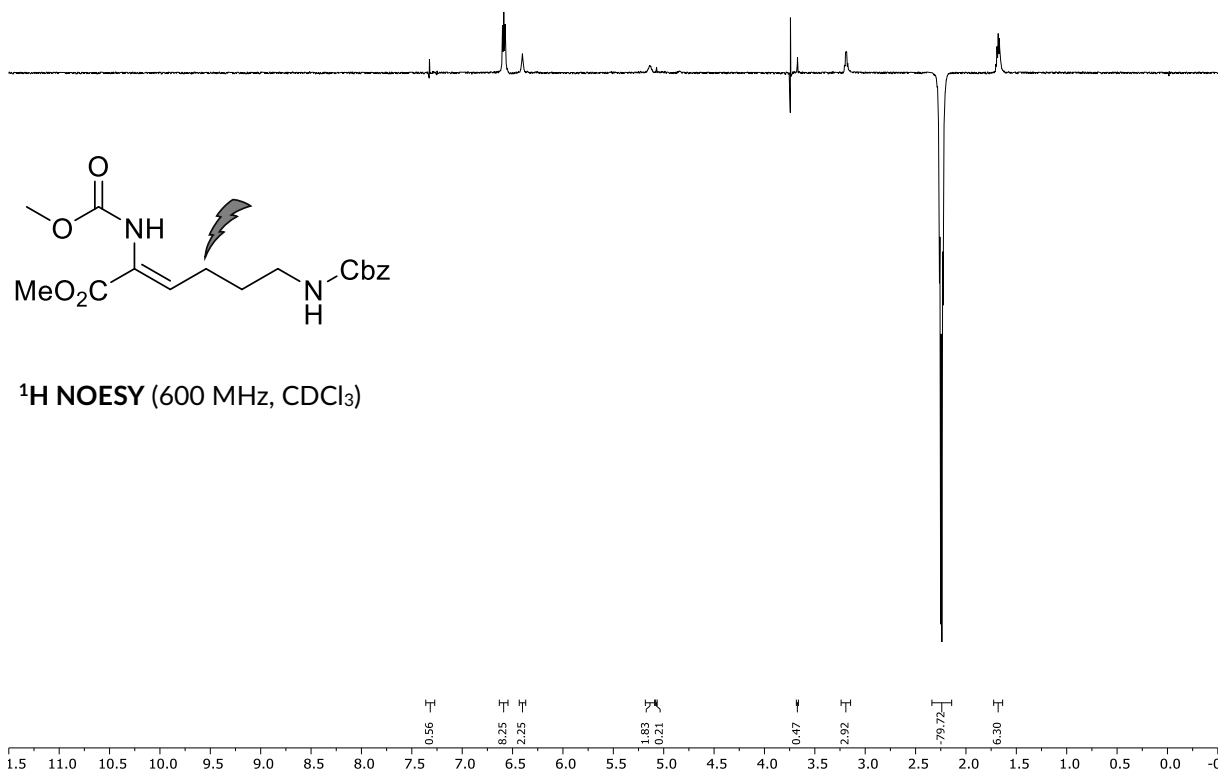
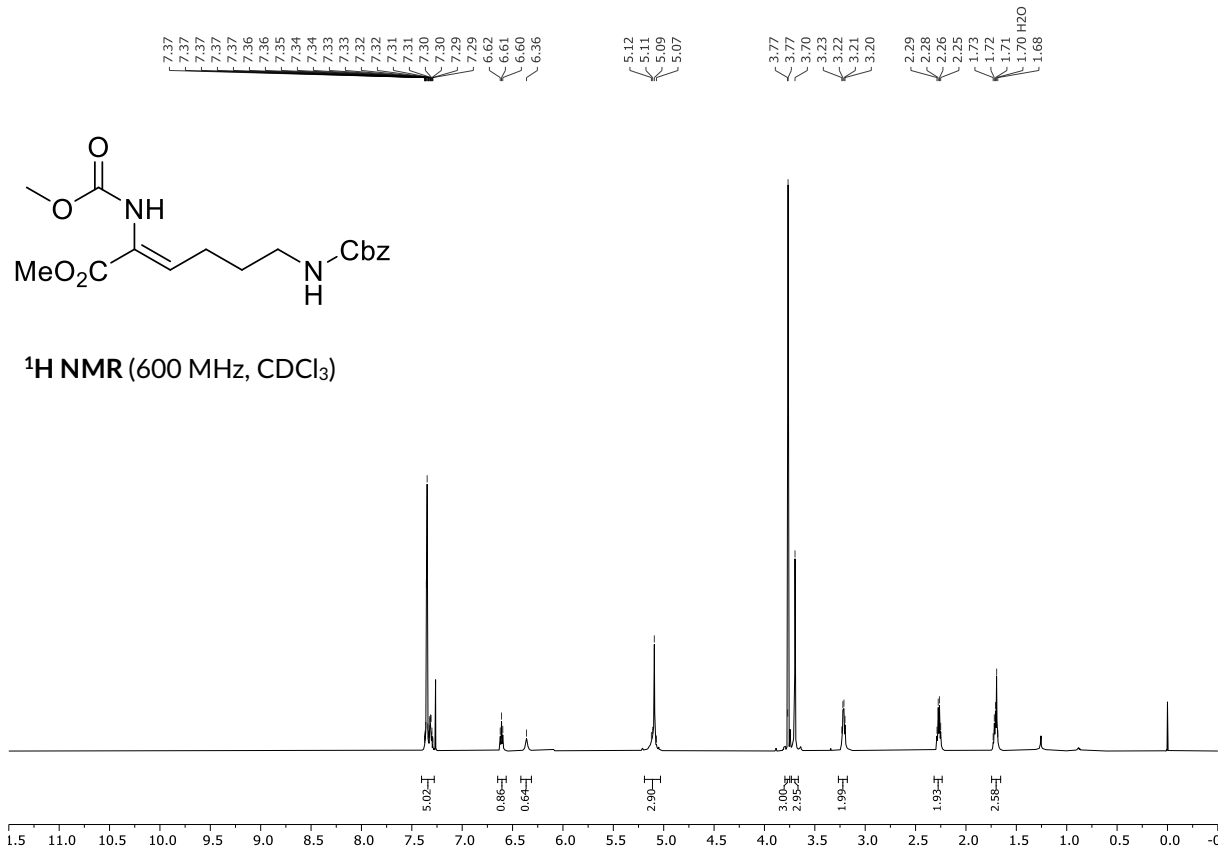


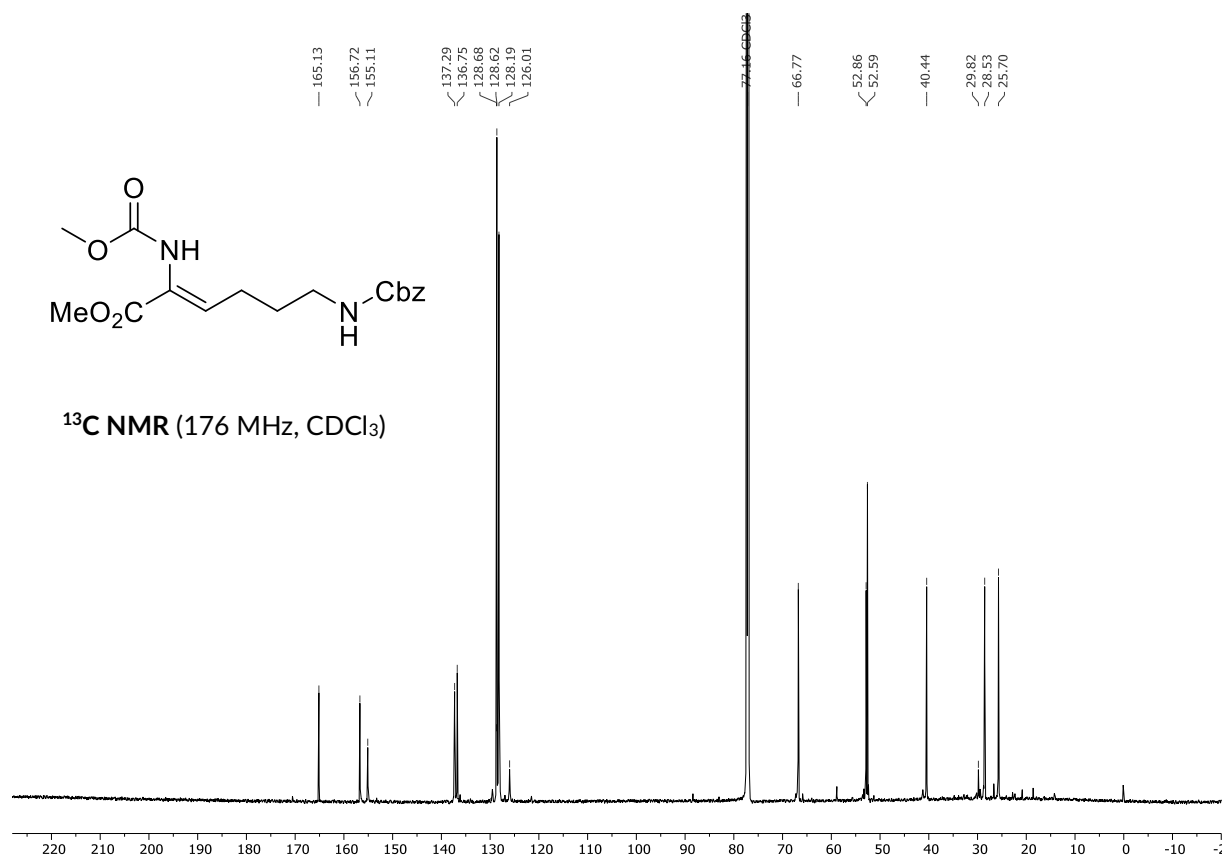
CH0500437g3

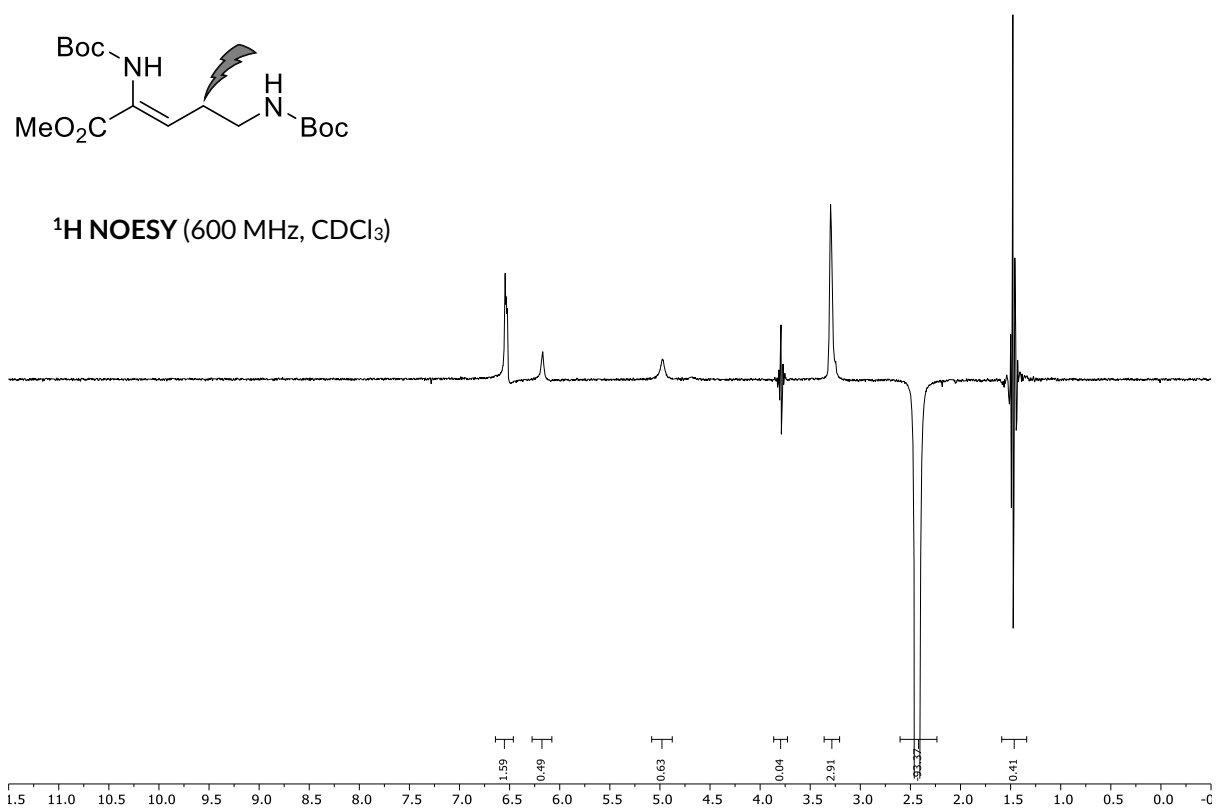
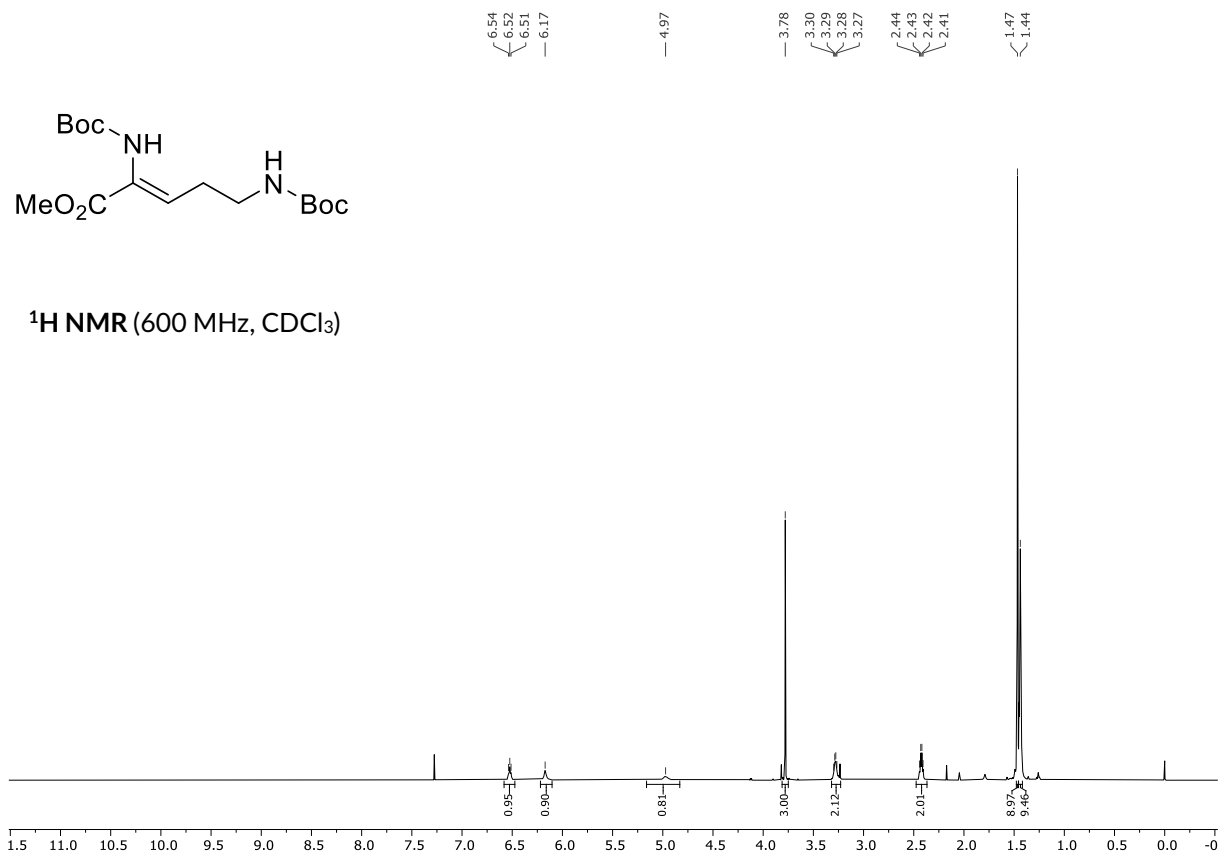


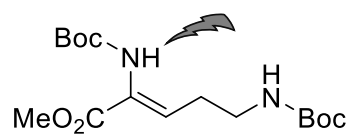




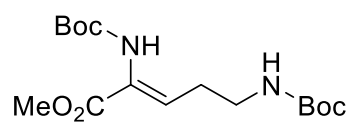
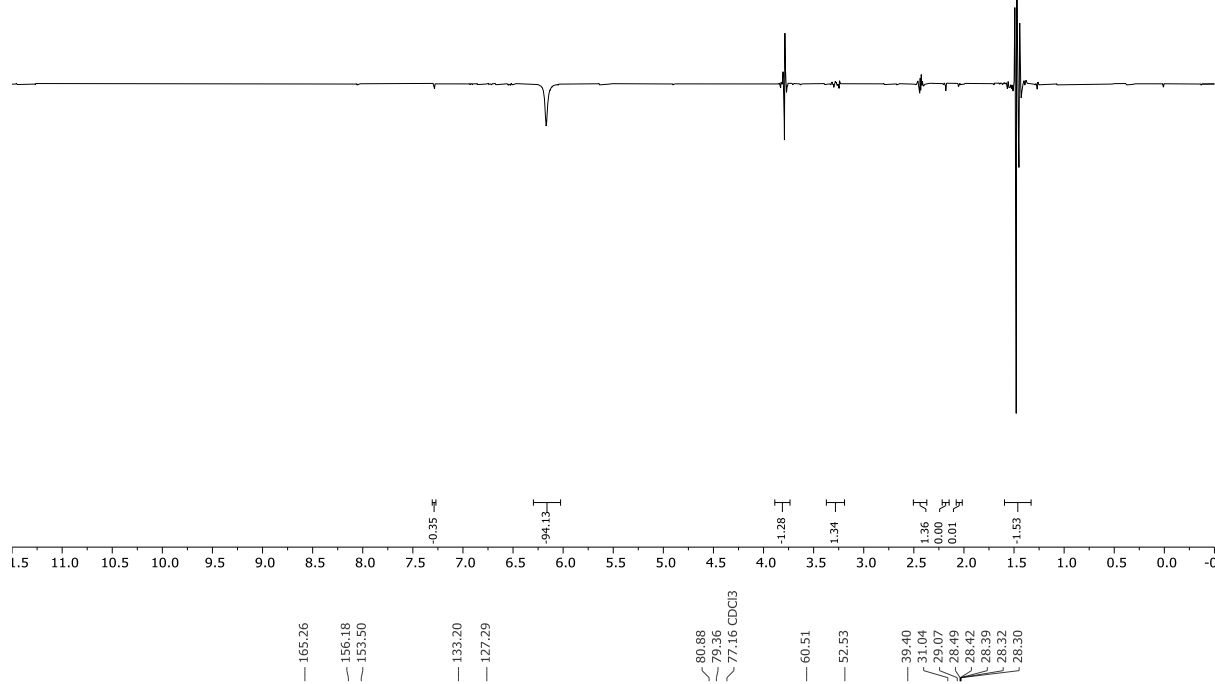




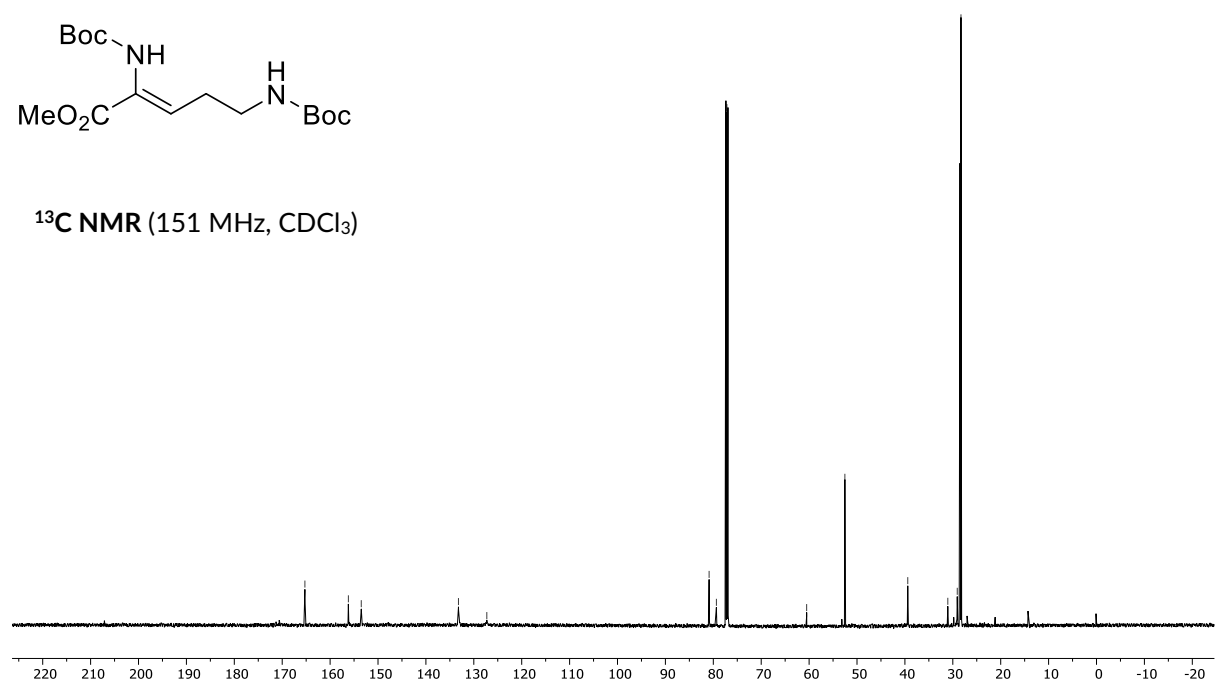


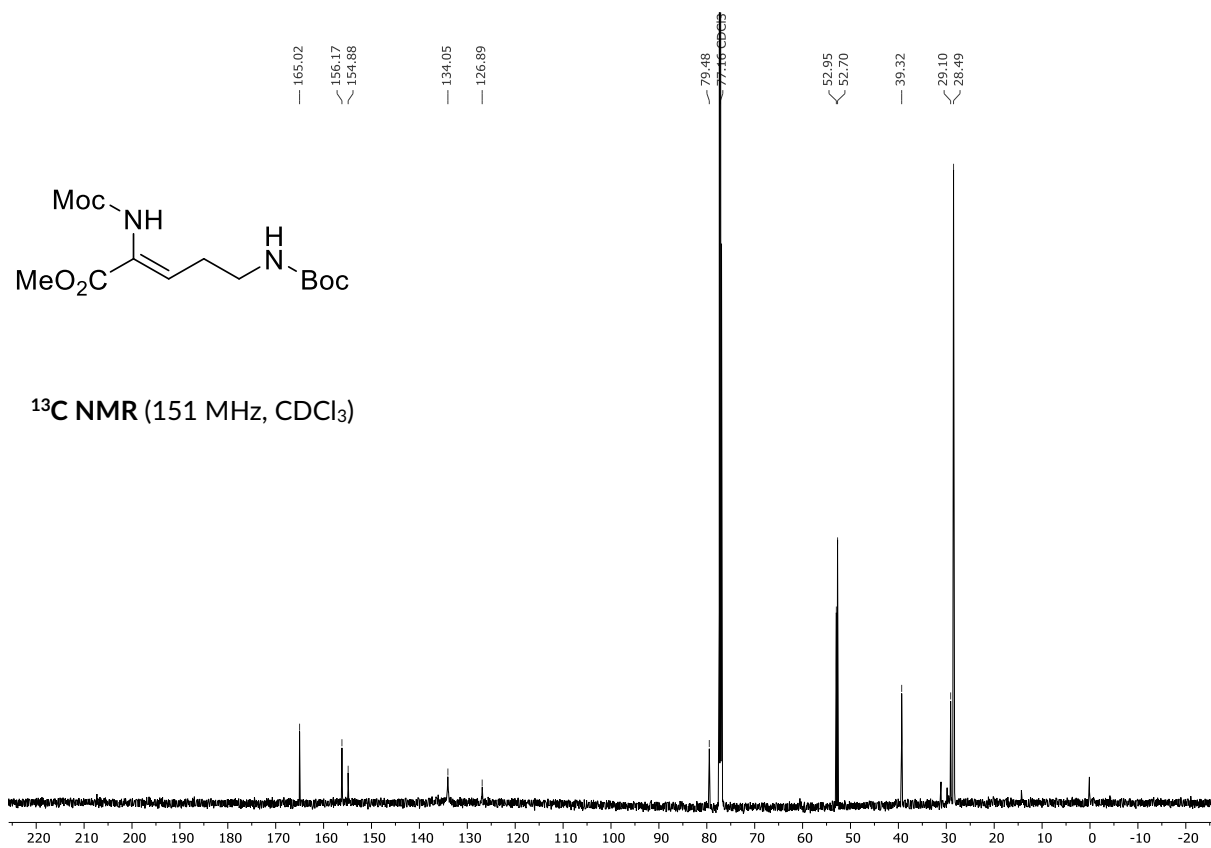
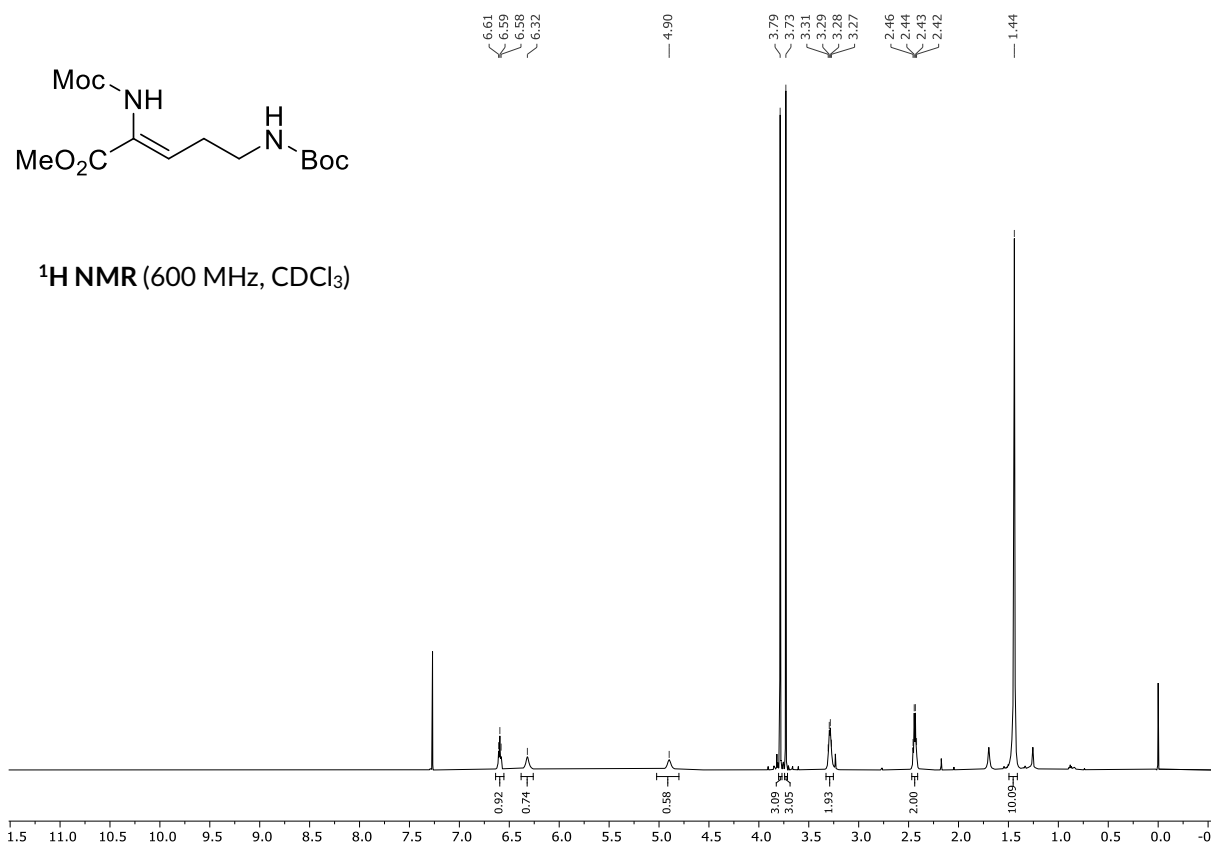


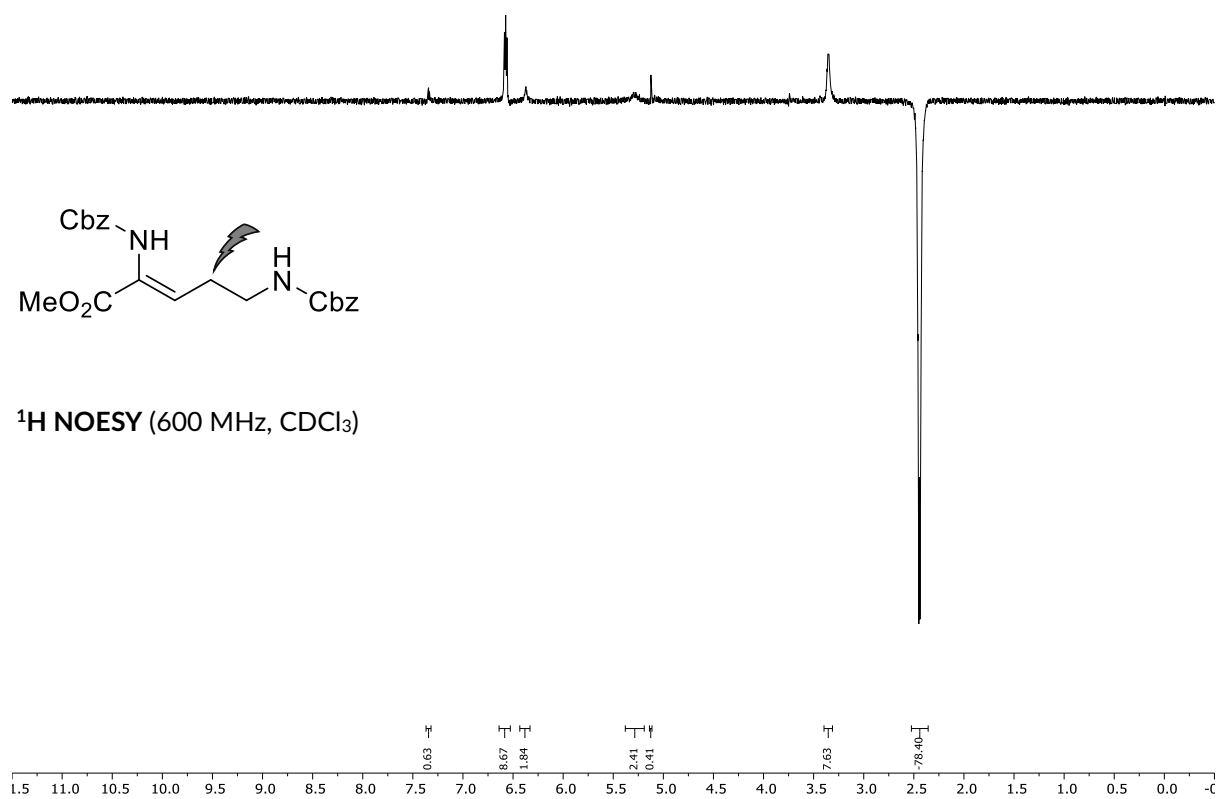
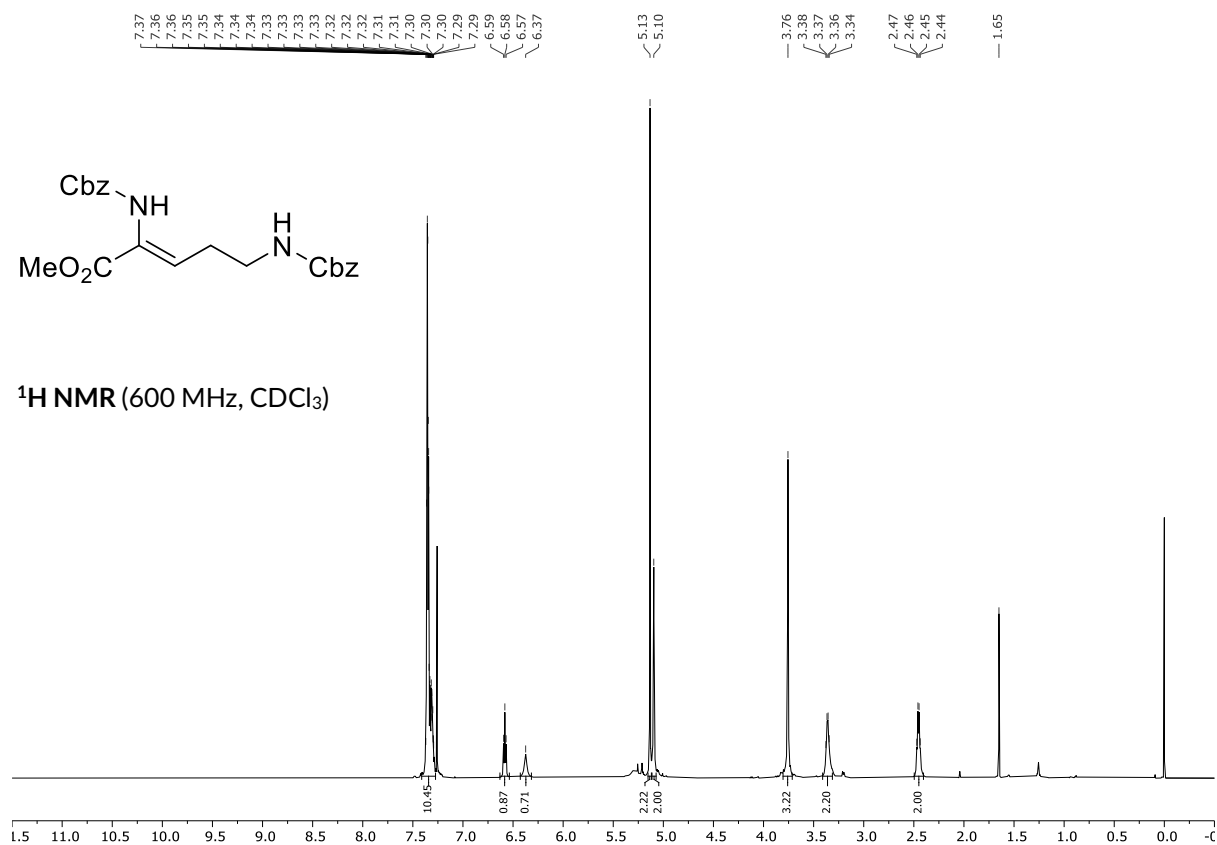
¹H NOESY (600 MHz, CDCl₃)

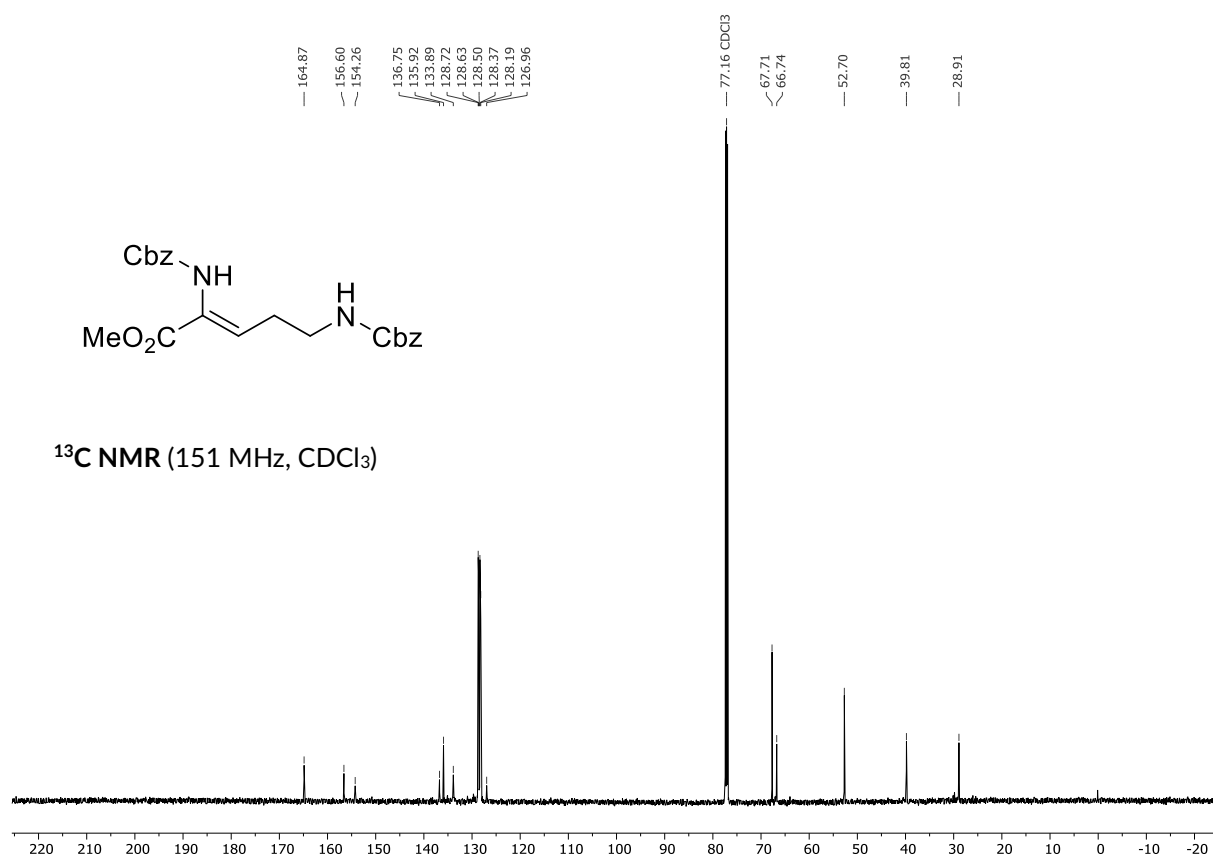


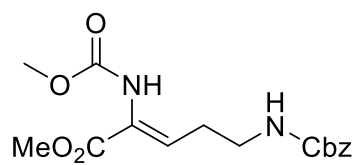
¹³C NMR (151 MHz, CDCl₃)



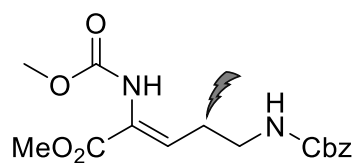
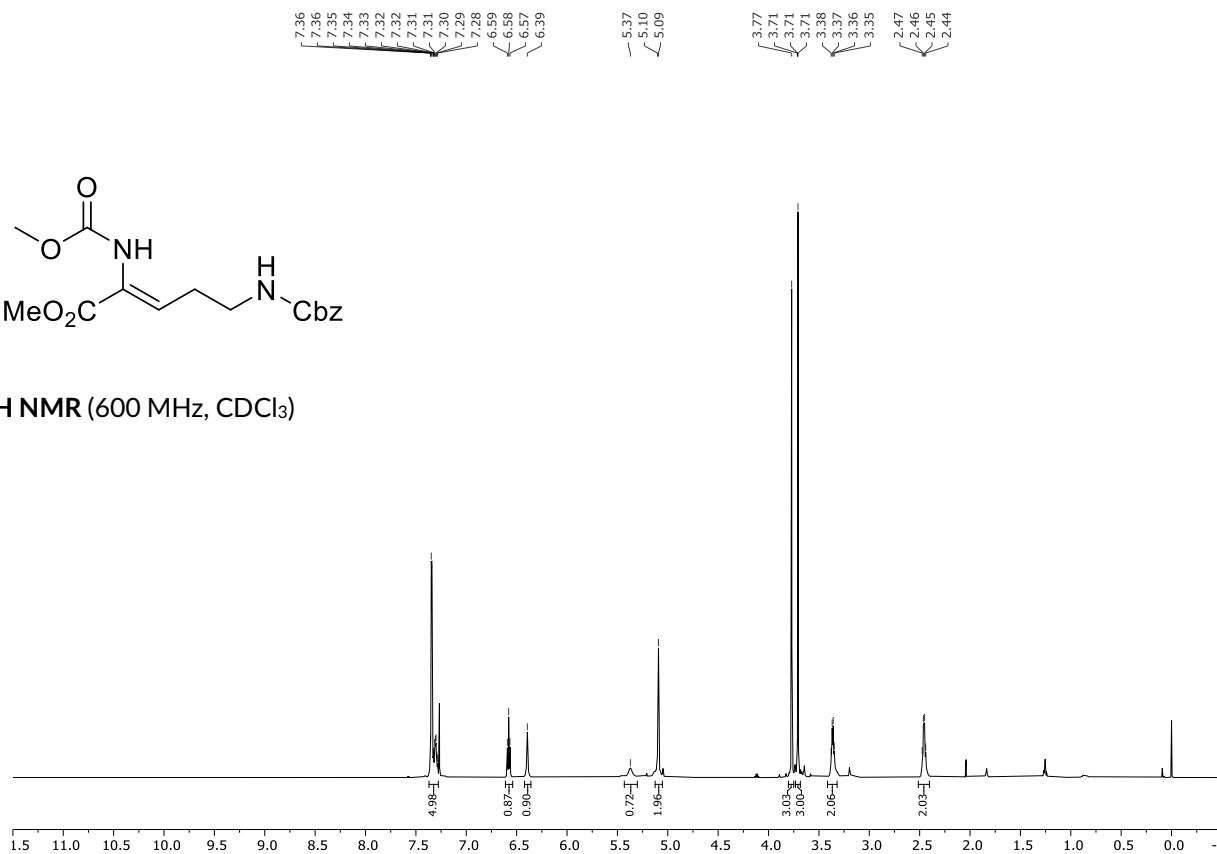




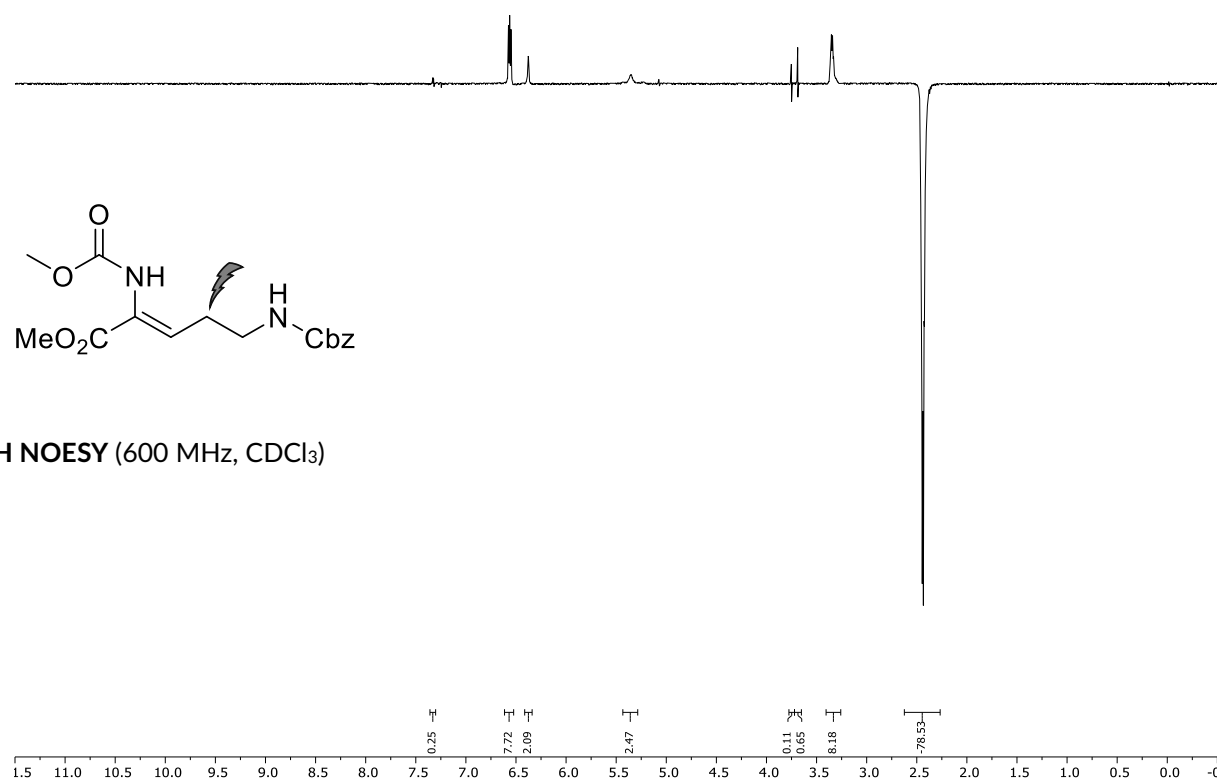


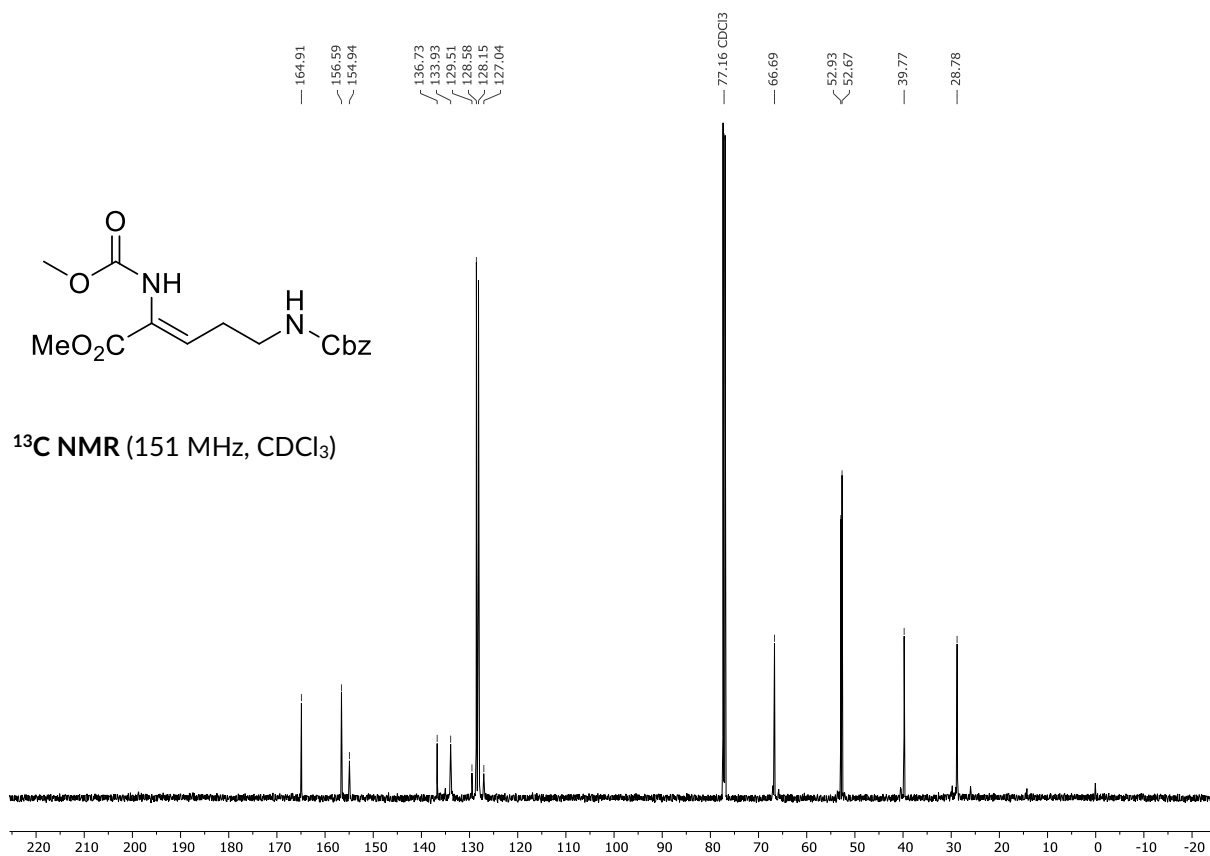


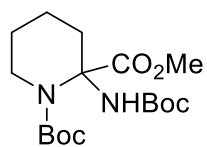
^1H NMR (600 MHz, CDCl_3)



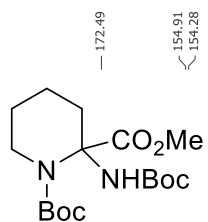
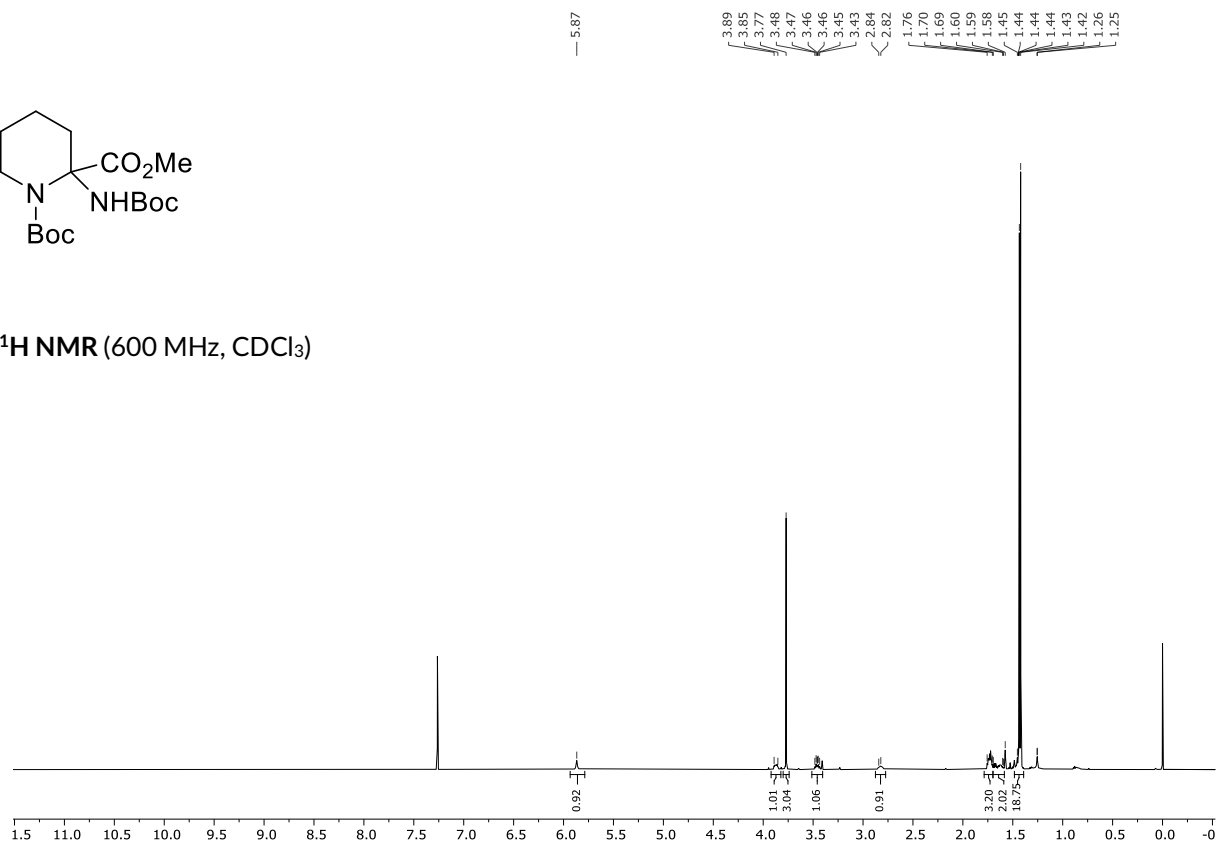
^1H NOESY (600 MHz, CDCl_3)



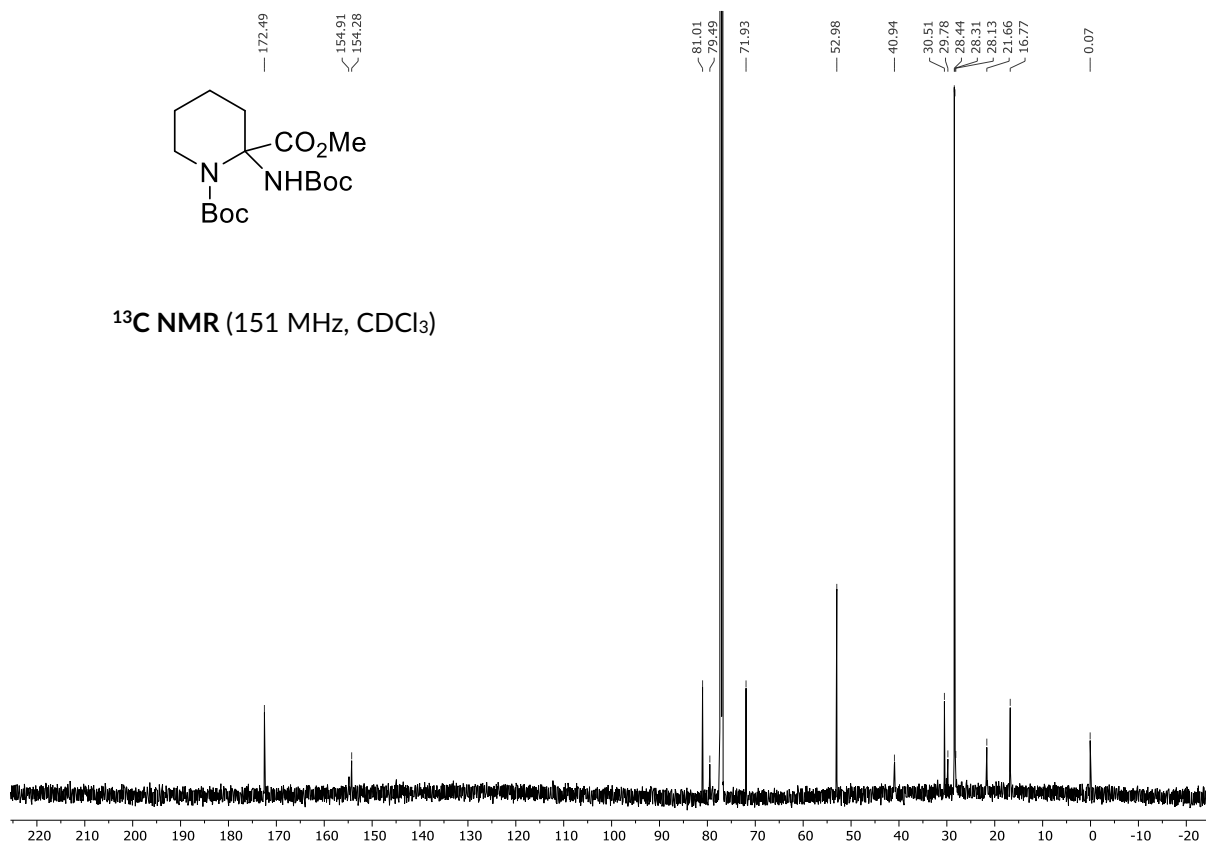


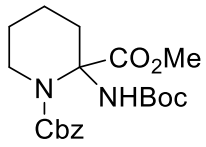


^1H NMR (600 MHz, CDCl_3)

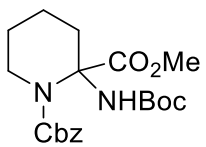
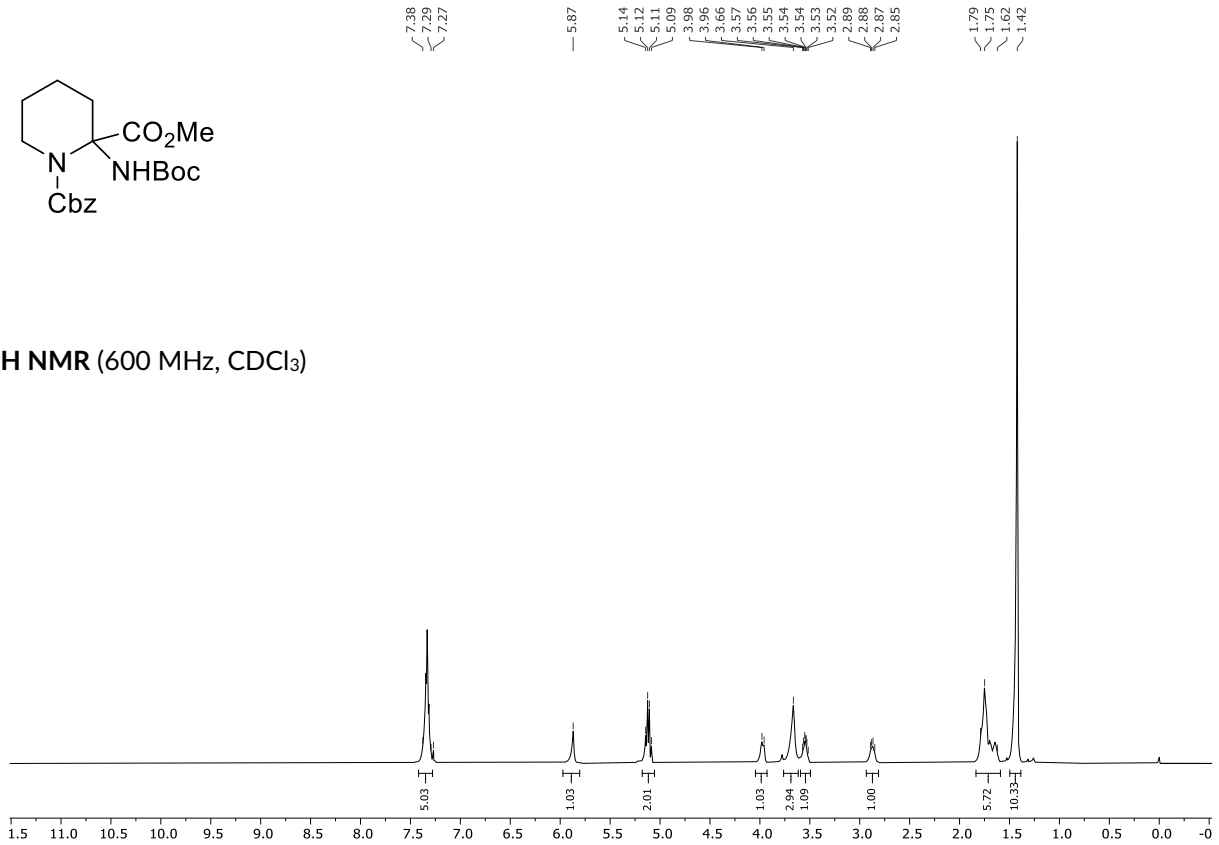


^{13}C NMR (151 MHz, CDCl_3)

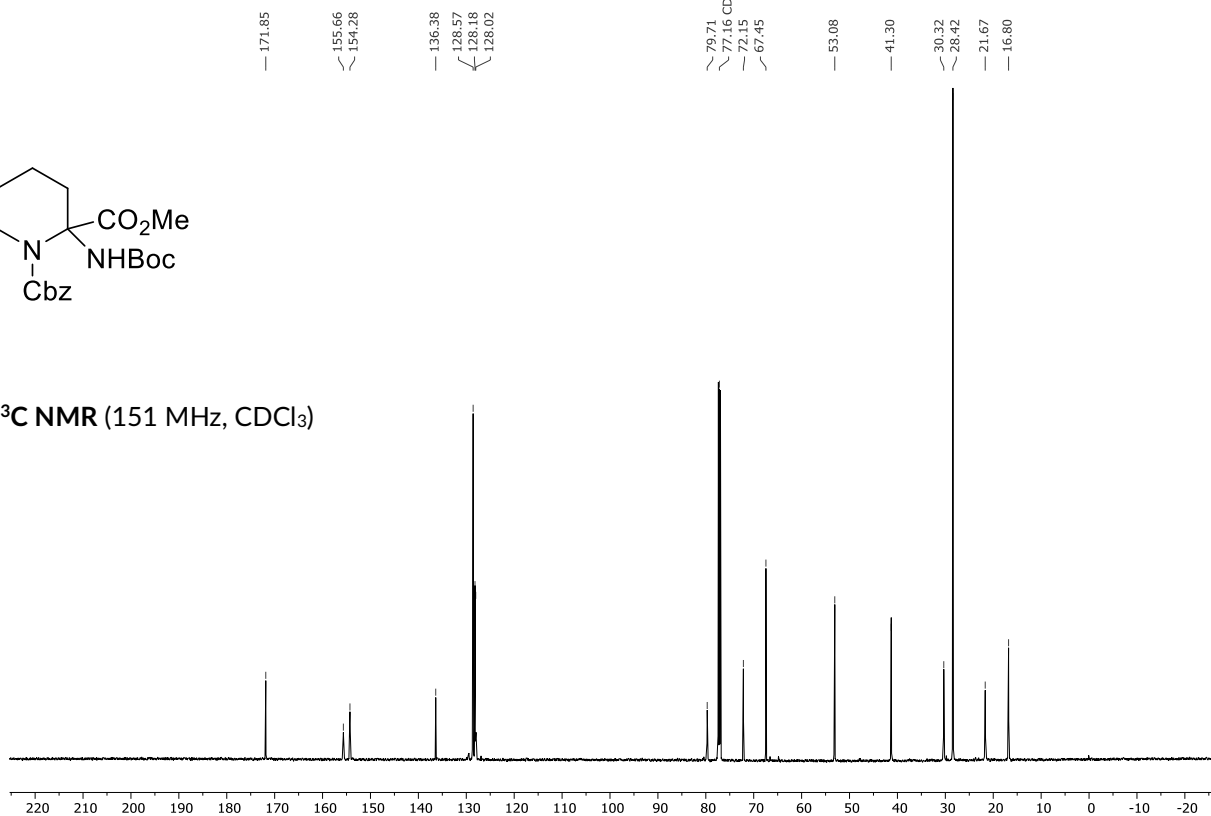


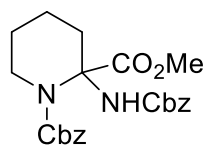
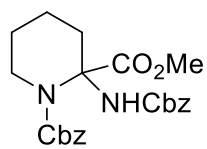
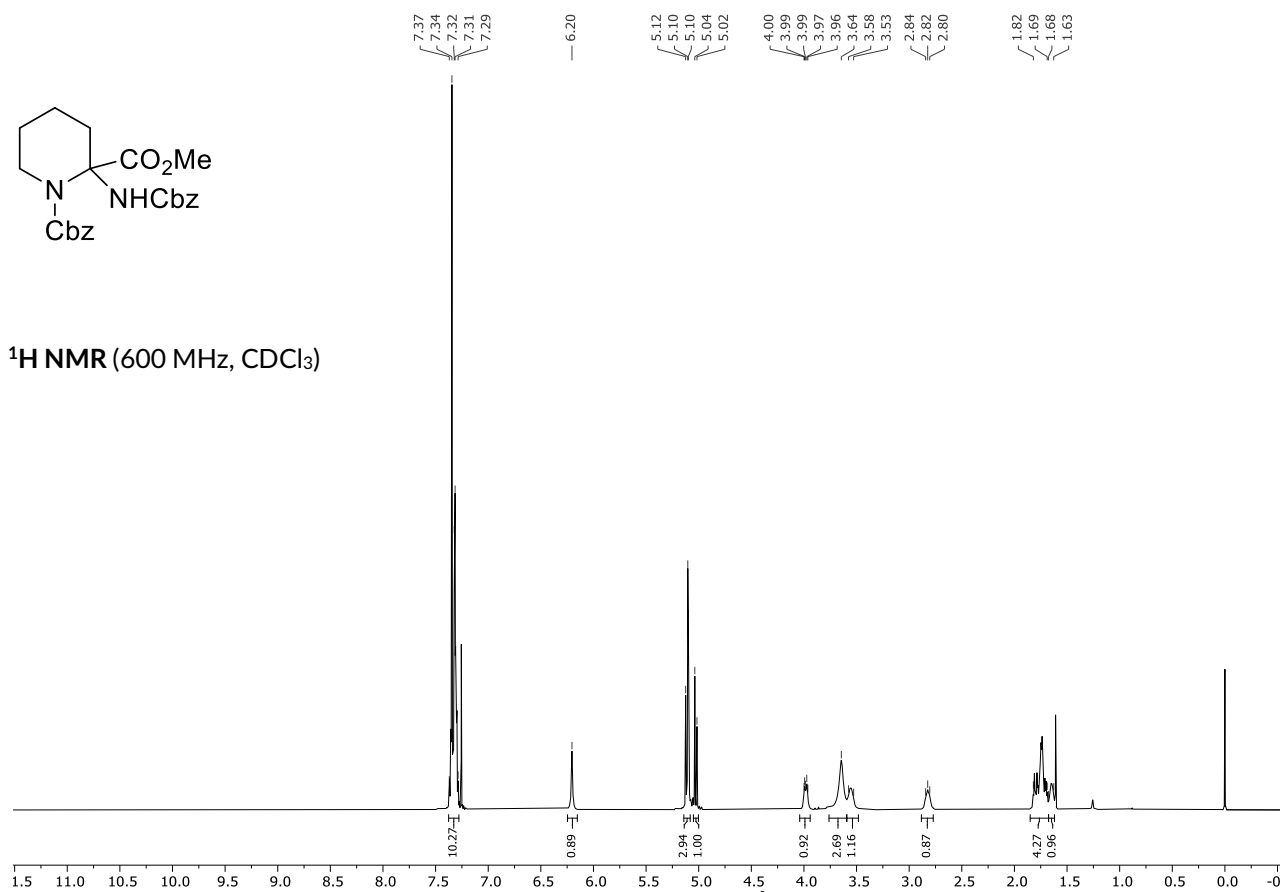
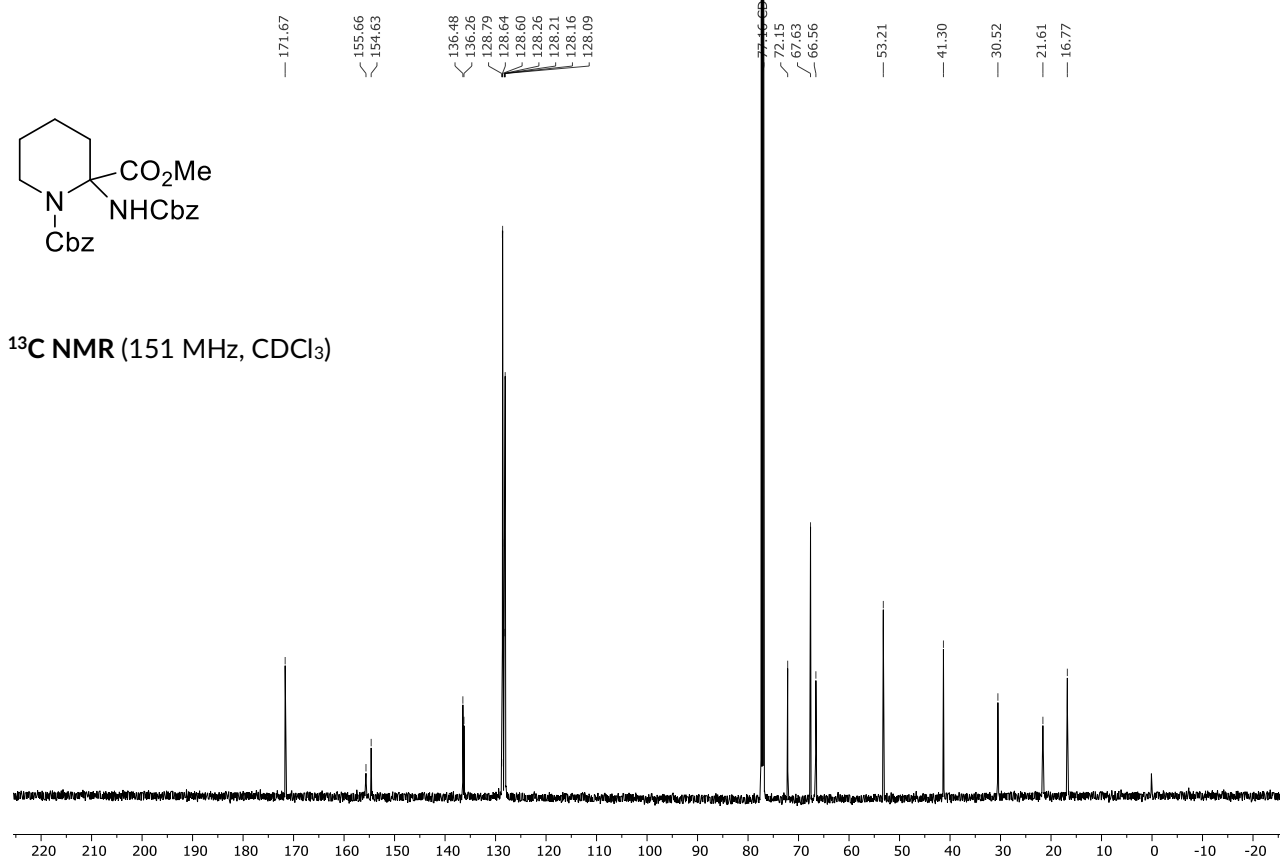


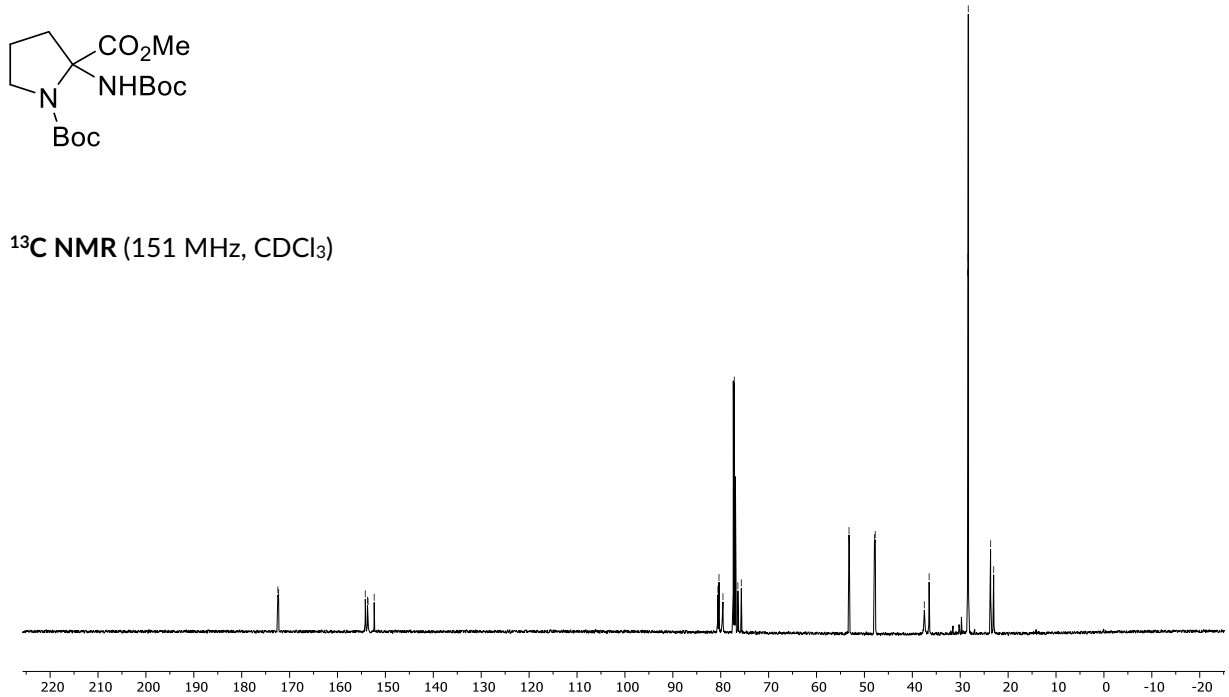
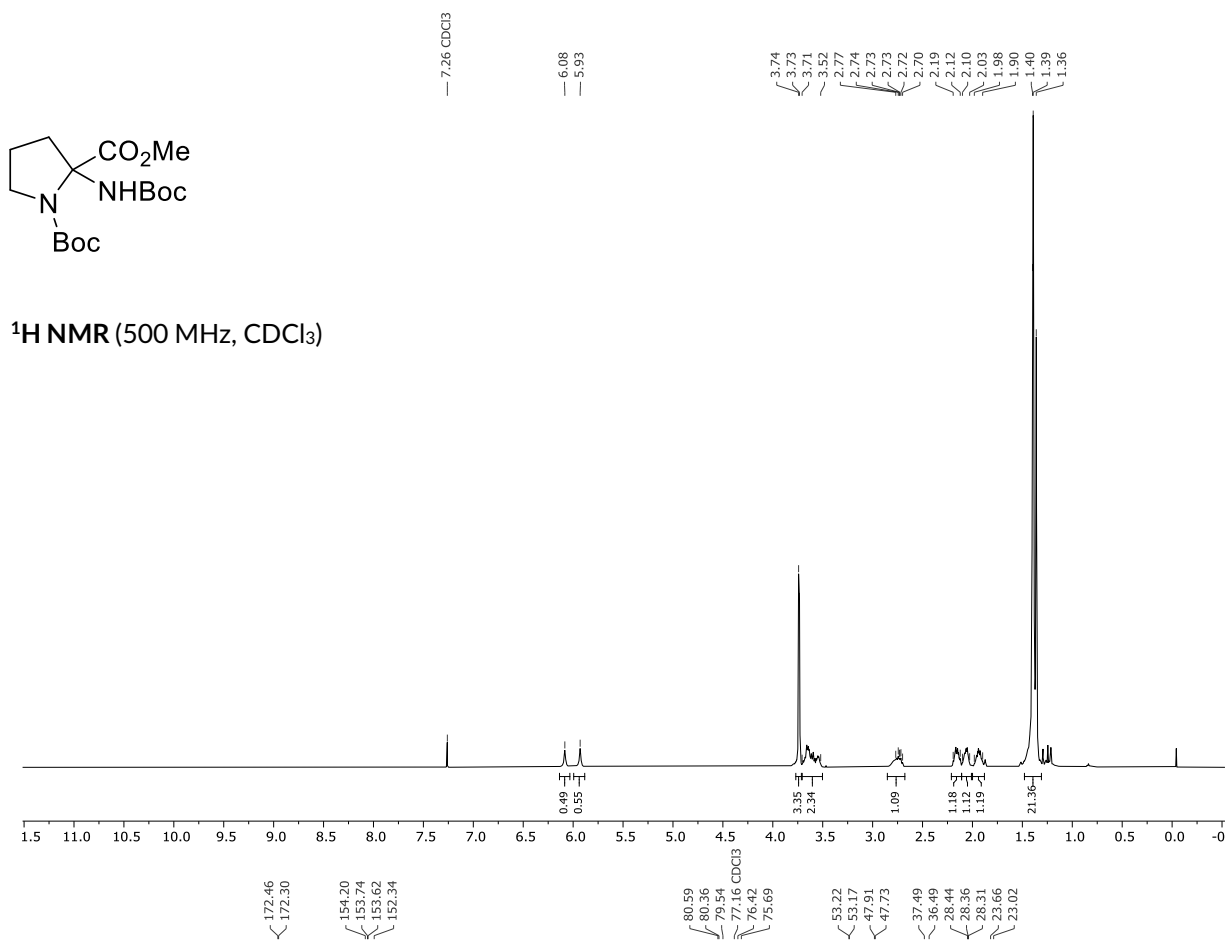
¹H NMR (600 MHz, CDCl₃)

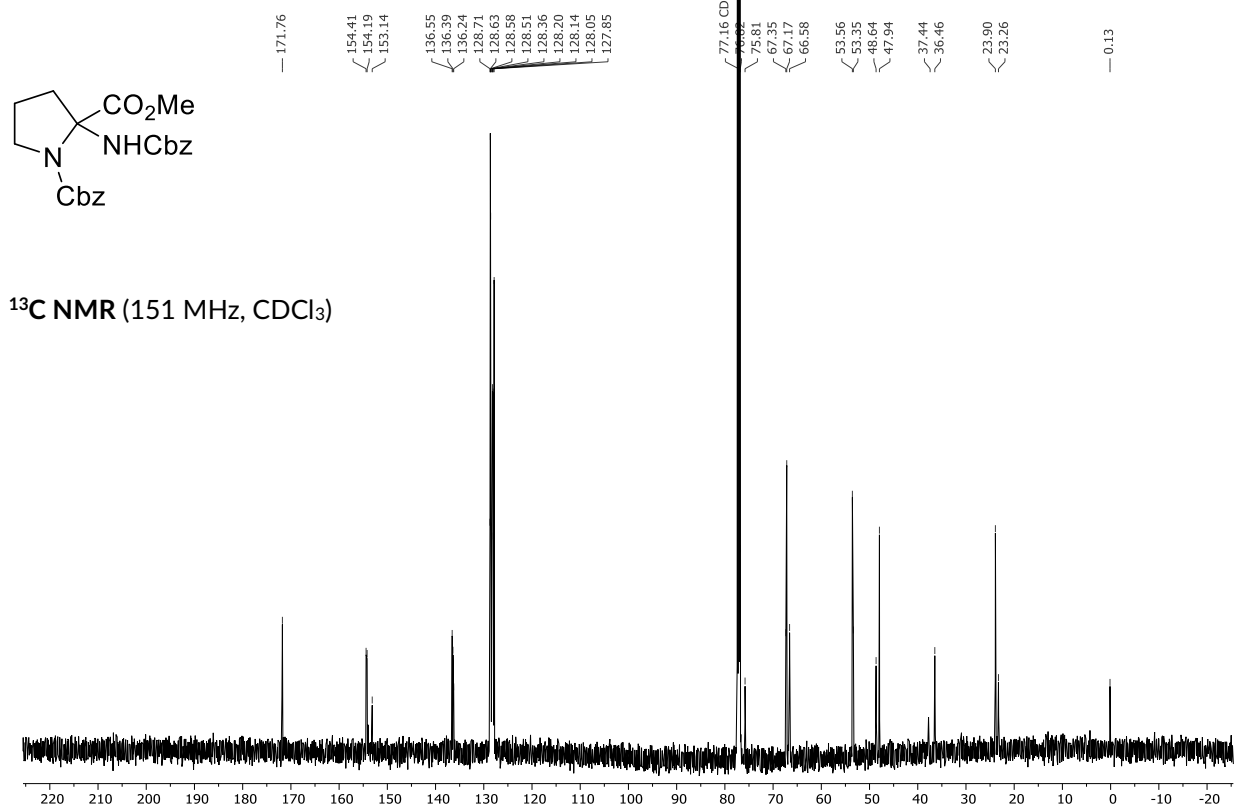
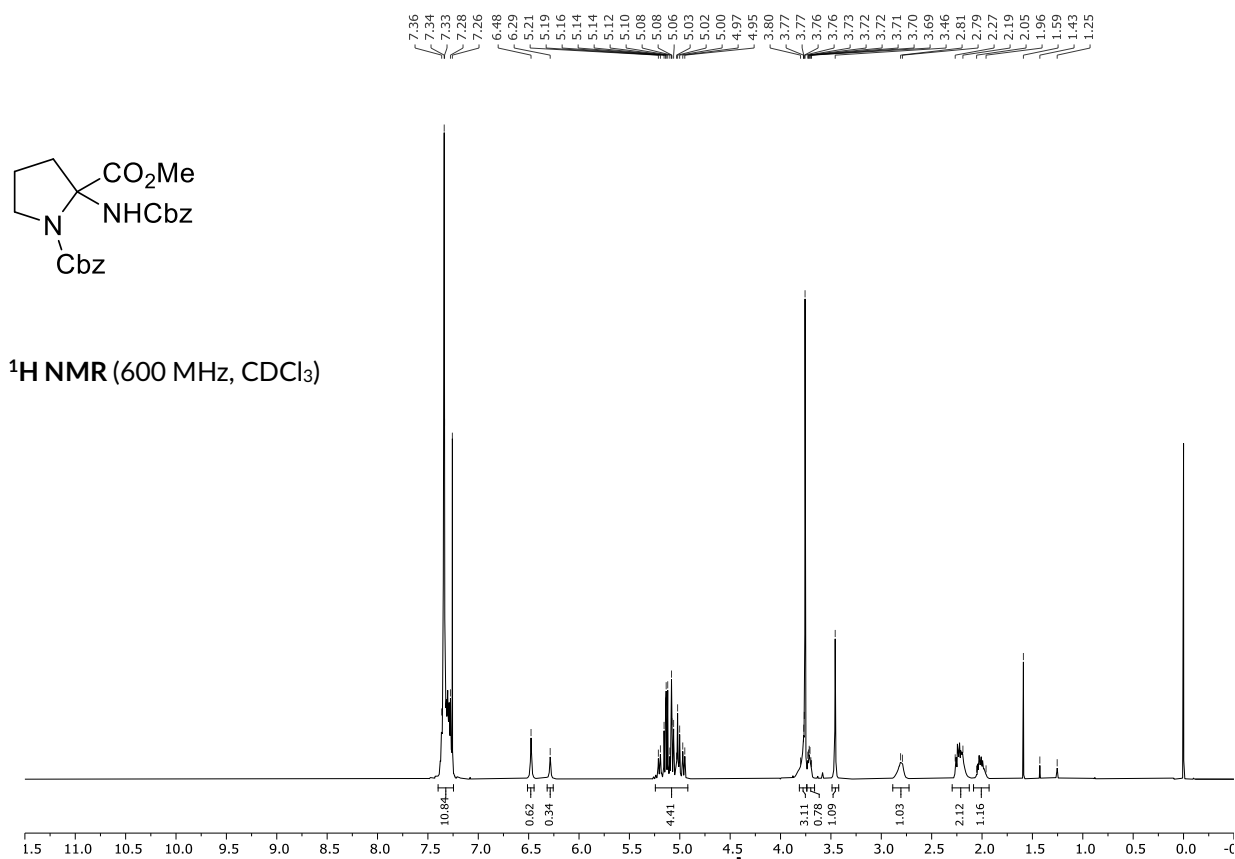


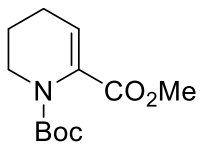
¹³C NMR (151 MHz, CDCl₃)



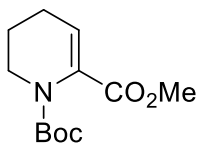
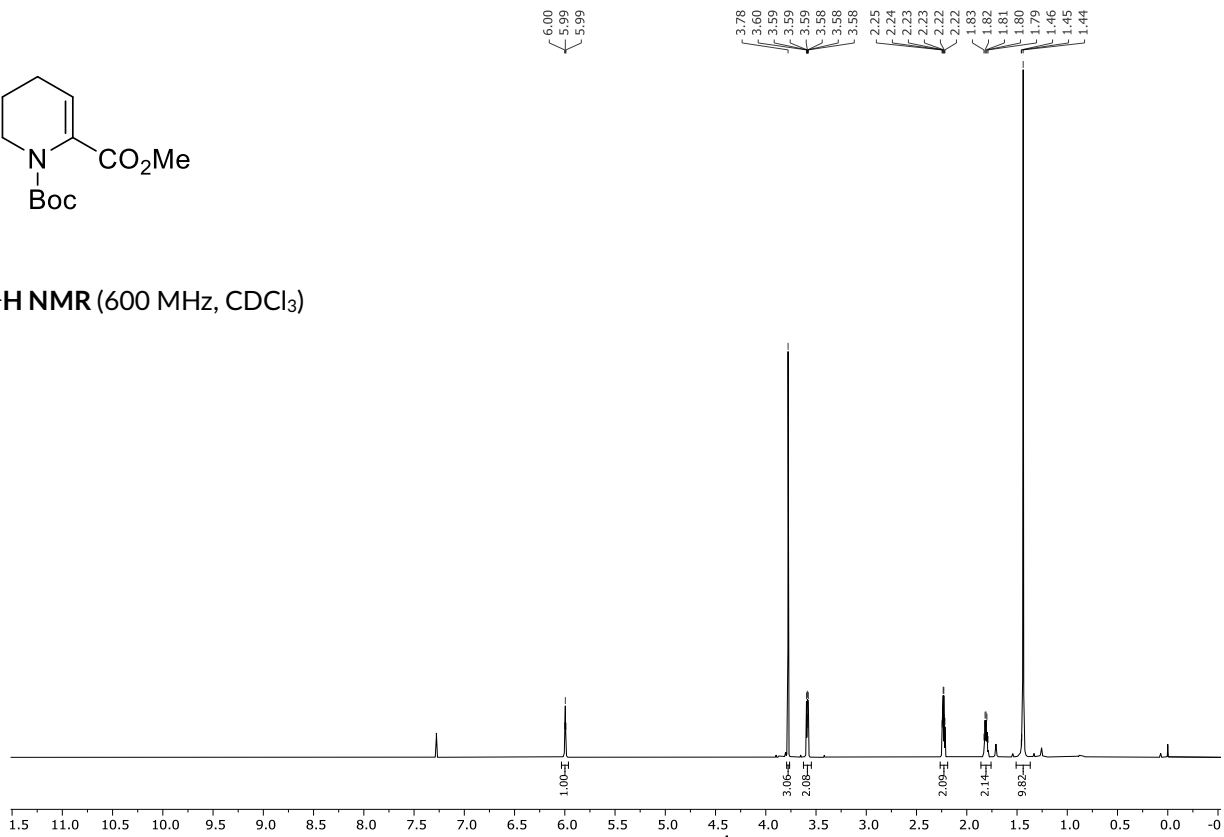
 ^1H NMR (600 MHz, CDCl_3) ^{13}C NMR (151 MHz, CDCl_3)



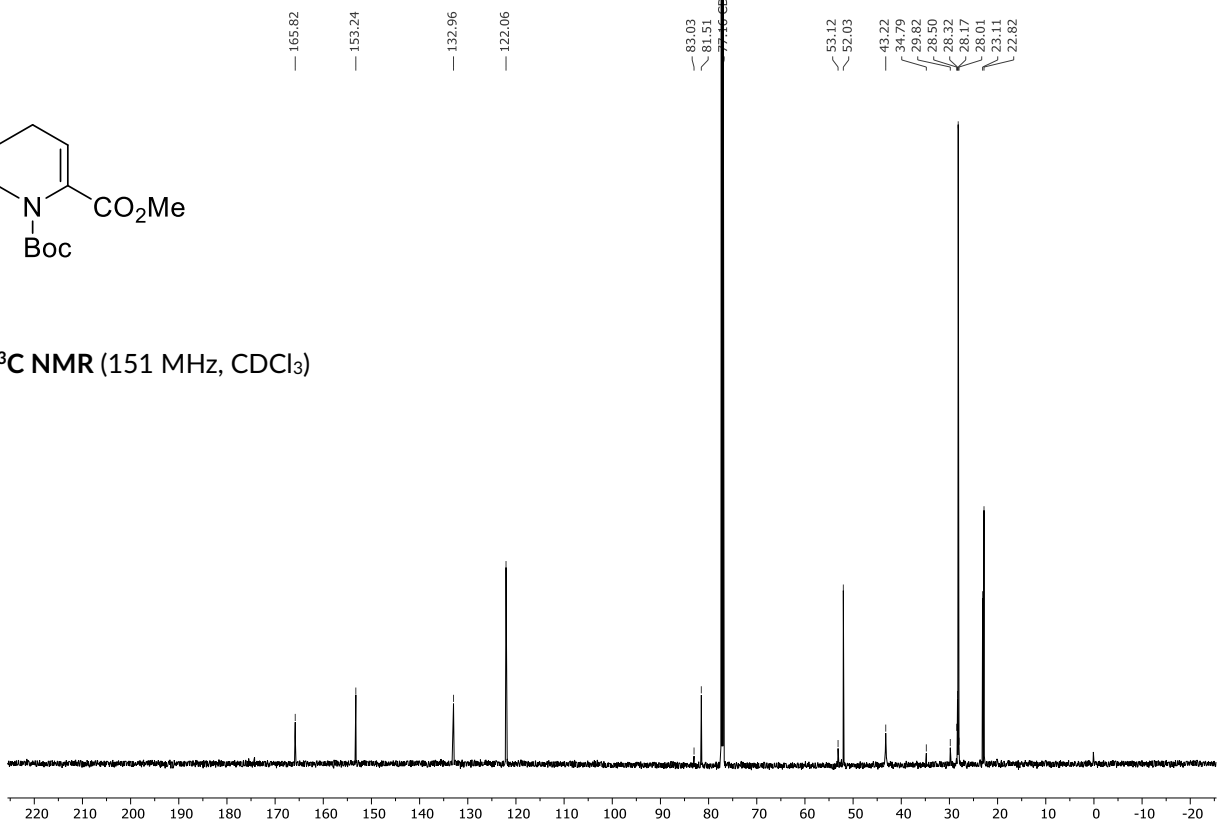




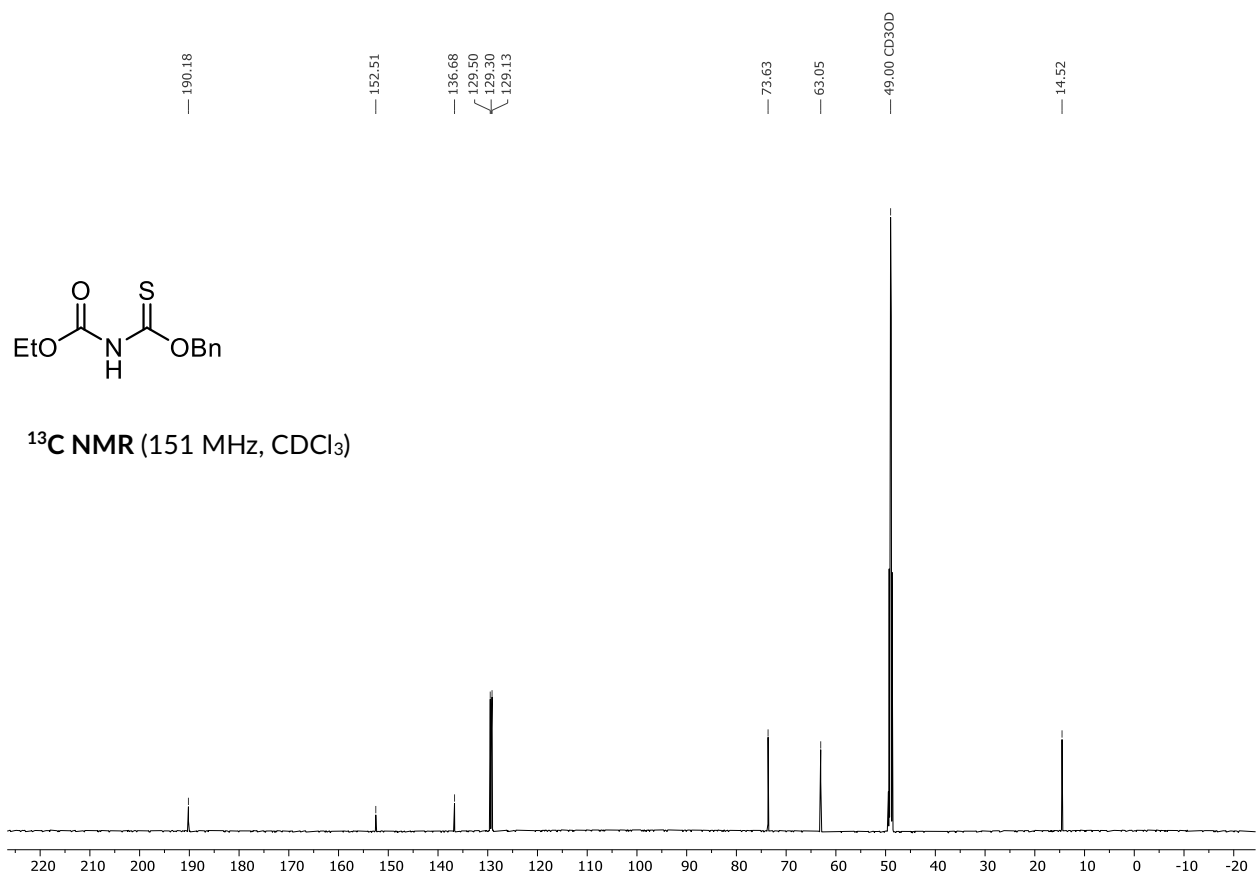
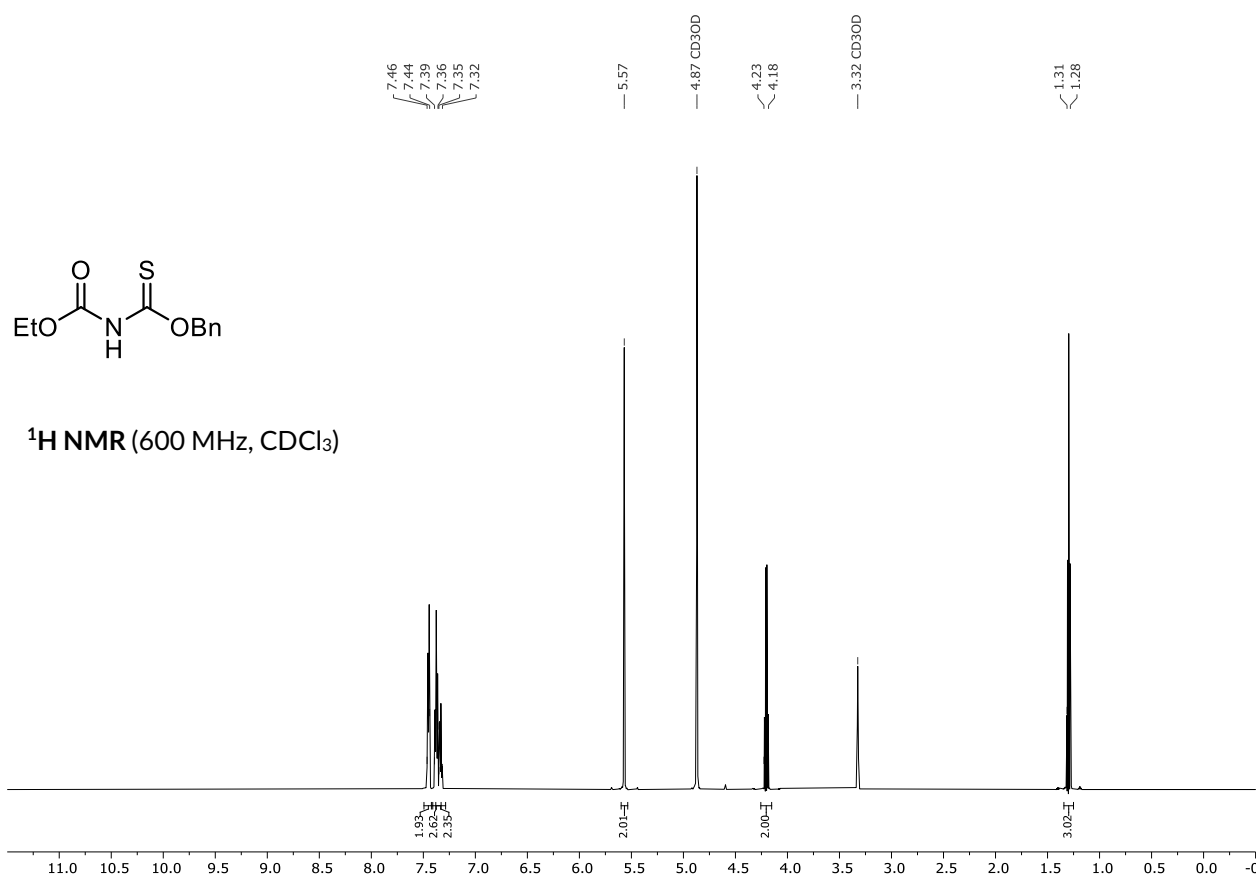
$^1\text{H NMR}$ (600 MHz, CDCl_3)

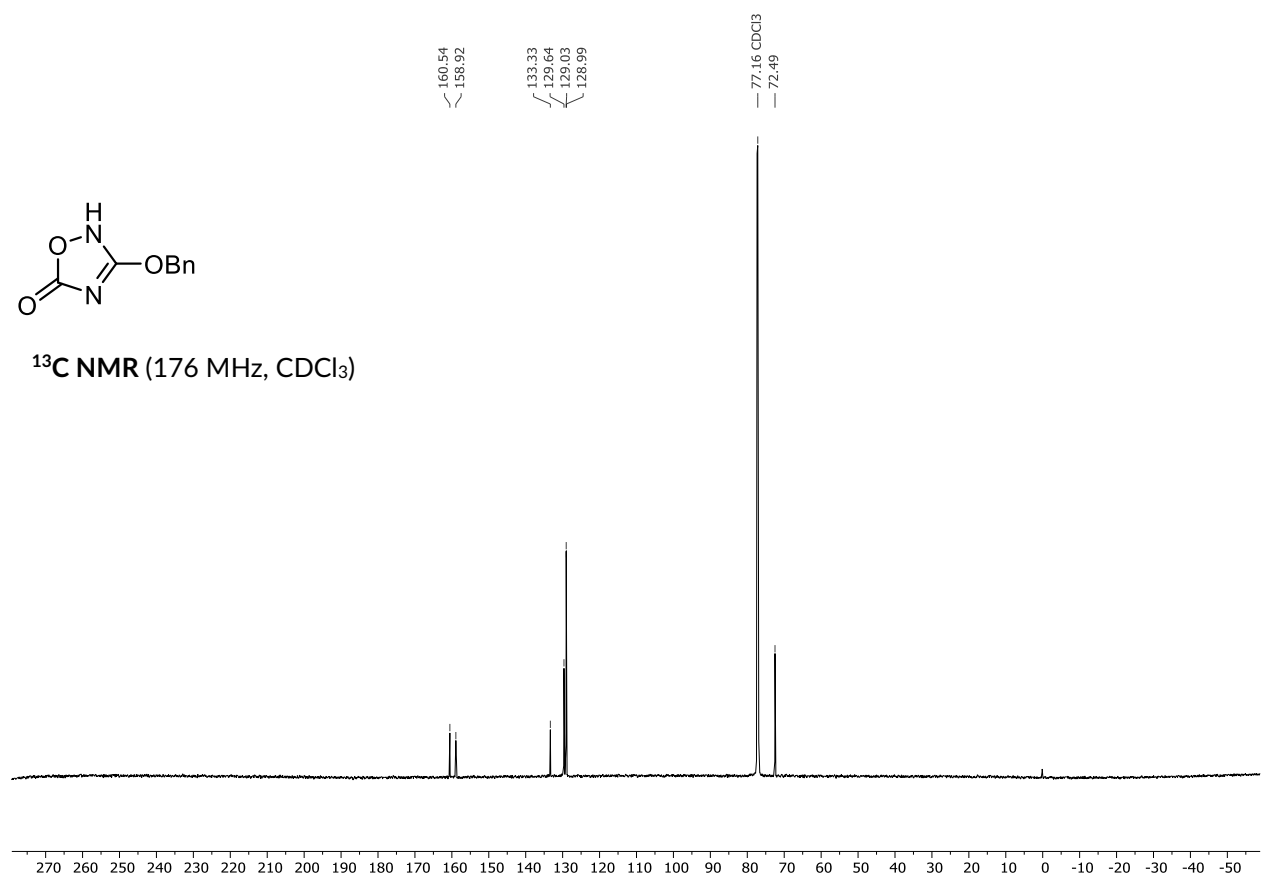
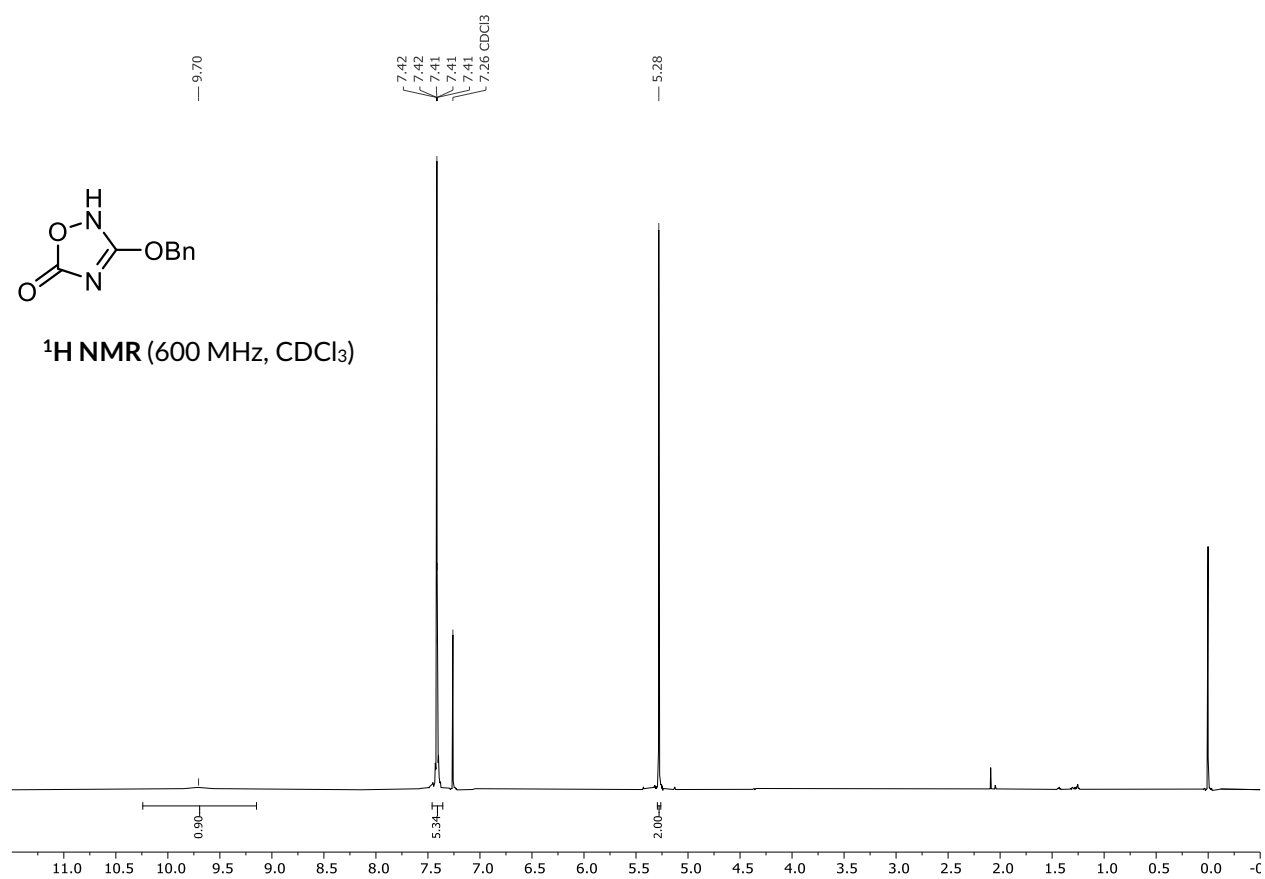


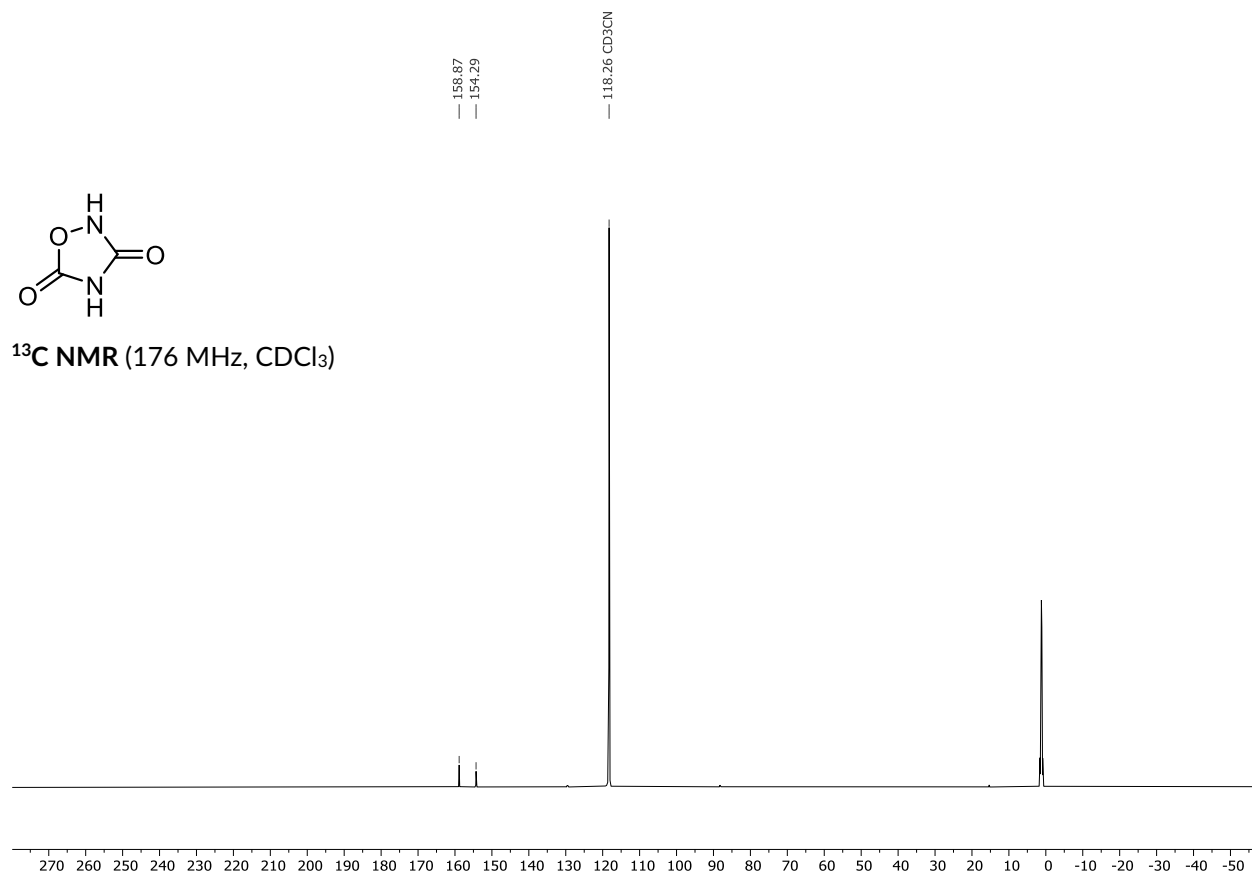
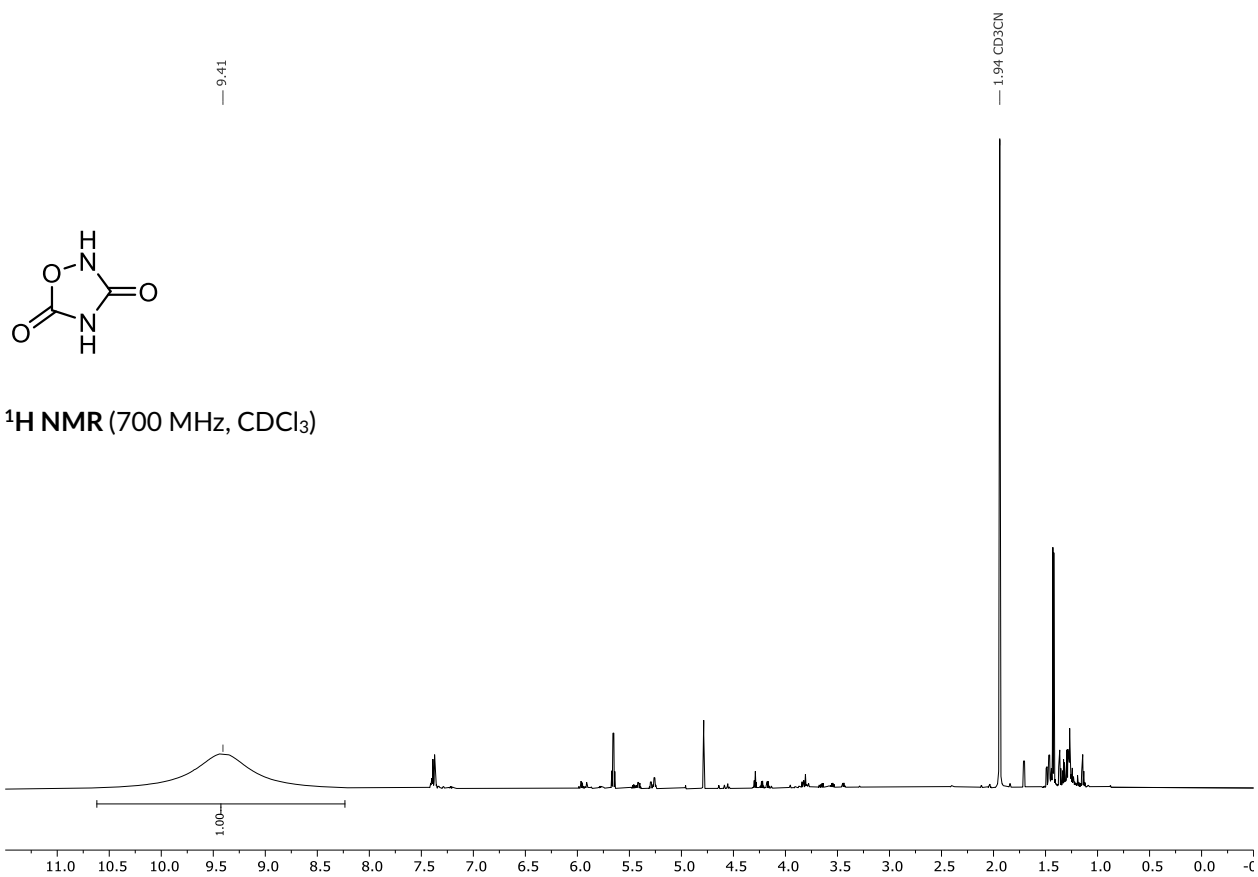
$^{13}\text{C NMR}$ (151 MHz, CDCl_3)



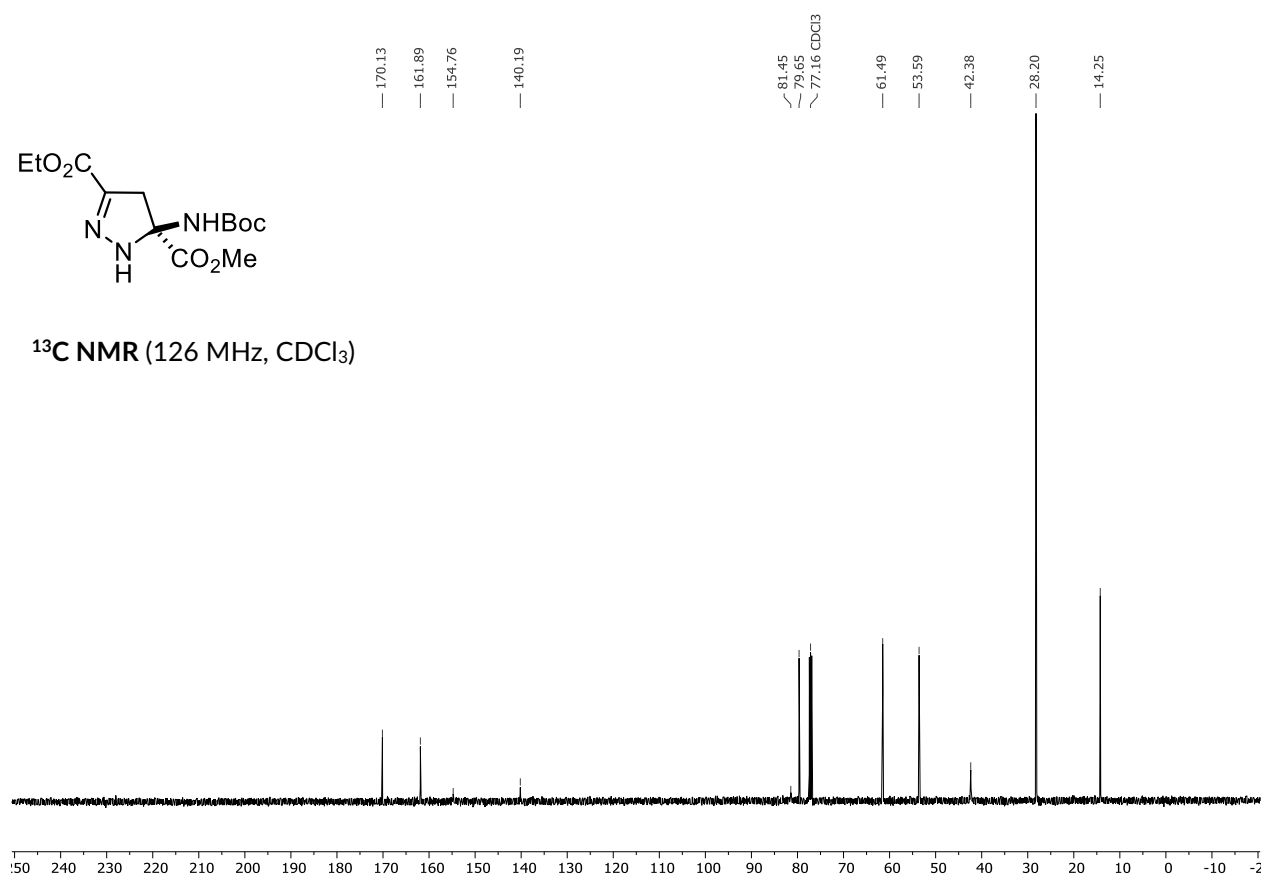
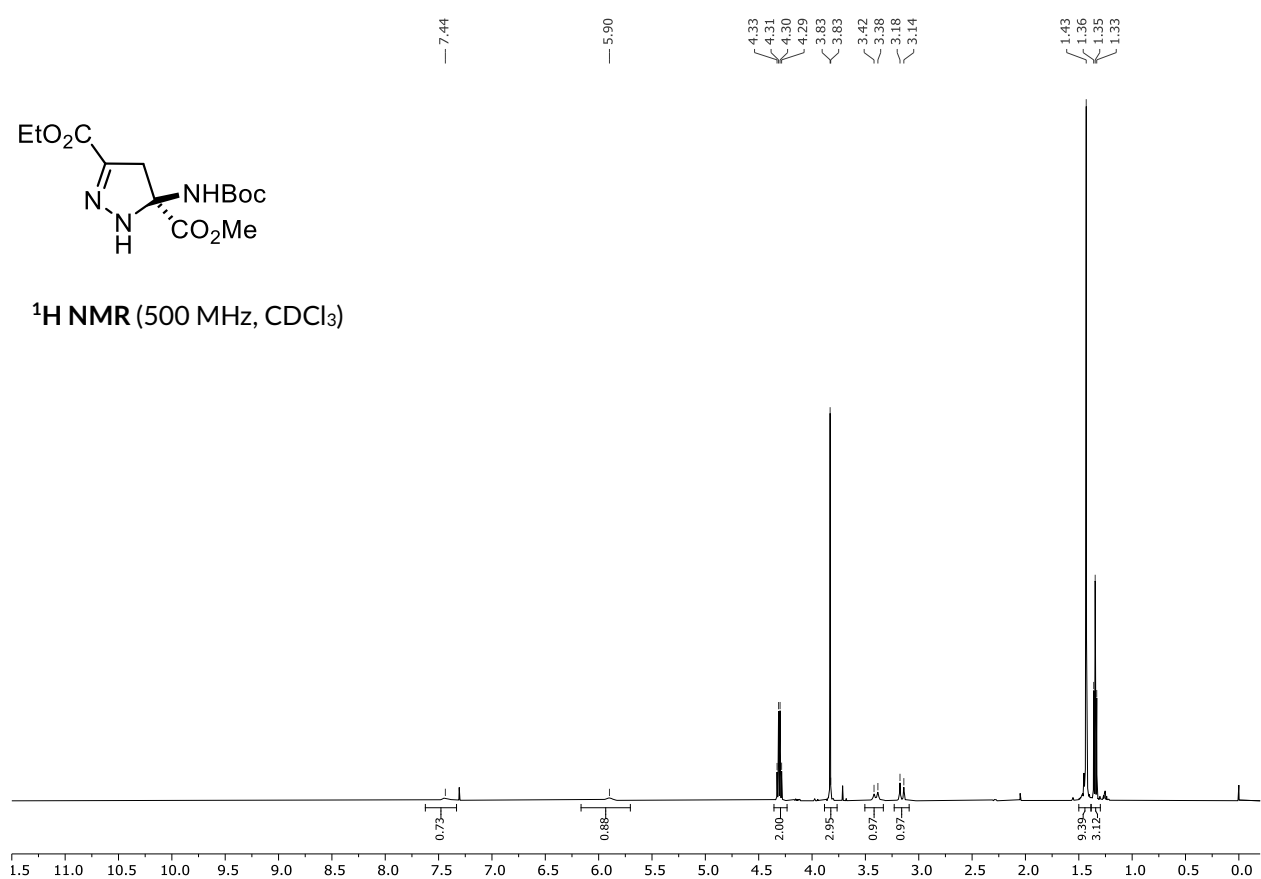
7.2.8. Synthesis of Quisqualic Acid

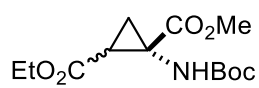
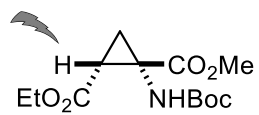
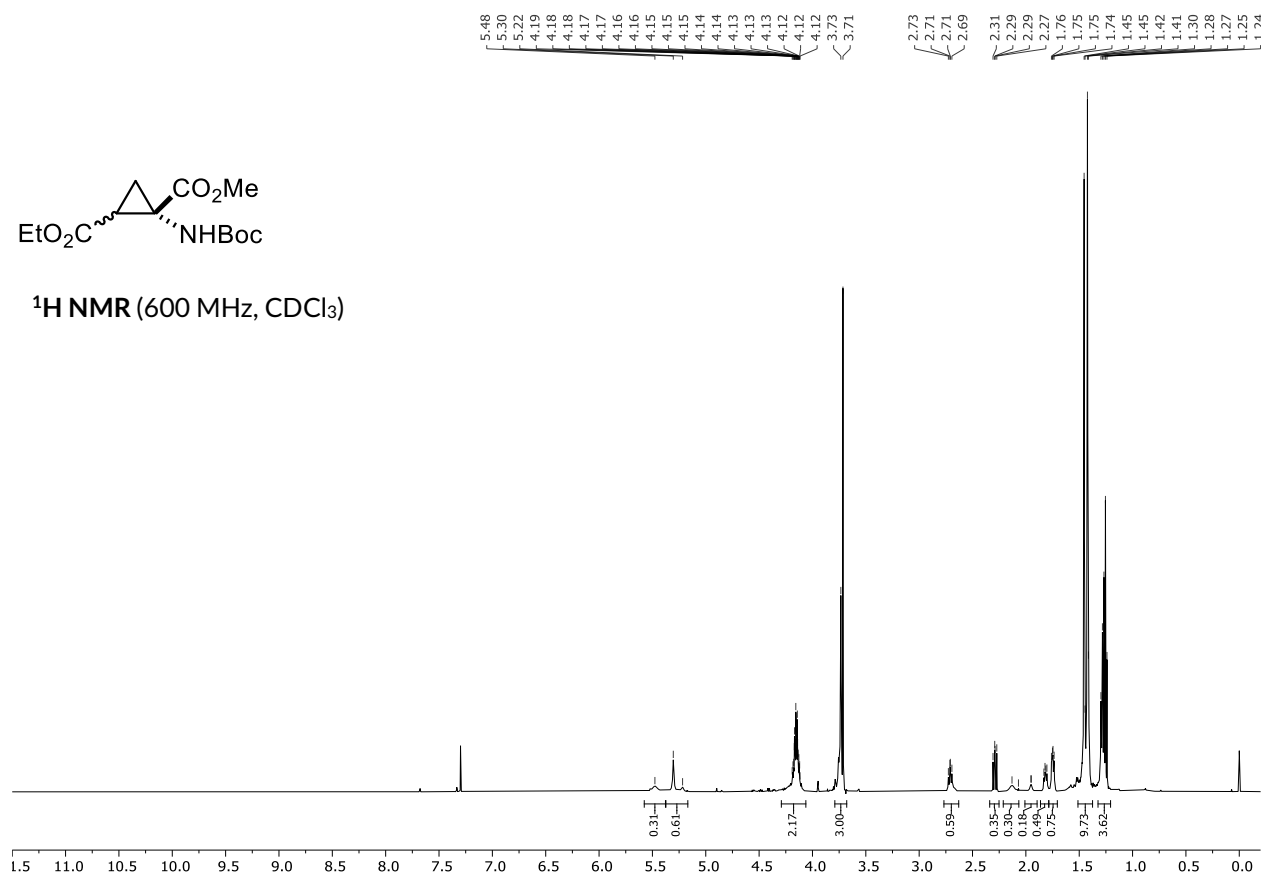
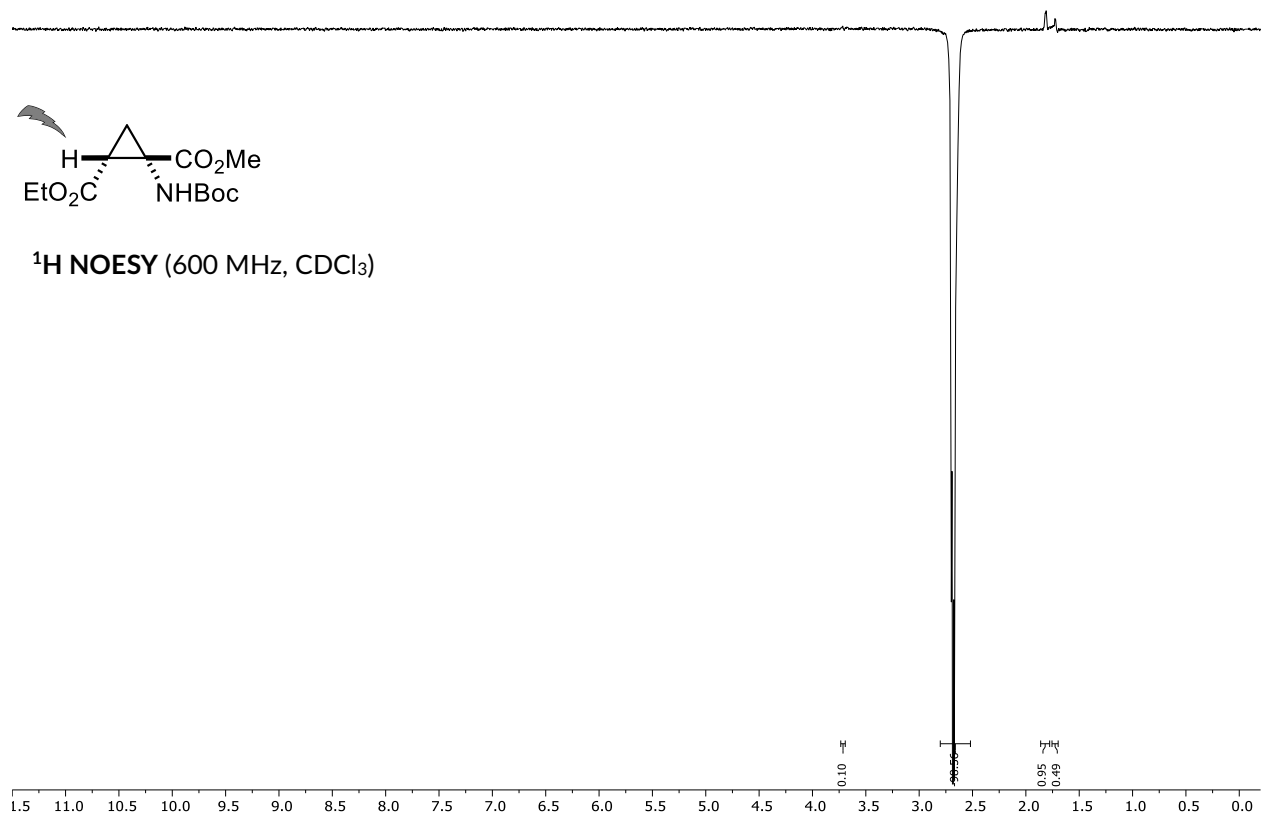


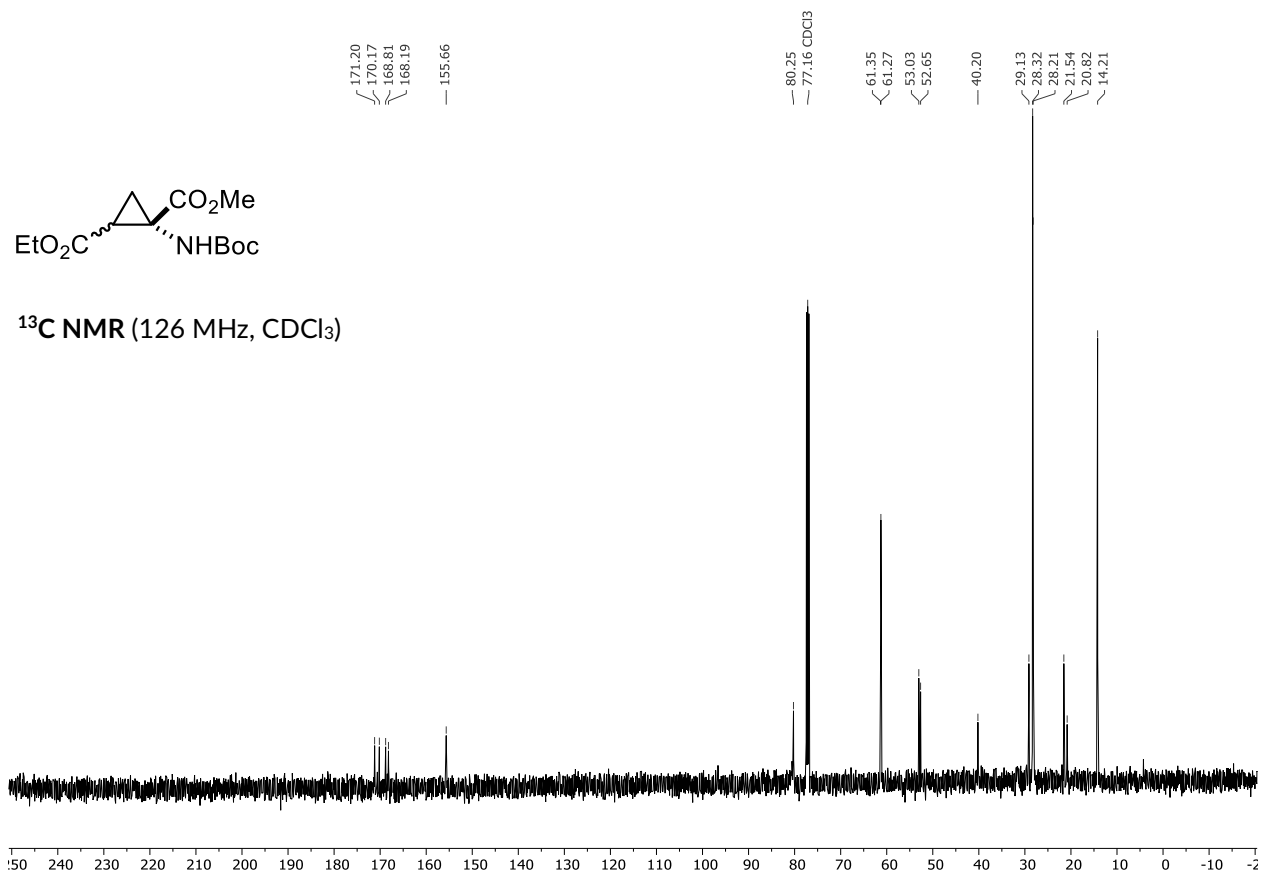
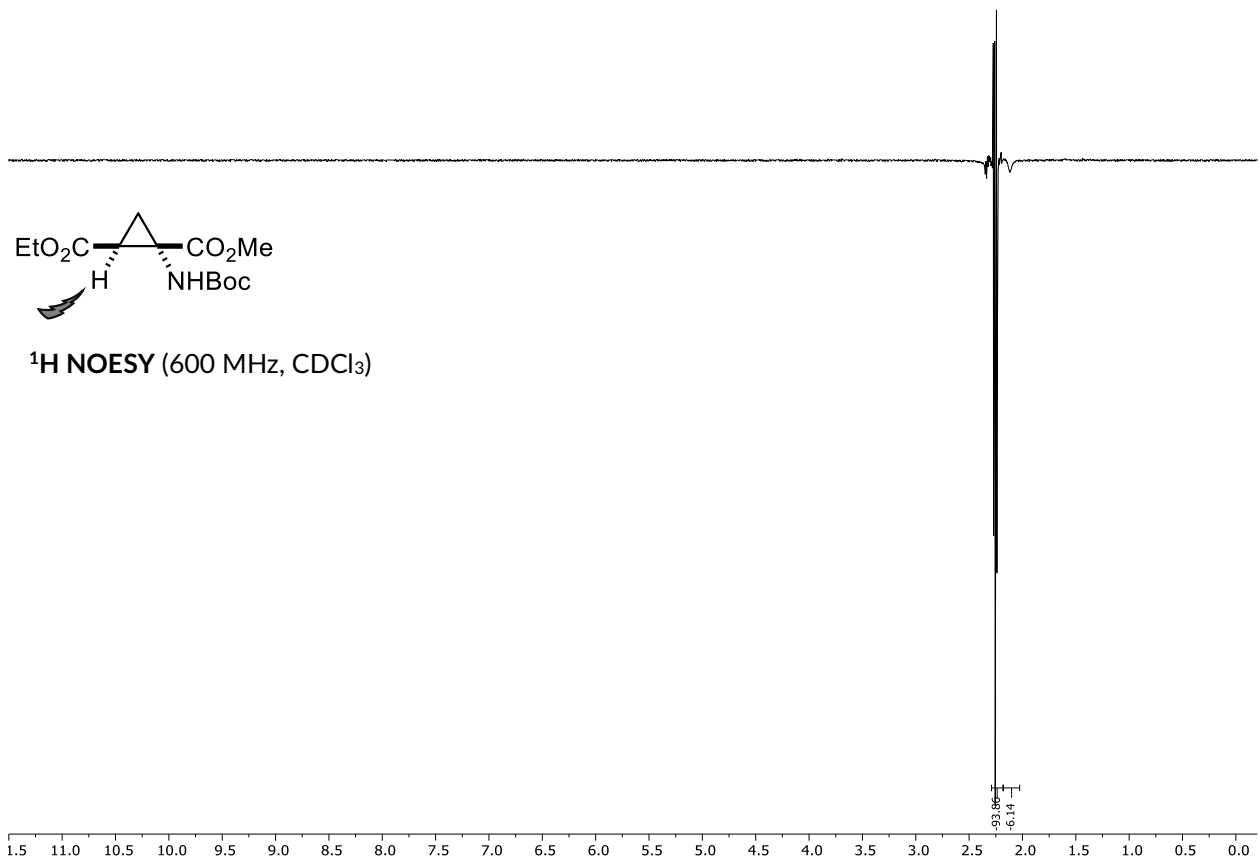


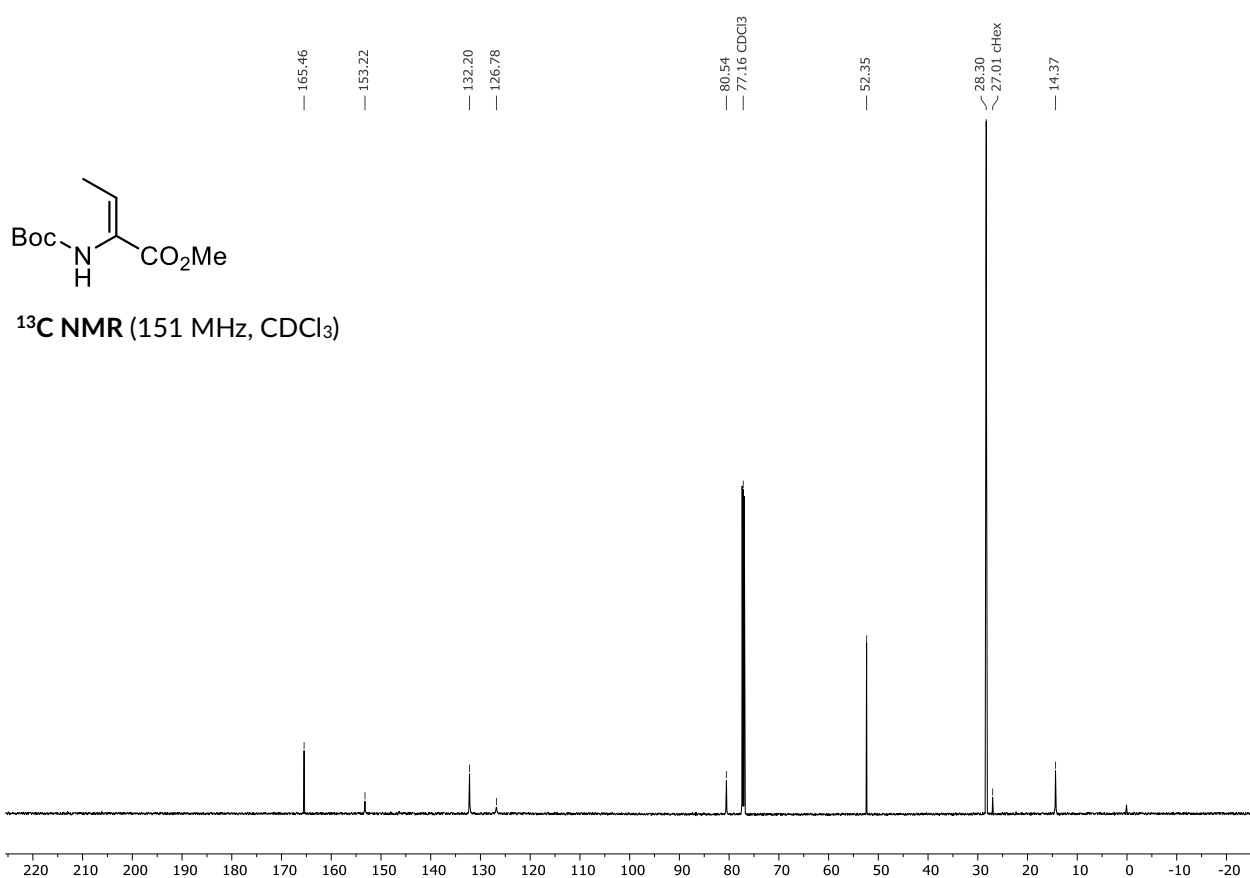
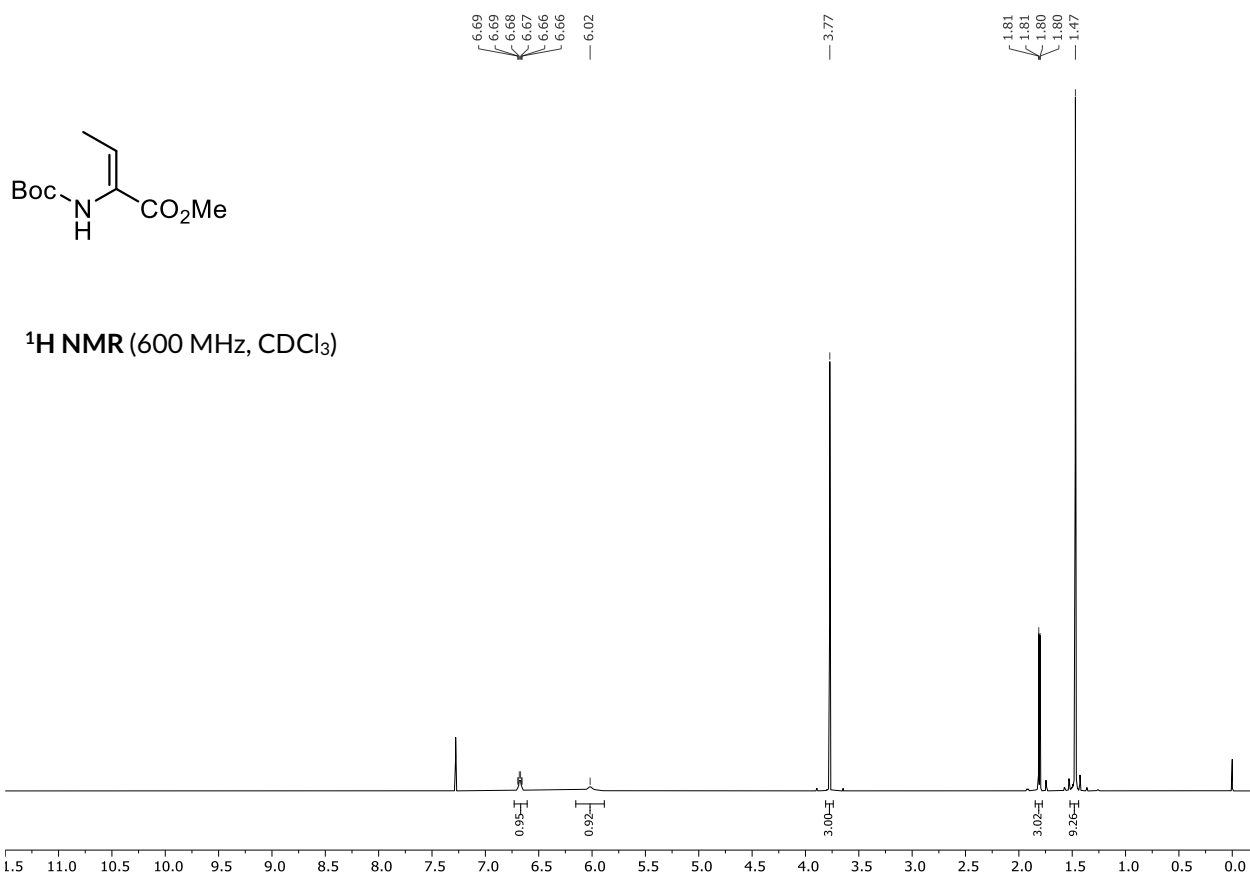


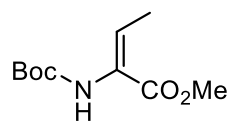
7.2.9. Synthesis of 2-Pyrazoline Amino Acids



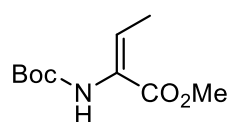
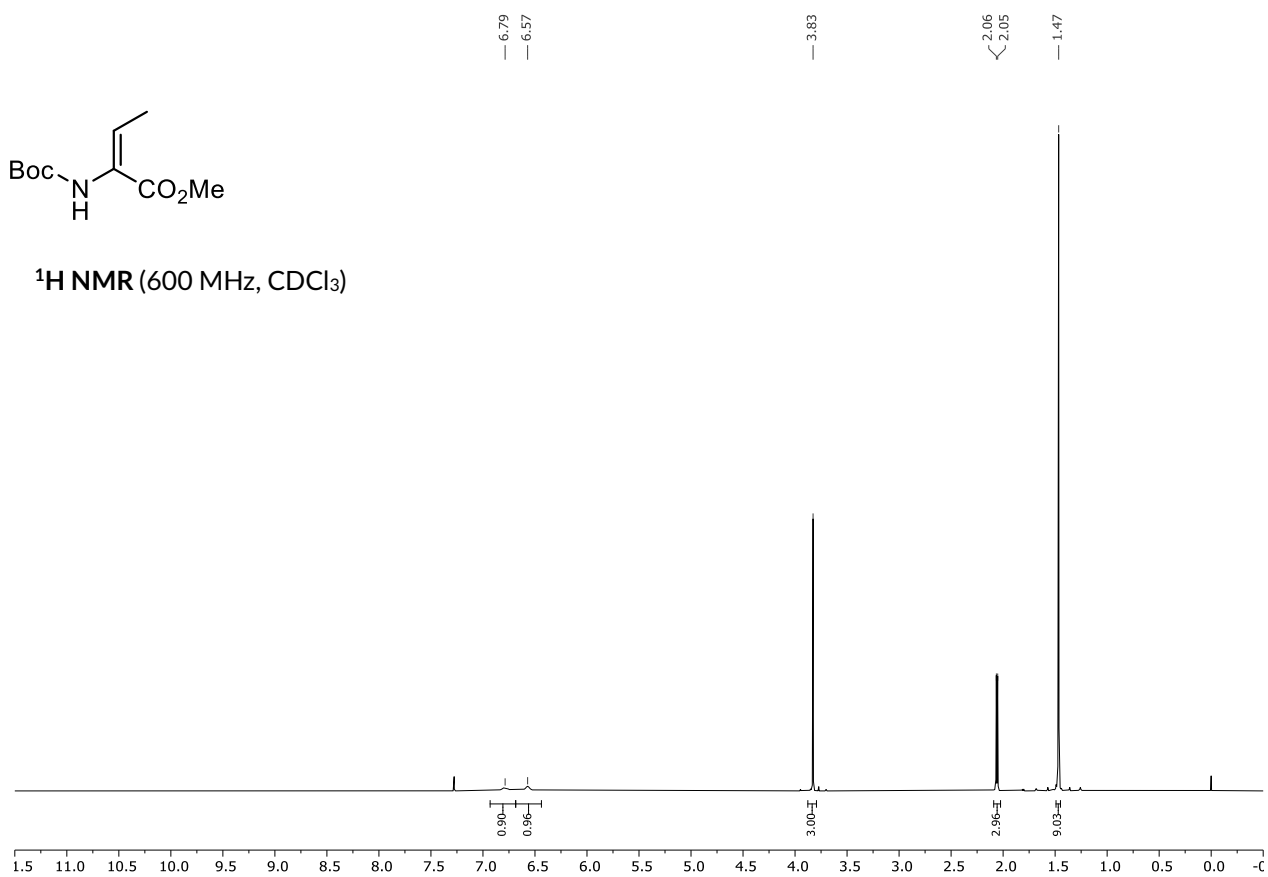
¹H NMR (600 MHz, CDCl₃)¹H NOESY (600 MHz, CDCl₃)



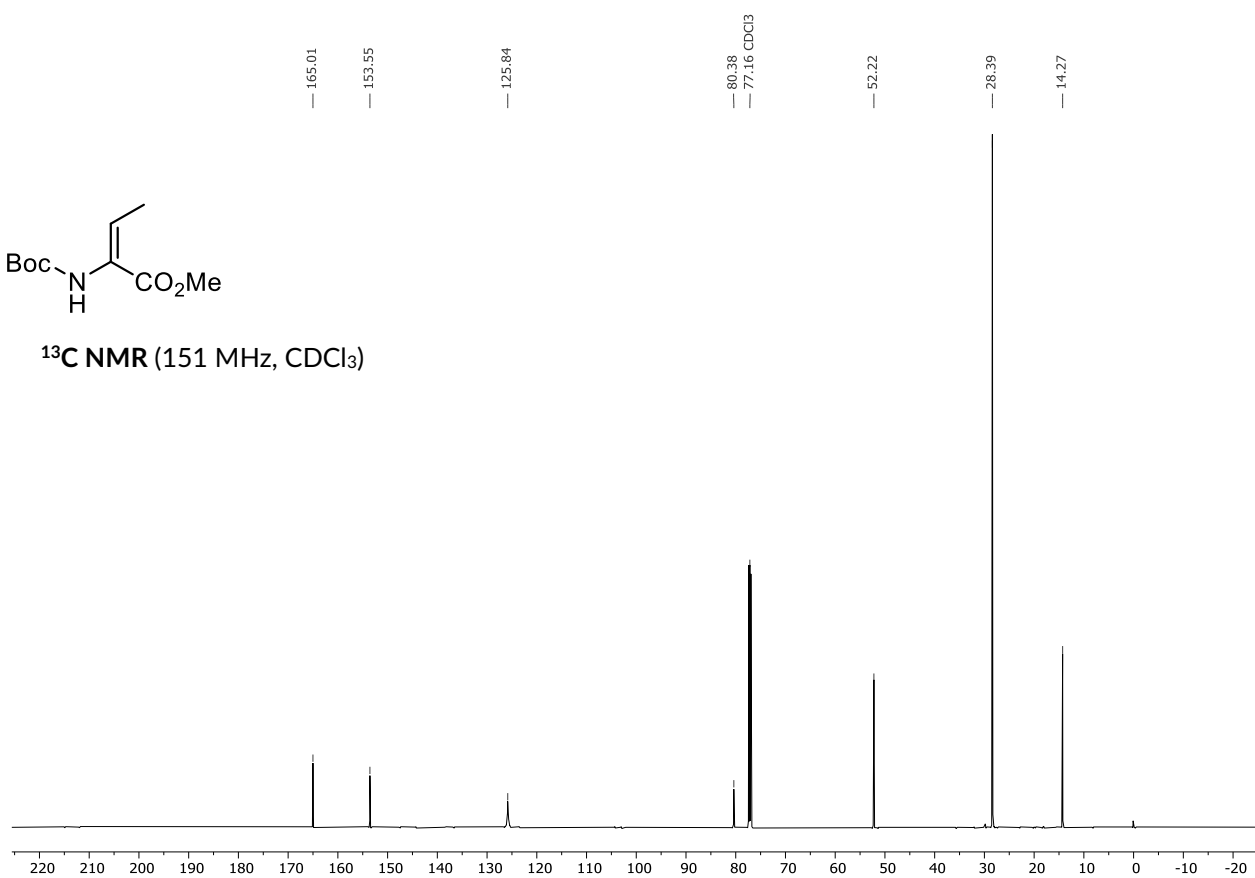


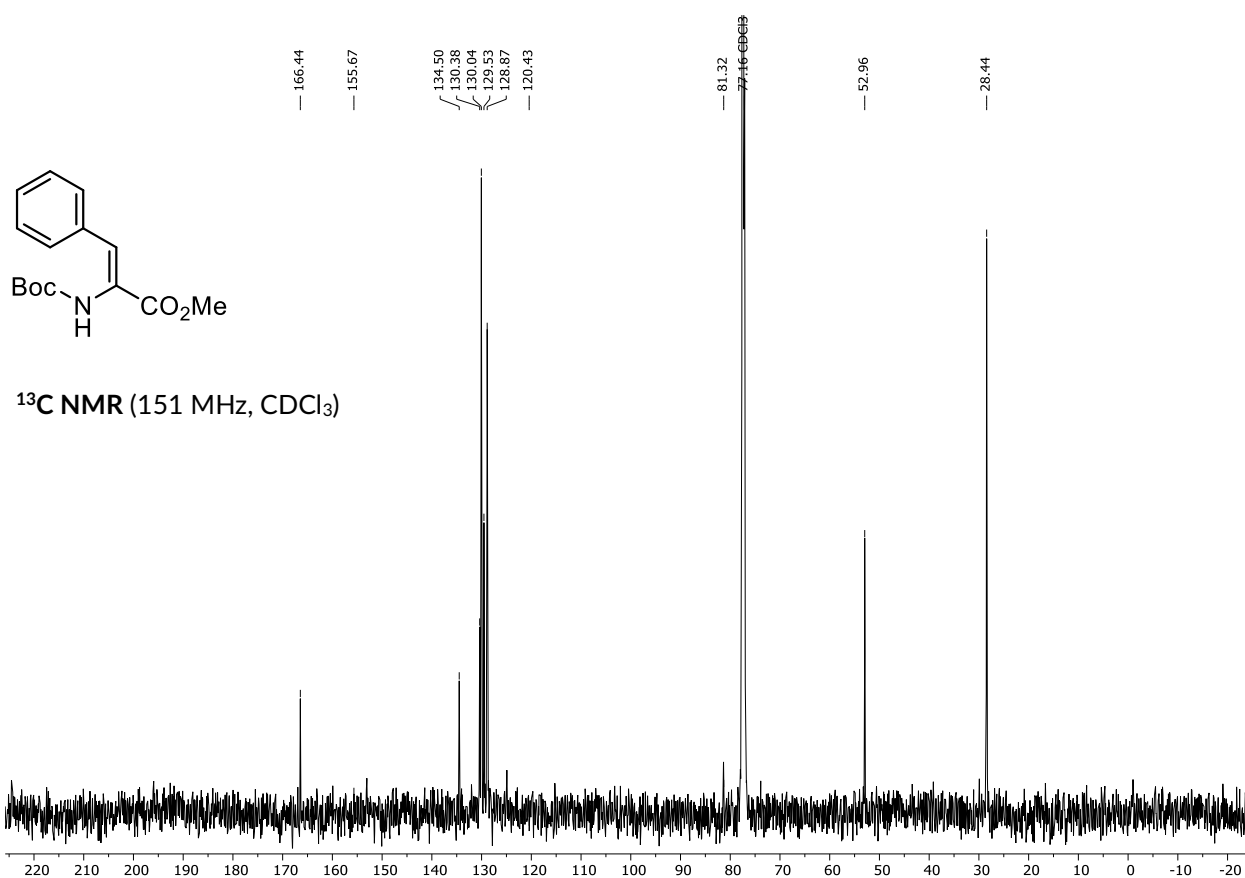
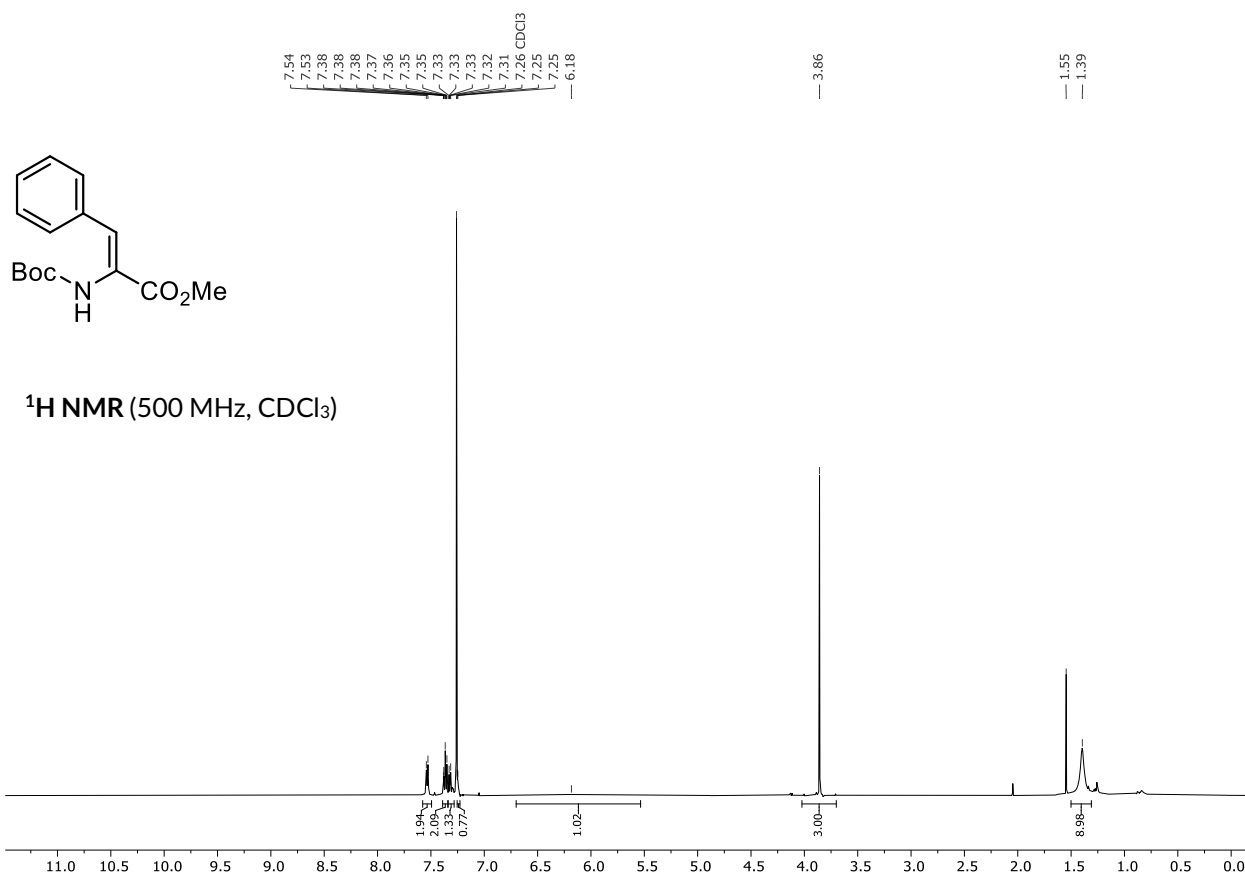


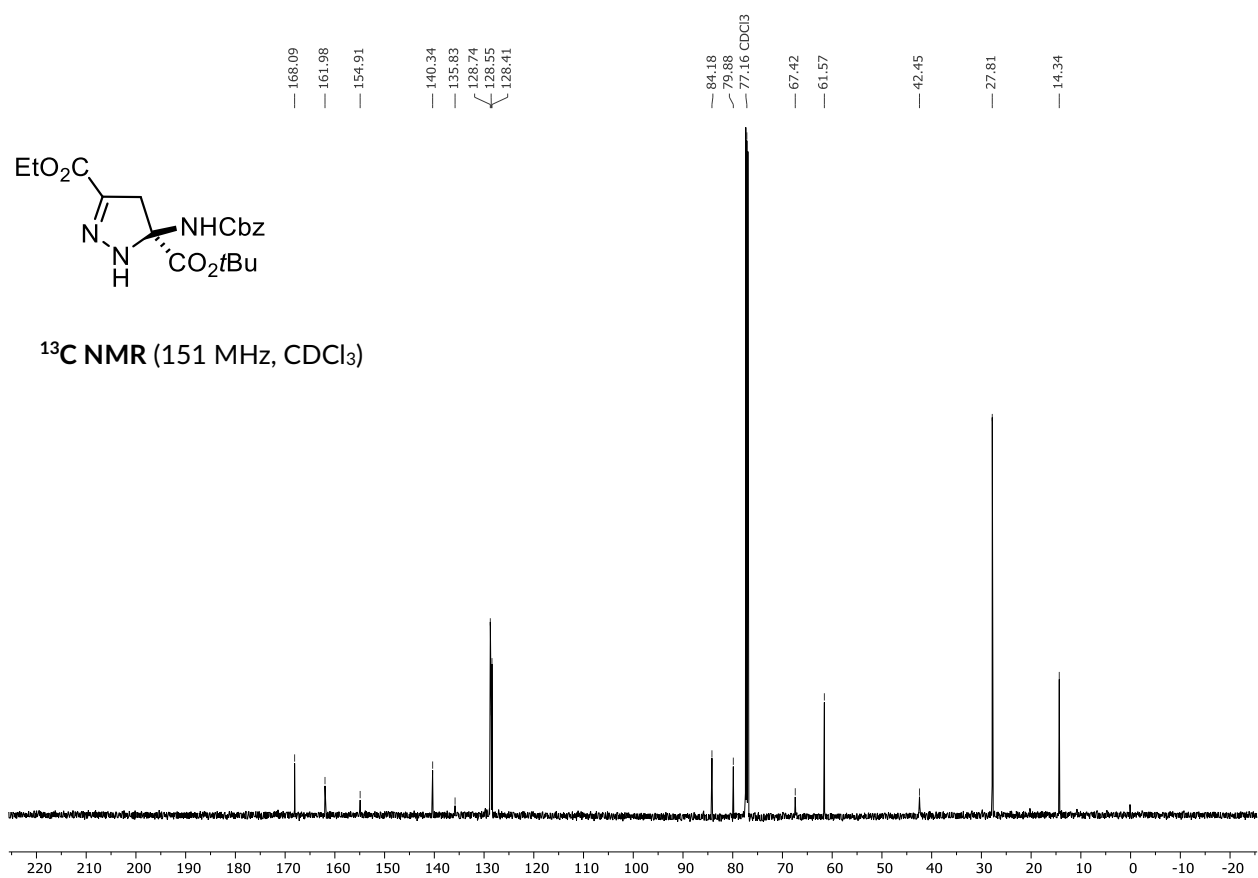
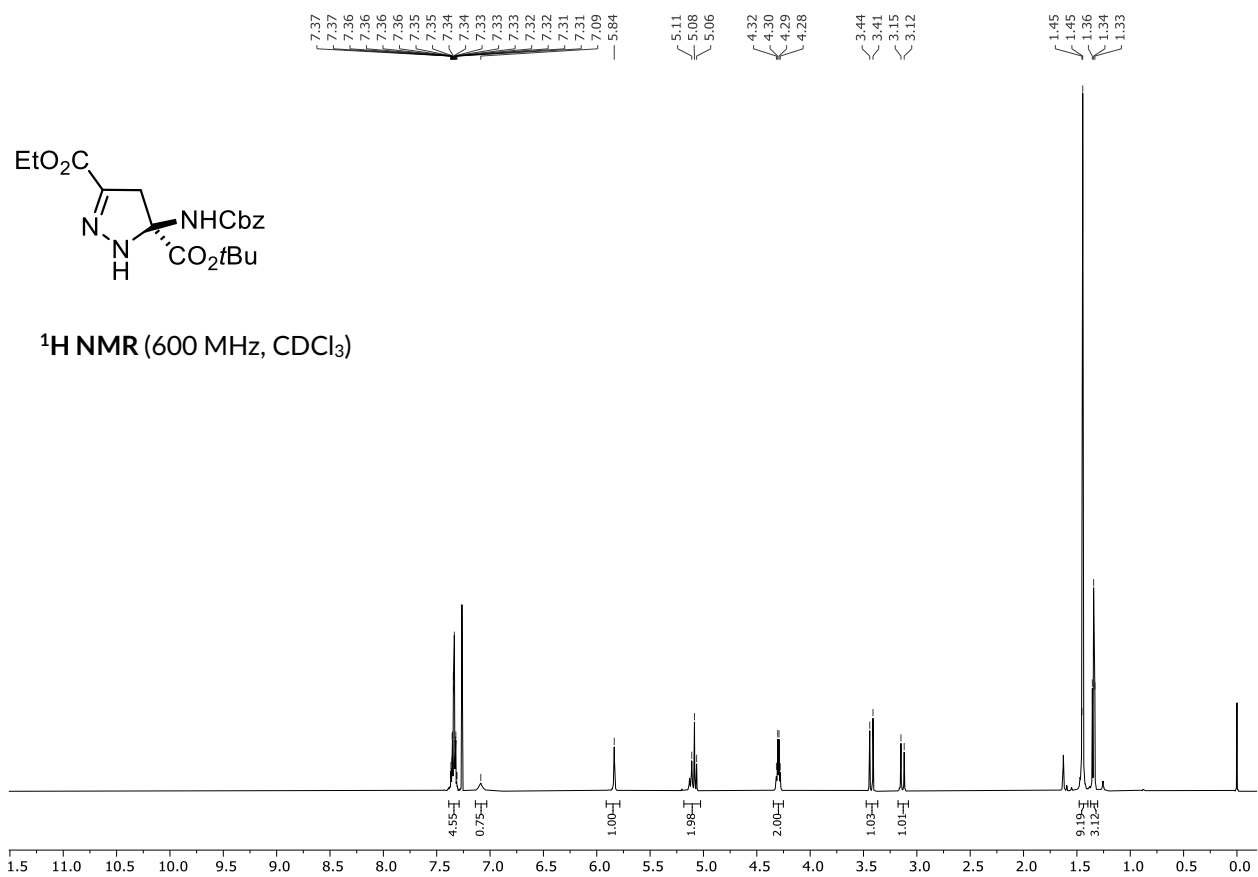
$^1\text{H NMR}$ (600 MHz, CDCl_3)

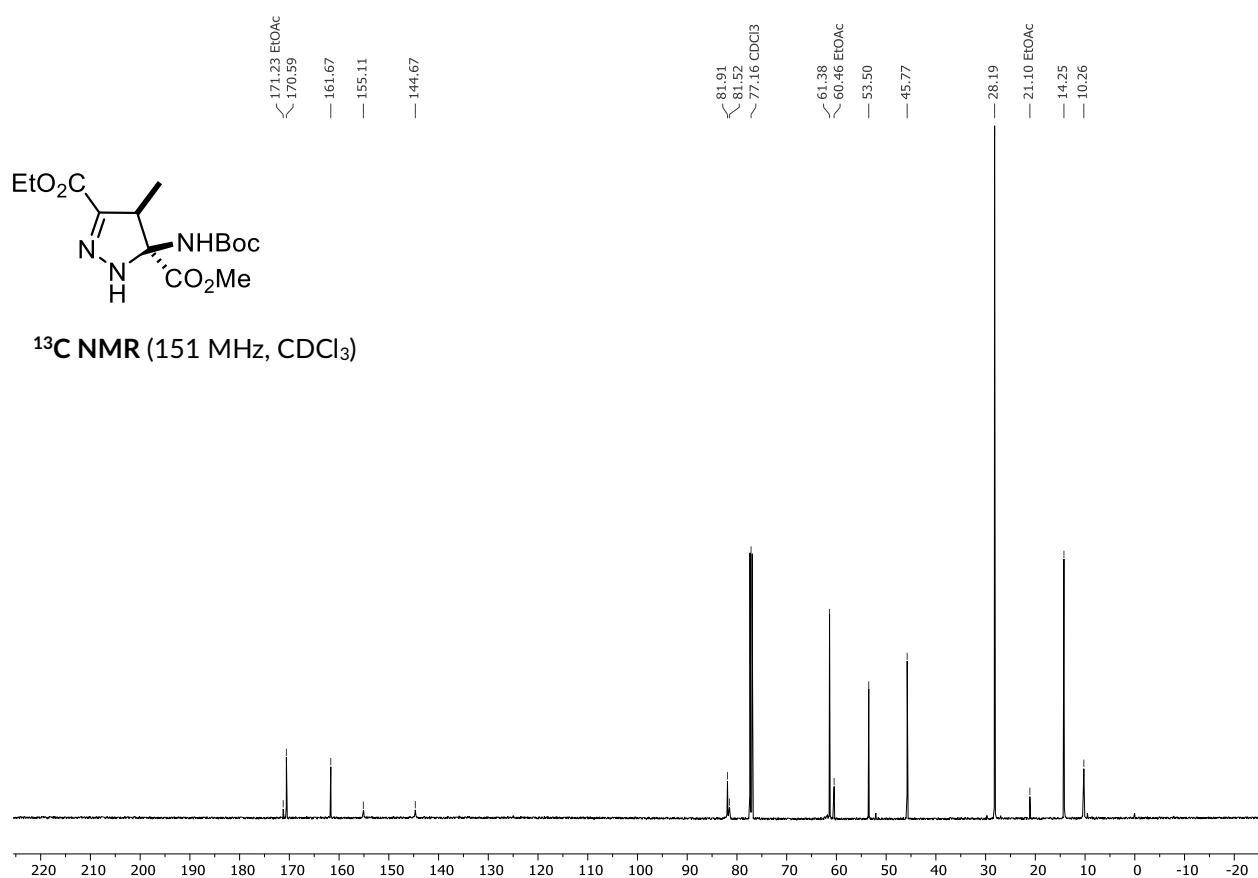
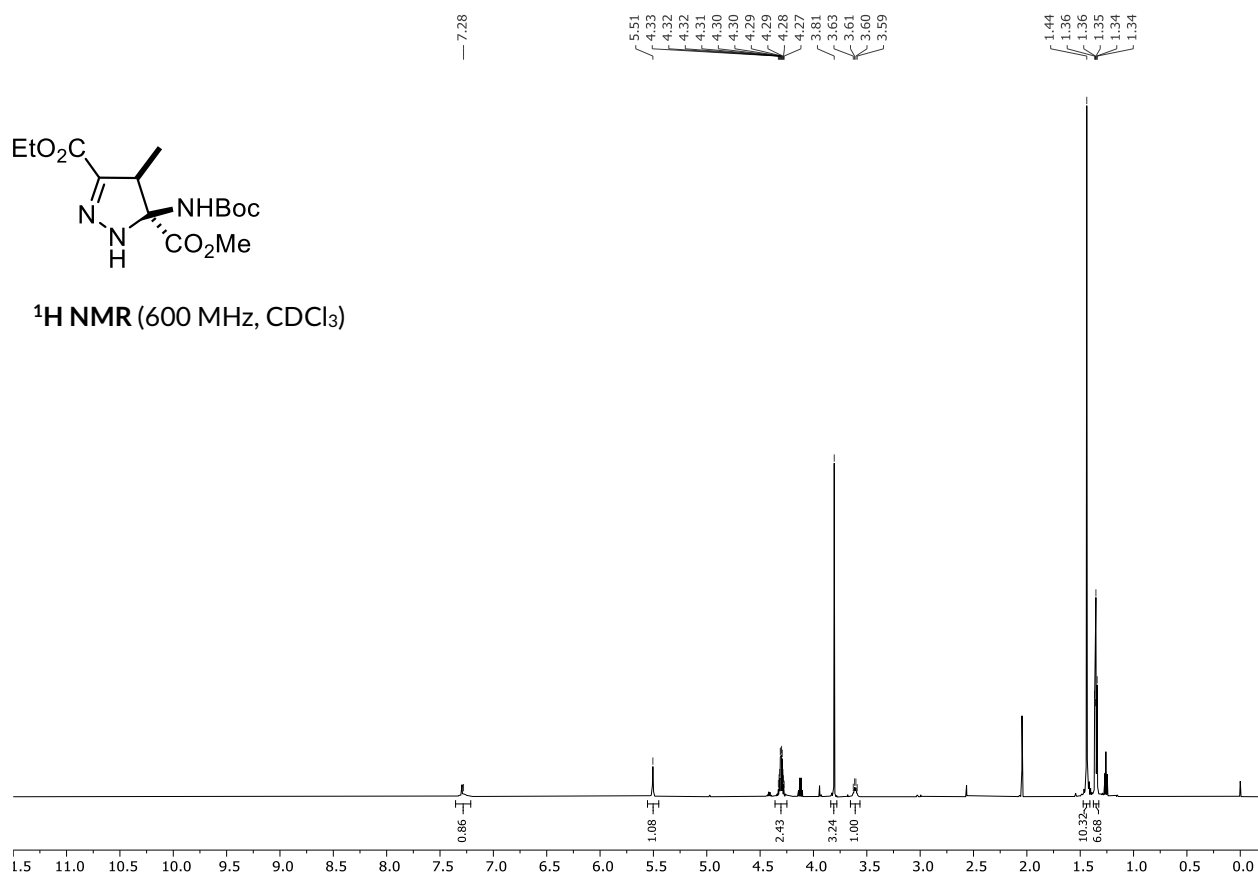


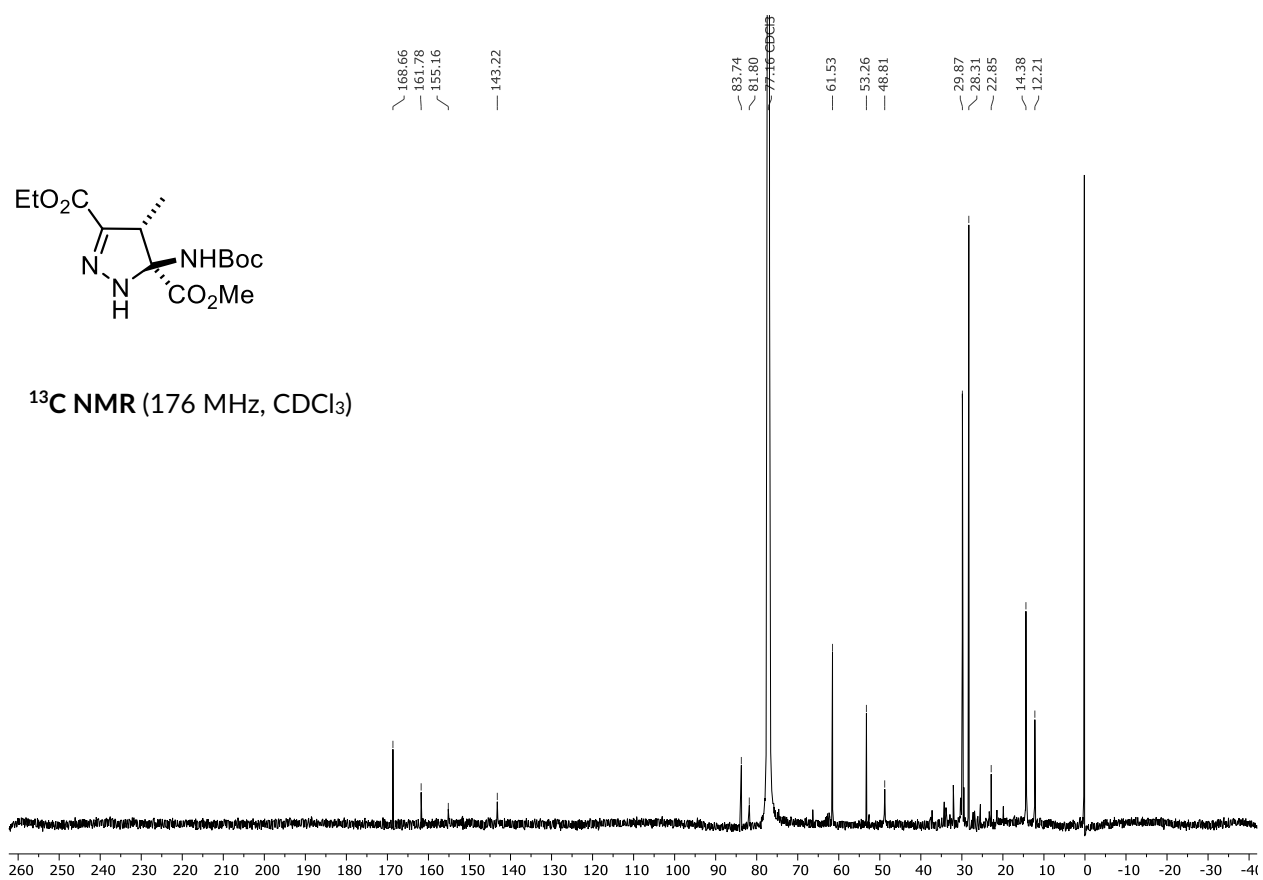
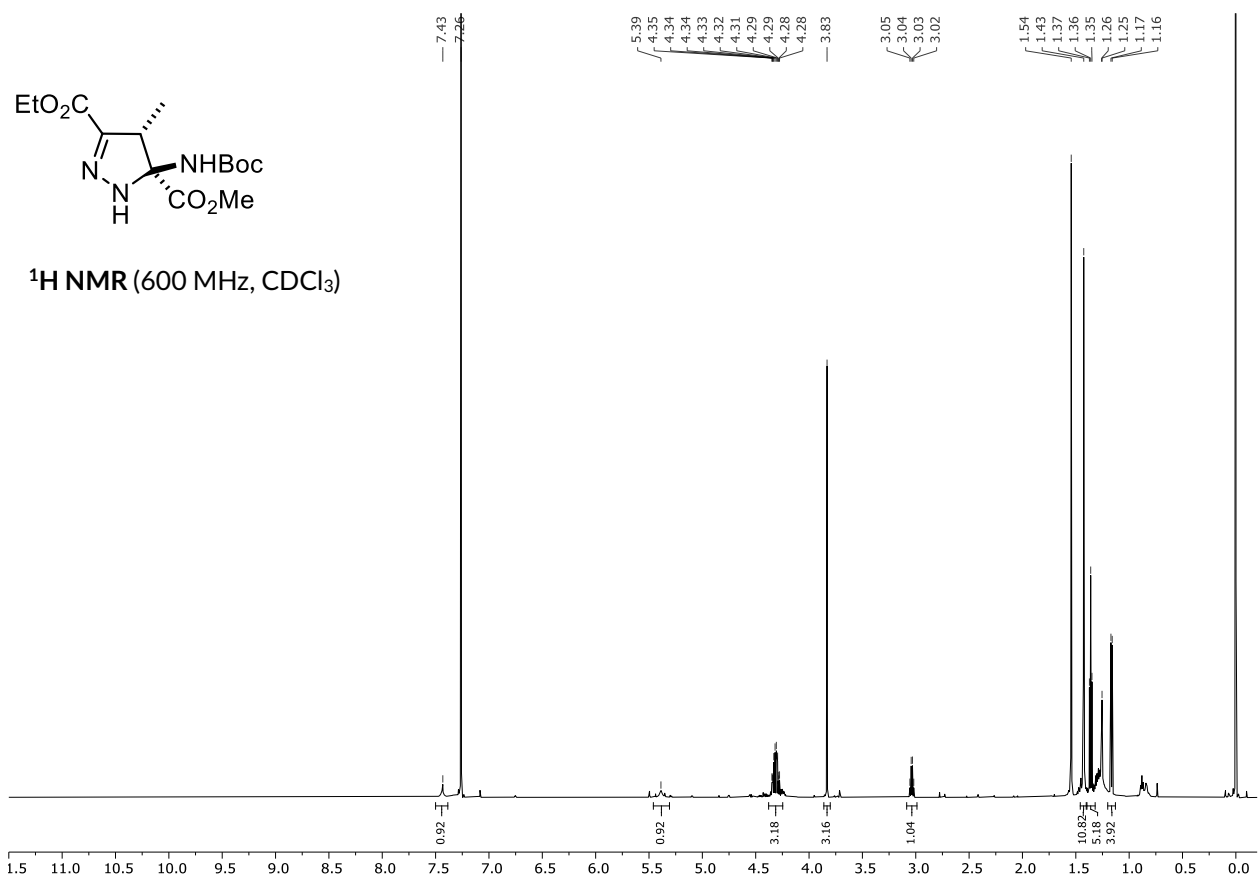
$^{13}\text{C NMR}$ (151 MHz, CDCl_3)

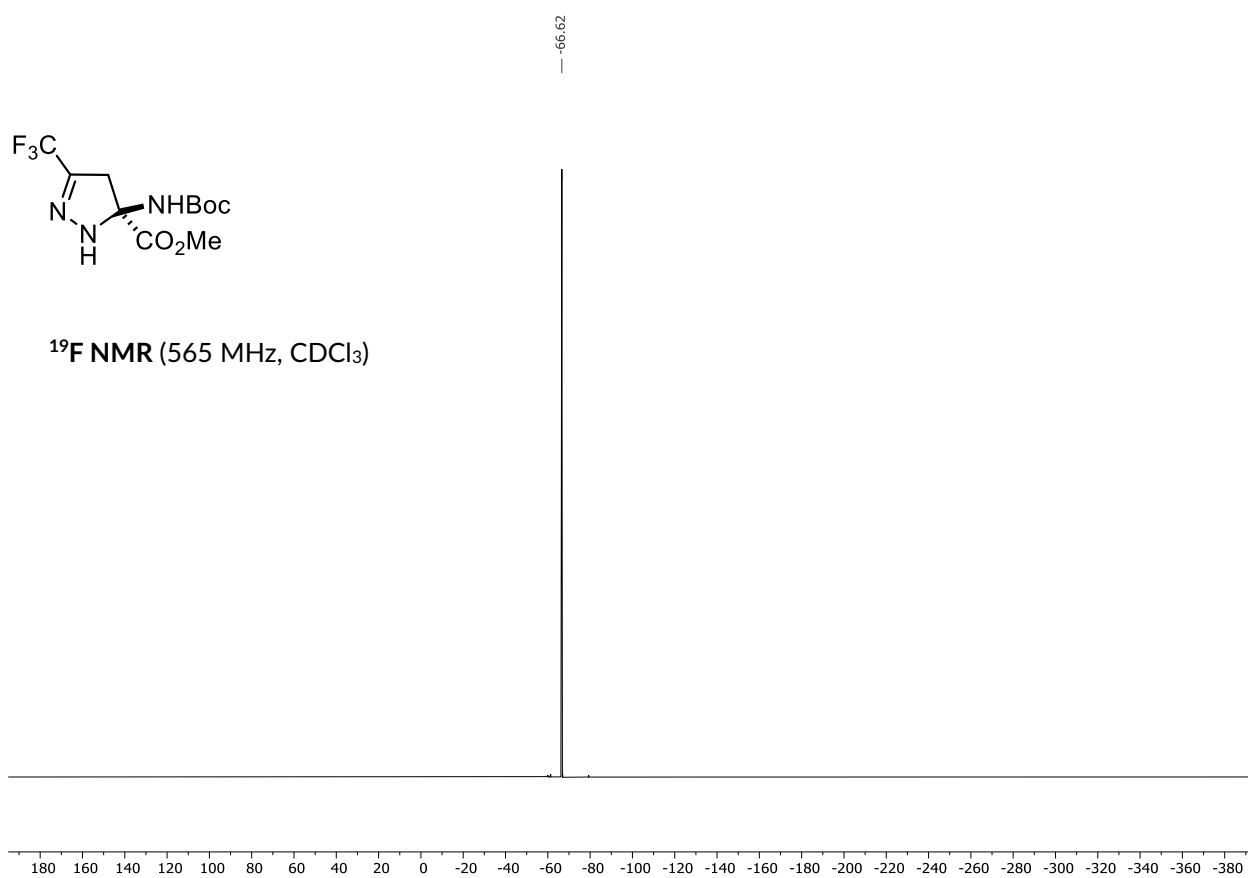
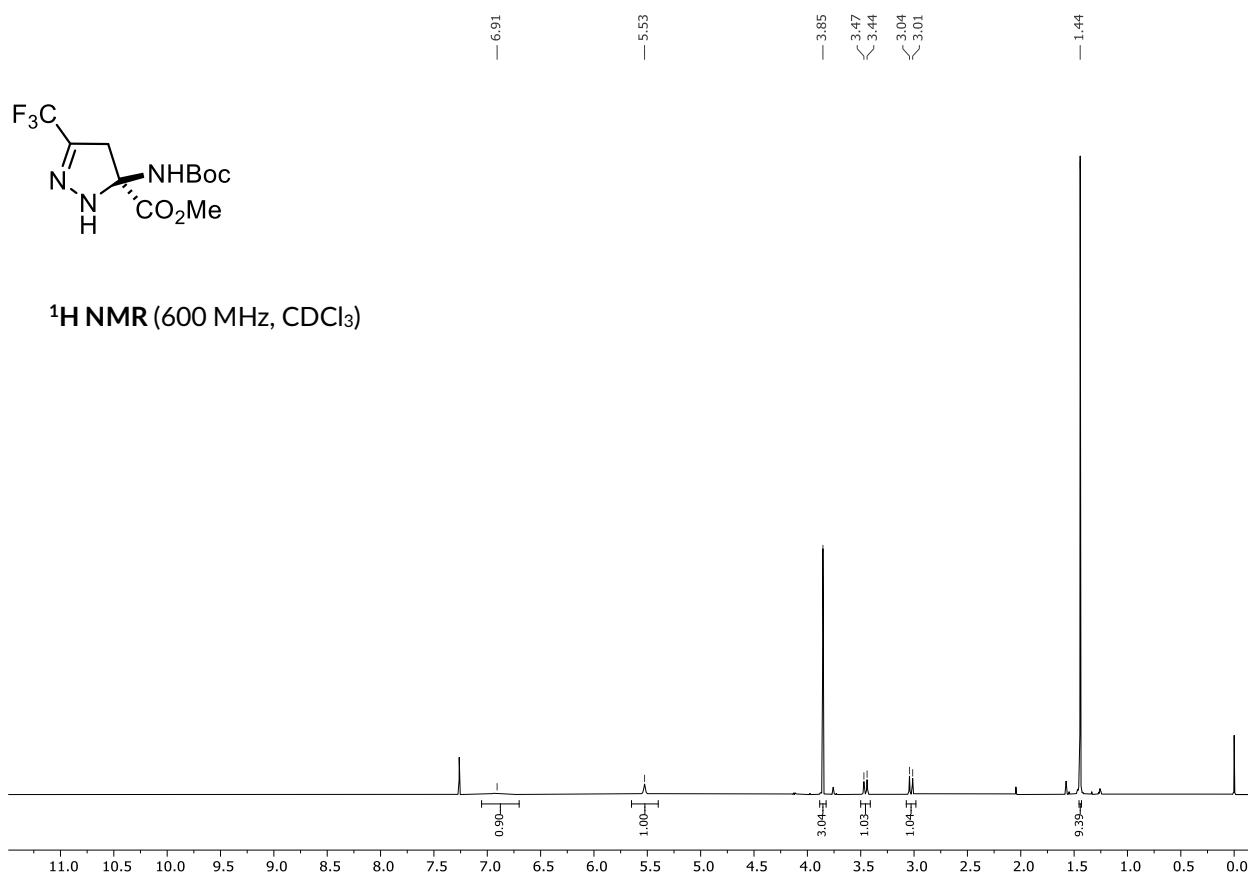


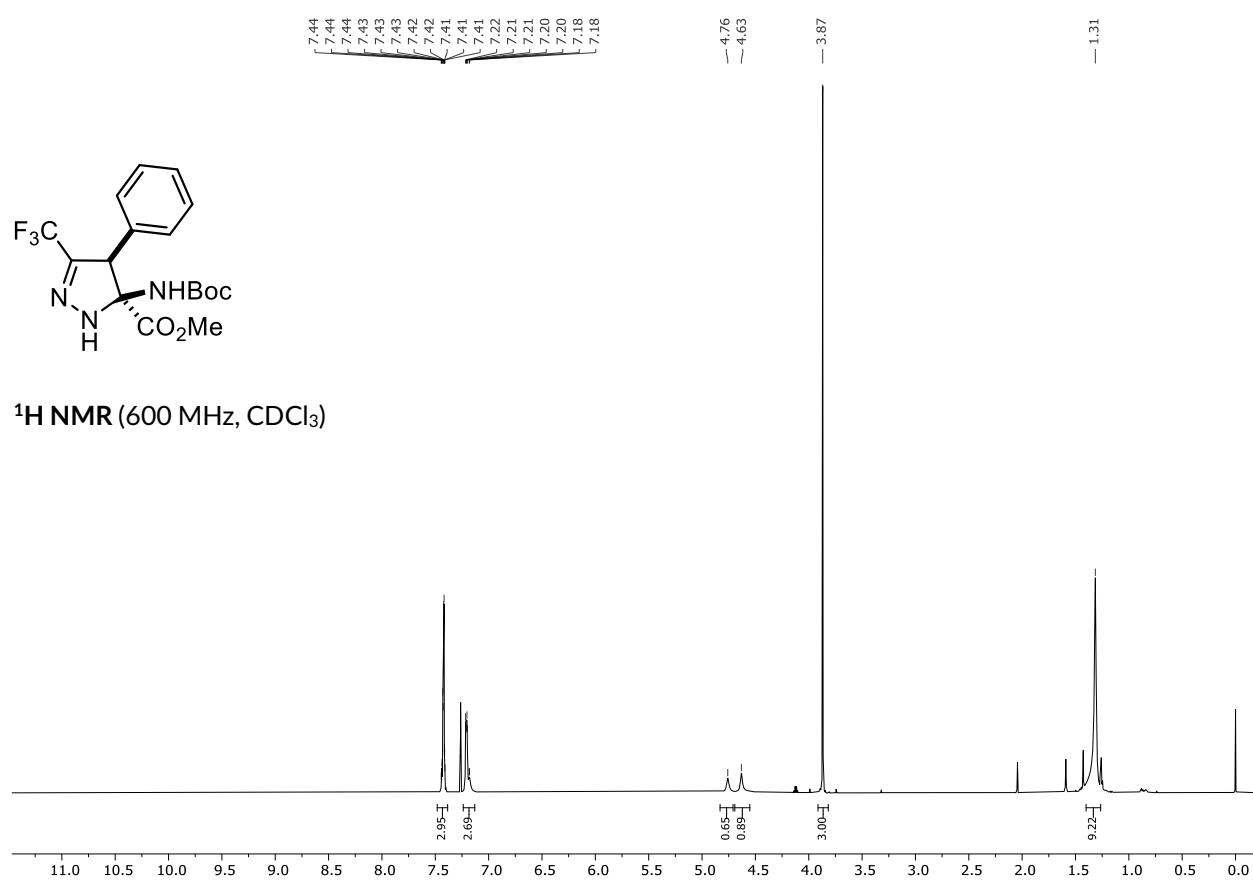
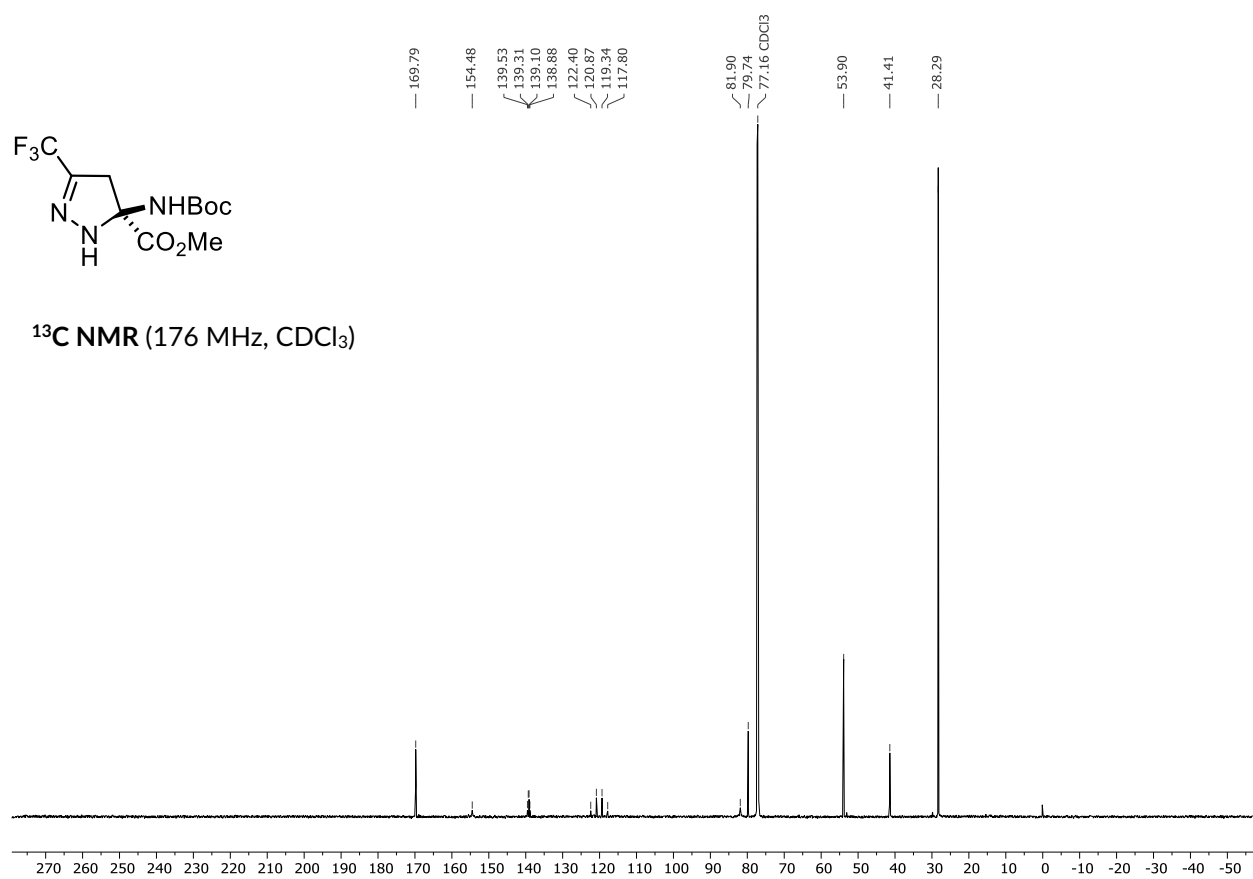


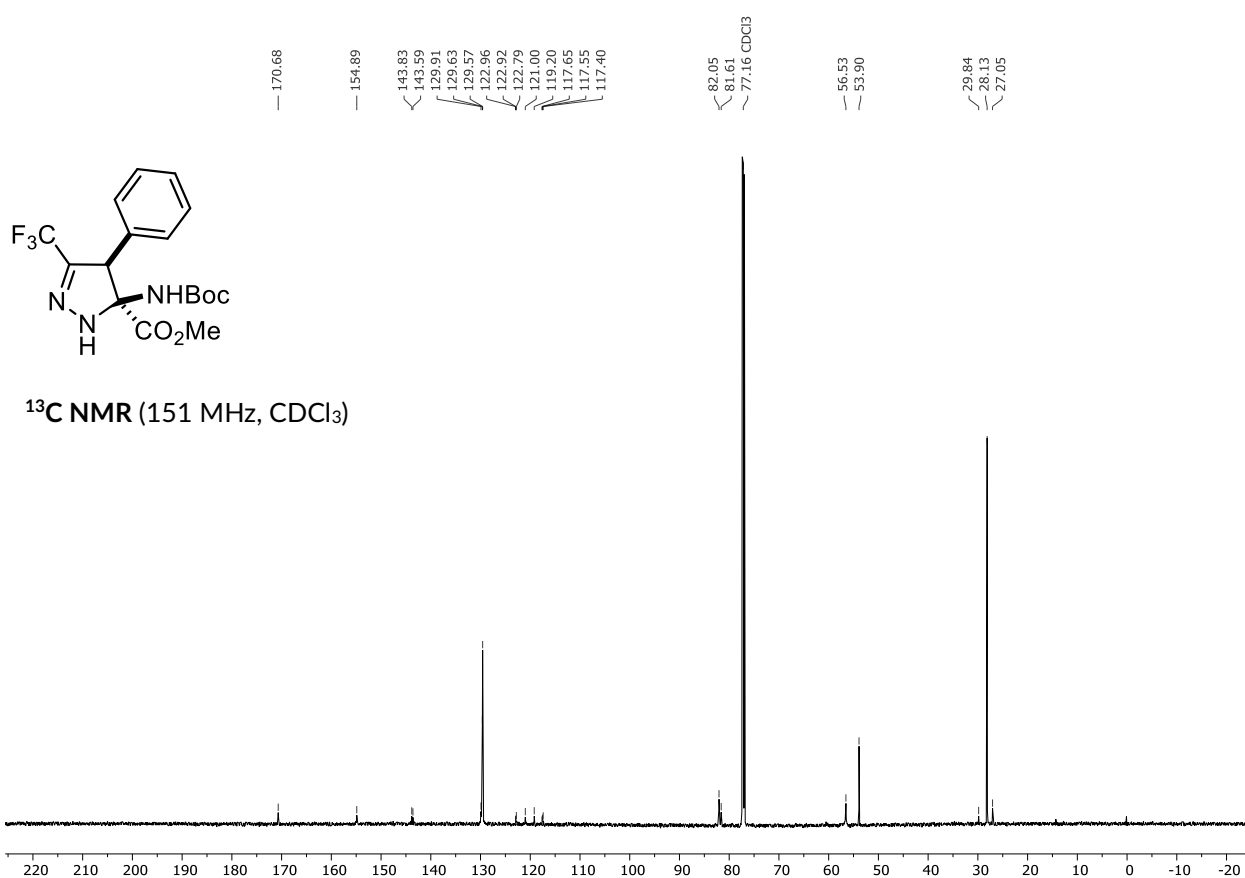
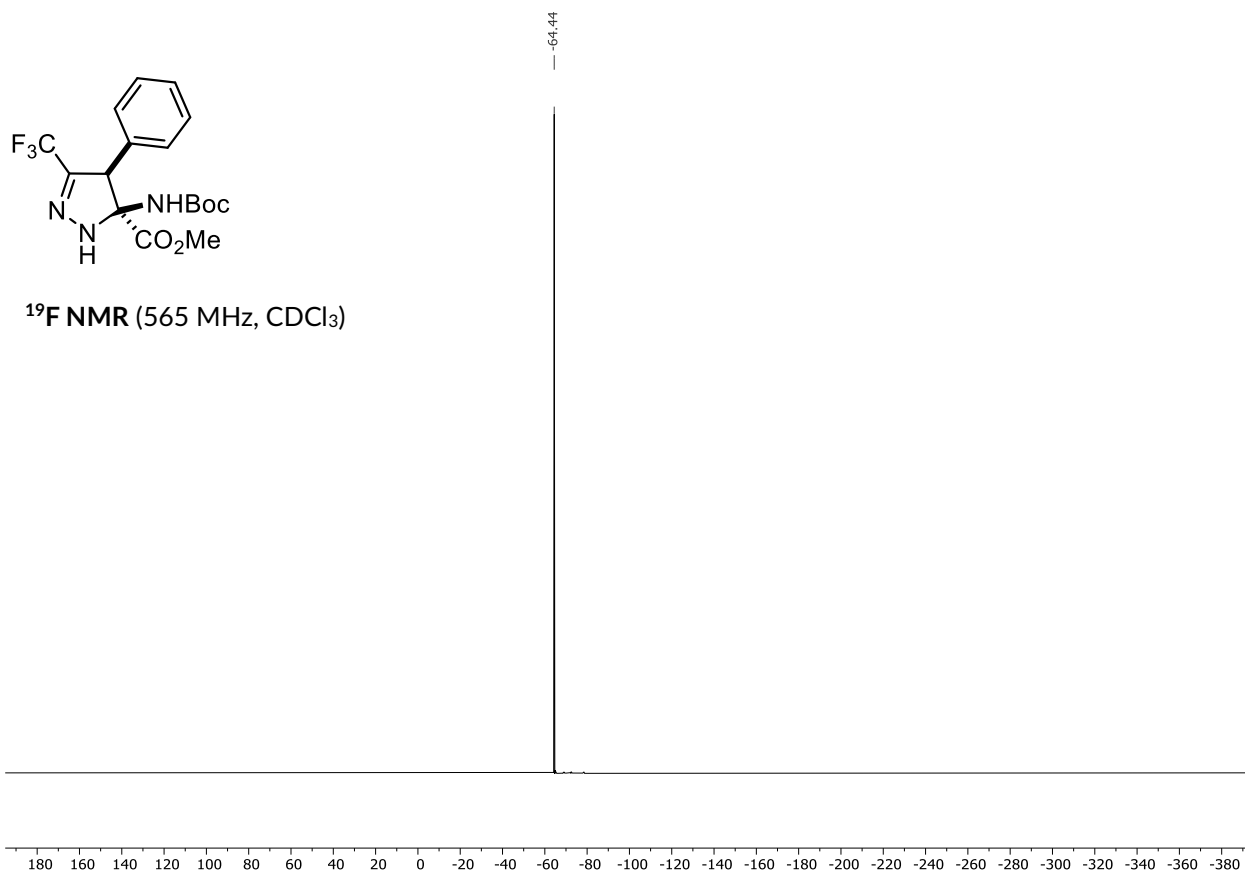




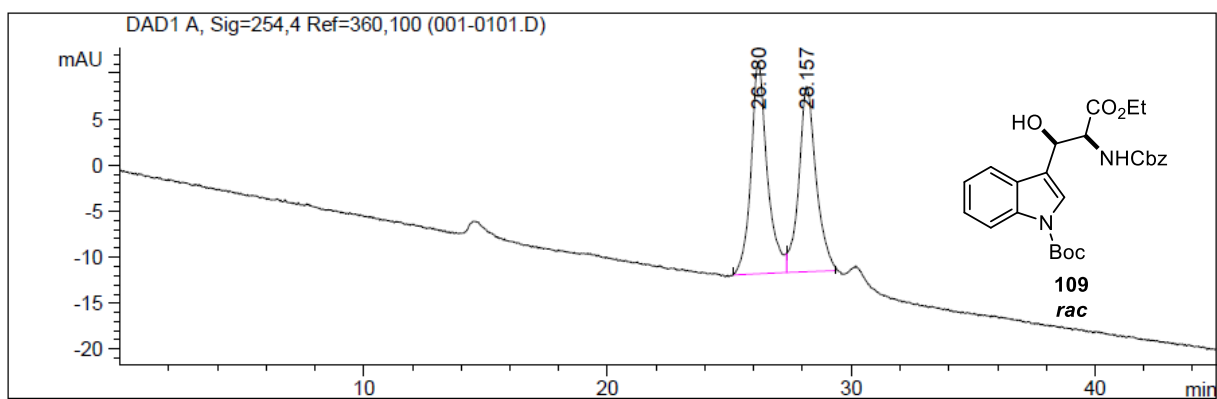




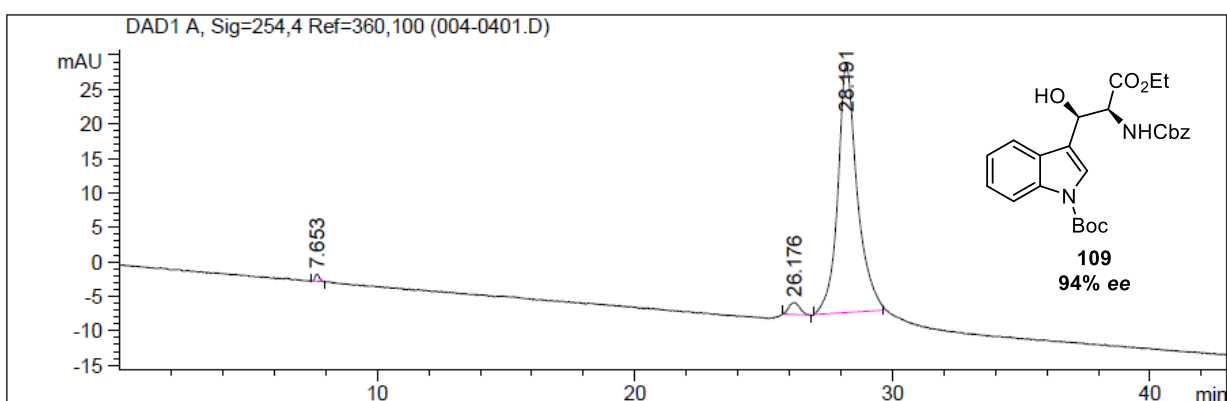




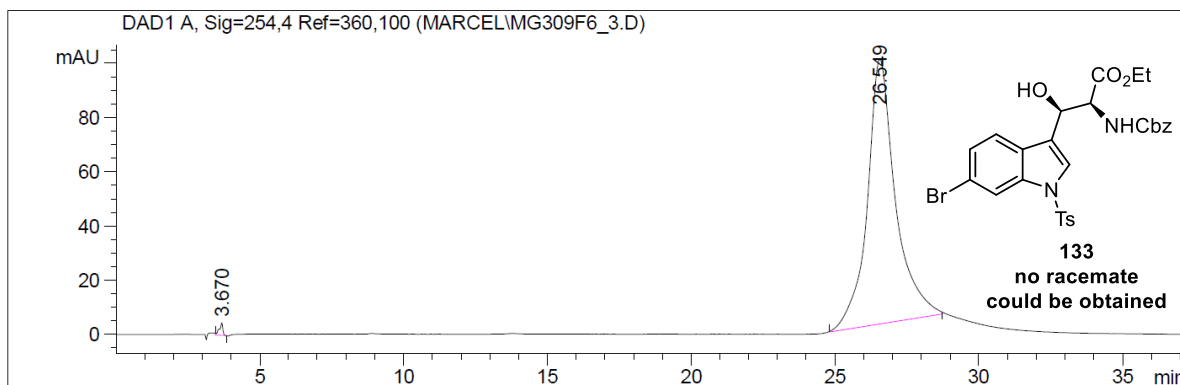
7.3. HPLC/GC Traces



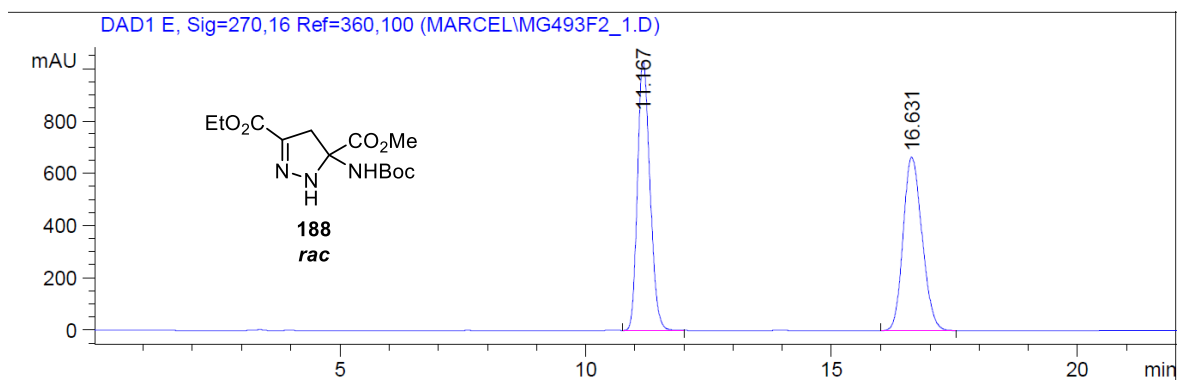
#	Time	Area	Area%
1	26.180	1082	52.1
2	28.157	996	47.9



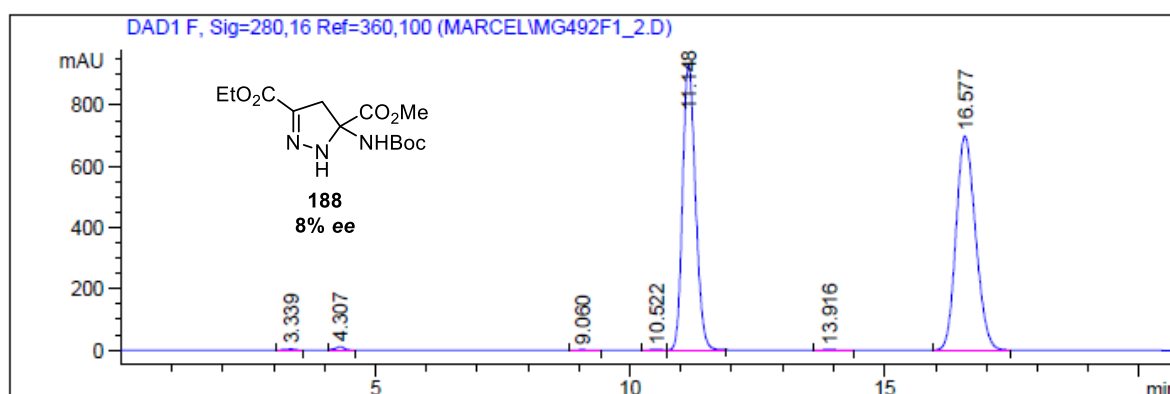
#	Time	Area	Area%
1	26.176	54	2.7
2	28.191	1899	97.2



#	Time	Area	Area%
1	26.549	6688	100



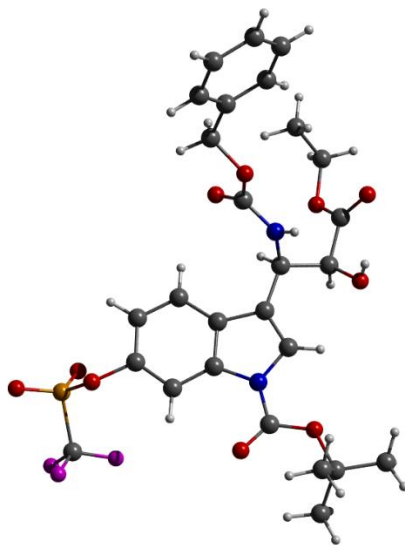
#	Time	Area	Area%
1	11.167	18250	50.7
2	16.631	17778	49.3



#	Time	Area	Area%
1	11.148	15276	46.2
2	16.577	17397	53.8

7.4. Crystallographic Data

7.4.1. Tryptophan 104

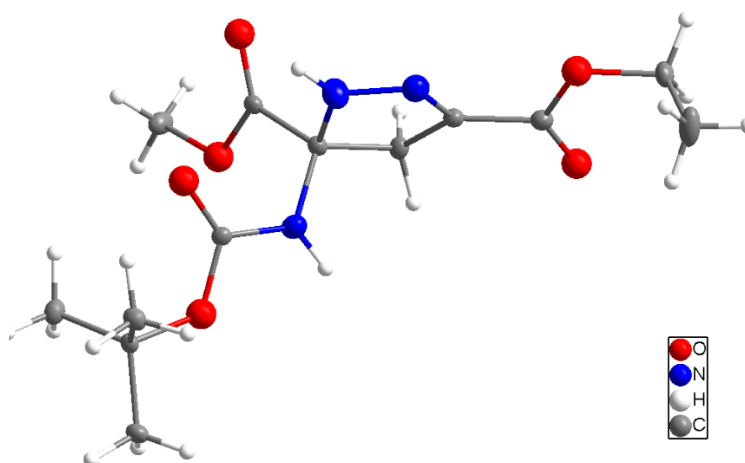


Crystal data and structure refinement of tryptophan **104**

Identification code	MG120s1
Empirical formula	C ₂₇ H ₂₉ F ₃ N ₂ O ₁₀ S
Molecular weight	630.58
Temperature [K]	100
Wavelength [Å]	1.54178
Crystal system, space group	Orthorhombic, <i>P2₁2₁2₁</i>
Unit cell dimensions	$a = 9.56964(6) \text{ \AA}$, $\alpha = 90^\circ$ $b = 12.16730(8) \text{ \AA}$, $\beta = 90^\circ$ $c = 25.08796(16) \text{ \AA}$, $\gamma = 90^\circ$
Volume [Å ³]	2921.16(3)
Z, Density (calculated)	4, 1.434 g/cm ³
Absorption coefficient [mm ⁻¹]	1.684
F(000)	1312
Crystal size [mm]	0.08 x 0.11 x 0.28
ϑ -range for data collection	3.52–68.36°
Index ranges	$-11 \leq h \leq 10$, $-14 \leq k \leq 14$, $-30 \leq l \leq 30$
Reflections collected	37409
Independent reflections	5224
Completeness to $\vartheta = 67.679^\circ$	97%
Absorption correction	multi-scan
Max. and min. transmission	0.829 and 0.695
Refinement method	Full-matrix least-squares on F ²
Data / restraints / parameters	5224 / 0 / 395

Goodness-of-fit on F^2	1.058
Final R indices [$I > 2\sigma(I)$]	$R_1 = 0.0237$, $wR_2 = 0.0619$
R indices (all data)	$R_1 = 0.0244$, $wR_2 = 0.0617$
Largest diff. peak and hole	0.267 and $-0.309 \text{ e}^-/\text{\AA}^{-3}$

7.4.2. Pyrazoline 188



Crystal data and structure refinement of 2-pyrazoline 188

Identification code	MG6171f3
Empirical formula	$C_{13}H_{21}N_3O_6$
Molecular weight	315.33
Temperature [K]	150
Wavelength [\AA]	0.71073
Crystal system, space group	triclinic, $P-1$
Unit cell dimensions	$a = 5.8859(1) \text{ \AA}$, $\alpha = 104.8851(6)^\circ$ $b = 10.3870(2) \text{ \AA}$, $\beta = 96.4341(6)^\circ$ $c = 13.7431(2) \text{ \AA}$, $\gamma = 103.6269(6)^\circ$
Volume [\AA^3]	775.72(2)
Z, Density (calculated)	2, 1.350 g/cm^3
Absorption coefficient [mm^{-1}]	0.107
F(000)	336
Crystal size [mm]	0.39 x 0.45 x 0.57
ϑ -range for data collection	2.110–26.362°
Index ranges	$-7 \leq h \leq 7$, $-12 \leq k \leq 12$, $-17 \leq l \leq 17$
Reflections collected	3160

Independent reflections	3018
Completeness to $\vartheta = 26.362^\circ$	99.7%
Absorption correction	multi-scan
Max. and min. transmission	0.753 and 0.692
Refinement method	Full-matrix least-squares on F^2
Data / restraints / parameters	3442 / 0 / 233
Goodness-of-fit on F^2	1.066
Final R indices [$I > 2\sigma(I)$]	$R_1 = 0.0555$, $wR_2 = 0.1412$
R indices (all data)	$R_1 = 0.0570$, $wR_2 = 0.1423$
Largest diff. peak and hole	0.992 and $-0.566 \text{ e}^-/\text{\AA}^{-3}$
